



Universidad de Valladolid

ESCUELA de INGENIERÍAS INDUSTRIALES

**DEPARTAMENTO de INGENIERÍA
ENERGÉTICA y FLUIDOMECÁNICA**

TESIS DOCTORAL

**ANÁLISIS DE CONCEPTOS Y EXPRESIONES
DE LA
VELOCIDAD DE COMBUSTIÓN LAMINAR EN AIRE
DE HIDRÓGENO Y DE MEZCLAS
HIDRÓGENO - GAS NATURAL**

Presentada por
Luis Manuel Mayo Monge
para optar al grado de doctor por
la Universidad de Valladolid
y
dirigida por el profesor doctor
Francisco V. Tinaut Fluixá

**An Analysis of Concepts and Expressions
for in-Air Laminar Burning Velocity of
Hydrogen and
Hydrogen - Natural Gas Mixtures**

Luis Manuel Mayo Monge

Tesis Doctoral dirigida
por el doctor
Francisco V. Tinaut Fluixá



Universidad de Valladolid



Universidad de Valladolid

Departamento de
Ingeniería Energética y Fluidomecánica

2015



Dedicado a la memoria de **Heliodoro Mayo Alonso** (★ 1931-2008 †)

¡Gracias por tus bendiciones!

Mi **hijo Luis H.M.** era aún muy chico. En un atardecer ya vecino de su noche, **mi** venerado **padre** elevaba con él sus ojos hacia lo más alto, muy lejos. Le abrazaba cálidamente con la mano izquierda, por el hombro, y levantaba la mano diestra, dirigiendo su dedo índice para mostrarle una estrella luminosa. Lucía vivamente como ardiente llama bajo el cielo protector.

Hoy mi buen pequeño está en camino de ser un muchacho, ojalá sensato y cabal. Le pido que conserve fielmente el recuerdo fecundo de su magistral abuelo, virtuoso leonés de manos prodigiosas y brazos heroicos, de ojos limpios, frente despejada y magno corazón; que no olvide a quien labró vigorosamente la ruta de nuestra vida y la senda de esta familia con su trabajo generoso, con su noble sabiduría e inmenso amor.

La meta de un trayecto no es el fin de un pasaje. Es un extremo abierto de una línea en un espacio del destino, un punto más del tiempo que intentamos forjar y que deseamos merecer porque lo creemos semi-infinito.

Con todo cariño para mi amada **madre, Tivi,**
y para mi querida **esposa, M^a Isabel.**

Agradecimientos

*Quiero expresar mi más señalado reconocimiento y gratitud, en lo académico y en lo humano, al **profesor** Francisco Tinaut, por ser para mí un ejemplo de competencia y profesionalidad, maestro de ingenieros y persona a imitar.*

*Después de haber sido alumno suyo, hace ya algunos lustros, él me acogió para realizar un proyecto fin de carrera en el **Departamento Universitario**, entonces de **Mecánica Aplicada e Ingeniería Térmica**. Me brindó seguidamente la posibilidad de colaborar como profesor ayudante de forma inmediata, tras mi licenciatura en 1989, a mis veinticuatro años y antes de incorporarme al servicio militar obligatorio en esa época. Asimismo me animó a cursar el programa de doctorado de aquel bienio 1989-1991, hasta completarlo a la sazón con el reconocimiento de suficiencia investigadora.*

*La historia ha transcurrido hasta el presente, sumando media centuria en mi pasado que, dicho sea de paso, me gustaría igualar en mi porvenir. De esta suerte, pues, ha sucedido otro cuarto de siglo de mi vida, jalonada por trabajo y familia, alejado de Valladolid mientras tanto. No por ello he dejado nunca de sustentar y alimentar la idea aplazada de recobrar, por ventura, algún día, el paso pendiente de tesis doctoral. He atesorado esta ilusión, aunque sólo fuera para visitar cada par de años el **Departamento**, ahora de **Ingeniería Energética y Fluido-Mecánica**, con la humilde disculpa de renovar prórrogas periódicamente, si bien conjeturando perpetuarlas, acaso hasta cuando arribara a una hipotética prejubilación en mi trabajo profesional o hasta que, quizá a la par, mi hijo empezase una carrera universitaria en un futuro. Los nuevos planes de estudios, que han establecido definitivamente periodos de expiración de programas de postgrado anteriores y fijado su extinción en la mitad de esta segunda década, me han obligado a tener que adelantar mi decisión, improrrogablemente, para afrontar una tesis en estos años recientes, sin más esperas. La determinación cardinal para ello ha nacido del estímulo recibido, de nuevo, gracias a la extraordinaria impronta de mi respetado **profesor**, y ha crecido primordialmente con el gran acicate y la única voluntad de que pueda servir como provechosa muestra patrón en la educación de mi hijo.*

*Para este último, primero en mi afán, escribo tan dilatadas líneas, al igual que la dedicatoria previa, con la confianza de que las lea pronto, con atención, y comprenda positivamente las sanas razones de las horas hurtadas a las tardes y noches en varios años, los que ansío poder restituir y pretendo empezar a compensar, **D. M.***

*Tras estos párrafos extensos, que espero se entiendan esencialmente imprescindibles para mí en lo muy personal y familiar, deseo mostrar también mi reconocimiento agradecido para quienes han alentado esta tesis, de una u otra forma, comenzando por el formidable equipo del muy estimado **profesor** Francisco V. Tinaut.*

*La **profesora** Blanca Giménez ha sido excelente asesora y supervisora, y me ha aportado interesantes consejos y atinadas consideraciones, con dedicación y afecto.*

*El **profesor** Andrés Melgar me ha animado en la tarea, desde su perspectiva y conocimiento, y se ha interesado positivamente por los avances del desarrollo.*

*La **profesora** Miriam Reyes ha sido valiosa y apreciada colaboradora, prestándome amablemente su pródiga y beneficiosa contribución.*

*El **investigador** Álvaro Lafuente, del centro tecnológico CIDAUT, me ha facilitado gentilmente información y experiencia precedente en materias relacionadas.*

*Quiero también reseñar mi agradecimiento al **profesor** Miguel Ángel Villamañán, con mi grato recuerdo por su trato siempre acogedor y cordial y su muy estimable cercanía para conmigo, prolongada desde el pasado.*

*Adicionalmente, no puedo omitir el reconocimiento de la labor, en resumen, de todos los **profesores y profesoras** que sembraron doctamente su semilla académica en la **Escuela Técnica Superior de Ingenieros Industriales**, ni debo dejar de mencionar a los que siguen haciéndolo en la transformada **Escuela de Ingenierías Industriales** de esta **Universidad de Valladolid**, a la que doy sinceras gracias.*

*Para finalizar, he de añadir un reconocimiento general a todos y cada uno de los numerosos **autores** mencionados en esta tesis, agradeciéndoles los trabajos publicados que han inspirado el desarrollo de este estudio.*

Luis M. Mayo Monge

A D. G.

Salamanca, Julio 2015.

**Análisis de Conceptos y Expresiones de la
Velocidad de Combustión Laminar en Aire
de Hidrógeno y de Mezclas
Hidrógeno - Gas Natural**

Luis Manuel Mayo Monge

Tesis Doctoral dirigida
por el doctor
Francisco V. Tinaut Fluixá



Universidad de Valladolid

Extracto resumen

A.	Prólogo	<i>xiii</i>
B.	Justificación de los temas tratados y puntos de partida	<i>xv</i>
B.1.	Antecedentes	<i>xv</i>
B.2.	Relaciones metodológicas	<i>xvii</i>
B.2.1.	Formulaciones de velocidades de quemado laminar para el hidrógeno y el metano como combustibles individuales	<i>xviii</i>
B.2.2.	Efectos relevantes para la velocidad de combustión laminar debidos a variables termodinámicas y parámetros de composición en la terminología de motores	<i>xviii</i>
C.	Planteamiento y desarrollo	<i>xix</i>
C.1.	Enfoque conceptual	<i>xix</i>
C.2.	Objetivos, métodos, resultados y análisis	<i>xix</i>
C.2.1.	Velocidad de quemado laminar de mezclas de hidrógeno-aire a presiones y temperaturas elevadas	<i>xx</i>
C.2.2.	Velocidad de quemado laminar en la combustión premezclada de mezclas de hidrógeno y gas natural	<i>xxi</i>

D.	Conclusiones	<i>xxiii</i>
D.1.	Aspectos generales de la velocidad de combustión laminar de mezclas combustibles de hidrógeno en relación con los métodos de obtención	<i>xxiii</i>
D.2.	Características de expresiones específicas de velocidad de quemado laminar para mezclas de hidrógeno	<i>xxvii</i>
D.3.	Tendencias de la velocidad de combustión laminar de mezclas hidrógeno-metano para los regímenes relacionados con el contenido de hidrógeno	<i>xxix</i>
D.4.	Características de diversas expresiones de velocidad de combustión laminar para mezclas combustibles de hidrógeno y gas natural	<i>xxx</i>
D.4.1.	Expresiones simples de velocidad de combustión laminar de mezclas de hidrógeno y gas natural	<i>xxx</i>
D.4.2.	Expresiones globales de velocidad de combustión laminar de mezclas de hidrógeno y gas natural en rangos completos de condiciones de composición y de variables termodinámicas	<i>xxxiii</i>
D.5.	Propuestas para futuros desarrollos	<i>xxxv</i>

A. Prólogo

Las mezclas gaseosas de aire-combustible, con diferentes tipos de combustibles combinados, tales como mezclas de algunos hidrocarburos (HC) e hidrógeno (H_2), implican oportunidades para aplicaciones prácticas que se consideran en muchos planes estratégicos contemporáneos, entre otras alternativas aplicadas o en procesos de mejora y diversificación. Se integran como combustibles alternativos en los estudios de investigación y desarrollo para la creación de un paisaje de energía que pueda ser racionalmente sostenible en el medio y largo plazo. Las perspectivas sobre protección ambiental y las circunstancias de los recursos energéticos en algunos países han contribuido, de manera significativa, a enfoques destinados a evitar dependencias operativas y económicas asociadas con los combustibles fósiles convencionales, a la promoción de técnicas encaminadas a la utilización y a la proliferación de otras fuentes de energía alternativas, de portadores y transmisores de energía que puedan considerarse como formas limpias y viables en condiciones razonables.

La evolución de las nuevas tecnologías relacionadas con la combustión interna ha mejorado en las últimas décadas el uso en motores de combustibles con gas natural (NG), individualmente o en combinación, y se están desarrollando sistemas comparativamente más "verdes", es decir, más ecológicos y ajustados a la legislación medioambiental, con arquitecturas optimizadas y estrategias de control específicas asociadas con el uso de estos tipos de combustibles. Entre otras necesidades, los investigadores han tenido en cuenta ciertos objetivos deseados de reducción de las emisiones de escape y de mejora del consumo de combustible y del comportamiento de los motores de combustión interna (ICE), con fines específicos y pensamiento general en la minimización de las emisiones de gases de efecto invernadero y dióxido de carbono (CO_2) en particular. El uso y la combinación de un combustible tal como el hidrógeno, obviamente libre de carbono, pueden ayudar significativamente en la reducción de las emisiones, con acaso la excepción de los óxidos de nitrógeno (NO_x).

El uso del hidrógeno (H_2) es una opción propuesta en la mayoría de los planes estratégicos de un sistema energético sostenible. El hidrógeno es el elemento más abundante en el universo, pero tiene que ser producido utilizando otras fuentes de energía, ya que no está disponible en un estado libre. Por eso se considera un portador de energía, en lugar de una fuente de energía. Las tareas y desafíos asociados son la producción de hidrógeno y su distribución y almacenamiento. Quizás las soluciones energéticas a largo plazo dependan preferentemente de la electricidad renovable para producir hidrógeno, almacenable a bordo en forma de líquido o de gas, para utilizarlo finalmente en pilas de combustible, para generar electricidad para alimentar un motor eléctrico, o en motores de combustión interna, para generar directamente energía mecánica para un vehículo. Sin embargo, como la utilización de hidrógeno en la tecnología de celdas de combustible está aún en investigación, una utilización prometedor y fácilmente aplicable es la combustión directa en los motores como combustible simple o en mezclas de combustibles. Los motores de combustión interna propulsados por hidrógeno (H_2ICE) han sido también considerados en la literatura como una tecnología de transición en el medio plazo, hacia una proliferación de las celdas de combustible (FC) en vehículos. Actualmente los H_2ICE son más baratos que las pilas de

combustible de hidrógeno (H_2FC), tanto directamente como en términos de coste de combustible (debido a los requisitos de pureza más alta del combustible para las H_2FC).

Además de su uso como combustible simple, el hidrógeno también se considera como un potenciador de la combustión, como un agente activador en mezclas con combustibles gaseosos, y también en aplicaciones combinadas o duales con combustibles líquidos de ambos tipos gasolina y diesel. El uso de motores de combustión interna permite operaciones con combustibles combinados; como ejemplos, un motor puede funcionar con un combustible líquido así como con hidrógeno gas, o con mezclas de hidrógeno y gas natural, mitigando los requerimientos de autonomía.

Debido a sus propiedades peculiares, el hidrógeno es un combustible de modelado no convencional. La relativamente baja sensibilidad a la turbulencia y la alta velocidad de llama laminar imponen no sólo tener en cuenta las propiedades del combustible, sino también tener que modelar la propagación de su combustión laminar. Sin embargo, sus mismas propiedades, de baja densidad y de muy alta velocidad de la llama laminar, imponen estrategias operativas específicas y la adaptación de los instrumentos de investigación convencionales. En el cilindro de motores de encendido por chispa (SIE) la llama se propaga en una mezcla homogénea, por lo tanto un conocimiento profundo de la propagación de la llama y la transición del frente de llama desde el inicio de la combustión a una llama completamente turbulenta son esenciales para el diseño de motores de encendido provocado eficientes.

La velocidad de combustión laminar está estrechamente asociada a estos fenómenos. El cálculo de la combustión turbulenta de hidrógeno, para un seguimiento de la propagación de la llama a lo largo de la cámara de combustión, y la resolución de la presión en el cilindro y la temperatura, son necesarios para facilitar el desarrollo de los motores de ignición propulsados por hidrógeno (H_2SIE). En la cámara de combustión de los motores de encendido provocado, la presión y las temperaturas son mucho más altas que las condiciones ambientales. Lo que generalmente se conoce como condiciones en motor puede ser cuantitativamente definido por presiones de hasta 5 MPa y temperaturas de hasta 900 K (correspondientes a las mezclas sin quemar). Esto conlleva entonces su importancia, no sólo para conocer la dependencia con la presión instantánea y la temperatura de la velocidad de combustión laminar de la mezcla en el cilindro, sino también para extender esta dependencia hasta las condiciones propias en motores.

Esta valiosa información se utiliza comúnmente para validar los mecanismos de reacción química y modelos computacionales de combustión, y es de interés práctico en el diseño y optimización de motores de combustión interna alimentados con hidrógeno o por mezclas enriquecidas con hidrógeno. De este modo, las bases de datos pertinentes de las velocidades de quemado laminar de hidrógeno en motores, de mediciones de llamas premezcladas de hidrógeno-aire a alta presión y alta temperatura, son muy útiles y demandadas, porque el entendimiento de la operación del motor alimentado por hidrógeno requiere datos sobre la velocidad de quemado laminar de las mezclas de hidrógeno-aire y gases residuales bajo una amplia gama de condiciones. Sin embargo, hay una escasez de datos en la literatura, en particular en condiciones de motores. Esto se complica aún más por la aparición de inestabilidades de llama a presiones de motor, lo que compromete algunos de los datos existentes en la velocidad de combustión laminar de mezclas de hidrógeno, que se necesitan para amplios intervalos. Además, la

influencia de la tasa de estiramiento (stretch) del frente de llama y de la estabilidad de la llama es significativa en la velocidad de combustión. Los trabajos publicados existentes subrayan la importancia de datos exactos sobre la velocidad de combustión laminar de mezclas de hidrógeno-aire y gases residuales de la combustión (gas de escape, interna o externamente recirculado). La validación de los datos experimentales y la validación de los mecanismos de reacción química en estas condiciones son importantes.

B. Justificación de los temas tratados y puntos de partida

Los usos eficaces y seguros de hidrógeno gas y de mezclas gaseosas de combustibles, tales como las de los tipos de hidrocarburos e hidrógeno o de gas natural e hidrógeno, implican atención a sus propiedades fisicoquímicas y sus mecanismos de reacción asociados al proceso de combustión, para las diversas posibles mezclas de combustibles, que pueden ser ponderadas dependiendo de muchas y variadas potenciales composiciones y condiciones. Entre otras características, relacionadas con las posibilidades de combustión y sus implicaciones en el análisis técnico, los conceptos como las velocidades de quemado son interesantes (y principal objetivo de este estudio), así como otros términos relativos a la dispersión cíclica, la sensibilidad a la detonación, las emisiones, etc.

B.1. Antecedentes

La velocidad de quemado laminar de una mezcla de combustible-aire es una propiedad fisicoquímica particularmente importante, debido a su dependencia de las variables presión, temperatura y composición (dosado relativo de la mezcla y concentración de diluyentes). Como una propiedad fundamental de combustión, la velocidad de quemado laminar caracteriza y cuantifica los efectos del combustible para las mezclas de combustible y aire premezclados, influyendo sobre la entrada del gas y en la velocidad de propagación de la llama en la combustión de carga homogénea. Esta velocidad afecta directamente a la velocidad del frente de llama y por lo tanto al funcionamiento de un motor de encendido provocado, donde la velocidad de quemado es una causa primordial de la tasa de combustión. Esto sirve para la interpretación de los procesos desarrollados por la llama en su difusión y extensión, por ejemplo, las inestabilidades y la formación de arrugamientos, etc. En los motores de ignición, el quemado más rápido conduce a una combustión más robusta y repetible y permite mejoras de la operación y del rendimiento del motor, incluso con sustancialmente mayor cantidad de gases residuales, permitiendo de este modo la reducción de emisiones de NO_x. Por lo tanto, la velocidad de quemado laminar (u_l) proporciona información sobre las características de combustión y se utiliza en la validación de los mecanismos de reacción química.

El uso de las expresiones de velocidad de quemado laminar calculadas a partir de los mecanismos de cinética química, sobre la base de llamas teóricas unidimensionales, se asocia particularmente en alguna literatura a la adecuada significación de la velocidad de combustión laminar como una tasa de reacción química característica. Esa es una solución utilizada por varios autores para emplear ésta (u_L)

como base de correlación para la velocidad de combustión turbulenta (u_t) en modelos en motor, donde estas dos velocidades están relacionadas, a la misma presión y temperatura, por una relación de velocidades de quemado. Esto es porque la velocidad de quemado laminar también proporciona una referencia de base para el estudio de la combustión turbulenta y con respecto a la velocidad de llama correspondiente. De esta manera, la mayoría de los modelos de combustión en motor estiman la velocidad de la llama turbulenta como el valor laminar multiplicado por la relación de velocidades de la llama (FSR), que representa los efectos en la llama de la turbulencia en el cilindro, aumentando la superficie de la llama y los fenómenos de difusión y de transporte.

Así, una de las variables clave, de importancia práctica en diseño y optimización de motores para el modelado de combustión en motores de encendido provocado, es la velocidad de quemado laminar para la mezcla de combustible, que incorpora información sobre los efectos de la reactividad, la difusividad y la exotermicidad de la mezcla de combustible-aire. Este es un elemento fundamental de cualquier modelo para los procesos en un motor de combustión interna. En consecuencia, en resumen, son muy útiles los datos sobre las velocidades de quemado laminares y sus dependencias de la presión, temperatura, composición de la mezcla, velocidad de estiramiento (stretch) del frente de llama e inestabilidades de ésta. Debido a eso, se necesitan velocidades de quemado validadas en condiciones similares a las propias de motores, que pueden ser obtenidas a partir de instalaciones experimentales y como resultados de simulación deducidos por extrapolaciones o de los mecanismos de reacción. Por otra parte, las expresiones de velocidad de quemado laminar de mezclas, como funciones de la presión (P), la temperatura (T_u), el dosado relativo (Φ) y la fracción de gases residuales ($f_{res,u}$), son una entrada muy importante para su uso en la predicción por medio de modelos de las características de la combustión y de las emisiones de contaminantes en motores de encendido provocado.

Diferentes técnicas experimentales, que se muestran en muchos estudios para la obtención de velocidades de quemado laminar, se han utilizado para las mezclas de combustible-aire, con resultados diversos como las condiciones experimentales consideradas por diferentes autores, especialmente variadas para mezclas de combustibles. Para una presión inicial dada (P) y una temperatura (T_u) de los gases frescos, las mezclas de combustible pueden tener diferentes valores de velocidad de quemado laminar, de acuerdo con las formas del frente de llama, los flujos, las inestabilidades y las pérdidas de calor; los factores experimentales asociados a la geometría y la estabilidad de la llama afectan decisivamente a los resultados de su velocidad.

Los datos publicados sobre las velocidades de quemado laminar para mezclas de combustible-aire a presiones y temperaturas de motores (hasta aproximadamente 5 MPa y 900 K) son singularmente escasos en la literatura y comúnmente no tienen en cuenta los efectos del estiramiento (stretch) del frente de llama ni de la inestabilidad y la tendencia a la celularidad, causando una gran dispersión en las velocidades de quemado reportadas. Algunos de ellos llevan a velocidades de quemado consistentemente más altas, con diferencias mayores para las mezclas pobres. El efecto directo de la tasa de estiramiento (stretch) en la velocidad de quemado laminar es menos importante a alta presión (como en motores) que a baja presión. Sin embargo, la reducida sensibilidad a la

tasa de estiramiento (stretch) a alta presión resulta en una mayor susceptibilidad a la inestabilidad, con una mayor influencia en los valores de velocidad de quemado laminar. Este problema es aún más relevante para mezclas de combustibles en combinación con un alto contenido de hidrógeno, debido a su incrementada sensibilidad a los efectos termo-difusivos e hidrodinámicos de la inestabilidad, mayor que para los hidrocarburos comunes, lo que lleva a la intensificación de la formación de arrugamientos del frente de llama y de celularidad en algunas condiciones.

Para facilitar la aplicación de los valores de velocidad de quemado laminar en modelos fenomenológicos y predictivos de combustión, se prefiere generalmente hacer un empleo analítico de funciones matemáticas continuas en lugar de utilizar tablas de valores discretos. Sin embargo, el problema principal es que, por lo general, no hay correlaciones de datos disponibles válidas en condiciones motor para las infinitas posibles composiciones de mezclas de combustibles. Algunas expresiones que aparecen en las publicaciones se basan con más frecuencia en mediciones de bajas presión, temperatura y velocidad de la llama, que generalmente no son totalmente representativas de las condiciones que se encuentran en sistemas de combustión reales. Enfoques experimentales y numéricos se han utilizado de forma conjunta en la literatura para superar las incertidumbres y la falta de datos, tratando de determinar las velocidades de quemado laminar ideales en diferentes casos, frecuentemente tomando extrapolaciones de valores, por ejemplo a partir de mediciones experimentales de llamas laminares en algunas condiciones controladas.

De acuerdo con el enfoque general esbozado aquí, los estudios con expresiones de velocidades de quemado laminar que han sido referenciados de la literatura, en el presente trabajo, se centraron en análisis experimentales y/o por simulación numérica de las llamas de mezclas de aire con hidrógeno o con combustibles combinados de hidrocarburos e hidrógeno. En algunos de ellos se utilizan llamas esféricas de propagación hacia el exterior para obtener velocidades de quemado laminar desde condiciones iniciales próximas a condiciones ambientales atmosféricas. Otros extienden las condiciones por simulación hasta mayores valores iniciales de temperatura y de presión. Algunos otros utilizan modelos computacionales termo-fluido-dinámicos y consideran también las cadenas de reacciones y los perfiles de radicales, incluso a elevadas presiones y temperaturas, y su influencia sobre las velocidades de quemado laminar por análisis con modelos y códigos químicos. Como base para las comparaciones y cálculos, muchos autores señalan en sus trabajos que los resultados de más o menos detallados cálculos cinéticos se reflejan en la definición de la mayoría de las expresiones y de las correlaciones, debido a la falta o la escasez de datos experimentales suficientemente representativos, a causa de las dificultades de su obtención para las mezclas enriquecidas de hidrógeno en aire.

B.2. Relaciones metodológicas

Antes de entrar en el planteamiento del desarrollo de este trabajo, en este doble punto se mencionan formulaciones consideradas para gases simples, y se esbozan efectos relacionados, con influencia relevante en las velocidades de combustión laminar.

B.2.1. *Formulaciones de velocidades de quemado laminar para el hidrógeno y el metano como combustibles individuales*

La velocidad de quemado laminar de cada combustible por sí mismo, única y respectivamente considerado, en la combustión premezclada de mezclas con aire, es un posible punto de partida hacia el examen de algunas dependencias funcionales de las velocidades de quemado laminar para las mezclas de combustibles combinados. Las velocidades de llama y de quemado del hidrógeno y, respectivamente, del metano (considerado frecuentemente como representativo del gas natural), se han estudiado abundantemente en la literatura como combustibles individuales en llamas premezcladas.

- El caso del hidrógeno (H_2) como combustible singular es ampliamente tratado en este trabajo, donde se han estudiado fórmulas empíricas y teóricas de las velocidades de quemado laminar para la combustión premezclada de mezclas de hidrógeno-aire. Expresiones de interés, aplicables en amplios rangos de temperaturas, presiones, dosados relativos y fracciones de dilución, han sido analíticamente procesadas con especial atención a las presiones y temperaturas elevadas típicas para condiciones análogas a las de motores de ignición.
- En el caso de metano (CH_4), éste se considera un combustible gaseoso de referencia y es posible encontrar numerosos resultados publicados y expresiones de velocidad de quemado, con diferentes criterios y diversas exactitudes o precisiones de aplicación en sus rangos de uso efectivo o supuestos correspondientes.

B.2.2. *Efectos relevantes para la velocidad de combustión laminar debidos a variables termodinámicas y parámetros de composición en la terminología de motores*

La mayoría de las fórmulas analíticas publicadas de velocidades de quemado laminar están basadas en expresiones experimentales (u_l) o calculadas por simulación numérica (u_L), como se ha dicho anteriormente. Con frecuencia se encuentran con una forma general ampliamente extendida para dar cuenta de los efectos de temperatura y presión (también para mezclas de combustible-aire a presiones y temperaturas elevadas), modificada a veces para expresar la influencia y dependencias funcionales del dosado relativo (Φ) y de la fracción de dilución de gas residual contenido ($f_{res,u}$), además de la temperatura (T_u) y la presión (P) iniciales, y donde las variables están en función de parámetros de acuerdo con los datos y los métodos de deducción. El contenido de hidrógeno en diferentes formas de fracciones o parámetros se puede añadir como otra posible variable o parámetro funcional cuando se correlacionan velocidades de quemado laminar de mezclas de combustibles con hidrógeno.

Algunos de los términos generales de la composición, en la terminología de los motores, se detallan en [tabla 1](#) para las mezclas de combustible-aire con hidrógeno. Estos términos han sido considerados desde dos perspectivas, respectivamente, tanto para el hidrógeno como combustible único o como componente en mezclas de combustible combinado con hidrocarburos (por ejemplo, gas natural o puro metano).

C. Planteamiento y desarrollo

Después del capítulo introductorio, los demás capítulos de este trabajo se desarrollan, sucesivamente, en base a los propósitos que se caracterizan en líneas generales en los apartados siguientes.

C.1. Enfoque conceptual

- El segundo capítulo de este estudio contiene un resumen de las propiedades de gas natural, metano e hidrógeno y de las características de sus mezclas de combustible-aire (v.g. [tabla 3](#)), incluyendo también un resumen con información complementaria y terminología sobre características de la combustión, emisiones, variabilidad cíclica, etc. (v.g. [tabla 5](#)), en diferentes aplicaciones en motores con diversas mezclas combustibles, en función de las posibles combinaciones de combustible y de los efectos de dilución de gas residual.
- El tercer capítulo presenta, con el fin de proporcionar una mejor comprensión, un compendio de conceptos asociados con la velocidad de quemado laminar de mezclas de combustible gaseoso. Esto se ha hecho, principalmente, con el objetivo más centrado en mezclas hidrógeno-aire (es decir, el hidrógeno se ha tenido en cuenta como combustible singular en una parte importante del trabajo realizado). Consideraciones sobre las inestabilidades del frente de llama, la aparición de estructuras celulares en llamas y los conceptos relacionados con interacciones por estiramiento (stretch), se han desarrollado y resumido, así como la influencia de la geometría del frente de llama en la velocidad de quemado.

C.2. Objetivos, métodos, resultados y análisis

Los propósitos de la Tesis se desglosan en partes sucesivas, con sus correspondientes desarrollos en dos grupos de capítulos respectivamente.

- En los capítulos cuatro y cinco se incluyen el estudio y la comparación de expresiones publicadas de velocidad de quemado laminar para la combustión premezclada de mezclas combustibles de hidrógeno-aire, con especial atención a la aplicabilidad en amplios rangos de condiciones de operación y hasta elevadas presiones y temperaturas (similares a condiciones en motores de encendido provocado). Estas expresiones se formulan con sus dependencias definidas de las condiciones iniciales de la mezcla, presión, temperatura y composición, con dosado relativo combustible-aire de pobre a rico, para su aplicación a diferentes mezclas de hidrógeno-aire y gas residual.

El análisis comparativo de esta parte del trabajo se ha realizado con el fin de mostrar una selección, válida en condiciones de motores, de expresiones de velocidad de quemado laminar que se han seleccionado de varias referencias técnicas, entre muchas otras. De este modo este trabajo permite la elección de expresiones específicas para combustión laminar premezclada de mezclas de aire y de hidrógeno como único

combustible o como la base para estimar, con la ayuda de reglas de mezclado, la velocidad de combustión de mezclas combinadas con hidrógeno y otros combustibles.

- En los capítulos seis y siete se muestra un estudio de expresiones publicadas de velocidad de quemado laminar para la combustión premezclada de mezclas de hidrocarburos e hidrógeno, y se incluyen algunas opciones válidas para presiones y temperaturas elevadas (similares a condiciones en motores de ignición). Estas otras expresiones también se formulan con sus dependencias definidas en condiciones iniciales de presión, temperatura y composición, con dosado relativo combustible-aire de pobre a rico, y para su aplicación a diferentes combinaciones de combustible, con gases residuales en algunos casos.

Además, el análisis de esta otra parte del estudio también incluye una selección de formulaciones de velocidad de quemado laminar, parcialmente válidas en amplios rangos de condiciones de funcionamiento o, a veces, extrapoladas a condiciones similares a las de motores. Como se ha dicho, éstas son aplicables a combustión laminar premezclada de mezclas de hidrógeno-hidrocarburos-aire, pero particularmente para mezclas de hidrógeno-metano-aire, como base para estimar las velocidades de quemado para mezclas combustibles de hidrógeno y gas natural.

C.2.1. Velocidad de quemado laminar de mezclas de hidrógeno-aire a presiones y temperaturas elevadas

- El cuarto capítulo se refiere más específicamente a valores y expresiones analíticas de las velocidades de combustión laminar de mezclas de hidrógeno-aire publicadas en varios documentos técnicos. El material se presenta considerando el origen y la metodología utilizada para obtener los resultados, más o menos agrupados en dos categorías: metodologías basadas experimentalmente y basadas numéricamente. En cuanto a las metodologías basadas en datos experimentales, que proporcionan velocidades de quemado laminar generalmente obtenidas a partir de la grabación de imágenes de frente de llama o de análisis de la presión de combustión, se dan detalles de sus gamas de validez, desde condiciones atmosféricas hasta condiciones similares a las de motores, y sobre el hecho de si tienen o no tienen en cuenta los efectos de estiramiento (stretch) y de inestabilidades en los resultados experimentales. En cuanto a los métodos numéricos, basados en mecanismos químicos para cálculo de la cinética y en modelos computacionales termo-fluido-dinámicos, aunque tienen la ventaja de ser capaces de calcular la velocidad de combustión laminar en condiciones ideales teóricas (frente adiabático, unidimensional, libre de estiramiento y de inestabilidades), requieren sin embargo algún tipo de validación con datos reales.

- El quinto capítulo trata en detalle la aplicabilidad de expresiones de velocidad de combustión laminar de las mezclas de hidrógeno-aire en condiciones similares a las de los motores, con comparaciones entre las diferentes expresiones seleccionadas, en sus respectivas gamas de validez. Cada metodología particular para alcanzar las expresiones ha sido analizada, basada en procedimientos experimentales, métodos de simulación numérica o metodologías combinadas. Hay que señalar que las expresiones de la literatura han sido citadas primeramente con la nomenclatura original de sus

autores, pero también se han reescrito con una homogeneización de notación, a efectos de una comparación más valiosa.

Numerosas tablas (v.g. [tablas 10-16](#)) presentan, de forma esquemática, la información relativa al sistema experimental o al método numérico, la consideración o no de correcciones para dar cuenta de efectos de estiramiento (stretch) e inestabilidades, comentarios adicionales, la dependencia de las variables relevantes, la homogeneización de la nomenclatura, los rangos de validez, el significado real de la velocidad reportada (ideal, aparente, casi laminar, sometida o libre de tasa de estiramiento, afectada o no afectada por inestabilidades), etc.

Además, doce expresiones analíticas seleccionadas de velocidad de combustión de las mezclas de hidrógeno-aire se han computado (v.g. [tablas 15-18](#)) para comparar los resultados predichos por medio de representaciones gráficas, para mostrar los valores y tendencias cuando varían la presión, la temperatura o el dosado relativo, siempre teniendo en cuenta estrictamente los rangos de aplicación de las respectivas expresiones. Algunas consideraciones generales se hacen sobre las expresiones de velocidad de combustión laminar, dependiendo del origen y la metodología. Finalmente se hace una comparación de las mejores opciones para las expresiones de velocidad de quemado laminar, válidas en condiciones similares a las de motores. Un objetivo declarado de esta parte es identificar expresiones que pueden proporcionar resultados coherentes para calcular la velocidad de combustión laminar de las mezclas de hidrógeno-aire y ser válidas incluso en condiciones de motores, para rangos suficientemente completos.

C.2.2. Velocidad de quemado laminar en la combustión premezclada de mezclas de hidrógeno y gas natural

- El sexto capítulo se refiere en primer lugar a las formulaciones de velocidad de quemado laminar para el metano y el hidrógeno como combustibles puros en mezclas con aire, como punto de partida. En segundo lugar, con el objetivo centrado en la velocidad de quemado laminar de mezclas de combustibles combinados, se reseñan algunas consideraciones sobre diversos tipos de métodos de definición experimentales y computacionales. También se consideran las opciones de usar implementaciones de esquemas cinéticos químicos para la simulación de llamas premezcladas unidimensionales teóricas. Finalmente se introduce la aplicación de reglas de mezclado relacionadas con expresiones de formas lineales, potenciales, exponenciales y fórmulas del tipo de la llamada regla de Le Chatelier.

- El séptimo capítulo se refiere más específicamente a expresiones de la velocidad de quemado laminar de mezclas de hidrógeno-hidrocarburos-aire publicadas en documentos técnicos. Este material se presenta considerando el origen y los procedimientos empleados para obtener los resultados, más o menos agrupados en función de las metodologías comparadas. En cuanto a los métodos de base experimental, que proporcionan datos de las velocidades de quemado laminar generalmente obtenidos a partir de la grabación de imágenes de frente de llama o del análisis de la presión de combustión, se dan detalles de sus gamas de validez, desde condiciones atmosféricas

hasta condiciones similares a las de motores, y sobre el hecho de si consideran o no gamas completas de las posibles combinaciones de componentes del combustible. En cuanto a los métodos numéricos (ya bien sea basados en reglas de mezclado y/o basados en mecanismos químicos para cálculo de la cinética y en modelos termo-fluidodinámicos computacionales), tienen la ventaja de ser capaces de calcular la velocidad de combustión laminar en condiciones teóricas, aunque requieren sin embargo algún tipo de validación con datos reales. Por lo tanto esta sección también se refiere a las diferentes aplicaciones y extrapolaciones de algunas expresiones de velocidad de quemado laminar para la combustión de mezclas combustibles de hidrógeno y metano o gas natural.

Se incluyen varios esquemas, resúmenes y tablas para presentar la información relativa a los distintos comportamientos de tendencias de la velocidad de combustión laminar en los diversos regímenes posibles considerados en la literatura (v.g. [tabla 21](#)), y sobre la influencia de la interacción de las concentraciones de radicales y de las reacciones sensibles en la zona de reacción de la llama premezclada (v.g. [tablas 22-24](#)).

Además, algunas expresiones analíticas seleccionadas de velocidad de combustión laminar y su aplicabilidad se han explicado en particular. Singularmente una de ellas ([tabla 25](#)), especialmente completa, ha sido descrita en detalle por sus importantes amplios intervalos de aplicación, basados en la consideración de todos los efectos significativos (composición de la mezcla, proporción de componentes combustibles en ella, fracción de dilución de gases residuales, presión y temperatura). De este modo, son reseñados algunos aspectos generales acerca de las expresiones consideradas de la velocidad de combustión laminar, en función de su origen y de su metodología. Por último, se da una conclusión sobre las expresiones que se estiman como las mejores opciones, debido a su aplicabilidad para condiciones variadas. Una meta declarada de esta parte es identificar una expresión que puede proporcionar resultados útiles con una precisión aceptable para el cálculo de la velocidad de combustión laminar de las mezclas de hidrógeno-metano-aire y ser válida para rangos completos, incluso en condiciones similares a las de motores.

Se aporta un resumen de todos los tipos de expresiones que han sido analizados en el capítulo siete ([tabla 26](#)), para las mezclas de combustible de hidrógeno con metano o con gas natural, con sus características de aplicación dependiendo de las condiciones de composición.

- El octavo capítulo, al final de esta parte, tiene un carácter de apéndice complementario de los capítulos seis y siete anteriores, para incluir separadamente algunas informaciones complementarias o más detalladas ([tablas 27-29](#)) en relación con trabajos consultados.

D. Conclusiones

En el capítulo noveno, y final, de conclusiones derivadas de las distintas partes de este trabajo, nos centramos principalmente en dos perspectivas: por una parte, acerca de las consideraciones de las cuestiones relativas a los diferentes métodos de deducción de las expresiones de las velocidades de combustión laminar para el hidrógeno y sus mezclas con metano o gas natural y, por otro lado, sobre las consideraciones de los diferentes tipos de expresiones y en las expresiones específicas aplicables para diversos contenidos de hidrógeno en mezclas, desde solamente hidrógeno hasta exclusivamente metano, pasando por los diversos tipos de combinaciones posibles en variadas proporciones de cada uno.

D.1. *Aspectos generales de la velocidad de combustión laminar de mezclas combustibles de hidrógeno en relación con los métodos de obtención*

En investigación es un objetivo lograr valores de velocidad de combustión laminar de mezclas de hidrógeno, a presiones y temperaturas elevadas, como ocurre en motores de combustión interna, así como tener en cuenta el efecto de los gases residuales derivados de la recirculación de los gases de escape. La definición y validación de velocidad de combustión laminar de mezclas de combustible y aire no es fácil cuando se trata de encontrar datos experimentales precisos a partir de mezclas de combustibles gaseosos combinados con hidrógeno como uno de los constituyentes, siendo esos datos también insuficientemente amplios o representativos, en general. Una razón importante de esto es que la generación de suficientes datos experimentales es difícil, especialmente para condiciones de motores, sobre todo si se trata de cubrir muchas posibilidades de composición para mezclas de varios componentes en las mezclas combustibles con hidrógeno e hidrocarburos, como el metano o gas natural, para variadas y elevadas presiones y temperaturas.

Los valores experimentales de la velocidad de combustión dependen significativamente de las **técnicas de medición** y de los equipos empleados. Las velocidades de combustión obtenidas mediante técnicas ópticas (velocidad de la llama en la zona de gases frescos) dependen de las metodologías específicas y son diferentes de las obtenidas por las lecturas de presión (fracciones de masa quemada) en combinación con modelos termodinámicos. Las mediciones basadas en imágenes de llama son sensibles a los medios por los que el frente de llama se registra y a la ubicación dentro de la llama de la propiedad registrada (gradientes de índice de refracción, concentraciones de especies, etc.). Los resultados están influenciados por la resolución de imagen, métodos de detección de bordes de llama y procedimientos de cálculo. Por otro lado, las mediciones basadas en los registros de presión son sensibles a la precisión de los transductores y equipos de registro, particularmente en las primeras etapas del crecimiento de la llama. Además, cuando las velocidades de quemado tienen que ser obtenidas a partir de la presión por medio de modelos termodinámicos, deben ser considerados procedimientos de cálculo e hipótesis adicionales, introduciendo de este modo nuevas fuentes de error.

A su vez, en cualquier dispositivo experimental, especialmente para la combustión de hidrógeno, los efectos de **estiramiento (stretch)**, **inestabilidades y celularidad** están presentes. Las medidas experimentales se ven afectadas por efectos de aceleración del estiramiento de la llama y de las inestabilidades térmico-difusivas e hidrodinámicas, que obviamente no están cubiertas por los esquemas puramente cinéticos. El efecto de estiramiento del frente de llama sobre las velocidades de quemado debe cuantificarse para conseguir, al menos, velocidades de combustión laminar libres de estos efectos de stretch correctamente definidas. Los efectos de la tasa de estiramiento son más significativos a baja presión y temperatura que en condiciones similares a las de motores, donde los números de Markstein (longitud de Markstein dividida por el espesor del frente de llama) son más bajos y el desprecio de los efectos de estiramiento de llama puede ser considerado no demasiado importante en la práctica. Por otra parte, en condiciones similares a las de motores las llamas laminares son más propensas a inestabilidad y a celularidad, con aumento de la superficie de la llama e intensificación de la velocidad de combustión. Así pues, la presencia de estiramiento (stretch) de la llama en la mayoría de los montajes experimentales y la naturaleza inestable de las llamas a alta presión hacen la determinación experimental muy difícil.

Las medidas experimentales de velocidades de quemado a presiones elevadas, y sobre todo para dosados relativos combustible-aire de pobres a estequiométricos, sólo han sido posibles en las experiencias publicadas haciendo consideraciones semi-teóricas para las **inestabilidades hidrodinámicas y termo-difusivas** que surgen. El punto de partida para tal corrección de inestabilidades tiene que ser la medición precisa del radio crítico en el que la velocidad de la llama aumenta de forma brusca debido a su inestabilidad. Esto ha permitido encontrar los valores críticos del número de Peclet (el radio de frente de llama dividido por el espesor del frente de llama), junto con las longitudes de onda de manifestación o de corte interior y exterior de la inestabilidad. Las mediciones de la velocidad de la llama dentro del régimen estable de propagación del frente de llama afectado por estiramiento (stretch), entre el final del encendido por chispa y el inicio de la propagación inestable, han permitido que se encuentren los números de Markstein con tasa de estiramiento.

Todas estas mediciones requieren, por ejemplo, muy alta velocidad de registro fotográfico. Sin embargo, según aumenta la presión, la intensificación de la velocidad de la llama debido a las inestabilidades se produce antes en el proceso de propagación de la llama, lo que hace precisa su consideración para las inestabilidades más importantes. Con el aumento de la presión, se reduce el intervalo temporal de propagación de llama estable, entre el final de la chispa y el desarrollo de la celularidad, haciendo casi imposible una estimación precisa del número de Markstein. Cuando el intervalo se vuelve aún más corto, la medición de la velocidad de combustión laminar deja de ser fiable, poniendo en cuestión el interés de este parámetro para alta presión y llamas inestables, según lo sugerido por algunos autores. Como en condiciones de motor no existirán llamas laminares estables, se puede argumentar que la velocidad de combustión laminar, es decir, la velocidad de quemado laminar "pura o ideal" u_l de llamas planas estables, pierde su validez como entrada para los modelos de combustión. En consecuencia, los datos en condiciones de motor que se pueden encontrar en la literatura específica son ya bien **velocidades "aparentes" de combustión laminar** (es

decir, en condiciones no “estables y libres de estiramiento”) o bien están asociadas con incertidumbres.

Así pues, los límites técnicos de las mediciones a **altas presiones y temperaturas**, así como las inestabilidades hidrodinámicas y térmico-difusivas que aparecen en tales condiciones, impiden la adquisición de resultados fiables en términos de velocidades de quemado, restringiendo el dominio de validez de hipotéticas correlaciones empíricas de velocidad de combustión laminar a algunos bares de presión y cientos de Kelvin de temperatura. Estos límites son aún más importantes cuando es alta la reactividad de la mezcla de combustible o del combustible considerado. La **naturaleza altamente explosiva** del hidrógeno hace las mediciones aún más complicadas.

En este contexto, los datos de velocidades de quemado puramente laminares en condiciones de motor son relevantes, para poder evaluar el efecto de la inestabilidad, o para proporcionar una referencia inequívoca para las velocidades de combustión turbulenta medidas o calculadas. Sin embargo, se requieren **tratamientos teóricos**, por lo general, dadas las importantes **limitaciones experimentales** (debidas a las interacciones de las inestabilidades y del estiramiento del frente de llama, fenómenos de celularidad, etc.) dependiendo de las propiedades del combustible, de los intervalos de composición de las mezclas y de las condiciones termodinámicas. Como se ha mencionado, algunos enfoques han mostrado en la literatura el uso de la **teoría de estabilidad** para calcular las velocidades de quemado en llamas estables, a partir de datos medidos de propagación de llama inestable y, por otro lado, inversamente, pertinentes velocidades de combustión inestable se han calculado a partir de datos de tipo estable. Estos datos han sido generados mediante el uso de **cálculos de cinética química**, pero también han requerido el cálculo de las longitudes de Markstein, aunque la validez de los esquemas de reacción utilizados es difícil de evaluar, debido a la falta de datos experimentales para validar los esquemas.

El desarrollo de motores de combustión interna se basa con frecuencia en una unión entre **ensayos experimentales y simulación numérica**. Modelos termo-fluido dinámicos, multidimensionales y unidimensionales, se utilizan comúnmente para diseñar optimizaciones a través de la predicción de los flujos. Algunos trabajos de simulación numérica utilizan códigos y paquetes especializados. Con éstos, llamas de libre propagación adiabática, premezclada, plana sin estiramiento (stretch), se han simulado en algunos estudios importantes. Así, con el fin de complementar las medidas experimentales, la evolución de los trabajos técnicos de la literatura ha llevado con frecuencia a la utilización de **modelos teóricos de llamas premezcladas unidimensionales y esquemas químicos detallados**. Los valores medidos de velocidad de combustión son generalmente superiores en relación a los predichos por los modelos cinéticos químicos en la literatura, pero, dentro de sus márgenes de error, se consideran con tendencias análogas a altas presiones. El inconveniente para muchos tipos de mezclas combustibles es que la definición de los modelos de cinética química es generalmente complejo, con largos tiempos de cálculo, y existen pocos modelos para estos casos. De esta manera, no se encuentran muy a menudo en publicaciones estudios en gamas completas o amplios rangos de composiciones de mezcla fresca y de condiciones termodinámicas.

Otras opciones en la literatura son desarrolladas mediante la obtención de la **velocidad de combustión laminar de las mezclas** a partir de las correspondientes **velocidades propias de los constituyentes individuales**, en las mismas condiciones, variando su contenido en la composición de las mezclas y modificando las condiciones iniciales en algunos rangos limitados. Su viabilidad y precisión se pueden comprobar mediante la comparación de los resultados, pero no están disponibles muchos datos precisos de referencia para mezclas combustibles en amplios rangos de condiciones, y también son particularmente escasos en condiciones asimilables a las de motores.

Por otro lado, las expresiones basadas, por ejemplo, en los promedios ponderados de las concentraciones de los componentes, hidrógeno e hidrocarburos, tendrían que ser restringidas a combustibles mezclados cuyas velocidades de combustión y temperaturas de llama no difirieran sustancialmente entre sí, lo cual no es el caso general. Además, pueden suceder modificaciones de la concentración de las mezclas en las estructuras de llama, dependiendo de la difusividad de los componentes de la mezcla y de sus diferencias. Por otra parte, las interacciones cinético químicas tienen una gran influencia con la fuerte reactividad del hidrógeno, lo que intensifica las propagaciones de las llamas.

Desde todas estas consideraciones previas, la Tesis presenta una visión general de **expresiones de velocidades de combustión laminar de mezclas de hidrógeno-aire**, obtenidas a partir de autores que han utilizado cálculos cinéticos químicos complementarios, empleando esquemas de reacción que se han validado, al menos parcialmente, frente a medidas de velocidad de quemado a temperatura y presión elevadas. Estas expresiones han sido procesadas analíticamente, para una amplia gama de condiciones representativas de combustión premezclada en motores, y comparadas con algunas expresiones de trabajos más antiguos, puramente experimentales o definidos en condiciones más limitadas. La atención prestada a las formulaciones analíticas de las expresiones surgidas parte del hecho de que las expresiones analíticas se aplican más fácilmente en los códigos, y permiten convenientemente las comparaciones con expresiones existentes y futuras de velocidad de combustión laminar para las mezclas de hidrógeno-aire y otras mezclas con aire de mezclas de hidrógeno y otros gases.

Las expresiones puramente experimentales publicadas en la literatura se muestran menos adecuadas que las derivadas en conjunción con resultados cinéticos detallados, debido a las mencionadas incertidumbres asociadas a las llamas de hidrógeno-aire. A pesar de esto, los esquemas cinéticos no se pueden estimar como datos de entrada absolutamente exactos para predecir las velocidades de quemado reales, dado que su comportamiento difiere con frecuencia de los experimentos (por ejemplo, predicen una disminución pura de la velocidad de la llama laminar con el aumento de presión sea cual sea el dosado relativo combustible-aire). En resumen, las **expresiones obtenidas a partir de algunos trabajos numéricos**, basadas en validaciones parciales con datos experimentales o de códigos asociados a motores, en conjunción con modelos cinéticos, se consideran más adecuadas para ser utilizadas.

D.2. Características de expresiones específicas de velocidad de quemado laminar para mezclas de hidrógeno

Como se ha indicado, un primer objetivo de este trabajo es identificar expresiones publicadas de velocidad de combustión laminar de hidrógeno-aire, relevantes para sus posibles usos en nuevos desarrollos sobre mezclas combustible aire de hidrógeno, como combustible puro o como un componente en mezclas combustibles (por ejemplo, con metano o gas natural) considerando los orígenes de sus definiciones metodológicas y los rangos y la influencia de cada parámetro de entrada (dosado relativo combustible-aire Φ , temperatura de gas fresco T_u , presión P y fracción de gases residuales $f_{res,u}$).

La Tesis revisa las expresiones de velocidad de combustión laminar derivadas de estudios experimentales y numéricos que se han publicado para llamas de hidrógeno-aire. Se presta especial atención a las expresiones válidas para presiones y temperaturas en **condiciones asimilables a las de motores** (hasta aproximadamente 5 MPa y 900 K), a fin de permitir el cálculo de la combustión de hidrógeno en motores, así como para profundizar en el entendimiento de la combustión de las mezclas hidrógeno-aire en esas condiciones. Las expresiones de velocidad de este tipo se describen conceptualmente en los capítulos 3 y 4, y más particularmente en el capítulo 5 (tablas 10-16). Las expresiones revisadas se basan en datos diversos, utilizados para la correlación de las velocidades de quemado laminar determinadas por diferentes métodos de origen. Algunos de ellos se basan en una metodología experimental, mientras que otros se basan en mecanismos de reacción de varios orígenes. Con el fin de proporcionar una mejor comprensión de los métodos involucrados, se han revisado los conceptos básicos de la combustión laminar, incluyendo aspectos tales como las inestabilidades y los efectos de estiramiento (stretch) de llama. Se ha hecho un repaso general adicional de **datos experimentales y numéricos** calculados de velocidades de quemado laminar publicadas para mezclas de hidrógeno-aire, y se ha incluido una homogeneización y estandarización de notaciones y nomenclatura en el capítulo 3 y en la sección 5.2 con el fin de facilitar la comprensión de su significado real y la comparación de las expresiones.

Se han elegido **doce expresiones analíticas**, consideradas las más interesantes entre las publicadas en la bibliografía, entre las obras de muchos autores. Estas expresiones analíticas están completamente detalladas en la sección 5.3, con sus rangos de aplicación correspondientes en la sección 5.4. Estas doce expresiones seleccionadas (funciones de presión, temperatura, dosado combustible-aire y fracción de gases residuales) se han procesado numéricamente y representado gráficamente, con una amplia serie de resultados en condiciones de funcionamiento que se han estimado significativas de acuerdo con todas las consideraciones realizadas.

De acuerdo con las consideraciones de la sección 5 y los resultados previstos para las condiciones de este trabajo, las expresiones que se consideran **más apropiadas** para todos los rangos son la propuesta por **Gerke et al.** 2010 [III.2] y la propuesta por **Verhelst et al.** 2011 [III.3]. Además, la expresión propuesta por **Bougrine et al.** 2011 [III.12] tiene una gama muy amplia de validez y es directamente aplicable para combustión de mezclas de hidrógeno y metano con aire.

La expresión basada en cálculos cinéticos químicos de O'Conaire et al. [III.39] dada por Gerke et al. 2010 [III.2] predice bien la velocidad de combustión en sus gamas de presión (1-80 bar) y de temperatura (300-900 K), con tendencias de valores que son coherentes con las predichas por la expresión de Verhelst et al. 2011 [III.3], en sus respectivos rangos de presión (5-45 bar) y de temperatura (500-900 K). Esta última expresión se basa en los mecanismos de Konnov [III.47,III.125], que son positivamente reconocidos para presiones más altas, mientras que los mecanismos de O'Conaire et al. [III.139] se consideran adecuados a presiones más moderadas.

Ambas expresiones [III.2] y [III.3] son aplicables en amplios rangos de condiciones de motores de encendido por chispa, incluyen dependencias del dosado y de la fracción de dilución de gases residuales, y proporcionan valores similares en los rangos, más estrechos, de temperatura y presión de [III.3]. Sus resultados son también próximos para valores elevados de temperatura y presión e incluso para dosados moderadamente pobres y para fracciones significativas de gases residuales.

La expresión de Göttgens et al. 1992 [III.9] podría ser opción complementaria para intervalos de baja presión, inferior a la de condiciones asimilables a las de motores, y para temperatura inferior a 500 K, pero ésta se limita para valores de dosado desde pobre a estequiométrico y no incluye fracción de gas residual.

En los casos de utilización de la expresión de Gerke et al. 2010 [III.2], la forma más elaborada del **factor función de gases residuales** propuesto por Verhelst et al. 2011 [III.3] se podría aplicar como alternativa (en lugar del propuesto en [III.2] previamente, adaptado a su vez de otro trabajo de Verhelst et al. 2005,2007 [III.7,14]), aunque esta recomendación no se ha comprobado en el presente trabajo. Además, de acuerdo con esto, y como conclusión provisional, se puede decir que, puesto que la influencia de los gases residuales en la velocidad de combustión se incorpora en la expresión de Verhelst et al. 2011 [III.3], en forma de un término de corrección separado, entonces este término podría fácilmente ser introducido en otras expresiones de velocidad.

La aplicación de la expresión debida a Bougrine et al. 2011 [III.12] puede ser muy práctica cuando sea necesaria para cálculos de velocidad de combustión en **rangos muy amplios**, llegando a presiones y temperaturas muy elevadas. Su rango de aplicabilidad es más extenso que los permitidos por otras expresiones, y comienza incluso a partir de condiciones atmosféricas o presiones bajas, donde sus resultados de velocidad están en mejor acuerdo con las tendencias de los resultados de otros autores que los valores dados, por ejemplo, por la expresión de Gerke et al. 2010 [III.2]. La expresión de velocidad de combustión de Bougrine et al. 2011 [III.12], como combinación optimizada de otras expresiones, incluidas las de Gerke et al. 2010 [III.2] y Verhelst et al. 2011 [III.3], permite una amplia extensión de las gamas de validez con una sola expresión genérica, alcanzando hasta altos niveles de presión $P(\text{bar})=[1, 110]$ y de temperatura $T(K)=[300, 950]$, para cualquier fracción de contenido de hidrógeno 100-0% en mezclas combustibles con metano (Bougrine et al. 2011 [III.142]). Su expresión [III.12] es interesante también por su rango de dosado relativo $\Phi=[0,6, 1,3]$, que cubre adecuadamente más allá de las condiciones estequiométricas, aunque no se extiende hasta mezclas muy ricas. La expresión es adecuada para ser aplicada a mezclas de aire con combinaciones de gas natural e hidrógeno, como se concluye en la sección D.4.2.

En resumen, las expresiones proporcionadas por Gerke et al. 2010 [III.2], Verhelst et al. 2011 [III.3], y Bougrine et al. 2011 [III.12], ofrecen **resultados coherentes y de utilidad** para el cálculo de velocidad de combustión laminar de mezclas de hidrógeno-aire, con la ventaja adicional de que la última expresión es válida para el cálculo de velocidades de combustión laminar de mezclas de hidrógeno-metano-aire, también con resultados consistentes y muy útiles en rangos suficientemente completos y en condiciones similares a las de motores, y con una precisión aceptable en comparación con otras formulaciones basadas en reglas de mezclado complejas o simples, quizá en origen más fáciles de aplicar pero más restringidas a rangos parciales de las variables, como se explica en el apartado D.4.

D.3. Tendencias de la velocidad de combustión laminar de mezclas hidrógeno-metano para los regímenes relacionados con el contenido de hidrógeno

Se han identificado en la literatura tres modos de comportamiento diferentes de la velocidad de propagación de llamas con mezclas H₂-CH₄-aire, a temperatura ambiente y presión atmosférica, para todos los valores de dosado relativo pero dependiendo de la **fracción molar de hidrógeno** en la mezcla de combustible.

Son reconocidas ampliamente dos tendencias **lineales** para la velocidad de combustión laminar en función de los contenidos volumétricos de hidrógeno en la mezcla de combustible, para dos tipos de proporciones de hidrógeno en metano:

- un primer régimen, para bajos y medios contenidos de hidrógeno, en órdenes de $x_{H_2}=[0; 0.4-0.6]$;
- un segundo régimen, para contenidos predominantes o muy altos, en órdenes de $x_{H_2}=(0.8-0.9; 1]$.

Ambos regímenes se caracterizan por evoluciones lineales de la velocidad de combustión laminar, aunque con diferentes pendientes.

En una parte central de valores de la proporción hidrógeno-metano, la evolución de la velocidad de quemado laminar es de otra forma fuertemente no lineal, asimilable como **cuasi-exponencial**, lo que refleja comportamientos cinéticos complejos,

- y un tercer régimen, para contenidos medios y altos de hidrógeno, en órdenes de $x_{H_2}=(0.5; 0.9)$.

Los dos mencionados regímenes lineales de velocidad de combustión laminar para las mezclas de hidrógeno-metano han sido respectivamente atribuidos, en un caso, al **efecto potenciador de la adición de hidrógeno** en metano y, en el otro caso, a un **efecto inhibidor por la adición de metano** al hidrógeno. Así, el régimen dominado por la combustión de metano se caracteriza por un ligero aumento lineal cuando se añade hidrógeno en la mezcla. Y, a su vez, el régimen de combustión de hidrógeno inhibida por metano, a veces conocido como dominado por el hidrogeno, se caracteriza por una aguda disminución lineal con la adición de metano.

El aumento de velocidad de combustión laminar mediante adición de hidrógeno se justifica ampliamente por el incremento de radicales reactivos y por el ascenso de la temperatura adiabática de llama. La adición de hidrógeno acrecienta ligeramente la reactividad de metano en mezclas pobres, mientras que el efecto inhibidor de la adición de metano a hidrógeno es mucho más fuerte para condiciones ricas.

D.4. Características de diversas expresiones de velocidad de combustión laminar para mezclas combustibles de hidrógeno y gas natural

En la [tabla 26](#) (al final del capítulo 7) se incluye un resumen de los tipos de estas expresiones para las mezclas de combustible de hidrógeno con metano o con gas natural, con sus características de aplicabilidad dependiendo de las condiciones de composición.

A continuación se dan algunas conclusiones particulares resumidas sobre diversos tipos de expresiones simples, es decir para las fórmulas lineales, exponenciales y del tipo de la regla de Le Chatelier. Después se dan también otras conclusiones acerca de las expresiones más complejas.

D.4.1. Expresiones simples de velocidad de combustión laminar de mezclas de hidrógeno y gas natural

Diferentes fórmulas lineales, exponenciales y del tipo de la regla de Le Chatelier han sido respectivamente propuestas por muchos autores para predecir la velocidad de combustión laminar de mezclas de H_2-CH_4 o H_2-NG . De acuerdo con la literatura, las formulaciones simplificadas y ***sencillas reglas de mezcla*** basadas en el cambio en la composición no se consideran lo suficientemente precisas para predecir en amplios intervalos la velocidad de combustión laminar de mezclas de combustibles. Por ello, cuando se aplican expresiones simples, éstas pueden emplearse sólo en rangos específicos.

Las fórmulas generales simples se han cuestionado en parte debido a la aplicabilidad en rangos limitados de composiciones y condiciones termodinámicas. Las relaciones funcionales basadas en reglas simples no funcionan tan bien como las fórmulas derivadas de los modelos basados en esquemas químicos detallados, especialmente cuando amplios rangos de condiciones asimilables a las de motores tienen que ser tomados en cuenta.

Algunos desarrollos, como el basado en la ***regla de Le Chatelier***, se pueden extrapolar para ser empleados a presiones y temperaturas elevadas, incluso para condiciones de motores. Las aplicaciones que se hacen para cálculos de velocidades de combustión laminar de mezclas de combustibles, v.g. de hidrógeno y metano o gas natural, pueden ofrecer precisiones diversas. Pueden ser en mayor o menor medida aceptables en función de que sea más o menos apropiado el hecho de vincular los resultados de las expresiones individuales de velocidad de quemado laminar (las correspondientes a cada uno de los combustibles integrados a través de la regla de promedio considerada). Asimismo, la exactitud de tales fórmulas para mezclas combustibles, resultantes de combinar de este modo las expresiones características de los componentes de la mezcla combustible, dependerá del ajuste de la combinación de las respectivas exactitudes de las expresiones de partida, con respecto a sus propios intervalos de aplicabilidad. Dichos rangos deben de ser suficientemente amplios, para facilitar un razonable empleo en común de las expresiones combinadas, y deben ser

tomados en su parte coincidente, para acoplar su uso con un mediano rigor, al menos analítico. En todo caso, este tipo de metodología, solamente por sí misma, no repercute los efectos de las interacciones de los combustibles integrados en la mezcla; por tanto, su exactitud está relativamente condicionada por este hecho.

- ***Expresiones lineales de velocidades de combustión laminar para mezclas de hidrógeno e hidrocarburos***

Los intensos efectos no lineales de la cinética química hacen difícil obtener simples expresiones lineales con precisión, puesto que la cinética de reacción del metano es mucho más lenta que la del hidrógeno en la combustión de la mezcla combustible. Esto explica las grandes diferencias entre los valores de las velocidades de combustión laminar calculadas por otros métodos y los obtenidos por promediado lineal de las velocidades de los gases combustibles constituyentes en proporciones molares.

Las expresiones lineales de velocidad de llama laminar en base a parámetros virtualmente definidos han sido consideradas intrínsecamente válidas sólo para bajo contenido en hidrógeno. Estos parámetros son tales como un dosado relativo efectivo (Φ_{eF}) asociado a una relación R_h (de la cantidad de hidrógeno más la cantidad estequiométrica de aire necesario para su oxidación total, con respecto a la cantidad de hidrocarburo más el aire disponible restante que queda para su oxidación). Estas formulaciones están relacionadas con algunos coeficientes específicos de sensibilidad al contenido de hidrógeno (que, por ejemplo, pueden tener en cuenta la tendencia de la velocidad de combustión laminar con adición de hidrógeno en el combustible a base de metano). Su limitada validez para baja proporción de hidrógeno se debe a las características inherentes a las expresiones de estos parámetros, adoptados en esa forma para definir composiciones virtuales efectivas de las mezclas con aire de combustible combinado. Con estas limitaciones y algunas desviaciones entre las mediciones experimentales y los cálculos numéricos, estas correlaciones lineales aproximadas, entre la velocidad de llama laminar y la adición de hidrógeno, se han aplicado respectivamente en la literatura para mezclas mixtas de metano (C_1), etano, etileno y acetileno (C_2), propano (C_3) y n-butano (C_4), a presión atmosférica. Además, este tipo de correlaciones también se ha considerado, si bien con menor precisión, para el etileno y propano a presiones elevadas relativamente limitadas.

- ***Expresiones exponenciales de velocidades de combustión laminar para mezclas de hidrógeno y gas natural***

Algunas fórmulas, basadas en datos experimentales, consideran incrementos adimensionales de la velocidad de combustión laminar de metano o gas natural con la adición de hidrogeno. Sus tendencias son marcadamente exponenciales con el aumento de la fracción de hidrógeno. Esto concuerda bastante bien con los valores calculados para bajas fracciones de hidrógeno, en intervalos de contenido molar en la mezcla de combustibles en el orden de $x_{H_2}=[0; 0.3-0.4]$, y para altas cantidades, en rangos del orden de $x_{H_2}=[0.6-0.7; 1]$. Sin embargo, los errores son relativamente mayores para fracciones intermedias en órdenes de $x_{H_2}=(0.3; 0.7)$.

Estas expresiones exponenciales han sido usualmente obtenidas partiendo de datos medidos cerca de condiciones atmosféricas, pero también se han usado a más

elevadas presiones y temperaturas, ya que los resultados experimentales de presión coinciden bastante bien con las predicciones de modelos de motores para valores bajos de contenido de hidrógeno, $x_{H_2} < 0.3$, donde este tipo de expresiones se considera de una precisión razonable, en la combustión en condiciones similares a las de motores de encendido provocado, para mezclas combustibles con metano. Por lo tanto, la exactitud de estas expresiones se considera que es alta sólo para bajas fracciones de hidrógeno, en rangos habituales de dosado relativo del orden de $\Phi = [0.6, 1.3]$, y algunas veces con un error inferior particularmente en intervalos estrechos, por ejemplo, en un orden de $x_{H_2} = [0.2, 0.3]$, incluido en las gamas de contenidos de hidrógeno comúnmente utilizadas en motores de gas natural.

- ***Expresiones de promedio basadas en la regla de Le Chatelier aplicada a velocidades de combustión laminar para mezclas de hidrógeno y gas natural***

Fórmulas del tipo de la regla de Le Chatelier, basadas en fracciones molares de los componentes del combustible, para predecir la velocidad de combustión laminar de mezclas hidrógeno y metano o gas natural, se han probado por algunos autores, mostrando la viabilidad de este tipo de expresiones para obtener correlaciones de velocidad de quemado laminar. En la literatura las fórmulas basadas en supuestos de la regla de Le Chatelier se han utilizado preferentemente cuando la exactitud de las reglas de mezcla basadas en la composición se ha considerado suficiente; sin embargo, incluso en este caso, se ha considerado que no pueden predecirse resultados precisos en rangos completos de condiciones.

Sus resultados pueden ser válidos para diferentes dosados relativos y contenidos de hidrógeno, en particular para fracciones intermedias y altas de hidrógeno, con mejores precisiones para valores $x_{H_2} > 0.3-0.4$. Las expresiones correspondientes por aplicación de la regla de Le Chatelier han sido bien consideradas en condiciones pobres y estequiométricas en todos los regímenes, con buena concordancia entre los valores previstos y los resultados, ya sean con datos experimentales o de simulación obtenidos por medio de esquemas detallados de las reacciones. Sin embargo, hay diferencias más significativas para mezclas ricas con alto contenido de hidrógeno; cuando se realizan predicciones para mezclas ricas, se consideran aplicables sólo para rangos limitados de fracción de hidrógeno, en algunas extensiones hasta $x_{H_2} \leq 0.7$ como máximo. Por lo tanto, fórmulas de este tipo se aplican con éxito sobre amplias gamas de mezclas combustibles de hidrógeno con metano, incluso en condiciones superiores a las atmosféricas, y se consideran de precisión razonable cuando se usan con modelos de combustión en condiciones de motores de encendido provocado, para rangos de dosado relativo en ordenes de $\Phi = [0.6, 1.3]$, con limitaciones sobre su fiabilidad para otros dosados relativos diferentes.

D.4.2. Expresiones globales de velocidad de combustión laminar de mezclas de hidrógeno y gas natural en rangos completos de condiciones de composición y de variables termodinámicas

Así, de acuerdo con las evaluaciones en la literatura, algunas expresiones como las basadas en la regla de Le Chatelier proporcionan predicciones adecuadas, en una mejor conformidad con el comportamiento cinético de las reacciones que otros tipos de expresiones. Sin embargo, cuando se trata de contenido de hidrógeno mayor que $x_{H_2} > 0.7$, y por tanto con más altas concentraciones de radicales H asociadas, su interacción es demasiado fuerte para ser reproducida por expresiones simples, incluso por la regla de Le Chatelier, requiriendo expresiones más sofisticadas.

No muchos estudios han sido capaces de ampliar las opciones para cubrir todos los diferentes regímenes de forma simultánea. Algunos de ellos lo han hecho a través de expresiones que son más complejas y, en algunos casos, válidas para rangos más amplios y completos. Sin embargo, no resulta una tarea fácil en la literatura poder disponer de reglas simples de combinación para la velocidad de quemado laminar de mezclas con aire de combustibles combinados, con componentes tan diversos como H₂ y CH₄ (o gas natural), ya que los componentes individuales no son sólo químicamente distintos, sino que también tienen diferentes propiedades de transporte. Otra dificultad para presentar correlaciones precisas para estas mezclas surge debido a los diferentes requisitos de estequiometría de los componentes del combustible. Las fórmulas para la predicción de las velocidades de quemado llegan a ser necesariamente complejas, sobre todo cuando se requieren rangos amplios, como para condiciones asimilables a las de los motores. Las relaciones pueden ser más simplificadas sólo cuando relativamente pequeñas cantidades de hidrógeno están presentes en las mezclas de combustibles.

Algunos estudios detallados de la literatura, llevados a cabo con mayor frecuencia empezando desde condiciones estequiométricas y atmosféricas, aportan evaluaciones de los principales procesos químicos que rigen la producción de radicales de hidrógeno, como elementos clave para la velocidad de llama laminar. Pocos de ellos consideran conjuntamente los tres regímenes de las mezclas de metano-hidrógeno. Los análisis completos, cuando están disponibles, contribuyen a cuantificar el impacto no lineal en la llama laminar en expansión. También ayudan a comprender las evoluciones de la velocidad de combustión laminar debidas al efecto del contenido de hidrógeno en las mezclas de combustibles. Los estudios generales son interesantes para los sistemas comunes de combustión en aplicaciones industriales, debido a la escasez de expresiones globales de velocidad de llama laminar que sean totalmente aplicables en amplios rangos operativos de composición de combustibles y de variables termodinámicas, por la gran cantidad de grupos de condiciones corrientes que tienen que ser investigadas.

Cuando se tienen simultáneamente en cuenta los diferentes comportamientos a través de los tres regímenes, entonces esto conduce al desarrollo de complejas expresiones de velocidad de combustión laminar para llamas de metano-hidrógeno-aire. Tal es el caso de la fórmula fenomenológica, ampliamente descrita en la sección 7.6 y parcialmente utilizada en el capítulo 5, con una forma general que ha sido definida por Bougrine et al. mediante la combinación de funciones paramétricas. Éstas se determinaron considerando los diversos efectos de los factores funcionales y variadas

condiciones, con recopilación de los diferentes comportamientos contrastados por simulaciones unidimensionales de llamas laminares premezcladas y a través de química compleja, asegurando las respectivas continuidades en $x_{H_2}=0.7$ y $x_{H_2}=0.9$ y también transiciones suaves en $x_{H_2}=[0.6, 0.8]$ y en $x_{H_2}=[0.8, 1]$, respectivamente. Esta relación es aplicable incluso en amplios rangos de composiciones y de condiciones termodinámicas de funcionamiento, tales como las características de motores de encendido provocado o de turbinas de gas, y extiende el dominio de validez de las correlaciones experimentales a altas proporciones de hidrógeno en el combustible, a altas proporciones de gases residuales quemados, así como a altas presiones y temperaturas. Por lo tanto, esta expresión puede ser muy útil, especialmente para ser utilizada en su aplicación para nuevos desarrollos de este tipo, y como un dato de entrada en los modelos de combustión, para otros tipos de estudios.

D.5. Propuestas para futuros desarrollos

Se pueden proponer estudios para la obtención del comportamiento de la combustión de diversas mezclas combustibles con hidrógeno, extendiendo las consideraciones a otras variables, v.g. incluyendo los tiempos de retardo del encendido.

Por otra parte, adicionalmente a todas las expresiones de la velocidad de combustión laminar que han sido analizadas en esta Tesis para mezclas de combustibles gaseosos (hidrógeno singularmente y mezclas de hidrógeno y gas natural/metano), también pueden ser desarrolladas otras expresiones sobre la base del uso de diversas reglas de mezcla (como funciones de fracciones de volumen, masa o energía, con fórmulas de promedio directo o indirecto). Estas expresiones podrían ser utilizadas para aplicaciones de una amplia variedad de mezclas de los combustibles mencionados y para otros combustibles.

En otro contexto, pueden ser útiles revisiones y aplicaciones de metodologías más recientes en la literatura para la obtención de velocidades experimentales específicas de combustión laminar de llamas de propagación esférica, como han hecho por ejemplo Jayachandran et al. 2014,2015 [V.25,26] (v.g. para etileno y n-heptano). Ello puede permitir comparar discusiones actualizadas con las consideraciones utilizadas como ejemplo en la sección 3 (en ilustración de algunos desarrollos convencionales), dado que estudios recientes comprenden ideas adicionales sobre las limitaciones de las determinaciones experimentales de velocidad de quemado, v.g. usando llamas de propagación esférica.

Por otro lado, también son un reto en investigación de la química de combustión en llamas laminares los nuevos desarrollos de modelos cinéticos en profundidad, con valores más precisos de las constantes, y validaciones a presión y temperatura elevadas de las tasas de las reacciones químicas elementales, con las concentraciones de especies y sus gradientes. Además, para el modelado de llamas, son interesantes descripciones plenamente detalladas de los fenómenos de transporte y de la cinética química, así como nuevos posibles avances en experimentos de llama laminar con implicaciones para la química de la combustión de hidrógeno y de muchas variadas mezclas con otros combustibles. Son también de interés los estudios relacionados concernientes a los efectos de las condiciones iniciales y de contorno en la estructura de las llamas a presiones y temperaturas elevadas, con análisis particulares de los parámetros físicos.

**An Analysis of Concepts and Expressions
for in-Air Laminar Burning Velocity of
Hydrogen and
Hydrogen - Natural Gas Mixtures**

Luis Manuel Mayo Monge

Doctoral Thesis led
by Ph.D.
Francisco V. Tinaut Fluixá



University of Valladolid

General index. Contents

Part I (First chapter)

1. Introduction	1
1.1. Justification of discussed topics and starting points	4
1.1.1. Background	4
1.1.2. Methodological relations	6
1.1.2.1. Formulations of laminar burning velocity for hydrogen and methane as single fuels	6
1.1.2.2. Relevant effects on laminar burning velocity due to thermodynamic variables and parameters of composition in engines terminology	7
1.2. Approach and development	8
1.2.1. Conceptual approach	8
1.2.2. Objectives, methods, results and analysis	8
1.2.2.1. Laminar burning velocity of hydrogen-air mixtures at elevated pressures and temperatures	9
1.2.2.2. Laminar burning velocity in premixed combustion of hydrogen and natural gas blends	10

Part II (Second chapter)

2. An overview of natural gas, methane and hydrogen properties and characteristics of fuel blends in internal combustion engines	13
2.1. Characteristics of methane and natural gas	15
2.2. Compared properties of hydrogen gas and fuel-air mixtures	17
2.3. Characteristics of hydrogen and types of blends with hydrocarbons	19
2.3.1. Characteristics of hydrogen as fuel in combustion engines	19
2.3.2. Types of blends of hydrogen and hydrocarbons and characteristics as fuels	20
2.3.2.1. Hydrogen-based blends	22
2.3.2.2. Natural gas-based blends	22
2.4. Behavior of natural gas and blends with hydrogen as fuels in internal combustion engines	23
2.4.1. Combustion performance and emissions according to fuel composition and dilution	24
2.4.2. Cycle-to-cycle dispersion	27

References of chapter two (<i>second part</i>)	31
--	----

Part III (Third, Fourth and Fifth chapters)

3.	Concepts of burning velocities and flame speed in premixed combustion of fuel-air mixtures	41
3.1.	Laminar burning velocities interrelationships	43
3.2.	Theoretical expressions of laminar burning velocities. Asymptotical theories	48
3.3.	Laminar burning velocities based on detailed chemical kinetics schemes	51
3.4.	Laminar burning velocities related to studies of radical concentrations in the reaction zone	51
3.5.	Flame stability, instabilities onset and stretch interaction	53
3.5.1.	Instabilities origination	54
3.5.2.	Flame stretch	59
3.6.	Markstein lengths and correction for stretch effects	61
3.6.1.	Markstein lengths and un-stretched flame speeds and burning velocities	61
3.6.2.	Markstein numbers and Karlovitz stretch factors	67
3.7.	Flame thickness and Peclet number	68
3.8.	Instabilities development and cellular structures	70
3.8.1.	Flame instabilities and cellularity	70
3.8.2.	Critical values of Peclet number and regime transitions	73
3.9.	Linear stability theory. Application for lean hydrogen-air flames	76
3.9.1.	Instability peninsula based on wavenumbers	76
3.9.2.	Instabilities on spherical flames at constant pressure for non-minor positive values of Markstein numbers	79
3.9.3.	Instabilities on spherical flames at constant pressure for minor-positive and negative values of Markstein numbers	81
3.9.4.	Flame instabilities in confined explosions	82
3.10.	Correction of instabilities effects. Fractal considerations	85
4.	Review of studies about laminar burning velocities of hydrogen-air mixtures	87
4.1.	Laminar burning velocities of hydrogen-air mixtures obtained from experimental methods close to atmospheric conditions	89
4.2.	Laminar burning velocities of hydrogen-air mixtures obtained from experimental methods near engine-like conditions	91
4.2.1.	Laminar burning velocities	91
4.2.2.	Quasi-laminar burning velocities	97
4.3.	Laminar burning velocities calculated by numerical simulation	97
4.3.1.	Combustion models, thermo-fluid-dynamics analysis, CFD models and chemical kinetic mechanisms	98

4.3.2. Laminar burning velocities of hydrogen-air mixtures calculated by numerical methods, based on chemical kinetic mechanisms and related to combustion models	102
5. Analysis of laminar burning velocity expressions for hydrogen-air mixtures at engine-like conditions	107
5.1. Summary of methodologies used in the literature works	109
5.2. Homogenization of notation of laminar burning velocity expressions of the reviewed works	113
5.3. Analytical expressions of laminar burning velocities	115
5.4. Ranges of applicability of expressions	117
5.5. Graphical representation of results in the applicability ranges of laminar burning velocity expressions	121
5.6. Analysis of results of laminar burning velocity expressions	135
5.6.1. General analysis	135
5.6.2. Particular analysis of expressions of laminar burning velocity	136
5.6.3. Behavior of laminar burning velocities calculated from chemical kinetics mechanisms on basis of theoretical one-dimensional flames	139
References of chapters three, four and five (<i>third part</i>)	143

Part IV (Sixth, Seventh and Eighth chapters)

6. Notions of laminar burning velocities relative to hydrogen - natural gas blends	153
6.1. Laminar burning velocity for methane and hydrogen	155
6.2. Experimental laminar burning velocities of hydrogen-hydrocarbon blends	157
6.2.1. Summary of experimental works related with laminar burning velocity of fuel blends	157
6.2.2. Experimental results of some authors about fuel blends behavior with spherically expanding flames in combustion chambers	159
6.3. Theoretical laminar burning velocities from simulation of one-dimensional premixed flames of fuel blends with implemented chemical kinetics schemes	163
6.4. Mixing-rules calculations to obtain laminar burning velocities of fuel blends	165
6.4.1. Mixing rules derived from linear and potential rules-like formulas	166
6.4.2. Mixing rules derived from LeChatelier's rule-like formula	167

7. Expressions for laminar burning velocity of hydrogen - natural gas blends	171
7.1. Expressions for laminar burning velocities of hydrogen-hydrocarbon blends escalated linearly with hydrogen content	173
7.1.1. Specific composition parameters intended for a preferential oxidation of hydrogen in hydrocarbon-based mixtures	173
7.1.2. Comparison of transport, thermal and kinetic effects of hydrogen addition to hydrocarbon-based mixtures	176
7.1.3. Adiabatic flame temperature and Zeldovich number for hydrogen addition to methane-based mixtures	178
7.2. Expressions for laminar burning velocities of methane and natural gas fuel-air mixtures escalated exponentially with hydrogen content	179
7.2.1. Effects of equivalence ratio, temperature and dilution	179
7.2.2. Concept of dimensionless laminar burning velocity increment	181
7.3. Expressions for laminar burning velocities of hydrogen and methane blends based on linear mixing rules	183
7.3.1. Non-linear behavior of laminar burning velocities of hydrogen and methane blends	183
7.3.2. Regimes of laminar burning velocities of hydrogen and methane blends	183
7.4. The role of radicals in the premixed flame reaction zone and interaction on laminar burning velocities	185
7.4.1. Radicals for combustion of hydrogen-methane fuel-air mixtures	185
7.4.2. Radicals for combustion of hydrogen-natural gas fuel-air mixtures	190
7.5. Expressions for laminar burning velocities of fuel-air mixtures of hydrogen and methane/natural gas blends based on LeChatelier's rule-like formulas	192
7.5.1. Applicability of expressions based on LeChatelier's rule in function of equivalence ratio and hydrogen content	192
7.5.2. Applications of expressions based on LeChatelier's rule at engine-like conditions for spark-ignition engine models	192
7.6. Complex expressions of laminar burning velocity applicable to hydrogen-methane blends at engine-like conditions in complete range of fuel combinations	193
7.6.1. Effects of equivalence ratio and hydrogen addition	197
7.6.2. Temperature and pressure effects	198
7.6.3. Dilution effect of residual gas	198
7.6.4. Calculation by global correlation compared to simulation based on detailed chemistry	199

8.	Summaries of reviews on other consulted works about combinations of hydrogen - natural gas (<i>appendix chapter to the fourth part</i>)	205
8.1.	Characteristics and conditions of several works related to combustion of hydrogen combined with methane or natural gas	207
8.2.	Conditions related to several works about laminar burning velocity expressions for single methane-air mixtures	207
8.3.	Conditions related to several works about laminar burning velocity expressions for single hydrogen-air mixtures	207
	References of chapters six, seven and eight (<i>fourth part</i>)	219
Part V	(Ninth chapter)	
9.	Conclusions	233
9.1.	General aspects of laminar burning velocity of fuel blends of hydrogen in relation to methods of obtaining	235
9.2.	Characteristics of specific expressions of laminar burning velocity for hydrogen-air mixtures	238
9.3.	Trends of laminar burning velocity of hydrogen-methane blends for the regimes related to hydrogen contents	240
9.4.	Characteristics of diverse expressions of laminar burning velocity for fuel blends of hydrogen and natural gas	240
9.4.1.	Simple expressions for laminar burning velocity of fuel blends of hydrogen and natural gas	240
9.4.2.	Global expressions for laminar burning velocity of fuel blends of hydrogen and natural gas in complete ranges of conditions for fuel composition and thermodynamic variables	242
9.5.	Proposals for future developments	244
	References of chapter nine (<i>fifth part</i>)	245
	Lists of figures and tables (in sequential orders)	249
	Bibliography (General summary of all parts references in alphabetical order)	257
	Nomenclature (Glossary of abbreviations, acronyms, symbols and others)	289

1. Introduction

- 1.1. Justification of discussed topics and starting points
 - 1.1.1. Background
 - 1.1.2. Methodological relations
 - 1.1.2.1. Formulations of laminar burning velocity for hydrogen and methane as single fuels
 - 1.1.2.2. Relevant effects on laminar burning velocity due to thermodynamic variables and parameters of composition in engines terminology
- 1.2. Approach and development
 - 1.2.1. Conceptual approach
 - 1.2.2. Objectives, methods, results and analysis
 - 1.2.2.1. Laminar burning velocity of hydrogen-air mixtures at elevated pressures and temperatures
 - 1.2.2.2. Laminar burning velocity in premixed combustion of hydrogen and natural gas blends

1. Introduction

Gaseous fuel-air mixtures with different types of combined fuels such as blends of some hydrocarbons (HC) and hydrogen (H_2) involve opportunities for practical uses that are considered in many contemporary strategic plans, among other alternatives applied or in process of improvement and diversification. They are integrated as alternative fuels in research and development studies to set up an energy landscape that can be rationally sustainable in the medium and long term. The prospects of environmental protection and energy resources circumstances in some countries have significantly contributed to approaches intended to avoid operational and economic dependencies associated with conventional fossil fuels, promoting techniques aimed to the use and proliferation of other alternative energy sources, energy carriers and power trains that can be regarded as clean and viable ways on reasonable terms.

The evolution in recent decades of new technologies related to internal combustion (IC) have enhanced the use in engines of fuels with natural gas (NG), alone or in combination, and systems comparatively “greener” are being developed, i.e. ecological-friendly and more adjusted to environmental legislation, with optimized architectures and specific control strategies associated with the use of these types of fuels. Among other needs, the researchers have had in mind certain desired objectives of reducing exhaust emissions and improving fuel consumption and performance of internal combustion engines (ICE), with specific purposes and general thinking on minimizing emissions of greenhouse gases and carbon dioxide (CO_2) in particular. The use and combination of fuel such as hydrogen, obviously carbon-free, can significantly help in reducing emissions, with perhaps the exception of nitrogen oxides (NO_x).

The use of hydrogen (H_2) is an option put forward in most strategic plans for a sustainable energy system. Hydrogen is the most abundant element in the universe, but it has to be produced using other energy sources, because it is not available in a free state; for that, it is considered an energy carrier rather than a power source. The associated challenges and tasks are hydrogen production, distribution and storage. Perhaps the long-term energy solutions will preferably rely on renewable electricity to produce hydrogen, stored as a liquid or gas on-board and finally used in fuel cells, generating electricity to feed an electric motor, or in internal combustion engines, to generate directly mechanical power for a vehicle. Nevertheless, as hydrogen utilization in fuel cell technology is still under research, a promising and easily applicable utilization is the direct combustion in engines as a single fuel or in fuel blends. Hydrogen-fueled internal combustion engines (H_2ICE) has been also considered in the literature as a bridging technology in the medium-term towards a spread of fuel cell (FC) vehicles. Currently H_2ICE are cheaper than H_2FC (hydrogen fuel cells), both directly and in terms of fuel cost (due to the higher fuel purity requirements for the H_2FC).

Besides its use as a pure fuel, hydrogen is also considered as a combustion enhancer, as an activating agent for gaseous fuel blends, also in combination and-or dual applications with liquid fuels of both gasoline and diesel types. Using of ICE allows operations with combined fuels; for example, an engine can run on liquid fuel as well as hydrogen gas, or with mixtures of hydrogen and natural gas, mitigating autonomy requirements.

Because of its peculiar properties, hydrogen is an unconventional fuel to model. The relatively low sensitivity to turbulence and the high laminar flame speed impose to account for the fuel properties, also to model the laminar combustion propagation. However, the same properties, low density and very high laminar flame speed, impose specific operating strategies and the adaptation of the conventional research tools. Inside the cylinder of spark ignition engines (SIE) the flame propagates in a homogeneous mixture, thus a thorough understanding of

the flame propagation and the transition of the flame front from combustion onset to a fully turbulent flame are essential for the design of efficient SIE.

The laminar burning velocity is closely associated to these phenomena. The calculation of the turbulent combustion of hydrogen to track the flame propagation throughout the combustion chamber and resolving in-cylinder pressure and temperature are necessary to facilitate the development of the hydrogen-fueled spark ignition engines (H₂SIE). In the combustion chamber of SIE, pressure and temperatures are much higher than ambient conditions. What it is usually known as engine-like conditions could be quantitatively defined by pressures up to 5 MPa and temperatures up to 900 K (corresponding to the unburned mixtures). Then this means that it is important, not only to know the dependence of the laminar burning velocity of the in-cylinder mixture on the instantaneous pressure and temperature but to extend the dependence up to these engine-like conditions.

This valuable information is commonly used to validate chemical reaction mechanisms and computational combustion models, and is of practical interest in the design and optimization of ICE fueled with hydrogen or hydrogen-enriched blends. Thus, engine relevant databases of hydrogen laminar burning velocities, of premixed hydrogen-air flames measurements at high pressure and high temperature, are very applied for and useful, because the understanding of hydrogen-fueled engine operation requires data on the laminar burning rate of mixtures hydrogen-air-residuals under a wide range of conditions. However, there is a scarcity of data in the literature, particularly at these engine conditions. This is further complicated by the occurrence of flame instabilities at engine pressures, which compromises some of the existing data on the laminar burning velocity of hydrogen mixtures that are needed for wide ranges. Besides, the influence of the flame stretch rate and flame stability is significant on the burning velocity. The existing published works emphasize the importance of accurate data on the laminar burning rate of mixtures of hydrogen-air and residuals from combustion (exhaust gas, internally or externally re-circulated). The validation of both experimental data and chemical reaction mechanisms validation at these conditions are important.

1.1. Justification of discussed topics and starting points

The effective and safe uses of hydrogen gas and gaseous fuel blends, such as hydrocarbon-hydrogen or natural gas-hydrogen types, implicate attention to their physicochemical properties and reaction mechanisms associated to the combustion process for the diverse possible fuel blends that may be pondered depending on many varied potential compositions and conditions. Among other characteristics, related to combustion possibilities and implications in technical analyzes, the concepts such as the burning velocities are interesting (and main objective of this study) as well as other terms relative to cycle-to-cycle variability, sensitivity to detonation, emissions, etc.

1.1.1. Background

The laminar burning velocity of a fuel-air mixture is particularly an important physicochemical property due to its dependence on the variables pressure, temperature and composition (mixture equivalence ratio and diluents concentration). As a fundamental combustion property, the laminar burning velocity characterizes and quantifies the effects of the fuel for premixed fuel-air mixtures, influencing the gas entrainment and the speed of flame propagation in homogeneous charge combustion. This velocity directly affects the flame front speed and hence the operation of a spark ignition (SI) engine in which the burning velocity is a primordial cause of the combustion rate. This serves for the interpretation of the processes

developed by the flame in its spread and extension, e.g. instabilities and wrinkling, etc. In spark ignition engines (SIE), faster burning leads to a more robust and repeatable combustion and permits improvements of the engine operation and performance, even with substantially larger amount of residual gases, thus allowing the reduction of NO_x emissions. Therefore, the laminar burning velocity (u_l) provides information on the characteristics of combustion and this is used in validation of chemical reaction mechanisms.

The use of laminar burning velocity expressions calculated from chemical kinetics mechanisms, based on theoretical one-dimensional flames, is particularly associated in some literature to the suitable significance of the laminar burning velocity as a characteristic chemical-reaction rate. That is a solution used by several authors in order to employ this (u_l) as a correlation basis for the turbulent burning velocity (u_t) in engine models, where these two velocities are related, at the same pressure and temperature, by a burning velocity ratio. This is because the laminar burning velocity also provides a primary reference for the study of the turbulent combustion and with respect to the corresponding flame speed. Thereby most engine-combustion models estimate the turbulent flame speed as the laminar value times the flame speed ratio (FSR), which accounts for the effects of the in-cylinder turbulence on the flame to increase the flame surface and diffusion and transport phenomena.

So, one of the key variables of practical importance in engine design and optimization to modeling of combustion in SIE is the laminar burning velocity for the fuel blend, which embodies information on the effects of reactivity, diffusivity and exothermicity of the fuel-air mixture. This is an underlying building block of any model for the processes in an ICE. Consequently, in summary, data on the laminar burning velocities and their dependence on pressure, temperature, mixture composition, stretch rate and instabilities are very useful. Because of that, validated burning velocities at engine-like conditions are needed, which can be obtained from both experimental facilities and simulation results deduced by extrapolations or reaction mechanisms. Moreover, laminar burning velocity expressions of mixtures as functions of pressure (P), temperature (T_u), equivalence ratio (Φ) and residuals fraction ($f_{res,u}$) are a very important input to use in prediction of the performance and pollutant emissions in SIE by means of models.

Different experimental techniques, shown in many studies for obtaining laminar burning rates, have been used for fuel-air mixtures, with diverse results as the experimental conditions considered by different authors, especially varied for blends of fuels. For a given initial pressure (P) and a temperature of the fresh gases (T_u), the fuel mixtures can have different values of laminar burning velocity, according to the flame front shapes, flows, instabilities and heat losses; the experimental factors associated with the geometry and stability of the flame decisively affect the results of its speed.

The published data on laminar burning velocities for fuel-air mixtures at engine-like pressures and temperatures (up to about 5 MPa and 900 K) are singularly scarce in the literature and commonly do not take into account the effects of stretch and instabilities and the tendency to cellularity, causing a large spread in the reported burning velocities. Some of them result in consistently higher burning velocities, with the differences increasing for leaner mixtures. The direct effect of stretch rate on laminar burning velocity is less important at high (engine-like) pressure than at low pressure. However, the reduced sensitivity to stretch rate at high pressure results in greater susceptibility to instability, with a larger influence on laminar burning velocity values. This issue is even more relevant for fuel blends combined with high hydrogen content, because of its increased sensitivity to the effects of thermo-diffusive and hydrodynamic instabilities, bigger than for common hydrocarbons, leading to intensify the formation of wrinkling and cellularity in the flame front in some conditions.

In order to facilitate the application of the values of laminar burning velocity in phenomenological and predictive combustion models, making analytical use of continuous mathematical functions is generally more preferred instead of using tables of discrete values. However, the main problem is that usually there are not available data correlations valid at engine-like conditions for the infinite possible compositions of fuel blends. Some expressions shown in publications are more often based on measurements of low pressure, temperature and flame speed, which usually are not fully representative of the conditions found in actual combustion systems. Experimental and numerical approaches have been jointly used in the literature to overcome the uncertainties and lack of data, trying to determine the ideal laminar burning rates in different cases, frequently taking extrapolations of values, starting e.g. from the experimental measurements of laminar flames in some controlled conditions.

In accordance with the general approach outlined here in this introduction, the studies with expressions of laminar burning velocities that have been referenced from the literature in this present work, were focused on the experimental and-or numerical analysis of flames of air mixtures with hydrogen or hydrocarbon-hydrogen fuel blends. In some of them, outwardly propagating spherical flames are used to obtain the laminar burning velocities from initial conditions close to atmospheric ambient conditions. Others extend the conditions by simulation up to higher initial values of temperature and pressure. Some others use computational thermo-fluid-dynamic models and-or consider also the chain reactions and radical profiles, even at elevated pressures and temperatures, and their influence on laminar burning velocities by analysis with chemical models and codes. As a basis for comparisons and computations, many authors remark in their works that results from more or less detailed kinetics calculations are reflected in the definition of most expressions and correlations, because of the lack or scarcity of sufficiently representative experimental data due to the difficulties in obtaining them for the hydrogen enriched air mixtures.

1.1.2. Methodological relations

In this double section, before entering the development approach of this work, formulations considered for single gases are mentioned, and effects related with relevant influence on laminar burning velocities are outlined.

1.1.2.1. Formulations of laminar burning velocity for hydrogen and methane as single fuels

The laminar burning velocity of each single fuel in the premixed combustion of air mixtures is a possible starting point towards the search of some functional dependencies of laminar burning velocities for the combined fuel blends. The flame speeds and burning velocities of hydrogen and, respectively, methane (frequently taken as representative of natural gas), have been copiously studied in the literature for the individual fuels in premixed flames.

- The subject of hydrogen (H_2) as a singular fuel is widely discussed in this work, where empirical and theoretical formulas of laminar burning velocities for premixed combustion of hydrogen-air mixtures are studied. Interesting expressions applicable in wide ranges of temperatures, pressures, equivalence ratios and dilution fractions have been analytically processed with special attention at the elevated pressures and temperatures typical of spark ignition engine conditions.

- In the case of methane (CH_4), this is considered a reference gaseous fuel and it is possible to find numerous published results and burning velocity expressions, with different criteria and diverse accuracies or precisions of applicability in their effective use ranges or corresponding assumptions.

1.1.2.2. Relevant effects on laminar burning velocity due to thermodynamic variables and parameters of composition in engines terminology

As aforementioned, most of the published analytical formulas of laminar burning velocities are based on experimental (u_l) or numerically calculated (u_L) expressions. Frequently they meet a widely extended general form to account for temperature and pressure effects (also for fuel-air mixtures at elevated pressures and temperatures), modified sometimes to express the influence and functional dependences of equivalence ratio (Φ) and dilution fraction of residual gas content ($f_{res,u}$) in addition to initial pressure (P) and unburned temperature (T_u), and where the variables are depending on parameters according with the data and methods of deduction. The hydrogen content in different fraction forms or parameters can be added as another possible variable or functional parameter when laminar burning velocities of combined fuel blends with hydrogen are correlated.

Some general terms of composition, in engines terminology, are detailed in [table 1](#) for fuel-air mixtures with hydrogen. These have been respectively considered from perspectives for both hydrogen as single fuel or as combined component in fuel blends with hydrocarbons (e.g. natural gas or pure methane).

Table 1

Composition terms for air mixtures of hydrogen and fuel blends ^(a,b)

Fuel to air equivalence ratio $\Phi = (m_F/m_{air})/(m_F/m_{air})_{stq}$ (m_F/m_{air}) = actual fuel-air mass ratio	(m_F/m_{air}) _{stq} = stoichiometric value of m_F/m_{air}
Mass fraction of residual gas in a fuel-air mixture $f_{res,u(m)} = m_{dil}/(m_F+m_{air}+m_{dil})$ m_i = masses of fuel, air and dilution gas	
Volume (mole) fraction of residual gas in a fuel-air mixture $f_{res,u(v)} = Vol_{dil}/(Vol_F+Vol_{air}+Vol_{dil}) \Leftrightarrow n_{dil}/(n_F+n_{air}+n_{dil})$ Vol_i = volumes of fuel, air and dilution gas	n_i = moles of fuel, air and dilution gas
H ₂ volume (mole) fraction in a fuel blend air mixture $X_{H_2} = Vol_{H_2}/(Vol_{H_2}+Vol_F+Vol_{air}) = Vol_{H_2}/(Vol_F+Vol_{air}) \Leftrightarrow n_{H_2}/(n_{H_2}+n_F+n_{air}) = n_{H_2}/(n_F+n_{air})$ $F \equiv f + H_2$ $f \equiv \{C_xH_yO_z\}$ $X_{H_2}+X_f+X_{air} = 1$ $X_f = X_{H_2}+X_f$	
H ₂ volume (mole) fraction in a fuel blend $f_{H_2} \Leftrightarrow X_{H_2}$; $Vol_{H_2}/(Vol_{H_2}+Vol_f) = Vol_{H_2}/Vol_f \Leftrightarrow n_{H_2}/(n_{H_2}+n_f) = n_{H_2}/n_f$ $X_{H_2}=X_{H_2}/(X_{H_2}+X_f)$ $h(\%)=100 X_{H_2}$ $X_f=X_f/(X_{H_2}+X_f)$ $X_{H_2}+X_f=1$	
O ₂ volume (mole) fraction in standard (dry) air $g_{O_2} \Leftrightarrow x_{O_2}$; $Vol_{O_2}/Vol_{air} \Leftrightarrow n_{O_2}/n_{air}$ $x_{O_2}=X_{O_2}/X_{air}=0.21$ $x_{N_2}=X_{N_2}/X_{air}=0.79$ $x_{O_2}+x_{N_2}=1$	
O ₂ volume (mole) fraction in oxidizer blend (e.g. N ₂ dilution) $g_{O_2} \Leftrightarrow x_{O_2}$; $Vol_{O_2}/(Vol_{O_2}+Vol_{N_2}) = Vol_{O_2}/Vol_{O_2+N_2} \Leftrightarrow n_{O_2}/(n_{O_2}+n_{N_2}) = n_{O_2}/n_{O_2+N_2}$ $x_{O_2}=X_{O_2}/(X_{O_2}+X_{N_2}) < 0.21$ $x_{N_2}=X_{N_2}/(X_{O_2}+X_{N_2}) > 0.79$ $x_{O_2}+x_{N_2}=1$	
^(a) Hydrogen as a single fuel:	$F = H_2$; $n_f = n_{H_2}$, $V_f = V_{H_2}$; $x_{H_2} = 1$, $h(\%) = 100$; $x_f = X_f = n_f = Vol_f = 0$
^(b) Hydrogen as a component of fuel blends:	$F = f + H_2$; $n_f = n_f + n_{H_2}$, $V_f = V_f + V_{H_2}$; $x_{H_2} = [0, 1]$, $h(\%) = [0, 100]$

1.2. Approach and development

After this introductory chapter, the other chapters of this work are successively performed, based on the purposes that are outlined broadly on the following sections.

1.2.1. Conceptual approach

- The second chapter of this study contains a summary on natural gas, methane and hydrogen properties and characteristics of their fuel-air mixtures (e.g. [table 3](#)), also including an overview with complementary information and terminology about combustion performance, emissions, cyclic variability, etc. (e.g. [table 5](#)), on different applications in engines of diverse fuel blends depending on possible fuel combinations and effects of dilution by residual gas.
- The third chapter presents, in order to provide a better understanding, a summary of concepts associated with the laminar burning velocity of gaseous fuel mixtures. This has been done primarily with the aim more focused on hydrogen-air mixtures (i.e. hydrogen has been taken into account as a single fuel in a main part of the work). Considerations on the instabilities of the flame front, the apparition of cellular structures in flames and the concepts related to stretch interactions have been developed and summarized, as well as the influence of flame front geometry on the burning velocity.

1.2.2. Objectives, methods, results and analysis

The purposes of the Thesis are disaggregated into successive parts, with corresponding developments in two groups of respective chapter.

- In chapters four and five, this work includes the study and comparison of published laminar burning velocity expressions for premixed combustion of fuel hydrogen-air mixtures, with the special attention to applicability in wide ranges of operating conditions and up to elevated (engine-like) pressures and temperatures (SIE conditions). These expressions are formulated with their defined dependences on the initial mixture conditions, pressure, temperature and composition, from lean to rich fuel-air equivalence ratios, for their application to different mixtures of hydrogen-air and residual gas.

The comparative analysis of this part of the study has been made in order to show a selection, valid at engine-like conditions, of laminar burning velocity expressions that have been selected from several technical references among many others. Thereby this work allows choosing specific expressions for laminar premixed combustion of mixtures of air and hydrogen as the only fuel or as the basis to estimate, with the aid of mixing rules, on the combustion velocity of combined mixtures with hydrogen and other fuels.

- In chapters six and seven, this work shows a study of published laminar burning velocity expressions for premixed combustion of hydrocarbon-hydrogen blends, including some options valid at elevated (engine-like) pressures and temperatures (SIE conditions). These other expressions are also formulated with their defined dependences on the initial conditions, pressure, temperature and composition, from lean to rich fuel-air equivalence ratios, for their applications to different fuel combinations, with residual gases in some cases.

Moreover, the analysis of this other part of the study also include a selection of laminar burning velocity formulations, partially valid in wide ranges of operating conditions or

sometimes extrapolated at engine-like conditions. As said, these are applicable to laminar premixed combustion of hydrogen-hydrocarbon-air mixtures but with particular scope on hydrogen-methane-air mixtures, as the basis to estimate the burning velocities for fuel blends of hydrogen and natural gas.

1.2.2.1. Laminar burning velocity of hydrogen-air mixtures at elevated pressures and temperatures

- The fourth chapter refers more specifically to values and analytical expressions of the laminar burning velocities of hydrogen-air mixtures published in several technical papers. The material is presented considering the origin and methodology used to obtain the results, roughly grouped in two categories: experimentally based and numerically based methodologies. As for the methodologies based on experimental data, they provide laminar burning velocities usually obtained from flame front image recording or from combustion pressure analysis; details are given on their ranges of validity, from atmospheric conditions to engine-like conditions, and on the fact of whether they do or do not consider the effects of stretch and instabilities on the experimental results. As for the numerical methods, based on thermo-fluid-dynamic computational models and chemical mechanisms for kinetics calculation, although they have the advantage of being able to calculate the laminar burning velocity in theoretical ideal conditions (adiabatic, one-dimensional, free of stretch and instabilities), they require some type of validation with actual data.

- The fifth chapter covers in detail the applicability of laminar burning velocity expressions for hydrogen-air mixtures in engine-like conditions, with comparisons among different selected expressions, in their respective ranges of validity. Each particular methodology for achieving the expressions has been analyzed, based on experimental procedures, numerical simulation methods or combined methodologies. It has to be pointed out that the literature expressions have been first cited with the original authors' nomenclature, but for the sake of a more valuable comparison, they have also been rewritten with a homogenization of notation.

Numerous tables (e.g. [tables 10-16](#)) present, in a schematic way, the information relative to the experimental apparatus or the numerical method, the consideration or absence of corrections to account for stretch and instabilities effects, additional comments, dependence on relevant variables, homogenization of nomenclature, ranges of validity, actual meaning of the reported velocity (ideal, apparent, quasi-laminar, stretched or stretch-free, affected or unaffected by instabilities), etc.

Additionally, twelve selected analytical expressions of burning velocity of hydrogen-air mixtures have been computed (e.g. [tables 15-18](#)) to compare the predicted results by means of graphical representations to show the values and trends when pressure, temperature or equivalence ratio vary, always strictly considering the applicability ranges of the respective expressions. Some general considerations are done about the laminar burning velocity expressions, depending on the origin and the methodology. Finally a comparison of the best choices for expressions of laminar burning velocity, valid at engine-like conditions, is done. A stated goal of this part is to identify expressions that can provide coherent results for calculating the laminar burning velocity of hydrogen-air mixtures and being valid, even at engine-like conditions, for sufficiently complete ranges.

1.2.2.2. Laminar burning velocity in premixed combustion of hydrogen and natural gas blends

- The sixth chapter refers firstly to formulations of laminar burning velocity for methane and hydrogen as pure fuels in air mixtures, as a starting point. Secondly, with the objective centered on laminar burning velocity of combined fuel blends, some considerations on several types of experimental and computational methods of definition are referred. The options of using implementations of chemical kinetic schemes for the simulation of theoretical one-dimensional premixed flames are also considered. Finally, the application of mixing rules related with linear, potential, exponential and LeChatelier's rule-like formulas is introduced.
- The seventh chapter refers more specifically to expressions of the laminar burning velocity of hydrogen-hydrocarbons-air mixtures published in technical papers. This material is presented considering the origin and procedures employed to obtain the results, roughly grouped depending on the compared methodologies. As for the experimentally based methods that provide data of laminar burning velocities usually obtained from flame front image recording or from combustion pressure analysis, details are given on their ranges of validity, from atmospheric conditions towards engine-like conditions, and on the fact of whether they do or do not consider complete ranges of possible combinations of fuel components. As for numerical methods, either based on mixing rules or/and derived from thermo-fluid-dynamic computational models and chemical mechanisms for kinetics calculation, they have the advantage of being able to calculate the laminar burning velocity in theoretical conditions, although they require some type of validation with actual data. Therefore, this section also covers the different applicability and extrapolations of some laminar burning velocity expressions for combustion of fuel blends of hydrogen and methane or natural gas.

Several schematics, summaries and tables have been included to present the information relative to the different behaviors of laminar burning velocity trends at the diverse possible regimes regarded in the literature (e.g. [table 21](#)), and on the influence of the interaction of radical concentrations and sensitive reactions in the premixed flame reaction zone (e.g. [tables 22-24](#)).

In addition, some selected analytical expressions of laminar burning velocity and their applicability have been explained particularly. Singularly one of them ([table 25](#)), especially complete, has been described in detail because of its important wide ranges of application, based on the consideration of all significant effects (mixture composition, proportion of fuel components in the blend, residual gases dilution fraction, pressure and temperature). Thus, some general considerations are given about the regarded laminar burning velocity expressions, depending on their origin and methodology. Finally, a conclusion is done about the expressions that are estimated as the best choices due to their applicability at different conditions. A stated goal of this part is to identify an expression that can provide useful results with acceptable accuracy for calculating the laminar burning velocity of hydrogen-methane-air mixtures and being valid for complete ranges, even at engine-like conditions.

A summary of all types of expressions, which have been analyzed in chapter seven, is reported ([table 26](#)) for hydrogen fuel mixtures with methane or natural gas, with application characteristics depending on the conditions of composition.

- The eighth chapter, at the end of this part, is a complementary appendix to the previous chapters six and seven, in order to include complementary or more detailed information apart ([tables 27-29](#)), in relation to consulted works.

2. An overview of natural gas, methane and hydrogen properties and characteristics of fuel blends in internal combustion engines

- 2.1. Characteristics of methane and natural gas
- 2.2. Compared properties of hydrogen gas and fuel-air mixtures
- 2.3. Characteristics of hydrogen and types of blends with hydrocarbons
 - 2.3.1. Characteristics of hydrogen as fuel in combustion engines
 - 2.3.2. Types of blends of hydrogen and hydrocarbons and characteristics as fuels
 - 2.3.2.1. Hydrogen-based blends
 - 2.3.2.2. Natural gas-based blends
- 2.4. Behavior of natural gas and blends with hydrogen as fuels in internal combustion engines
 - 2.4.1. Combustion performance and emissions according to fuel composition and dilution
 - 2.4.2. Cycle-to-cycle dispersion

References of chapter two (*second part*)

2. An overview of natural gas, methane and hydrogen properties and characteristics of fuel blends in internal combustion engines

This chapter introduces characteristics of natural gas (NG) and some typical compositions compared to methane. Moreover, some physical and chemical properties of hydrogen (H_2) relevant to engines are detailed and compared in parallel with properties of methane (CH_4) and iso-octane (C_8H_{18}), which are taken in the technical literature as reference fuels for natural gas and gasoline, respectively.

Hydrogen-hydrocarbon fuel blends are also considered in this review chapter. These blends can be seen from two perspectives: as hydrogen-based fuel blends with hydrocarbon combination, particularly methane or natural gas, or conversely as hydrocarbon-based fuel blends with hydrogen contents.

2.1. Characteristics of methane and natural gas

Natural gas (NG), widely used in passenger cars, power generation devices, domestic usage, etc., is considered a favorable alternative fuel due to its properties and its reserves are more evenly distributed over the globe than the crude oil, being NG less affected by price fluctuations. Nowadays NG-fueled engines have become commercial engines and are manufactured both spark-ignition (SI), Cho&He 2007 [1], and compression-ignition (CI) engines. Particularly spark ignited internal combustion engines (SIE) fueled by hydrogen enriched (compressed) natural gas (HCNG) have shown advantages compared to traditional gasoline, diesel and even to single NG or compressed NG (CNG), especially in emission control.

Under the name of natural gas (NG) mixtures of some gases in different proportions are known, where methane is its main major chemical component. NG is used rather than methane because pure CH_4 seldom exists in natural resources. NG obtained from different locations and at different times may have different compositions. Furthermore, there exist some other methane-based gaseous fuels such as coal gas and landfill gas which contain not only methane (CH_4) and small amounts of ethane (C_2H_6) and propane (C_3H_8), but also large amount of nitrogen (N_2) and/or carbon dioxide (CO_2).

Some wide ranges of compositions of NG are expressed in [table 2.A](#), Naber et al. 1994 [2]. As commented, apart from the main hydrocarbon (HC) constituents, other gases may be present in small quantities in the varied combinations, depending on diverse NG types and several origins (Jessen&Melvin1977 [3], etc.) as detailed in the data intervals of [table 2.B](#). Some sample types of NG particular and diverse compositions are specifically presented in [table 2.C&D](#), as examples. The high CH_4 concentrations of the NG, about 96% in volume, are more commonly used in many published studies (e.g. [table 2.C](#)).

The properties of NG are usually well represented by methane, especially when the volume fraction of this is very high in the NG compositions ([table 2.C](#)). Thus it was assumed in simulations, for instance by Ma et al. 2012 [4] considering the relative molecular mass and lower calorific value of CH_4 as approximate and nearly equal, respectively, to those of the used composition of a specific NG. On the other hand, Liao et al. 2004 [5] found that un-stretched laminar burning velocities of NG (yielded from the stretched flames) were close to the methane burning velocity.

Table 2**Natural gas (NG) compositions****A. Approximate ranges of hydrocarbon (HC) components in composition of different NG types from diverse origins (adapted from Naber et al. 1994 [2])**

NG main HC components	Methane CH ₄	Ethane C ₂ H ₆	Propane C ₃ H ₈	Butanes n C ₄ H ₁₀ / i C ₄ H ₁₀ / ...	Higher HCs (Pentanes, etc.) i C ₅ H ₁₂ / n C ₅ H ₁₂ ...	Other gases table 2.B
Volume (%) percentages	75 – 98.9	0.5 - 13	0 - 2.8	0 - 1.1	0 - 0.2	...

B. Approximate ranges of composition of other minor components in different NG types from diverse sources (adapted from Jessen&Melvin 1977 [3])

NG secondary components	Nitrogen N ₂	Hydrogen H ₂	Helium He	Carbon monoxide CO	Carbon dioxide CO ₂	Oxygen O ₂	Water H ₂ O
Minor (vol%) percentages	0 - 1.3	0 - 0.6	0 - 0.03 (1 - 8)	0 - 0.05	0 - 2.55	0 - 0.01	...

C. Usual NG composition (adapt. from Huang et al. 2006,2009 [6,7], Wang et al. 2007,2008 [8-10], Miao et al. 2008,2009 [11-13], Hu et al. 2009 [14,15])

C _x H _y O _z (x=1.01523, y=3.928084, z=0.05086)	Methane CH ₄	Ethane C ₂ H ₆	Propane C ₃ H ₈	Carbon dioxide CO ₂	Nitrogen N ₂	Other gases ...
Vol% fractions	96.160	1.096	0.136	2.540	0.001	0.067

D. Particular NG sample type composition (measurements from chromatographic analysis in a continuous supply line in Valladolid; April 2011)

C _x H _y O _z Vol% fractions	Methane CH ₄	Ethane C ₂ H ₆	Propane C ₃ H ₈	Butanes n C ₄ H ₁₀ / i C ₄ H ₁₀	Pentanes i C ₅ H ₁₂ / n C ₅ H ₁₂	Hexane n C ₆ H ₁₄	Carbon dioxide CO ₂	Nitrogen N ₂
average	85.782	9.387	1.420	0.134/ 0.114	0.023/ 0.016	0.003	2.027	1.094
maximum	86.861	9.683	1.731	0.288/ 0.205	0.054/ 0.054	0.013	2.280	3.768
minimum	84.411	8.543	1.196	0.092/ 0.075	0.012/ 0.008	0.002	0.936	0.807

Table 3

Hydrogen properties compared to other gases: properties of **hydrogen, methane** and **iso-octane** as pure fuels and in fuel-air mixtures (adapted from Huang et al. 2009 [7], Wang et al. 2008 [9], Hu et al. 2009 [14,15], Bauer&Forest 2001 [16], Karim 2003 [17], Verhelst&Wallner 2009 [18])

Pure fuel properties	Iso-octane	Methane	~ NG	Hydrogen (gas)
Density (kg/m ³)	692	0.650		0.081
Emissions of CO ₂ (mg/kJ)	~80 (<i>gasoline</i>)	55		0
Flammability limits in air (air-to-fuel equivalence ratio λ)	1.51 – 0.26	2 - 0.6		10 – 0.14
Flammability limits in air (fuel-to-air equivalence ratio Φ)	0.66 – 3.85	0.5 - 1.67		0.1 – 7.1
Flammability limits in air (volume %)	1.1 - 6	5 - 15		4 - 75
Higher heating mass value (MJ/kg)	47.8	55.5		141.9
Lower heating mass value (MJ/kg)	44.3	50.0		120.0
Lower heating vol. value (MJ/m ³) T~293 K, ρ _a ~1.17 kg/m ³ *	~195.8 (<i>vapor</i>)	32.6		10.0
Mass diffusivity in air (cm ² /s)	~0.07	0.16		0.61
Minimum ignition energy (mJ) H ₂ /air~22-26%, Φ~0.67-0.83	0.28	0.29		0.017
Minimum quenching distance (mm) Φ~1	3.5	2.03		0.64
Molecular weight (g/mol)	114.236	16.043		2.016
Stoichiometric air to fuel mass ratio (kg/kg)	15.1	17.1		34.2
Stoichiometric air to fuel mole ratio (kmol/kmol)	59.666	9.547		2.387
Toxicity of fuel and emissions	yes	yes		no
Visibility of the flame	yes	yes		no
Fuel-air mixture properties	C ₈ H ₁₈ -Air (Φ=1)	CH ₄ -Air (Φ=1)	H ₂ -Air (Φ=1)	H ₂ -Air (Φ=0.25)
Air to fuel mass ratio (kg/kg)	15.1	17.1	34.2	136.6
Fuel volumetric fraction in air (m ³ /m ³) %	1.65	9.5	29.5	9.5
Adiabatic flame temperature (K)	2276	2226	2390	1061
Auto-ignition temperature (K)	~690	~813	~858	>858
Kinematic viscosity (mm ² /s)	15.2	16	21.6	17.4
Laminar burning velocity (cm/s) T~360 K **	45	48	290	12
Lower heating mass value - gravimetric energy (kJ/kg)	3013	3028	3758	959
Lower heating volumetric value - volumetric energy (kJ/m ³)	3704	3071	2913	1024
Mixture density (kg/m ³)	1.229	1.123	0.850	1.068
Mole ratio before/after combustion	1.07	1.01	0.86	0.95
Sound speed (m/s)	334	353.9	408.6	364.3
Specific heats ratio	1.389	1.354	1.401	1.400
Thermal conductivity (W/m K)	0.0236	0.0242	0.0497	0.0317
Thermal diffusivity (mm ² /s)	18.3	20.1	42.1	26.8

Data at 1 atm & 300 K, with exceptions of volumetric heating value of fuels (*) at 293.15 K and laminar burning velocity of fuel-air mixtures (**) at 360 K.

Table 4
Simple schemes of combustion for **hydrogen-air mixtures** ***

H ₂	+	[O ₂ + (79/21) N ₂] (2/4)(1/Φ)	→				
→		H ₂ O	+	(79/21) N ₂ 0.5(1/Φ)	+ O ₂ 0.5(1/Φ)(1-Φ) Φ<1		
→		H ₂ O	+	(79/21) N ₂ 0.5	Φ=1		
→		H ₂ O (1/Φ)	+	(79/21) N ₂ 0.5(1/Φ)	+ H ₂ (1/Φ)(Φ-1) Φ>1		
				N ₂	O ₂	Air (<i>dry</i>)	H ₂
Fuel-air mixture stoichiometric mole fractions (Φ=1)				0.556	0.148	0.704	0.296
Typical composition of dry air (mole fractions)				0.79	0.21	1	--
Molecular weights (g/mole)				28.01	32	28.85	2.016
				N ₂	H ₂ O (<i>steam</i>)		CO ₂
Typical molar composition of H ₂ -air combustion (Φ=1)				0.65	0.35		--
Molecular weights (g/mole)				28.01	18.02		44.01

(***) Burned gas compositions as a function of fuel to air equivalence ratio, Φ, with moles of products for each mole of fuel.

2.2. Compared properties of hydrogen gas and fuel-air mixtures

Hydrogen (H₂), which has been shown in the literature as an important energy carrier, contributes significantly to the energy diversification. It can be produced from different fossil and renewable energy sources, with costs strongly affected by the technology adopted, Gorenssek 2009 [19]. One difficulty in hydrogen production is because the methods, such as fuel reforming and electrolysis, are energy consuming; some of them are industrially developed but some others, such as biological production or photo-dissociation, have to be developed further.

Some physical and chemical properties of hydrogen, relevant to engines, are detailed in the data compilation of table 3, partially adapted from Verhelst&Wallner 2009 [18] and other references. Hydrogen properties are compared in parallel in this table with properties of methane and iso-octane, which are taken as reference for natural gas and gasoline, respectively. The values included are at 300 K temperature and atmospheric pressure (0.1 MPa), with a few marked exceptions.

The products of complete reaction of hydrogen-air mixture combustion are expressed in table 4, showing the theoretical species as a function of the equivalence ratio Φ (defined as the ratio of the stoichiometric air-fuel ratio to the actual air-fuel ratio).

Some properties of hydrogen-air mixtures before combustion at stoichiometry Φ=1 and at an equivalence ratio Φ=0.25 are also shown among the data of the second part of table 3, compared to stoichiometric methane-air and iso-octane-air mixtures.

Some of the properties related with combustion can be highlighted before considering the various characteristics of hydrogen and hydrocarbon blends and their performances in combustion engines.

Based on an examination of the properties of the pure fuels, there is a big difference in stoichiometric air to fuel ratio of hydrogen compared to methane and iso-octane, as well as a large difference in stoichiometric air to fuel ratio in mass terms versus mole (volume) terms. There is also a big difference between specific lower and higher heating values of hydrogen compared to methane and iso-octane, which is easily explained since water (H₂O) is the only combustion product of hydrogen. The specific lower heating value of hydrogen (defined as the chemical energy released during complete combustion with the water product as vapor) is of about 120 MJ/kg on a mass basis, which is nearly three times that of methane (50 MJ/kg) or iso-octane (44.3 MJ/kg). However, the small and light hydrogen molecule is very mobile, with a high

mass diffusivity in air ($D_m=0.6 \text{ cm}^2/\text{s}$), and hydrogen density is very low at atmospheric conditions, of about $\rho=0.081 \text{ kg}/\text{m}^3$ (at pressure of 1 atm and temperature of 300 K), and the specific lower heating value results of about $10 \text{ MJ}/\text{m}^3$ on a volumetric basis, which is lower than that of methane ($32.6 \text{ MJ}/\text{m}^3$) or iso-octane ($195.8 \text{ MJ}/\text{m}^3$).

Based on an examination of the properties of fuel-air mixtures, there is an important difference in mass and volumetric heating values of hydrogen-air mixtures compared to those of corresponding mixtures of methane-air and iso-octane-air. In terms of specific lower heating value, stoichiometric mixtures of hydrogen and air contain more energy on a mass basis ($3758 \text{ kJ}/\text{kg}$) than stoichiometric methane-air ($3028 \text{ kJ}/\text{kg}$) and stoichiometric iso-octane-air ($3013 \text{ kJ}/\text{kg}$). On the other hand, although its stoichiometric air-to-fuel ratio is higher, hydrogen occupies a greater proportion of volume (29.5%) with respect to air than methane (9.5%) or iso-octane (1.65%), and this counteracts specific lower heating value of hydrogen, so that in effect stoichiometric mixtures of hydrogen and air contain slightly less energy on volume basis ($2913 \text{ kJ}/\text{m}^3$) than stoichiometric methane-air ($3071 \text{ kJ}/\text{m}^3$) and stoichiometric iso-octane-air ($3704 \text{ kJ}/\text{m}^3$).

Thus, the large volume fraction occupied by hydrogen has consequences for the attainable engine power density. Combined with the wide flammability limits, it also have an important effect on mixture properties such as the kinematic viscosity (ν_u), thermal conductivity (λ_{tc}), thermal diffusivity (D_t), etc. These properties vary much more than in conventional engine fuels.

The wide flammability limits ranging of hydrogen in air (from 4 to 75 volume percent) and the low minimum ignition energy (about 0.02 mJ) require special attention when using hydrogen as an engine fuel. This wide range of flammability limits allows a wide range of engine power output through changes in the mixture equivalence ratio, with flammable mixtures from lean to rich fuel to air equivalence ratio $\Phi=0.1-7.1$ (i.e. $\lambda=10-0.14$, defined λ as $1/\Phi$, i.e. air to fuel equivalence ratio). These flammability limits, important also for safety considerations, widen with increasing temperature, although the lower flammability limit reduces slightly. On the other hand, the lower flammability limit increases with pressure, with the upper flammability limit having a behavior fairly complex in terms of pressure dependence but of smaller importance to engines. In practice, the lean limit of hydrogen-fueled internal combustion engines (H_2ICE) is reached for equivalence ratios near $\Phi\sim 0.25$ ($\lambda\sim 4$). Thus, hydrogen is able to burn at ultra-lean equivalence ratio in comparison with methane and iso-octane that are normally capable of burning at equivalence ratios no lower than about $\Phi\sim 0.53$ and $\Phi\sim 0.70$, respectively. The flammability limits ranging of methane in air ($5-15 \text{ vol}\%$ or $\Phi=0.5-1.67$) and iso-octane in air ($1.1-6 \text{ vol}\%$ or $\Phi=0.66-3.85$) are not so large as those of hydrogen, and the minimum ignition energy values of methane (0.29 mJ) and iso-octane (0.28 mJ) are about a factor of fifteen times higher than that of hydrogen. The minimum ignition energy is normally measured using a capacitive spark discharge and is dependent on the spark gap, being more or less constant for hydrogen concentrations of about $10-50 \text{ vol}\%$ or $\Phi=0.27-2.38$.

The quenching distance, whose value affects heat transfer of wall and has influence on risks of top-land crevice in combustion, can be experimentally obtained from the relation between the minimum ignition energy and the spark gap size or directly measured (usually defined as the minimum gap between parallel plates in which a flame will propagate). Verhelst&Wallner 2009 [18] reports that the quenching distance is minimal for mixtures around stoichiometry and decreases when increasing pressure and temperature. Their reported value for hydrogen is of about 0.64 mm at 300 K and 1 atm , which is approximately one third that of methane (2.03 mm) or iso-octane (3.5 mm). Bauer&Forest 2001 [16] gave same data of quenching distances except for iso-octane (2 mm), but at 293.15 K and 1 atm . These latter authors also reported that hydrogen generally burns hotter (2318 K) than methane (2148 K), but cooler than iso-octane (2470 K), based on flame temperatures in air.

Moreover, there is some ambiguity concerning the auto ignition temperature of fuels in general and of hydrogen particularly, Verhelst&Wallner 2009 [18]. For methane, values have been found ranging from 810 to 868 K. For hydrogen, values have been found from 773 to 858 K. Some sources list the auto ignition temperature for hydrogen as lower than that for methane; other sources list the opposite. This ambiguity can be at least partly explained by the sensitivity of auto ignition temperatures to the experimental apparatus, the experimental procedure and the criterion used for defining the value. For SIE, with a propagating flame front, auto ignition of the unburned mixture ahead of the flame front is unwished, as it can result in knocking combustion. The efficiency of a SIE is influenced by the compression ratio and the ignition timing, among others, and the choices of which are dependent on the auto ignition temperature of the fuel-air mixture, so this is an important parameter.

As the wide flammability limits allow hydrogen engines to be operated with substantial dilution, the laminar burning velocity and laminar flame stability can vary widely, and consequently are important parameters too. The laminar burning velocity of stoichiometric hydrogen-air mixtures, given by Verhelst&Wallner 2009 [18] for 360 K and 1 atm, is approximately 290 cm/s, which is a factor of about six times higher than that of methane (48 cm/s) or iso-octane (45 cm/s). However, if lean-burn strategies are used, the burning velocity of hydrogen mixtures in practical devices is usually lower. Bauer&Forest 2001 [16] observed an approximate seven-fold increase, at 293.15 K and 1 atm, in the burning velocity of a hydrogen flame (265-325 cm/s) over results of methane (37-45 cm/s) or iso-octane (37-43 cm/s), in shorter burn times. This shorter burn time was reflected in less heat transfer from a hydrogen flame compared to that of either methane or iso-octane flame; only 17-25% of the thermal energy released during combustion of hydrogen was lost to the environment due to radiation heat transfer compared to 22-33% for methane and 30-42% for iso-octane.

2.3. Characteristics of hydrogen and types of blends with hydrocarbons

The characteristics of hydrogen are unique compared to both conventional liquid fuels, like gasoline, and gaseous fuels, like methane and other alkanes, thus making it a challenging though promising fuel for ICE applications. The hydrogen properties involve several advantages in comparison with hydrocarbon fuels and some of these properties permit its use as single fuel in air mixtures, Verhelst&Wallner 2009 [18], or other uses in combined fuel blends.

2.3.1. Characteristics of hydrogen as fuel in combustion engines

The application in ICE, particularly in SIE, is attractive because of its wide flammability range, low spark energy requirement and stable ignition, large flame propagation velocity, small quenching distance, high rate of heat release per unit mass relative to hydrocarbon fuels, no unburned hydrocarbon emissions and less knock probability than gasoline or methane because of the high flame velocity, short ignition delay and high auto-ignition temperature.

As aforementioned, the hydrogen molecular composition and its peculiar chemical and physical properties make it interesting for SIE since allows a clean combustion of excellent quality, due to the positive influence, on air mixture formation and combustion process, of the high diffusion coefficient, the wide range of ignition flammability limits in air combustion and the very high flame speeds.

In addition, the elimination of CO₂ and the possibility of lean operating conditions lead to making hydrogen a clean fuel. Das et al. 2000 [20] compared performance and combustion

characteristics of an engine fueled with both H₂ and compressed NG (CNG), showing better thermal efficiency with hydrogen operation compared to CNG.

However, the direct use of hydrogen fuel it is not easy sometimes, as for transport engines, due to safety, storage and economic reasons. Some problems were accounted for using hydrogen as pure fuel, Karim 2003 [17], Verhelst&Sierens 2001 [21], Heffel 2003 [22], Mohammadi et al. 2007 [23], such as the backfire in the intake manifold, knock especially at higher engine loads and NO_x emissions increase due to the higher flame temperature.

For mixtures around stoichiometry, the high burning velocity and high adiabatic flame temperature can lead to high NO_x emissions. It is remarkable that the possibility of qualitative load control, changing the mixture richness at wide open throttle, the tolerance for substantial mixture dilution, either through excess air or exhaust gas recirculation (*EGR*), the high auto ignition temperature (allowing high compression ratios) and the generally fast burn rate, are all factors contributing to potentially high engine efficiencies experimentally confirmed. However, heat losses from cylinder gases to combustion chamber walls can be higher with hydrogen compared to conventional fuels, affecting efficiencies negatively. Nevertheless, in brief, hydrogen can be burned in engines with potentially high specific power output and efficiencies, with low emissions of NO_x for all load demands, far below standard levels using the suitable control strategies, over a very wide range of equivalence ratios with considerable large tolerance of *EGR*. The wide ignition limits allow engines to be operated even at extremely lean air-fuel ratios compared to conventional fuels. In addition, lean burn also improves thermal efficiency by the possibility of applying higher compression ratios with reduced heat transfer loss.

It is also noteworthy that value of specific heats ratio for hydrogen-air mixtures at standard conditions (of about $(c_p/c_v) \cong 1.4$) is almost constant for a wide range of equivalence ratios and virtually identical to the value of γ for only air, being higher than that of methane-air (1.354) or iso-octane-air (1.389).

On the other hand, slower flame propagation speed, increased cycle-to-cycle variations and instability of combustion process are some difficulties of lean burn operation. Otherwise, very low amount of emissions is possible at ultra-lean conditions due to the combustion stability; using ultra-lean mixtures, e.g. as a result of stratified charge engines, can improve the ability to increase compression ratio and therefore thermal efficiency that is limited in homogeneous stoichiometric mixtures because of knock phenomenon, Aliramezani et al. 2013 [24].

2.3.2. Types of blends of hydrogen and hydrocarbons and characteristics as fuels

The strong reactivity and wide range of flammability limits also make hydrogen ideal for fuels combination, in order to improve the combustion properties of mixtures. Thus, apart from use as a single fuel, hydrogen is also considered as a combustion enhancer, i.e. as a blending agent with other gaseous fuels and even in bi-fuel applications with both gasoline-type and diesel-type fuels. In particular, by extending the extinction and flammability limits of lean mixtures, hydrogen addition holds the potential to promote the combustion efficiency and reduce the pollutant formation.

Particularly H₂-CH₄ blends have been adopted as alternative fuels for power generation applications. A first reason for this is related with the performance improvement due to the hydrogen addition to methane, to extend operability ranges and to reduce pollutant emissions of lean combustion in both stationary, Schefer et al. 2002 [25], and mobile systems, Bell&Gupta 1997 [26], Bade-Shrestha&Karim 1999 [27], Sierens&Rosseel 2000 [28], Bauer&Forest 2001 [16,29]. A second reason is due to concerns about global warming, with problems of greenhouse effects, and the possibility of using hydrogen in both, fuel cells and combustion devices,

Verhelst&Sierens 2001 [30], Goltsov et al. 2006 [31]. However, stringent problems of safety and storage strongly complicate the use of pure hydrogen. Substitution of H₂ with CH₄ or other hydrocarbons (HC) has been proposed, Law&Kwon 2004 [32], as an interim solution to overcome these difficulties.

Two mixture formation strategies are differentiated by Verhelst&Wallner 2009 [18], “blended” operation and “dual-fuel” operation. Combinations of hydrogen with one or more gaseous fuels are called blended operation when fuel is stored and delivered to the engine in a mixed form, by means of a single system of gas mixer or a fuel-injection system. In this regard, hydrogen is often used to improve the NG lean combustion performance. On the other hand, dual-fuel operation describes any combination of hydrogen and liquid fuels in which several mixture preparation devices are used. Either these systems use separate storage for the different fuels or, in some cases, hydrogen may be produced on board. The concept of producing hydrogen by electrolysis on board was not considered an energetically viable way in conclusion of Bade-Shrestha&Karim 1999 [27].

◦ *Dual-fuel operation with combination of hydrogen*

This kind of application of hydrogen with diesel and bio-diesel, as well as gasoline and alcohol fuels, aims at improving combustion properties, hence reducing emissions and increasing fuel conversion efficiencies. This dual-fuel definition is different from the commonly used to denote the combustion of a homogeneous gas-air mixture with a diesel pilot injection.

◦ *Multiple-gas blends with hydrogen combination*

Some gaseous blends can result from pyrolysis, biomass gasification, thermally utilizable waste substances or by-product gases containing hydrogen that arise from chemical processes. Gaseous blends containing hydrogen help shift the lean-burn limit towards greater amounts of excess air than with NG. This effect causes mean combustion chamber temperatures to descend while NO_x emissions are reduced to a very low level. Verhelst&Wallner 2009 [18] mention that NO_x values lower than 5 ppm can be attained depending on the amount of hydrogen and other gas components. The hydrogen-rich gas mixtures can have a neutral influence on the degree of efficiency even with extremely high amounts of excess air. The background of this property lies in the considerably higher laminar burning velocity of hydrogen. The last cited work also mentions that in the case of coke gas (with 60% H₂), the laminar burning velocity at equivalence ratio $\Phi=0.5$ is the same as that for NG at $\Phi=0.9$. Especially in the lower and medium load range, this effect can be utilized directly resulting in an efficiency increase of up to 2% with operation using pure H₂ compared with NG, Gruber 2006 [33]. The power output is limited with turbocharged lean-burn gas engines operating with hydrogen-rich gas mixtures, especially due to the turbo charging unit.

On the other hand, and as a side remark, enrichment by hydrogen combined with exhaust gas recirculation in ICE somehow can be deemed leading to multicomponent mixtures in which the effective amount of oxygen (O₂) in the oxidizer is reduced as compared to standard air, and the mixing with hot fuel gases contributes to the initial temperature increase of these mixtures.

◦ *Blends of hydrogen and hydrocarbons (methane or natural gas)*

The combustion of lean hydrocarbon-air mixtures offers the potential of reduced flame temperatures and NO_x emissions according to thermal mechanisms. However, close to the lean flammability limits, the flame stability decreases and extinction phenomena may occur. To control this phenomenon, many studies have been performed in the literature to estimate the impact of hydrogen addition on the stability of methane-air flames, with the conclusion that the addition of small amounts of hydrogen extends the lean operating limit of combustion and

increases the stability of methane-air flames, as previously commented. Other studies indicated also how high addition rates of hydrogen increase the flame instability.

On the other hand, the blend lower heating value on a mass basis increases with hydrogen content, whereas the lower heating value referred to the volume decreases with hydrogen fraction, due to its very low density. A slower reduction occurs for the volumetric energy content of the fuel-air mixture, which indicates the effect of such blends on engine power output. The volumetric and mass lower heating values of NG-H₂ mixtures at different hydrogen fractions were illustrated by Hu et al. 2009 [14,15] regarding that, although the mass heating value of hydrogen is larger than that of NG, the volumetric heating value of hydrogen gives a lower value than that of NG; the volumetric heating value decreases by 28% when the hydrogen volumetric fraction in the fuel blends reaches 40%. Thus, the volumetric fraction of hydrogen at the stoichiometric air-fuel ratio is greater than that of NG as hydrogen occupies a large proportion of volume at the stoichiometric air-fuel ratio. The stoichiometric hydrogen-air mixture contains less energy than the stoichiometric NG-air mixture in volume terms, as explained in previous section 2.2 when comparing values of methane and hydrogen.

Thus, among the blends with hydrogen as a constituent, the main motivation for adding H₂ to NG is to extend the lean limit of NG. Otherwise, the low gravimetric storage density of compressed hydrogen tanks can be significantly improved by blending H₂ with CH₄. According with the predominant gas in the fuel blends, these can be called respectively natural gas based blends and hydrogen based blends.

2.3.2.1. Hydrogen-based blends

Hydrogen addition in the fuel blends improves the thermal efficiency of piston engines or gas turbines. However, the hydrogen impact on combustion processes can be dramatic for high blending rates. Therefore, H₂-NG mixtures need of specific system architectures and optimized control strategies to exploit the fuel properties, ensuring a safe operation at the same time.

For "H₂ dominated blends", the addition of CH₄ to H₂ significantly improves the storage density of compressed storage systems, and therefore increases the range of gaseous-fueled vehicles. As referred in Verhelst&Wallner 2009 [18], blending hydrogen with 5% in volume of methane increases the stored energy content by 11%, compared to pure hydrogen, while the stored energy increase is by 46% with 20% in volume of methane, Wallner et al. 2007 [34]. Tests performed on a single-cylinder research engine operated on hydrogen, as well as with these same blend proportions of 5% and 20% in volume of methane, showed a slight reduction in NO_x emissions with increased methane content while engine efficiencies decreased with increased methane content especially at low engine loads, Wallner et al. 2007 [35]. Vehicle-level tests on a Mercedes Benz E 200 NGT, a bi-fuel gasoline-natural gas vehicle that was adapted to operate on gasoline, NG, H₂ and any H₂-NG mixture showed up to 3% improvement in brake thermal efficiency when operated with hydrogen compared to gasoline, Eichlseder et al. 2009 [36].

On the other hand, in engines fueled with methane-hydrogen mixtures, back-fire and knock appear due to the rapid increasing burning velocity when the hydrogen fraction becomes high, especially above 50-60%, Karim et al. 1996 [37].

2.3.2.2. Natural gas-based blends

The use of additive to gaseous fuel combustion processes is one of the effective methods for reducing NO_x because it can assist in the production of the radical species necessary for reducing not only NO, but also NO₂, N₂O and may also lead to increase the burning velocity. Thus,

El-Sherif 2000 [38] considered the addition of small amounts of hydrogen to methane-air flames for control of emissions, with NO_x decreasing while increasing significantly the burning velocity.

A registered fuel referring to mixtures of 20% in volume of H_2 and CH_4 is called hythane, with the trademark being the property of Eden Innovations Ltd. The Denver Hythane project in 1991 showed a more than 75% reduction in carbon monoxide (CO) and NO_x emissions when using hythane instead of natural gas, Ortenzi et al. 2008 [39]. Experimental tests of Larsen&Wallace 1997 [40] on heavy-duty engines fueled by HCNG blends showed improvements of efficiency and reductions of CO, CO_2 and HC emissions on a turbocharged lean-burn NG hythane-fueled engine. Sierens&Rosseel 2000 [28] determined that the optimal composition of HCNG (hydrogen enriched compressed natural gas) to obtain low unburned HC and NO_x emissions should be varied with engine load.

For “NG based blends”, it is very helpful the referred fact that hydrogen has a burning velocity that is several times higher than that of methane. With the addition of hydrogen to NG an overall better combustion has been verified, even in a wide range of operating conditions (equivalence ratio, compression ratio, etc.), generally showing benefits, including promotion of higher thermal efficiency of combustion and reducing both pollutant exhaust emissions and greenhouse gas to lower CO_2 production, Sierens&Rosseel 2000 [28], Bauer&Forest 2001 [16,29]. Moreover, the NG- H_2 blends commonly named HCNG can be delivered using the NG infrastructures without significant modifications if hydrogen content is lower than 30% in volume, Mariani et al. 2012 [41]. The important synergies between hydrogen and methane for their application to ICE are very rewarding, Klell et al. 2012 [42].

2.4. Behavior of natural gas and blends with hydrogen as fuels in internal combustion engines

The combustion of NG produces fewer harmful exhaust emissions than that of conventional fuels, Karim et al. 1996 [37], Ristovski et al. 2000 [43], Pratti et al. 2011 [44], because NG chemical structures are less complicated, together with the non-existence of fuel evaporation, El-Sherif 1998 [45]. Methane, as main constituent of NG, is one of the less polluting fuels in terms of CO_2 thanks to its low carbon level, with an atomic ratio hydrogen/carbon close to $(H/C)=4$. The high anti-knock potential property of NG, Das et al. 2000 [20], with high octane number, between 120 and 130, allows to operate at even high compression ratios, with positive effects on power output and engine thermal efficiency, and improving the fuel economy.

However, a homogeneous charge SIE has lower volumetric efficiency for NG compared, for instance, with gasoline, since NG occupies a fraction of intake charge which implies a decrease in fresh air into the cylinder and thus in the output power, Mello et al. 2006 [46], with lower combustion rate. When NG is directly injected into the cylinder (direct injection) it has the advantage to eliminate the loss in volumetric efficiency, Huang et al. 2002 [47], but anyway NG engines broadly show a lower efficiency than diesel engines. Thus, due to the relatively slow burning velocity of NG even slower at lean conditions, with long ignition delay, Ben et al. 1999 [48], the combustion systems fueled with natural gas as the NG-SIE can be disadvantageous in some conditions, with lower thermal efficiency, important cycle-to-cycle variations and poor ability for exhaust gas recirculation (EGR), Wang et al. 2008 [10], Huang et al. 2009 [7], decreasing the engine power output and increasing fuel consumption, Ben et al. 1999 [48], Rousseau et al. 1999 [49]. Due to these restrictions, NG engines were usually operated at stoichiometric equivalence ratio or relatively rich mixture condition with relative low thermal efficiency. Traditionally, to improve the lean burn capabilities and flame burning velocity under lean burn conditions, an increase of flow rate in cylinder was introduced, but this measure increases the heat loss to the cylinder wall and increase the combustion temperature as well as

the NO_x emissions, Das&Watson 1997 [50], and optimizations in ignition timing and combustion chamber had to be operated to achieve a stable combustion.

Blending with fast-burning fuels are effective methods to counteract disadvantages, improving the poor lean-burn operation of NG and its slow burning velocity compared to liquid fuels, thus increasing efficiency. As aforementioned, such a gaseous fuel is hydrogen with its high burning velocity, Blarigan&Keller 2002 [51], Karim 2003 [17], Akansu et al. 2004 [52], Halter et al. 2005 [53], Ilbas et al. 2006 [54], Mandilas et al. 2007 [55]; therefore, hydrogen addition can increase the burning velocity of NG as regarded by Huang et al. 2006 [6]. Several authors published experimental results of NG fueled ICE, Karim et al. 1996 [37], Hoekstra et al. 1996 [56], Hu et al. 2009 [14,15], claiming that hydrogen as additive can increase the flame propagation speed of hydrocarbons, stabilize the combustion process and strongly improve the engine performance, especially in terms of power, efficiency and emissions, allowing engine operation with lean mixtures and, moreover, no deteriorating the anti-knock qualities of NG fuel with small amounts of hydrogen in the blends. In addition, the quenching distance of hydrogen, one-third of that of NG, is beneficial to reducing unburned HC near the wall and top-land crevice. Additionally, the conductivity of hydrogen is higher than that of NG, and this may increase the heat transfer to the coolant in the case of NG- H_2 combustion. An interesting study on the difference between the combustion of hydrogen and hydrocarbons (such as CNG), in terms of entropy generation and thus in terms of exergy destruction, was presented by Rakopoulos&Kyritsis 2006 [57], who asserted that using H_2 in NG can significantly reduce the irreversibility of the combustion process, with this reduction as large as the content of hydrogen.

Hydrogen increases linearly the H/C atomic ratio and improves pollutant emissions, so that it is beneficial to the reduction of carbon-related emissions such as exhaust concentrations of CO , CO_2 and unburned HC, and its addition to NG extends the flammability limits, Schefer 2003 [58], Choudhuri&Gollahalli 2003 [59], Hawkes&Chen 2004 [60], Sankaran 2006 [61], making lower the lean limit of NG without going into the lean misfire region, thereby achieving extremely low emission levels.

2.4.1. Combustion performance and emissions according to fuel composition and dilution

A study of Verhelst&Wallner 2009 [18] on a turbocharged lean-burn SIE, operated on NG as well as mixtures of H_2 -NG (in volume percentages H_2/NG of 20/80% and 30/70%) demonstrated that it was possible to achieve lower emissions of both NO_x and total unburned hydrocarbons (THC) without sacrificing engine torque or fuel economy, Munshi 2006 [62]. With the higher flame speed, a consequent reduction of the spark advance angle is required to obtain the maximum brake torque (MBT), as indicated by Nagalingam et al. 1983 [63] and Hoekstra et al. 1995 [64]. A numerical engine model was developed by Mariani et al. 2008 [65], who carried out an investigation on HCNG blends with H_2 content up to 30% stating that, by using MBT spark advance, such blends exhibit improvements of engine brake efficiency compared with NG, which are more relevant at part loads and for the highest H_2 content within the considered range, meanwhile NO_x emissions were reduced by means of EGR . Improvement in engine efficiency obtained by using EGR , Mariani et al. 2012 [41], is due to reduced burned gas dissociation and reduced heat losses to the walls because of the lower in-cylinder combustion chamber temperatures attained. Morrone&Unich 2009 [66] carried out a numerical investigation on the characteristics of NG- H_2 blends as well as their effect on engine performance; their results showed an increase in engine efficiency only if MBT spark advance is used for each fuel and specially at low-loads. Moreover, these authors performed an economic analysis and determined the over cost of hydrogen in such blends, showing cost percentage increments between 6% and 32% for different H_2 volumetric contents of 10% and 30% in the HCNG blends.

The optimum ignition timing is the ignition advance at which the engine gets the *MBT*, which is dependent on flame speed. The optimum ignition timing is advanced with the increase of the *EGR* rate due to the decrease in flame propagation speed, while it is postponed with the increase of H_2 addition in NG- H_2 blend. At large *EGR* rate, the flame propagation speed is decreased, and this needs the advancement of the ignition timing to avoid power loss due to the extended combustion duration. Adding hydrogen shortens the ignition delay and increases the flame propagation speed of the mixture. In the case of NG- H_2 combustion, properly delaying the ignition timing does not defer the combustion process because the burning velocity of the mixtures is increased as hydrogen is added. For a specified hydrogen fraction, the flame development duration, the rapid combustion duration and the total combustion duration are increased with the increase of *EGR* rate and are decreased with the increase of hydrogen fraction.

In the experimental study on the performance and emissions of a SIE fueled with NG- H_2 blends combined with *EGR* conducted by Hu et al. 2009 [14] the brake mean effective pressure was decreased with the increase of the *EGR* rate; on the other hand, this was decreased at small hydrogen fraction and was increased with further increase of hydrogen content. Effective thermal efficiency was increased with the increase of *EGR* rate when this was less than a certain value (10%) whereas it decreased with further increase of *EGR* rate when this was larger than that value. In the case of small *EGR* rate, effective thermal efficiency was decreased with the increase of H_2 fraction. In the case of large *EGR* rate, effective thermal efficiency showed an increasing trend with the increase of H_2 fraction. For a specified H_2 fraction, NO_x concentration was decreased with the increase of *EGR* rate, and this effectiveness became remarkably at large H_2 fraction; NO_x concentration showed an increasing trend with the increase of H_2 fraction. HC emissions increased with the increase of *EGR* rate and decreased with the increase of H_2 fraction. *EGR* had some influence on CO and CO_2 emissions but these showed little variations with *EGR* rate; CO and CO_2 emissions were decreased with the increase of H_2 addition. At engine speed of 2000 *r/min*, when the H_2 fraction was in the range of 30-40% and the *EGR* rate was in the range of 10-20%, engine performance and emissions got the reasonable values. At engine speed of 3000 *r/min*, when the H_2 fraction was in the range of 20-40% and the *EGR* rate was in the range of 20-30%, engine performance and emissions got the reasonable values. Engine fueled with NG- H_2 blends combined with *EGR* is a favorable approach to attain high-efficiency and low-emission combustion in SIE.

As in the context of the previously mentioned works, hydrogen fuel blends with generic natural gas or singular methane, respectively, have been widely studied in ICEs over time, but more broadly in recent two decades, Hoekstra et al. 1995 [64], Bade-Shrestha&Karim 1999 [27], Sita-Rama-Rahu et al. 2000 [67], Das et al. 2000 [20], Sierens&Rosseel 2000 [28], Wong&Karim 2000 [68], Bauer&Forest 2001 [16,29], Blarigan&Keller 2002 [51], Akansu et al. 2004 [52], Huang et al. 2006,2007 [6,69-72], Bysveen 2007 [73], Liu et al. 2008 [74], Ortenzi et al. 2008 [39], Morrone&Unich 2009 [66], Hu et al. 2009 [14,15,75-78], Tinaut et al. 2011 [79], Wang et al. 2007,2008,2009,2012 [8-10,80,81], Ma et al. 2007,2008,2010,2011,2012 [82-89,4], Mariani et al. 2008,2012,2013 [65,41,90], etc.

Therefore, in the literature, there are very varied works regarding to generic or specific air mixtures of NG or methane in fuel blends with hydrogen. Some of them have been collected in table 27 (chapter 8), among other published studies. These are referred about blends of hydrogen and hydrocarbons, in general or in particular, with diverse and interesting contributions to knowledge of the combustion behavior that may be reviewed according to the composition conditions. A summary of effects on combustion performance and emissions is also reported in table 5 (at the end of this chapter 2) for premixed fuel blends of NG- H_2 in SIE.

- *Combustion characteristics of lean mixtures* of NG-H₂ or CH₄-H₂ have been investigated more than other blends. Results of studies generally show that for lean conditions the engine performance can improve the unburned HC and exhaust emissions of CO and CO₂ that can be reduced by adding a small amount of H₂ with minor drawbacks on power output. NG containing 10-15% H₂ was proven to be an economical way to improve the gas engine lean-burn combustion, enabling the engine to realize high-efficient low-emission combustion, Phillips&Roby 2000 [91]. The H₂ addition speeds up the combustion process and can strengthen significantly the engine lean burn capability, which is beneficial to the reduction of fuel consumption and emission levels. NO_x emissions at partial load can be slightly reduced as H₂ extends the lean flammability limit of the mixture, Sierens&Rosseel 2000 [28], Ma&Wang 2008 [85], Wang et al. 2012 [81]. As a result of ultra-lean combustion the experimental study of Raman et al. 1994 [92], on SIE fueled with HCNG blends with 0-30% of H₂, observed reductions of NO_x emissions for proportions between 15-20% of H₂, with some increase of HC emissions. Hoekstra et al. 1995 [64] observed a limit of NO_x reduction for H₂ percentages up to 30%. Otherwise Genovese et al. 2011 [93] performed tests comparing energy consumption and exhaust emissions for NG and HCNG blends with H₂ content between 5-25% and they found that average engine efficiency over the driving cycle increased with H₂ fraction and NO_x emissions were higher for the blends with 20-25% of H₂ in volume, despite the lean relative air fuel ratios and delayed ignition timings adopted. The ignition timing is an important parameter for improving engine performance and combustion, as analyzed in the experimental study of Huang et al. 2006,2007 [71,72] for a direct injection (DI) SIE fueled with HCNG blends under various ignition timings and lean mixtures conditions. Other authors also carried out investigations on lean-burn HCNG engines obtaining very low NO_x emissions operating close to the lean limit, as Larsen&Wallace 1997 [40], Ma&Wang 2008,2010 [85,88] or Bysveen 2007 [73], who showed that the H₂ addition in CNG fuel has a positive impact on the engine efficiency especially when the lean limit is approached.

- *Combustion characteristics of stoichiometric and relatively rich mixtures* of NG-H₂ or CH₄-H₂ have been investigated because the NO_x emissions increase due to the increment in the adiabatic flame temperature. NO_x emissions can be controlled adopting EGR systems as one of the most effective methods for that reduction, Mariani et al. 2012 [41]. In fact, EGR is widely used in reducing NO_x from ICE. In general it can be said that unburned HC, CO₂ and CO emissions decrease by increasing the percentage of H₂ in NG, but NO_x emission broadly rise because the addition of H₂ increases the burning velocity and, thus, the burned temperature of the mixture as a consequence of a faster combustion, Nagalingam et al. 1983 [63]. Allenby et al. 2001 [94] studied the influence of the addition of EGR in NG-H₂ mixtures, by introducing residual gas into the combustible mixture, to reduce oxygen and fuel concentration (by dilution effect) and the flame temperature (by thermal effect, absorbing extra portion of heat release from combustion), and consequently the NO_x formation respect to undiluted charge, and they reported that the addition of H₂ into CH₄ could improve the combustion stability and the engine could tolerate up to 25% of EGR, while maintaining a coefficient of variability of indicated mean pressure below 5%, with this level of EGR giving a reduction in emissions greater than 80% at the stoichiometric fuel ratio. Further investigations performed by Mariani et al. 2012 [41] also at stoichiometric condition, adopting 10% EGR for HCNG blends, achieved an analogous large reduction of NO_x emission, greater than 80% compared with NG without EGR, with a positive effect also on engine efficiency and a reduction of fuel consumption between 5-8% respect to CNG.

- In summary, the most important engine variables that affect NO_x emissions are fuel-air equivalence ratio, spark timing and burned gas fraction in charge. The burned gas fraction in charge depends on the amount of diluent introduction such as EGR. Thus, NO_x emission, as a problem in NG-H₂ blend fueled engines, can be greatly decreased through lean combustion,

retarding ignition timing and introducing *EGR*. Many works concentrated on the mentioned method of using lean combustion and retarding ignition timing, Sierens&Rosseel 2000 [28], Larsen&Wallace 1997 [40], Hoekstra et al. 1995 [64], Huang et al. 2006 [69], Liu et al. 2008 [74], while other cited literatures introduced *EGR* with NG-H₂ blends to reduce NO_x emission, as Allenby et al. 2001 [94] or Hu et al. 2009 [14,15]. These authors investigated the effect of different *EGR* rates on the combustion characteristics of a SIE fueled with different fractions of NG-H₂ blends, and quantitatively analyzed heat release rate, and durations of flame development, rapid combustion and total combustion, as well the coefficient of variation of the indicated mean effective pressure. Dimopoulos et al. 2007,2008 [95,96] also investigated the combustion characteristics and emission behaviors of NG-H₂ blend engines operated with *EGR*, and their results also showed that the introduction of *EGR* could decrease NO_x emission remarkably. Ivanic et al. 2005 [97], like Hu et al. 2009 [14], also expressed that NO_x emissions can be limited by the adoption of *EGR* or lean burn, and Blarigan&Keller 2003 [98] conducted the investigation on a lean-burn NG-H₂ blend fueled engine combined with *EGR* and the NO_x emission was within the zero-emission limitation. Engines fueled with NG-H₂ blends combining with proper *EGR* rate can realize the stable low temperature combustion. HCNG blends combustion properties are particularly suitable for *EGR*, assuring a stable combustion also when the charge is diluted, Hu et al. 2009 [15], with the aim at improving engine efficiency and reducing NO_x emissions, particularly at low loads and for the highest H₂ contents considered as in Mariani et al. 2012 [41], from 10% up to 30%, moreover reducing fuel consumption respect to CNG. Thus, the use of H₂-NG blends can also reduce the energy consumption, besides CO₂ emissions, in engines that frequently operates at low-intermediate loads, as passenger cars engines for a great part of their lifetime.

2.4.2. Cycle-to-cycle dispersion

The phenomenon of cycle-to-cycle dispersion or variability is inherent to SIEs, Heywood 1988 [99], and has been widely studied. Many studies have been carried out in order to find out the main causes of this effect, Sen et al. 2008 [100], Galloni 2009 [101]. Cycle-to-cycle variations are considered being caused by dispersions in the flame speed, combustion duration and turbulence, Tinaut et al. 2000 [102]. The effect of dispersion has been described and studied by Litak et al. 2007,2008 [103,104] using statistical treatments (such as histograms, return maps and recurrence plots) of pressure data and heat release. These variations resulted in a diminution of up to 20% in the mean effective torque, Litak et al. 2009 [105].

The cyclic variability was evaluated by statistical processing of the maximum pressure (*MAXP*) and the angle at which this pressure is reached, by Selim 2005 [106]; in other works, it was studied with the variation in heat released during combustion, Hill 1988 [107], Hill&Kapil 1989 [108], and by using continuous wavelet transform to analyze the indicated mean effective pressure (*IMEP*) time series, Sen et al. 2011 [109]. More recently it has been studied in homogeneous charge compression ignition (HCCI) engine processes, Ebrahimi&Desmet 2010 [110], Sen et al. 2011 [111], using complex computational fluid dynamics simulations, Vermorel et al. 2009 [112], and using zero-dimensional predictive models based on stochastic estimation of the physically-relevant parameters, Curto-Risso et al. 2011 [113].

Thus, as cyclic variability estimators in the literature have been used, e.g., the standard deviations of *MAXP*, *IMEP*, combustion duration and burning velocity. Other estimators that can be used, and which are usually applied, are those such as the coefficients of variation (*CoV*) of these variables, defined as the ratio of the relative standard deviation and the averaged value of the respective variable. The *CoV* represents a measure of the dispersion of each related variable in relation to its average value; in addition, since the *CoV* is dimensionless, it may be considered as a better estimator of cyclic dispersion than the corresponding standard deviation.

Methane, which is the main component of NG, has a unique tetrahedral molecular structure, with large H-C bond energies, and also some unique combustion characteristics such as high ignition temperature and low burning velocity, Turns 2000 [114], leading to the poor lean-burn ability, slow burning velocity and long combustion duration. Consequently, these may lead to incomplete combustion, high misfire ratio and large cycle-to-cycle variations that are increased due to the presence of partial burn cycles in the NG fueled engines, especially engines operated under lean mixture operating conditions or with large *EGR* ratios to reduce NO_x emission. As already mentioned, one effective approach to solve this problem is to mix the NG gas with H_2 to improve the ignition performance and increase the burning velocity. The flammability limit of hydrogen is extended to a much leaner mixture and the lean operating limit can be extended by H_2 addition. The minimum ignition energy of hydrogen is much lower than that of NG and this can reduce the cycle-to-cycle variations in initial flame development with H_2 addition to the fuel blend.

Thus, hydrogen-enriched NG can promote flame propagation and combustion stability, leading to the fast burning cycle and low cycle-to-cycle variations, as shown by aforementioned studies, Bade-Shrestha&Karim 1999 [27], Das et al. 2000 [20], Bauer&Forest 2001 [16,29], and other recent works, Tinaut et al. 2014 [115].

The results of many studies conducted on the SIE cycle-to-cycle dispersion revealed that the variations in the early combustion stage mainly determine the cyclic variability of engines and are increased under lean mixture combustion or for the highly diluted mixture combustion, such as high *EGR* ratios or high residual gas fraction in load condition, Heywood 1988 [99].

Ma et al. 2008 [84] conducted the experimental study of H_2 addition on cycle-to-cycle variations in a turbocharged lean burn NG-SIE, while the hydrogen volumetric fraction in the NG- H_2 blends was kept invariable at 20% and the engine speed and load kept constantly in their study, with the conclusions that H_2 addition contributed to reducing flame development duration and was an effective and applicable approach to keep down cycle-to-cycle variations in lean burn SIE.

Wang et al. 2008 [10] investigated the cycle-to-cycle variations of NG engines with H_2 addition studying the variations of SIE fueled at low and medium load experimental conditions with NG- H_2 blends with H_2 fractions between 0-40% (0, 12, 23, 30 & 40%). The peak cylinder pressure *MAXP*, the maximum rate of pressure rise and the *IMEP* increased and their corresponding cycle-to-cycle variations decreased with the increase of H_2 fraction under lean mixture condition, and interdependency between combustion parameters and the corresponding crank angle tended to be strongly correlated with H_2 addition. The coefficient (CoV_{imep}) of variation of *IMEP* was maintained at a low level and was slightly influenced under the stoichiometric and the relatively rich mixture operation while it decreased remarkably with the increase of H_2 fraction under lean mixture operation. H_2 addition into the NG was able to decrease engine cycle-to-cycle variations. In other work, Wang et al. 2008 [116] studied cyclic variations of NG- H_2 mixtures in a constant-volume chamber with direct-injection. Their results showed that cyclic variations were initiated at the beginning of the flame development and decreased with the increase of H_2 addition.

Huang et al. 2009 [7] reported the variations of SIE fueled with NG- H_2 blends combined with *EGR*; the objective of that study was to evaluate the effect on cycle-to-cycle variations of *EGR* ratio between 0-40% and hydrogen fraction analogously in between 0-40%. The cylinder peak pressure *MAXP* and the maximum rate of pressure rise were decreased with the increase of *EGR* ratio, while the cycle-to-cycle variations of the two parameters were increased with the increase of *EGR* ratio. Interdependency between cylinder peak pressure, maximum rate of pressure rise and their corresponding crank angle was decreased with the increase of *EGR* ratio.

The cycle-to-cycle variations of *IMEP* were increased with the increase of *EGR* ratio. Partial burn cycles or misfire cycles would appear at large *EGR* ratio. The results of CoV_{imep} were slightly increased with the increase of *EGR* when this ratio was less than a certain value, and these were remarkably increased with the increase of *EGR* ratio when this was over this certain value. Hydrogen addition had little influence on CoV_{imep} at small *EGR* ratio while H_2 addition was able to decrease the CoV_{imep} remarkably at large *EGR* ratio.

- In summary, the effects of H_2 addition to NG on cycle-to-cycle variations have been studied in several works and the results showed that the coefficients of variation CoV_{maxp} and CoV_{imep} (of *MAXP* and *IMEP* respectively) were reduced by increasing H_2 content with both lean air-to-fuel mixtures, Ma et al. 2008 [84], and high *EGR* rates, Wang et al. 2008 [10]. The CoV_{imep} increased with the increase of *EGR* rate in experiments by Huang et al. 2009 [7], and H_2 addition into NG decreased the CoV_{imep} , and this effectiveness became more obviously at high *EGR* rate. Thus, H_2 addition makes possible to decrease cyclic variability, particularly at low loads, Mariani et al. 2013 [90], due to a positive effect of hydrogen on combustion stability in some conditions and given that the impact of H_2 addition on combustion speed varies with the engine loads; observed reductions of CoV_{imep} were smaller when higher loads were considered.

Other studies about cycle-to-cycle variations in a single-cylinder SIE were carried out by Reyes et al. 2013 [117] and Tinaut et al. 2014 [115]. NG- H_2 blends were used as fuel with a lean fuel-air equivalence ratio $\Phi=0.7$ and for different proportions of hydrogen, being considered $h(\%)=\{100, 80, 60, 40, 20, 0\}$ in [117] and $h(\%)=\{100, 75, 50, 25, 0\}$ in [115]. The engine rotational speed was constant (1500 rpm) in [117] and varied (1000, 1750 and 2500 rpm) in [115]. These works are two applications of respectively developed diagnostic models, with temperature dependent thermodynamic properties and consideration of heat losses, performing analysis of the experimentally obtained data of combustion chamber pressure. These studies combine a procedure based on genetic algorithms that are used to solve optimization problems. The methodology allows obtaining very accurate adjustments of the experimental correction factors and determines the optimum parameters needed for combustion diagnosis: pressure offset of the pressure register, top dead center angular positioning, effective dynamic compression ratio and heat transfer coefficients. The parameters have different values for each particular engine cycle and this usually makes difficult their adjustment, in general, which is a need in order to obtain an exact diagnosis of the combustion process. The method yields automatically an objective diagnosis of combustion pressure records, so that permits studying a high number of cycles without introducing any subjectivity or bias due to data manipulation, thus increasing the analysis capability. In these studies, six series of 830 consecutive engine pressure cycles were analyzed, obtaining the combustion diagnosis of each cycle. Principal objectives of these works were to obtain an estimation of the influence of the percentage of hydrogen in the fuel mixture on the cycle-to-cycle variations.

The study of the cyclic variability in the work of Reyes et al. 2013 [117] was carried out firstly by using traditional parameters, such as CoV_{imep} between others, and the study was carried out secondly by considering the values of the deviation of the mass-fraction burning rate (*MFBR*) as a function of the burned mass fraction (*BMF*). Determining the average combustion-burning rate (proportional to combustion speed) with its standard deviation was possible with some hypotheses. Results indicated that as the proportion of hydrogen increased in the mixture, the duration of the combustion and the relative dispersion were reduced, as expected. In order to have a better understanding of the influence of mixture composition on the combustion development, independently of combustion duration, the relevant combustion variables were plotted versus the *BMF* of each mixture. The standard deviation of *MFBR* is an estimator of the turbulence intensity of the combustion speed. For all the cases tested, except when the engine

was only fueled with H₂, this variable showed little dependence on *BMF*. These results showed that the turbulence in the combustion chamber is a characteristic of the engine for a given engine geometry and speed, and the variations of the combustion process are a consequence of the velocity inside the combustion chamber. Results indicated that the combustion process is dominated by the turbulence inside the combustion chamber (generated during intake and compression), showing little dependency of combustion variation on the mixture composition. This became more evident when relevant combustion variables were plotted versus the *BMF* of each mixture. The only exception was the case of single H₂, which showed differential characteristic, due to the inherent higher laminar speed of hydrogen that causes strong acceleration of combustion and thus increasing fluid turbulence generation; hydrogen combustion is not so dominated by flow turbulence, due to its high laminar speed. For all proportions of H₂ in the fuel mixture, results indicated that there is a little dependency between the first stage of the combustion (characterized by a value of *0.05 BMF*) and the second stage of combustion (characterized respectively by a value of *0.45 BMF*) and its posterior evolution.

An objective of the study published by Tinaut et al. 2014 [115] was additionally focused on the estimation of the influence on the combustion velocity of the percentage of H₂ in the fuel mixture. This was developed using the values of the burning velocity (computed from the pressure register and calculated as a result from the mass burning rate, the unburned mixture density and the flame front surface). The values were especially applied on the analysis of the cycle-to-cycle variation, quantified through the standard deviation and the coefficient of variation (CoV_{bv}) of the burning velocity. The work was presented as the result of ensemble averaging process of combustion cycles, done by considering all the values of burning velocity of the individual cycles with the same *BMF* (slightly different from ensemble averaging for the same angular position). Thus, results of burning velocity, standard deviation and CoV_{bv} of the burning velocity were represented, as a function of *BMF*, in order to identifying the general trends due to the effects of hydrogen substitution of NG in the blend. Since the laminar burning velocity of hydrogen is much higher than that of natural gas, increasing the H₂ content in the mixture with NG increases its burning velocity. This effect was roughly linear as hydrogen fraction increased from zero, except for very high values of the fraction, when the effect of hydrogen dominated combustion, even reducing the enhancing effect of flow turbulence. Additionally, increasing the H₂ fraction reduces the relative dispersion of combustion.

The averaged burning velocity, represented versus *BMF* for the different mixtures, increases as the engine rotational speed (*rpm*) grows, as can be expected due to the turbulent nature of combustion flow. The burning velocity also increases as the fraction of hydrogen increases in the mixtures, independently of the engine speed. However, the behavior corresponding to only H₂ is qualitatively different, showing what it is known as hydrogen-dominated combustion.

A general effect of engine speed on the standard deviation of the burning velocity is shown when the values are represented versus *BMF* for the different mixtures, which increases as engine speed increases, as the value of the burning velocity by itself makes. Again, this is a consequence of the turbulence of the engine in-cylinder flow, with a turbulent intensity that scales with engine speed, increasing not only the average value of the burning velocity but also its variability, given by its standard deviation. The variability of the burning velocity is generally much less dependent on the fraction of H₂ in the fuel mixture than the burning velocity itself. Thus, for higher engine speeds (*1750-2500 rpm*), the values of standard deviation of the burning velocity were similar in all the cases, with small differences when H₂ fraction changes. So, the combustion process can be considered mainly dominated by the turbulence inside the combustion chamber due to the admission and compression processes. However, in the case of pure H₂ tested at a lower engine speed (*1000 rpm*) the values of standard deviation of the burning velocity were clearly higher than for other fractions. This is considered a likely

consequence of the very high transport properties of hydrogen, which at low levels of flow turbulence (i.e. low engine rotational speed) are more relevant than the enhanced transport effects due to turbulence.

When the coefficient of variation CoV_{bv} of the burning velocity was plotted versus BMF , the values showed the effects of H_2 contents in the mixture more distinctly than the standard deviation of the burning velocity. In particular, the values of CoV_{bv} for each value of BMF are descending as the H_2 fraction increases.

The conclusions in [115] were that increasing the H_2 content in the mixture with NG increases its burning velocity and reduces the relative dispersion of combustion; moreover, while it is necessary to increase significantly the H_2 content to have a relevant increase in burning velocity, the effect of H_2 hydrogen addition on reducing combustion variability was evident soon, from at least 25% (less amount used in corresponding test-mixtures).

The effect on burning velocity of H_2 fraction was shown in more detail in several graphs that were plotted with the burning velocity versus the H_2 fraction for each engine rotational speed (rpm). Since the burning velocity varied along the combustion process, particular values of it at relevant values of BMF were selected to show the trends. The values of burning velocity at $BMF=\{0.05, 0.10, 0.25, 0.50, 0.75\}$ were considered as representative of initial, central and final parts of combustion process. The general trends are similar for all values of engine speed, with bigger values of burning velocity as engine speed increases. However, the differences are stronger for $0.25 BMF$ and $0.50 BMF$, since the combustion induced turbulence was not yet strong. This is in accordance to the fact that the dependence of burning velocity on engine speed was practically the same for $0.05 BMF$ and $0.10 BMF$. On the contrary, for $0.75 BMF$, the dependence of burning velocity on engine speed was smaller, since combustion rate at that BMF is more influenced by the previous combustion development than by initial flow turbulence. On the other hand, there was the obvious increasing trend of burning velocity with H_2 fraction for all values of engine speed. As already mentioned, for high H_2 fractions (bigger than 75%) combustion become dominated by hydrogen characteristics. This can also be confirmed since the dependence of burning velocity with engine speed is very much reduced as BMF is bigger.

Table 5

Summary of some effects of fuel composition parameters on the combustion performance and emissions in spark ignition engines for premixed **blends of natural gas and hydrogen**

Fuel	Equivalence ratio Φ	Dilution EGR or f_{res}	Ignition delay	Engine load	Cyclic variability	Thermal efficiency	Emissions			Knock probability	Ref.
							NO_x	HC	CO, CO ₂		
H₂	Possible lean burn in wide range $\Phi < 1$, even extremely lean.	Large tolerance to substantial dilution.	Short.	-	Variability increasing for lean burn, with increase of instability; mainly in early stage of combustion.	Potentially high. Negatively affected and limited for $\Phi \sim 1$ because of knocking.	High for $\Phi \sim 1$. Control strategies needed for reduction at all demands.	-	-	Especially given at high loads.	[17, 20-24, 37]
NG	Poor capability of lean burn.	Poor ability for dilution.	Long.		Especially important under lean operation and for highly diluted mixture, such as high EGR ratios or high residual gas fraction in load condition.	Not high. Positively affected in usual operation at $\Phi \sim 1$ or relatively rich, but decreasing with cyclic variability, also with lean operation and by dilution of residual gas or EGR .	Increasing with the flow rate increase (to improve lean burn). In need of optimization of ignition timing and chamber design for reduction.	Not high.	Low.	Anti-knock potential quality.	[7, 10, 20, 37, 43-44, 48-50, 99, 114]
NG + H₂	Lean burn limit extent by H ₂ addition without going into misfire region.	-	Reduction required for engine MBT . Optimum ignition timing postponed with increase of %H ₂ .	Optimal compositions should be varied with engine load because the impact of H ₂ addition varies.	Remarkable decreasing of variability with increase of %H ₂ under lean mixture operation, particularly at low loads; smaller reductions when higher loads.	Important promotion of efficiency, especially at partial (low-medium) loads and more significant for higher H ₂ content within 20-30% (<40%).	Increasing trend with increase of %H ₂ ; increasing especially at higher loads; slightly reduced with %H ₂ at partial load. Reduction when very lean condition.	Decreasing with increase of %H ₂ .	Decreasing with increase of %H ₂ .	No deterioration of anti-knock qualities of NG with small %H ₂ .	[6, 10, 14-18, 20, 25-29, 37-38, 40-41, 51-56, 58-64, 66, 69, 71-74, 81, 84-85, 88, 90, 92, 97, 115-117]
h(%)											
10-15%						Efficiency increasing.		Low.	Low.		[91]
15-20%											[20, 92]
20-25%											[93]
> 30%						No significant effect of more increase of efficiency for H ₂ >30%.	Limit of NO _x reduction in lean burn for %H ₂ up to 30%, even if very lean operation.				[18, 64]
< 40%		EGR for the greater promotion of efficiency and NO _x reduction.	Optimum ignition timing needs advance of retardation with increase of EGR .		Variability increasing with EGR ; slight increasing when EGR is lesser than a certain value, and remarkable increasing when EGR is over that. Little influence of H ₂ addition on variability at small EGR , while remarkable decreasing with %H ₂ at large EGR .	Efficiency reducing when using of e.g. $EGR > 10\%$. Increasing trend with increase of %H ₂ in the case of large EGR rate. Decreasing with increase of %H ₂ in the case of small EGR .	NO _x control by EGR systems. Decreasing with the increase of EGR for a specified %H ₂ ; remarkable effectiveness at large %H ₂ .	HC increasing with the increase of EGR rate.	Some influence of EGR but little variations on CO-CO ₂ .		[7, 10, 14-15, 41, 65, 95-98]
20-40%		20-30% (>rpm)									[14]
30-40%		10-20% (<rpm)									[10]
< 40%	Stoichiometric and relatively rich mixture operation.				Low variability is maintained, slightly influenced.	Positive effect on engine efficiency.					[41, 94]
H₂ + CH₄	Lean burn applications.	EGR applicable.			Remarkable decreasing of variability with increase of %H ₂ under lean mixture operation, particularly at low loads.	Efficiency decreasing with increase of CH ₄ (5-20%), especially at low loads.	Slight reduction of NO _x with increase of CH ₄ (5-20%).	HC increasing with %CH ₄ .	CO-CO ₂ increasing with %CH ₄ .	Especially for %H ₂ >50-60.	[35, 37, 115-117]
$h > 50\%$											

References of chapter two (second part)

- [1] **Cho HM, He BQ.** Spark ignition natural gas engines – a review. *Energy Conversion and Management* 2007;48(2):608-18.
- [2] **Naber JD, Siebers DL, Di-Julio SS, Westbrook CK.** Effects of natural gas composition on ignition delay under diesel conditions. *Combustion and Flame* 1994;99:192-200.
- [3] **Jessen PF, Melvin A.** Combustion fundamentals relevant to the burning of natural gas. *Progress in Energy and Combustion Science* 1977;4(2):239-55.
- [4] **Ma F, Li S, Zhao J, Qi Z, Deng J, Naeve N, He Y, Zhao S.** A fractal-based quasi-dimensional combustion model for SI engines fueled by hydrogen compressed natural gas. *International Journal of Hydrogen Energy* 2012;37:9892-901.
- [5] **Liao SY, Jiang DM, Cheng Q.** Determination of laminar burning velocities for natural gas. *Fuel* 2004;83(9):1247-50.
- [6] **Huang Z, Zhang Y, Zeng K, Liu B, Wang Q, Jiang D.** Measurements of laminar burning velocities for natural gas-hydrogen-air mixtures. *Combustion and Flame* 2006;146:302-11.
- [7] **Huang B, Hu E, Huang Z, Zeng J, Liu B, Jiang D.** Cycle-by-cycle variations in a spark ignition engine fueled with natural gas-hydrogen blends combined with EGR. *International Journal of Hydrogen Energy* 2009;34:8405-14.
- [8] **Wang J, Huang Z, Fang Y, Liu B, Zeng K, Miao H, Jiang D.** Combustion behaviors of a direct-injection engine operating on various fractions of natural gas-hydrogen blends. *International Journal of Hydrogen Energy* 2007;32(15):3555-64.
- [9] **Wang J, Huang Z, Miao H, Wang X, Jiang D.** Characteristics of direct injection combustion fueled by natural gas-hydrogen mixtures using a constant volume vessel. *International Journal of Hydrogen Energy* 2008;33:1947-56.
- [10] **Wang J, Chen H, Liu B, Huang Z.** Study of cycle-by-cycle variations of a spark ignition engine fueled with natural gas-hydrogen blends. *International Journal of Hydrogen Energy* 2008;33(18):4876-83.
- [11] **Miao H, Jiao Q, Huang Z, Jiang D.** Effect of initial pressure on laminar combustion characteristics of hydrogen enriched natural gas. *International Journal of Hydrogen Energy* 2008;33:3876-85.
- [12] **Miao H, Jiao Q, Huang Z, Jiang D.** Measurement of laminar burning velocities and Markstein lengths of diluted hydrogen-enriched natural gas. *International Journal of Hydrogen Energy* 2009;34:507-18.
- [13] **Miao H, Ji M, Jiao Q, Huang Q, Huang Z.** Laminar burning velocity and Markstein length of nitrogen diluted natural gas/hydrogen/air mixtures at normal, reduced and elevated pressures. *International Journal of Hydrogen Energy* 2009;34:3145-55.
- [14] **Hu E, Huang Z, Liu B, Zheng J, Gu X, Huang B.** Experimental investigation on performance and emissions of a spark-ignition engine fueled with natural gas-hydrogen blends combined with EGR. *International Journal of Hydrogen Energy* 2009;34(1):528-39.
- [15] **Hu E, Huang Z, Liu B, Zheng J, Gu X.** Experimental study on combustion characteristics of a spark-ignition engine fueled with natural gas-hydrogen blends combining with EGR. *International Journal of Hydrogen Energy* 2009;34(2):1035-44.
- [16] **Bauer CG, Forest TW.** Effect of hydrogen addition on the performance of methane-fueled vehicles. Part I: effect on S.I. engine performance. *International Journal of Hydrogen Energy* 2001;26:55–70.
- [17] **Karim GA.** Hydrogen as a spark ignition engine fuel. *International Journal of Hydrogen Energy* 2003;28:569–77.
- [18] **Verhelst S, Wallner T.** Hydrogen-fueled internal combustion engines. *Progress in Energy and Combustion Science* 2009;35:490-527.
- [19] **Gorensek MB, Forsberg CW.** Relative economic incentives for hydrogen from nuclear, renewable, and fossil energy sources. *International Journal of Hydrogen Energy* 2009;34:4237-42.
- [20] **Das LM, Gulati R, Gupta PK.** A comparative evaluation of the performance characteristics of a spark ignition engine using hydrogen and compressed natural gas as alternative fuels. *International Journal of Hydrogen Energy* 2000;25:783-93.
- [21] **Verhelst S, Sierens R.** Hydrogen engine specific properties. *International Journal of Hydrogen Energy* 2001;26:987-90.

- [22] **Heffel JW.** NO_x emission reduction in a hydrogen fueled internal combustion engine at 3000 rpm using exhaust gas recirculation. *International Journal of Hydrogen Energy* 2003;28:1285-92.
- [23] **Mohammadi A, Shioji M, Nakai Y, Ishikura W, Tabo E.** Performance and combustion characteristics of a direct injection SI hydrogen engine. *International Journal of Hydrogen Energy* 2007;32:296-304.
- [24] **Aliramezani M, Chitsaz I, Mozafari AA.** Thermodynamic modeling of partially stratified charge engine characteristics for hydrogen-methane blends at ultra-lean conditions. *International Journal of Hydrogen Energy* 2013;38:10640-47.
- [25] **Schefer RW, Wicksall DM, Agrawal AK.** Combustion of hydrogen enriched methane in a lean premixed swirl-stabilized burner. *Proceedings of the 29th international symposium on combustion* 2002;843-51.
- [26] **Bell SR, Gupta M.** Extension of the lean operating limit for natural gas fueling of a spark ignited engine using hydrogen blending. *Combustion Science and Technology* 1997;123:23-48.
- [27] **Bade-Shrestha SO, Karim GA.** Hydrogen as an additive to methane for spark ignition engine applications. *International Journal of Hydrogen Energy* 1999;24:577-86.
- [28] **Sierens R, Rosseel E.** Variable composition hydrogen/natural gas mixtures for increased engine efficiency and decreased emissions. *Journal of Engineering for Gas Turbines and Power* 2000;122:135-40.
- [29] **Bauer CG, Forest TW.** Effect of hydrogen addition on the performance of methane-fueled vehicles. Part II: driving cycle simulations. *International Journal of Hydrogen Energy* 2001;26:71-90.
- [30] **Verhelst S, Sierens R.** Aspects concerning the optimization of a hydrogen fueled engine. *International Journal of Hydrogen Energy* 2001;26:981-5.
- [31] **Goltsov VA, Veziroglu TN, Goltsova LF.** Hydrogen civilization of the future – a new conception of the IAHE. *International Journal of Hydrogen Energy* 2006;31:153-9.
- [32] **Law CK, Kwon OC.** Effects of hydrocarbon substitution on atmospheric hydrogen-air flame propagation. *International Journal of Hydrogen Energy* 2004;29(8):867-79.
- [33] **Gruber F, Herdin G, Klausner J, Robitschko R.** Use of hydrogen and hydrogen mixtures in a gas engine. *Proceedings of the 1st international symposium on hydrogen internal combustion engines, Graz, Austria* 2006;34-48.
- [34] **Wallner T, Lohse-Busch H, Ng H, Peters RW.** Results of research engine and vehicle drive cycle testing during blended hydrogen-methane operation. *Proceedings of National Hydrogen Association Annual Conference, San Antonio, Texas, 2007.*
- [35] **Wallner T, Ng H, Peters RW.** The effects of blending hydrogen with methane on engine operation, efficiency and emissions. *SAE Paper 2007-01-0474, 2007.*
- [36] **Eichlseder H, Wallner T, Freymann R, Ringler J,** The potential of hydrogen internal combustion engines in a future mobility scenario. *SAE Paper 2003-01-2267, 2003.*
- [37] **Karim GA, Wierzba I, Al-Alousi Y.** Methane-hydrogen mixtures as fuels. *International Journal of Hydrogen Energy* 1996;21(7):625-31.
- [38] **El-Sherif SA.** Control of emissions by gaseous additives in methane-air and carbon monoxide-air flames. *Fuel* 2000;79:567-75.
- [39] **Ortenzi F, Chiesa M, Scarcelli R, Pede G.** Experimental tests of blends of hydrogen and natural gas in light-duty vehicles. *International Journal of Hydrogen Energy* 2008;33:3225-9.
- [40] **Larsen JF, Wallace JS.** Comparison of emissions and efficiency of a turbocharged lean-burn natural gas and hythane-fueled engine. *Journal of Engineering for Gas Turbines and Power* 1997;119(1):218-26.
- [41] **Mariani A, Morrone B, Unich A.** Numerical evaluation of internal combustion spark ignition engines performance fueled with hydrogen-natural gas blends. *International Journal of Hydrogen Energy* 2012;37:2644-54.
- [42] **Klell M, Eichlseder H, Sartory M.** Mixtures of hydrogen and methane in the internal combustion engine – synergies, potential and regulations. *International Journal of Hydrogen Energy* 2012;37:11531-40.
- [43] **Ristovski ZD, Morawska L, Hitchins J, Thomas S, Greenaway C, Gilbert D.** Particle emissions from compressed natural gas engines. *Journal of Aerosol Science* 2000;31:403-13.
- [44] **Prati MV, Mariani A, Torbati R, Unich A, Costagliola MA, Morrone B.** Emissions and combustion behavior of a bi-fuel gasoline and natural gas spark ignition engine. *SAE International Journal Fuels Lubricants* 2011;4:328-38.

- [45] **El-Sherif SA.** Effects of natural gas composition on the nitrogen oxide, flame structure and burning velocity under laminar premixed flame conditions. *Fuel* 1998;77:1539-47.
- [46] **Mello P, Pelliza G, Cataluna R, Da-Silva R.** Evaluation of the maximum horsepower of vehicles converted for use with natural gas fuel. *Fuel* 2006;85:2180-6.
- [47] **Huang Z, Shiga S, Ueda T, Jingu N, Nakamura H, Ishima T, Obokata T, Tsue M, Kono M.** A basic behavior of CNG DI combustion in a spark ignited rapid compression machine. *JSME International Journal, Series B, Fluids and Thermal Engineering* 2002;45(4):891-900.
- [48] **Ben L, Dacros NR, Truquet R, Charnay G.** Influence of air/fuel ratio on cyclic variation and exhaust emission in natural gas SI engine, SAE Paper 992901; 1999.
- [49] **Rousseau S, Lemoult B, Tazerout M.** Combustion characteristics of natural gas in a lean burn spark-ignition engine. *Proceedings of the Institution of Mechanical Engineers, Part D, Journal of Automobile Engineering* 1999;213(D5):481-9.
- [50] **Das A, Watson HC.** Development of a natural gas spark ignition engine for optimum performance. *Proceedings of the Institution of Mechanical Engineers, Part D, Journal of Automobile Engineering* 1997;211:361-78.
- [51] **Blarigan PV, Keller JO.** A hydrogen-fueled internal combustion engine designed for single speed power operation. *International Journal of Hydrogen Energy* 2002;23(7):603-9.
- [52] **Akansu SO, Dulger A, Kahraman N.** Internal combustion engines fueled by natural gas-hydrogen mixtures. *International Journal of Hydrogen Energy* 2004;29(14):1527-39.
- [53] **Halter F, Chauveau C, Djebaili-Chaumeix N, Gökalp I.** Characterization of the effects of pressure and hydrogen concentration on laminar burning velocities of methane-hydrogen-air mixtures. *Proceedings of the Combustion Institute* 2005;30:201-8.
- [54] **Ilbas M, Crayford AP, Yilmaz I, Bowen PJ, Syred N.** Laminar-burning velocities of hydrogen-air and hydrogen-methane-air mixtures: an experimental study. *International Journal of Hydrogen Energy* 2006;31:1768-79.
- [55] **Mandilas C, Ormsby MP, Sheppard CGW, Woolley R.** Effects of hydrogen addition on laminar and turbulent premixed methane and iso-octane/air flames. *Proceedings of the Combustion Institute* 2007;31:1443-50.
- [56] **Hoekstra RL, Blarigan PV, Mulligan N.** NO_x emissions and efficiency of hydrogen, natural gas, and hydrogen/natural gas blended fuels. SAE Paper 961103; 1996.
- [57] **Rakopoulos CD, Kyritsis DC.** Hydrogen enrichment effects on the second law analysis of natural and landfill gas combustion in engine cylinders. *International Journal of Hydrogen Energy* 2006;31:1384-93.
- [58] **Schefer RW.** Hydrogen enrichment for improved lean flame stability. *International Journal of Hydrogen Energy* 2003;28:1131-41.
- [59] **Choudhuri AR, Gollahalli SR.** Stability of hydrogen-hydrocarbon blended fuel flames. *AIAA Journal of Propulsion and Power* 2003;19(2):220-5.
- [60] **Hawkes ER, Chen JH.** Direct numerical simulation of hydrogen-enriched lean premixed methane-air flames. *Combustion and Flame* 2004;138:242-58.
- [61] **Sankaran R, Im HG.** Effect of hydrogen addition on the flammability limit of stretched methane-air premixed flames. *Combustion Science and Technology* 2006;178:1585-611.
- [62] **Munshi S.** Medium-heavy duty hydrogen enriched natural gas spark ignition IC engine operation. *Proceedings of the 1st international symposium on hydrogen internal combustion engines, Graz, Austria* 2006;71-82.
- [63] **Nagalingam B, Duebel F, Schmillen K.** Performance study using natural gas, hydrogen supplemented natural gas and hydrogen in AVL research engine. *International Journal of Hydrogen Energy* 1983;8(9):715-20.
- [64] **Hoekstra RL, Collier K, Mulligan N, Chew L.** Experimental study of a clean burning vehicle fuel. *International Journal of Hydrogen Energy* 1995;20:737-45.
- [65] **Mariani A, Morrone B, Unich A.** Numerical modeling of internal combustion engines fueled by hydrogen-natural gas blends. *ASME international mechanical engineering congress exposition; 2008.*
- [66] **Morrone B, Unich A.** Numerical investigation on the effects of natural gas and hydrogen blends on engine combustion. *International Journal of Hydrogen Energy* 2009;34:4626-34.
- [67] **Sita-Rama-Raju AV, Ramesh A, Nagalingam B.** Effect of hydrogen induction on the performance of a natural-gas fueled lean-burn SI engine. *Journal of the Energy Institute* 2000;73(496):143-8.

- [68] **Wong YK, Karim GA.** An analytical examination of the effects of hydrogen addition on cyclic variations in homogeneously charged compression-ignition engines. *International Journal of Hydrogen Energy* 2000;25(12):1217-24.
- [69] **Huang Z, Liu B, Zeng K, Huang Y, Jiang D, Wang X, et al.** Experimental study on engine performance and emissions for an engine fueled with natural gas-hydrogen mixtures. *Energy & Fuels* 2006;20(5):2131-6.
- [70] **Huang Z, Wang J, Liu B, Zeng K, Yu K, Jiang D.** Combustion characteristics of a direct-injection engine fueled with natural gas-hydrogen mixtures. *Energy & Fuels* 2006;20(2):540-6.
- [71] **Huang Z, Wang J, Liu B, Zeng K, Yu K, Jiang D.** Combustion characteristics of a direct-injection engine fueled with natural gas-hydrogen blends under various injection timings. *Energy & Fuels* 2006;20(4):1498-504.
- [72] **Huang Z, Wang J, Liu B, Zeng K, Yu K, Jiang D.** Combustion characteristics of a direct-injection engine fueled with natural gas-hydrogen blends under different ignition timings. *Fuel* 2007;86:381-7.
- [73] **Bysveen M.** Engine characteristics of emissions and performance using mixtures of natural gas and hydrogen. *International Journal of Hydrogen Energy* 2007;32(4):482-9.
- [74] **Liu B, Huang Z, Zeng K, Chen H, Wang X, Miao H, et al.** Experimental study on emissions of a spark-ignition engine fueled with natural gas-hydrogen blends. *Energy & Fuels* 2008;22(1):273-7.
- [75] **Hu E, Huang Z, He J, Jin C, Zheng J.** Experimental and numerical study on laminar burning characteristics of premixed methane-hydrogen-air flames. *International Journal of Hydrogen Energy* 2009;34(11):4876-88.
- [76] **Hu E, Huang Z, He J, Zheng J, Miao H.** Measurements on laminar burning velocities and onset of cellular instabilities of methane-hydrogen-air flames at elevated pressure and temperatures. *International Journal of Hydrogen Energy* 2009;34:5574-84.
- [77] **Hu E, Huang Z, Zheng J, Li Q, He J.** Numerical study on laminar burning velocity and NO formation of premixed methane-hydrogen-air flames. *International Journal of Hydrogen Energy* 2009;34:6545-57.
- [78] **Hu E, Huang Z, He J, Miao H.** Experimental and numerical study on lean premixed methane-hydrogen-air flames at elevated pressure and temperatures. *International Journal of Hydrogen Energy* 2009;34:6951-60.
- [79] **Tinaut FV, Melgar A, Giménez B, Reyes M.** Prediction of performance and emissions of an engine fueled with natural gas/hydrogen blends. *International Journal of Hydrogen Energy* 2011;36:947-56.
- [80] **Wang J, Huang Z, Zheng J, Miao H.** Effect of partially premixed and hydrogen addition on natural gas direct injection lean combustion. *International Journal of Hydrogen Energy* 2009;34:9239-47.
- [81] **Wang X, Zhang H, Yao B, Lei Y, Sun X, Wang D, Ge Y.** Experimental study on factors affecting lean combustion limit of SI engine fueled with compressed natural gas and hydrogen blends. *Energy* 2012;38:58-65.
- [82] **Ma F, Wang Y, Liu HQ, Li Y, Wang JJ, Zhao S.** Experimental study on thermal efficiency and emission characteristics of a lean burn hydrogen enriched natural gas engine. *International Journal of Hydrogen Energy* 2007;32(18):5067-75.
- [83] **Ma F, Liu H, Wang Y, Li Y, Wang JJ, Zhao S.** Combustion and emission characteristics of a port-injection HCNG engine under various ignition timings. *International Journal of Hydrogen Energy* 2008; 33(2):816-22.
- [84] **Ma F, Wang Y, Liu H, Li Y, Wang J, Ding S.** Effects of hydrogen addition on cycle-by-cycle variations in a lean burn natural gas spark-ignition engine. *International Journal of Hydrogen Energy* 2008;33(2):823-31.
- [85] **Ma F, Wang Y.** Study on the extension of lean operation limit through hydrogen enrichment in a natural gas spark ignition engine. *International Journal of Hydrogen Energy* 2008;33(4):1416-24.
- [86] **Ma F, Wang Y, Wang M, Liu H, Wang J, Ding S, et al.** Development and validation of a quasi-dimensional combustion model for SI engines fueled by HCNG with variable hydrogen fractions. *International Journal of Hydrogen Energy* 2008;33:4863-75.
- [87] **Ma F, Liu H, Wang Y, Wang J, Ding S, Zhao S.** A quasi-dimensional combustion model for SI engine fueled by hydrogen enriched compressed natural gas. *SAE Paper* 2008-01-1633, 2008.

- [88] **Ma F, Wang M.** Performance and emission characteristics of a turbocharged spark-ignition hydrogen-enriched compressed natural gas engine under wide open throttle operating conditions. *International Journal of Hydrogen Energy* 2010;35:12502-9.
- [89] **Ma F, Deng J, Qi Z, Li S, Cheng R, Yang H, Zhao S.** Study on the calibration coefficients of a quasi-dimensional model for HCNG engine. *International Journal of Hydrogen Energy* 2011;33:9278-85.
- [90] **Mariani A, Prati MV, Unich A, Morrone B.** Combustion analysis of a spark ignition i.c. engine fueled alternatively with natural gas and hydrogen-natural gas blends. *International Journal of Hydrogen Energy* 2013;38:1616-23.
- [91] **Phillips JN, Roby RJ.** Hydrogen-enriched natural gas offers economic NO_x reduction alternative. *Power Engineering (Barrington, Illinois)* 2000;104(5):3.
- [92] **Raman V, Hansel J, Fulton J, Lynch F, Bruderly D.** Hythane – An ultraclean transportation fuel. *Proceedings of 10th World Hydrogen Conference, Cocoa Beach, Florida, USA, 1994.*
- [93] **Genovese A, Contrisciani N, Ortenzi F, Cazzola V.** On road experimental tests of hydrogen-natural gas blends on transit buses. *International Journal of Hydrogen Energy* 2011;36:1775-83.
- [94] **Allenby S, Chang WC, Megaritis A, Wyszynski ML.** Hydrogen enrichment: a way to maintain combustion stability in a natural gas fueled engine with exhaust gas recirculation, the potential of fuel reforming. *Proceedings of the Institution of Mechanical Engineers, Part D: Journal of Automobile Engineering* 2001;215(3):405–18.
- [95] **Dimopoulos P, Bach C, Soltic P, Boulouchos K.** Hydrogen-natural gas blends fuelling passenger car engines: combustion, emissions and well-to-wheels assessment. *International Journal of Hydrogen Energy* 2008;33(23):7224-36.
- [96] **Dimopoulos P, Rechsteiner C, Soltic P, Laemmle C, Boulouchos K.** Increase of passenger car engine efficiency with low engine-out emissions using hydrogen–natural gas mixtures: a thermodynamic analysis. *International Journal of Hydrogen Energy* 2007;32(14):3073-83.
- [97] **Ivanic Z, Ayala F, Goldwit J, Heywood JB.** Effects of hydrogen enhancement on efficiency and NO_x emissions of lean and EGR-diluted mixtures in a SI engine. *SAE paper 2005-01-0253, 2005.*
- [98] **Blarigan PV, Keller JO.** A hydrogen-fueled internal combustion engine designed for single speed-power operation. *Journal of Engineering for Gas Turbines and Power* 2003;125(3):783–90.
- [99] **Heywood JB.** *Internal combustion engine fundamentals.* McGraw-Hill, New-York; 1988.
- [100] **Sen AK, Longwic R, Litak G, Górski K.** Analysis of cycle-to-cycle pressure oscillations in a diesel engine. *Mechanical Systems and Signal Processing* 2008;22(2):362-73.
- [101] **Galloni E.** Analyses about parameters that affect cyclic variation in a spark ignition engine. *Applied Thermal Engineering Journal* 2009;29(5-6):1131-7.
- [102] **Tinaut FV, Giménez B, Horrillo A, Cabaco G.** Use of multi-zone combustion models to analyze and predict the effect of cyclic variations on SI engines. *SAE Paper 2000-1-0961, 2000.*
- [103] **Litak G, Kaminski T, Czarnigowski J, Zukowski D, Wendeker M.** Cycle-to-cycle oscillations of heat release in a spark ignition engine. *Meccanica* 2007;42:423-33.
- [104] **Litak G, Kaminski T, Rusinek R, Czarnigowski J, Wendeker M.** Patterns in the combustion process in a spark ignition engine. *Chaos, Solitons & Fractals* 2008;35(3):578-85.
- [105] **Litak G, Kaminski T, Czarnigowski J, Sen A, Wendeker M.** Combustion process in a spark ignition engine: analysis of cyclic peak pressure and peak pressure angle oscillations. *Meccanica* 2009;44:1-11.
- [106] **Selim MY.** Effect of engine parameters and gaseous fuel type on the cyclic variability of dual fuel engines. *Fuel* 2005;84(7-8):961-71.
- [107] **Hill PG.** Cyclic variations and turbulence structure in spark ignition engines. *Combust Flame* 1988;72(1):73-89.
- [108] **Hill PG, Kapil A.** The relationship between cyclic variations in spark-ignition engines and the small structure of turbulence. *Combust Flame* 1989;78(2):237-47.
- [109] **Sen AK, Zheng J, Huang Z.** Dynamics of cycle-to-cycle variations in a natural gas direct-injection spark-ignition engine. *Applied Energy* 2011;88(7):2324-34.
- [110] **Ebrahimi R, Desmet B.** An experimental investigation on engine speed and cyclic dispersion in an HCCI engine. *Fuel* 2010;89(8):2149-56.
- [111] **Sen A, Litak G, Edwards K, Finney C, Daw C, Wagner R.** Characteristics of cyclic heat release variability in the transition from spark ignition to HCCI in a gasoline engine. *Applied Energy* 2011;88(5):1649-55.

- [112] **Vermorel O, Richard S, Colin O, Angelberger C, Benkenida A, Veynante S.** Towards the understanding of cyclic variability in a spark ignited engine using multi-cycle LES. *Combustion and Flame* 2009;156(8):1525-41.
- [113] **Curto-Risso P, Medina A, Hernández AC, Guzmán-Vargas L, Angulo-Brown F.** On cycle-to-cycle heat release variations in a simulated spark ignition heat engine. *Applied Energy* 2011;88(5):1557-67.
- [114] **Turns SR.** An introduction to combustion. McGraw-Hill, New-York, 2000.
- [115] **Tinaut FV, Reyes M, Giménez B, Pérez A.** Characterization of combustion process and cycle-to-cycle variations in a spark ignition engine fueled with natural gas/hydrogen mixtures. Scientific conference on Combustion and related fields -SPEIC14- Towards Sustainable Combustion, Lisboa. Nov 19-21, 2014.
- [116] **Wang J, Huang Z, Miao H, Wang X, Jiang D.** Study of cyclic variations of direct-injection combustion fueled with natural gas-hydrogen blends using a constant volume vessel. *International Journal of Hydrogen Energy* 2008;33:7580-91.
- [117] **Reyes M, Melgar A, Pérez A, Giménez B.** Study of the cycle-to-cycle variations of an internal combustion engine fueled with natural gas-hydrogen blends from the diagnosis of combustion pressure. *International Journal of Hydrogen Energy* 2013;38:15477-87.

3. Concepts of burning velocities and flame speed in premixed combustion of fuel-air mixtures

- 3.1. Laminar burning velocities interrelationships
- 3.2. Theoretical expressions of laminar burning velocities. Asymptotical theories
- 3.3. Laminar burning velocities based on detailed chemical kinetics schemes
- 3.4. Laminar burning velocities related to studies of radical concentrations in the reaction zone
- 3.5. Flame stability, instabilities onset and stretch interaction
 - 3.5.1. Instabilities origination
 - 3.5.2. Flame stretch
- 3.6. Markstein lengths and correction for stretch effects
 - 3.6.1. Markstein lengths and un-stretched flame speeds and burning velocities
 - 3.6.2. Markstein numbers and Karlovitz stretch factors
- 3.7. Flame thickness and Peclet number
- 3.8. Instabilities development and cellular structures
 - 3.8.1. Flame instabilities and cellularity
 - 3.8.2. Critical values of Peclet number and regime transitions
- 3.9. Linear stability theory. Application for lean hydrogen-air flames
 - 3.9.1. Instability peninsula based on wavenumbers
 - 3.9.2. Instabilities on spherical flames at constant pressure for non-minor positive values of Markstein numbers
 - 3.9.3. Instabilities on spherical flames at constant pressure for minor-positive and negative values of Markstein numbers
 - 3.9.4. Flame instabilities in confined explosions
- 3.10. Correction of instabilities effects. Fractal considerations

References of chapters three, four and five (*after the fifth chapter*)

3. Concepts of burning velocities and flame speed in premixed combustion of fuel-air mixtures

This chapter 3 is a preliminary step in order to provide a conceptual support for a further objective of treating concrete expressions of laminar burning velocities applicable to fuel-air mixtures with hydrogen at engine conditions. This objective is explicitly developed in following chapters 4 and 5, based on significant references such as [1-14] among others. Also to assist in that goal, properties and characteristics of fuels such as hydrogen and methane and some blends have been referred in the previous chapter 2, in comparative terms of use in engines, from references such as Verhelst&Wallner 2009 [15], Bauer&Forest 2001 [16], Perini et al. 2010 [17], Hu et al. 2009 [18].

The significance of the laminar burning velocity has been previously introduced in chapters 1 and 2, as one of the most crucial properties to characterize the combustion process for a homogeneous mixture. Expressions of laminar burning velocity as functions of pressure (P), temperature (T), equivalence ratio (Φ) and residual gas fraction (f_{res}) are very important input to use in predicting characteristics of combustion performance and pollutant emissions in SIE by means of models. These usually consider a flame speed ratio (FSR) as the relationship between the turbulent combustion speed and a laminar value, Tinaut&López 2011 [19], Verhelst&Sheppard 2009 [20], Horrillo 1998 [21].

In the context where models of SIE combustion use burning velocities as an important property of fuel mixtures, both laminar and turbulent burning velocities are reported in the literature with strong differences among published works. These differences can be attributed to the fact that the authors sometimes do not consider the effects of stretch and instabilities, other times roughly consider them, and very few times strictly consider the interactions of these effects. The differences are sometimes important, not only in the values, but also in notations and definitions.

In order to clarify and discriminate concepts, this chapter 3 introduces an analysis of conceptual descriptions about burning velocities and flame speeds, those which are more generically employed, e.g. Gillespie et al. 2000 [22], with a homogenization of nomenclature for the relevant variables. This is also used in following chapters, for a wider understanding and easier interpretations of summaries of expressions. These are stated from different original terminologies applied by several authors, but conveyed with a homogenized terminology accounting for the respective and diverse data origins and varied methodologies.

3.1. Laminar burning velocities interrelationships

Because the burning velocity can vary with the flame device, it is necessary to define the laminar burning velocity associated to a one-dimensional reference flame, in order to identify the influence of the different variables on the laminar burning velocity of the flame, and to analyze the actual flame geometrical and stability factors, at the same time, with derived influence on the burning velocity. It is also noteworthy that the laminar burning velocity can only be defined for premixed flames. This work is oriented to the combustion of gaseous fuels in premixed mixtures mainly considering the laminar transport. Then, the laminar burning velocity can be identified as a property of the air-fuel-residual gas mixture, defined as the speed of a steady planar (ideally one-dimensional, adiabatic and stable) propagated flame front of a premixed, homogeneous, quiescent mixture, Cuenot et al. 2000 [23]. From an experimental point of view, the definition of ideal laminar burning velocity has the problem of the impossibility of achieving an ideal flame in practice. The real laminar flames are not a perfectly one-dimensional

flux, due to one or several of the following factors: Non-adiabatic flame, non-planar flame front, non-smooth and non-stable. Thus, it is necessary to define practically the normal component of the propagation velocity of the flame front, in a normal direction to the plane and in relative movement respect to the unburned mixture.

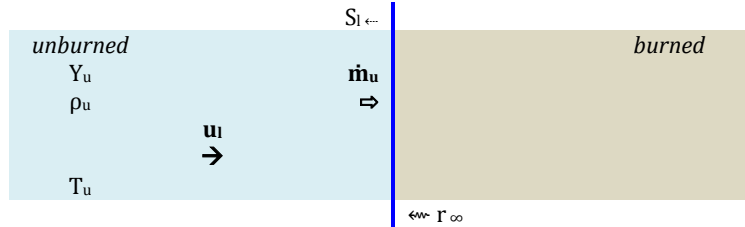


Fig. 1. Ideal laminar burning velocity u_l

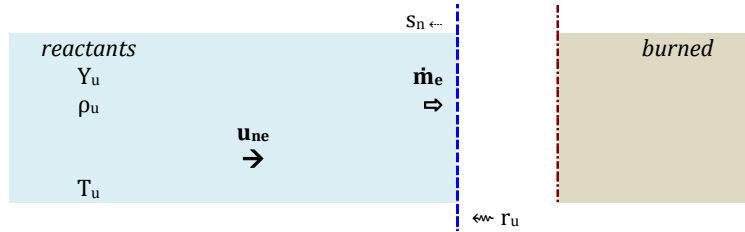


Fig. 2. Laminar burning velocity u_{ne} based on flame mass flux \dot{m}_e of unburned reactants entrainment

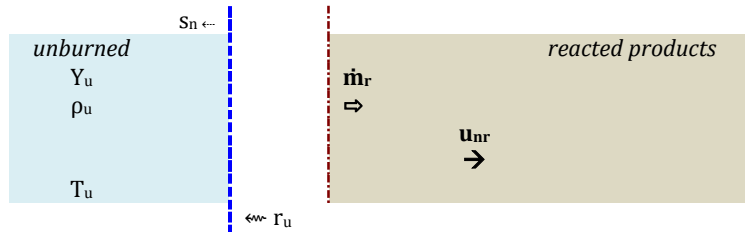


Fig. 3. Laminar burning velocity u_{nr} based on flame mass flux \dot{m}_r of burned reacted products

A premixed combustion of a fuel-air mixture, in which the laminar transport is the main phenomenon, is usually initiated by a spark ignition and the progress is due to the localized burning of the fresh unburned mixture at the flame front. This may be considered, in a first simplified approximation, a spatial discontinuity in temperature and chemical composition, but with the same pressure in both unburned and burned zones. The burning velocity of a mixture is then defined by the velocity of the cold reactants, perpendicular to the plane that includes the cold front of the flame. If this is one-dimensional and un-stretched, then the laminar burning velocity is a physicochemical variable that depends only on the mixture composition, pressure and temperature. Mathematically, this laminar burning velocity u_l is, under ideal conditions, the mass burning rate per unit surface area of the cold front of the flame, considering the density (ρ_u) of the unburned gas, such as depicted in fig. 1.

$$\text{Flame mass flux} = \dot{m}_u (1/A) = (1/A) \{ \partial m_u / \partial t \} \quad (1)$$

$$\text{Laminar burning velocity} \equiv \mathbf{u}_l = (1/A) (1/\rho_u) \{ \partial m_u / \partial t \} \quad (2)$$

The values of this ideal burning velocity u_l cannot be achieved in practice because it is not possible to produce experimentally perfect, adiabatic, one-dimensional, steady, un-stretched laminar premixed flames. The mass rate of consumption of unburned gas \dot{m}_e entrained into the flame front, for a non-planar flame, is not the same in general as the rate of production or formation of the burned product \dot{m}_r , principally because of the finite flame thickness and chemical kinetics. For those reasons, different burning velocities are derived depending on the experimental techniques of the measuring methods.

◦ The burning velocity such as determined by analysis from observations of cold flame fronts with imaging techniques (e.g. Schlieren cinematography) is defined first. The (non-ideal) laminar burning velocity u_{ne} (fig. 2) normal to the flame surface and based on the entrainment velocity of unburned mixture into the flame front, Rallis et al. 1965 [24], Bradley et al. 1996,1998 [25,26], is the rate of reactants consumption at initial unburned gas density (ρ_u).

$$\begin{aligned} \text{Flame "consumption or entrainment" mass flux} &= \dot{m}_e (1/A) \\ &= (1/A) \{ \partial m_e / \partial t \} \end{aligned} \quad (3)$$

$$\begin{aligned} \text{Laminar burning velocity of "unburned reactants consumption"} &\equiv \mathbf{u}_{ne} \\ &= (1/A) (1/\rho_u) \{ \partial m_e / \partial t \} \end{aligned} \quad (4)$$

◦ The burning velocity such as determined by thermodynamic analysis from measurements of pressure rise in closed vessels and taken into account for engine combustion is defined secondly. The (non-ideal) laminar burning velocity u_{nr} (fig. 3) based on the rate of production of reacted gas, at the same initial unburned gas density (ρ_u), is the rate of burned products formation, sometimes denominated as the mass burning velocity.

$$\begin{aligned} \text{Flame "production or reaction" mass flux} &= \dot{m}_r (1/A) \\ &= (1/A) \{ \partial m_r / \partial t \} \end{aligned} \quad (5)$$

$$\begin{aligned} \text{Laminar burning velocity of "burned products formation"} &\equiv \mathbf{u}_{nr} \\ &= (1/A) (1/\rho_u) \{ \partial m_r / \partial t \} \end{aligned} \quad (6)$$

For both defined normal laminar burning velocities, u_{ne} and u_{nr} , the flame area is determined at the cold front of the flame and the involved density is the one of the initial unburned gas (ρ_u).

For a spherically out-warding flame propagation, both expressions of laminar burning velocities can be developed, as was made by Bradley et al. 1996 [25], taking into account the density $\rho(r)$ at radius r and the initial unburned gas density ρ_u at radius r_u . In addition, the gas within the spherical theoretical surface of radius r_u might be regarded as composed of a mixture of unburned gas with a density ρ_u and burned gas at its adiabatic temperature with a density ρ_b .

$$\mathbf{u}_{ne} = (1/\rho_u) (1/r_u^2) \{ \partial \langle \int_{0-r_u} \rho r^2 dr \rangle / \partial t \} \quad (7)$$

Thus, at a radius r and density $\rho(r)$, two respective theoretical fractions of density differences or increments for the unburned gas $[(\rho - \rho_b) / (\rho_u - \rho_b)]$ and for the burned gas $[(\rho_u - \rho) / (\rho_u - \rho_b)]$ may be considered.

$$u_{ne} = (1/\rho_u) (1/r_u^2) \left\{ \partial \left\langle \int_{0-r_u} \rho_u [(\rho-\rho_b)/(\rho_u-\rho_b)] r^2 dr + \int_{0-r_u} \rho_b [(\rho_u-\rho)/(\rho_u-\rho_b)] r^2 dr \right\rangle / \partial t \right\} \quad (8)$$

Therefore, the first term on the right of the above equation represents the rate of entrainment by the flame front of gas that remains unburned. The second term on the right represents the rate of formation of burned gas. In spite of that, the normal laminar burning velocity of unburned reactants consumption u_{ne} is the expression, on the left, of the rate of entrainment of cold unburned gas by the flame front, the second term on the right expresses the rate of appearance of completely burned gas behind the front. The burning velocity associated solely with the latter term has been defined previously as the normal laminar burning velocity of burned products formation u_{nr} . Such a burning velocity concept was determined from the experiments of Metghalchi&Keck 1980,1982 [27,28] or Ryan&Lestz 1980 [29], from measurements of pressure rise in closed vessels.

$$u_{nr} = (1/\rho_u) (1/r_u^2) \left\{ \partial \left\langle \int_{0-r_u} \rho_b [(\rho_u-\rho)/(\rho_u-\rho_b)] r^2 dr \right\rangle / \partial t \right\} \quad (9)$$

Then, both normal laminar burning velocities, u_{ne} and u_{nr} , are related on the terms based on the previous equations.

$$u_{ne} = (1/\rho_u) (1/r_u^2) \left\{ \partial \left\langle \int_{0-r_u} \rho_u [(\rho-\rho_b)/(\rho_u-\rho_b)] r^2 dr \right\rangle / \partial t \right\} + u_{nr} \quad (10)$$

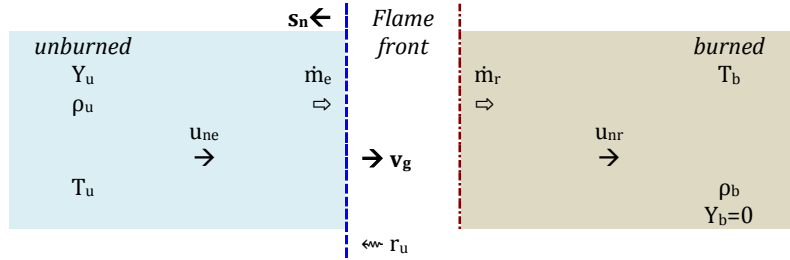


Fig. 4. Flame speed s_n and gas expansion velocity v_g

These terms can be expressed in relation with the normal flame-front speed s_n (fig. 4), defined as the time derivative of the flame radius r_u , which is measurable by observing the temporal development of the flame against time, with this r_u defined at the cold front, e.g. as an isotherm a few Kelvin above the temperature of reactants $r_u=r(T_u+\Delta T)$.

$$\text{Normal flame speed} \equiv s_n = \{ \partial r_u / \partial t \} \quad (11)$$

The normal flame speed s_n is not a unique property of a fuel mixture, but it is the sum of the normal laminar burning velocity of unburned reactants consumption u_{ne} and a term that corresponds to the gas expansion velocity v_g , immediately adjacent to the flame front, (fig. 4).

$$\text{Flame gas expansion velocity (adjacent to the flame front)} \equiv v_g$$

$$= s_n - u_{ne} = [(\rho_u - \rho_b) / \rho_b] u_{nr} \quad (12)$$

The flame gas expansion velocity v_g is a function of the densities of burned (ρ_b) and unburned gas (ρ_u) at any instant and is (except at the earliest stages of flame propagation or in the presence of any constraining boundary) bigger than the laminar burning velocity of unburned

reactants consumption u_{ne} . An expansion ratio of the normal flame speed to the normal burning velocity can be expressed as a function of the ratios of densities (ρ_u/ρ_b) and burning velocities (u_{nr}/u_{ne}).

$$(S_n/u_{ne}) = 1 + (v_g/u_{ne}) = 1 + [u_{nr}(\rho_u - \rho_b)/\rho_b u_{ne}] = 1 + [(\rho_u/\rho_b) - 1] (u_{nr}/u_{ne}) \quad (13)$$

Thus, an important distinction to make is the difference between normal flame speeds and burning velocities. Descriptions about gases movement are in Gillespie et al. 2000 [22], Rahim et al. 2002 [30] and Dahoe&De-Goey 2003 [31] or Dahoe 2005 [32]. The flame speed can be seen as the flame propagation in a fixed frame of reference. This can be obviously different from the burning velocity; e.g. in this developed case of centrally ignited spherically propagating flame, the flame front speed equals the sum of the burning velocity and the gas expansion velocity.

$$S_n = u_{ne} + v_g = u_{ne} + [(\rho_u - \rho_b)/\rho_b] u_{nr} \quad (14)$$

So, the difference between the flame speed s_n and the burning velocity u_{ne} is the velocity of the unburned gas v_g ahead of the flame front. The density of the burned zone is much lower than that of the unburned mixture due to the temperature rise. Therefore, in closed vessels, the expansion of the burned gas ($v_b \sim v_g$) has an important effect on the flame front speed.

It would be possible to adapt concepts from Heywood 1988 [33], Gillespie et al. 2000 [22], Gerke et al. 2010 [2], to describe a way for taking v_g into account using an expansion factor relative to the burned mass fraction Y_b (which could be derived from pressure data). The relations between the burned mass and volume (mole) fractions, respectively Y_b and X_b , can be expressed in a simplified formulation if the hypothesis of ideal gas law is applied.

$$1 + \{(\rho_u/\rho_b) [(1/X_b) - 1]\} = (1/Y_b) \quad \leftrightarrow \quad 1 + \{(\rho_b/\rho_u) [(1/Y_b) - 1]\} = (1/X_b) \quad (15)$$

$$\begin{aligned} \text{And} \quad (S_n/u_{ne}) &\sim \{(\rho_b/\rho_u) + Y_b [1 - (\rho_b/\rho_u)]\}^{-1} = (\rho_u/\rho_b) - X_b [(\rho_u/\rho_b) - 1] \\ &\sim [Y_b + (\rho_b/\rho_u) (1 - Y_b)]^{-1} = [X_b + (\rho_u/\rho_b) (1 - X_b)] \end{aligned} \quad (16)$$

The density of the burned zone (ρ_b) is much lower than that of the unburned mixture (ρ_u) due to the temperature rise. The value of the burned volume fractions X_b is higher than that of the mass fractions Y_b for a given combustion stage (but equal theoretically at the burning extremes, 0% & 100%). Corresponding values of the expansion factor (ρ_u/ρ_b) during the ignition phase (when X_b is close to 0 at the combustion beginning), as derived from pressure analysis with thermodynamic models, Gerke et al. 2010 [2], range between about 2.5 and 4, for mixtures with lean equivalence ratios, and between about 4.5 and 6 for stoichiometric equivalence ratios, depending on the condition of the unburned mixture. If the values of burning velocities are obtained experimentally by optical analysis (as radical OH-chemiluminescence measurements), the values of the density ratio are slightly bigger than those of the pressure analysis results.

Otherwise, the following expressions can be extrapolated, only in a very simplified “theoretically-ideal planar laminar consideration”, including zero flame thickness ($\delta_f=0$) and infinite radius (r_∞). That is the same considering the mass conservation across a section “A” of the flame front for an ideal isobaric process, perfect adiabatic one-dimensional steady unstretched laminar premixed flame (fig. 5).

$$u_{nr} \sim u_{ne} \sim u_l \quad \Rightarrow \quad v_g \sim S_l - u_l = [(\rho_u - \rho_b)/\rho_b] u_l \quad \Rightarrow \quad (17)$$

$$u_l = [S_l / (\rho_u/\rho_b)] \quad \Leftrightarrow \quad A \rho_u u_l = A \rho_b S_l \quad (18)$$

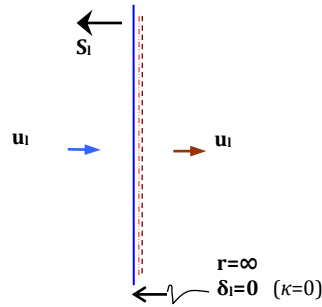


Fig. 5. Sketch of a section of an ideal laminar flame-front

However, the laminar flame thickness δ_l is not a mere discontinuity between burned and unburned gas, since densities, species concentrations and temperatures vary between the two borders of this thickness in the theoretical one-dimensional adiabatic premixed flame (fig. 6).

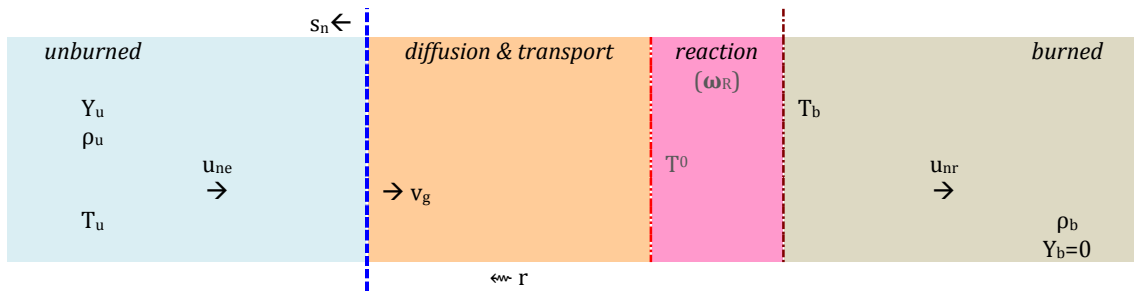


Fig. 6. Sketch of a section of a laminar flame-front

3.2. Theoretical expressions of laminar burning velocities. Asymptotical theories

In the combustion literature, Glassman 1997 [34], etc., there are wide descriptions of the physicochemical phenomena, and about the reactions and transports of heat, mass and species. In a conceptual summary, several zones can be considered. In the pre-heating zone, where the temperature T of the fuel-air mixture increases due to the thermal and mass diffusion from the flame front, the chemical activity is not yet relevant energetically because the reactions in this part are very slightly exothermic. The transformation to the products occurs in the thinner reaction zone; at its border, the temperature reaches the temperature of the burned products T_b , theoretically equivalent to the flame adiabatic temperature if the wall heat loss were negligible. Another zone, not energetically significant, is that of recombination, where the gases composition can change depending of the thermodynamic conditions or, simply, if the reactions are controlled by kinetics. It is obvious that in addition to the species and energy transport due to the convective effects, there is diffusive transport motivated by the gradients of the temperatures and species concentrations.

Kuo 1986 [35] classified different theories about the study of the ideal one-dimensional flame in function of the considered dominant effect in combustions. This includes thermal theories, where it is assumed that heat diffusion controls the combustion; diffusional theories, if the mass diffusion is assumed as the controlling factor, and global theories, that consider both heat and mass diffusion.

The conservation equations of governing species mass fractions, global mass, momentum and energy are developed in the literature for these processes, based on different theories, with the corresponding transport and thermochemical properties, by considering the mixture densities (ρ), the molecular diffusion velocities, the volumetric mass production rates, the rates of reaction, the mass Y_i or mole fractions X_i of species and their molecular masses.

It is theoretically interesting to consider a brief elemental approximation to conceptual expressions of combustion laminar burning velocity as related to a geometric mean of a thermal diffusion coefficient $D_{t,0}$ and a specific global reaction rate ω_R of the fuel, e.g. units such as *mole/m³.s*. This global reaction rate is very dependent on the reactants molar concentrations and temperature, and is usually expressed by means of an Arrhenius expression depending on the burned temperature T_b , with a reduced overall activation-energy E/R . In this way an expression of burning velocity can be straightforwardly derived, keeping the control of both physical and chemical phenomena, Desantes&Molina 2011 [36].

$$\hat{u}_L \sim [P^{(n-2)} T_u^h \omega_R D_{t,0}]^{(1/2)} \quad (19)$$

with $n \equiv$ global reaction order $\lesssim 2$ e.g. for a typical fuel premixed combustion, and $h \sim 2$;

$$D_{t,0} = (\lambda_{tc}/c_p) (1/\rho_u) \quad (20)$$

where λ_{tc} , c_p , ρ_u are the thermal conductivity, specific heat and density of gas, respectively;

$$\omega_R \sim e T^r \text{EXP}(-E/2RT_b) \quad (21)$$

being R the universal gas constant and $r \sim [-2,2]$.

From another theoretical point of view, it is also interesting to refer in this introduction to the dependences observed by Turns 2000 [37], on general factors of pressure P and unburned T_u and burned T_b gas temperatures.

$$\hat{u}_L \sim P^{[(n-2)/2]} (T_b)^{(-n/2)} (T_u)^{(1/2)} [(T_b+T_u)/2]^{(7/8)} \text{EXP}(-E/2RT_b) \quad (22)$$

The global reaction orders, used in this and other formulations, can be expressed according to Egolfopoulos&Law 1990 [38].

$$n \equiv \text{global reaction order} = 2 \{ \partial \langle \ln(\dot{m}) \rangle / \partial P \}_{T_b} \quad (23)$$

with $\dot{m} \equiv$ mass flux

Zeldovich et al. 1981,1985 [39,40], in early asymptotic analysis, developed a hybrid mass-thermal theory with the fundamental physicochemical effects, based on some simplified hypothesis and with reduced analytic complexity, to obtain the temperatures T and fuel mass fraction Y fields, taking the fuel as the representative element of the chemical reaction and with two defined dimensionless associated variables.

$$\text{Normalized fuel mass fraction variation in the mixture} \quad (Y_u - Y)/Y_u \quad (24)$$

$$\text{Normalized variation of temperature} \quad (T - T_u)/(T_b - T_u) \quad (25)$$

Other analyses of asymptotic type were made by Williams 1985 [41] and Clavin 1985 [42]. The sensitivity of chemical reactions to the variation of the maximum flame temperature was represented by the so-called Zeldovich number.

$$[(E/R) (T_b - T_u) / (T_b)^2] = Ze \quad (26)$$

Another alternative to the Zeldovich number was the given in the work of Seshadri&Williams 1994 [43], with the additional consideration of a temperature T^0 in the inner (fuel consumption) layer.

$$Z = Ze [(T^0 - T_u) / (T_b - T_u)] = [(E/R) (T^0 - T_u) / (T_b)^2] \quad (27)$$

Peters&Williams 1987 [44] deduced an asymptotic structure of the flame and introduced that temperature T^0 in the inner layer, which serves to characterize the balance between the chain-branching reactions and the chain-breaking effect of the fuel and the recombination reactions. This T^0 was considered as the critical temperature, at and above which chemical reaction takes place. They expressed the mass flux based on the laminar burning velocity in a square root form, provided T^0 remaining constant.

$$\hat{u}_L \sim (1/\rho_u) \text{EXP}(-E/2RT_b) \quad (28)$$

On other work, this was interpreted by Göttgens et al. 1992 [9], who computed values numerically, shown primarily T^0 as a pressure function. This asymptotic formulation is the basis of a laminar burning velocity expression of these authors, presented in section 5. The actual kinetics generally is too complicated to be represented in terms of a simple reaction in wide ranges of temperature T_b and pressure P . The study was based on a detailed chemical kinetic mechanism of these authors considering an important number (82) of elementary reactions. Thus, the chemical production rate contains contributions from all considered reactions, instead of a single overall global reaction, making use of the proper kinetic data and the necessary transport properties.

Specific chemical production rate of the species i :

$$m'_i = M_i (\sum_q \epsilon_{i,q} \omega_q) \quad (29)$$

$$q = \{1, r\} \quad r = \text{reactions number}$$

$$i = \{1, N\} \quad N = \text{species number}$$

$\epsilon_{i,q}$ = stoichiometric coefficient of species i in reaction q

M_i = molecular weights of the species i ;

Y_j = mass fractions of the species j

Rates of the reactions q :

$$\omega_q = k_{f,q} \{ \prod_{1-N} [(\rho Y_j / M_j)^{\epsilon'_{j,q}}] \} - k_{b,q} \{ \prod_{1-N} [(\rho Y_j / M_j)^{\epsilon''_{j,q}}] \} \quad j = \{1, N\} \quad (30)$$

$\epsilon'_{j,q}$ = stoichiometric coefficient of the forward step for the species j , in the reaction q

$\epsilon''_{j,q}$ = stoichiometric coefficient of the backward step for the species j , in the reaction q

$$\text{Rate coefficients of the reactions } q: \quad k_{-,q}(T) = a_q T^{N_q} \text{EXP}(-E_q/RT) \quad (31)$$

$k_{f,q}(T)$ = rate coefficient of the forward step for the species j , in the reaction q

$k_{b,q}(T)$ = rate coefficient of the backward step for the species j , in the reaction q

The specific reaction rates are given, with their specific activation energies, in terms of the Arrhenius expressions (with semi-empirical origin and theoretical justification) that can be interpreted, in a simplified form, according to the molecular collisions theory:

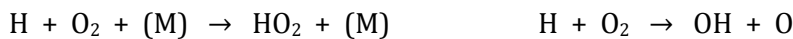
$a_q T^{N_q} \sim$ parameter estimator of the collisions frequency of the reacting molecules,

$\text{EXP}(-E_q/RT) \sim$ function estimator of the fraction of collisions with enough energy to the chemical reaction.

3.3. Laminar burning velocities based on detailed chemical kinetics schemes

Before introducing considerations on flame stability, it is interesting to observe that many computational studies in the literature are based on the assumption of a one-dimensional, planar flame. With this assumption, the accuracy of the predicted burning velocities depends on the accuracy of the molecular transport coefficients, the realism of the chemical kinetic reaction schemes and the accuracy of the rate constants.

A key problem, particularly at high pressure, Bradley et al. 2007 [45], is the dependence of these rates constants for three body reactions upon the nature of the third bodies. So, in the case of hydrogen-air mixtures, this is well exemplified by the importance of the rates of the hydrogen reactions with third body (M), Davis et al. 2005 [46], relative to that of the chain branching reaction.

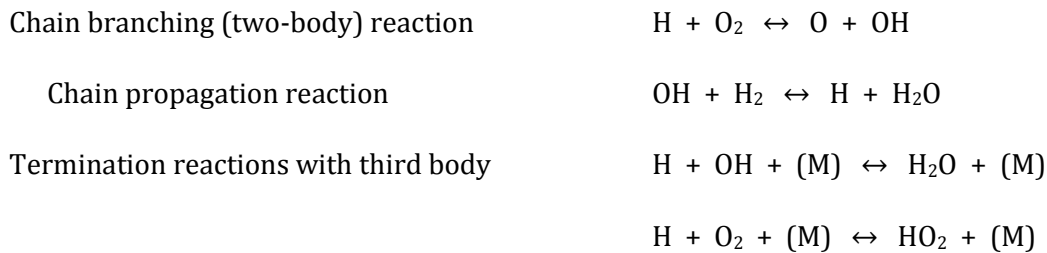


The rate constant for the chain branching reaction is considered known with quite good accuracy. However, with regard to the reactions with a third body, there is uncertainty about the rate constant and the collision efficiencies of different third bodies, Konnov 2004 [47].

The alternative to computing laminar burning velocities u_L for one-dimensional laminar flames, with detailed chemical kinetics but without flame stretch and instability, has been used by some authors trying to avoid the kinetic uncertainties, especially at high pressure for very unstable flames. Many times these studies are complementary to experimental works. Some of them will be detailed in chapters 4 and 5 for the considered cases of hydrogen-air mixtures. In this work, the particular notation u_L will be used, instead of u_b , when a laminar burning expression (from those summarized in chapter 5) has been determined by means of a computational model assuming one-dimensional planar flames based on chemical kinetics.

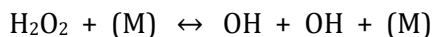
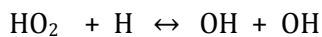
3.4. Laminar burning velocities related to studies of radical concentrations in the reaction zone

The following are four important and representative elementary reactions in the hydrogen-air flame, Hu et al. 2009 [1].



The dominant chain branching reactions produce many radicals O and OH during the combustion. The main chain termination reactions induce the reduction of active radicals during the combustion process. Enhancement of chain branching reaction can increase the concentrations of highly reactive radical species, such as hydrogen and hydroxyl radicals, and increases laminar burning rate. In contrast, enhancement of chain termination reaction can decrease the available radical species concentrations and decreases laminar burning rate.

Termination reactions, Hu et al. 2009 [1], are increased when compared to those of main branching reactions, leading to initial decrease of the reaction order. When pressure increases, the concentrations of HO₂ and the third body (M) become high. Other reactions are more frequent and overtake the stability of HO₂ and H₂O₂. Therefore, they generate much OH active species. This behavior contributes to the subsequent increase in the reaction order again.



The reaction rate analysis of Hu et al. 2009 [1] considered the influences of initial pressure and temperature on laminar burning velocity via the dominant chain branching (two-body) reactions and the main chain termination reactions (with third body). They considered these four crucial chain branching and termination reactions in the oxidation kinetics of hydrogen and their reaction rate profiles at different initial pressures and temperatures.

Their results show that the reaction rates of both branching reactions and both termination reactions are increased with the increase of initial pressure and temperature. However, the growth rate of branching reaction rate and termination reaction rate are different. They calculated the growth rate of the maximum reaction rate of these four elementary reactions, with some conclusions. With the increase of initial pressure, the growth rate of the termination reaction rate is much higher than that of branching reaction rate, and this will decrease active radicals and burning velocity. With the increase of initial temperature, the growth rate of branching reaction rate is larger than that of termination reaction rate, and this will increase the concentrations of highly reactive radical species and lead to the increase of burning velocity. This study reveals that chain branching reactions are the temperature-sensitive, two-body reactions, while chain termination reactions are the temperature-insensitive, three-body reactions. Thus, the branching and termination reactions can be enhanced by increasing flame temperature and pressure, respectively.

Competition of chain branching reactions and chain termination reactions plays an important role on the determination of laminar burning velocity. Suppression (or enhancement) of overall chemical reaction with the increase of initial pressure (or temperature) is due to the decrease (or increase) of H and OH mole fractions in flames. Strong correlation is derived between laminar burning velocity and maximum radical concentrations of H and OH radicals in the reaction zone of premixed flames. High laminar burning velocity corresponds to high radical concentration in the reaction zone.

3.5. Flame stability, instabilities onset and stretch interaction

There are present in real flames several types of phenomena (figs. 7, 8 and 9) that can change the laminar burning velocity, among other properties.

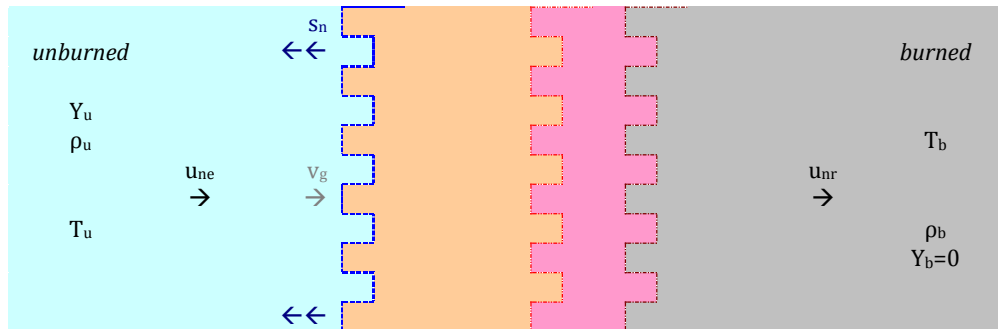


Fig. 7. Radially unstable flame front sketch
(Wrinkled geometries of waves are schematically represented as squared shapes)

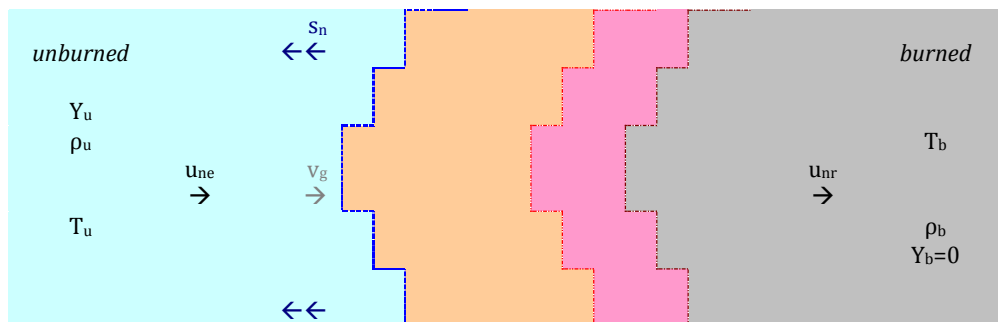


Fig. 8. Transversely unstable flame front sketch
(Wrinkled geometries of waves are schematically represented as squared shapes)

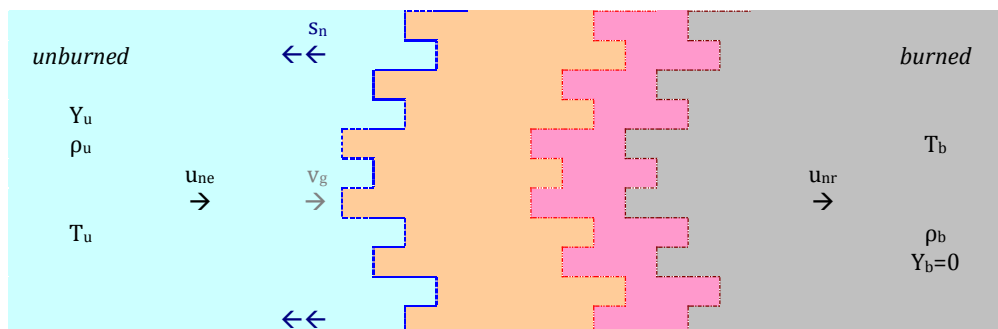


Fig. 9. Radially and transversely unstable flame front sketch
(Wrinkled geometries of waves are schematically represented as squared shapes)

- The instabilities of the structure of the flame front are one type of the phenomena to take into account. The presence of body forces, like gravity for instance, the thermal expansion of gases when pass through the flame front, and phenomena of thermo-diffusive origin, can create instabilities in the flame front, which can develop deformations and wrinkling in it. The effect on the laminar burning velocity is double; one is the increase of flame front surface, with the

subsequent increase of the effective flame speed; the other, the deformations of the flame and flow geometry, resulting in changes of velocity direction and magnitude.

- The other type of phenomena is the combination of two factors, one of geometric type and other of diffusive nature, and both can modify the burning velocity. The first factor originates in the deviation of the flame geometry and the flow respect to the one-dimensional flame; it can be quantified by means of both the flame front curvature and the presence of flow speed gradients in the flame front. The second factor may be due to the fact of the different mass diffusivities of the reactants in the mixture, or due to the different mass and thermal diffusivities of the mixture.

3.5.1. Instabilities origination

Several intrinsic mechanisms can trigger instabilities of a laminar flame (fig. 10), with very important implications on hydrogen combustion. Different phenomenological aspects related to the effects of disturbance or perturbations on a flame front are considered by many authors, Manton et al. 1952 [48], Clavin 1985 [42], Williams 1985 [41], Bechtold&Matalon 1987 [49], Law 1988 [50], Kull 1991 [51], Ronney 1999 [52], Bychkov&Liberman 2000 [53], Law&Sung 2000 [54], Gu et al. 2000 [55], Law&Kwon 2004 [56], Law 2006 [57], Lafuente 2008 [8], etc. The types of phenomena that produce instabilities are considered, respectively, due to body forces, hydrodynamic origin and thermo-diffusional causes.

Nevertheless, some of them can also have a stabilization result on the flame front, Zeldovich 1981 [39], and the global results of the different effects determine the flame stability or instability. Sometimes the presence of instabilities in a smooth-planar flame front can cause a wrinkling intrinsic process (fig. 11) and the flame can reach a cellular structure (fig. 12). The effects of preferential diffusion are very pronounced for hydrogen fuel, for instance.

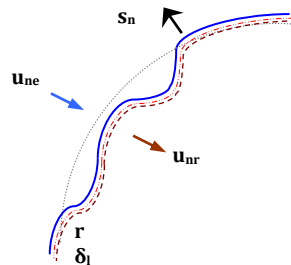


Fig. 10. Unsteady flame front sketch

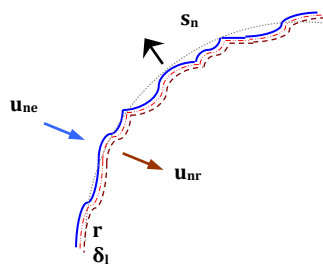


Fig. 11. Wrinkled flame front sketch

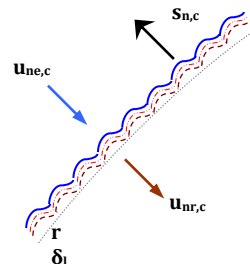


Fig. 12. Cellular flame front sketch

If the laminar flame is considered as a passive surface, i.e. as an infinitely thin interface separating burned gases of lower density ρ_b from unburned gases with higher density ρ_u , a wrinkling of the flame will not affect the flame intensity but it will increase the volumetric burning rate by the increased flame area. The discontinuity of density ($\rho_u \rightarrow \rho_b$) causes a hydrodynamic instability, Clavin 1985 [42], Williams 1985 [41], known as the Darrieus-Landau instability (fig. 13). As indicated by Verhelst 2005 [13], a wrinkle of the flame front will cause a widening of the stream tube to the protrusion of the flame front into the unburned gases, resulting in a locally decreased gas velocity. This will cause a further protrusion of this flame front into this flame segment as the flame speed remains unchanged (if the flame structure is not affected). Thus, a flame is unconditionally unstable when hydrodynamic stretch is the only one considered, neglecting the effect of flame stretch on the structure of the flame (this will be later referred to in section 3.5.2).

The hypothesis of a flame front like a density discontinuity, without structure, loses its validity when the perturbation wavelength grows up to a size close to the flame front width (and, on the contrary, there are samples in which the smaller the perturbation wavelength is, the faster increases).

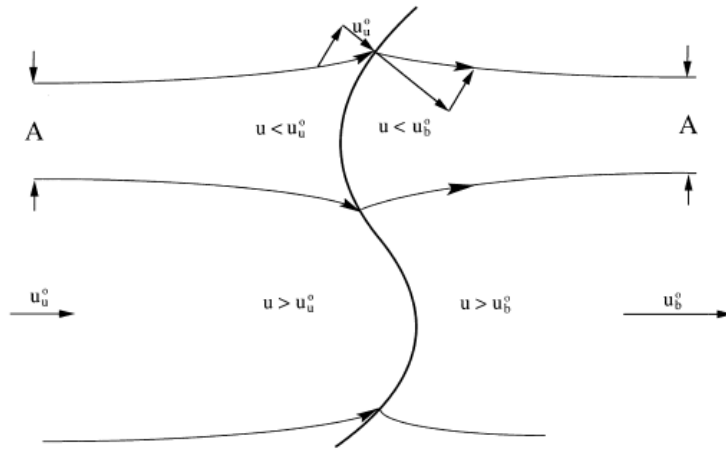


Fig. 13. Scheme of hydrodynamic instability growth mechanism (adapted from Law&Sung 2000 [54])

The hydrodynamic instability is mainly determined by the density ratio σ (which slightly increases with pressure) and the flame thickness δ_f , Gu et al. 2000 [55], Kwon et al. 2002 [58], Law&Kwon 2004 [56]. Thus, hydrodynamic instability is enhanced with pressure, as the flame thickness decreases with it.

$$\text{Density ratio (expansion coefficient)} \equiv \sigma = (\rho_u/\rho_b) \quad (32)$$

$$\text{Laminar flame thickness} \equiv \delta_f$$

On the other hand, the lower the density ρ_b of the burned gases is, compared to the unburned gases ρ_u , there appears the cause for a second instability arising from gravitational effects. This is a buoyant instability, known as the Rayleigh-Taylor instability, Kull 1991 [51], which arises when a less dense fluid is present beneath a more dense fluid, as such would be the case of e.g. an upwardly propagating flame. Gravity, as body force, has influence on the combustion process because of the natural convection in the heat and reactants transports in the flame front around, Ronney 1999 [52].

Finally, flame instability can be caused through unequal diffusivities. As flame propagation rate is largely influenced by the flame temperature, and this is in turn influenced by conduction of heat from the flame front to the unburned gases and diffusion of reactants from the unburned gases to the flame front, a perturbation of the balance between diffusivities can have important effects (fig. 14).

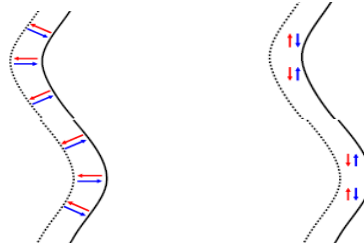


Fig. 14. Schematics of diffusion of heat (↗) and mass (↖) in thermo-diffusive instability (of much lower size than the hydrodynamic instability)

General (unburned ↔ burned)

Transversal (unburned ⊥ burned)

The relevant diffusivities are the associated with the heat or thermal diffusivity of the unburned mixture D_t (where $D_t = \lambda_{tc} / \rho_u c_p$ with λ_{tc} , c_p and ρ_u being the thermal conductivity, the specific heat and the density of unburned gas, respectively), and with the mass diffusivities of the fuel mixture components D_{m-ij} , the mass diffusivity which limits the rate of the reaction, that is $D_{m,def}$ of the limiting reactant (of fuel, in a lean flame; alternatively of oxygen in a rich flame), and the mass diffusivity $D_{m,exc}$ of the excess reactant (of oxygen for a lean flame, and of the fuel component for a rich flame). Thus, the ratios of (each two) diffusivities can be used to evaluate the stability of a flame subjected to a perturbation or flame stretch, and they serve to analyze the mechanisms involving unequal diffusivities.

- The ratio of the thermal diffusivity of the unburned mixture to the mass diffusivity of the deficient reactant, define the so-called Lewis number Le of the limiting reactant. It can be regarded as a physicochemical property associated to the transport phenomena, the non-equal diffusivities and the derived effects in the flame.

$$\text{Lewis number of the limiting reactant} = Le = (D_t / D_{m,def}) \quad (33)$$

In a mixture and in a flame there are many species, with different diffusivities each one, because of that it could be difficult to define a unique Lewis number for the processes. This property can be defined experimentally, Sun et al. 1999 [59], or also by means of complex expressions as derived by Joulin&Mitani 1981 [60]. For mixtures with equivalence ratio far enough from stoichiometry, the approximation of Le as the diffusivities ratio offers very similar values to the experimental ones, because in these cases the limiting component is more important in the control of the reaction progress.

So, according to the definition of Lewis number, Le , the value can only be properly calculated for the sufficiently off-stoichiometric mixtures where reaction rate is controlled by the limiting reactant. Therefore, the value of Le at stoichiometric equivalence ratio is the averaged value of the fuel Le_{fuel} (hydrogen, for instance, Le_{H_2}) and oxygen Le_{O_2} , and this only provides a reference value in the analysis of the Lewis number rather than a quantitative value. If the value of the mixture Lewis number (which is fairly constant with pressure in comparison with other properties) is close to 1, then the effect of a mixture temperature increase is similar to the effect of the velocity of reduction of the concentration of the limiting reactant. If the values

of mixtures Lewis number are very different from 1, then it is possible to distinguish the lengths of thermal diffusion and mass diffusion (fig. 15) instead of a unique preheating length. The Lewis number can also be expressed as the ratio of these lengths.

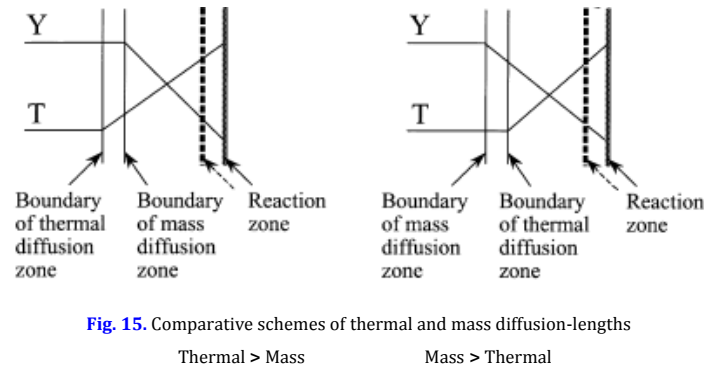


Fig. 15. Comparative schemes of thermal and mass diffusion-lengths

Thermal > Mass

Mass > Thermal

- A mixture is called thermo-diffusively stable when $D_t > D_{m,def}$, it means $Le > 1$. A wrinkled flame front will have parts that are bulging towards the unburned zone, which lose heat more rapidly than the diffusing reactants can compensate. The parts that recede in the burned gases, on the contrary, will increase in temperature more rapidly than they are being depleted of reactants. As a result, the flame speed of the crests will decrease and the flame speed of the troughs will increase, which counteracts the wrinkling and promotes a smooth flame front.

- A mixture is thermo-diffusively unstable when $D_t < D_{m,def}$, meaning $Le < 1$, because the perturbations will be amplified based on a parallel reasoning.

◦ The ratio of mass diffusivities is defined, on the other hand, as the limiting reactant mass diffusivity to the corresponding excess reactant mass diffusivity.

$$\text{Mass diffusivities ratio} = (D_{m,def} / D_{m,exc}) \quad (34)$$

When $D_{m,def} > D_{m,exc}$ the limiting reactant diffuses more rapidly than the excess reactant, and it will reach a bulge of the flame front into the unburned gases more quickly and cause a local shift in mixture ratio. When the more diffusive reactant is the limiting reactant, the local mixture ratio will shift so that it is nearer to stoichiometry and the local flame speed will increase. Thus, a perturbation is amplified and the resulting instability is termed preferential diffusion instability. This is the mechanism illustrated by the propensity of rich mixtures with heavier-than-air fuels and lean mixtures with lighter-than-air fuels to develop cellular flame fronts, Hertzberg 1989 [61].

Rich mixtures with heavier-than-air fuels are e.g. propane-air (Kwon et al. 1992 [62]), iso-octane-air (Bradley et al. 1998 [26]). Lean mixtures with lighter-than-air fuels are e.g. methane-air (Tseng et al. 1993 [63], Gu et al. 2000 [55]) and hydrogen-air (Kwon et al. 1992 [62]). The diffusivities for some gaseous fuel-air mixtures, with non-equal diffusion effects $D_{m-i} \neq D_{m-j}$ such that $D_{m,H_2} > D_{m,CH_4} > D_{m,O_2} > D_{m,C_3H_8}$ and with $Le \neq 1$, are compared in table 6.

The selective diffusion of reactants can be viewed as a stratification of the mixture, Law&Sung 2000 [54]. The mechanisms involving unequal diffusivities are sometimes called differential diffusion instabilities, or instabilities due to non-equal diffusion (which is not reflected in the concept of Lewis number). The preferential diffusion, Aung et al. 2002 [64], is influenced by recombination reactions that become increasingly important with pressure.

Table 6Compared diffusivities of **hydrogen, methane and propane** in **fuel-air mixtures** (adapted from Law&Sung 2000 [54])

Mixtures condition	$Le = (D_t/D_{m,def})$	$D_{m,exc} \neq D_{m,def}$
Lean hydrogen H ₂ /air	$Le_{H_2} < 1 \Leftrightarrow D_t < D_{m,H_2}$	$D_{m,O_2} < D_{m,H_2}$
Lean methane CH ₄ /air	$Le_{CH_4} < 1 \Leftrightarrow D_t < D_{m,CH_4}$	$D_{m,O_2} < D_{m,CH_4}$
Rich propane C ₃ H ₈ /air	$Le_{O_2} < 1 \Leftrightarrow D_t < D_{m,O_2}$	$D_{m,C_3H_8} < D_{m,O_2}$
Rich hydrogen H ₂ /air	$Le_{O_2} > 1 \Leftrightarrow D_t > D_{m,O_2}$	$D_{m,H_2} > D_{m,O_2}$
Rich methane CH ₄ /air	$Le_{O_2} > 1 \Leftrightarrow D_t > D_{m,CH_4}$	$D_{m,CH_4} > D_{m,O_2}$
Lean propane C ₃ H ₈ /air	$Le_{C_3H_8} > 1 \Leftrightarrow D_t > D_{m,CH_4}$	$D_{m,O_2} > D_{m,C_3H_8}$

Because of the very high diffusivity of hydrogen, the highest of all existing fuels, a lean to stoichiometric hydrogen-air mixture will be diffusively unstable, from both points of view of considering the Lewis number ($D_t \ll D_{m,H_2}$) and the preferential diffusion ($D_{m,O_2} \ll D_{m,H_2}$) (table 7). Lean hydrogen-air mixtures are diffusively unstable due to the higher mass diffusivity of the hydrogen molecule compared to the oxygen molecule. It is worth noting that the molecular diffusion of hydrogen and oxygen in the air are of the order of 0.6 and 0.2 cm^2/s , respectively, while the molecular heat diffusivity of air is of the order of 0.2 cm^2/s . Hence the hydrogen based Lewis number value is substantially smaller than unity. Consequently, there are instabilities due to molecular transport, which are not negligible for very lean hydrogen-air mixture.

Table 7

Flame conditions regarding to instabilities phenomena (some combinations of cases)

Buoyancy (gravity)	Hydrodynamic	Thermo - diffusive		Flame front
		$Le = (D_t/D_{m,def})$	$(D_{m,exc}/D_{m,def})$	
Unburned beneath	Never stable	> 1	> 1	Stability
Burned beneath	Always unstable	< 1	< 1	Instability

Thermo-diffusively unstable mixtures (e.g. lean hydrogen-air, for fuel to air equivalence ratios around $\Phi \sim 0.6$, or rich propane-air, for $\Phi \sim 1.4$, Law 2006 [57], at pressures of the order of $P \sim 0.5$ MPa) present in general cellular flame fronts from the combustion beginning. The different behaviors of thermo-diffusively stable mixtures (e.g. rich hydrogen-air or lean propane-air) require particular explanations based on the balance of both thermo-diffusive and hydrodynamic effects.

Therefore, the mixtures with equivalence ratio faraway from stoichiometric values are more thermo-diffusively stable. On the other hand, the mixtures are more hydro-dynamically unstable when the pressure is higher, because the flame front thickness decreases with the pressure. Both factors jointly cause smooth and stable flame fronts in mixtures combustion at low pressure with equivalence ratios quite different of the stoichiometric value (e.g. rich hydrogen-air for $\Phi \sim 4$, or lean propane-air for $\Phi \sim 0.7$, Law 2006 [57], at pressures of the same order of $P \sim 0.5$ MPa); on the contrary, these factors cause cellular unstable flame fronts in combustion at high pressure with equivalence ratios less away from the stoichiometric value (e.g. rich hydrogen-air for $\Phi \sim 2.5$, or lean propane-air for $\Phi \sim 0.95$, Law 2006 [57], at pressures of the order of $P \sim 2$ MPa).

3.5.2. Flame stretch

The properties of premixed flames, including the laminar burning velocity, can be affected by the flame propagation and flow geometry. Curvatures, wrinkling and non-uniform flux propagation happen, and real flames are not ideally one-dimensional, as already seen. All these phenomena, mathematically and phenomenologically related with the laminar burning velocity, are known as stretch effects in the literature, Strehlow&Savage 1978 [65]. The influence of flame flux and geometry on the burning velocity is defined by the stretch models.

Actually, the reasons that lead to burning velocity modifications are the simultaneous action of stretch and the phenomena of mass and thermal diffusion, as well as a non-unity Lewis number (mixture with different mass and thermal diffusivities) or the effect of preferential diffusion (different mass diffusivities of the limiting and excess reactants in the mixture). The relation between laminar flame deformation and its burning velocity has large interest for the study of turbulent flame speed by means of models of the turbulent flame as a combination of laminar flames submitted to stretch, De-Goey&Thije-Boonkkamp 1999 [66], Williams 2000 [67].

If a laminar flame can be defined as a structure with a certain thickness in which reactants diffusion and heat conduction happen in a normal direction to the flame front, when this one-dimensional structure is submitted to a certain stretch rate, a deformation is caused, with a modification of the flame behavior. The changes are especially strong for mixtures with very different diffusivities, as it happens with hydrogen and air (oxygen) because the flame temperature is directly affected. On the contrary, for mixtures with similar diffusivities the stretch influence is much lesser.

Flame sheets are subject to transverse velocity components and curvature, which stretch the flame, and this can change the burning velocity, Bradley et al. 1998 [26], because the flame structure is changed by the additional convective term and the effect of curvature, Bychkov&Liberman 2000 [53], on the fluxes of energy and species. The flame stretch rate κ is a scalar parameter defined, Williams 1985 [41], as the normalized rate of change of an infinitesimal area element of the flame, and is mathematically calculated as the lagrangian time derivative of the logarithm of the area at any point on the flame front.

$$\text{Flame stretch rate} \equiv \kappa = \left\{ \frac{\partial \langle \ln(A) \rangle}{\partial t} \right\} = (1/A) \left\{ \frac{\partial A}{\partial t} \right\} \quad (35)$$

When the thermo-diffusive phenomena have not enough stabilization effects and cannot reduce the hydrodynamic instability on the perturbations of small wavelengths, then instabilities grow and it is not possible to achieve stable flames. The mechanisms described in section 3.5.1 are simultaneously present. Disturbances of a flame front causing deviation from a steady planar flame can be summarized by considering the flame stretch rate κ . The combined effect of the instability mechanisms appears when the flame is stretched and is dependent on the magnitude of the stretch rate (table 8). For instance, thermo-diffusively stable spherically expanding flames start out smoothly, as the stretch rate is initially high enough for thermo-diffusion to stabilize the flame against hydrodynamic instability.

Table 8
Flame trends with stretch interactions (some combinations of cases)

$Le = (D_T/D_{m,def})$	$(D_{m,exc}/D_{m,def})$	Stretch rate κ	Flame front
>1	>1	>0	Stability
<1	<1	<0	
>1	>1	<0	Instability
<1	<1	>0	

For an outwardly propagating spherical flame, the stretch rate ($\kappa > 0$) is related to the flame speed s_n according with the flame front spherical geometry, with the flame radius defined at the cold flame front (r_u).

Outwardly propagating spherical overall flame stretch rate $\equiv \kappa$

$$= (2/r_u) \{ \partial r_u / \partial t \} = (2/r_u) s_n \quad (36)$$

Bradley et al. 1996,1998 [25,26] quantified the contributions of rate of strain (transverse velocity components) and curvature to the stretch rate, with the flame surface identified by the cold front of radius r_u , the local fluid velocity $u_{(r,\theta,\phi)}$ defined by its spherical coordinates (u_r, u_θ, u_ϕ), the unit vector normal $n_{(r,\theta,\phi)}$ to the surface, directed from the burned to the unburned side, defined by its spherical coordinates (n_r, n_θ, n_ϕ), and the stretched burning velocity u_{ne} normal to the flame surface. Considering an out-warding spherically symmetrical propagating flame, the angular components are null and the radial ones are already defined (u_r is the gas expansion velocity v_g).

$$u_r = v_g \quad u_\theta = u_\phi = 0 \quad n_r = +1 \quad n_\theta = n_\phi = 0$$

Thus, the total flame stretch rate κ function of the stretched flame speed s_n can be assumed to have two components, the stretched normal burning velocity based on the propagation of the flame front u_n and the gas velocity v_g due to the flame expansion, at radius r_u , namely the flame stretch due to curvature at the cold front κ_c and the flame stretch due to the flow-field aerodynamic strain κ_s (transverse velocity components).

$$s_n = u_{ne} + v_g \quad \Rightarrow \quad \kappa = (2/r_u) \{ \partial r_u / \partial t \} = (2/r_u) s_n = \kappa_c + \kappa_s \quad (37)$$

Flame stretch rate due to curvature at the cold front $\equiv \kappa_c$

$$= u_{ne} (1/r^2) \{ \partial \langle r^2 [n_r] \rangle / \partial r \} = n_r (2/r_u) u_{ne} \quad (38)$$

Flame stretch rate due to aerodynamic strain $\equiv \kappa_s$

$$= (1/r^2) \{ \partial \langle r^2 [u_r] \rangle / \partial r \} - [n_r]^2 \{ \partial [u_r] / \partial r \} = (2/r_u) v_g \quad (39)$$

The flame stretch terms are different for out-warding or in-warding spherical flames propagation (with positive or negative flame speed respectively).

For an implosion, with “in-warding flame propagation”, of difficult practical origination but computationally studied in literature, the values and signs will be the following:

$$s_n = (v_g - u_{ne}) < 0 \quad v_g = 0 \quad (40)$$

$$\kappa_c = -(2u_{ne}/r_u) = \kappa < 0 \quad \kappa_s = (2v_g/r_u) = 0 \quad (41)$$

On the other hand, the flame speed is also the velocity of the burned gases immediately behind a stationary flame and, for more or less theoretical stationary modes (with null flame speeds), the values and signs would be thus:

For an “out-warding stationary flame” (not possible to obtain stable computed solutions for such a flame)

$$s_n = 0 = (v_g + u_{ne}) \quad v_g = -u_{ne} < 0 \quad (42)$$

$$\kappa_c = (2u_{ne}/r_u) = -\kappa_s > 0 \quad \kappa = 0 \quad \kappa_s = (2v_g/r_u) < 0 \quad (43)$$

For an “in-warding stationary flame” (practically attainable)

$$s_n = 0 = (v_g - u_{ne}) \quad v_g = u_{ne} > 0 \quad (44)$$

$$\kappa_c = -(2u_{ne}/r_u) = -\kappa_s < 0 \quad \kappa = 0 \quad \kappa_s = (2v_g/r_u) > 0 \quad (45)$$

For our purpose, in summary for explosion cases, “out-warding flame propagation” ($\kappa > 0$), the most common spherical flame ignited at a central ignition point, the stretch rates have been well defined by these expressions:

$$s_n = (v_g + u_{ne}) > 0 \quad v_g > 0 \quad (46)$$

Out-warding flame propagation total-overall stretch rate

$$\kappa = (2s_n/r_u) = \kappa_s + \kappa_c > 0 \quad (47)$$

Rate of stretch due to curvature effect

$$\kappa_c = (2u_{ne}/r_u) \quad (48)$$

Rate of stretch due to strain effect

$$\kappa_s = (2v_g/r_u) \quad (49)$$

3.6. Markstein lengths and correction for stretch effects

The deficit in burning velocity due to the stretch effect is expressed in the literature by considering the Markstein length. This physicochemical parameter embodies the effect of a change in the flame structure when the flame is stretched.

3.6.1. Markstein lengths and un-stretched flame speeds and burning velocities

When measuring burning velocities it is very important to estimate the stretch rate, as well as the Markstein lengths, so that the stretch-free burning velocity can be calculated.

◦ As the flame propagates, the flame speed S that would have in the absence of instabilities (fig. 16) is modified by several effects. The changes arise from the combined effects of a decreasing proportion of unreacted mixture within the flame thickness and the effects of the flame stretch. Then:

Normal (stretched) flame speed in the absence of instability $\equiv S$

$$= \{ \partial r / \partial t \} \quad (50)$$

Outwardly propagating spherical flame stretch rate in absence of instability = κ

$$= (2/r) \{ \partial r / \partial t \} = (2/r) S \quad (51)$$

The values of S can be obtained in practice, at moderated pressures, Al-Shahrany et al. 2005,2006 [68,69], Bradley et al. 2007 [45], from the experimentally measured values of s_n by accounting for the instability as described in sections 3.9 and 3.10.

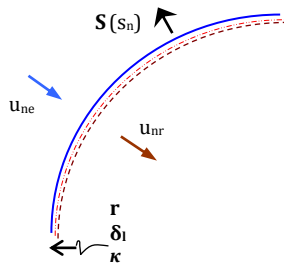


Fig. 16. Instabilities correction (to obtain S from s_n)

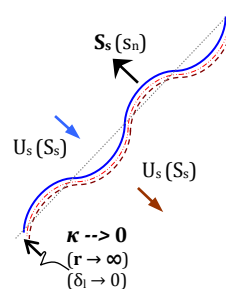


Fig. 17. Stretch correction (to obtain S_s from s_n)

◦ The un-stretched values S_s of flame speed (fig. 17) are obtained in practice in different ways described in the literature, Bradley et al. 1996,1998 [25,26], from the stretched flame speeds by accounting for the stretch effect. This can be done for stable flames by plotting the measured flame speeds against the flame stretch rate and making a linear extrapolation of the speed value to $\kappa \rightarrow 0$ ($r \rightarrow \infty$, $\kappa = 0$) as the interception value at the origin of the plot, to obtain the value at zero stretch rate. These values are independent of the isotherm chosen for the measurement of the speed.

Un-stretched flame speed value extrapolated for $\kappa \rightarrow 0$ in the absence of instability $\equiv S_s$

For smaller values of stretch the influence of the unreacted mixture is negligible and it is applicable the first order linear relation for the flame speed deficit (un-stretched speed minus stretched speed, $S_s - S$) as a function of the burned gas Markstein length L_b . For flames submitted to high stretch rates, linear expressions are not valid because the flame response cannot be considered linear, Sun&Law 2000 [70].

Flame speed deficit in the absence of instability = $S_s - S$

$$= L_b \kappa \quad (52)$$

Burned gas Markstein length associated to the stretched flame speed S (in the absence of instability): L_b

Un-stretched flame speed extrapolated for $\kappa \rightarrow 0$ in the absence of instability $\equiv S_s$

$$= S + L_b \kappa \quad (53)$$

Thus, the slope of the linear correlation line of the difference of S_s and S as a function of the total stretch rate κ gives the Markstein length L_b of the burned gas flame speed. A positive (or respectively negative) value means that an increase in the overall stretch rate causes a reduction (or an increment respectively) in the flame speed (table 9).

In weakly stretched flames of hydrogen-air mixtures, computational studies based on detailed chemical kinetics, Sun et al. 1999 [59], Kim et al. 1994 [71], provided values of burned gas Markstein length L_b based on flame speed without instabilities (S), at 300 K temperature, that were negative at all pressures for very lean mixtures, while the values of L_b became positive respectively for fuel to air equivalence ratios Φ of 0.7, 0.9 and 1.3, at pressures of 0.06, 0.1 and 0.5 MPa.

Table 9
Flame front speed corrections of instability and stretch effects

Stretched normal flame speed affected by instabilities	Stretched flame speed with correction of instabilities effect, by means of stability theory (sections 3.9-3.10)	Correction on the flame speed of the effect of stretch-rate
s_n	$S(s_n)$	$S_s(s_n) - S(s_n) = L_b \kappa$

A corresponding un-stretched laminar burning velocity U_s is obtained from the un-stretched flame speed S_s for constant pressure propagation in combustion, Bradley et al. 1996,1998 [25,26], directly by scaling with the densities ratio.

Un-stretched laminar burning velocity deduced in the absence of instabilities $\equiv U_s$

$$= [S_s / (\rho_u/\rho_b)] \quad (54)$$

This un-stretched laminar burning velocity, obtained from the flame un-stretched speed (obtained in the absence of instabilities) under the consideration of zero stretch rate, is equivalent to the flame speed with an infinite radius for which the curvature can be neglected.

For finite radii, an analogous but different relation between the normal flame speed s_n and the normal laminar burning velocity of unburned reactants consumption u_{ne} can be obtained from a mass conservation equation for the propagating spherical laminar flame, accounting for the density ratio.

$$u_{ne} \simeq [\eta s_n / (\rho_u/\rho_b)] \quad (55)$$

Bradley et al. 1996 [25] gave an expression similar to this with a flame speed factor η . This is a generalized function depending upon the flame radius r_u and the density ratio σ , with a form based on experiments with methane at atmospheric conditions, sometimes extrapolated to generalized use, confirmed for paraffin fuels in some works.

$$\eta = 1 + 1.2\psi - 0.15\psi^2 \quad \psi = (\delta_l/r_u) (\rho_u/\rho_b)^{2.2} \quad (56)$$

This flame speed factor η accounts for the effect of the non-negligible flame thickness δ_l . It is not known to have been either surely validated for fuels as hydrogen, nor for alternative pressures and temperatures, but it has been used in several works, as by Miao et al. 2008,2009 [72,73,74] in studies for non-diluted or diluted hydrogen-enriched natural gas at normal, reduced and

elevated pressures. According to Gu et al. 2000 [55], its use is unlikely to produce significant errors in theory, because it predicts adequate trends in flame thickness for variations in pressure and temperature, but these expressions could not be exact if they were used in a very general application assuming a zero flame thickness.

As indicated, the slope of the straight line fit to data plots of S - κ gives the best estimation of the burned gas Markstein length, Bradley et al. 2007 [45]. The s_n - κ plots are experimentally reported at limited pressures, removing data affected by ignition energy and electrodes. In early stable propagations, the instability-corrected flame speed S can be given by the measured flame speed s_n , but the stretch rate decreases as the flame radius increases with the time, and the plotted values of s_n show a bent trend that becomes separated of the straight line. When there are enough experimental values of flame speed s_n and they are quite close to the linear fit line s_n - κ , these values can be considered as good estimations for the calculation by extrapolation of the un-stretched flame speed s_s , and the associated burned gas Markstein length l_b , and the un-stretched laminar burning velocity u_s , given by:

$$\begin{aligned} \text{Flame speed deficit with no absence of instabilities, but with limited instability} &= s_s - s_n \\ &= l_b \kappa \end{aligned} \quad (57)$$

Un-stretched flame speed (extrapolated for $\kappa \rightarrow 0$) when instability is moderate $\equiv s_s$

Burned gas Markstein length associated to the stretched value s_n of the flame speed: l_b

Un-stretched laminar burning velocity deduced with moderate instability $\equiv u_s$

$$= [s_s / (\rho_u / \rho_b)] \quad (58)$$

By using this methodology to obtain stretch-free flame speeds, Verhelst 2005 [13] was able to utilize data points in a range between the (initial) spark-affected region and the (final) cellular regions of speed plots. He observed that after the effects of the spark-boost decayed, a regime was found where the flame speed varied linearly with the flame stretch rate. This was used in the same way to extrapolate towards zero stretch and obtain a stretch-free flame speed s_s , and the laminar burning velocity u_s after dividing s_s by the density ratio of unburned to burned gases $\sigma = (\rho_u / \rho_b)$. He expressed that this procedure does not produce the ideal laminar burning velocity that would be found by a steady, planar ideal computation with perfect thermodynamics, transport and chemical kinetics, and that was considered applicable only in the linear range at low stretch, but the procedure was considered convenient since it leads to a very good approximation of laminar burning velocity in conditions close to atmospheric conditions.

When the values of s_n and S are required for higher pressures, then the flames are much more unstable and the stable regimes in the speed plots versus stretch rate are much less coincident and shorter, with fewer experimental points because of the large difficulties to obtain accuracy data. There is consequently more confidence, Bradley et al. 2007 [45], on the preferred linear extrapolation on the more adequate values of S against κ (instead of the values of s_n against κ) to obtain the suitable stretch free value S_s of flame speed and hence the more appropriate un-stretched laminar burning velocity U_s values (than their approximations by s_s and u_s respectively).

As previously said, the values of S (free of instabilities) for unstable, even cellular flames, are deduced in the literature (Al-Shahrany et al. 2005,2006 [68,69], Bradley et al. 2007 [45]) from s_n by accounting for the instability as described in sections 3.9 and 3.10.

The differences between the un-stretched laminar burning velocity u_l and the normal stretched velocities u_{ne} and u_{nr} , already defined respectively, only for small to moderate rates of total stretch, can be expressed as a function of other analogous corresponding Markstein lengths.

$$l_e \kappa = u_l - u_{ne} \quad (59)$$

Markstein length associated to stretched value u_{ne} of the normal entrainment burning velocity:

l_e

$$l_r \kappa = u_l - u_{nr} \quad (60)$$

Markstein length associated to stretched value u_{nr} of the normal production burning velocity:

l_r

Depending on the Markstein length sign and whether the flame is positively or negatively stretched ($\kappa > 0$ if out-warding propagation) the burning velocities can be increased or decreased compared to the stretch-free burning velocity u_l . A positive Markstein length indicates a diffusively stable flame, as flame stretch decreases the burning velocity. Any disturbances or wrinkles of the flame front will thus tend to be smoothed out. A negative Markstein length indicates a diffusively unstable flame. Any perturbation of the flame front will then to be enhanced and such flames quickly develop into cellular structures. At theoretical zero stretch rate both burning velocities (u_{ne} , u_{nr}) are equal to the un-stretched burning velocity (u_l) of a planar flame with theoretical infinitely large radius (fig. 18).

$$\kappa = 0 \quad (r \rightarrow \infty) \quad \Rightarrow \quad u_{nr} \leftrightarrow u_{ne} \leftrightarrow u_l$$

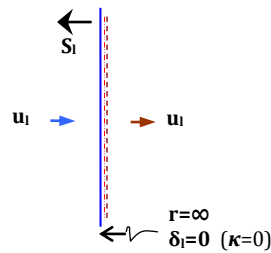


Fig. 18. Sketch of a theoretical laminar flame front with an infinite radius

The linearities l_e or l_r between the burning velocities deficits and the total stretch rate are not necessarily compatible with the linearities associated to the separated components of the stretch.

Markstein lengths associated to u_{ne} and u_{nr} stretched by strain and curvature, respectively:

l_{se} , l_{ce} and l_{sr} , l_{cr}

Thus, the reductions in burning velocities due to stretch are usually expressed and presented in the literature by the Markstein lengths associated with curvature and strain, respectively.

$$u_l - u_{ne} = l_{se} \kappa_s + l_{ce} \kappa_c \quad (61)$$

$$u_l - u_{nr} = l_{sr} \kappa_s + l_{cr} \kappa_c \quad (62)$$

It is common the use of the stretched burning velocity u_{nr} that expresses solely the rate at which burned gas is formed and that exclude the changing rate of entrainment of unburned gas into the flame thickness, Bradley et al. 1996 [25]. Some transformations are possible with the already developed expressions.

$$u_{nr} = u_l - (l_{sr} \kappa_s + l_{cr} \kappa_c) \quad (63)$$

$$u_{ne} = u_l - (l_{se} \kappa_s + l_{ce} \kappa_c) \quad (64)$$

$$s_n = s_s - l_b \kappa = s_s - l_b (\kappa_s + \kappa_c) \quad (65)$$

$$s_s = (\rho_u / \rho_b) u_l \quad (66)$$

And so,

$$\begin{aligned} u_{nr} &= \{ (s_n - u_{ne}) / [(\rho_u - \rho_b) / \rho_b] \} = \{ [(\rho_u / \rho_b) u_l - l_b \kappa_s - l_b \kappa_c - u_l + l_{se} \kappa_s + l_{ce} \kappa_c] / [(\rho_u - \rho_b) / \rho_b] \} \\ &= u_l - [\rho_b / (\rho_u - \rho_b)] [(l_b - l_{se}) \kappa_s + (l_b - l_{ce}) \kappa_c] \end{aligned} \quad (67)$$

Thus, the relations of these Markstein lengths, with moderate presence of instabilities, can be deduced.

$$l_{sr} = (l_b - l_{se}) [(\rho_u / \rho_b) - 1]^{-1} \quad (68)$$

$$l_{cr} = (l_b - l_{ce}) [(\rho_u / \rho_b) - 1]^{-1} \quad (69)$$

And analogous relations for Markstein lengths in the absence of instabilities can be expressed.

$$L_{sr} = (L_b - L_{se}) [(\rho_u / \rho_b) - 1]^{-1} \quad (70)$$

$$L_{cr} = (L_b - L_{ce}) [(\rho_u / \rho_b) - 1]^{-1} \quad (71)$$

Markstein lengths associated to u_{ne} stretched by strain and curvature, respectively, in the absence of instabilities: L_{se} and L_{ce}

Markstein lengths associated to u_{nr} stretched by strain and curvature, respectively, in the absence of instabilities: L_{sr} and L_{cr}

Both types of Markstein lengths, based on the burning speed and velocities with moderate instabilities, $l_b, l_s, l_c, l_{se}, l_{ce}, l_{sr}, l_{cr}$, or the corresponding Markstein lengths based on the burning speed and velocities in the absence of instabilities, $L_b, L_s, L_c, L_{se}, L_{ce}, L_{sr}, L_{cr}$, with parallel expressions, will have values that depend on the equivalence ratio, Bechtold&Matalon 2001 [75], because the effect of stretch rate changes with the equivalence ratio and is different for lean and rich mixtures.

3.6.2. Markstein numbers and Karlovitz stretch factors

The Markstein lengths of the burning speed, and respectively of the burning velocities, are sensitive to the stretch rates dimensional parameters. They embody the effects of changes in flame structure when the flame is stretched. Their values are of the order of flame front thickness and depend on other variables such as activation energy, expansion coefficient σ (density ratio) and Lewis number, Tien&Matalon 1991 [76]. The Markstein lengths can be expressed in dimensionless forms, as the Markstein numbers, by normalizing them by the flame thickness (δ_l).

$$Ma_b = (L_b/\delta_l) \quad (72)$$

$$Ma_{se} = (L_{se}/\delta_l) \quad (73)$$

$$Ma_{ce} = (L_{ce}/\delta_l) \quad (74)$$

$$Ma_{sr} = (L_{sr}/\delta_l) \quad (75)$$

$$Ma_{cr} = (L_{cr}/\delta_l) \quad (76)$$

Similarly, the stretch rates can be normalized by multiplying them by the chemical lifetime (δ_l/u_l) to give the dimensionless Karlovitz stretch factors.

$$\kappa (\delta_l/u_l) = Ka \quad (77)$$

$$\kappa_s (\delta_l/u_l) = Ka_s \quad (78)$$

$$\kappa_c (\delta_l/u_l) = Ka_c \quad (79)$$

The products of corresponding Karlovitz and Markstein numbers express the differences between flame speeds or burning velocities due to the corresponding stretch rates; the influences of the thermal and mass diffusivities, coupled in the Markstein number, and the activation energy, expressed respectively by the Lewis and Zeldovich numbers, and the densities gradient through the flame, Bradley et al. 1996 [25]. Thus the effect upon flame speed S of the contribution to the total flame stretch rate can be given by this expression.

$$[(S_l - S)/S_l] = Ma_b Ka \quad (80)$$

And the effect upon burning velocities u_{ne} and u_{nr} of the contributions to the flame stretch rate from the aerodynamic strain and the flame curvature can be given by these corresponding expressions.

$$[(u_l - u_{ne})/u_l] = Ma_{se} Ka_s + Ma_{ce} Ka_c \quad (81)$$

$$[(u_l - u_{nr})/u_l] = Ma_{sr} Ka_s + Ma_{cr} Ka_c \quad (82)$$

The latter expression is essentially a quasi-steady statement, which is applied to non-steady explosion conditions Bechtold&Matalon 1987 [49], Bradley et al. 2000 [77]. The first term of the right of the latter expression is dominant usually, because κ_c can be neglected to a first approximation since v_g is usually significantly much larger than u_{ne} ($2v_g/r_u = \kappa_s \gg \kappa_c = 2u_{ne}/r_u$) in combustion explosions (this is not so in implosions). Hence, there is more sensitivity in

determining Ma_{sr} than Ma_{cr} and the effect of stretch on u_{nr} is approximately given only by the strain effect.

$$(u_l - u_{nr}) \sim L_{sr} \kappa_s \quad (83)$$

$$[(u_l - u_{nr})/u_l] \sim Ma_{sr} Ka_s \quad (84)$$

The higher the Markstein number, the bigger is the initial stabilization in the early stages of flame propagation when smooth flame surfaces are maintained. However, as the flame radius increases, the flame stretch rate decreases and instabilities can develop from any perturbations, which might arise at ignition and grow in amplitude. The Markstein number decreases with pressure, Bradley et al. 1996,1998 [25,26], Gu et al. 2000 [55], Aung et al. 2002 [64], and thus it is a better parameter to characterize stability, Bradley et al. 2003 [78], than the simplest concept of the previously mentioned Lewis number. Markstein numbers take even negatives values for mixtures with very unstable flames. Experimental data, Aung et al. 1998 [79], show hydrogen-air flames at atmospheric conditions to have positive Markstein numbers if they are close to stoichiometry, but all lean mixture equivalence ratios have negative Markstein numbers as soon as the pressure exceeds about 0.4 MPa .

3.7. Flame thickness and Peclet number

Laser sheet imaging of flames, such as laser-induced fluorescence, may offer a variety of flame surfaces being imaged depending on the recorded property, as chemical radical emissions depend on the target molecule (e.g. OH, etc.) and its location within the flame. Other properties may be used by different scattering imaging techniques, where the recorded flame edge may vary, Gillespie et al. 2000 [22].

It is difficult to quantify the distance between the completely unburned gas, at the unburned temperature, and the completely burned gas (of the order of *tenths of millimeters*) because the change from the former to the latter occurs gradually. Therefore the laminar flame thickness is defined as a characteristic length for a given fuel-air mixture at given initial conditions. The length of flame thickness is a consequence of the density and pressure gradient across the flame and decreases with pressure, which increase the gradients. The range of unstable wavelengths is bounded by a multiple of the flame thickness, implying a larger range for increasing pressure as the flame thickness decreases, Kobayashi&Kawazoe 2000 [80].

Different definitions of laminar flame thickness e.g. using either hydrodynamic, thermal or diffusion properties can be applied based on the respective ratios, to the un-stretched laminar burning velocity (u_l), of some properties of the unburned mixture (the kinematic viscosity ν_u (in Verhelst 2005 [13], Bradley et al. 2007 [45]); the thermal diffusivity defined as $D_t=(\lambda_{tc}/\rho_u c_p)$, where λ_{tc} and c_p are the thermal conductivity and the specific heat of unburned gas respectively (in Hu et al. 2009 [1], Law 1988 [50], Bechtold&Matalon 1987 [49]); or the binary mass diffusion coefficients D_{m-d-ij} of reactive components). These expressions, depending on the laminar burning velocity and fresh gas properties, as the diffusive also so-called Zeldovich expression for $\delta_{l,td}$, describe the thickness corresponding to flame Reynolds number of unit value $Re_{flame}=(\delta_l/D_t)u \approx 1$.

$$\text{Laminar flame thickness based on a hydrodynamic length} = \delta_{l,hd} = (\nu_u/u_l) \quad (85)$$

$$\text{Laminar flame thickness based on a thermal diffusion length} = \delta_{l,td} = (D_t/u_l) = \{(\lambda_{tc}/\rho c_p)_u / u_l\} \quad (86)$$

$$\text{Laminar flame thickness based on a mass diffusion length} = \delta_{l,md-ij} = (D_{m-ij}/u_l) \quad (87)$$

Some expressions of $\delta_{l,hd}$ have been proposed, for instance by Bradley et al. 2000 [77], underestimating the actual overall flame thickness. The laser induced fluorescence images in the work of Bradley et al. 1996 [25], corresponding to the thickness of super-equilibrium OH concentrations in rich iso-octane flames, suggest a factor of even about thirty times $\delta_{l,hd}$. Other authors, Chung et al. 1995 [81], Jamel 1984 [82], had referred thicknesses between six and fifty times bigger than the given by the expression of $\delta_{l,hd}$.

Other thermal-diffusive thickness expressions have been proposed in the literature including corrections by the burned gas properties, e.g. Blint 1986 [83], for constant Prandtl number.

$$\delta_{l,td}^B = 2 (T_b/T_u)^{0.7} D_t (1/u_l) \quad (88)$$

Flame thicknesses have also been predicted by chemical kinetic mechanisms in the literature, by comparing simulated results with experimental measurements. Some Zeldovich expressions seem more adapted to define the thermal flame thickness when modified by correction coefficients, as in Bougrine et al. 2011 [12].

$$\delta_{l,td}^{Z_{Bougr}} = C_{Bougr}^Z D_t (1/u_l) \quad C_{Bougr}^Z \sim 1.2 \quad (89)$$

Other modified expressions were derived by correlations as, for instance, the developed by Knop et al. 2008 [6], with a Blint form function of temperature in a range [600, 1000] K, of pressure in a respective range [30, 70] bar, and of fuel-air equivalence ratio for ranges in [0.8, 2], taking variable values of the equivalence ratio (Φ) but making exception of $\Phi \approx 1.2 \sim \text{constant}$ in the sub-range [1.2, 2]. The corresponding values of the resultant flame thickness coefficient increase with Φ and the temperature (T_u), but decrease with the pressure (P).

$$\delta_{l,td}^{B_{Knop}} = 2 C_{Knop}^B D_t (1/u_l) \quad C_{Knop}^B \text{ et al} \sim [2, 7] \quad (90)$$

$$C_{Knop}^B = 3.37 [-0.7 + 2.85(\Phi) - 1.15(\Phi)^2] \cdot [0.43 + 0.000075(T_u) + 0.00000145(T_u)^2] \cdot [1.46 - 0.0182(P/1.013) + 0.000106(P/1.013)^2]$$

The effect of flame thickness is important because different experimental techniques record different locations within the flame; for instance, main heat release zones with regions of high chemical radical species concentration in natural light photography, meanwhile zones of different densities function of temperature gradient in Schlieren technique. For instance, the flame front radius r_u was related to the observed Schlieren radius r_{sch} , Bradley et al. 1996 [25], through the densities ratio σ and the laminar flame thickness based on a hydrodynamic length.

$$r_u = r_{sch} + 1.95 \delta_{l,hd} (\rho_u/\rho_b)^{0.5} \quad (91)$$

This assumes the Schlieren-edge associated with a given temperature isotherm. Other works have considered the more suitable isotherm as a function of the flame radius varying between higher temperatures.

Each flame radius r , expressed in the appropriate dimensionless terms, defines the values of the Peclet number Pe , when it is normalized by the flame thickness δ_l .

$$\text{Flame radius} = r \quad \Rightarrow$$

$$\text{Peclet number} = Pe = (r/\delta_l) \quad (92)$$

When some hydrogen-air mixtures are considered, Verhelst 2005 [13], their laminar flame thickness δ_l could deliver stable burning velocities from conditions where only cellular burning velocities can be measured, provided these quantities are known or can be estimated with reasonable accuracy, which was demonstrated by Al-Shahrany et al. 2005 [68] for iso-octane mixtures and applied by Bradley et al. 2007 [45] for hydrogen-air mixtures.

This latter work observed that the ratio of flame thicknesses $\delta_{l,hd}/\delta_{l,td}$, involving respectively the kinematic viscosity and the thermal diffusivity, is the Prandtl number Pr , estimated to be less than 1 (usually about 0.7 for gases). As a consequence, the values of Peclet number based on $\delta_{l,hd}$ are somewhat higher than the based on $\delta_{l,td}$.

$$(\delta_{l,hd}/\delta_{l,td}) = (v_u/D_t) = Pr \quad (93)$$

However, such simplistic expressions for δ_l can be considered not more than a very approximate estimation of the significant flame thickness, Bradley et al. 2007 [45]. The direct measurement of the thickness is recommended by Law et al. 2005 [84].

3.8. Instabilities development and cellular structures

A review of several mechanisms that can trigger instability of a laminar flame was previously introduced in section 3.5. There were two main instabilities of flame, the diffusive-thermal instability and the hydrodynamic instability. Cellular flames tend to develop in the mixtures in which the limiting reactant is also the constituent with the largest diffusivity. This kind of flame cellularity was experimentally observed in both plane flames, from the study of Markstein 1949 [85], and spherically expanding flames, from Manton et al. 1953 [86]. The formation of cells in the cases due to diffusive-thermal instability with preferential diffusion results from the competing effects between heat conduction from the flame and reactant diffusion toward the flame, Parlange 1968 [87], Bechtold&Matalon 1987 [49].

3.8.1. Flame instabilities and cellularity

In some conditions, due to instabilities, the flame front after the ignition is not smooth, but it is more or less wrinkled. The wrinkling extent can vary from simple superficial wrinkles to a fully cellular flame, with cell structure in the flame front surface. Commonly it is studied in spherical flames, but this phenomenon has been observed also in other geometries, as the above-mentioned planar flame front. In practice, the cellular flame front is very easily produced in thermo-diffusive unstable mixtures. Palm-Leis&Strehlow 1969 [88] obtained almost smooth flame fronts for lean mixtures, with tests of propane-air mixtures at atmospheric pressure; but they observed spontaneous cells in rich mixtures flames. Groff 1982 [89] tested at high pressure, also with lean propane-air mixtures (thermo-diffusively stable) but observed cellular flames; thus, in this case, the cellular flame mechanism could not be thermo-diffusive and it had to be produced by hydrodynamic instabilities.

Konnov&Dyakov 2005 [90] obtained experimental cellular flame fronts for CH₄-O₂-CO₂ and C₂H₆-O₂-CO₂ mixtures with a controlled heat flux burner. Measured burning velocity values were bigger than the laminar ones obtained from a theoretical model. Other conclusion was that the cellular flame front was smoothed when small heat losses were introduced in the flame. Aldredge&Zuo 2001 [91] presented a theoretical study of a spherical flame front which resulted in flame acceleration once reached an unstable point in the form $r-r^* \sim (t-t^*)^{1.5}$, representing the radius increment from the value (denoted by the asterisk) at which flame accelerates noticeably.

This acceleration was stronger the higher the expansion coefficient σ (density ratio) and the smaller the flame thickness δ_f were. Bradley et al. 2001 [92] experimentally observed similar acceleration values in large flame fronts (up to *thirty centimeters* radii). Kwon et al. 2002 [58] also registered accelerations a bit lower, $r-r^* \sim (t-t^*)^{1.3}$, for smaller spherical flames (up to *five centimeters* radius).

Also Kwon et al. 2002 [58], in an experimental study on spherical flame fronts in a constant volume bomb, identified the influence on the flame stability of the flame front thickness, activation energy, expansion coefficient (density ratio), non-equal diffusional effects and stretch rate. The flame front tendency to cellularity increases according to combined considerations. Small values of flame thickness are favorable to the hydrodynamic cells increase and development, Law et al. 2005 [84]. In addition, when thickness is smaller also the observed cellular flame front characteristic size is smaller. Similarly small values of activation energy are favorable to cells development in stable flame fronts. Large values of the expansion coefficient are favorable to the flame front hydrodynamic instability increase. The smaller is the Lewis number, the more thermo-diffusively unstable is the flame. The flame front trend to cellularity increases when the stretch rate is smaller (positive for a spherical flame). In that case, wrinkles are smoothed out by the increase of stretch; that means that if the increase rate is less than the flame expansion rate, then the cells will not be formed. All these experimentally obtained trends agree with the behavior predicted by the theoretical expressions of Bechtold&Matalon 1987 [49], which will be treated extensively later.

Kadowaki et al. 2005 [93] developed a theoretical model to understand the behavior of cellular flame fronts, with hydrodynamic and thermo-diffusive effects, by simulating the unstable behaviors of these flame fronts: cells creation, increasing and combination in bigger cells, and then new smaller cells again appear over the previous ones. Simulations showed, for mixtures Lewis numbers $Le < 1$, that the lower Le is, the more unstable the behavior is, the smaller size cells are, the flame front surface increase and, so, the cellular flame front advance speed increases notably, in a similar behavior to turbulent flames. About the buoyancy, Kadowaki 2001 [94] presented a model for $Le=1$ mixtures. Simulations showed that in a flame propagating upwards there is a more accentuated and wider cellular structure than when the flame propagate downwards, i.e. cells are deeper and the formed flame front have a larger surface, and because of that it can advance faster. The null gravity case offered intermediate results. Thus, it was inferred that the body force could contribute to both stabilize and destabilize the flame front according to how it was applied on the system. Kadowaki&Hasegawa 2005 [95] presented the following trends of the burning velocity increment reached with a cellular flame model:

- The body force effect was evaluated with the system acceleration defined positive in direction from burned zone to unburned one. The higher the acceleration is, the more unstable the system is and the bigger the burning velocity increment value is, the latter defined as the ratio of the cellular to laminar values.
- The hydrodynamic instability effect was evaluated by means of the temperature in burned zone. The higher the temperature is, the larger the gases expansion is and the more important is this instability effect on the flame front. This model shows that the increment of burning velocity increases as the temperature also increases.
- The thermo-diffusive effect was evaluated by means of the Lewis number. The thermo-diffusive instability is accentuated when Le decreases and the ratio of increment of the burning velocity increases. For $Le=1$ this increment ratio takes proportional values to the cellular flame front surface increment relative to the smooth one. Nevertheless, for $Le < 1$, the ratio increment is even longer than the area increment.

These three results indicate that the more accentuated the instability is, the bigger the cellular flame front surface increment above the smooth one is and, thus, the bigger the increment of the burning velocity ratio (cellular to merely laminar).

Some experimental works in the literature have prevented cellular flame structures by suppressing instabilities, Tse et al. 2000 [96], Kwon&Faeth 2001 [97]. For instance, it has been done by using helium instead of nitrogen, for inert substitution, increasing the thermal diffusivity D_t of the mixture and, thus, the Lewis number, thereby enhancing thermo-diffusive stability, or retarding the hydrodynamic instability through dilution and lowering the density ratio σ . Obviously, this method is not representative for practical applications such as engine conditions.

Most flames at high pressure are unstable since Markstein lengths decrease with pressure and the range of unstable wavelengths increase accordingly, Bradley et al. 1998 [26], Aung et al. 1998 [79]. The pressure increase, combined with the Markstein number reduction, enhances instabilities, Bradley et al. 2000 [77]. At engine pressures, even stoichiometric flames become unstable and instabilities increase burning rates. Instabilities also may cause the pressure rises in large-scale explosions.

With low Markstein lengths, cellular structures appear to be quite general for all spherically expanding flames, that are intrinsically unstable due to non-stabilizing influence of thermo-diffusive effects, Bradley&Harper 1994 [98]. The stability analysis developments are widely presented in the literature in terms of dimensionless groups, including Peclet and Markstein numbers.

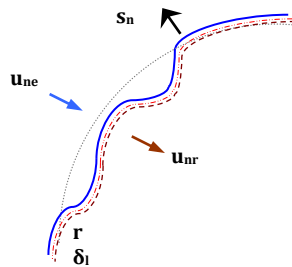


Fig. 19. Flame instabilities

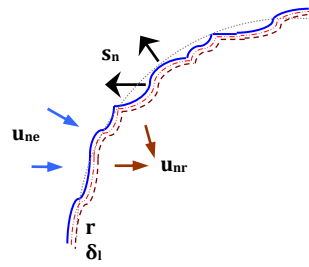


Fig. 20. Flame wrinkling and cracking

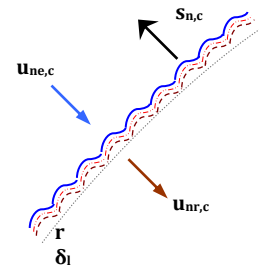


Fig. 21. Flame cellularity

Other theoretical and experimental studies have been published about the growth of flame instabilities arising from perturbations (fig. 19) of spherically propagating laminar flames in explosion bomb by Bradley&Harper 1994 [98]. They observed that first wrinkles are originated due to interferences of igniters with the flame front, while wrinkles progress later in the flame front.

- High speed Schlieren cinematography shows flame instability to be associated with the propagation of discontinuities in the flame structure that have the appearance of cracks, originating from disturbances due to flame movement over the spark electrodes, along the flame surface. Some distortions of the flames form single lines or the small cracks associated with the flames passing across spark electrodes, which are considered of less influence on the flame speeds. Flame cracking eventually leads to metastable cellular flames, and instabilities can hasten the development of cellular structures.

- On the other hand, mainly at increasing pressures, some flames develop cracks and cross-cracks until also eventually cellular structures in dynamic equilibrium, in which convex,

positively stretched cells are bounded by fractured cracks, where localized quenching is caused by sufficient localized negative stretch rate at cracks, or cusps (crests or ridges), Bradley et al. 2000 [77]. Measured cracks propagation velocities were correlated qualitatively with predictions by asymptotic analysis. When such cracks (fig. 20) are precursors of cellular flame structures they propagate at rates that are qualitatively in agreement with the theoretically predicted growth rate of the amplitude of the perturbations.

Flame instabilities and the formation of cellular structures (fig. 21) during spherical gaseous explosions have also been experimentally studied by Bradley et al. 2000 [77], by using natural light and Schlieren high-speed cinematography, as well as single-shot planar laser-induced fluorescence from the OH radical. High-pressure, rich-hydrocarbon and lean-hydrogen flames at low Markstein numbers were used. Ranges of unstable wavelengths have been identified as a function of Markstein and Peclet numbers. The cinematography enables recording the dynamics of cell growth and split to be studied and qualitatively interpreted, in terms of flame stretch rates and thermo-diffusion. This technique enabled unstable wavelengths to be measured and flame fracture at negatively stretched cracks to be observed. A cascade of unstable wavelengths terminates in a cellular structure. This structure appears at the later defined (second) critical Peclet number Pe_{cl} . The smaller cells are continually destabilizing and re-stabilizing. As they increase in size, the localized stretch rate on the cell surface decreases and the cell becomes unstable. It re-stabilizes by splitting into smaller cells with higher localized stretch rates. The cells are bounded by cracks in regions of negative curvature. At sufficiently small Markstein numbers, the cracks are fractured. The results were interpreted within the theoretical framework of the stability analysis of Bechtold&Matalon 1987 [49].

3.8.2. Critical values of Peclet number and regime transitions

A diffusively stable spherical expanding flame is stable for all perturbation wavelengths λ_w when it is smaller than a critical radius. As soon as the critical radius is reached, an estimated range of wavelengths ($\lambda_{w,s}, \lambda_{w,l}$) exists than can wrinkle the flame and trigger instability, inside an instability peninsula, Matalon 2007 [99]. There are not cells with a size smaller than a certain size $\lambda_{w,s}$, because those perturbations are stabilized by thermo-diffusive effect. The lower unstable wavelength is the wavelength at which thermo-diffusive effects stabilize the hydrodynamic instability. So, the lowest possible limit is given by the flame structure and is a multiple ($\lambda_{w,s} \propto \delta_l$) of the laminar flame thickness, Bradley et al. 2000 [77]. The upper limit ($\lambda_{w,l} \sim r$) is set by the overall flame size. Thus, the range of unstable wavelengths changes and increases as the flame radius (r) grows. As the flame front propagates its flame speed increases in consequence with the increasing range of the unstable wavelengths ($\lambda_{w,s}, \lambda_{w,l}$) and the associated surface wrinkling.

For flames with a certain minimum positive Markstein number, the thermo-diffusive effects keep the flame initially stable until a critical flame radius is reached and then the flame becomes unstable. This instability arises from the implicit hydrodynamic disturbances associated with thermal expansion, Clavin 1985 [42], Bechtold&Matalon 1987 [49]. These become important when the amplitude of a disturbance grows at a rate that is bigger than the flame speed. The flame should be stable, to all perturbations whatever their wavelength λ_w is, until a critical value of the flame radius r_{cr} normalized by the flame thickness δ_l is reached, i.e. at a critical Pe_{cr} . Thereafter the flame is no longer stabilized by the stretch rate and it becomes unstable.

Critical flame radius = r_{cr} \Rightarrow

$$\begin{aligned} \text{Critical value of Peclet number (onset of instabilities and first initial cracking)} &= Pe_{cr} \\ &= (r_{cr}/\delta_i) \end{aligned} \quad (94)$$

Instability becomes evident just after this defined first critical value of Peclet number Pe_{cr} , Bradley et al. 1998,2000 [26,77], with the origination and start of propagation of cracks. The value of Pe_{cr} , Bradley&Harper 1994 [98], is close to that predicted for the onset of instability in the theory of Bechtold&Matalon 1987 [49].

The propagation of cracks across the flame surface is followed by cross cracking and the formation of cells. The creation of new cells cannot keep up with the growth of the flame kernel and the surface area of the individual cells increases. The cells grow as the flame kernel grows until the local stretch rate can no longer stabilize the cell and the cells are subdivided into smaller cells stabilized by the higher local flame stretch. Eventually these smaller cells are created over the entire flame surface accompanied by an increase in flame speed Bradley et al. 1998 [26], Gu et al. 2000 [55]. This occurs when the localized flame stretch rate at the cell surface has been reduced sufficiently to allow the growth of instabilities with a shorter wavelength, Bradley 1999 [100]. A cascade of progressively decreasing wavelengths develops causing fractal-like flame wrinkling. When this extends over the whole flame surface and a cellular flame structure is developed, associated with the lower wavelengths, Bradley&Harper 1994 [98], the change in flame speeds is significant, Groff 1982 [89]. At higher pressures the increases in flame speeds occurs at smaller radii, thus reducing the range of flame stretch rate.

A second critical value of Peclet number is defined as the value above which the burning velocity is further enhanced by cellularity. At smaller stretch rates and bigger radii than those of the associated to the critical "cellular" Peclet number Pe_{cl} the flame speed and the burning velocity continue to be enhanced.

$$\text{Critical cellular radius} = r_{cl} \quad \Rightarrow$$

$$\begin{aligned} \text{Critical cellular value of Peclet number (onset of cellularity and increase in flame speed)} &= Pe_{cl} \\ &= (r_{cl}/\delta_i) \end{aligned} \quad (95)$$

It is considered that this second critical Peclet number Pe_{cl} , Bradley et al. 2000 [77], is less well-based than the first critical Peclet number Pe_{cr} , because there is some evidence that a much increased ignition energy can generate stronger acoustic waves and reduce the value of this second critical Peclet number Pe_{cl} .

As said, an increase in pressure can decrease Markstein numbers Ma_{sr} and cellular Peclet number Pe_{cl} . Together with the decrease in the flame thickness δ_i , this causes the critical cellular radius to decrease significantly, as the pressure is increased. The cellular flame structure develops earlier during flame propagation as the pressure increases. As the flame becomes completely cellular, there is an increase in flame speed and this continues as the flame propagates. The flame front wrinkling is associated with its acceleration. Bradley et al. 2000 [77] justify this behavior because of the flame front surface increasing in the smooth to cellular transformation. So, the cellular flame front mixture burning velocity is bigger than the smooth flame front velocity. In spite of the fact that a cellular flame cannot be considered laminar, the measurement method is similar and both flames are developed without the influence of outer turbulence.

The two theoretical Peclet numbers above introduced, as criteria for the growth of instabilities, associated with the onset and propagation of cracks, are not unique in all cases. Additionally, a turbulent propagation of the flame may appear. To account for that, at very high Peclet numbers corresponding to large radius, a third critical value of Peclet number is defined for the transition to a self-turbulizing spherical flame, Zeldovich et al. 1985 [40], Bradley 1999 [100].

Critical self-turbulizing flame radius = r_{ct} \Rightarrow

Critical self-turbulizing value of Peclet number = Pe_{ct}

$$= (r_{ct}/\delta_l) \quad (96)$$

Stronger pressure pulses can create macro and micro vorticity at the flame front that enhance the burning rates and produce local turbulent flames (fig. 22). A flame vorticity number was proposed by Bradley&Harper 1994 [98] for the prediction of whether flame vorticity generations might initiate turbulent flame propagation.

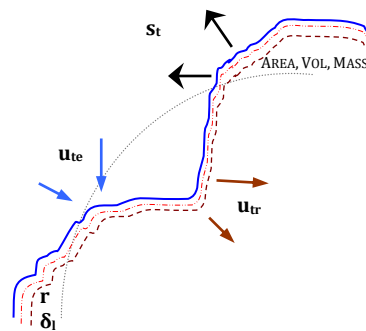


Fig. 22. Localized turbulization of the flame

The scope of this work is limited to laminar burning velocities of fuel-air gas mixtures, with the instabilities associated to hydrogen behavior. The turbulent burning velocity u_t of hydrogen mixtures is a convenient parameter to calculate the fuel mass burning rate in a hydrogen engine and, contrary to the laminar burning velocity, it depends not only on the mixture properties but also on the flow, the geometry and the history of the flame, Driscoll 2008 [101].

Although it is not the authors' purpose, an interesting question is to what extent both flame stretch and instabilities influence on the turbulent burning velocity of hydrogen flames. The extension to which cellularity carries over to turbulent flames and its possible consequences for phenomenological and multi-dimensional modeling has been discussed in the literature (e.g. by 2000 Gillespie et al. 2000 [22]). However, this extension to what cellular enhancement of laminar burning velocity carries over to turbulent flames has not yet been solved Verhelst&Sheppard 2009 [20]. Some works devoted to this subject (taking into account the effect of stretch and laminar flame instabilities on turbulent combustion) were included in a review paper of Lipatnikov&Chomiak 2005 [102], with other related work by Lipatnikov&Chomiak 2002 [103]. Verhelst&Wallner 2009 [15] have also reported very interesting descriptions of experimental and numerical works with considerations of the role of instabilities and the effects of stretch on the turbulent burning velocity u_t for hydrogen mixtures.

3.9. Linear stability theory. Application to lean hydrogen-air flames

This section presents a review of complementary methods that have been developed in the literature to allow the obtaining of burning velocities of unstable flames. These velocities can be appreciably higher than their stable un-stretched laminar values. These methods are adequate when the conditions of fuel-air mixtures compositions and pressures are prone to instability. In many mixtures, it is impossible to measure stable laminar values directly because of the rapid onset of instabilities. As said before, when the pressure is higher, the flame becomes unstable at ever-decreasing radii, or the range of stable flame speeds becomes too narrow for reliable measurements of laminar burning velocity and Markstein numbers. However, the correction methods accuracy is estimated to be reduced as the pressure increases significantly or in highly unstable flames.

In the next two sections, the linear instability theory is reviewed, Bechtold&Matalon 1987 [49], Bradley 1999 [100], based on the consideration of the increasing range of unstable wavelengths at small positive and negative values of Markstein numbers. Later, in section 3.10 a different approach, with a method based on fractal considerations, is described.

3.9.1. Instability peninsula based on wavenumbers

Burning velocities of unstable flames are not constant, but change with time as flame develops. Many studies clearly demonstrate the importance of instabilities, even at lower pressures, in enhancing burning velocities. For instance, in section 3.5 it was observed the propensity of rich mixtures with heavier-than-air fuels and lean mixtures with lighter-than-air fuels to develop cellular flame fronts. On the other hand, the measurement of laminar burning velocities and the associated Markstein numbers present several problems at high pressure, because the flames are more prone to hydrodynamic and thermo-diffusive instabilities. In general, acoustic disturbances and oscillations are more marked for mixtures with low Markstein lengths, which is a consequence of increased propensity to instability. At elevated pressure, the direct effect of stretch rate is lower, and this results in a bigger susceptibility to instability.

Instabilities produce severe flame wrinkling, that increase flame front surfaces and enhance flame speeds with an associated increase in burning velocities. Instabilities are suppressed by sufficiently high values of stretch, as in the early stage of explosive flame propagation from a point source, and also by flow divergence in counter-flow burners Egolfopoulos&Law 1990 [38]. However, by definition a laminar burning velocity u_l must be a value in the absence of stretch rate. In section 3.6, it has been shown how this u_l can be found for stable flames by plotting the measured flame speed against the flame stretch rate and extrapolating the speed to obtain the value at a zero stretch rate. But this approach is not possible when a flame has become unstable. As described in section 3.8, this happens in spherical explosion flames at a critical value Pe_{cl} of the Peclet number, as it is known from experiments (Groff 1982 [89], Kwon et al. 1992 [62], Bradley et al. 1998 [26], Gu et al. 2000 [55]) and from theory (Bechtold&Matalon 1987 [49], Bradley et al. 1996,1999,2000 [25,100,77], Addabbo et al. 2003 [104]).

When the stretch rate falls below its critical stabilizing value and only flame speeds s_n in the presence of instabilities can be measured, the effect of instabilities can be accounted for with the already mentioned methodology reviewed in section 3.6, by means of the resulting near-linear plot $S-\kappa$ of corrected flame speed S against flame stretch rate κ , that can provide a stretch-free, stable, laminar burning velocity. So, the corrected stable values of the flame normal

stretched speed in the absence of instabilities S are obtained in practice in the literature, Bradley et al. 2007 [45], for lean hydrogen air mixtures, based on the approach methodology used for unstable explosion flames at elevated pressure. Al-Shahrany et al. 2005,2006 [68,69] similarly obtained laminar burning velocities of iso-octane-air mixtures. The lean hydrogen-air mixtures flames are unstable specially, with low and often negative values of Markstein numbers, particularly at high pressure. Even at atmospheric pressure, cellular flames have been observed when fuel to air equivalence ratio fell below about 0.8, Andrews&Bradley 1972 [105].

In the work of Bradley et al. 2007 [45], flame speeds s_n were calculated from the mean flame radii r obtained from measurements of the flame projected area, and their variations were shown for explosions at lean equivalence ratio of $\Phi=0.4$, temperature of 365 K and pressures between 0.1 and 1 MPa, with the most stable flames at 0.1 MPa. It was observed that in the early stage of flame propagation the values of flame speed s_n were decreasing as the radius increased, and the Schlieren flame photographs did not show evidence of cellularity. However the structure became fully cellular, with s_n starting to increase at the instant defined by the critical radius r_{cl} , with its critical Peclet number Pe_{cl} for the given conditions, assuming a value of flame thickness based on a hydrodynamic length $\delta_{i,hd}=(\nu_u/u_l)$, considering the kinematic viscosity ν_u of the mixture. The flame speed s_n kept increasing and the oscillations in its values arose from acoustic waves travelling across the combustion bomb of the experimental method. The instabilities became evident as flame wrinkling over a range of wavelengths. The hydrodynamic and thermo-diffusive instabilities, which gave rise to the cellularity, took place within the peninsula of instability that serves to the semi-theoretical methodological analysis for the instabilities consideration that is reviewed in this section.

The limits of the instability peninsula (fig. 23) are defined by upper and lower limiting wavenumbers diagrammatically plotted against Peclet number. Thus, the increasing range of unstable wavelengths as the flame grows (bigger radius, i.e, bigger Peclet number) is illustrated by the increasing range of the wavenumber as a function of Peclet number, given by the vertical distance between the straight line $f \cdot n_s$ (upper limit, with n_s being the theoretical limit corrected by a factor f less than 1) and the horizontal line n_l (lower limit). The wavenumber is essentially the ratio between the length of a virtual circumference (given by a cross section of the spherical flame front) and the wavelength. The higher is the wavenumber, the bigger is the potential number of cells on the flame surface. However, this number is limited, as the minimum size of the cells is limited by either about fifty times the flame thickness, for diffusively unstable flames, or the size where thermo-diffusion stabilizes the cell against hydrodynamic instability. The upper limit ($f \cdot n_s$) for the unstable wavenumbers thus increases linearly with the flame size, or what it is the same, the radius and the corresponding Peclet number. Wavenumbers are related to wavelengths and Peclet numbers by the following expressions, with these adapted notations.

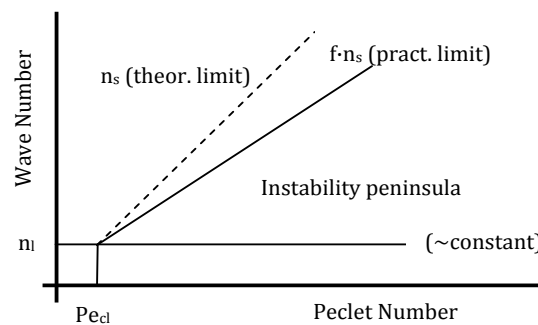


Fig. 23. Limiting wavenumbers in peninsula of instability (adapted from Al-Shahrany et al. 2005 [68])

Unstable wavelength = λ_w

$$\Rightarrow \text{Normalized unstable wavelength (wl)} = \Gamma_w = (\lambda_w/\delta_l) \quad (97)$$

Longest unstable wavelength = $\lambda_{w,l}$

$$\Rightarrow \text{Longest normalized unstable wl} = \Gamma_{w,l} = (\lambda_{w,l}/\delta_l) \quad (98)$$

Shortest unstable wavelength = $\lambda_{w,s}$

$$\Rightarrow \text{Shortest normalized unstable wl} = \Gamma_{w,s} = (\lambda_{w,s}/\delta_l) \quad (99)$$

Wavenumbers of the unstable wavelength = $n = (2\pi r/\lambda_w)$

$$= 2\pi (Pe/\Gamma_w) \quad (100)$$

Smallest (theoretical) unstable wavenumber of the longest unstable wavelength = n_l

$$= 2\pi (Pe/\Gamma_{w,l}) \quad (101)$$

Largest (theoretical) unstable wavenumber of the shortest unstable wavelength = n_s

$$= 2\pi (Pe/\Gamma_{w,s}) \quad (102)$$

Largest (practical) modified unstable wavenumber of the shortest unstable wavelength

$$= f n_s \quad (f < 1) \quad (103)$$

The framework for the construction of the instability peninsula is based on the already mentioned linear instability theory of Bechtold&Matalon 1987 [49]. The upper limit n_s predicted by the theory over-predicts the experimentally measured one. This is because the measured cellular Peclet number Pe_{cl} at which the flame speed increases significantly is different from the theoretical (first) critical Peclet number Pe_{cr} , defined before. Thus, the practical upper limit for the highest unstable wavenumber is $f n_s$ reduced by a factor f . The lower limit n_l can be seen to be almost constant, a consequence of the longest unstable wavelength $\lambda_{w,l}$ to be limited by the flame size, thus proportional to the flame radius and resulting in a constant wavenumber, in general terms.

The peninsula of unstable wavelengths was confirmed experimentally by Bradley 1999 [100]. The range of wavelengths bound by these corresponding limits was expressed as functions of the density ratio or expansion coefficient σ (being the measure of hydrodynamic instabilities) and the strain rate Markstein number Ma_{sr} (representing diffusional effects). The instability peninsula extent is a function of Ma_{sr} for each given value of σ . The lower Ma_{sr} is, the lower the tip critical Peclet number is and the more tilted the peninsula upper branch is, resulting in a wider range of unstable wavelengths and corresponding lower shortest wavelength $\lambda_{w,s}$ values. The instability peninsula lower branch remains almost constant, as also the longest wavelength size $\lambda_{w,l}$.

3.9.2. Instabilities on spherical flames at constant pressure for positive non-minor values of Markstein numbers

The complete theory of Bechtold&Matalon 1987 [49] is only exhaustively valid for normalized unstable wavelengths Γ_w bigger than 30 ($\lambda_w > 30\delta_l$), which generally implies values of the strain rate Markstein number Ma_{sr} bigger than three ($L_{sr} > 3\delta_l$). This was derived, Bradley et al. 2000 [77], from experimental work with planar laser-induced fluorescence images, because the theoretical values of the shortest normalized unstable wavelengths $\Gamma_{w,s}$ were unrealistically small for values of $Ma_{sr} < 3$, considering that the practical limit for the shortest wavelength $\lambda_{w,s}$ must be set by the flame structure and as a multiple of the flame thickness.

During a spherical explosion and flame propagation, the Peclet number value increases and the onset of instabilities occurs, with full flame cellularity, at the defined critical cellular value Pe_{cl} of Peclet number. This depends upon the strength of both hydrodynamic and thermo-diffusive contributions. The limits of the range of wavelengths, between which the flame is not stable, are given by the smallest unstable wavenumbers n_s and the largest theoretical unstable wavenumbers n_l .

In practice, as said above, full cellularity develops at higher values of critical Peclet number than predicted by the theory. The theoretical spherical explosion flames in which the pressure remains constant, Bechtold&Matalon 1987 [49], Bradley 1999 [100], begin to show cracks propagating across their surfaces at critical Peclet numbers close to theoretically predicted values for the flame instability onset, Bradley et al. 2000 [77], Addabbo et al. 2003 [104]. However, full cellularity and associated increase in flame speed only occur at the higher critical Peclet number value, $Pe_{cl} = (r_{cl}/\delta_l)$, Gu et al. 2000 [55], Bradley et al. 2000 [77]. In a real experiment, it is as if there would be a lag before full development of instability, Al-Shahrany et al. 2005 [68]. In particular, the theoretical n_s , or inner cut-off values, given in Bechtold&Matalon 1987 [49] are reduced in practice, without a comparable change in the respective n_l values, which changes much less with Peclet number.

Bradley et al. 1999,2007 [100,45] accounted for this practical lag effect by replacing the theoretical values of the critical Peclet number Pe_{cl} with those experimentally-observed higher. A practical value fn_s is obtained from the theoretical n_s by multiplication by a numerical constant f less than unity, evaluated at the tip conditions for the measured critical Peclet number Pe_{cl} , which enables to make fn_s equal to the theoretical value of n_l , as given in Bechtold&Matalon 1987 [49], Bradley 1999 [100].

$$(fn_s)_{cl} = (n_l)_{cl} \quad (104)$$

The range of unstable wavelengths that contribute to the flame wrinkling only exists beyond the tip of the instability peninsula, where Peclet number values Pe are bigger than the critical Pe_{cl} (triangular region in fig. 23) for a particular strain rate Markstein number Ma_{sr} and a ratio of densities $\sigma = (\rho_u/\rho_b)$. Experimental values of the critical Peclet number Pe_{cl} have been correlated linearly in terms of Ma_{sr} by Gu et al. 2000 [55], with a relationship that is less reliable at increasing negative values of Ma_{sr} ($Pe_{cl} \approx 177Ma_{sr} + 2177$, proposed for $-5 < Ma_{sr} < 8$ by Bradley et al. 2000 [77], for methane-air and iso-octane-air mixtures). For these increasingly unstable flames, the measurement of Pe_{cl} is easier than that of Ma_{sr} .

For values of Peclet number bigger than the critical value Pe_{cl} the linear instability theory shows the limit n_s to increase linearly with the Peclet number Pe , and this linearity is maintained for the modified wavenumber fn_s . Thus, it is formulated by Bradley et al. 1999,2007 [100,45].

$$(fn_s)_{pe} = (fn_s)_{cl} + (Pe - Pe_{cl}) \left\{ \frac{\partial (fn_s)}{\partial (Pe)} \right\}_{pe} \quad (105)$$

The theory shows that the range of unstable wavelengths increases as Ma_{sr} decreases and, usually, as the densities ratio $\sigma=(\rho_u/\rho_b)$ increases.

Within regimes of full validity of the linear instability theory ($Ma_{sr}>3, L_{sr}>3\delta_l$), it is possible to evaluate the derivative of fn_s from the wavenumber expression, for the appropriate values of Ma_{sr} and densities ratios $\sigma=(\rho_u/\rho_b)$, at the different values Pe of Peclet number. The actual shortest normalized unstable wavelength $\Gamma_{w,s}=(\lambda_{w,s}/\delta_l)$ is independent of the Peclet number.

$$(fn_s) = 2\pi(Pe/\Gamma_{w,s}) \quad \Rightarrow \quad (106)$$

$$\{\partial(fn_s)/\partial(Pe)\}_{Pe} = (2\pi/\Gamma_{w,s}) = [(fn_s)/(Pe)]_{Pe} \quad (107)$$

3.9.3. Instabilities on spherical flames at constant pressure for minor-positive and negative values of Markstein numbers

Based on experimental findings concerning the cellular structures of unstable flames, Bradley et al. 2007 [45], the adopted procedure was different for processing many measurements for values of $Ma_{sr}<3$ or even with negative values in most of the experiments with hydrogen-air mixtures. In Bradley et al. 2000 [77] these types of structures appeared to be in dynamic equilibrium and small cells increased in size as a flame kernel grew. This decreased the localized flame stretch rate and, consequently, the cell became unstable. It re-stabilized by splitting into smaller cells, with higher, stabilizing, local stretch rates. In such instances, it had been observed that the normalized wavelength $\Gamma_{w,s}$ of a single unstable localized cell, just prior to its split into the smallest stable cells, was close to that of the original flame kernel at the critical Peclet number.

$$(n)_{cl} = 2\pi(Pe_{cl}/\Gamma_{w,s}) \quad (108)$$

$$(fn_s) = 2\pi(Pe/\Gamma_{w,s}) \quad (109)$$

Thus, in regimes with strain rate Markstein number $Ma_{sr}<3$ ($L_{sr}<3\delta_l$) where it is not fully valid the linear instability theory, with normalized unstable wavelengths $\Gamma_w<30$ ($\lambda_w<30\delta_l$), it is possible to evaluate the derivative of fn_s from the wavenumber expression in this way.

$$\{\partial(fn_s)/\partial(Pe)\}_{Pe} = [(fn_s)/(Pe)]_{Pe} = (2\pi/\Gamma_{w,s}) = [(n)_{cl}/Pe_{cl}] \quad (110)$$

There must be a maximum limit to this derivative and, consequently, a lowest physicochemical limit to the value of the wavelength of a localized cell $\Gamma_{w,s}$ below which a wrinkled flame sheet cannot be maintained. It was inferred that this limit would be of the order of the flame thickness δ_l , because of the condition that the dimensional wavelength $\lambda_{w,s}$ cannot be less than δ_l ($\Gamma_{w,s}\geq 1$), and therefore the following inequality could be derived, although later modified in the following.

$$\{\partial(fn_s)/\partial(Pe)\}_{Pe} = [(fn_s)/(Pe)]_{Pe} \leq 2\pi \quad (111)$$

This condition is approached by the more negative values of Ma_{sr} . Nevertheless, experimental evidence based on diagnostic studies of Bradley et al. 2000 [77] suggested a lower limit $\Gamma_{w,s}\geq 50$ ($\lambda_{w,s}\geq 50\delta_l$) for such very unstable flames. Thus, the maximum limiting value at highly negative values of Ma_{sr} is taken as given by this inner cut-off, and this value is assumed by Bradley et al. 2007 [45].

$$\{\partial(fn_s)/\partial(Pe)\}_{Pe} = [(fn_s)/(Pe)]_{Pe} \lesssim 2\pi/50 \quad (112)$$

Returning to these former equations, the following transformations are possible with the previous considerations, to obtain the indicated expression.

$$(fn_s)_{Pe} = (fn_s)_{cl} + (Pe - Pe_{cl}) \{ \partial(fn_s) / \partial(Pe) \}_{Pe} \quad (113)$$

$$\{ \partial(fn_s) / \partial(Pe) \}_{Pe} = [(fn_s) / (Pe)]_{Pe} = (2\pi / \Gamma_{w,s}) = [(n_l)_{cl} / Pe_{cl}] \quad (114)$$

$$(fn_s)_{cl} = (n_l)_{cl} \quad (115)$$

$$\Rightarrow (fn_s)_{Pe} = (n_l)_{cl} + (Pe - Pe_{cl}) [(n_l)_{cl} / Pe_{cl}] \quad (116)$$

This leads, from positive smaller values of strain rate Markstein numbers $Ma_{sr} < 3$ until highly negatives, to this other expression.

$$(fn_s)_{Pe} = (Pe / Pe_{cl}) (n_l)_{cl} \quad (117)$$

3.9.4. Flame instabilities in confined explosions

The pressure remains constant in the theory of Bechtold&Matalon 1987 [49], Bradley 1999 [100], but this is not the case in confined explosions, Al-Shahrany et al. 2005 [68], where increasing pressure P and unburned temperature T_u occur, and the associated decreasing flame thickness δ_f and strain rate Markstein number Ma_{sr} , which leads to a reduction of the value of the function $\{ \partial(fn_s) / \partial(Pe) \}_{Pe} = [(fn_s) / (Pe)]_{Pe}$.

Al-Shahrany et al. 2005 [68] calculated the unburned gas temperatures from measured pressures, based on the assumption of isentropic compression, and could find Ma_{sr} from measurements in some instances. With the densities ratio $\sigma = \rho_u / \rho_b$, and based on the same theory of Bechtold&Matalon 1987 [49], Bradley 1999 [100], they could find $\{ \partial(fn_s) / \partial(Pe) \}_{Pe} = [(fn_s) / (Pe)]_{Pe}$ at different values or Peclet number Pe for strain rate Markstein number $Ma_{sr} > 3$, as regarded in section 3.9.2.

$$\{ \partial(fn_s) / \partial(Pe) \}_{Pe} = [(fn_s) / (Pe)]_{Pe} = (2\pi / \Gamma_{w,s}) \quad (118)$$

At lower values of strain rate Markstein number $Ma_{sr} < 3$, either of these expressions, presented in section 3.9.3, were used.

$$\{ \partial(fn_s) / \partial(Pe) \}_{Pe} = [(fn_s) / (Pe)]_{Pe} = [(n_l)_{cl} / Pe_{cl}] \quad \text{or} \quad (119)$$

$$\{ \partial(fn_s) / \partial(Pe) \}_{Pe} = [(fn_s) / (Pe)]_{Pe} \approx (2\pi / 50) \quad (120)$$

Because the mentioned fact of the value of the function $\{ \partial(fn_s) / \partial(Pe) \}_{Pe}$ changes during a confined explosion, it was assumed that the highest unstable wavenumber at a given Peclet number Pe could be found from a modification of the steady state equation.

$$(fn_s)_{Pe} = (fn_s)_{cl} + (Pe - Pe_{cl}) \{ \partial(fn_s) / \partial(Pe) \}_{Pe} \quad (121)$$

And the used quasi-steady state assumption was presented in the corresponding associated integral form as the following.

$$(fn_s)_{Pe} = (fn_s)_{cl} + \int_{Pe_{cl}-Pe} \{ \partial(fn_s)/\partial(Pe) \}_{Pe} dPe \quad (122)$$

The evaluation of the Peclet number Pe was made, in Al-Shahrany et al. 2005 [68], from the mean radius of two kernels and the flame thickness given by the kinematic viscosity of a mixture ν_u of iso-octane based on a hydrodynamic length $\delta_{l,hd}=(\nu_u/u_l)$. The values of laminar burning velocity u_l used were either known from previous data or evaluated by iteration. The twin kernel technique that was used allowed measurements at pressures up to 3 MPa.

3.10. Correction of instabilities effects. Fractal considerations

As we have referred, the stable values of flame speeds without instabilities S are derived in the literature, Bradley et al. 2007 [45], from the flame speeds with instabilities s_n , by accounting for the instability, based on the notations and terms already introduced in section 3.6. The instabilities produce severe flame wrinkling that increase flame front surfaces and enhance the flame speeds with an associated increase in burning velocities for unstable flames. Thus, the ratio of flame speeds with and without instabilities can be expressed by the ratio of the corresponding flame surface areas for unstable and stable processes. On the other hand, the ratio of the limiting values of the unstable wavenumbers, $n=(2\pi r/\lambda_w)$, is inversely proportional to that of the wavelengths.

Assuming fractal-like flame wrinkling, the fractal considerations previously used for the effects of laminar spherical flame instabilities allow estimating the burning speed of a cellular flame. It was suggested, Bradley 1999 [100], that a ratio of the fractal surface area increment due to wrinkling can be calculated with a resolution of the ratio of the outer to inner cut-off scale for flame wrinkling, with an assigned value, Bradley 1992 [106], of the fractal dimension d equal to 7/3, based on turbulent flames. This fractal approach was used because the fractal dimension had given satisfactory predictions of burning velocities for, initially laminar, large scale explosions, Bradley et al. 2000,2001 [77,92]. This has been sometimes considered overestimated, Verhelst 2005 [13]. Fractal-like flame wrinkling of cellular flame fronts has been experimentally confirmed by Kwon et al. 2002 [58].

$$[(fn_s)/(n_l)]^{(d-2)} \approx [(fn_s)/(n_l)]^{(1/3)} \quad (123)$$

Thus Bradley et al. 2007 [45] defined a flame speed enhancement factor F as the ratio of flame speed enhanced by instabilities s_n and the laminar flame speed S without instabilities, for each value of the Peclet number Pe .

$$F = (s_n/S) \quad (124)$$

The ratio of speeds can be estimated as the ratio of flame surface areas that with the fractal approach results in:

$$(s_n/S)_{Pe} = \langle [(fn_s)/(n_l)]_{Pe} \rangle^{(1/3)} \quad (125)$$

This may be used to give the flame speed S that would have been obtained in the absence of instabilities, from experimentally measured flame speeds s_n (e.g. cellular flame speeds $s_{n,c}$), assuming right values of $(F)_{Pe}$ are known.

$$(S)_{Pe} = [(s_n)_{Pe}/(F)_{Pe}] \quad (126)$$

The procedure adopted was to find the flame speed enhancement factor F at different values of Peclet number Pe (i.e. different measured radii), from the appropriate expressions of $(fn_s)_{Pe}$, for the cases considered in section 3.9, and applying the semi-theoretical methodology for the adequate values of the strain rate Markstein number Ma_{sr} and densities ratio $\sigma=(\rho_u/\rho_b)$, with the corresponding estimates of $(n_l)_{Pe}$ and $(n_l)_{cl}$. The value of F increases as a function of the range of unstable wavelengths.

$$(F)_{Pe} = \langle [(fn_s)/(n_l)]_{Pe} \rangle^{(1/3)} \quad (127)$$

Recalling that the value of $(fn_s)_{Pe}$ is a function of Peclet number Pe with two possible cases that depend on the value of Marsktein number, the corresponding expressions of $(F)_{Pe}$ could be deduced as follows.

For positive (non-minor) strain rate Markstein numbers $Ma_{sr} > 3$, in accordance with section 3.9.2:

$$(fn_s)_{Pe} = (fn_s)_{cl} + (Pe - Pe_{cl}) \{ \partial(fn_s) / \partial(Pe) \}_{Pe} \Rightarrow \quad (128)$$

$$(F)_{Pe} = [(fn_s)_{Pe} / (n_l)_{Pe}]^{(1/3)} \quad (129)$$

And for minor-positive and negative strain rate Markstein numbers $Ma_{sr} < 3$, according to section 3.9.3:

$$(fn_s)_{Pe} = (Pe / Pe_{cl}) (n_l)_{cl} \Rightarrow \quad (130)$$

$$(F)_{Pe} = [(Pe / Pe_{cl}) (n_l)_{cl} / (n_l)_{Pe}]^{(1/3)} \quad (131)$$

In summary, when the density ratio σ , strain rate Markstein number Ma_{sr} , Peclet number Pe_{cl} and fractal dimension d are known, the burning speed of a cellular flame can be calculated from the burning speed of the stable flame. A corresponding analogous statement is the one derived in terms of burning velocities associated to a cellular flame, Verhelst 2005 [13]. Thus, stable burning velocities could be derived for conditions where only cellular burning velocities can be measured, provided these quantities are known or can be estimated with a reasonable accuracy.

At spark ignition engine conditions, in combustion of hydrogen-air mixtures, the flames are unstable and cellular from combustion start, Verhelst 2005 [13], with Pe_{cl} effectively being close to zero. In such conditions, it is impossible to measure stable laminar burning velocities directly. Even for moderate pressures, the rapid instabilities onset reduces the linear region where the differences on the burning velocities can be used as functions (of the Markstein lengths or numbers) to obtain the corresponding stretch-free values. All the facts and circumstances result in decreased accuracy and increased complexity in the estimates for engine-like conditions.

References of chapters three, four and five (*after the fifth chapter*)

4. Review of studies about laminar burning velocities of hydrogen-air mixtures

- 4.1. Laminar burning velocities of hydrogen-air mixtures obtained from experimental methods close to atmospheric conditions
- 4.2. Laminar burning velocities of hydrogen-air mixtures obtained from experimental methods near engine-like conditions
 - 4.2.1. Laminar burning velocities
 - 4.2.2. Quasi-laminar burning velocities
- 4.3. Laminar burning velocities calculated by numerical simulation
 - 4.3.1. Combustion models, thermo-fluid-dynamics analysis, CFD models and chemical kinetic mechanisms
 - 4.3.2. Laminar burning velocities of hydrogen-air mixtures calculated by numerical methods, based on chemical kinetic mechanisms and related to combustion models

References of chapters three, four and five (*after the fifth chapter*)

4. Review of studies about laminar burning velocities of hydrogen-air mixtures

Hydrogen mass diffusivity is very high, the highest of all fuels, and the flame fronts of hydrogen-air mixtures have high tendency to instabilities, as already said. The hydrogen-air mixtures with equivalence ratios such as used in hydrogen engines, lean to stoichiometric, are diffusively unstable, from both considering the Lewis number and the preferential diffusion points of view, Vagelopoulos et al. 1994,1998 [107,108], Kwon&Faeth 2001 [97]. In addition, the small thickness of the flame front in the hydrogen-air mixtures tends to create hydrodynamic instabilities that increase with the pressure, Verhelst 2005 [13], Smallbone et al. 2006 [109].

Thus, these flames are very sensitive to the flame stretch rate, as was shown by Verhelst 2005 [13], who obtained Schlieren photographs of centrally ignited hydrogen-air flames propagating in a constant-volume bomb. When the stretch rate fell below a critical stabilizing value, the flame became cellular, Bechtold&Matalon 1987 [49], Bradley et al. 2000 [77]; this could be seen clearly from the sudden acceleration of the flame. This behavior is one reason for the large spread in burning velocities when comparing results with correlations by Liu&MacFarlane 1983 [110], Milton&Keck 1984 [5], Iijima&Takeno 1986 [4] and Koroll et al. 1993 [111], that were derived from data that did not take into account the effects of the stretch rate and instabilities.

4.1. Laminar burning velocities of hydrogen-air mixtures obtained from experimental methods close to atmospheric conditions

Some un-stretched burning velocities were measured in the past but they were generally performed close to atmospheric conditions, as in the works of Dowdy et al. 1990 [112], Egolfopoulos&Law 1991 [113] or Aung et al. 1997 [114]. The stoichiometric burning velocities were varying with a large difference from 2.1 up to 2.5 m/s, and with even larger differences for lean mixtures (e.g. from 0.56 to 1.15 m/s for an equivalence ratio $\Phi=0.5$). Other stretch-free burning velocities were determined in the studies of Kwon et al. 1992 [62], Vagelopoulos et al. 1994 [107], Taylor 1991 [115], etc.

When Verhelst 2005 [13] compared the burning velocities predicted by the experimental expression of Iijima&Takeno 1986 [4] with his performed measurements, he could clearly see that the other burning velocities were all in the cellular region. As Iijima&Takeno calculated burning velocities from pressure records obtained from bomb explosions, flame instabilities could not be directly seen. When larger radii were used in the derivation of burning velocities, the flames had developed cellularity. The burning velocity predictions obtained with the correlation of Iijima&Takeno were multiplied by the density ratio σ to give flame speeds s_n and were plotted versus stretch rate κ for some hydrogen-air flames at atmospheric conditions. The predictions all fell in the cellular region, which explains the consistently higher values. The measurements of Liu&MacFarlane 1983 [110] and Koroll et al. 1993 [111] also reported higher burning velocities. The deviations with the stretch-corrected measurements increased when the mixtures were going leaner, which could be explained by the decreasing Markstein length (with L_b negative and thus becoming larger in absolute value), resulting in a larger increase in the burning velocity when the flame was positively stretched. The measurements of Liu&MacFarlane 1983 [110] were highly stretched due to a very small nozzle used in their measurements, as was indicated by Wu&Law 1984 [116].

In the same analysis of Verhelst 2005 [13] the burning velocity for a stoichiometric hydrogen-air mixture predicted by the correlation by Milton&Keck 1984 [5] was lower than the values obtained with stretch rate correction, which could also be due to stretch (a stoichiometric

hydrogen-air flame was stable and would thus propagate slower when subjected to positive stretch) if the burning velocity was taken at a small flame radius (e.g. before the onset of cellularity). The stretch-free measurements showed reasonably good correspondence although the values reported by Vagelopoulos et al. 1994 [107] lower than the others were. All bomb-derived data, Taylor 1991 [115], Kwon&Faeth 2001 [97] and Verhelst et al. 2005 [7], corresponded closely. The very rich equivalence ratio at which the laminar burning velocity peaked, about $\Phi \sim 1.7$ ($\lambda \sim 0.6$) could also be explained by the high mass diffusivity of hydrogen, Hertzberg 1989 [61]. It is noteworthy that the equivalence ratio at which the laminar burning velocity peaked is much richer than the equivalence ratio at which the flame temperature peaked (about stoichiometry). The comparisons of Verhelst 2005 [13] with stretch-free burning velocities at atmospheric pressure and temperature about 360 K, and Bradley et al. 1998 [26], Gu et al. 2000 [55], Verhelst et al. 2005 [7], Knop et al. 2008 [6], for hydrogen, methane and iso-octane as a function of equivalence ratio, demonstrated the much higher laminar burning velocity of hydrogen-air mixtures and its strong dependence on the equivalence ratio.

Other experimental studies on constant pressure, spherical expanding hydrogen flames were conducted by Tse et al. 2000 [96] and Law et al. 2005 [84]. For instance, in a bomb with flame front image recording (fig. 24), Law observed instabilities starting from a critical radius of 5 mm in the spherical flame fronts hydrogen-air mixtures at 0.5 MPa of pressure and for equivalence ratios between $0.6 < \Phi < 0.9$. With a similar technique, Kwon et al. 1992 [62] observed unstable flame fronts in stoichiometric mixtures $\text{H}_2\text{-O}_2\text{-N}_2$ ($\text{O}_2/\text{N}_2 = 0.125$) at 0.3 MPa, for radii from about 7 mm. These values of flame front critical radius were much lower than the minimum radius to obtain valid data in experiments, and so, even at this pressure conditions, the flame front structure should be cellular.

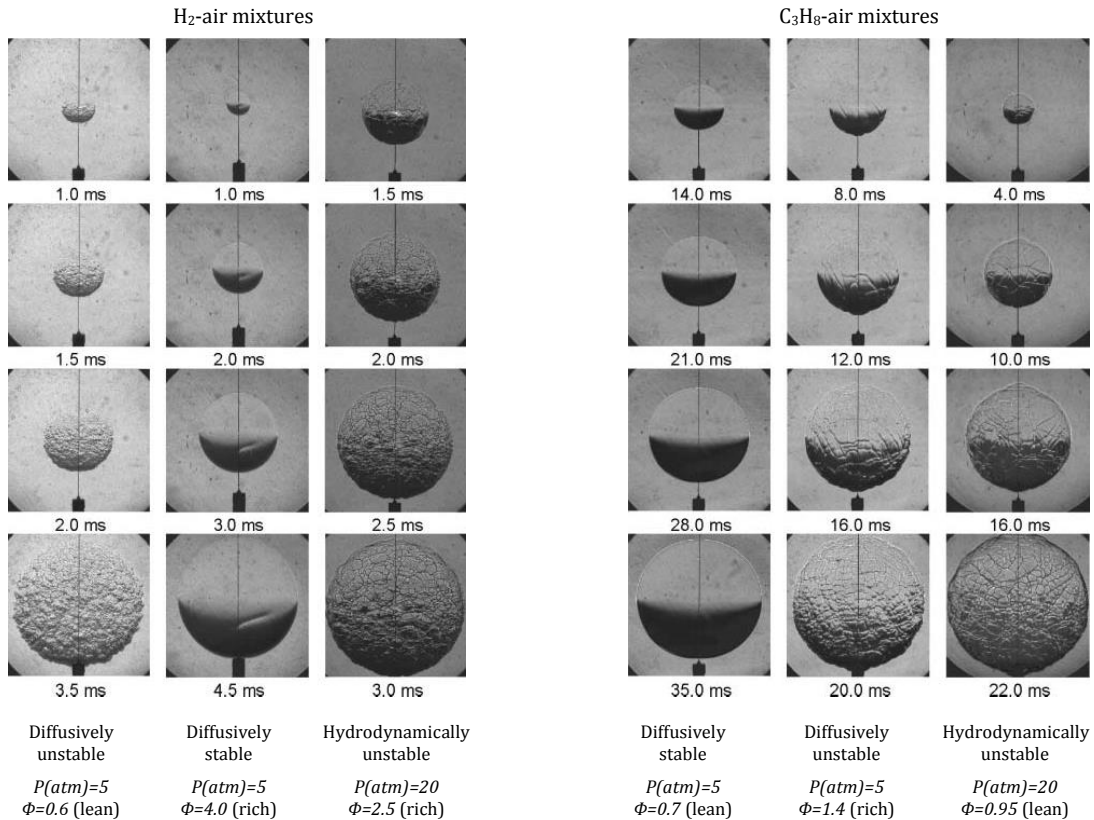


Fig. 24. Spherically expanding flames of hydrogen and propane air mixtures recorded by Schlieren cinematography (taken from Matalon 2007 [99] and Law 2006 [57])

Some other works reported new measurement of laminar burning velocities of hydrogen-air flames, Gu et al. 2000 [55], Kwon&Faeth 2001 [97], Lamoureux et al. 2003 [117], Qiao et al. 2005 [118], Hermanns et al. 2007 [119]. However, these studies were also mainly done at close to room temperature and pressure, sometimes also with large difference in burning velocities, and for limited equivalence ratios. Few works were reported on the measurement of laminar burning velocities and on the understanding of combustion characteristics of the hydrogen-air flames at high pressures and temperatures over a wide range of equivalence ratios and residuals fractions.

4.2. Laminar burning velocities of hydrogen-air mixtures obtained from experimental methods near engine-like conditions

The studies for calculating the stretch-free local flame speed require stretch-free data to model and validate. As a consequence, there have been few, insufficient, data available of laminar burning velocity of hydrogen-mixtures at engine conditions, because stretch and instabilities make difficult the experimental determination of stretch-free data at higher pressures, Verhelst et al. 2005 [7], Clavin 1985 [42], Law 1988 [50], Aung et al. 1998 [79]. The range of conditions covered by the correlations of Liu&MacFarlane 1983 [110], Milton&Keck 1984 [5], Iijima&Takeno 1986 [4] and Koroll et al. 1993 [111], mentioned above, include (only sometimes) lean to rich mixtures and (not commonly) elevated temperatures (up to 550 K) and pressures (up to 25 atm). However, as discussed previously, they did not account for the effects of stretch and instabilities, which grow stronger with pressure as the flame thickness decreases, Verhelst et al. 2005 [7]. The main reasons for the large spread in the reported data on burning velocities throughout the years are that the effects of stretch were initially ignored, and only later understood with variations, and due to the different developed measuring methodologies that take into account their respective effects. The burning velocities corrected to account for the effects of the flame stretch rate, only valid under certain conditions, Pareja et al. 2010 [120], Chen et al. 2009 [121], might have not been respected in the same modes in all the works, according with the observed difficulties.

4.2.1. Laminar burning velocities

Care must be taken in using published data for the laminar burning velocity of hydrogen-air mixtures. The laminar burning velocity of these mixtures and its dependence on the mixture conditions and the flame front instabilities have been discussed at length by Verhelst and other few authors in the recent relevant literature. A lot of work, wide and excellent, has been done by them in the first decade of this century. The same study of Verhelst 2005 [13] addressed to the need for experimental data. Un-stretched burning velocities and Markstein lengths would have to be determined from stable flames. At the higher pressures, hydrodynamic and thermo-diffusive instabilities caused the flames to be cellular from inception, from the first recorded flame image, which prohibited the direct obtaining of laminar burning velocity and Markstein length. On the other hand, the effect of pressure on the burning rate was demonstrated to have opposing trends when comparing stoichiometric and lean mixtures.

Experimental data of Aung et al. 1998 [79] showed hydrogen-air flames at atmospheric conditions to have positive Markstein lengths (numbers) if they were close to stoichiometry, but all lean mixture equivalence ratios had negative Markstein lengths (numbers) as soon as the pressure exceeded about 0.4 MPa. It had been shown in works at atmospheric pressure that

hydrogen-air flames were diffusively unstable on the lean side of equivalence ratio $\Phi \approx 0.8$. Thus, these mixtures showed a flame speed reduction with decreasing stretch rate. This also implied an earlier transition to a cellular flame structure. Under such circumstances the methodology adopted in Bradley et al. 1998 [26], Gu et al. 2000 [55], was to extrapolate to zero stretch rate “only the linear portion of the curve” of the flame speed s_n versus the flame stretch rate κ , relying this approach on a sufficiently large stable linear regime. But further, it was shown that the flame acceleration due to cellularity occurs at the already defined (second) critical Peclet number $Pe_{cl} = (r_{cl}/\delta_l)$, as it was used in Bradley et al. 2007 [45], where r_{cl} is the radius at which cells start to induce flame acceleration, and δ_l the laminar flame thickness, with the critical value of Peclet number increasing linearly with Markstein number.

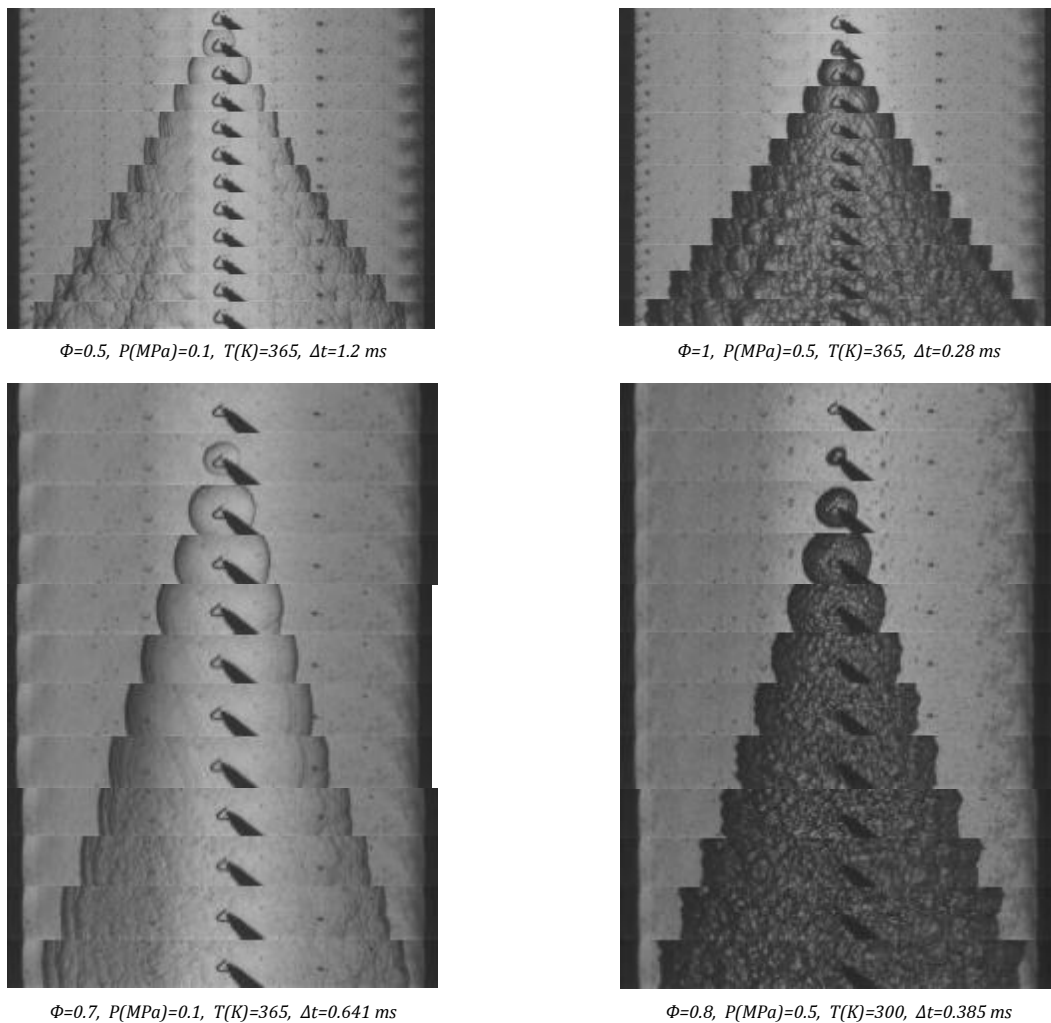


Fig. 25. Propagation of hydrogen flames recorded by Schlieren cinematography (adapted from Verhelst 2005 [13])

The consequence of increasing instability with pressure was illustrated (fig. 25) in the work of Verhelst 2005 [13] with Schlieren photographs of a hydrogen-air flame, for instance at $\Phi=0.8$, 300 K, 0.5 MPa. In this case, the flame was cellular from inception onwards, accelerating throughout its growth. The flame speed increased faster than linearly with decreasing flame stretch rate; consequently the methodology of obtaining stretch-free burning velocities (and its dependence on stretch rate) as described at atmospheric conditions was considered no longer

applicable, Verhelst et al. 2005 [7], Bradley et al. 2007 [45], because experimentally all flames at engine-like conditions were unstable and cellular from inception. This means, for higher pressures, that the mixture equivalence ratio below which the Markstein number was negative was given to increasingly higher values, which implies that for all practical mixtures in hydrogen engines (stoichiometric to lean, and high pressures) the laminar flames were unstable. The increase in flame speed with radius was much bigger for flames at 0.5 and 1 MPa than at 0.1 MPa. This corresponded to a difference in flame structures; the flame at 0.1 MPa was smooth throughout the flame growth, whereas those at 0.5 and 1 MPa were cellular throughout, and a consequence of the reduced flame thickness at higher pressures. Because the hydrogen flames used in Verhelst 2005 [13] had a very thin reaction zone, the critical Peclet number was reached at small flame radii, and hence only for mixtures at 0.1 MPa it was reliable to make extrapolations to zero stretch rate. The range of conditions at which stable hydrogen-fueled flames existed was much lower than observed, for instance, with both methane, Gu et al. 2000 [55], and iso-octane, Bradley et al. 1998 [26].

The variation of flame speed with radius and pressure was also shown by Verhelst 2005 [13] for lean flames at $\Phi=0.3$ and 365 K. Each plot exhibited the same trend with an initial reduction, followed by acceleration in the flame speed as cells developed. Similarly to stoichiometric flames, the tendency to cellularity was bigger as the pressure was increased. This was indicated by an earlier onset of acceleration with increasing pressure. However, the effect of pressure on the flame speed in lean flames was the opposite of that observed for stoichiometric flames.

To identify the effect of initial temperature on flame instability, Schlieren images at different initial temperatures were also provided in Verhelst et al. 2005 [13,7], and the result was that flame instability was insensitive to initial temperature. No significant effect of temperature on the stability was found, a trend that can be justified as follows. The effective Lewis number decreased slightly with the increase of initial temperature for the fixed equivalence ratio and initial pressure. This indicated that initial temperature had little influence on the diffusive-thermal instability. With the increase of initial temperature, both the expansion coefficient $\sigma=(\rho_u/\rho_b)$ and the flame thickness δ_l were decreased. The decreased density ratio σ factor led to the decrease of hydrodynamic instability while the decreased flame thickness δ_l factor led to the increase of the hydrodynamic instability. The combined influence of the two factors resulted in little variation in flame front instability at different initial temperatures.

Schlieren images of flame propagation of hydrogen-air mixture at different equivalence ratios were also obtained by Verhelst 2005 [13]. In case of the stoichiometric equivalence ratio, a smooth flame front was presented at different flame radius. When mixture became leaner, the cellular structure at flame front began to occur. However, a smooth flame front was still retained at small flame radius. When mixture became much leaner at about $\Phi=0.4$, a strong cellular flame front appeared at the smaller flame radius. When mixture became richer, there was no cellular structure at the flame front, indicating that the flame remained stable. Comparing with the stoichiometric flame, Lewis number was decreased as flame became lean, indicating the increase of thermo-diffusive instability, while Lewis number was increased as flame became rich, and this resulted in the decrease of thermo-diffusive instability. Expansion ratio was decreased and the flame thickness was increased at both lean mixture and rich mixture. Both factors led to the decrease of hydrodynamic instability. Therefore, when the mixture became lean, the early appearance of the onset of cellular instability was the competition result of the increased thermo-diffusive instability and the decreased hydrodynamic instability. The results indicated that thermo-diffusive instability plays more important role than the hydrodynamic instability does. When mixture became rich, the smooth flame front was the combination of the decreased thermo-diffusive instability and the decreased hydrodynamic instability.

Verhelst et al. 2005 [7] also studied the effect of residual gas on the flame speed of flames at 0.1 MPa, 365 K, and $\Phi=0.8$. This was shown for residual gas concentrations of volumetric

percentages 0, 10, 20 and 30%. Increasing residual gas concentration caused a reduction in flame speed and an earlier transition to cellularity. Hence, diluting with residuals had the same effect on the flame speed and stabilities as dilution has with air. At all values of dilution ratios derived of exhaust gas recirculation (EGR) the Markstein length increased with equivalence ratios. However, all values of Markstein lengths L_b remained negative, except those for the richer mixtures with few residuals. The trend was less strong with increasing residual fraction such that the effect of f_{res} appeared to suppress the effect of equivalence ratio Φ . However, the author reflection was that more data were required.

Considering that obtaining laminar burning velocities u_l or Markstein lengths L_b was not possible at higher pressures due to the early onset of instabilities, Verhelst et al. 2005 [13,7] recorded the flame speed $s_{n,10mm}$ at a flame radius $r=10\text{ mm}$ and divided it by the density ratio $\sigma=\rho_u/\rho_b$ to yield a burning velocity $u_{n,10mm}$. This was applied to a spherically expanding hydrogen-air flames at a range of temperatures T , pressures P , equivalence ratios Φ and varying concentrations of residuals f_{res} of combustion, for $0.3\leq\Phi\leq 1$ ($1\leq\lambda\leq 3.3$), $300\leq T(K)\leq 430$, $0.1\leq P(\text{MPa})\leq 1$ and $0\leq f_{res}(\%)\leq 30$, with f_{res} the volumetric gas content. This burning velocity obtained was not a fundamental parameter (i.e. a burning velocity that would depend only on fuel and operating conditions), but it was considered a “quasi-laminar” velocity. The authors reasoned that “was indicative of the burning rate at a fixed repeatable condition, representing a compromise that involved a sufficiently large radius to minimize the effects of the spark ignition, while being small enough to limit the acceleration due to the instabilities”. As it was also observed in that work, “it is noteworthy that these were of the few data that included the effects of residual gas content, an important parameter given the operating strategies for H₂ICEs”.

The correlation for the burning velocity derived from these experimental data, and partially validated using an engine code, Verhelst&Sierens 2007 [14], is one of the several expressions (including among other the correlations of Milton&Keck 1984 [5] and Iijima&Takeno 1986 [4], as pioneers) that have been analyzed and graphically represented in section 5, for the comparison with other more recent expressions found in the literature.

An alternative methodology proposed to obtain the laminar burning velocity and Markstein lengths at higher pressures, already introduced in sections 3.8-3.10, was derived from high speed Schlieren cinematography of freely expanding spherical flames, Bradley et al. 2007 [45]. Laminar burning velocities, as well as Markstein lengths, had been reported for equivalence ratios from $\Phi=0.3$ ($\lambda=3.3$) up to stoichiometric, and for pressures of 0.1, 0.5 and 1 MPa.

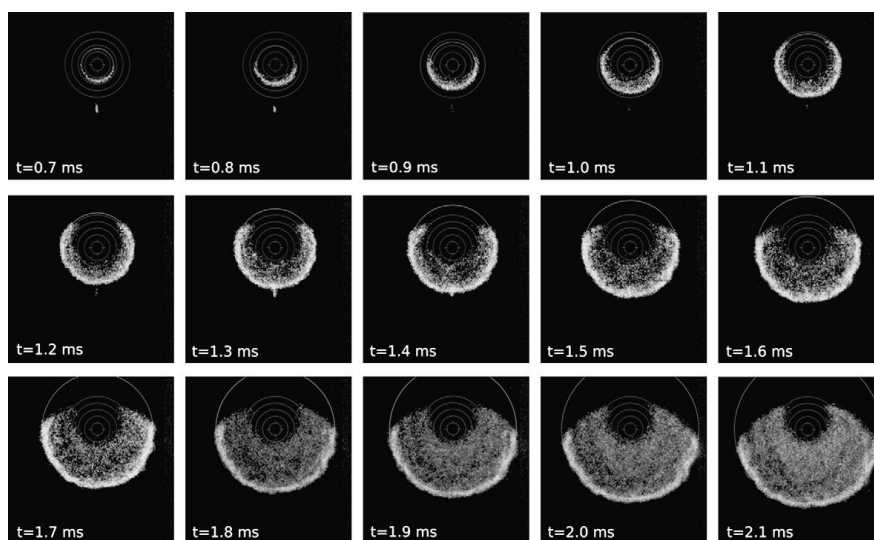
Other authors, as another alternative strategy, although not fully representative of engine combustion conditions, decided to replace the nitrogen in the mixture with helium, resulting in a stable flame from which the un-stretched laminar burning velocity could be measured, Tse et al. 2000 [96], Kwon&Faeth 2001 [97]. In a stability study of hydrogen-air flames, Kwon et al. 1992 [62] indicated the transition of a smooth flame front to a non-regular or unstable one, mainly due to preferential diffusion for mixtures with equivalence ratio $\Phi<1.4$, while for $\Phi>1.8$ mixtures a cellular flame front appeared due to the hydrodynamic instability. The trend to cellular behavior for $\Phi>1.8$ mixtures decreased with equivalence ratio and increased with pressure, Tse et al. 2000 [96].

The characteristics of the ignition systems can also influence the measured value of burning velocity. Some studies showed that flame speeds were independent of ignition energy when flame radius was bigger than about 5 mm. This phenomenon was observed, among others, by Hu et al. 2009 [1], Bradley et al. 2007 [45] and Lamoureux et al. 2003 [117]. By taking into account of the effect of ignition energy and pressure rise in the combustion chamber, some experimental studies consider for analysis only the flame pictures in the approximate range of flame radius 5-25 mm. On the other hand, these more depurated data were also restricted by the

cellular structures that occurred with the increased flame front area and flame speed, Bradley et al. 2007 [45], Hu et al. 2009 [1].

The latter authors, Hu et al. 2009 [1], gave computed Lewis numbers of hydrogen-air flame at different initial temperatures and pressures. Their results showed that Lewis number increased with the increase of equivalence ratio and showed a slight decreasing trend with the increase of initial temperature. The values of Lewis number showed the same trend regardless of the initial pressure. Schlieren images of the expanding spherical flame of hydrogen-air mixtures at different initial pressures, with equivalence ratio $\Phi=0.8$ and $T_{i0}=373\text{ K}$, showed that, up to flame radius of 30 mm, the flame front still remained a smooth surface at an initial pressure of 0.1 MPa. At the elevated pressures, smooth flame surface was presented in the early development. With the flame development, some wrinkles would grow and-or ramify until eventually a cellular structure appeared over the entire flame surface. The onset of cellularity would occur at an earlier position with the increase of initial pressure. Lewis number kept the same value at different initial pressures for the fixed equivalence ratio and initial temperature and it revealed little influence on thermo-diffusive instability from initial pressure. The hydrodynamic instability was related to gas thermal expansion (σ) and flame thickness (δ_f) and, as the density ratio σ remained almost the same value at different initial pressures, thus the remaining parameter that governed the hydrodynamic instability was considered the flame thickness. The increase in hydrodynamic instability with increasing initial pressure resulted from the decrease in δ_f . The combined result of two instabilities led to the enhancement of flame instability with the increase of initial pressure.

One more recent attempt at measuring laminar flame speeds with the goal of deriving a correlation for use in an engine code was reported by Gerke et al. 2010 [2]. They extensively discussed the effects of flame instabilities and demonstrated the resulting complexity of experimentally determining burning velocities through measurements of propagating flames in a rapid compression machine. They measured flame speeds by using OH-chemiluminescence (fig. 26) as well as deriving flame speeds from the pressure rise, for a fairly large range of conditions. The large variability, large error margins and large deviation between optical (OH) and thermodynamic (pressure) results clearly illustrated the problems in obtaining hydrogen flame speeds at engine conditions.



$\Phi=0.66$, $P_{i0}(\text{bar})=13$, $T_{i0}(\text{K})=600$, $\Delta t=0.1\text{ ms}$

Fig. 26. Propagation of hydrogen flame recorded by OH-chemiluminescence (taken from Gerke et al. 2010 [2])

The stability analysis proposed by Bradley et al. 2007 [45] (as reviewed in sections 3.9 and 3.10) was used by Gerke et al. 2010 [2], in similar terms, applied for a correction of the influence of flame front instabilities effects on the measured burning velocities. Thus, the method was based on linear stability theory, assuming an onset of instability for Peclet numbers above a critical value Pe_{cr} , given by a critical flame radius r_{cr} (according to $Pe_{cr}=r_{cr}/\delta_l$ where δ_l was the laminar flame thickness determined by reaction mechanism computations). The instability was assumed to be limited by an upper wavenumber $n_u(Pe)$ and a lower wavenumber $n_l(Pe)$ defining the peninsula of instability as a function of the Peclet number. The flame was considered entirely stable with respect to all wavenumbers for values of Peclet number lower than the corresponding critical value $Pe < Pe_{cr}$.

Also following Al-Shahrany et al. 2005 [68] (as reviewed in sections 3.9 and 3.10) a flame speed enhancement factor was defined, by Gerke et al. 2010 [2], for each value of Peclet number $F_s=(s_n/S_n^*)_{Pe}=[(n_u/n_l)_{Pe}]^{1/3}$. This factor expressed the ratio of flame front speed enhancement by instabilities compared to the laminar flame speed. The approach was based on the assumption that the ratio of unstable values of flame front speeds with instabilities (s_n) and those of stable flame speeds without instabilities (S_n^*) was equal to that of the surface areas. This last designation, S_n^* , in the work of Gerke et al. 2010 [2], corresponds to S in the nomenclature of the present work (sections 3.6, 3.9, 3.10). Values for the wavenumbers limits were also calculated with the theory of Bechtold&Matalon 1987 [49]. Correspondingly, instability-corrected flame speeds $S_n^*=(s_n/F_s)$ were derived at each value of Peclet number, using measurements of unstable propagation speed $s_n=(\partial r/\partial t)$. The onset of cellular flame enhancement was observed at a critical flame radius of $r_{cr}\approx 5\text{ mm}$ for stoichiometric mixtures with initial unburned conditions of $P_u=1.36\text{ MPa}$, $T_u=472\text{ K}$. Fuel-rich flames for $\Phi=1.66$ ($\lambda=0.6$) showed larger critical flame radii about $r_{cr}=6\text{ mm}$. Regarding fuel-lean flames for $\Phi=0.66$ ($\lambda=1.5$) the instability occurred already at $r_{cr}=3\text{ mm}$. The instability-corrected values S_n^* showed a remarkable reduction in the flame front speed. The theoretical stretch-free and stable laminar flame speed was derived by the extrapolation of the stable regime ($\kappa > \kappa_{cr}$) towards zero stretch rate. Velocities presented by kinetic-mechanism (theoretically derived of stretch-free stable flames with $\kappa=0$ and $F_s=1$) predicted analogous values of flame speed that were located even below. A better agreement between computed and measured results was not expected due to the different source of the velocities. However, the discrepancy between all three types of “stable” flame speeds (instability-corrected values S_n^* , extrapolation of stable regime and kinetic-mechanism) and unstable values s_n demonstrated the large influence of instability effects on the level of flame speed.

Gerke et al. 2010 [2] classified the enhancement of flame speed by instabilities and stretch as the ratio u_{ne}/u_L between the measured burning velocities u_{ne} of the unstable flame and the stable flame burning velocities u_L obtained from a kinetic model. Rich mixtures provided the lowest values of the ratio $(u_{ne}/u_L) < 2$. The proportion increased almost linearly towards leaner mixtures, reaching values of about $(u_{ne}/u_L)=4$ at $\Phi=0.5$ ($\lambda=2$). Results were almost identical for optical measurements and thermodynamic analysis. The positive slope of the ratio u_{ne}/u_L for decreasing values of fuel to air equivalence ratio Φ might be explained by intensified thermo-diffusive perturbations for lean mixtures due to Lewis number $Le < 1$.

In summary, a linear stability analysis was applied by Gerke et al. 2010 [2] in order to estimate the magnitude of instabilities and exclude instability effects for selected measurements. The results provided burning velocities of laminar stable flames. The correction method was applicable as long as the critical radius at which the flame speed increased was large enough. However, for increasing pressure levels, the critical flame radius moved towards smaller values and instabilities were present from a very early stage of the flame. The higher the pressure, the thinner was the flame and the less stabilizing was the effect of curvature. Regarding engine

relevant pressure ranges, cellular structures due to hydrodynamic and thermo-diffusive instabilities arose. The definition of stable burning velocities for high-pressure flames, e.g. as provided by reaction mechanism computations or as obtained from instability correction of measured data, was therefore considered questionable.

4.2.2. Quasi-laminar burning velocities

In the last work of Gerke et al. 2010 [2], non-corrected values of “quasi-laminar” burning velocities directly obtained from measurements were presented in the form of a flame speed correlation including dependences of pressure, temperature and equivalence ratio. The experimental results, at high-pressure conditions, on flame speed measurements of “quasi-laminar” burning velocities showed the enhancement of flame speed, with an acceleration effect on the value of laminar burning velocities due to flame front instabilities, and consequently provided higher values of burning velocities than those obtained for smooth laminar flames, which cannot be reproduced by computations with the chemical model (that will be referred to, among others, in section 4.3). Gerke et al. 2010 [2] reasoned that the dataset of “quasi-laminar” burning velocities can be used as an input for turbulent flame speed closure combustion models, because three-dimensional CFD simulations of hydrogen internal combustion engines confirmed better results using unstable “quasi-laminar” flame speed whereas computations with stable laminar flames yielded too low effective turbulent burning velocities, Gerke et al. 2007 [122].

In summary, for engines applications, it is important that measurements of burning velocity are obtained at relevant pressures and temperatures. This is because extrapolations from lower pressures and temperature are unreliable. But, at engine-like pressures, particularly the hydrogen flames are unstable leading to a cellular flame structure from inception onwards, accelerating throughout its growth. The flame speeds increase faster than linearly with decreasing flame stretch rate. Then, the linear relationship between flame speed s_n and stretch rate κ does not longer applies and consequently the methodology of obtaining stretch-free burning velocities u_l (and its dependence on stretch rate) using the linear equations is not directly applicable as observed by Verhelst et al. 2005,2007 [7,13,14], Bradley et al. 2007 [45], Gerke et al. 2010 [2]. The upgraded methodology reviewed in sections 3.8-3.10 (derived from high speed Schlieren cinematography of freely expanding spherical flames) to obtain the laminar burning velocity and Markstein lengths at higher pressures (developed by Bradley et al. 2007 [45] for pressures up to 1 MPa, and also tested by Gerke et al. 2010 [2] at even bigger pressures) involves numerous experiments and very high camera frame rates. Furthermore, as Verhelst&Wallner 2009 [15] have considered, the experimental uncertainty could be rather high, especially on the Markstein lengths, and uncertainties are increasing with the pressure. These are the reasons argued by the authors to consider that there is no such a thing as a classical laminar flame or associated laminar burning velocity, under engine conditions, for hydrogen-air mixtures. And, thus, some of them prefer to define the “quasi-laminar” values, derived in some known conditions, in order to be used for engine applications and models. This option to “quasi-laminar” or apparent burning velocities has been also developed in other works in the literature, also for other types of mixtures like liquid fuels at engine conditions, Tinaut et al. 2012 [123].

4.3. Laminar burning velocities computed by numerical simulation

According to what discussed previously, stable laminar hydrogen-air flames are not likely to exist in engine-like high-pressure combustion environments. The validity of defining corresponding imaginary, artificial values of stable laminar burning velocities as input for

combustion models has been considered questionable experimentally, Bradley et al. 2007 [45]. On the other hand, the failure of steady, planar calculations to predict burning velocities at very lean mixtures is in agreement with values obtained by Williams&Grcar 2009 [124] who showed, through both asymptotic analysis and direct numerical simulation, that a premixed flame front could propagate theoretically when the mixture is leaner than the flammability limit for planar flames. They provided evidence that this was due to the high diffusivity of molecular hydrogen, leading to a propagation mechanism that could be qualitatively seen as the advancement of a collection of sinks of fuel into the fresh mixture. Thus, the high fuel diffusivity would lead to stratification with local fuel-enriched zones. Considering the mostly reduced availability of experimental data of laminar burning velocities of hydrogen-air mixtures at engine conditions, consequently numerical data would have to be considered not validated. This has been considered an area requiring further study, Konnov 2008 [125]. New accurate measurements of hydrogen burning velocities have been therefore considered extremely important for reaction mechanism validation. However, as discussed above, accurate burning velocity measurements at lean conditions were next to impossible because of instability.

In any case, an additional alternative to data of experimental origin is the use of one-dimensional chemical kinetics codes to calculate the laminar burning velocity u_L , that is, to calculate the burning velocity in conditions of a one-dimensional planar adiabatic flame, whose burning velocity is laminar by definition. One of the critical elements for simulation is the appropriate reaction mechanism that can describe the essential fundamental reaction paths followed by the overall reaction. The H_2 - O_2 system has a reaction mechanism that is one of the simplest; it is fairly well known, with more than 100 mechanisms reported in the literature, Saxena&Williams 2006 [126], and computations of laminar burning velocity are reasonably fast. However, even for this simple system, there still exist a number of uncertainties, as reviewed by Konnov 2008 [125]. As the discussions have shown, stretch-free data are scarce, especially at engine-like conditions. Thus, validation of reaction mechanisms has also been very limited. Other alternative approached in other works has been to test reaction mechanisms on the basis of measured auto-ignition times, Williams 2008 [127], Ströhle&Myhrvold 2007 [128].

For this work, selected expressions of laminar burning velocities of hydrogen-air premixed mixtures valid for elevated initial pressure and temperature have been taken from the literature about H_2 SIE research.

Originally these types of expressions were defined mainly by extension of measurements made by using spherically expanding flames, and frequently they were supported mostly in data of combustion bombs plus engines tests and numerical calculations, in a generalized way, both for conventional fuels in normal use and others with potential future. A base of modern actual development of ICEs is the link between the engine testing and the numerical simulation, with one-dimensional and multidimensional thermo-fluid dynamic models commonly used.

4.3.1. Combustion models, thermo-fluid-dynamics analysis, CFD models and chemical kinetic mechanisms

The development of software has reached important computing power levels in recent times. This has made possible combustion models (phenomenological, CFD, etc.), that together with the inclusion of reaction mechanisms allow feasible theoretical solutions to combustion problems. One-dimensional thermo-fluid dynamic models and multidimensional CFD simulation tools have been often used to achieve better knowledge about the phenomena or as an aid in the engine design and optimization procedures through prediction of fluxes. CFD tools are options to simultaneously solve the flow equations and solve or model the chemical reactions. Values of laminar flame speed have to be provided to the CFD-codes in form of tabulated values or

algebraic functions and are taken from experiments or from reaction mechanism simulations using kinetic schemes.

From the discussion on the laminar burning velocity, a number of fundamental questions perhaps remain unresolved, e.g. concerning the effects of instability and about how this carries over to turbulent burning velocity. This has also increased the motivation for the use of multi-zone thermodynamic models as a framework in which hypotheses concerning the nature of flame propagation in engines can be easily tested. Computationally, flame instabilities have been avoided in the literature by the assumption of one-dimensional, planar flames. With this assumption, the accuracy of the calculated burning velocities depends on the accuracy of the molecular transport coefficients, the realism of the chemical kinetic reaction scheme, and the accuracy of the rate constants. The simulation and chemical kinetics analysis were still mostly limited to the condition of atmospheric pressure and room temperature and, only in the recent decade, some works have reported more similarity to engine conditions on numerical study of hydrogen-air flames at elevated initial pressures and temperatures. Mainly in recent time, some numerical works for simulations have used specialized codes and packages. With these ones, the freely propagating adiabatic, premixed, un-stretched planar flames have been simulated. The accelerating effects of flame stretch and thermo-diffusive and hydrodynamic instabilities, which are considered by experimental measurements, are not covered by the kinetic schemes involved.

A short review of references to models and mechanisms, developed and used in literature with numerical studies, is included in this work. These are alternatives to the experimental determinations, with the use of one-dimensional chemical kinetics codes to calculate laminar burning velocities. Some of the burning velocity expressions analyzed in section 5 are derived from simulations performed by these computational tools.

Among the codes used to solve the conservation equations that characterize the combustion phenomena, the CHEMKIN codes software collection, of Sandia National Laboratories, is a much known computational tool for simulation and analysis of complex chemical kinetics, including transport properties, Kee et al. 1985-2004... [129,130;131,132,133]. CHEMKIN codes collection is the most referred to in the bibliography of combustion modeling, mainly from the beginning of 2000s (e.g. Marinov et al. 1996,1998 [134,135], Mosbacher et al. 2002 [136], Rahim et al. 2002 [137], Rozenchan et al. 2002 [138], O'Conaire et al. 2004 [139], Davis et al. 2005 [46], Zhao et al. 2005 [140], Huang&Bushe 2006 [141], Knop et al. 2008 [6], Hu et al. 2009 [1], Bougrine et al. 2011 [142,12], etc.). These are prestigious codes that make possible to compute laminar burning velocities and delay times to auto-ignition. The entry data files format of the simulation program (for reaction mechanism and thermodynamic and transport data bases) has become a standard in combustion area. Sub-models are used for the estimation of the combustion properties.

The equation systems solved by CHEMKIN are complex, with a conservation equation per each one of species in the reaction kinetic mechanism, which have to be introduced by the user. CHEMKIN gives solutions of the laminar burning velocities (u_L), flame temperatures and concentration spatial profiles, obtained by solving mass and energy conservation equations, with the hypotheses, among others, of adiabatic system, uniform pressures and one-dimensional laminar and stationary flow, where the flame area remains constant. This collection of codes includes a set of subroutines, to solve different kinetics problems in gas state. One of them is the Flame Speed Calculator, which is used for laminar premixed one-dimensional flames. In the input file the conditions are specified for calculation of the laminar burning velocity (u_L), the reactants temperature (T_u), the pressure (P) and the different species concentration ($Y_{j,u}$) of the reactive mixture in the flame. The introduction of initial estimates is necessary for the initialization of the differential equations algorithm. Estimates of reactive flux or laminar burning velocity and the flame temperature profile (T_x) have to be introduced, as well as

estimates of products concentration ($Y_{j,b}$) or a balanced composition is generated by the program as initial approximation. A series of parameters, used by the calculation algorithm, have to be also specified in the mentioned entry file, the size of the spatial range and the nodes number of the frame space. Good approximations in the initial estimations are crucial in order to reach the program convergence to the final solution.

In numerical studies in the literature, an important part of simulations was conducted with the related codes CHEMKIN-PREMIX Kee et al. 1985,1989 [129,131], as was used by Hu et al. 2009 [1], who also utilized COSILAB of Rogg 1991 [143], as laminar premixed flame codes where detailed kinetic schemes can be implemented, for instance GRI-Mech (of Frenklach et al. or Smith et al. 1995,1999-2011 [144,145]) or other chemical mechanisms; several ones will be referred to later. The premixed flame code PREMIX, of Kee et al. 1985-2000 [129], is a part of CHEMKIN collection and uses a hybrid time integrating Newton-iteration technique to solve the steady state mass, species and energy conservation equations and can simulate the propagating flame. Equations were sometimes solved, e.g. in Hu et al. 2009 [1], by using the TWOPNT, a boundary value problem solver in the CHEMKIN package. The transport property processor and the gas-phase interpreter that are built in this package provide the species transport properties and process the chemical reaction mechanism.

Among other codes for the laminar burning velocities deductions are FLAMEMASTER of Pitsch et al. 1994-2007 [146], FACSIMILE of Curtis&Sweetenham 1987 [147], the mentioned COSILAB RUN-1DL of Rogg 1993-2006 [148], and CHEM-1D of Somers 1994 [149], that have the advantage of making possible the modeling of the stretch effect on the flame properties. FLAMEMASTER [146] has been used in bibliography references to study the stretch effect on flames both premixed, as Sánchez et al. 2000 [150], and diffusive, as Rao&Rutland 2003 [151], as well to calculate the hydrogen flames Markstein number, Kwon&Faeth 2001 [97]. COSILAB [148] and CHEM-1D [149] obtain simulations of conical or planar geometries of flames, use standard CHEMKIN format for entry files and have been used by several authors as Verhelst 2005 [13], Aung et al. 1997 [114], Wu et al. 1998 [152], for hydrogen or methane diffusive and premixed flames simulation. Particularly the CHEM-1D [149] one-dimensional chemical kinetics code, developed at the Technical University of Eindhoven, was used by Verhelst [13] in his work with hydrogen.

The multi-dimensional CFD codes, as FIRE 2003 [153], FLUENT 2003 [154], STAR-CD [155], or ECFM (Extended Coherent Flame Model) of Colin et al. 2003 [156], perform simulations of combustion processes with complex geometries, and most of them include sub-models to account for the turbulence effects on combustion. A bibliographic revision on simulation methods of the turbulence combustion was made by Hilbert et al. 2004 [157].

New calculation procedures for combustion reactions are often based on the improvement of previous kinetic mechanisms or on the combination of sub-schemes. Simmie 2003 [158] considered the optimization method of Frenklach et al. 1992 [159] as a possible good procedure for the kinetic mechanism construction. This consists of the systematic minimization of the differences between theoretical and experimental results relatives to concentration values, delay time and laminar burning velocity, with the theoretical values calculated through the combustion modeling by the CHEMKIN code. The selection of reaction mechanisms can be made by comparison of the experimental laminar burning velocity results with the values obtained theoretically, by using computing codes, based on the different considered reactions with their respective velocity (kinetic) constants.

Among the reaction mechanisms in the literature, often originated primarily for the oxidation of methane or acetylene, and sometimes developed for more general applications, the following mechanisms can be mentioned by their authors' names: Miller et al. 1982 [160] with

several antecedents; Miller&Bowman 1989 [161], which did not consider initially the pressure influence on the kinetic constants; Warnatz&Maas 1993 [162] (Sandia Corporation) which considered pressures up to 5 MPa, but which required modifications to be used with the CHEMKIN code; Konnov 2000,2004 [163,47] (Brussels University), a mechanism that incorporated many reactions and species, considered the pressure influence on the kinetic constants, included reactions to model the oxidation of hydrocarbons with 2-3 atoms of carbon, having a CHEMKIN format disposition together with transport and thermodynamic data files, and that was a mechanism constructed by comparison with a big quantity of experimental data; Hughes et al. 2001 [164] (by Leeds-UK and other universities), a mechanism also in a CHEMKIN format that took into account the pressure influence on the kinetic constants, although the data base of transport properties is not given. Some modeling workgroups such as the Resources Research Institute in the University of Leeds have preferred to use the multi-component transport option, with difference to e.g. Lawrence Livermore National Laboratory group [165], that use the mixture-averaged transport properties, as indicated by Hu et al. 2009 [1].

Of the mentioned mechanisms, there have been many references in the literature to the mechanism of Miller&Bowman 1989 [161], among the oldest, and the Leeds mechanism of Hughes et al. 2001 [164], among the modern ones, and the due to the Gas Research Institute, the already mentioned GRI-Mech (of Frenklach et al. or Smith et al. 1995,1999-2011 [144,145], as reference examples of some releases along years) which is a sample of a kinetic mechanism, with important impact, commonly cited in the literature. Some mechanisms as the Leeds one and the very interesting of Konnov 2000,2004 [163,47] have been constructed following the Frenklach [159] philosophy. Others, as the one proposed by Davis et al. 2005 [46], for combustion of mixtures H₂-CO-O₂, use many kinetic constants proposed in GRI-Mech.

The GRI-Mech [144,145] mechanisms account for the pressure influence on the kinetic constants. The authors provide thermodynamic and transport data bases, with information of specific heats, enthalpies and formation entropies, viscosities and mass and thermal diffusivities of all chemical species in the kinetic mechanism. The construction was also carried out following the mentioned method of optimization proposed by Frenklach et al. 1992 [159], in a wide range of combustion conditions, up to temperatures of 2500 K and pressures of 1 MPa, approximately, for lean and rich mixtures of different hydrocarbons and several gas hydrocarbons-air mixtures.

Since the pioneering introduction of kinetic modeling to describe experimental flames at low pressures, as by Dixon-Lewis&Williams 1963 [166] at 0.1 MPa, there have been computations of H₂-air laminar burning velocities based on detailed chemical kinetic modeling. Combustion at higher pressures was modeled in these other works: Dixon-Lewis 1984 [167]; Warnatz 1981 [168] (reaction mechanism for H₂-O₂-N₂ mixtures of 18 elementary reaction steps involving nine species, considering concentration, pressure and temperature dependence of the burning velocity); Maas&Warnatz 1988 [169] (extended version of 37 steps to investigate the ignition process); Yetter et al. 1993 [170] (reaction mechanism for CO-H₂-O₂ mixtures of 28 steps involving 13 species); Marinov et al. 1998 [135] (reaction mechanism for H₂-O₂ system to combustion of H₂ under ICE conditions, 20 reaction steps involving nine species). None of these approaches involved modeling of instabilities. Different weakly stretched flames were studied computationally by Sun et al. 1999 [59], based on the detailed chemical kinetics of Kim et al. 1994 [71].

Among the more specific chemical kinetic calculation models for hydrogen other works can be cited additionally: Burks&Oran 1981 [171]; O'Conaire et al. 2004 [139] (descendent of reaction mechanism of Yetter, more relevant for pressures close to atmospheric conditions, although with a wide pressure range including higher pressures); Konnov 2000,2004... [163,47] (refinement of kinetic mechanism of hydrogen combustion for wider ranges more relevant to ICE conditions), etc. The hydrogen mechanisms of O'Conaire and Konnov are both optimized, detailed chemical reaction mechanisms with, respectively, 19 and 21 elementary chemical reactions with associated rate coefficient expressions and thermo-chemical parameters for ten

species in the calculation of hydrogen chemical reaction process. The ranges of O'Conaire mechanism are between 298-2700 K in temperature, 0.05-87 atm in pressure and 0.2-6 in fuel to air equivalence ratio. These reaction mechanisms of O'Conaire and Konnov, which will be later considered among others, are very interesting in the applications developed in recent years, e.g. with refinements and revisions made by Konnov in some years (2000-2008) with an increasing scope.

4.3.2. Laminar burning velocities of hydrogen-air mixtures calculated by numerical methods, based on chemical kinetic mechanisms and related to combustion models

Some of the expressions of burning velocities published in the literature were constructed by their authors in origin in relation to several models applied to hydrogen engines. There are burning velocity correlations related to multi-zone thermodynamic models, for instance: Verhelst&Sierens 2003, 2007 [10,14], with the reaction mechanisms of Yetter et al. 1993 [170] and O'Conaire et al. 2004 [139]; D'Errico et al. 2008 [11], with the kinetic chemical code DSMOKE of Frassoldati et al. 2006 [172] or Safari et al. 2009 [173], etc. Other correlations that are related to computational fluid dynamics (CFD) models, were obtained by Knop et al. 2008 [6], Wimmer et al. 2005 [174], Messner et al. 2006 [175], Gerke et al. 2006,2010 [176,2], etc. Special mention will be done later to the work of Verhelst et al. 2011 [3], with the reaction-mechanism of Konnov 2004 [47] already cited. All these works are briefly commented in the following paragraphs.

Regarding the available existing expressions of the laminar burning velocity of hydrogen-air mixtures, related to thermodynamic models and based in previous works, Verhelst&Sierens 2003,2007 [10,14] considered the wide operation range of a H₂SIE. In particular, they performed a series of laminar burning velocity calculations by using the one-dimensional chemical kinetic code CHEM-1D, including the reaction mechanism of Yetter et al. 1993 [170]. Calculations of the power cycle of a hydrogen-fueled engine by using a quasi-dimensional two-zone combustion model framework were also reported, Verhelst 2005 [13]. The models predicted the effects of both compression ratio and ignition timing, but did not always predict well the effects on equivalence ratio. The velocity correlation was then used with a number of turbulent burning velocity models, comparing simulations to measurements on a hydrogen-fueled cooperative-fuel-research engine for varying compression ratio, ignition timing and equivalence ratio.

Other results for the laminar burning velocity of hydrogen mixtures had been reported in Verhelst 2005 [13], calculated for one-dimensional flames with chemical kinetics codes, comparing several published reaction mechanisms. First, these results of laminar burning velocities were based on the reaction mechanism of O'Conaire et al. 2004 [139] that were initially chosen because of a better correspondence with selected experimental data at atmospheric conditions. Secondly, calculation results were compared with the experimental results from Verhelst et al. 2005 [13,7] for a range of pressures, temperatures, equivalence ratios and residual gas fractions. In spite of that, these experimental results for comparison were not stretch-free burning velocities and the authors reported that the calculations break down for very lean mixtures and higher pressures. The effects of temperature and dilution with residuals were reported, being predicted reasonably well for moderately lean to stoichiometric mixtures. The authors concluded that simulations of the effect of residuals could thus be considered to replace experiments with residuals. This was an important conclusion, because the possibility of EGR consideration in the expressions was stated almost only by these authors.

D'Errico et al. 2008 [11] tried to extend the range of possible conditions determined by Verhelst in their primary works up to 1.6 MPa, with particular concern to the maximum allowed pressure, and performed similar calculations of laminar burning velocities computed by means

of the detailed kinetic chemical code DSMOKE, developed at Politecnico di Milano, by using a 21 reaction mechanism of Frassoldati et al. 2006 [172]. They reported full-cycle simulations using one-dimensional gas dynamic calculations combined with a quasi-dimensional combustion model, for a hydrogen engine with cryogenic port injection. The gas dynamic algorithm was adapted in order to add the injection and transport of cryogenic hydrogen along the intake ducts. The methodology proposed by Verhelst&Sierens was used to build a correlation for the laminar burning velocity from chemical kinetic calculations using an in-house reaction scheme. The combustion pressure was not fully predicted, with better result for stoichiometric and moderately lean mixtures, but less satisfactory for very lean conditions at medium to high engine speeds. The authors attributed this response to the effects of differential diffusion and instabilities for these very lean conditions and the high ratios of turbulent to laminar burning velocities reported for these mixtures, which were unaccounted for in the combustion model.

Regarding the analysis of engine processes, multidimensional CFD models are used in the literature using sometimes sophisticated combustion models such as the Turbulent Flame Speed Closure of Zimont&Lipatnikov 1995 [177]. CFD simulations have been used e.g. by Wimmer et al. 2005 [174], Messner et al. 2006 [175], Gerke et al. 2006 [176], to investigate the mixture formation and combustion in direct injection engines. The laminar burning velocity was obtained sometimes from chemical kinetic calculations using the reaction scheme of O'Conaire et al. 2004 [139], neglecting the influence of residual gas. The prediction of the flame propagation and rate of heat release corresponded well with measurements obtained on an optical engine. As we have observed in section 4.2, Gerke et al. 2010 [2] have also reported burning velocity calculations using the scheme of O'Conaire et al. 2004 [139], and they have compared these to experimental results. Their measured unstable burning velocities and the "stable" burning velocities derived from linear stability theory were both higher than the values computed with the chemical kinetic scheme.

In this context, Knop et al. 2008 [6] discussed the problems of finding a suitable correlation for the laminar burning velocity and proposed a correlation for use in an engine code based on published experimental results, largely based on the correlation of Verhelst et al. 2005 [13,7] but extended to rich mixtures (through chemical kinetic calculations, based on GRI-Mech version 3.0 [144], by means of PREMIX and CHEMKIN [129,131]) to allow computations of stratified combustion in direct injection engines. A limited validation of the correlation was reported by comparison between simulated and measured engine cycles.

Another important contribution, in the paper by Knop et al. 2008 [6], was an extended Zeldovich model of which the reaction rate constants were adapted for hydrogen combustion, based on the work of Miller&Bowman 1989 [161]. The resulting CFD model was validated for both an engine with cryogenic port injection and a direct injection engine. The detailed mixture distribution obtained from the CFD simulations was used to explain the sensitivity of flame propagation and NO_x formation to mixture heterogeneity. In the work of Knop et al. 2008 [6] the three-dimensional CFD modeling of combustion and pollutant prediction was made by modification of the Extended Coherent Flame Model (ECFM) 2003 [156], adapted to hydrogen combustion through the addition of a new laminar flame speed correlation and a new laminar flame thickness expression. The extended Coherent Flame Model (CFM), able to simulate both homogeneous and stratified configurations, is known as the Extended Coherent Flame Model (ECFM). The adaptation of such a model to hydrogen combustion was performed by accounting for its peculiar properties, laminar flame speed, laminar flame thickness, etc. According to Knop and co-authors, the combustion of hydrogen produces nitrogen oxides, as only one regulated pollutant emission because it is carbon free, and these were classically modeled based on the extended model Zeldovich et al. 1947 [178]. Nevertheless, this model assumes the independence of the chemistry leading to NO_x formation on the instantaneous fuel consumption and therefore on the fuel nature to some extent. Knop proposed, consequently, to adapt the constants of the

Arrhenius expressions in the Zeldovich model, generally defined for hydrocarbons. The adapted models were validated by modeling two different engine configurations producing two widely different combustion conditions. The CFM, aimed to the modeling of premixed flame combustion, relies on the use of relations for the laminar flame speed and thickness, depending on the fuel, to avoid the direct chemistry resolution. It is well adapted to the flamelet regime in homogeneous mixtures and assumes that the fuel oxidation occurs in a very thin layer that separates fresh from burned gases and propagates towards fresh mixture. The extension of this model, leading to the ECFM, is aimed to represent better the local fresh gas conditions in order to be able to simulate also operating conditions with stratified conditions. The addition of the conditional averaging technique, Colin et al. 2003 [156], allowed to compute more accurately the fresh gas state and consequently to evaluate with more precision the local laminar flame speed and the local laminar flame thickness. Only a few experimental data were available to establish the effect of temperature on the laminar flame speed of hydrogen; moreover, these data of Iijima&Takeno 1986 [4], Verhelst et al. 2003 [10], corresponded to a quite narrow range of temperature (298-550 K). Therefore, several kinetic mechanisms, O'Conaire et al. 2004 [139], Miller et al. 1982 [160], Kee et al. 1990 [131], were tested in order to have more data to evaluate the correlations and to investigate their predictions beyond 550 K.

In accordance with the reviewed information, the validation of reaction mechanisms has been described by several authors as very limited because of the scarcity of experimental data at engine-like conditions. Accurate burning velocity measurements at lean conditions are almost impossible, because of the existence of instabilities and also due to the insufficiently representative stretch-free data.

The values of laminar burning velocities (u_L) computed from the kinetic schemes of both Konnov 2004 [47] and O'Conaire et al. 2004 [139], among others, are very recognized in literature. Bradley et al. 2007 [45] compared their stretch-free experimentally determined data of measured laminar burning velocity, for fuel to air equivalence ratios (Φ) between 0.3 and 1, at pressures of 0.1, 0.5 and 1 MPa, to calculations using respectively the reaction mechanisms of O'Conaire et al. 2004 [139] and Konnov 2004 [47]. The results using the scheme of Konnov were reported as the best ones compared to the experimental results, within the rather large uncertainty bands, with uncertainties quite large at the higher pressure. The experimental values were closer to the values computed with the scheme of Konnov but tended to be increasingly high as the pressure increased, although the stoichiometric values were better predicted. On the assumption that there is an inverse dependence of laminar burning velocity upon pressure (P), which can be expressed as u_L being proportional to a negative power P^{-q} , the experimental values of the pressure exponent q at the different values of fuel to air equivalence ratio (Φ) were given, with experimental error margins. The scheme of Konnov gave values of q that were quite close to the experimental values, though smaller than these ones, over the full range of values of Φ . At low values of Φ the scheme of O'Conaire et al. gave significantly lower values of q . The error bands on both Peclet numbers Pe_{cl} and Markstein numbers Ma_{sr} increased with pressure. In practice, the authors considered the problem not so severe, because instabilities were considered suppressed in increasingly more turbulent flames, Al-Shahrany et al. 2006 [69]. Thus based on their studies, the reaction kinetic scheme of Konnov 2004 [47] was chosen by Bradley et al. 2007 [45] and also by Verhelst et al. 2011 [3] for the calculation of the laminar burning velocity of hydrogen mixtures, as potentially and hypothetically the only scheme (partially) validated at elevated pressures, using stable burning velocities, at least until the dates of those works.

References of chapters three, four and five (*after the fifth chapter*)

5. Analysis of laminar burning velocity expressions for hydrogen-air mixtures at engine-like conditions

- 5.1. Summary of methodologies used in the literature works
- 5.2. Homogenization of notation of laminar burning velocity expressions of the reviewed works
- 5.3. Analytical expressions of laminar burning velocities
- 5.4. Ranges of applicability of expressions
- 5.5. Graphical representation of results in the applicability ranges of laminar burning velocity expressions
- 5.6. Analysis of results of laminar burning velocity expressions
 - 5.6.1. General analysis
 - 5.6.2. Particular analysis of expressions of laminar burning velocity
 - 5.6.3. Behavior of laminar burning velocities calculated from chemical kinetics mechanisms on basis of theoretical one-dimensional flames

References of chapters three, four and five (*third part*)

5. Analysis of laminar burning velocity expressions for hydrogen-air mixtures at engine-like conditions

This section covers in detail the applicability of laminar burning velocity expressions for hydrogen-air mixtures in engine-like conditions, with comparisons among different selected expressions, in their respective ranges of validity.

Each particular methodology for achieving the expressions has been reviewed in [table 10](#), based on experimental procedures, numerical simulation methods or combined methodologies.

5.1. Summary of methodologies used in the literature works

[Table 10](#) presents a summary of published studies relative to selected expressions of laminar burning velocity for hydrogen-air mixtures. The table includes information about experimental methods, apparatus and data recording, chemical mechanisms and chemistry computations when used, numerical calculation-simulation methods and computational procedures based on thermodynamic analysis, and references to some applications on computational thermo-fluid-dynamic models and multi-zone engine models, etc. There are also comments on whether the flame stretch and instabilities are or not accounted for and other observations of interest such as whether the residual gas fractions are or not included in each expression.

Table 10Summary of particular characteristics of the methodologies used in the definition and some applications of reviewed expressions of laminar burning velocity for **hydrogen-air mixtures**

Ref. Year Authors	Experimental apparatus and obtained data or-and numerical calculations-simulations	Computational applications (<i>Thermodynamic analyses, multi-zone models or-and computational thermo-fluid-dynamic models</i>)	Chemistry computations (<i>Chemical mechanisms- schemes</i>)	Flame stretch accounting	Instabilities accounting	Comments (<i>Additional models for comparison, residual gas fractions, flame thickness expressions, inner-layer temperature, etc.</i>)
[5] 1984 Milton -Keck	Experimental procedure. Spherical constant volume combustion bomb 152.5 mm inner diameter, central ignition system, piezoelectric pressure transducer readings and He-Ne laser shadowgraph system to check the flame radius.	Numerical calculation with gas and transport properties, only in stoichiometric conditions. Based on works of Metghalchi&Keck 1980,1982 [27,28], Ryan&Lestz 1980 [29], Rallis et al. 1965 [24], etc. Formulation only for stoichiometric cases.	-	Not regarded.	Not considered.	- Comparisons with theoretical calculations, near atmospheric conditions, of Warnatz 1981 [168]. - Complete combustion approximation 0.35H ₂ O steam + 0.65N ₂ (no sign of water condensation within the engine combustion chamber) Initial atmospheric conditions in combustion bomb makes impossible to use water vapor in proportion of residual gases. Mixture of 0.15CO ₂ + 0.85N ₂ for simulation. - Effect of diluting stoichiometric H ₂ -air mixtures with residual gases comments, but non-included residual gas fraction in the defined expression.
[8] 2008 Lafuente	Experimental procedure. Constant volume combustion vessel with pressure transducer readings; spherical combustion bomb 200 mm diameter, centrally ignited, with spark ignition between two electrodes. Capable of withstanding pressures up to 200 bar for mixtures at initial conditions up to 25 bar and upper of 600 K.	Experimental and numerical-graphical calculation. Two-zone quasi-dimensional model. Analysis of overlapping curves (for different flame front radii at the same pressures and temperatures in initial conditions). Correlation only for stoichiometric cases.	-	Stretch accounting at low pressure.	Instabilities onset at the beginning, with cellularity when pressure increases from low values.	- Reduced ranges of <i>P</i> and <i>T</i> . - No consideration of residual gas factor in the correlation.
[4] 1986 Iijima- Takeno	Experimental procedure. Spherical bomb with pressure transducer readings, 160 mm inside diameter and central ignition system. Data at the later stage, when the flame is propagating far from the origin, to try to avoid the effects of flame front curvature and thickness.	Numerical calculation based on theoretical study of Takeno&Iijima 1981 [179], Metghalchi&Keck 1980,1982 [27,28]. Quasi-steady flame surface model. Non-controlled initial <i>T</i> of mixture and data obtained no necessarily covering the whole ranges of <i>P</i> for fixed values of <i>T_i</i> , and vice versa (of <i>T_i</i> for fixed values of <i>P</i>).	Burning velocities correlated by an Arrhenius form expression, based on the one-dimensional flame theory with a one-step kinetics reaction model, to yield the apparent order and activation energy of the overall reaction.	Not regarded. Data readings for flame front far from the origin to try to avoid curvature.	Not considered. A very severe instability appeared in temporal <i>P-t</i> chart when <i>P</i> ~6 bar (<i>P</i> = 5 to 7 <i>P₀</i>)	- Comparisons with theoretical calculations of Liu&MacFarlane 1983 [110], Andrews&Bradley 1972 [105], close to atmospheric conditions. - The calibration of laminar burning velocity correlation did not account for the effects of stretch and instability. This grew stronger with pressure as the flame thickness decrease. - No consideration of residual gas factor in the correlation.
[9] 1992 Göttgens et al	Numerical calculation (not experimental). Theoretical premixed flame laminar burning velocity defined as the normal propagation velocity of a plane, undisturbed flame without heat loss and buoyancy effects. Assumption of an infinitely thin inner layer into which the radical consumption is embedded upstream. In this limit only two layers of finite thickness: the preheat zone and the oxidation layer. (Excluded laminar burning velocities less than 5 cm/s).	Geometrical procedure in origin, applied to experimentally obtained data and numerically calculated mass fractions and temperature profiles based on the lean premixed flames structure asymptotic analysis of Peters&Williams 1987 [44], Peters&Rogg 1992 [180], with kinetic data and transport properties, in different lean to stoichiometric conditions.	Detailed kinetic mechanism of 82 elementary reactions scheme for starting. Modified version of numerical code for flamelet structure of premixed flames.	-	-	- Defined and determined the inner layer temperature <i>T⁰</i> (inflection point of the temperature profile, at the maximum temperature gradient in the flame, where radical production equals radical consumption, which happens at the transition from the radical consumption layer to the broader fuel consumption layer) function of pressure, proportional to the square root of the mass fraction of the fuel in the unburned gas, relative to the equivalence ratio. - Determined adiabatic flame temperature <i>T_b</i> independent of pressure. - Flame thickness classical definition of the assumed chemically inert preheat zone (spatial coordinate <i>x</i> -interval spanned by the steepest tangent to the temperature profile between the unburned <i>T_i</i> and adiabatic temperature <i>T_b</i>). Thickness correlation is not applicable to hydrogen flames since the preheat zone is not chemically inert. - No consideration of residual gas factor in the correlation.
[10] [13] 2003- 2005 Verhelst- Sierens	Numerical simulation, calculation of one-dimensional laminar flames. Burning velocities correlated by Arrhenius form expression, based on one-dimensional flame. Chem 1D 2.0 with Yetter mechanism; Chem 1D 3.0 with O'Conaire mechanism.	Calculation based on works of Somers 1994 [149], Qin et al. 2000 [181], Egolfopoulos&Law 1990 [38], with a simulation code Chem1D developed to calculate thermodynamic gas and transport properties with reaction mechanism. Parameters of mixture composition (of fuel, oxidizer, bath-gas, residuals and fuel to air-equivalence ratio) and transport model parameters (diffusion velocities, Lewis numbers...) and inlet initial conditions of <i>P</i> , <i>T</i> .	One-dimensional chemical kinetic code Chem1D 2.0, 3.0, using the chosen reaction mechanism. Chem1D 2.0 with Yetter mechanism; Chem1D 3.0 with O'Conaire mechanism.	-	-	- Pointed out a strong interaction between the effects of equivalence ratio and pressure. - Comparisons of reaction mechanisms: Warnatz 1981 [168], Maas&Warnatz 1988 [169], Marinov et al. 1996,1998 [134,135], Yetter et al. 1993 [170], O'Conaire et al. 2004 [139]. - A function of the residual gas factor is considered (explained in section 5.3).

[11] 2008 D'Errico et al	Numerical and experimental research work, to evaluate the thermodynamic and chemical gas properties inside combustion chamber, carried out on a single-cylinder research four-valve SIE (cryogenic port injection) fueled with gaseous hydrogen, equipped with an indirect pulsed injection system and pressure transducers and sensors. Predictive simulation model validation completed comparing results with experimental data of in-cylinder pressures for naturally aspirated engine conditions.	Calculations based on previous works D'Errico et al. 2002,2005,2006 [182,183,184] regarding the transport of chemical species in cryogenic conditions. Values fitted into the correlation of Verhelst&Sierens 2003 [10] (developed with the one-dimensional chemical kinetic code Chem1D of Somers 1994 [149] using the reaction mechanism of Yetter et al. 1993 [170]). Simulation of SI hydrogen fueled engine, on the basis of an extended data-base for laminar burning velocities in wider ranges of pressures.	Detailed one-dimensional chemical kinetic code DSmoke (with calculations using the mechanism of Frassoldati et al. 2006 [172]) and with in-house reaction scheme kinetic scheme proposed by Ranzi et al.	-	-	<ul style="list-style-type: none"> - Kinetic mechanism tested in order to have more data to evaluate correlations and to investigate their predictions beyond 16 bar. It has been applied to acquire a significant database for the laminar flame speeds over a wide range of equivalence ratios, T and P. - This extension of the correlation of Verhelst&Sierens 2003 [10] does not seem completely valid for values at pressure higher than 16 bar. - The modeling of cryogenic injection of hydrogen was investigated by the GASEDYN code, introducing the fluid dynamic transport of chemical species. 1D thermo-fluid dynamic simulation code GASEDYN + quasi-D multi-zone combustion model. - The residual gas factor is considered according to the adapted expression of Verhelst&Sierens 2003 [10] but for mass fraction instead of hypothetically volumetric fraction defined by [10].
[7] [13] [14] 2005- 2007 Verhelst et al	Experimental procedure. Spherical, stainless steel vessel bomb (380 mm diameter) with central spark ignition and optical access (three pairs of orthogonal windows of 150 mm diameter), flame images captured by Schlieren cinematography using a digital camera. Capable of withstanding temperatures and pressures generated from explosions with initial pressures up to 15 bar and initial temperatures up to 600 K.	Measurements of spherically expanding hydrogen-air flames to determine the influence of initial T , P , Φ and residual gas content of combustion on the burning velocity and effects of flame stretch rate. Based on works of Bradley et al. 1996,1998 [25,26], Gillespie et al. 2000 [22]. (The laminar burning velocity obtained does not correspond to a steady, planar ideal computation with perfect thermodynamics, transport and chemical kinetics.)	-	This procedure applies only in the linear range, at low stretch. It is only an estimation of u_l .	Cellularity was reported for high-pressure flames with $P > 5$ bar due to flame instabilities.	<ul style="list-style-type: none"> - Flame speeds, $s_n = \partial r / \partial t$, were calculated from the mean flame radii, r, obtained from measurements of flame projected area. Un-stretched flame speed in the absence of instabilities (S_u), un-stretched laminar burning velocity ($u_{l,0}$) and effect of flame stretch rate (κ), were derived from the flame speed. The total stretch rate on a stable, non-cellular, outwardly propagating flame $\kappa = 2s_n/r$, and a linear relationship were quantified by a burned gas Markstein length (L_b). - S_u was obtained as the intercept value of s_n at $\kappa=0$ in the plot of s_n against κ. The un-stretched laminar burning velocity was obtained from $u_s = S_u / (\rho_u / \rho_b)$, where ρ are the densities, and the subscripts refer to the unburned and burned products respectively.
	Experimental pressure data. Single cylinder hydrogen engine. Spherically expanding flame. Laminar burning velocities are derived at a flame radius of 10 mm by means of optical analysis of the flame front using Schlieren technique. Flames at sufficiently small flame radii ($r < 10$ mm) are recorded in order to limit the acceleration due to instability effects.	Measurements of unstable burning velocities obtained under initially quiescent conditions, with burning velocity models. A simulation program developed to calculate the pressure and temperature development in hydrogen engines. Partially validated using an engine code, a quasi-dimensional two-zone combustion model framework for the power cycle of H ₂ /ICE.	-	Correction of stretch effects was applied to measurements at low initial pressure conditions ($P < 5$ bar).	Laminar values of burning velocity at measurements conditions are not possible to be obtained because of flame instabilities.	<ul style="list-style-type: none"> - Difficulties in obtaining stretch-free laminar burning velocities. It was not possible to obtain u_l or L_b due to the early onset of instabilities. Proposed correlation based on measurement of cellular flames $u_{l,nc}$ = stretched cellular burning velocity. This burning velocity is not the ideal laminar velocity. "It is indicative of the burning rate at a fixed, repeatable condition, representing a compromise that involves a sufficiently large radius to minimize the effects of the spark ignition, while being small enough to limit the acceleration due to the instabilities". - These were the only data, at its time, that include the effects of residual gas content.
[6] 2008 Knop et al	Experimental data and CFD simulation tools. Published experimental results for data. For limited correlation validation in single cylinder H ₂ fueled ICEs (cryogenic port injection/direct injection)	Numerical calculation based on works of Iijima&Takeno 1986 [4], Milton&Keck 1984 [5] Verhelst et al. 2003,2007 [10,7,13,14], etc. 3D-CFD code for modeling of combustion in combination of the correlation form like Verhelst et al. 2005,2007 [7,13,14]. Several kinetic mechanisms tested in order to have more data to evaluate correlations and to investigate their predictions beyond 550 K.	Chemistry computation by PREMIX and CHEMKIN-II [129,131]. Based on chemical kinetic calculations GRI-Mech 3.0 [144].	-	-	<ul style="list-style-type: none"> - Comparisons of reaction mechanisms: O'Conaire et al. 2004 [139], Miller et al. 1982 [160], Kee et al. 1989 [130,131] CHEMKIN-II, Colin et al. 2003 [156] ECFM adapted to hydrogen combustion through the addition of a new laminar flame speed correlation and a new laminar flame thickness expression. - u_l by chemical kinetic calculation, with a model based on Verhelst data ($u_{l,c}$) and correlation, but extended to equivalence ratio $\Phi > 1$ to allow computation of stratified combustion in direct injection engines (with locally rich mixtures). - Flame thickness function of parameters P, T, Φ, in limited ranges (section 3.7). - Residual gas factor considered according to the expressions of Verhelst et al. 2005,2007 [7,14].
[45] 2007 Bradley et al	Experimental and numerical study. Spherical stainless steel bomb equipped with three pairs of orthogonal windows of diameter 150 mm. Internal bomb radii of sphere around 190 mm. Gas temperatures from sheathed thermocouple. Pressures measured during the explosion with a pressure transducer. A central spark plug was used with ignition energies of about 26 mJ, supplied from a 12 V transistorized automotive ignition coil. Flame images were captured by Schlieren cine cinematography to obtain flame speeds and by shadowgraphs to obtain values of the critical cellular Peclet number Pe_c . A digital camera at various resolutions and frame rates, depending on the burning rate of the mixture.	Calculations of flame speeds, from the mean flame radii, obtained from measurements of the flame projected area. Laminar burning velocities and Markstein lengths at higher pressures, from the high speed Schlieren cinematography of freely expanding spherical flames. The influence of hydrodynamic and thermo-diffusive instability was considered using linear stability theory.	Applications of a one-dimensional chemical kinetics code. Calculations using the reaction mechanisms of both O'Conaire and Konnov.	Comparison of stretch-free experimentally determined data of laminar burning velocity at 5 and 10 bar.	At increasing pressure, the onset of instability is shifted to very small flame radii ($r < 1$ mm) so that a stable regime could not be measured.	<ul style="list-style-type: none"> - H₂-O₂ kinetic schemes of both Konnov 2004 [47] and O'Conaire et al. 2004 [139]. The latter scheme was based on the latest version available from the Lawrence Livermore National Laboratory [165] Web site. The chemical kinetic code was the release 3 of the Chem1D [149] code, developed at Eindhoven by De-Goeij and co-workers in Combustion Technology group [185]. This includes an exact solution of multicomponent transport, based on the EGLib library [186]. The values obtained with the two schemes were in good agreement with each other at these pressures, but they tended to be somewhat lower than the experimental values, particularly at the leaner conditions. - Laminar burning velocity data calculations without an explicit analytical correlation.

[1] 2009 Hu etal	Experimental and numerical study. Constant volume cylindrical combustion chamber with high speed Schlieren cinematography. Capable of withstanding temperatures and pressures generated from explosions up to 100 bar with initial temperature up to 500 K.	Mixture-averaged transport properties are used. Except the high temperature conditions, the correlated laminar burning velocities and data results show good agreement between the computed results, simulated by CHEMKIN-PREMIX code [131,129] and experimental data. The calculation was extended to initial pressure and temperature up to 80 bar and 950 K by using of CHEMKIN and the model under different initial conditions.	Compared Kinetic Chemical reactions: O'Conaire et al. 2004 [139] 1D chemical kinetic code (for P influence study) and GRI-Mech [144].	Markstein lengths at limited conditions, with stretch correction.	No consideration for instabilities in experimental method.	<ul style="list-style-type: none"> - Laminar burning velocities correlated only for stoichiometric conditions. - Sensitivity analysis and flame structure analyzed. Laminar burning velocities and Markstein lengths were obtained at limited elevated pressures-temperatures. - Un-stretched flame speed derived from stretched flame propagation speeds obtained by measurements of flame radius in Schlieren photographs. - Correlated empirical formula of laminar burning velocity $u_s(T_w, P_w) = S_{s,0} / (\rho_w / \rho_b)$. - Diluent gas (Air+H₂+N₂) regarded but no factor of residual gas fraction considered in the laminar burning velocity correlation.
[2'] 2010 Gerke etal	Premixed hydrogen-spherical air flames investigated in a single-cylinder compression machine adapted to spark ignition, with optical access of 45 mm diameter. Hydrogen centrally injected combustion chamber, with pressure transducer readings, axially symmetric with a plain cylinder head and a bore of 84 mm. Large flexibility regarding initial conditions and compression ratio and capable to withstand in-cylinder pressures up to 200 bar. Flame speed measurements using both OH-chemiluminescence high-speed CCD camera and in-cylinder recorded pressure analysis. Optical access limited to flames up to 40 mm.	Experimental procedure. Optical and thermodynamic analysis. Values of burning velocities calculated from flame front velocities regarding thermal-expansion effects. Temperatures of burned-unburned gas zones calculated by means of a zero-dimensional model, using accurate calorific properties. An in-house engine cycle simulation program was used to model the burned and unburned zones of the combustion event by a two-zone approach, with thermodynamic analysis of pressure traces to determine temperature, density and burning rate. The experimentally observed flame speed was compared to laminar burning velocities of a stable one-dimensional model flame, provided by computations with a detailed kinetic scheme. An evaluation of stretch and instability effects by comparison to fundamental laminar burning velocities of the one-dimensional flame computed with the chemical kinetic-mechanism.	Chemical kinetic calculations using the mechanism of O'Conaire et al.	Experimental data non-corrected for the effects of stretch.	Experimental data non-corrected for the effects of instabilities.	<ul style="list-style-type: none"> - Three dimensional model of combustion chamber geometry-half-spherical approximation of the flame. - The "quasi-laminar" burning velocities measured in the experiments include instability and stretch effects and depict "area-weighted" burning velocities after the onset of instability. The results obtained differ from predictions of kinetic models. The models predict theoretical values for burning velocities of smooth stable flames. The enhancement of flame speed is derived of the flame front instabilities. - One-dimensional simulations using the detailed kinetic schemes without such effects. - A function of residual gas factor is considered, according to the expressions of Verhelst et al. 2005,2007 [7,14].
[2] 2010 Gerke etal + O'Conaire etal	Both different measurement methods, OH-chemiluminescence and pressure analysis, show a fair agreement between the results for a wide range of measurement conditions at $s_{tr} < 20m/s$. For strong flame front instability effects, and $s_{tr} > 20m/s$, a substantial variability of the replicated measurements was observed.	The experimentally observed flame speed was compared to laminar burning velocities of a stable one-dimensional model flame, provided by computations with a detailed kinetic scheme. An evaluation of stretch and instability effects by comparison to fundamental laminar burning velocities of the one-dimensional flame computed with the chemical kinetic-mechanism.	Chemical kinetic calculations using the mechanism of O'Conaire et al.	Results of stretch-free, stable hydrogen burning velocities obtained from computations with the computational kinetic scheme of O'Conaire et al. 2004 [139].	Experimental data were compared with results of the reaction mechanism calculations, for the evaluation of instabilities magnitude.	
[3] 2011 Verhelst etal	Numerical computational simulation with one-dimensional chemical kinetic model Chem 1D with Konnov mechanism. Validated against burning velocity measurements (combustion chamber) and other kinetic models.	Based on the authors in-house reaction scheme by simulation code Chem 1D developed to calculate with reaction mechanism, in a more precise determination for the influence of the residual gas content, besides P , T and Φ .	Compared with kinetic chemical reactions of Konnov 1D chemical kinetic code.	-	-	<ul style="list-style-type: none"> - Comparisons of reaction mechanisms: O'Conaire et al. 2004 [139], Saxena&Williams 2006 [126], Konnov 2004 [47]. - An improved function of residual gas factor (referred to in section 5.3).
[12] 2011 Bougrine etal	Numerical study of laminar flame properties of diluted methane-hydrogen-air flames at high pressure and temperature using complex detailed chemistry and one-dimensional simulations of premixed laminar flames. New laminar flame burning velocity and thickness correlations proposed in order to extend the domain of validity of experimental correlations to high proportions of hydrogen in the fuel, high residual burned gas mass ratios as well as high pressures and temperatures. A new laminar flame velocity analytical expression developed using an optimization algorithm by means of Matlab [187] functions for results processing.	A wide data-base of laminar flame velocities and thicknesses generated from one-dimensional premixed flames simulations using the CHEMKIN-PREMIX [131,129] collection codes. Phenomenological function inspired by previous works on experimental correlations of laminar flame velocities from: Gülder 1984 [188], Han et al. 2007 [189], Rahim et al. 2002 [137], Coppens et al. 2007 [190], Hermanns 2007 [191], Hermanns et al. 2010 [192], Huang et al. 2006 [193], Tahtouh et al. 2009 [194], Gerke et al. 2010 [2], Bougrine et al. 2011 [142], and Verhelst et al. 2011 [3]. This study extended the validity-ranges of these correlations to high values of P - T , in a generic expression for any fraction of hydrogen content in the fuel.	Benchmark of several chemical kinetic schemes available to describe premixed combustion of fuel blends, in order to evaluate and to choose the more relevant mechanism in terms of accuracy, robustness, precision and CPU-efficiency. The GRI 3.0 scheme of Smith et al. 2011 [145] chosen.	-	-	<ul style="list-style-type: none"> - Comparisons of reference reaction mechanisms (that were tested against an extended database of laminar flame speed measurements from the literature): GRI 3.0 of Smith et al. 2011 [145] with 53 species and 325 reactions; USC-Mech II of Wang et al. 2011 [195] with 111 species and 784 reactions; Konnov 0.5 of Konnov 2011 [196] with 127 species and 1207 reactions; Princeton of Li et al. 2011 [197] with 21 species and 93 reactions. - Assumption of molecular diffusivity model where the multicomponent diffusion has not been considered, preferring the mixture averaged diffusion model, neglecting the diffusion effects. - Assumption of diluents as additional N₂. - An optimized residual gas factor function is considered (referred to in section 5.3). - This work [2] is referred in this part only for its results of hydrogen in air combustion.

5.2. Homogenization of notation of laminar burning velocity expressions of the reviewed works

In chapter 3 of this study, a nomenclature has been introduced that specifically considers the different possibilities of laminar burning velocities. Apart from u_L for the laminar burning velocity obtained from theoretical stable planar flame fronts, it is evident from table 10 that the values reported in literature include laminar velocities obtained by means of different experimental or computational techniques, supported by more or less limited experimental data, apparent or quasi-laminar burning velocities derived from practical devices, based on measurements of cellular flames, affected or not by the early onset of instabilities in the hydrogen-air mixtures.

Since each published work uses a different notation or even a common notation but referred to different velocity concepts, it has been considered important to convert the heterogeneous notation into a unified notation, as done in tables 11&12. The original nomenclature of the reviewed papers is included, in table 11, and also two unified notations, one simplified and a second that considers the functional influence, as detailed in table 12.

Table 11

Nomenclature of the reviewed expressions of laminar burning velocity for **hydrogen-air mixtures**. Parametric and functional dependences (based on their respective data origins and methodologies)

Ref.	Year	Authors	Original nomenclature of each laminar burning velocity expression	Simplified unified notation of velocity expressions (based on the origin of their main data source) with operating variables dependence	Complex unified notation of velocity expressions (with their respective functional dependence, as defined in table 12)
[5]	1984	Milton, Keck	$S_u(T_w, P)$	$u_{nr}(T_w, P)$	$\mathbf{u}_{nr,c}$
[8]	2008	Lafuente	$S_L(T_w, P)$	$u_{nr}(T_w, P)$	$\mathbf{u}_{nr,c}$
[4]	1986	Iijima, Takeno	$S_u(T_w, P, \Phi)$	$u_{nr}(T_w, P, \Phi)$	$\mathbf{u}_{nr,c}$
[9]	1992	Göttgens, Mauss, Peters	$S_L(T_w, P, \Phi)$	$u_L(T_w, P, \Phi)$	\mathbf{u}_L
[10] [13]	2003- 2005	Verhelst, Sierens (Yetter et al./ O'Conaire et al.)	$u_l(T_w, P, 1/\Phi, f_{res,u})$	$u_L(T_w, P, 1/\Phi, f_{u,v})$	\mathbf{u}_L'
[11]	2008	D'Errico, Onorati, Ellgas	$S_L(T_w, P, \Phi, Y_{res,u})$	$u_L(T_w, P, \Phi, f_{u,m})$	$\mathbf{u}_{qL}'' (\mathbf{u}_L''; \mathbf{u}_{nr,c}; \mathbf{u}_L')$
[7] [13] [14]	2005- 2007	Verhelst; Wooley, Lawes, Sierens	$u_n(T_w, P, \Phi, f_{res,u})$	$u_n(T_w, P, \Phi, f_{u,v})$	$\mathbf{u}_{qNc} (\mathbf{u}_{ne,c}, \mathbf{u}_{nr,c})$
[6]	2008	Knop, Benkenida, Jay, Colin	$S_L(T_w, P, \Phi, X_{res,u})$	$u_L(T_w, P, \Phi, f_{u,v})$	$\mathbf{u}_{qL}''' (\mathbf{u}_L'''; \mathbf{u}_{nr,c}; \mathbf{u}_{qNc})$
[45] *	2007	Bradley, Lawes, Liu, Verhelst, Wooley (O'Conaire et al./ Konnov)	u_l, u_n, u_{nr}	u_l, u_n, u_{nr}	$\mathbf{u}_l (\mathbf{u}_{ne,c}, \mathbf{u}_{nr,c})$
[1]	2009	Hu, Huang, He, Miao	$u_l(T_w, P)$	$u_L(T_w, P)$	$\mathbf{u}_L (\mathbf{u}_L; \mathbf{u}_l)$
[2]	2010	Gerke, Steurs, Rebecchi, Boulouchos (O'Conaire et al.)	$u_l(T_w, P, \Phi, X_{EGR,u})$	$u_L(T_w, P, \Phi, f_{u,m})$	$\mathbf{u}_{qL} (\mathbf{u}_L; \mathbf{u}_l; \mathbf{u}_{ne,c}, \mathbf{u}_{nr,c})$
[2]		Gerke, Steurs, Rebecchi, Boulouchos	$u_n(T_w, P, \Phi, X_{EGR,u})$	$u_n(T_w, P, \Phi, f_{u,m})$	$\mathbf{u}_{qNc} (\mathbf{u}_l; \mathbf{u}_{ne,c}, \mathbf{u}_{nr,c})$
[3]	2011	Verhelst, T'Joel, Vancoillie, Demuyneck (Konnov)	$u_l(T_w, P, 1/\Phi, f_{res,u})$	$u_L(T_w, P, 1/\Phi, f_{u,v})$	$\mathbf{u}_{qL}'' (\mathbf{u}_L''; \mathbf{u}_{qNc}, \mathbf{u}_{ne,c}, \mathbf{u}_{nr,c})$
[12]	2011	Bougrine, Richard, Nicolle, Veynante	$U_l(T_w, P, \Phi, Y_{res,u}, h)$	$u_L(T_w, P, \Phi, f_{u,m}, h)$	$\mathbf{u}_{qL}''' (\mathbf{u}_L'''; \mathbf{u}_{qL}, \mathbf{u}_{qL}'' \dots)$

(*) No analytical expression given

$f_{u,v}$ (volume basis)

$f_{u,m}$ (mass basis)

Table 12Summary of complex unified notations of [table 11](#), for the reviewed expressions of laminar burning velocity with their functional dependences

Ref.	Functional dependence	Methodology and data sources (experimental and-or calculated)
[5] [8] [4]	$u_{nr,c}$	Experimental measurements from pressure records. Potentially affected by stretch and instabilities. Cellularity when pressure increases. "Apparent" laminar velocity obtained as a result of experimental pressure data (affected by cellularity).
[9]	u_l	Numerical calculation of theoretical lean premixed one-dimensional flame by asymptotic analysis with detailed kinetics. "Theoretical laminar" velocity (based on a kinetic model of a theoretical one-dimensional flame).
[10] [13]	u_l'	Numerical simulation of a theoretical lean premixed one-dimensional flame with detailed chemical schemes. "Theoretical-laminar" velocity (based on a kinetic model of a theoretical one-dimensional flame).
[11]	$u_{ql}'' (u_l''; u_{nr,c}; u_l')$	Numerical research with data from a detailed kinetic mechanism and experimental data from pressure records and others. Extension for higher pressures of the expression [10] for a theoretical lean premixed one-dimensional flame. "Theoretical quasi-laminar" velocity, generated by the kinetic model of a theoretical one-dimensional flame.
[7] [13] [14]	$u_{qNe} (u_{ne,c}, u_{nr,c})$	Experimental measurements from optical methods and pressure records, for lean premixed flames at limited radii and not very elevated pressures and temperatures. Potentially affected by stretch and instabilities. Cellularity when pressure increases. "Quasi-laminar" or apparent velocity, obtained from experimental data (affected by cellularity).
[6]	$u_{ql}''' (u_l'''; u_{nr,c}; u_{qNe})$	Numerical research (CFD simulation tools) with data from a detailed kinetic mechanism and experimental data from pressure records and other published experimental results. Extension for higher temperatures of the expression [7] for a theoretical premixed one-dimensional flame, for lean to rich mixtures. "Theoretical quasi-laminar" velocity, generated by the kinetic model of a theoretical one-dimensional flame.
[45]	$u_l (u_{ne,c}, u_{nr,c})$	Experimental development with treatment of data (obtained from optical methods and pressure records) for stretch and instabilities correction, based on linear stability theory analysis of lean premixed flames at limited radii and not very high pressures and temperatures. "Laminar" velocity, obtained by introducing corrections for stretch and instabilities on experimental data.
[1]	$u_{l-} (u_l; u_{-})$	Numerical study, with some experimental data at limited conditions treated for stretch consideration. Extension for high pressures and temperatures (stoichiometric mixtures) of a theoretical premixed one-dimensional flame based on a chemical kinetic code and the behavior of reactions radicals. "Theoretical-laminar" velocity, generated by the kinetic model of a theoretical one-dimensional flame.
[2]	$u_{ql}'' (u_l''; u_{l-}; u_{ne,c}, u_{nr,c})$	Numerical development with treatment of data (derived from optical methods and pressure records) for stretch and instabilities effects evaluation by comparison to fundamental laminar burning velocities of a one-dimensional flame computed with a detailed chemical kinetic-mechanism, which serves for the definition of a particular theoretical laminar burning velocity function (different from the following expression). For high pressures and temperatures in wide ranges of equivalence ratio and significant fractions of residual gases. "Theoretical quasi-laminar" velocity, generated by the kinetic model of a theoretical one-dimensional flame but considering some experimental data.
[2]	$u_{qNe}' (u_l; u_{ne,c}, u_{nr,c})$	Experimental development with treatment of data (obtained from optical methods and pressure records), with comparisons for evaluation of stretch and instabilities effects, which serves to the definition of a particular practical laminar burning velocity function (different from the previous expression). For high pressures and temperatures in wide ranges of equivalence ratio and significant fractions of residual gases. "Quasi-laminar" or apparent velocity, obtained from experimental data (affected by cellularity).
[3]	$u_{ql}'''' (u_l''''; u_{qNe}, u_{ne,c}, u_{nr,c})$	Numerical computational simulation with one-dimensional chemical kinetic model validated against burning velocity measurements of previous works (combustion chamber) and other reaction mechanisms. Valid for high pressure and temperature in wide ranges of equivalence ratio and significant fractions of residual gases. "Theoretical quasi-laminar" velocity, generated by the kinetic model of a theoretical one-dimensional flame but modified by experimental results.
[12]	$u_{ql}'''''' (u_l''''''; u_{ql}''', u_{ql}'''' ...)$	Numerical study for blended hydrogen-methane air flames at high pressure and temperature using complex detailed chemistry and one-dimensional simulations of premixed laminar flames. New laminar flame burning velocity analytical expression, developed by using an optimization algorithm, proposed in order to extend the domain of validity of experimental and other correlations [2,3,...] to several proportions of hydrogen in the fuel (also for wide mass fractions of residual burned gas and high pressures and temperatures, from lean to non-very rich equivalence ratio). "Theoretical quasi-laminar" velocity, obtained from the kinetic model of a theoretical one-dimensional flame but modified by the original data of the optimized correlations of reference.

Table 13

Dependences of exponents and coefficients appearing in the reviewed expressions of laminar burning velocity (table 15 and eq.132 and following eqs.)

Ref.	$\alpha (T_u; P; \Phi, h)$	Ref.	$\beta (P; T_u; \Phi, h)$	Ref.	$\zeta (T_u, P, \Phi, f_{res,u}, h)$
[12]	$\alpha (T_u, \Phi, h)$	[12]	$\beta (P, T_u, \Phi, h)$	[12]	$\zeta (T_u, P, \Phi, f_{res,u}, h)$
[3] [10] [11]	$\alpha (P, \Phi)$	[3] [10] [11]	-	[3] [10] [11]	$\zeta (T_u, P, \Phi, f_{res,u})$
[1]	$\alpha (T_u)$	[1]	$\beta (P)$	[2][2] [6] [7]	$\zeta (\Phi, f_{res,u})$
[2][2] [4]	$\alpha (\Phi)$	[2][2] [4] [6] [7]	$\beta (\Phi)$		
[6] [7]	$\alpha (\Phi)= ct$	[5] [8]	$\beta (\Phi=1)= ct$	[1] [4] [5] [8] [9]	1
[5] [8]	$\alpha (\Phi=1)= ct$	[9]	ct		
[9]	ct				

Table 14

Dependences of factors and functions in the reviewed expressions of laminar burning velocity (table 15 and equation 132 and following equations)

Ref.	$u_o (\Phi, P; T_u, h)$	Ref.	$u (T_u, P, \Phi, f_{res,u}, h)$
[9]	$u_o (\Phi, P; T_u)$	[12]	$u (T_u, P, \Phi, f_{res,u}, h)$
[3] [10] [11]	$u_o (\Phi, P)$	[2][2] [3] [6] [7] [10] [11]	$u (T_u, P, \Phi, f_{res,u})$
[12]	$u_o (\Phi, h)$	[4] [9]	$u (T_u, P, \Phi)$
[2][2] [4] [6] [7]	$u_o (\Phi)$	[1] [5] [8]	$u (T_u, P, \Phi=1)$
[1] [5] [8]	$u_o (\Phi=1)= ct$		

5.3. Analytical expressions of laminar burning velocities

Most of the published formulas of burning velocities are based on experimental or numerical correlations of results for hydrogen-air premixed mixtures at elevated pressures and temperatures. Frequently they present a general mathematical expression as a power law function of pressure and temperature, as proposed by Metghalchi&Keck 1980 [27].

$$u (T_u, P) = (T_u/T_o)^\alpha \cdot (P/P_o)^\beta \cdot u_{o,0} \quad (132)$$

This original expression is sometimes modified to introduce the influence of equivalence ratio and residual gas content (ζ), according to the data and obtaining methodology.

$$u (T_u, P, \Phi, f_{res,u}, h) = (T_u/T_o)^\alpha \cdot (P/P_o)^\beta \cdot \zeta \cdot u_{o,0} \quad (133)$$

This type of expression is computationally convenient but, in origin, some studies assumed the effects of P , T , Φ and f_{res} to be independent. In the development and calibration of these expressions, some of the diverse parameters were expressed as functions of some of the variables, for a better fit to experimental data depending on the cases, with the dependences expressed in tables 13&14. The complete analytical formulas of the compared expressions are developed in table 15.

Although these formulations of laminar burning velocities have been partly validated through engine simulations in some cases, Verhelst pointed out some problems with the terms describing the effects of the residual gas fraction.

$$\zeta_c = 1 - \varsigma \cdot f_{res} \quad (134)$$

The term proposed by Verhelst 2005 [13] and used in engine cycle simulation by Verhelst&Sierens 2007 [14], Knop et al. 2008 [6], Gerke et al. 2010 [2], etc., had a coefficient ς function of the equivalence ratio.

$$\zeta(\Phi) = 2.715 - 0.5 \Phi \quad (135)$$

Verhelst indicated that then ζ_c becomes negative for certain values of residual gas fraction, depending on equivalence ratio. For example, for stoichiometric mixtures, a negative value of burning velocity was obtained if f_{res} in volumetric fraction percent exceeded 45%. However, hydrogen engine experiments had been reported in the literature with external EGR rates of 45% and higher, Brewster&Bleechmore 2007 [198], Verhelst et al. 2007 [14], with normal combustion. Such operating strategies were simulated but then the residual gas term was improper to be used in an expression such as eq.133 in some ranges.

Alternative residual gas terms, similar to the one previously proposed by Verhelst&Sierens 2003 [10], were used in engine cycle simulation by D'Errico et al. 2008 [11], with a coefficient ζ_2 that was a function of equivalence ratio, pressure and temperature. This was extended from other shorter formulation of the ζ coefficient as ζ_1 .

$$\zeta_{c1} = 1 - \zeta_1 \cdot f_{res} \quad (136)$$

$$\text{where } \zeta_1(\Phi, P, T_u) = g_0 \cdot T_u \quad (137)$$

$$\text{with } g_0 \equiv g_0(\Phi, P)$$

and

$$\zeta_{c2} = 1 - \zeta_2 \cdot f_{res} \quad (138)$$

$$\text{where } \zeta_2(\Phi, P, T_u) = g_1 - g_2 \cdot T_u \quad (139)$$

$$\text{with } g_1 \equiv g_1(\Phi, P) \quad \text{and} \quad g_2 \equiv g_2(\Phi, P)$$

The use of ζ_{c2} allows higher values of f_{res} when temperature is high, in comparison with the use of ζ_{c1} , because ζ_2 decreases with T . Verhelst&Sierens 2003 [10] gave the expressions for g_1 and g_2 (included in table 15) as functions of equivalence ratio and pressure. These expressions are valid in a range limited to lean to stoichiometric equivalence ratios and pressures less than 16 bar. For stoichiometric mixtures, the residual gas term also becomes negative if f_{res} exceeds 45%vol.

D'Errico et al. 2006,2008 [184,11] subsequently used the same formulation to construct their correlation for the laminar burning velocity from chemical kinetic calculations using an in-house reaction scheme. Their correlation was claimed to be valid in wider ranges up to 6 MPa but such extrapolation up to much higher pressures leads to non-physical results. Depending on the temperature, the residual gas term can even become bigger than unity, implying that diluting the mixture with residual gas would increase the burning velocity, which clearly is not possible. D'Errico gave the same coefficients as Verhelst&Sierens 2003 [10], although the correlation form used the fuel to air equivalence ratio (Φ) as opposed to the air to fuel ratio (λ), and stated the term relative to f_{res} as the mass fraction of residual gases whereas it is was defined as a volume fraction by Verhelst.

In order to allow computation of the laminar burning velocity of hydrogen mixtures at the conditions explored in hydrogen engine operating strategies, one-dimensional chemical kinetic calculations were reported by Verhelst et al. 2011 [3], whose results were fitted to a new correlation form, with calculations performed for fuel to air equivalence ratios (Φ) in the range of [0.33, 5], temperature (T_u) between [500, 900] K, pressure (P) between [5, 45] bar and

residuals volumetric fractions (f_{res}) between $[0, 0.5]$. The ranges cover most of the expected conditions of the unburned mixture in hydrogen-fueled engine experiences. Over one thousand conditions within this range were calculated by the authors to build up a database to which the correlation could be fitted. This makes this correlation one of the most complete and validated to be used.

Bougrine et al. 2011 [12] proposed a similar expression, but including terms up to third order of the residuals fraction exponent in its polynomial expression.

$$\zeta_{\zeta 3} = 1 - \zeta_3 \cdot f_{res} \quad (140)$$

$$\text{where } \zeta_3(\Phi, P, T_u, h) = \Omega_R \cdot [1 - 1.115 f_{res} + 1.323 f_{res}^2] \quad (141)$$

$$\text{with } \Omega_R \equiv \Omega_R(T_u, P, \Phi, h)$$

This expression of Bougrine et al. 2011 [12] was developed using an optimization algorithm and was inspired by previous works and other experimental correlations of burning velocities from Gülder 1984 [188], Han et al. 2007 [189], Rahim et al. 2002 [137], Coppens et al. 2007 [190], Hermanns 2007 [191], Hermanns et al. 2010 [192], Huang et al. 2006 [193], Tahtouh et al. 2009 [194], Gerke et al. 2010 [2], Bougrine et al. 2011 [142] and Verhelst et al. 2011 [3]. Their study extended the validity ranges of these correlations to high levels of pressure between $[1, 110]$ bar and temperature between $[300, 950]$ K, in a generic expression for any fraction $h(\%)$ of hydrogen percentage volumetric content in a fuel blend with methane, between $[0, 100]\%$. Their fuel to air equivalence ratio (Φ) range is limited between $[0.6, 1.3]$ and the residuals mass fractions between $[0, 0.3]$.

5.4. Ranges of applicability of expressions

As said, the selected burning velocity expressions have been written in table 15, approximately in the original authors' terms and nomenclature, but in addition, a complementary unified notation is included in order to facilitate a correct interpretation, according with their respective data origin and obtaining methodology as detailed in tables 11&12.

The respective ranges of application of these expressions are indicated in table 16 regarding to the hydrogen-air mixture parameters of initial fresh gas temperature (T_u) and pressure (P), fuel to air equivalence ratio (Φ), residual gas fraction ($f_{res,u}$) and hydrogen content in the fuel (h). This last value is usually equal to 100%, except for the last reference, that considers mixtures of methane and hydrogen in air, and for that the range of h goes from 0% (only natural gas) to 100% (only hydrogen).

Table 15Expressions of laminar burning velocity for **hydrogen-air mixtures** (applicability ranges in [table 16](#))

Ref.	Expressions defined in tables 10, 11, 12, 13, 14 & 16	Units.-	u =[cm/s]	T =[K]	P =[bar]	Φ =[-]	f_{res} =[-]
$u_{nrc}(T_w, P)$							
[5]	$S_u(T_w, P) = (T_w/298)^\alpha \cdot (P/1.01325)^\beta \cdot S_{u,0}$	α	= 1,26				
		β	= 0,26				
		$S_{u,0}(\Phi=1)$	= 217				
$u_{nrc}(T_w, P)$							
[8]	$S_u(T_w, P) = (T_w/300)^\alpha \cdot (P/1)^\beta \cdot S_{L,0}$	α	= 1,19				
		β	= 0,26				
		$S_{L,0}(\Phi=1)$	= 247				
$u_{nrc}(T_w, P, \Phi)$							
[4]	$S_u(T_w, P, \Phi) = (T_w/291)^\alpha \cdot [1 + \beta \cdot \text{LOG}(P/1.01325)] \cdot S_{u,s}$	$\alpha(\Phi)$	= 1,54 + 0,026(\Phi-1)				
		$\beta(\Phi)$	= 0,43 + 0,003(\Phi-1)				
		$S_{u,s}(\Phi)$	= 298 - 100(\Phi-1,70)^2 + 32(\Phi-1,70)^3				
$u_L(T_w, P, \Phi)$							
[9]	$S_u(T_w, P, \Phi) = (T_w/T^0) \cdot (P/30044.1)^{(G/E)} \cdot [(T_b-T^0) / (T_b-T_u)]^n \cdot Y_{F,u}^{m,3} \cdot F$	n	= 3,5349				
		$T_b(T_w, \Phi)$	= 0,522(T_w) + 673,8 + 807,9(\Phi) + 2515,6(\Phi)^2 - 1765,9(\Phi)^3				
		$T^0(P)$	= 10200,9 / LN(30044,1/P)				
		$G[K]$	= 2057,56				
		$E[K]$	= 10200,9				
		$Y_{F,u}(\Phi)$	= $\Phi / [(\Phi-1) + (1/Y_{F,st})]$				
		$Y_{F,st}$	= 0,02818				
		m	= 1,08721				
		$F[cm/s]$	= 1292880				
$u_L(T_w, P, 1/\Phi, f_{res})$							
[10] [13]	$u_L(T_w, P, 1/\Phi, f_{res,u}) = (T_w/300)^\alpha \cdot [1 - (g_1 - T_u g_2) \cdot f_{res}] \cdot u_{L,0}$ $\zeta(T_w, P, 1/\Phi, f_{res}) = 1 - (g_1 - T_u g_2) \cdot f_{res}$	$\alpha(P, 1/\Phi)$	= 1,85175 - 0,70875(1/\Phi) + 0,50171(1/\Phi)^2 - 0,19366(P/1) + 0,0067834(P/1)^2 + 0,27495(1/\Phi)(P/1) - 0,0088924(1/\Phi)(P/1)^2 - 0,052058(1/\Phi)^2(P/1) + 0,00146015(1/\Phi)^2(P/1)^2				
		$g_1(P, 1/\Phi)$	= -0,92196 + 3,4343(1/\Phi) - 0,31958(1/\Phi)^2 + 0,45716(P/1) - 0,0049817(P/1)^2 - 0,19362(1/\Phi)(P/1) - 0,013165(1/\Phi)(P/1)^2 - 0,0064435(1/\Phi)^2(P/1) + 0,007356(1/\Phi)^2(P/1)^2				
		$g_2(P, 1/\Phi)$	= [-4,2897 + 6,9775(1/\Phi) - 1,1295(1/\Phi)^2 + 1,0255(P/1) - 0,018852(P/1)^2 - 0,8639(1/\Phi)(P/1) - 0,0029116(1/\Phi)(P/1)^2 + 0,11834(1/\Phi)^2(P/1) + 0,0085017(1/\Phi)^2(P/1)^2] / 1000				
		$u_{L,0}(P, 1/\Phi)$	$u_{L,0}(P \leq 8.5, \Phi \leq 0.46)$	= 499,63 - 308,62(1/\Phi) + 48,887(1/\Phi)^2 - 76,238(P/1) + 4,825(P/1)^2 + 45,813(1/\Phi)(P/1) - 2,926(1/\Phi)(P/1)^2 - 7,163(1/\Phi)^2(P/1) + 0,463(1/\Phi)^2(P/1)^2			
			$u_{L,0}(P \leq 8.5, 0.46 \leq \Phi)$	= 373,653 - 174,435(1/\Phi) + 13,729(1/\Phi)^2 + 98,871(P/1) - 7,452(P/1)^2 - 122,14(1/\Phi)(P/1) + 8,582(1/\Phi)(P/1)^2 + 33,073(1/\Phi)^2(P/1) - 2,234(1/\Phi)^2(P/1)^2			
			$u_{L,0}(8.5 \leq P, \Phi \leq 0.46)$	= 277,195 - 170,618(1/\Phi) + 26,5(1/\Phi)^2 - 11,038(P/1) + 0,233(P/1)^2 + 5,678(1/\Phi)(P/1) - 0,114(1/\Phi)(P/1)^2 - 0,714(1/\Phi)^2(P/1) + 0,0138(1/\Phi)^2(P/1)^2			
			$u_{L,0}(8.5 \leq P, 0.46 \leq \Phi)$	= 1074,579 - 1009,883(1/\Phi) + 244,355(1/\Phi)^2 - 65,999(P/1) + 2,243(P/1)^2 + 71,111(1/\Phi)(P/1) - 2,59(1/\Phi)(P/1)^2 - 19,258(1/\Phi)^2(P/1) + 0,730(1/\Phi)^2(P/1)^2			
$u_{qt}(T_w, P, \Phi, f_{res})$							
[11]	$S_u(T_w, P, \Phi, Y_{res,u}) = (T_w/300)^\alpha \cdot [1 - (g_1 - T_u g_2) \cdot f_{res}] \cdot S_{L,0}$ $\zeta(T_w, P, \Phi, f_{res}) = 1 - (g_1 - T_u g_2) \cdot f_{res}$	$\alpha(P, \Phi)$	= 9,809594 - 15,8309(\Phi) + 7,98087(\Phi)^2 + 0,008283(P/1) - 0,00079(P/1)^2 - 0,00204(\Phi)(P/1) + 0,001911(\Phi)(P/1)^2 + 0,003867(\Phi)^2(P/1) - 0,00221(\Phi)^2(P/1)^2				
		$g_1(P, \Phi)$	= -0,9220 + 3,4343(\Phi) - 0,3196(\Phi)^2 + 0,4572(P/1) - 0,0050(P/1)^2 - 0,1936(\Phi)(P/1) - 0,0132(\Phi)(P/1)^2 - 0,0064(\Phi)^2(P/1) + 0,0074(\Phi)^2(P/1)^2				
		$g_2(P, \Phi)$	= [-4,2897 + 6,9775(\Phi) - 1,1295(\Phi)^2 + 1,0255(P/1) - 0,0189(P/1)^2 - 0,8639(\Phi)(P/1) - 0,0029(\Phi)(P/1)^2 + 0,1183(\Phi)^2(P/1) + 0,0085(\Phi)^2(P/1)^2] / 1000				
		$S_{L,0}(P, \Phi)$	= -40,5821 + 86,4724(\Phi) + 127,6104(\Phi)^2 + 2,8990(P/1) - 0,0339(P/1)^2 - 9,7199(\Phi)(P/1) + 0,1128(\Phi)(P/1)^2 + 2,3918(\Phi)^2(P/1) - 0,0280(\Phi)^2(P/1)^2				

$u_{qNc}(T_w, P, \Phi, f_{uv})$			
[7]	$u_n(T_w, P, \Phi, f_{res,u}) = (T_w/365)^\alpha \cdot (P/5)^\beta \cdot [1 - (2.715 - 0.5 \Phi) f_{res}] \cdot u_{n,0}$	α	= 1,232
[13]		$\beta(\Phi)$	$\beta(\Phi < 0.6) = -1,16 + 5,06(\Phi) - 6,69(\Phi)^2 + 2,90(\Phi)^3$
[14]			$\beta(\Phi \geq 0.6) = 0,0781 + 0,0246(\Phi)$
		$u_{n,0}(\Phi)$	= $100 \cdot [-0,296 - 0,394(\Phi) + 8,65(\Phi)^2 - 4,77(\Phi)^3]$
$u_{qt}^-(T_w, P, \Phi, f_{uv})$			
[6]	$S_L(T_w, P, \Phi, X_{EGR,u}) = (T_w/298)^\alpha \cdot (P/1.01325)^\beta \cdot [1 - (2.715 - 0.5 \Phi) f_{res}] \cdot S_{L,0}$	α	= 1,22
		$\beta(\Phi)$	$\beta(\Phi < 0.6) = -1,16 + 5,06(\Phi) - 6,69(\Phi)^2 + 2,90(\Phi)^3$
			$\beta(\Phi \geq 0.6) = 0,078 + 0,025(\Phi)$
		$S_{L,0}(\Phi)$	$S_{L,0}(\Phi \leq 1.9) = 100 \cdot [1,16 - 9,47(\Phi) + 26,92(\Phi)^2 - 25,54(\Phi)^3 + 10,81(\Phi)^4 - 1,75(\Phi)^5]$
		$S_{L,0}(\Phi = 1.9) = 271,5$	
		$S_{L,0}(\Phi > 1.9) = [S_{L,0}(\Phi = 1.9)] + [108 - S_{L,0}(\Phi = 1.9)] \cdot [(\Phi - 1.9) / (5,05 - 1,9)]$	
$u_{L}(T_w, P)$			
[1]	$u_l(T_w, P) = (T_w/303)^\alpha \cdot (P/1)^\beta \cdot u_{l,0}$	$\alpha_T(T_w)$	= $1,319 + 0,0008019(T)$
		$\beta_P(P)$	= $-0,406 + 0,374 \text{ EXP}[-P/1,451]$
		$u_{l,0}(\Phi = 1)$	= 240,6
$u_{qt}^-(T_w, P, \Phi, f_{uv})$			
[2]	$u_l(T_w, P, \Phi, X_{EGR,u}) = (T_w/500)^\alpha \cdot (P/20)^\beta \cdot [1 - (2.715 - 0.5 \Phi) f_{res}] \cdot u_{l,0}$	$\alpha(\Phi)$	$\alpha(\Phi \leq 0.5) = 24,877 - 85,633(\Phi) + 116,3(\Phi)^2 - 54,278(\Phi)^3$
			$\alpha(\Phi > 0.5) = 9,37 - 14,929(\Phi) + 12,019(\Phi)^2 - 4,7032(\Phi)^3 + 0,9066(\Phi)^4 - 0,0685(\Phi)^5$
		$\beta(\Phi)$	$\beta(\Phi \leq 1.75) = -1,1522 + 0,8(\Phi) - 0,2426(\Phi)^2$
			$\beta(\Phi > 1.75) = -0,6638 + 0,243(\Phi) - 0,0994(\Phi)^2 + 0,0075(\Phi)^3$
	$u_{l,0}(\Phi)$	$u_{l,0}(\Phi \leq 2) = 100 [-2,813 + 20,818(\Phi) - 65,998(\Phi)^2 + 108,95(\Phi)^3 - 84,173(\Phi)^4 + 30,521(\Phi)^5 - 4,239(\Phi)^6]$	
		$u_{l,0}(\Phi > 2) = 100 [2,940 + 3,593(\Phi) - 1,603(\Phi)^2 + 0,172(\Phi)^3]$	
$u_{qNc}(T_w, P, \Phi, f_{uv})$			
[2]	$u_n(T_w, P, \Phi, X_{EGR,u}) = (T_w/600)^\alpha \cdot (P/20)^\beta \cdot [1 - (2.715 - 0.5 \Phi) f_{res}] \cdot u_{n,0}$	$\alpha(\Phi)$	= $0,0163(1/\Phi) + 2,2937$
		$\beta(\Phi)$	= $0,2037(1/\Phi) - 0,575$
		$u_{n,0}(\Phi)$	$u_{n,0}(\Phi \leq 2.5) = 100 [1,2994 - 13,976(\Phi) + 52,317(\Phi)^2 - 46,525(\Phi)^3 + 18,498(\Phi)^4 - 3,4774(\Phi)^5 + 0,25(\Phi)^6]$
			$u_{n,0}(\Phi = 2.5) = 1041,1$
		$u_{n,0}(\Phi > 2.5) = [u_{n,0}(\Phi = 2.5)] + [723 - u_{n,0}(\Phi = 2.5)] \cdot [(\Phi - 2,5) / 2,5]$	
$u_{qt}^-(T_w, P, 1/\Phi, f_{uv})$			
[3]	$u_l(T_w, P, 1/\Phi, f_{res,u}) = (T_w/300)^\alpha \cdot \text{MÍN}[1; F_1] \cdot u_{l,0}$ $F(T_w, P, 1/\Phi, f_{res}) = \text{MÍN}[1; F_1]$ (\rightarrow) approx. $f_r = 0, F \rightarrow 1;$ $f_r > 0, F < 1;$ $f_r = 0.5, F \rightarrow 0$	$\alpha(P, 1/\Phi)$	= $0,584069 + 1,097884(1/\Phi) - 0,03683272(P/1) + 0,02454259(P/1)(1/\Phi) + 0,104381(1/\Phi)^2 - 0,0004119350(P/1)^2 + 0,007621143(1/\Phi)^2(P/1) + 0,000762759(1/\Phi)(P/1)^2 - 0,0004498380(1/\Phi)^2(P/1)^2 + 0,331465(\Phi) + 0,02165434(P/1)(\Phi)$
		$F_1(T_w, P, 1/\Phi, f_r)$	= $1,782191 - 0,1945813(T/300) - 0,004071734(P/1) - 0,4987061(1/\Phi) - 4,347767(f_r) + 0,00008576177(P/1)^2 + 0,04490150(T/300)^2 + 0,07878902(1/\Phi)^2 + 4,243637(f_r)^2 - 0,002052509(T/300)(P/1) + 0,003724404(P/1)(1/\Phi) - 0,2114637(f_r)(1/\Phi) - 0,2224738(\Phi) + 0,04624703(\Phi)(T/300) + 0,2116186(1/P)(T/300) - 2,098941(T/300)(f_r)^3 + 0,07029643(P/1)(f_r)^3 + 1,334951(1/\Phi)(f_r)^3 + 0,0004861730(P/1)(\Phi) - 0,01915344(P/1)(f_r) + 0,6146191(f_r)(T/300)$
		$u_{l,0}(P, 1/\Phi)$	= $\text{EXP}[7,505661 - 1,903711(1/\Phi) + 0,05380840(P/1) - 0,03936929(P/1)(1/\Phi) + 0,01896873(1/\Phi)^2 + 0,0005964680(P/1)^2 - 0,03010525(1/\Phi)^2(P/1) - 0,0003431092(1/\Phi)(P/1)^2 + 0,0009023031(1/\Phi)^2(P/1) - 0,00001556492(1/\Phi)(P/1)^3 + 0,0008452404(1/\Phi)^2(P/1)^2 - 0,478534(\Phi) - 0,03105883(P/1)(\Phi)]$
$u_{qt}^-(T_w, P, \Phi, f_{uv}, h)$			
[12]	$U_l(T_w, P, \Phi, Y_{res,u}, h) = (T_w/300)^\alpha \cdot (P/1)^\beta \cdot [1 - \Omega_R \cdot (1 - 1.115 f_{res} + 1.323 f_{res}^2) f_{res}] \cdot u_{l,0}$ $\zeta(T_w, P, \Phi, f_{res}, h) = 1 - \Omega_R \cdot (1 - 1.115 f_{res} + 1.323 f_{res}^2) f_{res}$	$\alpha_T(T_w, \Phi, h)$	= $[3,2466 - 1,0709(\Phi) + 0,1517(\Phi)^4 - 0,0003201(h) - 1,0359(300/T)^2(\Phi)^2] \cdot \{1 + [0,5(1 + \text{TANH}((h-90)/10))] \cdot [-1 + \text{EXP}(-1 + 0,58(T/300)^{0,5})]\}$
		$\beta_P(T_w, P, \Phi, h)$	= $[-0,5406 + 0,1347(\Phi) - 0,0125(\Phi)^4 - 0,0005174(h)(\Phi + (1/\Phi))^{0,5} + 0,0002289(T/300)(P/1)(\Phi)^2] \cdot \{1 + [0,5(1 + \text{TANH}((h-90)/10))] \cdot [-1 + \text{EXP}(-1,9026 + 0,03556(P/1) - 0,000163(P/1)^2)]\}$
		$\Omega_R(T_w, P, \Phi, h)$	= $4,157 - 1,744(\Phi) + 0,5124(\Phi)^4 - 0,0047(h) - 0,0008694(T/300)(P/1)(\Phi)^2$
		$u_{l,0}(\Phi, h)$	= $\{ (1 + 0,00000272 h^{2,897}) 150,817 \Phi^{4,539} \text{ EXP}[-2,448(\Phi - 0,0017 h - 0,2248)] \} \cdot \{ 1 + [0,5(1 + \text{TANH}((h-70)/10))] \cdot [-1 + 1,4 + 0,000000339(h) - 0,00000117(h)^2 + 0,000000117(h)^3 - 0,0000000375(h)^4 + 0,0000000014(h)^5] \} \cdot \{ 1 + [0,5(1 + \text{TANH}((h-90)/10))] \cdot [-1 + 1,75 - 1,75(\Phi) + 0,625(\Phi)^2 - 0,038(\Phi)^3 + 0,138(\Phi)^4] \}$
		h	= $100 (\%H_2)$

Table 16Applicability ranges of the reviewed expressions of laminar burning velocity for **hydrogen-air mixtures** (analytical expressions in table 15)

Ref.	Variables & units	P	T _u	P _o	T _o	Φ	f _{res,u}	h
	Authors	bar	K	bar	K	(-)	(-)	%
[5]	Milton, Keck	[0.5, 7.1]	[298, 550]	1.01325	298	1	-	100
[8]	Lafuente	[1, 7]	[330, 500]	1	300	1	0	100
[4]	Iijima, Takeno	[0.5, 25.3]	[291, 500]	1.01325	291	[0.5, 4]	0	100
[9]	Göttgens, Mauss, Peters	[1, 40]	[298, 500]	(1)	(298)	[0.4, 1]	0	100
[10]	Verhelst, Sierens	[1, 16]	[300, 800]	1	300	[0.33, 1]	[0, 0.3]	100
[13]	(Yetter et al./ O'Conaire et al.)							
[11]	D'Errico, Onorati, Ellgas	[1, <60] (16)	[500, 900]	(1)	(300)	[0.36, 1]	[0, 0.5]	100
[7] [13]	Verhelst; Wooley, Lawes, Sierens	[1, 10]	[300, 430]	5	365	[0.3, 1]	[0, 0.3]	100
[14]								
[6]	Knop, Benkenida, Jay, Colin	[1, 10]	[300, <1000]	1.01325	298	[0.25, <5]	[0, 0.3]	100
[45] *	Bradley, Lawes, Liu, Verhelst, Wooley (O'Conaire et al./ Konnov)	{1, 5, 10}	{300, 365}	(1)	{300, 365}	[0.3, 1]	0	100
[1]	Hu, Huang, He, Miao	[1, 80]	[303, 950]	1	303	1	-	100
[2]	Gerke, Steurs, Rebecchi, Boulouchos	[<10, >45]	[<350, >700]	20	600	[<0.36, >2.5]	[0, 0.3]	100
[2]	(O'Conaire et al.)	[>1, 80]	[>300, <900]	20	500	[0.4, 3.75]	[0, 0.3]	100
[3]	Verhelst, T'Joens, Vancoillie, Demuynck (Konnov)	[5, 45]	[500, 900]	1	300	[0.33, 5]	[0, 0.5]	100
[12]	Bougrine, Richard, Nicolle, Veynante	[1, 110]	[300, 950]	1	300	[0.6, 1.3]	[0, 0.3]	[0, 100]

(*) Without an analytical correlation

Table 17

Summary of conditions considered in this study for the comparison of expressions of laminar burning velocity

Variables	P	T _u	P _o	T _o	Φ	f _{res,u}	h
Units	bar	K	bar	K	(-)	(-)	%
	{1,	{300,	{1,	{300,	{0.5,	{0,	100
	10,	500,	6,	500}	0.9,	0.15,	
	25,	650,	10}		1,	0.3,	
	>40}	800}			1.3,	<0.4}	
					1.75,		
					2,	-----	
					>3.3}	(Φ=1)	

Table 18

Summary of charts indicating the functional dependences represented for the reviewed expressions of laminar burning velocity

Graphs	Function (variables)	Φ	EGR	P & T
Fig. 27	u(P) & u(T _u)	0.5	0	The values of P and T are assumed fully independent, inside their respective ranges T _u (K) = [300, 950] P (bar) = [1, 60]
Fig. 28		0.9		
Fig. 29		1		
Fig. 30		1.3		
Fig. 31		1.75		
Fig. 32		2		
Fig. 33	3.3			
Fig. 34		1	0.15	
Fig. 35			0.30	
Fig. 36			0.40	
Fig. 37	u(T) & u(P)	1	0	The values of P and T are related by an isentropic compression ($\gamma=1.4$)
Fig. 38	u(Φ) & u(EGR)	[0.5, 4.5]	[0, 0.45]	T _u (K) = {300, 500} P (bar) = {1, 6, 10}

5.5. Graphical representation of results in the applicability ranges of laminar burning velocity expressions

To provide a graphical representation of the expressions of laminar velocities listed in table 15, their output values are represented in figs. 27-38 (for the conditions of table 18), with each expression calculated only within its range of applicability (table 16). All the representations of results of each reference (denoted with the same number as in tables 10-16) are drawn always with the same color code (figs. 27-38). The representative operating conditions that have been chosen are detailed in table 17. When applicable, the residual gas correction term has been considered.

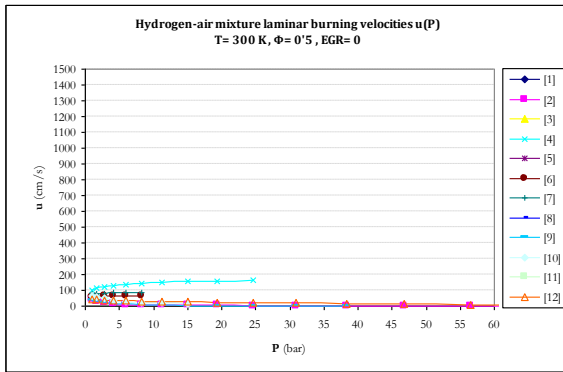
Of both correlations of Gerke et al. 2010 [2,2], only the based on the kinetic mechanism O'Conaire et al. 2004 [139] has been represented, i.e. the expression called as Gerke et al.(+O'Conaire et al.) 2010 [2]. This extends the validity domain of the other one [2], more restricted, for temperatures bigger than 700 K to 900 K and pressures bigger than 45 bar and up to 80 bar.

Thus, burning velocities have been calculated for the conditions in table 17, at different equivalence ratios in this database: rich conditions ($\Phi= 1.3, 1.75, 2, 3.3$), stoichiometric mixtures ($\Phi=1$), and lean conditions ($\Phi= 0.5, 0.9$). The results show that the equivalence ratios of maximum burning velocities vary between around 1.7-1.9 depending on correlations and conditions (fig. 38 a,c,e,g).

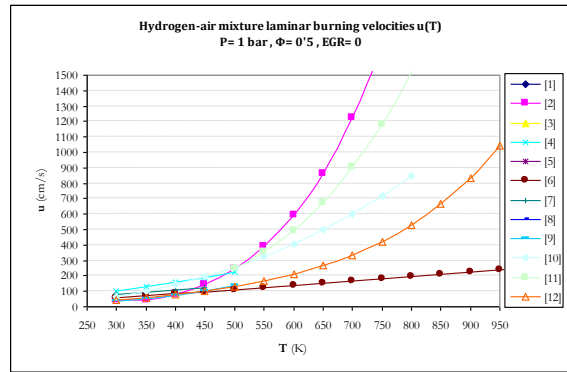
The residual gas content has set to be zero ($EGR=0$) for some cases (figs. 27-33). EGR is the variable associated to what each author names as residual gas fraction $f_{res,u}$ on volume basis $f_{u,v}$ or on mass basis $f_{u,m}$. As the number of data increases when the residual gas content is also included as a free variable, a more limited set of conditions has been chosen for the illustrative comparison of the behavior of the exhaust gas recirculation correction terms. So, the expressions that include the residual gas content have been evaluated at stoichiometric equivalence ratio ($\Phi=1$) for different values (e.g. for $EGR= 0.15, 0.3, 0.4$), because the EGR concentration can be varied in an engine with stoichiometric operation (figs. 34-36 and fig. 38 b,d,f,h).

In order to show widely the different trends with pressure, temperature, equivalence ratio and residual gas fraction, at different conditions, the results in the graphs have been calculated

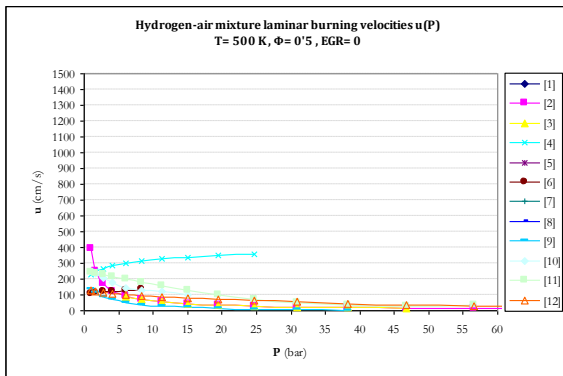
for representative values of the independent variables (table 18). Since for engines combustion, pressures and unburned temperatures grow in parallel, in the form of a quasi-adiabatic compression, Verhelst et al. 2011 [3] chose the representative values of both variables in couples. In this present work a few graphs (fig. 37) of some functions $u(P)$ and $u(T)$ consider this related values of pressures and temperatures (with a specific heats ratio of $\gamma=1.4$ almost constant for a wide range of equivalence ratios) as a simple initial reference based on combined P - T values (table 19) for a stoichiometric condition without residuals. Nevertheless, most of the graphical representation (figs. 27-36) has been done in a conventional approach, i.e. with graphs in which one parameter is varied while the others are kept constant. This type of graphs makes easier to study the trends of every expression in all the ranges for each parameter. Discrete diverse values of the parameters considered significant have been chosen, within the representative ranges of engine-like conditions, according to the experience in the literature, but with rigorous consideration to the validity limits of each author. Several data calculations and graphs are also included for lower pressures and temperatures close to atmospheric conditions.



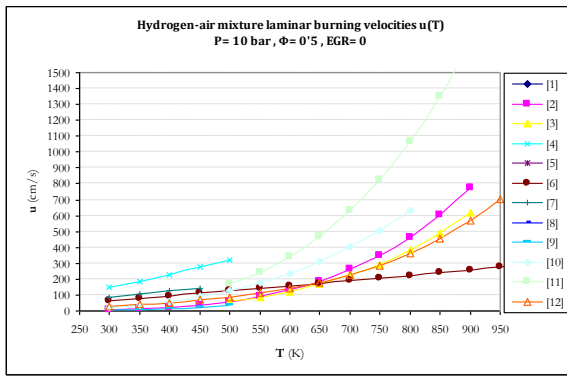
a



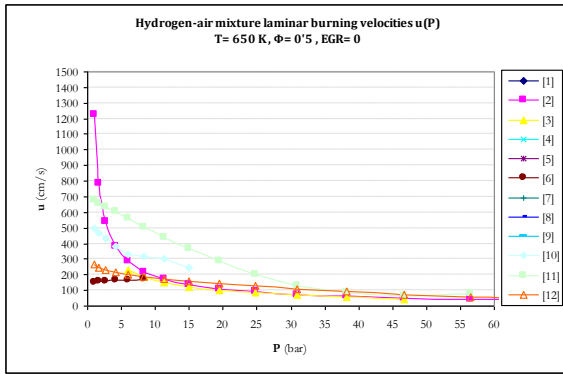
e



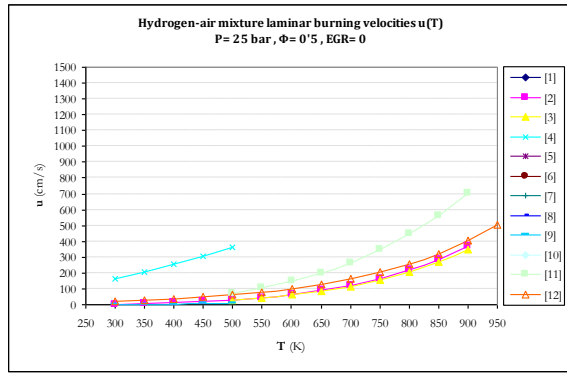
b



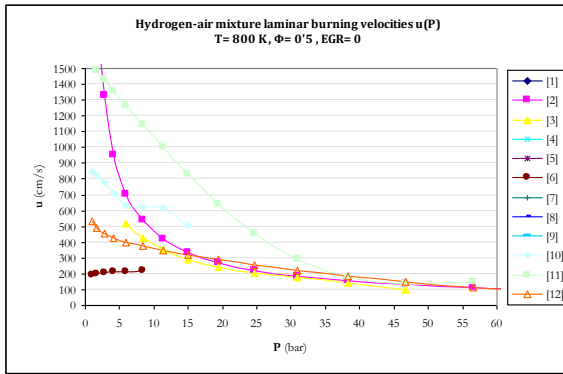
f



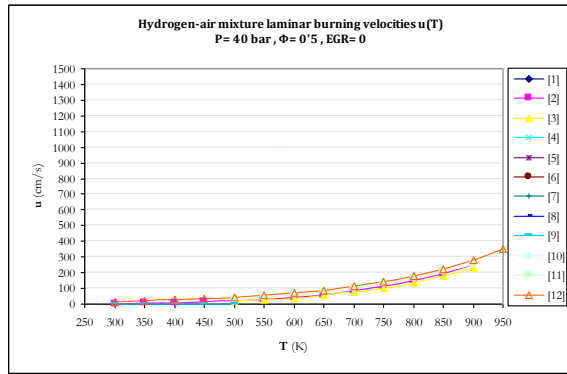
c



g

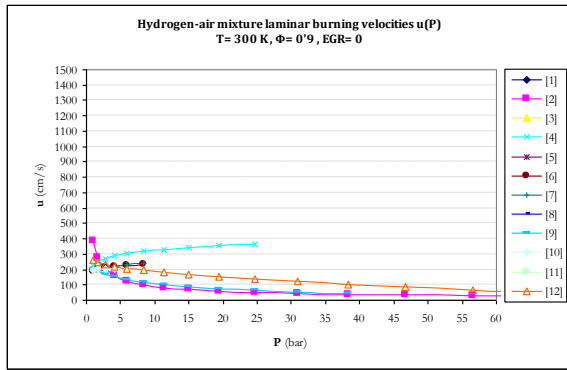


d

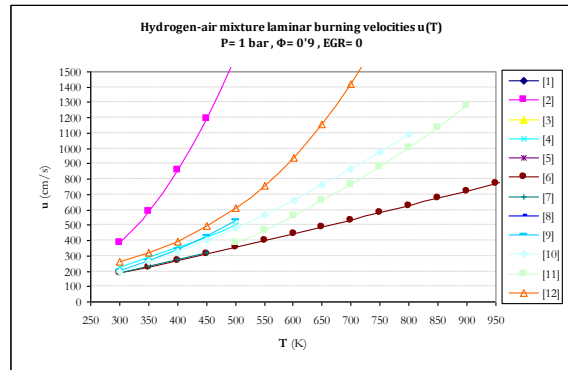


h

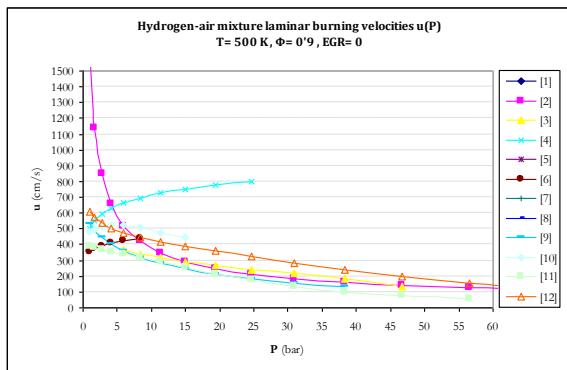
Fig. 27. Hydrogen-air mixture laminar burning velocity $u(P)$ and $u(T_u)$ graphs for $\phi=0.5$ & $EGR=0$



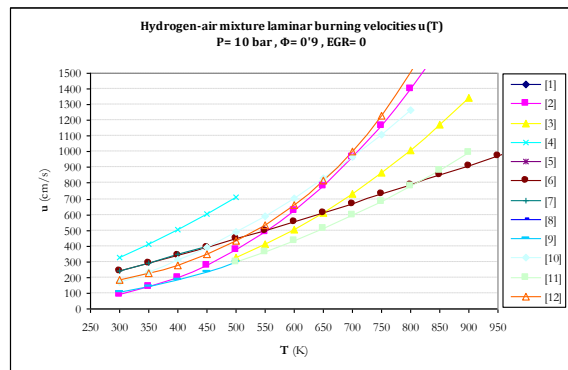
a



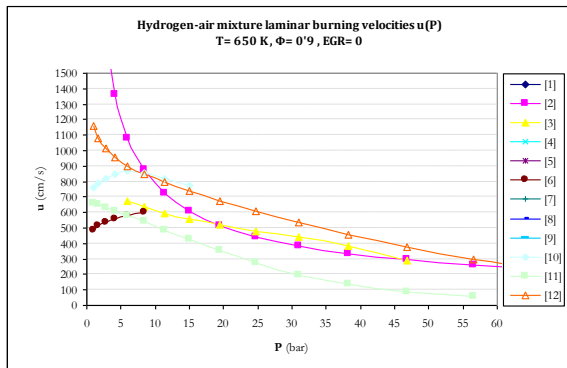
e



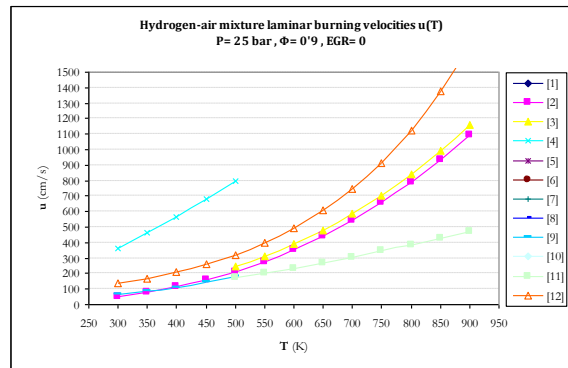
b



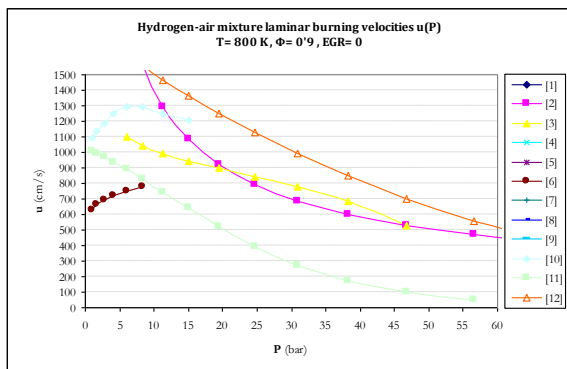
f



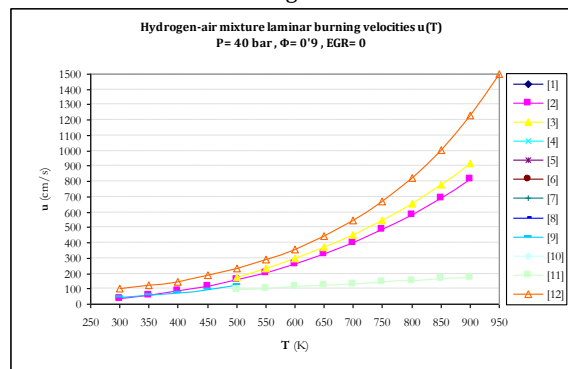
c



g

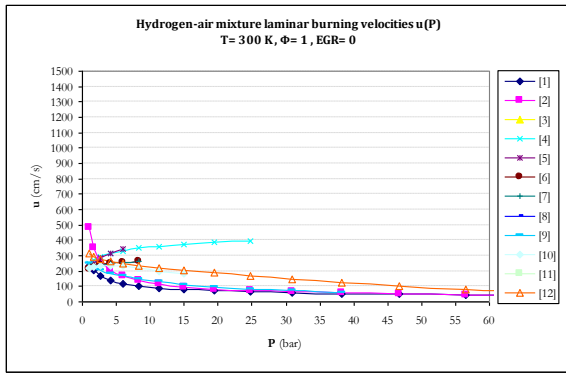


d

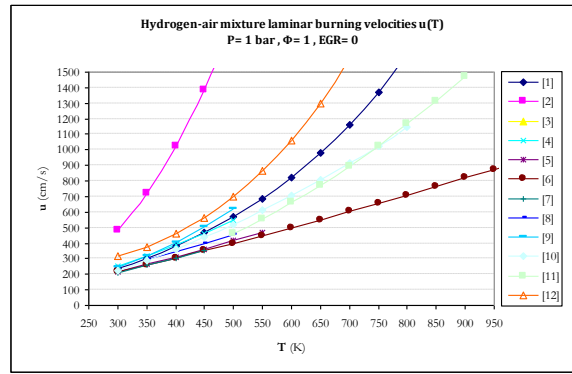


h

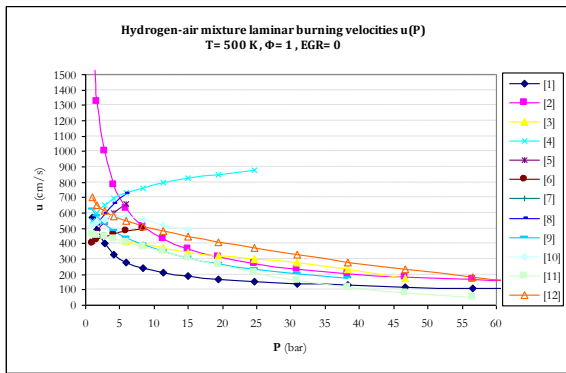
Fig. 28. Hydrogen-air mixture laminar burning velocity $u(P)$ and $u(T_u)$ graphs for $\Phi=0.9$ & $\text{EGR}=0$



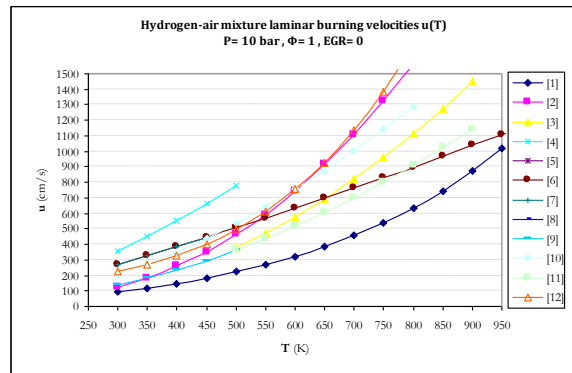
a



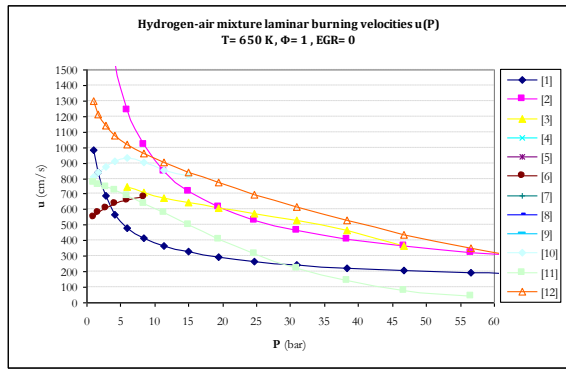
e



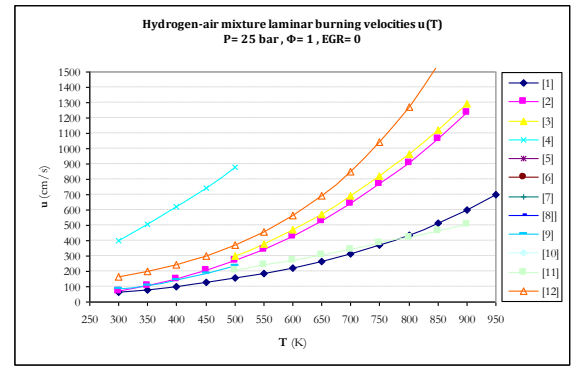
b



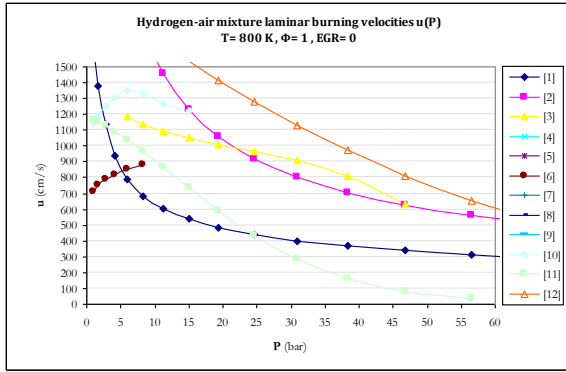
f



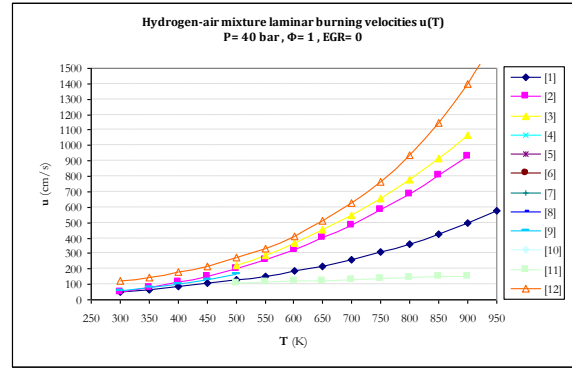
c



g



d



h

Fig. 29. Hydrogen-air mixture laminar burning velocity $u(P)$ and $u(T_u)$ graphs for $\Phi=1$ & $EGR=0$

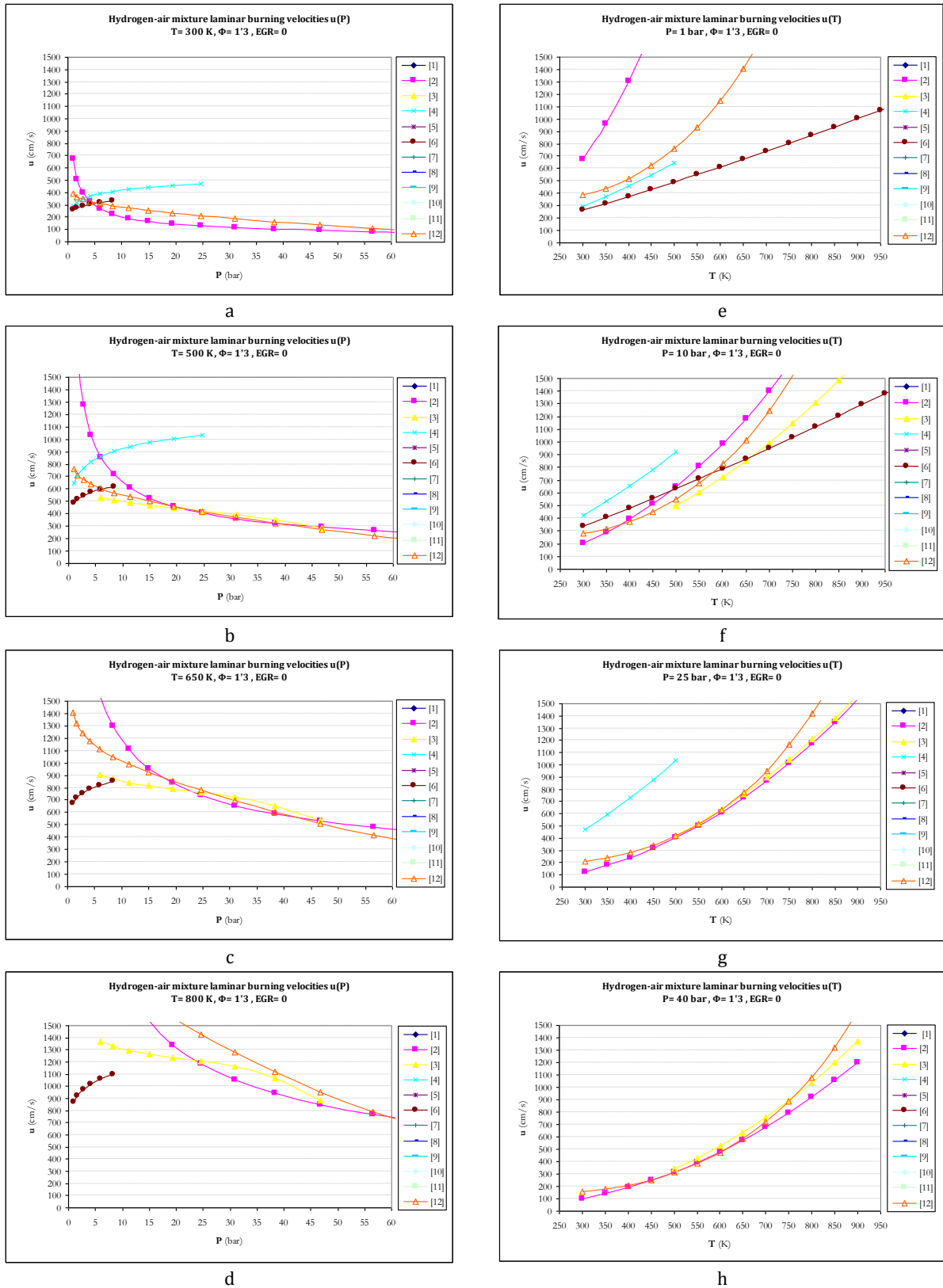
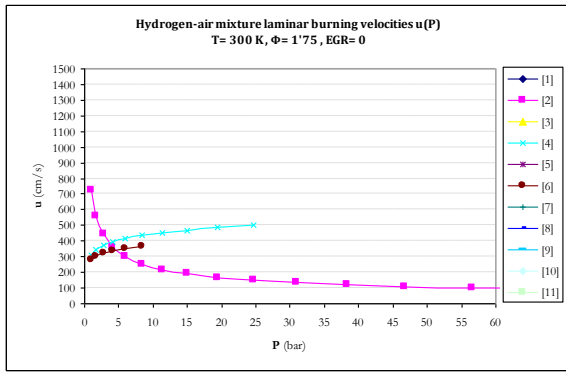
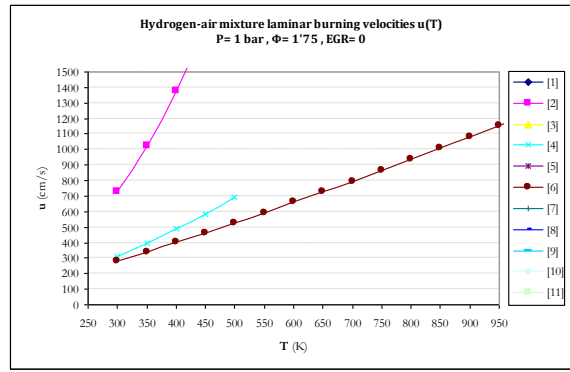


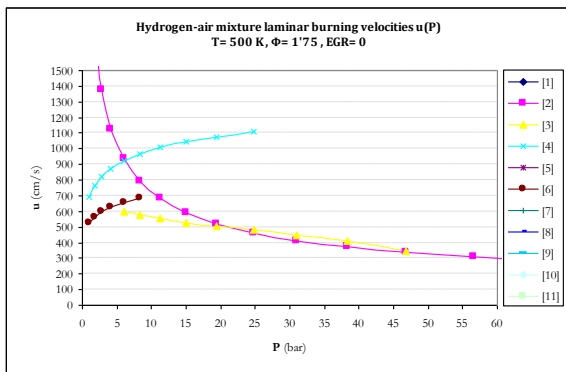
Fig. 30. Hydrogen-air mixture laminar burning velocity $u(P)$ and $u(T_u)$ graphs for $\Phi=1.3$ & $\text{EGR}=0$



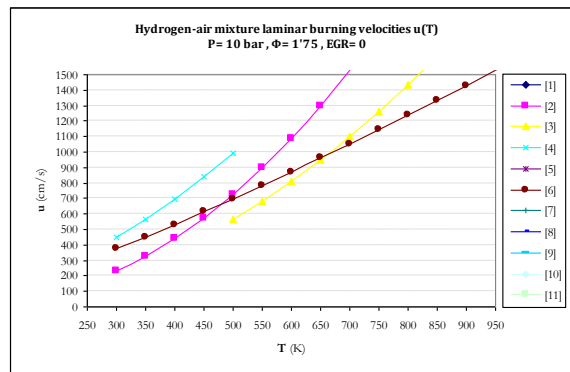
a



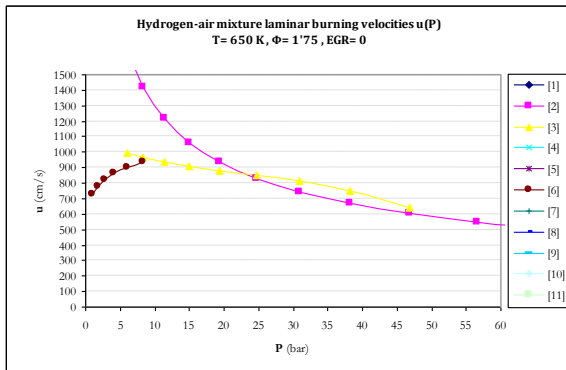
e



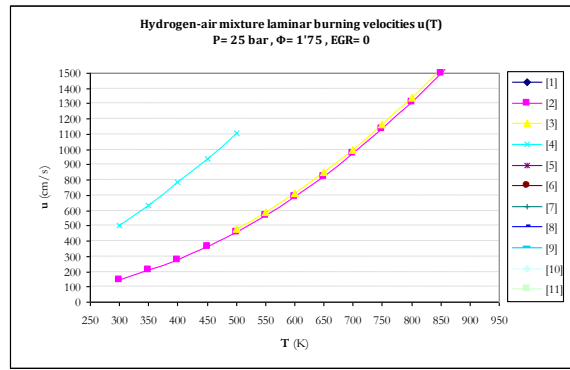
b



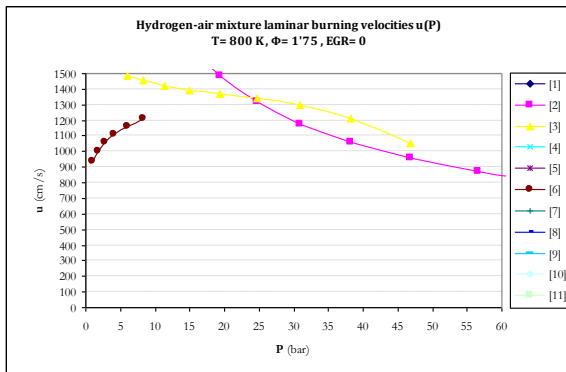
f



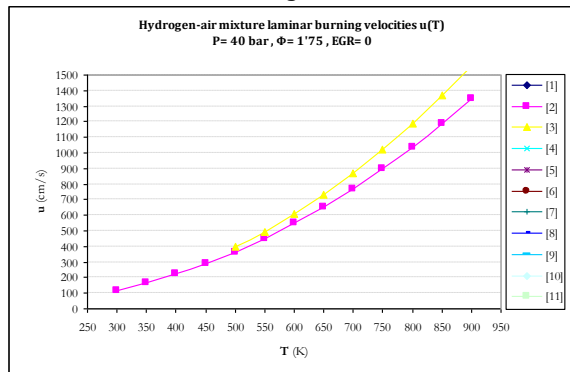
c



g

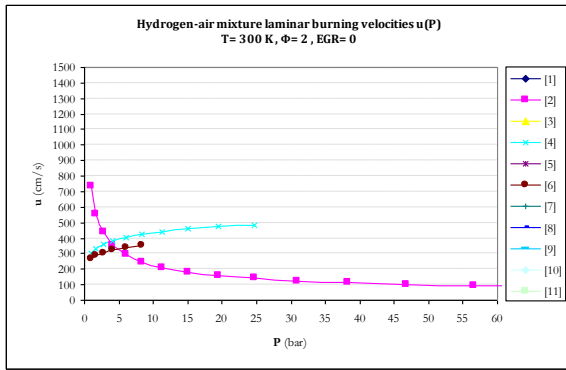


d

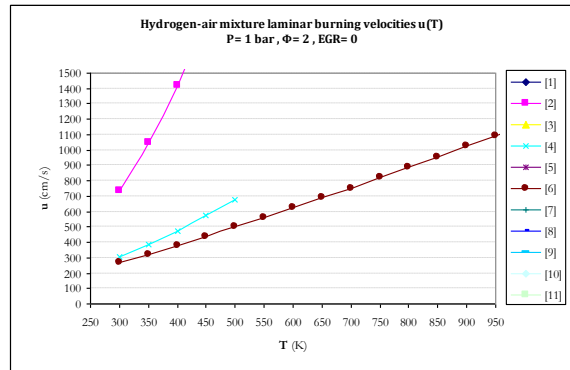


h

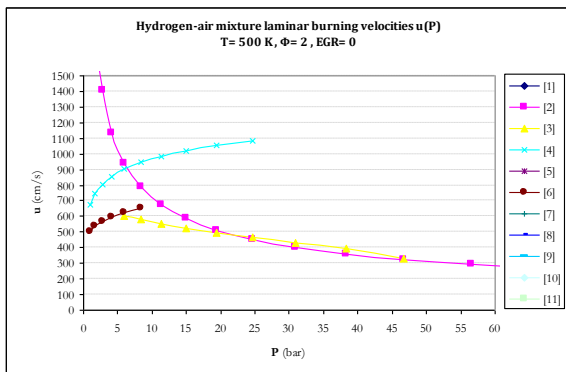
Fig. 31. Hydrogen-air mixture laminar burning velocity $u(P)$ and $u(T_u)$ graphs for $\Phi=1.75$ & $\text{EGR}=0$



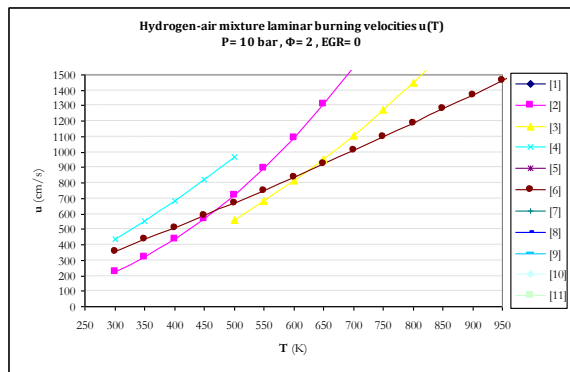
a



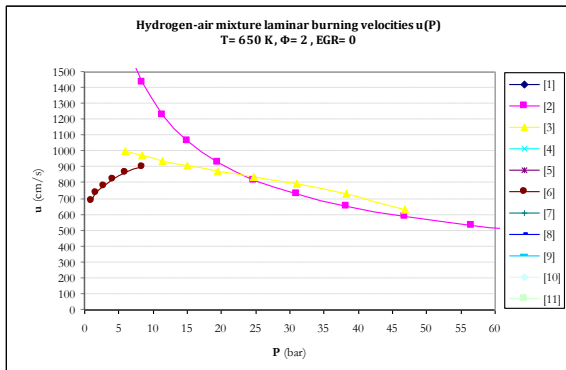
e



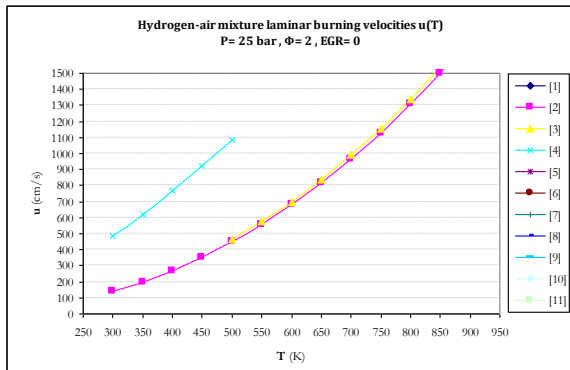
b



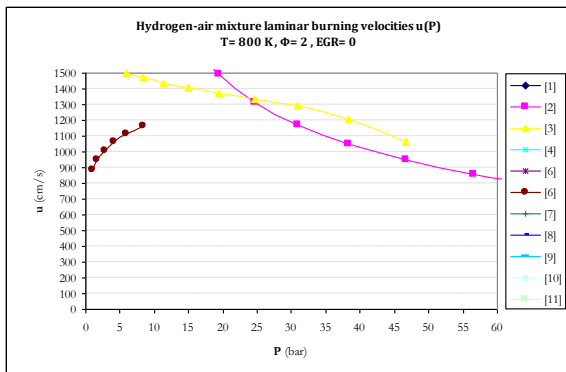
f



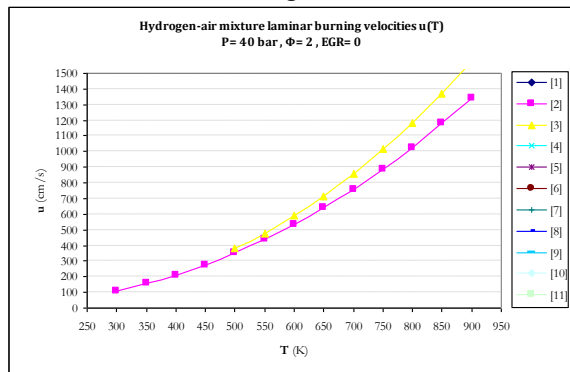
c



g

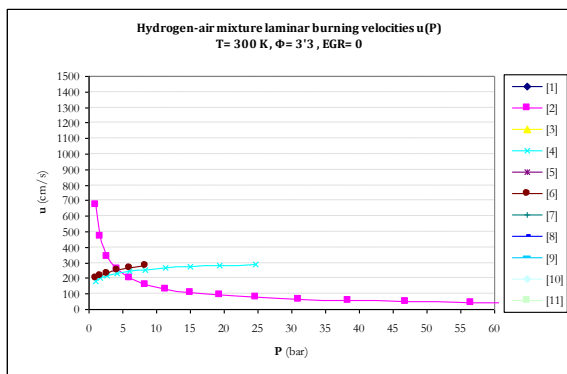


d

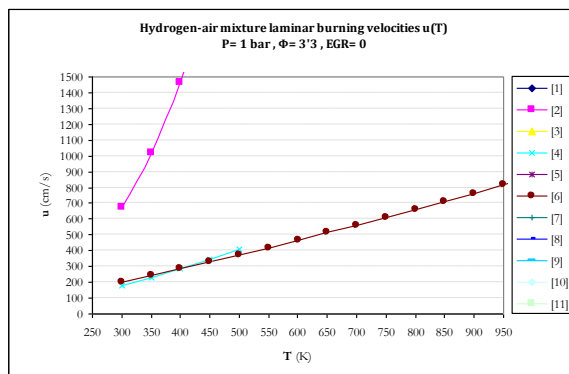


h

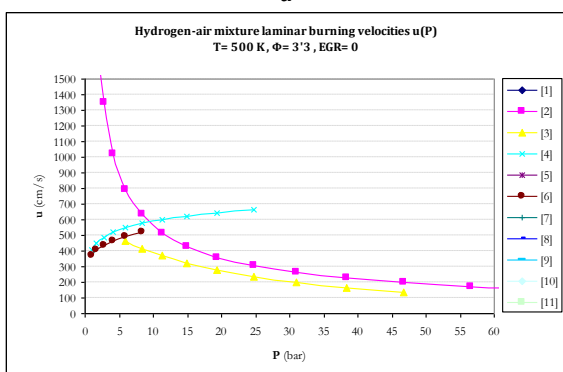
Fig. 32. Hydrogen-air mixture laminar burning velocity $u(P)$ and $u(T_u)$ graphs for $\Phi=2$ & $\text{EGR}=0$



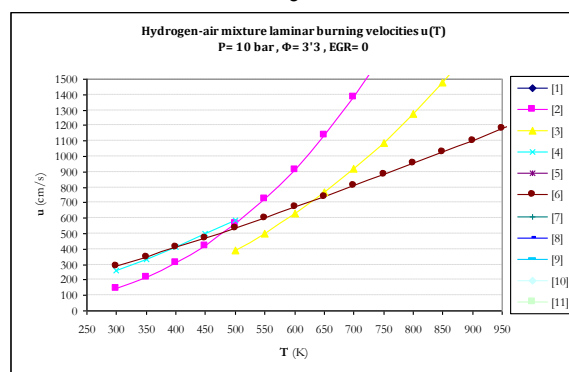
a



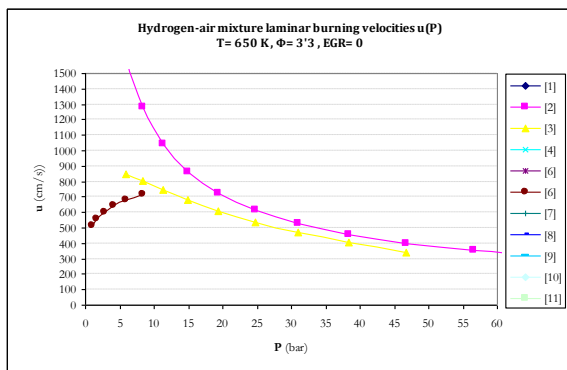
e



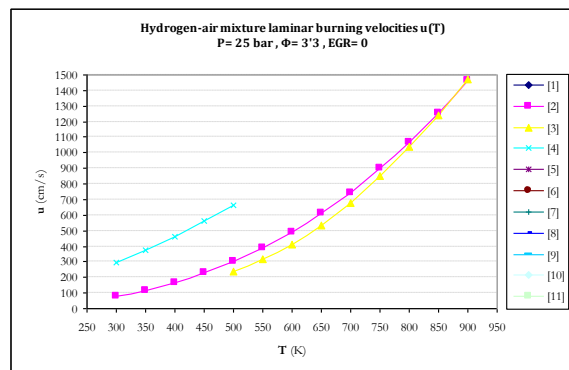
b



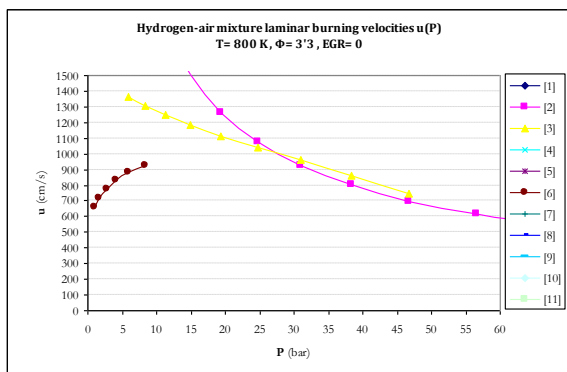
f



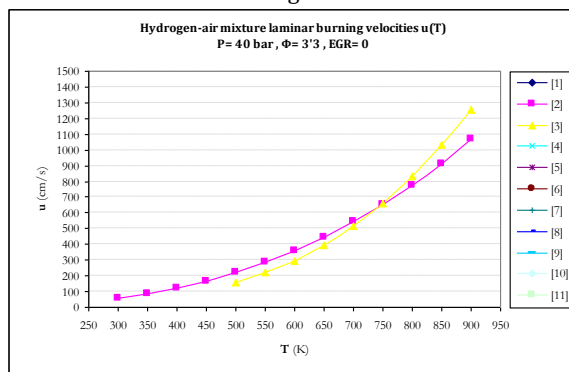
c



g

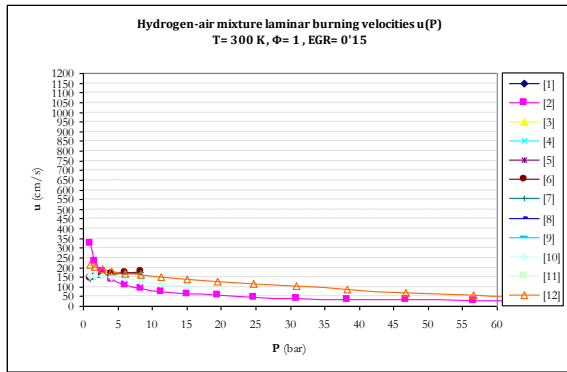


d

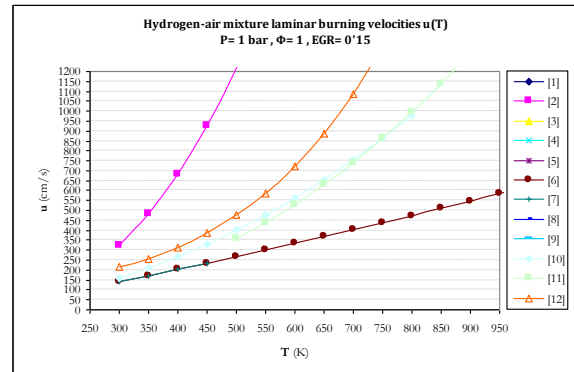


h

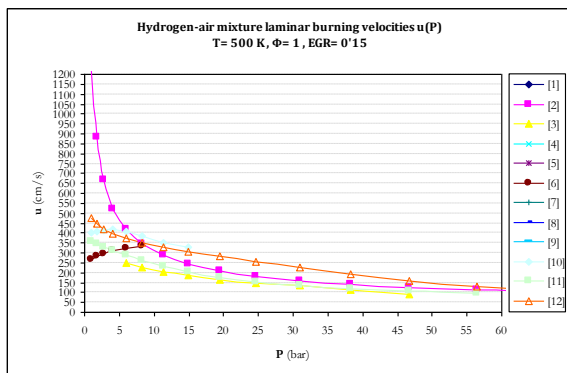
Fig. 33. Hydrogen-air mixture laminar burning velocity $u(P)$ and $u(T_u)$ graphs for $\Phi=3.3$ & $\text{EGR}=0$



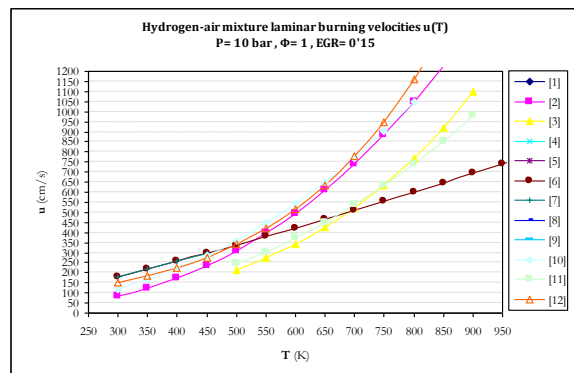
a



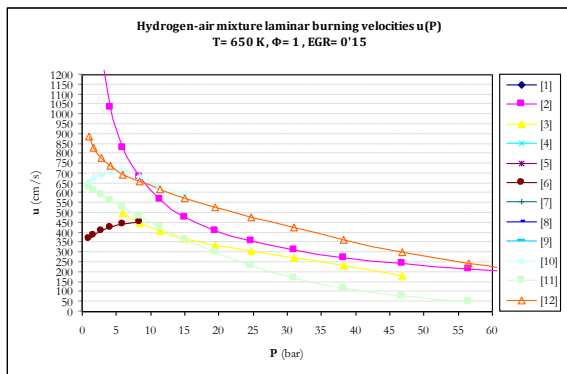
e



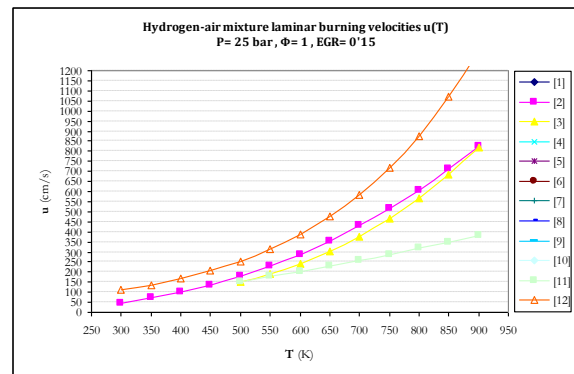
b



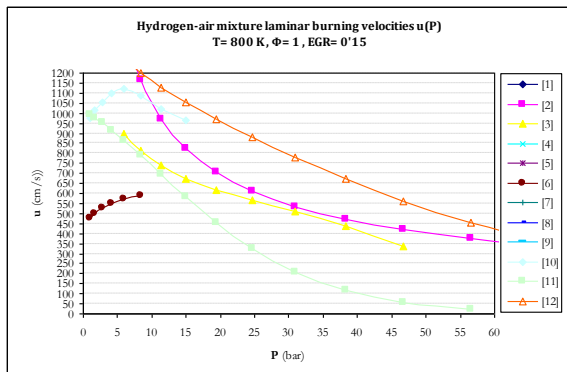
f



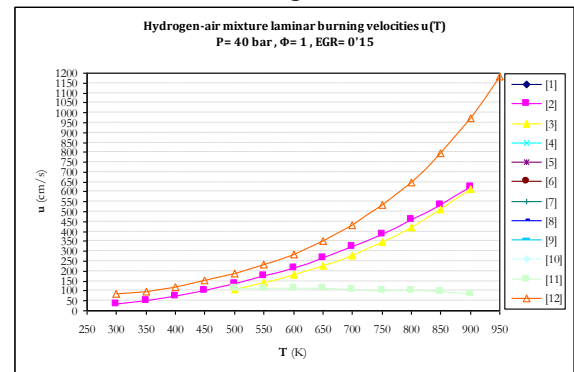
c



g

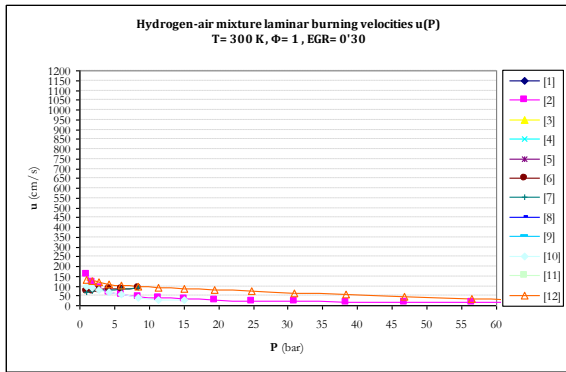


d

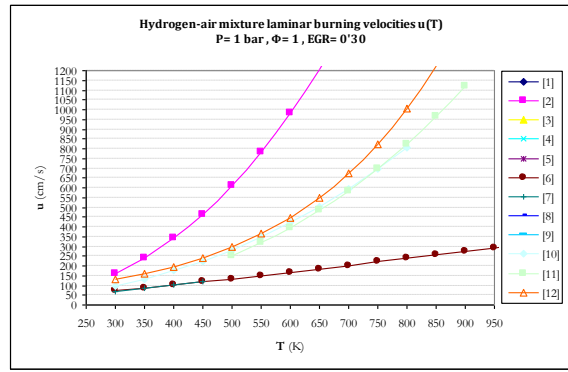


h

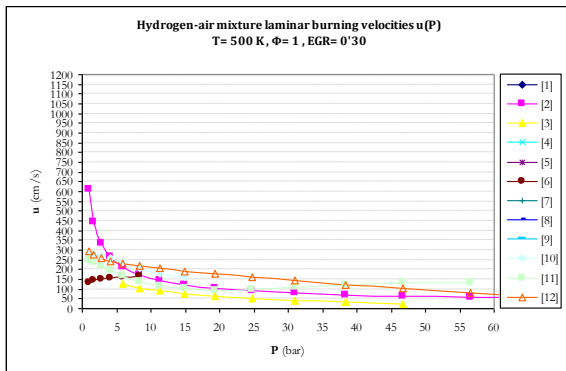
Fig. 34. Hydrogen-air mixture laminar burning velocity $u(P)$ and $u(T_u)$ graphs for $\Phi=1$ & $\text{EGR}=0.15$
 (Notice the change of scale in velocity axis of the graphs of [figs. 34-36](#) relative to the graphs of [figs. 27-33,37](#))



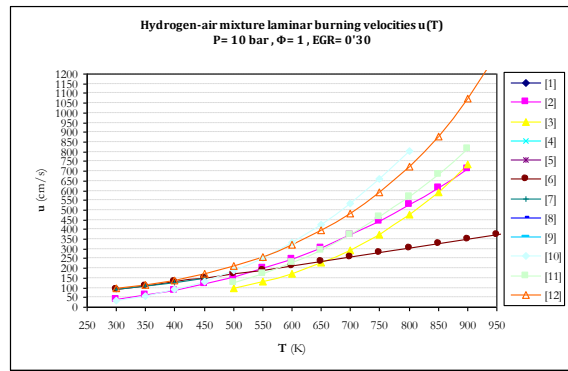
a



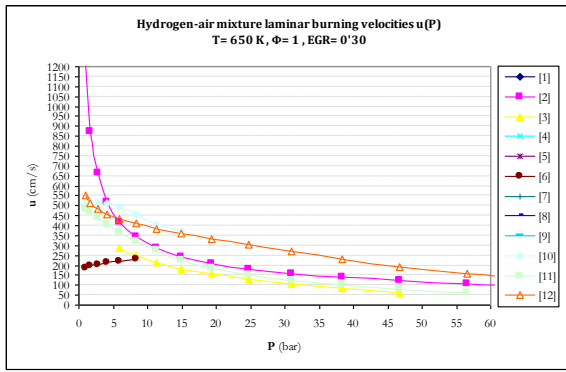
e



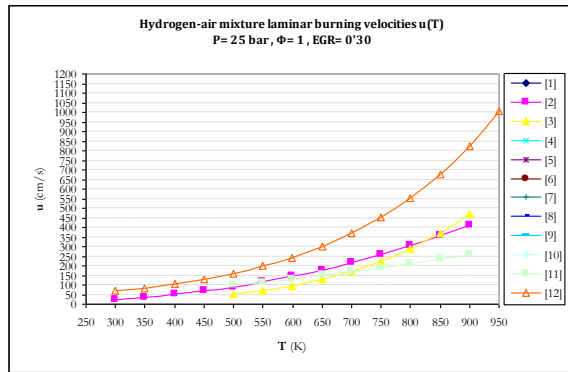
b



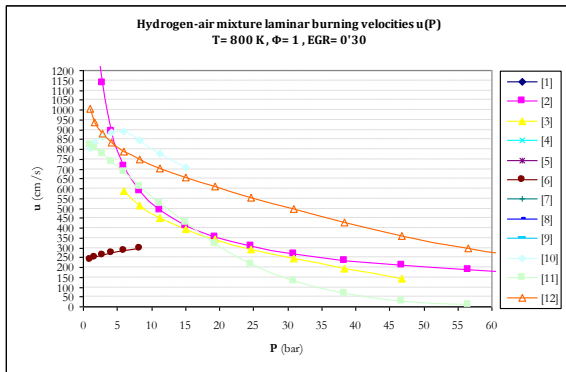
f



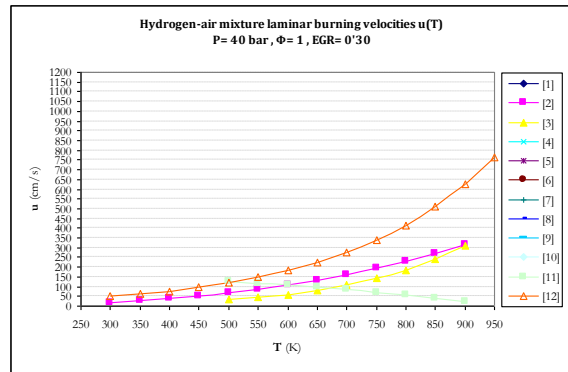
c



g



d



h

Fig. 35. Hydrogen-air mixture laminar burning velocity $u(P)$ and $u(T_u)$ graphs for $\Phi=1$ & $EGR=0.30$
(Notice the change of scale in velocity axis of the graphs of figs. 34-36 relative to the graphs of figs. 27-33,37)

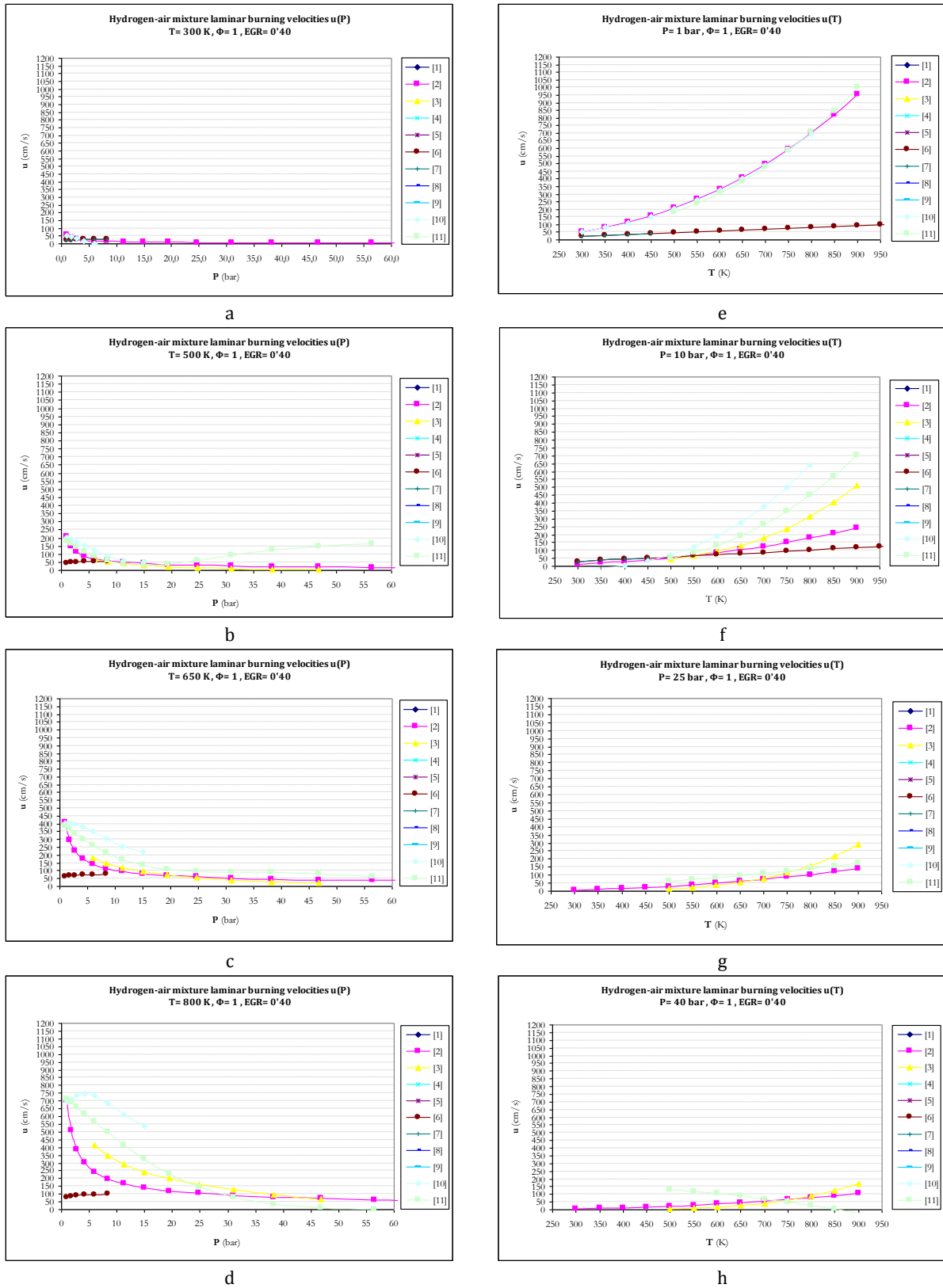


Fig. 36. Hydrogen-air mixture laminar burning velocity $u(P)$ and $u(T_u)$ graphs for $\Phi=1$ & $EGR=0.40$
 (Notice the change of scale in velocity axis of the graphs of figs. 34-36 relative to the graphs of figs. 27-33,37)

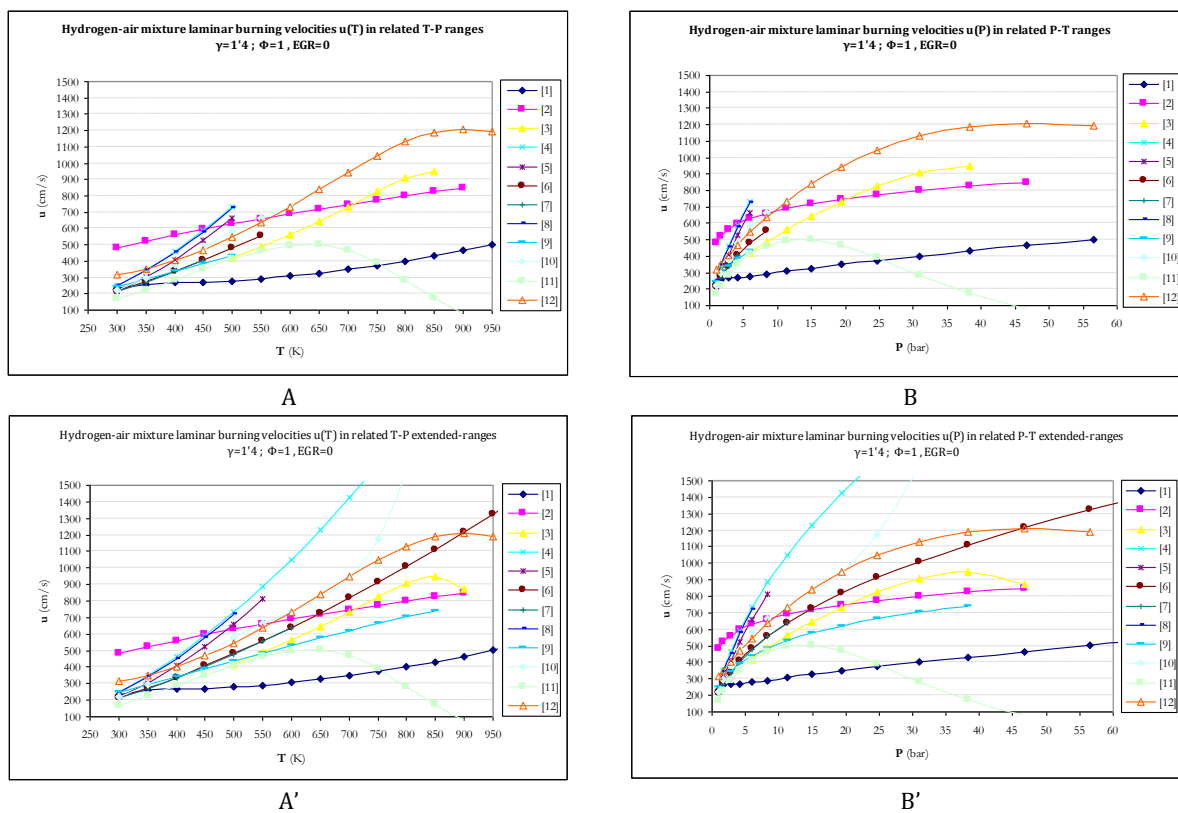
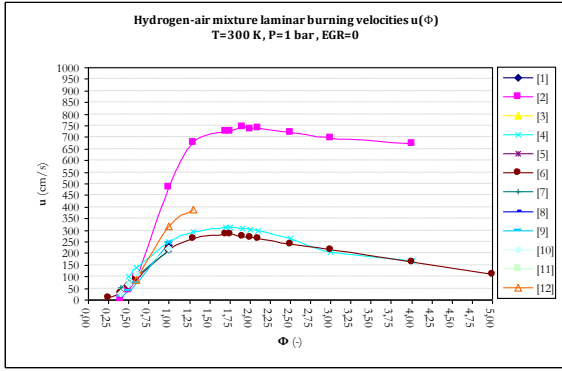


Fig. 37. Hydrogen-air mixture laminar burning velocity $u(T)$ and $u(P)$ graphs for $\Phi=1$ & $EGR=0$ and adiabatically related P - T values ($\gamma=1.4$). In the top graphs, *A* and *B*, the limitations of the validity ranges of P and T are strictly considered for each expression of laminar burning velocity. In the charts *A'* and *B'*, some of the velocity expressions are calculated even for values arbitrarily out of the respective validity ranges, to sketch the trends that they would have in wider ranges.

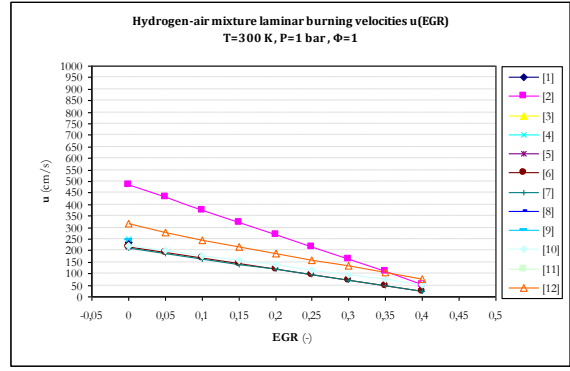
Table 19

Values of temperature T and pressure P related by an adiabatic compression ($\gamma = c_p/c_v = 1.4$) for the expressions of laminar burning velocity in charts of fig. 37 (*A*, *A'*; *B*, *B'*)

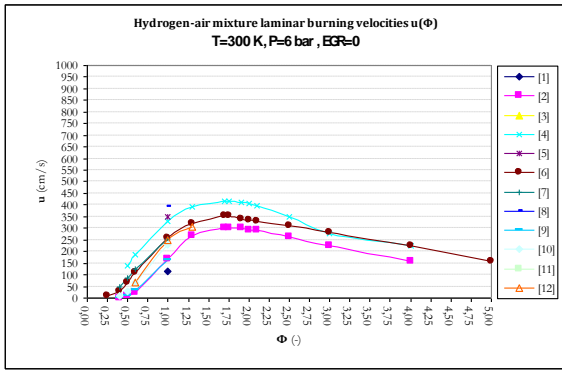
Temperature T (K)	Pressure P (bar)
$T_r = 300$	$P_r = 1$
	$P = P_r (T/T_r)^{1/\gamma}$
300	1.0
350	1.7
400	2.7
450	4.1
500	6.0
550	8.3
600	11.3
650	15.0
700	19.4
750	24.7
800	31.0
850	38.3
900	46.8
950	56.5



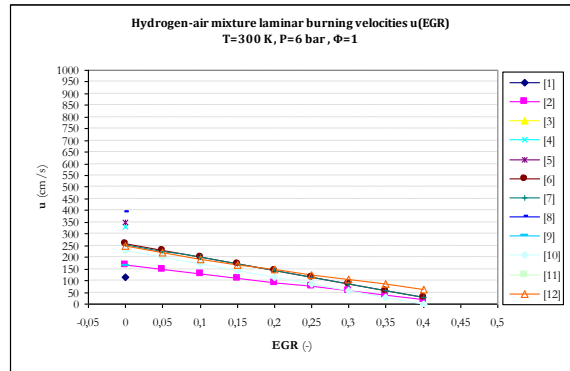
a



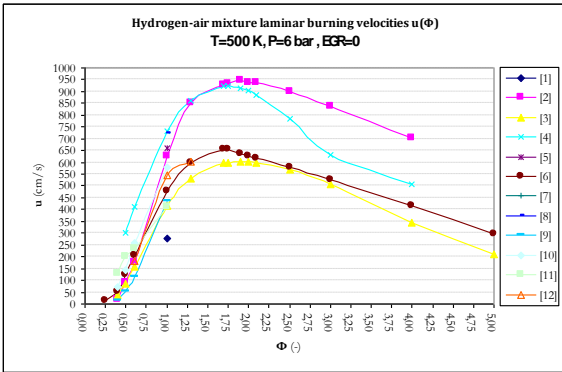
b



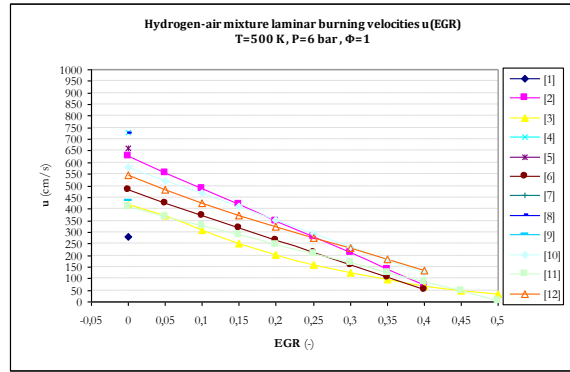
c



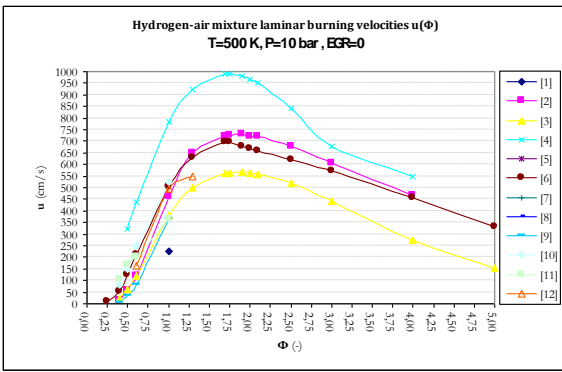
d



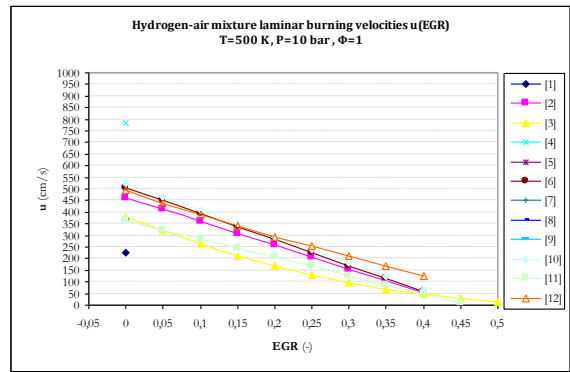
e



f



g



h

Fig. 38. Hydrogen-air mixture laminar burning velocity $u(\Phi)$ and $u(EGR)$ graphs for $T_u=\{300, 500\}$ K & $P=\{1, 6, 10\}$ bar (Notice the change of scale in velocity axis of the graphs of fig. 38 relative, respectively, to the graphs of figs. 27-33,37 and figs. 34-36)

5.6. Analysis of results of laminar burning velocity expressions

In this section, various aspects of general, particular and specific type are explained, respectively, including three subsections.

5.6.1. General analysis

As suggested by many authors, there is little accurate data for the laminar burning velocity of hydrogen mixtures at engine conditions, unfortunately, and it is not easy to achieve experimentally measured data. It is remarkable that experimental set-ups do not allow easy measurements of truly, one-dimensionally propagating, planar flames of hydrogen-air mixtures particularly at high pressures. Thus, set-ups referred in the literature are often only approximations to a planar flame and should take account of the deviation from the planar geometry. As studied in this work, most of the currently used correlations for laminar burning velocity were derived from the pressure development recorded in a constant volume combustion bomb, e.g. the pioneer work and some of the widely adopted correlations in the Metghalchi-Keck form. However, it has been noted that many of these correlations are not of stretch-free burning velocities but include effects of stretch and combustion instabilities. Neglecting the effects of non-planar flame geometry and stretch rates effects on some experimentally observed burning velocities are a cause of the spread of data on the published laminar values.

On the other hand, it has been suggested that neglecting stretch in the estimation of laminar burning velocity may be less inaccurate at high pressure, based on the fact that at relatively large flame radii at which high pressure and temperature laminar flame speeds have been calculated from bomb experiments, stretch rate is small and hence its effect would be negligible. However, unfortunately, it is just at such low stretch conditions that high-pressure flames are most prone to instabilities such as cellularity, which have been shown to have even more marked effect on burning velocity than stretch rate. Because of the associated reduced Markstein numbers, it is inferred that most "laminar" flames at engine pressures and temperatures become "cellular" in nature. Indeed, a general consideration is whether there exists such a thing as a laminar flame, and its associated laminar burning velocity, under such conditions. Cellularity has been shown to have a significant effect on the "laminar" (quasi-laminar or apparent) burning velocity.

The models based on chemical kinetic calculations could be considered less close to the intrinsic gas fuel characteristic, in order to reproduce data, than the experimental affected by the cellular flames. But, as explained, at higher pressures cumbersome experiments and large uncertainties are involved to apply corrections for stretch and instabilities to the velocity expressions based on experimental data of flames, usually not one-dimensional, not plane, not smooth, not adiabatic, non-steady, but prone to cellular structure. Thus, the different expressions can only be compared qualitatively and being judged by the predicting trends. Even though, some interesting observations can be made. It is clear from the study that there are significant differences in some expressions. Mainly the trends of the purely kinetical results are different from the strictly experimental results without corrections.

From the comparison of burning velocities derived from flame speed measurements (with thermodynamic or-and optical-image analysis) and results predicted by computation of reaction mechanisms for various equivalence ratios, unburned temperature and pressure conditions, the burning velocities determined by measurements are of higher magnitude than the values given

by the kinetic schemes. The burning velocities defined by measurements, under realistic conditions, include the enhancement of flame speeds by flame front instabilities. This discrepancy can be explained by the different nature of experimental and computed flames, since measurements represent unstable flames and kinetic models represent stable flames. The measurements consider accelerating effects of flame stretch and thermo-diffusive and hydrodynamic instabilities, which are not accounted for by the kinetic schemes involved. One-dimensional simulations using only detailed kinetic schemes do not include such effects.

Some of the considered expressions have been used in the literature for hydrogen engine cycle calculations, sometimes based on numerical and/or experimental data. Using mathematical expressions is mostly preferred to using tabulated data as they are more easily implemented in engine codes. Laminar burning velocity data for the air-fuel-residual mixture at the instantaneous in-cylinder pressure and unburned gas temperature are required by turbulent burning velocity models, as well as many CFD formulations, Verhelst&Sheppard 2009 [20]. The models that assume the local burning to take place in a laminar mode (flamelet type models) need data on the stretched laminar burning velocity. Namely, when these models use the laminar burning velocity as the local burning velocity, this implies that the stretched laminar burning velocities should be taken either from library files of stretched flamelets or by models correcting for the effects of stretch rates. Most of these models assume a linear relation between flame speed and stretch rate, valid for weakly perturbed laminar flames. In some cases, based on measurements of cellular flames, “quasi-laminar” burning velocity expressions are used as an intermediate solution convenient for simulations. They are used generally without any stretch model inasmuch that the effects of stretch are considered embodied in the experimental origin data.

5.6.2. Particular analysis of expressions of laminar burning velocity

After the previous general analysis, a particular discussion can be done about the numerical results and trends of lines in [figs. 27-38](#), based on the meaning of the laminar burning velocity proposed by each author. The unified nomenclature included in [table 12](#) is used.

Expressions based on cellular flames of the type “ $u_{nr,c}$ ”, such as the one of Iijima&Takeno 1986 [4] (line 4 _ light blue line with crosses), predict substantially higher velocities than all others, in their corresponding ranges of validity. In addition, Iijima&Takeno 1986 [4] expression has a contrary trend to the others when pressure grows. This trend is due to a positive exponent of pressure and is probably caused by not considering for the effects of stretch and instabilities, which increase with pressure as the flame thickness decreases.

The work of Göttgens et al. 1992 [9] resulted in an expression based on the lean premixed flames structure asymptotic analysis of the type “ u_L ” (line 9 _ light blue line with long segments). This makes it singular in comparison with all others. As observed in charts it shows a proper uniform behavior, but limited to 500 K, not enough for engine-like conditions, but it is a good complement to other expressions in its temperature range. In spite of that, the burning velocity is limited to lean to stoichiometric equivalence ratios and without a residual gas fraction factor.

The expressions proposed by Hu et al. 2009 [1] of the type “ u_L ” (line 1 _ dark blue line with diamonds), by Milton&Keck 1984 [5] of the type “ $u_{nr,c}$ ” (line 5 _ purple line with crosses), and by Lafuente 2008 [8] of the type “ $u_{nr,c}$ ” (line 8 _ blue line with short segments), have been only defined for stoichiometric conditions, making impossible to compare in other ranges of equivalence ratios (Φ). The interest of the first one [1] lies on the very broad P - T ranges of initial

temperature up to 950 K and pressure up to 80 bar . These limits are higher than others are, since they were achieved in their study by numerical chemical kinetic simulation, with extension from more restricted ranges of experimental data. The values included a correction for stretch effects but without consideration of eventual instabilities. Expressions [5] and [8] were defined from cellular conditions and they are limited up about 7 bar of pressure, which makes them of limited applicability if engine conditions are intended.

The expression of Verhelst et al. 2011 [3] of the type " u_{ql} ." (line 3 _ yellow line with triangles) based on Konnov's [47] kinetic scheme is considered, among the others, one of the most appropriate choices to be used in its ranges, for pressures from 5 up to 45 bar and temperatures from 500 to 900 K , for a fuel to air equivalence ratio (Φ) up to 5 , and with a wide range of residuals. This expression is not strictly applicable for low values of pressure (below 5 bar) and temperature (below 500 K), however it has a uniform behavior in wider ranges. This expression was validated against burning velocity measurements (in a combustion chamber) and with other kinetic models.

The analytical correction for the residuals included in this expression is clearly more comprehensive than other previous formulations, being valid for a wider range of conditions (including rich mixtures) and validated as always giving physically meaningful results. A distinction can be made between the linear trend obtained using previous Verhelst's works and the quadratic trend obtained using this one in accordance with the detailed kinetics (with lower values for the correction term than others, e.g. a smaller decrease of burning velocity in the presence of residuals for the lean cases). During the fitting procedure, the authors opted for removing the smallest values of burning velocities (less than 10 cm/s) from the dataset. Furthermore, the fitting was focused on the part of the dataset that was considered by the authors to be the most appropriate for engine simulations. The entire temperature range (500 - 900 K) was considered, but for extreme values of fuel to air equivalence ratio (Φ), lower than 0.5 and higher than 1.8 , the highest concentrations of residual gases ($f_{res} > 0.3$) were excluded.

For pressures and temperatures lower than 5 bar and 500 K , the other previous expressions that could be used from Verhelst et al. 2003,2005 [10,13] of the type " u_L ." (line 10 _ pale blue line with diamonds), and from Verhelst et al. 2005,2007 [7,13,14] of the type " u_{qnc} " (line 7 _ blue-green line with crosses), are based respectively on different kinetics schemes and experimental data, partially validated using an engine code (non-corrected for the effects of stretch and instabilities, as described by the authors, according with the explained hydrogen-air mixtures behavior). They were defined in rather restricted ranges, only valid in the stoichiometric to lean region conditions ($\Phi \leq 1$), with the applicability of the first [10] only up to 16 bar and 800 K , and the second [7] limited up to 10 bar and 430 K . The effect of residuals in these correlations differs, as observed, from the mentioned before. For instance, expression [7,13,14] predicts negative values when the residual gas volumetric content is higher than 45% . The expression [10,13] provides reasonable results for conditions from about 5 bar and 500 K to 25 bar and 700 K , but gives negative results at about 45 bar and 900 K for residual gas contents above 45% in volume, as was observed by the same authors.

The expression presented by Knop et al. 2008 [6] of the type " u_{ql} ." (line 6 _ brown line with circles), based on a combination of the correlation by Verhelst et al. [7,13] and additional chemical kinetic calculations, extends the range of conditions up to higher temperatures (1000 K) and fuel to air equivalence ratio Φ up to 5 . However, it is also limited to 10 bar as Verhelst's original expression, limiting the applicability to narrower range engine-like conditions, despite the validation done by comparison between simulated and measured engine cycles. At lean condition, the results using the expression of Verhelst et al. [7] are coincident in their partial range with the results provided by the expression of Knop et al [6].

The other expression based on a combination of the approach of Verhelst et al. [10] and chemical kinetic calculations is the one presented by D'Errico et al. 2008 [11] of the type " u_{ql} " (line 11 _ pale green line with squares), based on the mechanism of Frassoldati et al. 2006 [172]. As aforementioned, the range of conditions is out of the range of the proven reliability of chemical kinetic schemes and the calculations were limited to fuel-air equivalence ratios from stoichiometric to lean values ($\Phi \leq 1$), as in the case of the initial correlations of Verhelst et al. The applicability is limited partially because burning velocity extends widely to even negative values, even in the considered ranges. Somehow different trends result, compared to other correlations. Part of meaning is lost at high pressure and temperature, with some alteration of the common patterns of most other expressions. Based on the observations it seems to have a validity range more reduced than the one proposed by the authors, perhaps due to its mathematical form, which cannot reproduce all trends given by the detailed kinetic calculations. It might be more proper at more limited temperature and pressure (up to 16 bar), for not extreme equivalence ratios and without a significant quantity of residuals.

Gerke et al. 2010 [2] presented expressions for burning velocities obtained from two methods. The first one is based on experimentally measuring the pressure, while in the second one a chemical kinetic mechanism is used. For the residual gas term, they refer to Verhelst et al. 2005 [7,13]. The experimentally based expression (first method) of Gerke et al. 2010 (denoted as [2]), of the type " u_{qNc} " obtained from combustion in a rapid compression machine, has not been represented in this work, because the velocity values predicted are substantially higher than others, which is logical since the data origin correspond to cellular flames (non-corrected for the effects of stretch and instabilities). The second expression of Gerke et al. (+O'Conaire et al.) 2010 [2] is based on chemical kinetic calculations using the mechanism of O'Conaire et al. 2004 [139]. It is a fit to detailed kinetics results and is of the type " u_{ql} " (line 2 _ pink line with squares). This expression is the one with the best coincidence with the results of the expression of Verhelst et al. 2011 [3] (line 3 _ yellow line with triangles) within the range of its conditions, from 5 to 45 bar and from 500 to 900 K. The expression of Gerke et al. (+O'Conaire et al.) 2010 [2] works properly when it is extended out of its proposed validity range, up to the values of the expression [3], for lower temperatures, from 300-350 K, and for higher pressures, also beyond 50-60 bar, mainly from lean to stoichiometric conditions. The results from expressions obtained by fitting to chemical kinetic calculations using the mechanisms of O'Conaire et al. [139] and Konnov [47] are fairly close for the higher pressure and temperature points, particularly for the lean equivalence ratios, and for significant dilution, mainly for equivalence ratios lower than those that make maximum the burning velocity, which happens about $\Phi = 1.7-1.9$.

The expression for the burning velocity due to Bougrine et al. 2011 [12] of the type " u_{ql} " (line 12 _ orange line with triangles) combines and optimizes mathematically other expressions of burning velocity from many works by Gülder 1984 [188], Han et al. 2007 [189], Rahim et al. 2002 [137], Coppens et al. 2007 [190], Hermanns 2007 [191], Hermanns et al. 2010 [192], Huang et al. 2006 [193], Tahtouh et al. 2009 [194], Gerke et al. 2010 [2], Bougrine et al. 2011 [142] and Verhelst et al. 2011 [3]. The validity ranges of this generic expression extend to the highest pressure and temperature levels for any fraction of hydrogen content (h) in a fuel blend with methane, from 0 to 100%. Its equivalence ratio range, 0.6 to 1.3, exceeds stoichiometric conditions but does not extent up to very rich mixtures. The form of the residual gas factor is a polynomial expression with exponents of the dilution fraction up to third degree, as the included in the last expression of Verhelst et al. 2011 [3] but with different coefficients.

Two main zones can be distinguished on the left graphs of fig. 38 (a,c,e,g); a lean to moderately rich zone ($\Phi \leq 1.7-1.9$), where the laminar flame velocity increases with the fuel to air equivalence ratio (Φ), and a very rich zone ($\Phi > 1.7-1.9$), where decreases with increasing of Φ .

The first zone is the most significant since the mean fuel to air equivalence ratio in hydrogen-fueled engines is normally lower than 1.6, and more usually lower than 1 (lean combustion). The very rich conditions are also modeled in some works, usually in order to represent the highly stratified operating conditions in direct injection engines.

The effects of dilution on the laminar burning velocities have been represented for stoichiometric mixtures on the right graphs of [fig. 38 \(b,d,f,h\)](#), showing generally a linear decrease as the volume fraction of residual gases increases (from $f_{res,u}=0$ to 0.4). The effect of residuals included in the expression of Verhelst et al. 2011 [\[3\]](#) is clearly better than the previous formulations, being valid for a wider range of conditions and validated as always giving physically meaningful results. The distinction that can be observed is the quadratic trend instead of the linear trend obtained when other expressions are used, with a result of lower values for the correction term, i.e. a smaller decrease of burning velocity in the presence of residuals. The expression of Bougrine et al. 2011 [\[12\]](#) is somewhat similar to this behavior of the expression [\[3\]](#), according to its corresponding data origin and its more complex term of residuals factor. Nevertheless this mathematically derived expression for the dilution residuals gas, in mass fraction terms, applicable in the range $[0, 0.3]$, yields burning velocity values generally higher than the expression due to Verhelst et al. 2011 [\[3\]](#).

5.6.3. Behavior of laminar burning velocity expressions calculated from chemical kinetics mechanisms on basis of theoretical one-dimensional flames

Some of the selected expressions of laminar burning velocity for hydrogen-air premixed mixtures combustion at elevated pressures and temperatures exhibit, in general, the following common behaviors when they have been developed in origin on the particular basis of numerical data generated by chemical kinetic calculations associated to theoretical one-dimensional flames.

These expressions provide laminar burning velocity values that increase with the increase of initial temperature and decrease with the increase of pressure.

Moreover, the predicted values of laminar burning velocity increase with the increase of fuel to air equivalence ratio in the case of fuel-lean mixture combustion, and decrease in the case of fuel-rich mixture combustion. Maximum values of laminar burning velocity happen for fuel to air equivalence ratio about 1.7-1.9. Otherwise, laminar burning velocities decrease with the increase of dilution ratio and the position of peak value of the laminar burning velocity moves slightly, towards a lower value of the mixture equivalence ratio, with the increase of dilution ratio (bigger presence of residuals).

References of chapters three, four and five (*third part*)

- [1] **Hu EJ, Huang ZH, He JJ, Miao HY.** Experimental and numerical study on laminar burning velocities and flame instabilities of hydrogen-air mixtures at elevated pressures and temperatures. *International Journal of Hydrogen Energy* 2009;34:8741-55.
- [2] **Gerke U, Steurs K, Rebecchi P, Boulouchos K.** Derivation of burning velocities of premixed hydrogen-air flames at engine-relevant conditions using a single-cylinder compression machine with optical access. *International Journal of Hydrogen Energy* 2010;35:2566-77.
- [3] **Verhelst S, T'Joen C, Vancoillie J, Demuyneck J.** A correlation for the laminar burning velocity for use in hydrogen spark-ignition engine simulation. *International Journal of Hydrogen Energy* 2011;36:957-74.
- [4] **Iijima T, Takeno T.** Effects of temperature and pressure on burning velocity. *Combustion and Flame* 1986;65:35-43.
- [5] **Milton BE, Keck JC.** Laminar burning velocities in stoichiometric hydrogen and hydrogen-hydrocarbon gas mixtures. *Combustion and Flame* 1984;58:13-22.
- [6] **Knop V, Benkenida A, Jay S, Colin O.** Modeling of combustion and nitrogen oxide formation in hydrogen-fueled internal combustion engines within a 3D-CFD code. *International Journal of Hydrogen Energy* 2008;33:5083-97.
- [7] **Verhelst S, Woolley R, Lawes M, Sierens R.** Laminar and unstable burning velocities and Markstein lengths of hydrogen-air mixtures at engine-like conditions. *Proceedings of the Combustion Institute* 2005;30:209-16.
- [8] **Lafuente A.** Methodology for the laminar burning velocity diagnosis in mixtures of fuels from the instantaneous pressure in a constant volume combustion bomb (Spanish). PhD thesis 2008, University of Valladolid (Spain).
- [9] **Göttgens J, Mauss F, Peters N.** Analytic approximations of burning velocities and flame thicknesses of lean hydrogen, methane, ethylene, ethane, acetylene and propane flames. *Proceedings of the Combustion Institute* 1992;24:129-35.
- [10] **Verhelst S, Sierens R.** A laminar burning velocity correlation for hydrogen-air mixtures valid at spark-ignition engine conditions. *ASME Spring Engine Technology Conference paper ICES2003-555*, Salzburg, Austria, 2003.
- [11] **D'Errico G, Onorati A, Ellgas S.** 1D-thermo-fluid dynamic modeling of an SI single-cylinder H₂ engine with cryogenic port injection. *International Journal of Hydrogen Energy* 2008;33:5829-41.
- [12] **Bougrine S, Richard S, Nicolle A, Veynante D.** Numerical study of laminar flame properties of diluted methane-hydrogen-air flames at high pressure and temperature using detailed chemistry. *International Journal of Hydrogen Energy* 2011;36:12035-47.
- [13] **Verhelst S.** A study of the combustion in hydrogen fueled internal combustion engines. PhD thesis 2005, Ghent University, Belgium.
- [14] **Verhelst S, Sierens R.** A quasi-dimensional model for the power cycle of a hydrogen fueled ICE. *International Journal of Hydrogen Energy* 2007;32:3545-54.
- [15] **Verhelst S, Wallner T.** Hydrogen-fueled internal combustion engines. *Progress in Energy and Combustion Science* 2009;35:490-527.
- [16] **Bauer CG, Forest TW.** Effect of hydrogen addition on the performance of methane-fueled vehicles. Part I: effect on SI engine performance. *International Journal of Hydrogen Energy* 2001;26:55-70.
- [17] **Perini F, Paltrinieri F, Mattarelli E.** A quasi-dimensional combustion model for performance and emissions of SI engines running on hydrogen-methane blends. *International Journal of Hydrogen Energy* 2010;35:4687-701.
- [18] **Hu EJ, Huang ZH, He JJ, Jin C, Zheng JJ.** Experimental and numerical study on laminar burning characteristics of premixed methane-hydrogen-air flames. *International Journal of Hydrogen Energy* 2009;34(11):4876-88.
- [19] **Tinaut FV, López JJ.** Combustion in spark ignition engines. In: Payri F, Desantes JM, editors. *Reciprocating internal combustion engines (Spanish)*. Valencia Polytechnic University publication, Reverté publisher 2011 (2nd imprint 2012); chapt.18.
- [20] **Verhelst S, Sheppard CGW.** Multi-zone thermodynamic modeling of spark-ignition engine combustion. An overview. *Energy Conversion and Management* 2009;50:1326-35.

- [21] **Horrillo A.** Utilization of multi-zone models for the prediction of the pollutant emissions in the exhaust process in spark ignition engines (Spanish). PhD thesis 1998, University of Valladolid (Spain).
- [22] **Gillespie L, Lawes M, Sheppard CGW, Woolley R.** Aspects of laminar and turbulent burning velocity relevant to SI engines. SAE 2000-01-0192, 2000./ SAE Transactions 109 (section 3) 2001:13-33. In: Oppenheim AK, Stodolsky F, editors. Advances in combustion. Society of Automotive Engineers, SAE SP-1492, 2000;1-22.
- [23] **Cuenot B, Egolfopoulos FN, Poinot T.** Direct numerical simulation of stagnation-flow premixed flames transition from planar to Bunsen flames and the direct measurement of laminar flame speeds. 2nd Joint Meeting of the Combustion Institute US Sections, 2000;134.
- [24] **Rallis CJ, Garforth AM, Steinz JA.** Laminar burning velocity of acetylene-air mixtures by the constant volume method. Combustion and Flame 1965;9:345-56.
- [25] **Bradley D, Gaskell PH, Gu XJ.** Burning velocities, Markstein lengths, and flame quenching for spherical methane-air flames: a computational study. Combustion and Flame 1996;104(1-2):176-98.
- [26] **Bradley D, Hicks RA, Lawes M, Sheppard CGW, Woolley R.** The measurement of laminar burning velocities and Markstein numbers, for iso-octane-air and iso-octane/n-heptane-air mixtures, at elevated temperatures and pressures, in an explosion bomb. Combustion and Flame 1998;115(1-2):126-44.
- [27] **Metghalchi M, Keck JC.** Laminar burning velocity of propane-air mixtures at high temperature and pressure. Combustion and Flame 1980;38:143-54.
- [28] **Metghalchi M, Keck JC.** Burning velocities of mixtures of air with methanol, isooctane, and indolene at high pressure and temperature. Combustion and Flame 1982;48:191-210.
- [29] **Ryan TW, Lestz SS.** The laminar burning velocity of iso-octane, n-heptane, methanol, methane, and propane at elevated temperature and pressures in the presence of a diluent. SAE 800103./ SAE Transactions, Detroit, Michigan, 1980;Vol.89.
- [30] **Rahim F.** Determination of burning speed for methane-oxidizer-diluent mixtures. PhD thesis 2002, Northeastern University, Boston, Massachusetts.
- [31] **Dahoe AE, De-Goey LPH.** On the determination of the laminar burning velocity from closed vessel gas explosions. Journal of Loss Prevention in the Process Industries 2003;16:457-78.
- [32] **Dahoe AE.** Laminar burning velocities of hydrogen-air mixtures from closed vessel gas explosions. Journal of Loss Prevention in the Process Industries 2005;18:152-66.
- [33] **Heywood JB.** Internal combustion engine fundamentals. McGraw-Hill, New-York; 1988.
- [34] **Glassman I.** Combustion. Academic Press Inc. Orlando, Florida, 1997.
- [35] **Kuo KK.** Principles of combustion. Wiley&Sons Inc. New York, 1986.
- [36] **Desantes JM, Molina S.** Introduction to combustion. In: Payri F, Desantes JM, editors. Reciprocating internal combustion engines (Spanish). Valencia Polytechnic University publication, Reverté publisher 2011 (2nd imprint 2012);chapt.13.
- [37] **Turns SR.** An introduction to combustion. McGraw-Hill, New-York, 2000.
- [38] **Egolfopoulos FN, Law CK.** Chain mechanisms in the overall reaction orders in laminar flame propagation. Combustion and Flame 1990;80(1):7-16.
- [39] **Zeldovich YB.** Structure and stability of steady laminar flames at moderately large Reynolds numbers. Combustion and Flame 1981;40:225-34.
- [40] **Zeldovich YB, Barenblatt GI, Librovich VB, Makhviladze GM.** The mathematical theory of combustion and explosions. Plenum Press, New-York, 1985.
- [41] **Williams FA.** Combustion theory. Addison-Wesley, Reading, Massachusetts, 1985.
- [42] **Clavin P.** Dynamic behavior of premixed flame fronts in laminar and turbulent flows. Progress in Energy and Combustion Science 1985;11(1):1-59.
- [43] **Seshadri KA, Williams FA.** Turbulent reacting flows. Academic Press, London; 1994.
- [44] **Peters N, Williams FA.** The asymptotic structure of stoichiometric methane-air flames. Combustion and Flame 1987;68(2):185-207.
- [45] **Bradley D, Lawes M, Liu K, Verhelst S, Woolley R.** Laminar burning velocities of lean hydrogen-air mixtures at pressures up to 1 MPa. Combustion and Flame 2007;149(1-2):162-72.
- [46] **Davis SG, Joshi AV, Wang H, Egolfopoulos F.** An optimized kinetic model of H₂-CO combustion. Proceedings of the Combustion Institute 2005;30:1283-92.

- [47] **Konnov AA.** Refinement of the kinetic mechanism of hydrogen combustion. *Journal of Advances in Chemical Physics* 2004;23:5-18.
- [48] **Manton J, Von-Elbe G, Lewis B.** Non-isotropic propagation of combustion waves in explosive gas mixtures and the development of cellular flames. *Journal of Chemical Physics* 1952;20(1):153-7.
- [49] **Bechtold JK, Matalon M.** Hydrodynamic and diffusion effects on the stability of spherically expanding flames. *Combustion and Flame* 1987;67(1):77-90.
- [50] **Law CK.** Dynamics of stretched flames. *Proceedings of the Combustion Institute* 1988;22:1381-402.
- [51] **Kull HJ.** Theory of the Rayleigh-Taylor instability. *Physics Reports (Review Section of Physics Letters)* 1991;206(5):197-325.
- [52] **Ronney PD.** A perspective on the microgravity role in combustion research. *Combustion and Flame* 1999;116:317-8.
- [53] **Bychkov VV, Liberman MA.** Dynamics and stability of premixed flames. *Physics Reports* 2000;325:115-237.
- [54] **Law CK, Sung CJ.** Structure, aerodynamics and geometry of premixed flamelets. *Progress in Energy and Combustion Science* 2000;26(4-6):459-505.
- [55] **Gu XJ, Haq MZ, Lawes M, Woolley R.** Laminar burning velocity and Markstein lengths of methane-air mixtures. *Combustion and Flame* 2000;121(1-2):41-58.
- [56] **Law CK, Kwon OC.** Effects of hydrocarbon substitution on atmospheric hydrogen-air flame propagation. *International Journal of Hydrogen Energy* 2004;29(8):867-79.
- [57] **Law CK.** Propagation, structure, and limit phenomena of laminar flames at elevated pressures. *Combustion Science and Technology* 2006;178:335-60.
- [58] **Kwon OC, Rozenchan G, Law CK.** Cellular instabilities and self-acceleration of outwardly propagating spherical flames. *Proceedings of the Combustion Institute* 2002;29(2):1775-83.
- [59] **Sun CJ, Sung CJ, He L, Law CK.** Dynamics of weakly stretched flames quantitative description and extraction of global flame parameters. *Combustion and Flame* 1999;118:108-28.
- [60] **Joulin G, Mitani T.** Linear stability analysis of two-reactant flames. *Combustion and Flame* 1981;40:235-46.
- [61] **Hertzberg M.** Selective diffusional demixing: occurrence and size of cellular flames. *Progress in Energy Combustion Science* 1989;15:203-39.
- [62] **Kwon S, Tseng LK, Faeth GM.** Laminar burning velocities and transition to unstable flames in H_2 - O_2 - N_2 and C_3H_8 - O_2 - N_2 mixtures. *Combustion and Flame* 1992;90:230-46.
- [63] **Tseng LK, Ismail MA, Faeth GM.** Laminar burning velocities and Markstein numbers of hydrocarbon-air flames. *Combustion and Flame* 1993;95:410-26.
- [64] **Aung KT, Hassan MI, Kwon S, Tseng LK, Kwon OC, Faeth GM.** Flame/stretch interaction in laminar and turbulent premixed flames. *Combustion Science and Technology* 2002;174:61-99.
- [65] **Strehlow RA, Savage LD.** The concept of flame stretch. *Combustion and Flame* 1978;31:209-11.
- [66] **De-Goey LPH, Thijs-Boonkkamp JHM.** A flamelet description of premixed laminar flames and the relation with flame stretch. *Combustion and Flame* 1999;119:253-71.
- [67] **Williams FA.** Progress in knowledge of flamelet structure and extinction. *Progress in Energy and Combustion Science* 2000;26:657-82.
- [68] **Al-Shahrany AS, Bradley D, Lawes M, Woolley R.** Measurement of unstable burning velocities of Isooctane-air mixtures at high pressure and the derivation of laminar burning velocities. *Proceedings of the Combustion Institute* 2005;30:225-32.
- [69] **Al-Shahrany AS, Bradley D, Lawes M, Liu K, Woolley R.** Darrieus-Landau and thermo-acoustic instabilities in closed vessel explosions. *Combustion Science and Technology* 2006;178:1771-802.
- [70] **Sun CJ, Law CK.** On the nonlinear response of stretched premixed flames. *Combustion and Flame* 2000;121:236-48.
- [71] **Kim TJ, Yetter RA, Dryer FL.** New results on moist CO oxidation: high pressure, high temperature experiments and comprehensive kinetic modeling. *Proceedings of the Combustion Institute* 1994;25:759-66.
- [72] **Miao H, Jiao Q, Huang Z, Jiang D.** Effect of initial pressure on laminar combustion characteristics of hydrogen enriched natural gas. *International Journal of Hydrogen Energy* 2008;33:3876-85.
- [73] **Miao H, Jiao Q, Huang Z, Jiang D.** Measurements of laminar burning velocities and Markstein lengths of diluted hydrogen-enriched natural gas. *International Journal of Hydrogen Energy* 2009;34:507-18.

- [74] **Miao H, Ji M, Jiao Q, Huang Q, Huang Z.** Laminar burning velocity and Markstein length of nitrogen diluted natural gas/hydrogen/air mixtures at normal, reduced and elevated pressures. *International Journal of Hydrogen Energy* 2009;34:3145-55.
- [75] **Bechtold JK, Matalon M.** The dependence of the Markstein Length on stoichiometry. *Combustion and Flame* 2001;127:1906-13.
- [76] **Tien JH, Matalon M.** On the burning velocity of stretched flames. *Combustion and Flame* 1991;84:238-48.
- [77] **Bradley D, Sheppard CGW, Wooley R, Greenhalgh DA, Lockett RD.** The development and structure of flame instabilities and cellularity, at low Markstein numbers in explosions. *Combustion and Flame* 2000;122:195-209.
- [78] **Bradley D, Gaskell PH, Gu XJ, Sedaghat A.** Flame instabilities in large scale atmospheric gaseous explosions. 4th International Seminar on Fire and Explosion Hazards, Londonderry, Northern Ireland, 2003.
- [79] **Aung KT, Hassan MI, Faeth GM.** Effects of pressure and nitrogen dilution on flame stretch interactions of laminar premixed H₂-O₂-N₂ flames. *Combustion and Flame* 1998;112:1-15.
- [80] **Kobayashi H, Kawazoe H.** Flame instability effects on the smallest wrinkling scale and burning velocity of high pressure turbulent premixed flames. *Proceedings of the Combustion Institute* 2000;28:375-82.
- [81] **Chung, SH, Chung DH, Fu C, Cho P.** Proceedings of seminar on combustion phenomena in IC engines. Korean Society of Mechanical Engineers, Seoul, 1995;29.
- [82] **Jamel MAM.** PhD thesis 1984, University of Leeds.
- [83] **Blint RJ.** The relationship of the laminar flame width to flame speed. *Combustion Science and Technology* 1986;49:79-92.
- [84] **Law CK, Jomaas G, Bechtold JK.** Cellular instabilities of expanding hydrogen-propane spherical flames at elevated pressures: theory and experiment. *Proceedings of the Combustion Institute* 2005;30(1):159-67.
- [85] **Markstein GH.** Cell structure of propane flames burning in tubes. *Journal of Chemical Physics* 1949;17(4):428-9.
- [86] **Manton J, Von-Elbe G, Lewis B.** Burning-velocity measurements in a spherical vessel with central ignition. *Proceedings of the Combustion Institute* 1953;4:358-63.
- [87] **Parlange JY.** Influence of preferential diffusion on the stability of a laminar flame. *Journal of Chemical Physics* 1968;48(4):1843-9.
- [88] **Palm-Leis A, Strehlow RA.** On the propagation of turbulent flames. *Combustion and Flame* 1969;13:111-29.
- [89] **Groff EG.** The cellular nature of confined spherical propane-air flames. *Combustion and Flame* 1982;48:51-62.
- [90] **Konnov AA, Dyakov IV.** Measurement of propagation speeds in adiabatic cellular premixed flames of CH₄-O₂-CO₂. *Experimental Thermal and Fluid Science* 2005;29:901-7.
- [91] **Aldredge RC, Zuo B.** Flame acceleration associated with the Darrieus-Landau instability. *Combustion and Flame* 2001;127:2091-101.
- [92] **Bradley D, Cresswell TM, Puttock JS.** Flame acceleration due to flame-induced instabilities in large-scale explosions. *Combustion and Flame* 2001;124:551-9.
- [93] **Kadowaki S, Suzukia H, Kobayashi H.** The unstable behavior of cellular premixed flames induced by intrinsic instability. *Proceedings of the Combustion Institute* 2005;30:169-76.
- [94] **Kadowaki S.** Body-force effect on the cell formation of premixed flames. *Combustion and Flame* 2001;124:409-21.
- [95] **Kadowaki S, Hasegawa T.** Numerical simulation of dynamics of premixed flames, flame instability and vortex-flame interaction. *Progress in Energy and Combustion Science* 2005;31:193-241.
- [96] **Tse SD, Zhu DL, Law CK.** Morphology and burning rates of expanding spherical flames in H₂-O₂-inert mixtures up to 60 atmospheres. *Proceedings of the Combustion Institute* 2000;28:1793-800.
- [97] **Kwon OC, Faeth GM.** Flame-stretch interactions of premixed hydrogen-fueled flames: measurements and predictions. *Combustion and Flame* 2001;124:590-610.
- [98] **Bradley D, Harper CM.** The development of instabilities in laminar explosion flames. *Combustion and Flame* 1994;99(3-4):562-72.
- [99] **Matalon M.** Intrinsic flame instabilities in premixed and nonpremixed combustion. *Annual Review of Fluid Mechanics* 2007;39:163-91.

- [100] **Bradley D.** Instabilities and flame speeds in large-scale premixed gaseous explosions. *Philosophical Transactions of the Royal Society of London* 1999;357:3567-81.
- [101] **Driscoll JF.** Turbulent premixed combustion: flamelet structure and its effect on turbulent burning velocities. *Progress in Energy and Combustion Science* 2008;34:91-134.
- [102] **Lipatnikov AN, Chomiak J.** Molecular transport effects on turbulent flame propagation and structure. *Progress in Energy and Combustion Science* 2005;31:1-73.
- [103] **Lipatnikov AN, Chomiak J.** Turbulent flame speed and thickness: phenomenology, evaluation, and application in multi-dimensional simulations. *Progress in Energy and Combustion Science* 2002;28:1-74.
- [104] **Addabbo R, Bechtold JK, Matalon M.** Wrinkling of spherically expanding flames. *Proceedings of the Combustion Institute* 2002; 29(2):1527-35.
- [105] **Andrews GE, Bradley D.** Determination of burning velocities: A critical review. *Combustion and Flame* 1972;18(1):133-53.
- [106] **Bradley D.** How fast can we burn? *Proceedings of the Combustion Institute* 1992;24:247-62.
- [107] **Vagelopoulos CM, Egolfopoulos FN, Law CK.** Further considerations on the determination of laminar flame speeds with the counter-flow twin-flame technique. *Proceedings of the Combustion Institute* 1994;25:1341-7.
- [108] **Vagelopoulos CM, Egolfopoulos FN.** Direct experimental determination of laminar flame speeds. *Proceedings of the Combustion Institute* 1998;27(1):513-9.
- [109] **Smallbone AJ, Tsuneyoshi K, Kitagawa T.** Turbulent and stable-unstable laminar burning velocity measurements from outwardly propagating spherical hydrogen-air flames at elevated pressures. *Journal of Thermal Science and Technology* 2006;1:31-41.
- [110] **Liu DDS, MacFarlane R.** Laminar burning velocities of hydrogen-air and hydrogen-air-steam flames. *Combustion and Flame* 1983;49:59-71.
- [111] **Koroll GW, Kumar RK, Bowles EM.** Burning velocities of hydrogen-air mixtures. *Combustion and Flame* 1993;94:330-40.
- [112] **Dowdy DD, Smith D, Taylor SC, Williams A.** The use of expanding spherical flames to determine burning velocities and stretch effects in hydrogen air mixtures. *Proceedings of the Combustion Institute* 1990;23:325-32.
- [113] **Egolfopoulos FN, Law CK.** An experimental and computational study of the burning rates of ultra-lean to moderately-rich H₂-O₂-N₂ laminar flames with pressure variations. *Proceedings of the Combustion Institute* 1991;23(1):333-40.
- [114] **Aung KT, Hassan MI, Faeth GM.** Flame stretch interactions of laminar premixed hydrogen-air flames at normal temperature and pressure. *Combustion and Flame* 1997;109(1-2):1-24.
- [115] **Taylor SC.** Burning velocity and the influence of flame stretch. PhD thesis 1991, University of Leeds, United Kingdom.
- [116] **Wu CK, Law CK.** On the determination of laminar flame speeds from stretched flames. *Proceedings of the Combustion Institute* 1984;20:1941-9.
- [117] **Lamoureux N, Djebāyli-Chaumeix N, Paillard CE.** Laminar flame velocity determination for H₂-air-He-CO₂ mixtures using the spherical bomb method. *Experimental Thermal and Fluid Science* 2003;27(4):385-93.
- [118] **Qiao L, Kim CH, Faeth GM.** Suppression effects of diluents on laminar premixed hydrogen-oxygen-nitrogen flames. *Combustion and Flame* 2005;143(1-2):79-96.
- [119] **Hermanns RTE, Konnov AA, Bastiaans RJM, De-Goey LPH.** Laminar burning velocities of diluted hydrogen-oxygen-nitrogen mixtures. *Energy Fuels* 2007;21(4):1977-81.
- [120] **Pareja J, Burbano HJ, Ogami Y.** Measurements of the laminar burning velocity of hydrogen-air premixed flames. *International Journal of Hydrogen Energy* 2010;35:1812-8.
- [121] **Chen Z, Burke MP, Ju Y.** Effects of Lewis number and ignition energy on the determination of laminar flame speed using propagating spherical flames. *Proceedings of the Combustion Institute* 2009;32(1):1253-60.
- [122] **Gerke U.** Numerical analysis of mixture formation and combustion in a hydrogen direct-injection internal combustion engine. PhD thesis 2007, Swiss Federal Institute of Technology, Zurich, Switzerland.
- [123] **Tinaut FV, Giménez B, Iglesias D, Lawes M.** Experimental determination of the burning velocity of mixtures of n-heptane and toluene in engine-like conditions. *Flow, Turbulence and Combustion* 2012;89(2):183-213.

- [124] **Williams FA, Grcar JF.** A hypothetical burning-velocity formula for very lean hydrogen-air flames. *Proceedings of the Combustion Institute* 2009;32:1351-7.
- [125] **Konnov AA.** Remaining uncertainties in the kinetic mechanism of hydrogen combustion. *Combustion and Flame* 2008;152:507-28.
- [126] **Saxena P, Williams FA.** Testing a small detailed Chemical-kinetic mechanism for the combustion of hydrogen and carbon monoxide. *Combustion and Flame* 2006;145:316-23.
- [127] **Williams FA.** Detailed and reduced chemistry for hydrogen autoignition. *Journal of Loss Prevention in the Process Industries* 2008;21:131-5.
- [128] **Ströhle J, Myhrvold T.** An evaluation of detailed reaction mechanisms for hydrogen combustion under gas turbine conditions. *International Journal of Hydrogen Energy* 2007;32:125-35.
- [129] **Kee RJ, Grcar JF, Smooke MD, Miller JA.** PREMIX (CHEMKIN Collection part): A Fortran program for modeling steady laminar one-dimensional premixed flames. Sandia National Laboratories, Albuquerque, New Mexico, 1985; Report SAND 85-8240.
- [130] **Kee RJ, Miller JA, Evans G, Dixon-Lewis G.** A computational model of the structure and extinction of strained opposed flow, premixed methane air flame. *Proceedings of the Combustion Institute* 1988;22:1479-94.
- [131] **Kee RJ, Rupley FM, Miller JA.** CHEMKIN_II (CHEMKIN Collection part): A Fortran chemical kinetics package for the analysis of gas-phase chemical kinetics. Sandia National Laboratories, Albuquerque, New Mexico, 1989; Report SAND 89-8009.
- [132] **Kee RJ, Rupley FM, Miller JA, Coltrin ME, Grcar JF, Meeks E, Moffat HK, Lutz AE, Dixon-Lewis G, Smooke MD, Warnatz J, Evans GH, Larson RS, Mitchell RE, Petzold LR, Reynolds WC, Caracotsios M, Stewart WE, Glarborg P, Wang C, Adigun O.** A software package for the analysis of gas-phase chemical kinetics and plasma kinetics. CHEMKIN program & subroutine library. CHEMKIN Collection part, Release 3.6, Reaction Design, Inc. San Diego, California, 2000.
- [133] **Kee RJ, Rupley FM, Miller JA, Coltrin ME, Grcar JF, Meeks E, Moffat HK, Lutz AE, Dixon-Lewis G, Smooke MD, Warnatz J, Evans GH, Larson RS, Mitchell RE, Petzold LR, Reynolds WC, Caracotsios M, Stewart WE, Glarborg P, Wang C, Adigun O, Houf WG, Chou CP, Miller SF, Ho P, Young DJ.** CHEMKIN Software, Release 4.0, Reaction Design, Inc. San Diego, California, 2004.
- [134] **Marinov NM, Westbrook CK, Pitz WJ.** Detailed and global kinetics model for hydrogen. *Transport phenomena in combustion*, Taylor&Francis, Washington, Columbia, 1996;Vol.1.
- [135] **Marinov NM, Curran H.J, Pitz WJ, Westbrook CK.** Chemical kinetic modeling of hydrogen under conditions found in internal combustion engines. *Energy and Fuels* 1998;12:78-82.
- [136] **Mosbacher D, Wehrmeyer J, Pitz R, Sung CJ, Byrd J.** Experimental and numerical investigation of premixed cylindrical flames. *American Institute of Aeronautics and Astronautics, AIAA2002-0481*, 2002.
- [137] **Rahim F, Elia M, Ulinski M, Metghalchi M.** Burning velocity measurements of methane-oxygen-argon mixtures and an application to extend methane-air burning velocity measurements. *International Journal of Engine Research* 2002;3(2):81-92.
- [138] **Rozenchan G, Zhu DL, Law CK, Tse SD.** Outward propagation, burning velocities, and chemical effects of methane flames up to 60 atm. *Proceedings of the Combustion Institute* 2002;29:1461-69.
- [139] **O'Conaire M, Curran HJ, Simmie JM, Pitz WJ, Westbrook CK.** A comprehensive modeling study of hydrogen oxidation. *International Journal of Chemical Kinetics* 2004;36(11):603-22.
- [140] **Zhao Z, Li J, Kazakov A, Dryer FL, Zeppieri SP, Dryer FL.** Burning velocities and a high-temperature skeletal kinetic model for n-decane. *Combustion Science and Technology* 2005;177:89-106.
- [141] **Huang J, Bushe WK.** Experimental and kinetic study of autoignition in methane-ethane and methane-propane-air mixtures under engine-relevant conditions. *Combustion and Flame* 2006;144:74-88.
- [142] **Bougrine S, Richard S, Veynante D.** On the combination of complex chemistry with a 0-D coherent flame model to account for the fuel properties in spark ignition engines simulations: Application to methane-air-diluents mixtures. *Proceedings of the Combustion Institute* 2011;33:3123-30.
- [143] **Rogg B.** COSILAB RUN-1DL: Cambridge universal laminar flame code. Cambridge University, Department of Engineering Report, 1991; CUED/A-THERMO/TR39.
- [144] **Frenklach M, Bowman T, Smith G, Gardiner B.** GRI-Mech version 3.0, 1999.
- [145] **Smith GP, Golden DM, Frenklach M, Moriarty NW, Eiteneer B, Goldenberg M, et al.** GRI-Mech. http://www.me.berkeley.edu/gri_mech/releases.html/, 2011.

- [146] **Pitsch H, Bollig M. FLAMEMASTER:** A computer code for homogeneous and one-dimensional laminar flame calculation. Institut für Technische Mechanik, 1994. RWTHAachen. <http://www.lavision.de>.
- [147] **Curtis AR, Sweetenham WP. FACSIMILE** release H user's manual. AERE report R11771, 1987. <http://www.esm-software.com>.
- [148] **Rogg B. COSILAB RUN-1DL:** The Cambridge universal laminar flamelet computer code. Reduced kinetic mechanisms for applications in combustion systems, Appendix C. Springer-Verlag, Berlin-Heidelberg-New York, 1993.
- [149] **Somers LMT. CHEM1D** The simulation of flat flames with detailed and reduced chemical models. PhD thesis 1994. Eindhoven Technical University, Netherlands. TU/e. <http://yp.wtb.tue.nl/showabstract.php/1684>.
- [150] **Sánchez AL, Lépinette A, Bollig M, Liñán A, Lázaro B.** The reduced kinetic description of lean premixed combustion. *Combustion and Flame* 2000;123:436-64.
- [151] **Rao S, Rutland CJ.** A flamelet time scale model for non-premixed combustion including unsteady effects. *Combustion and Flame* 2003;133:189-91.
- [152] **Wu MS, Liu JB, Ronney PD.** Numerical simulation of diluent effects on flame balls. *Proceedings of the Combustion Institute* 1998;27:2543-50.
- [153] **FIRE** version 8.2 manual, 2003. AVL List GmbH. <http://www.avl.com>.
- [154] **FLUENT** (Ansys) flow modeling simulation software. Inc. Modeling premixed combustion. User's manual 2003. <http://www.fluent.com>.
- [155] **STAR-CD** version 3.15 PROSTAR. CD-adapco Group. <http://www.cd-adapco.com>.
- [156] **Colin O, Benkenida A, Angelberger C. ECFM_3D** modeling of mixing, ignition and combustion phenomena in highly stratified gasoline engines. *Oil Gas Science Technology* 2003;58:47-62.
- [157] **Hilbert R, Tap F, El-Rabii H, Thévenin D.** Impact of detailed chemistry and transport models on turbulent combustion simulations. *Progress in Energy and Combustion Science* 2004;30:61-117.
- [158] **Simmie JM.** Detailed chemical kinetic models for the combustion of hydrocarbon fuels. *Progress in Energy and Combustion Science* 2003;29:599-634.
- [159] **Frenklach M, Wang H, Rabinowitz MJ.** Optimization and analysis of large chemical kinetic mechanisms using the solution mapping method-combustion of methane. *Progress in Energy Combustion Science*, 1992;18:47-73.
- [160] **Miller JA, Bowman CT.** Mechanism and modeling of nitrogen chemistry in combustion. *Progress in Energy and Combustion Science* 1989;15:287-8.
- [161] **Miller JA, Mitchell RE, Smooke MD, Kee RJ.** Towards a comprehensive chemical kinetic mechanism for the oxidation of acetylene. *Proceedings of the Combustion Institute* 1982;19:181-96.
- [162] **Warnatz J, Maas U.** Technische Verbrennung: Grundlagen, Modellbildung, Schadstoffentstehung. Springer-Verlag, Berlin Heidelberg New York, 1993;101-4.
- [163] **Konnov AA.** Development and validation of a detailed reaction mechanism for the combustion modeling. *Eurasian Chemico-Technological Journal*, 2000;2:257-64. <http://homepages.vub.ac.be/~akonnov/>.
- [164] **Hughes KJ, Turanyi T, Clague AR, Pilling MJ.** Development and testing of a comprehensive chemical mechanism for the oxidation of methane. *International Journal of Chemical Kinetics* 2001;33(9):513-38.
- [165] **Lawrence Livermore** National Laboratory, Chemistry and Materials Science Web site: <http://www.cms.llnl.gov/>.
- [166] **Dixon-Lewis G, Williams A.** Some observations on the structure of a slow-burning flame supported by the reaction between hydrogen and oxygen at atmospheric pressure. *Proceedings of the Combustion Institute* 1963;9:576-84.
- [167] **Dixon-Lewis G.** Chemical mechanism and properties of freely propagating hydrogen oxygen supported flames. *Archivum Combustionis* 1984;4:279-96.
- [168] **Warnatz J.** Concentration, pressure and temperature dependence of the flame velocity in hydrogen-oxygen-nitrogen mixtures. *Combustion Science and Technology* 1981;26:203-13.
- [169] **Maas U, Warnatz J.** Ignition processes in hydrogen-oxygen mixtures. *Combustion and Flame* 1988;74:53-69.
- [170] **Yetter RA, Dryer FL, Rabitz H.** A comprehensive reaction mechanism for carbon monoxide/hydrogen/oxygen kinetics. *Combustion Science and Technology* 1993,1991;79:97-128.

- [171] **Burks TL, Oran ES.** A computational study of the chemical kinetics of hydrogen combustion. NRL Memorandum Report 1981;NRL-44-0572-0-1.
- [172] **Frassoldati A, Faravelli T, Ranzi E.** **DSmoke:** A wide range modeling study of NO_x formation and nitrogen chemistry in hydrogen combustion. *International Journal of Hydrogen Energy* 2006;31:2310-28.
- [173] **Safari H, Jazayeri S, Ebrahimi R.** Potentials of NO_x emission reduction methods in SI hydrogen engines: simulation study. *International Journal of Hydrogen Energy* 2009;34:1015-25.
- [174] **Wimmer A, Wallner T, Ringler J, Gerbig F.** Hydrogen-direct injection, a highly promising combustion concept. SAE 2005-01-0108; 2005.
- [175] **Messner D, Wimmer A, Gerke U, Gerbig F.** Application and validation of the 3D CFD method for a hydrogen fueled IC engine with internal mixture formation. SAE 2006-01-0448, 2006.
- [176] **Gerke U, Boulouchos K, Wimmer A.** Numerical analysis of the mixture formation and combustion process in a direct injected hydrogen internal combustion engine. *Proceedings 1st international symposium on hydrogen internal combustion engines.* Graz, Austria, 2006;94-106.
- [177] **Zimont V, Lipatnikov A.** A numerical model of premixed turbulent combustion of gases. *Chemical Physics Report* 1995;14: 993-1025.
- [178] **Zeldovich YB, Sadovnikov PYA, Frank-Kamenetskii DA.** Oxidation of nitrogen in combustion, translated by Shelef M. Moscow Academy of Science, 1947.
- [179] **Takeno T, Iijima T.** First specialist meeting of the combustion Institute, French section 1981;55.
- [180] **Peters N, Rogg B,** editors. *Reduced kinetic mechanisms for applications in combustion systems.* Springer-Verlag, Berlin Heidelberg New York; 1992.
- [181] **Qin X, Kobayashi H, Niioka T.** Laminar burning velocity of hydrogen-air premixed flames at elevated pressure. *Experimental Thermal and Fluid Science* 2000;21:58-63.
- [182] **D'Errico G, Ferrari G, Onorati A, Cerri T.** Modeling the pollutant emissions from a S.I. engine. SAE 2002-01-0006, 2002.
- [183] **D'Errico G, Lucchini T.** A combustion model with reduced kinetic schemes for S.I. engines fueled with compressed natural gas. SAE 2005-01-1123, 2005.
- [184] **D'Errico G, Onorati A, Ellgas S, Obieglo A.** Thermo-fluid dynamic simulation of a SI single-cylinder H₂ engine and comparison with experimental data. ASME Engine Technology Conference, Aachen, Germany. ICES2006-1311, 2006.
- [185] **Combustion Technology** group, Technical University of Eindhoven. <http://www.combustion.tue.nl>.
- [186] **Ern A, Giovangigli V.** **EGlib,** A general purpose Fortran library for multicomponent transport property evaluation, CERMICS Internal Report 96-51, 1996. Ecole Nationale des Ponts et Chaussées, Marne, France. <http://www.blanche.polytechnique.fr/> www.eglib.com.
- [187] **Matlab.** The language of technical computing, <http://www.mathworks.com/>; 2011.
- [188] **Gülder L.** Effect of initial mixture temperature on flame speed of methane-air, propane-air and ethylene-air mixtures. SAE 841000, 1984.
- [189] **Han P, Checkel MD, Fleck BA, Nowicki NL.** Burning velocity of methane/diluent mixture with reformer gas addition. *Fuel* 2007;86(4):585-96.
- [190] **Coppens FHV, de Ruycck J, Konnov AA.** Effects of hydrogen enrichment on adiabatic burning velocity and NO formation in methane-air flames. *Thermal and Fluid Science* 2007;31(5):437-44.
- [191] **Hermanns RTE.** Laminar burning velocities of methane-hydrogen-air mixtures. PhD thesis 2007. Eindhoven University, Universal Press, Veenendaal, Netherlands.
- [192] **Hermanns RTE, Konnov AA, Bastiaans RJM, De-Goeij LPH, Lucka K, Köhne H.** Effects of temperature and composition on the laminar burning velocity of CH₄+H₂+O₂+N₂ flames. *Fuel* 2010;89:114-21
- [193] **Huang Z, Zhang Y, Zeng K, Liu B, Wang Q, Jiang D.** Measurements of laminar burning velocities for natural gas-hydrogen-air mixtures. *Combustion and Flame* 2006;146:302-11.
- [194] **Tahtouh T, Halter F, Samson E, Mounaïm-Rousselle C.** Effects of hydrogen addition and nitrogen dilution on the laminar flame characteristics of premixed methane-air flames. *International Journal of Hydrogen Energy* 2009;34:8329-38.
- [195] **Wang H, You X, Joshi AV, Davis SG, Laskin A, Egolfopoulos FN,** et al. **USC_II-Mech.** High-temperature combustion reaction model of H₂/CO/C₁-C₄ compounds. http://ignis.usc.edu/USC_Mech-II.htm/, 2011.
- [196] **Konnov AA.** **Konnov-Mech_5.0.** <http://homepages.vub.ac.be/~akonnov/>, 2011.

- [197] **Li J, Zhao Z, Kazakov A, Dryer FL. Princeton-Mech.** <http://www.princeton.edu/wcombust/database/files/other/>, 2011.
- [198] **Brewster S, Blechmore C.** Dilution strategies for load and NO_x management in a hydrogen fueled direct injection engine. SAE 2007-01-4097, 2007.

6. Notions of laminar burning velocities relative to hydrogen - natural gas blends

- 6.1. Laminar burning velocities for methane and hydrogen
- 6.2. Experimental laminar burning velocities of hydrogen-hydrocarbon blends
 - 6.2.1. Summary of experimental works related with laminar burning velocity of fuel blends
 - 6.2.2. Experimental results of some authors about fuel blends behavior with spherically expanding flames in combustion chambers
- 6.3. Theoretical laminar burning velocities from simulation of one-dimensional premixed flames of fuel blends with implemented chemical kinetics schemes
- 6.4. Mixing-rules calculations to obtain laminar burning velocities of fuel blends
 - 6.4.1. Mixing rules derived from linear and potential rules-like formulas
 - 6.4.2. Mixing rules derived from LeChatelier's rule-like formula

References of chapters six, seven and eight (*after the eighth chapter*)

6. Notions of laminar burning velocities relative to hydrogen - natural gas blends

In chapter 2, this work has made an overview on natural gas, methane and hydrogen properties and characteristics of their fuel-air mixtures, also including a review with complementary information and terminology about combustion performance, emissions, cyclic variability, etc., on different applications in engines of diverse fuel blends, depending on possible fuel combinations and effects of dilution by residual gas. As inferred from the contents of that comprehensive review [1-117], knowledge about laminar flames of fuel blends in internal combustion engines is particularly interesting for this propagation itself and for the turbulent regime understanding. Laminar-premixed flames and their characteristics are fundamental input parameters for modeling turbulent combustion in explosions.

In a brief summary of the concept from chapters 1-3, we remember that the laminar burning velocity, sometimes called normal, adiabatic or fundamental burning velocity, is an essential property of a fuel-air mixture because it is defined as the velocity at which the flame propagates into a premixed combustion. It is generally considered as a fundamental variable, depending only on the initial temperature, pressure and composition of the gas mixture. When the coupling between the chemical kinetics and molecular transport properties is known in detail, then it is possible to calculate the burning velocity because this represents the eigenvalue of the time-independent one-dimensional flame equations. Thus, it is a useful combustion parameter characterizing the overall reaction rate in the premixed flame and can be used for estimating the burning rate in SIEs or for performance predicting. The burning velocity directly affects the flame propagation speed and hence, the operation of a SIE. Faster burning in the SIEs leads to a more robust and repeatable combustion and permits engine operation with substantially larger amount of *EGR*, bringing the reduction in NO_x emission. Fast burning results in the decreased combustion duration and the compact combustion process will improve engine thermal efficiency and decrease fuel consumption, Bilgin 2002 [118].

Then, burning velocity provides the laminar characteristics of a fuel mixture and it can also be used to study turbulent combustions and supply important information about the effects of flame stretching, flame front instabilities and wrinkling, Bradley et al. 1998 [119], Law&Kwon 2004 [32].

This chapter gives a review on different published data of laminar burning velocities of hydrogen-hydrocarbon fuel blends, in the line of original data obtained from combustion experiments, often from ambient initial conditions, mainly at atmospheric pressure, and in route towards engine terms, considering data derived by computational simulations and extrapolated calculations with premixed combustion models and chemical kinetics schemes. As well, an introduction to mixing rules conceptions, that can be compared with modeling studies based on detailed chemistry, is going to be extracted from the literature.

On the other hand, some specific analytical expressions of several authors will be presented in the following chapter 7.

6.1. Laminar burning velocities for methane and hydrogen

The laminar burning velocity of each single fuel considered respectively alone in the premixed combustion of air mixtures is a starting point towards the survey of some functional dependencies of laminar burning velocities for the hybrid fuel blends. As aforementioned, the flame speeds and burning velocities of both hydrogen and natural gas, considered as methane, have been copiously studied in the published literature as individual fuels in premixed flames.

- Methane (CH₄) is a reference gaseous fuel and it is possible to find many published results and burning velocity expressions, with different criteria and diverse accuracies and precisions of applicability in varied ranges of use. Some references are summarized in [table 28](#) (chapter 8), with indication of application ranges in terms of temperature, pressure, equivalence ratio and residual gas content.
- Hydrogen (H₂) has already been widely discussed in previous chapters 4 and 5 of this work, where empirical and theoretical formulas of laminar burning velocities for premixed combustion of hydrogen-air mixtures have been studied. Interesting expressions applicable in wide ranges of temperatures, pressures, equivalence ratios and dilution fractions have been analytically processed with special attention at elevated pressures and temperatures, to spark ignition engine-like conditions. Some references have been derived from the [table 16](#) (section 5.4) and summarized again in [table 29](#) (chapter 8), with indication of their ranges of applicability, for the scope of this other part of the present work.

Most of the published analytical formulas of laminar burning velocities are based on experimental correlations (u_l) or numerically calculated expressions (u_L). Frequently they meet the widely extended general form to account for temperature and pressure effects (also for fuel-air mixtures at elevated pressures and temperatures) as the one derived from the originally proposed by Metghalchi&Keck 1980,1982 [120,121] modified sometimes to express the influence and functional dependences of equivalence ratio (Φ) and dilution fraction of residual gas content ($f_{res,u}$) in addition to unburned or initial temperature (T_u) and pressure (P), and where the variables are depending on parameters according with the data and methods of deduction.

$$u_L(T_u, P) = (T_u/T_o)^\alpha \cdot (P/P_o)^\beta \cdot u_{L,o} \quad (142)$$

$$u_L(\Phi, f_{res,u}; T_u, P) = (T_u/T_o)^\alpha \cdot (P/P_o)^\beta \cdot \zeta \cdot u_{L,o} \quad (143)$$

This structure is considered computationally convenient but, in origin, some studies assumed the effects of P , T , Φ and f_{res} to be independent. In the development and calibrations of these types of formulas by several authors, sundry of the different parameters were expressed sometimes as parametric functions of some of these variables with calibrated coefficients.

The hydrogen content \hat{h} in different fraction forms or parameters ([table 1](#), chapter 1), e.g. x_{H_2} , $h(vol\%)$, X_{H_2} or R_h , can be added as another possible variable or functional parameter when laminar burning velocities of considered hybrid fuel blends with hydrogen are so correlated.

$$u_L(\Phi, \hat{h}, f_{res,u}; T_u, P) = (T_u/T_o)^\alpha \cdot (P/P_o)^\beta \cdot \zeta \cdot u_{L,o} \quad (144)$$

where

$$u_{L,o}(\Phi, \hat{h}; T_{u,o}, P_o) \quad (145)$$

$$\alpha(T_u, P; \Phi, \hat{h}) \quad (146)$$

$$\beta(P, T_u; \Phi, \hat{h}) \quad (147)$$

$$\zeta(f_{res,u}, \Phi, \hat{h}; T_u, P) \quad (148)$$

6.2. Experimental laminar burning velocities of hydrogen-natural gas blends

Several experimental techniques have been used to measure the laminar burning velocity of stationary or non-stationary flames of different gaseous fuels in air mixtures, such as: Bunsen flames; flat flame burners, one-dimensional burner-stabilized flames; stagnation flames, counter-flow double flames; expanding spherical flames and acquisition of the flame front radius or pressure in constant volume bombs.

Of these approaches in measuring the laminar burning velocity, the *stagnation plane flame* method can establish different flame configurations but it is difficult to draw a clear flame front and to stabilize the flame under high-pressure conditions; the *heat flux* method needs to determine the heat loss as a function of inlet velocity and to extrapolate the results to zero heat loss to get the adiabatic burning velocity; the *combustion bomb* methods utilize the prototypical propagating spherical flame configuration and has drawn particular attention due to its simple flame configuration with defined flame stretch and well control, Bradley et al. 1996 [122], Sun et al. 1999 [123].

Using analysis models is necessary to obtain the burning velocity from pressure data acquired inside a constant volume chamber, Reyes 2008 [124]. With the development of flame visualization technology, combustion bombs with spherically expanding flames have become widely used because of accuracy and capacity of deducting some other flame parameters, Verhelst et al. 2005 [125], including Markstein constants which have been used to indicate flame stability. The propagation speeds of the flames can be obtained by recording the process of spherical flame growth with high speed cameras; thus, based on Markstein theory, the relationship between the stretch and the propagating speed of flame can be established, after which the laminar burning velocity of un-stretched laminar flame can be obtained, as done in some works as those carried out by Miao et al. 2008,2009 [11-13] or Hu et al. 2009 [75,76,78,126].

A summary of experimental works related with laminar burning velocity for hydrogen blends in different fuel-air mixtures is reported in the following section 6.2.1. Nevertheless, in spite of the different techniques and many varied works developed to generate experimental data, the obtaining of sufficient and sufficiently representative data to full validations of empirical correlations has been difficult especially for engine-like conditions. Therefore theoretical treatments have been required, as it will be considered in section 6.3, because the experimental limitations depending on fuels properties, mixtures composition ranges and thermodynamic conditions.

6.2.1. Summary of experimental works related with laminar burning velocity of fuel blends

Relations and descriptions of several experimental methods can be found in the related literature, as for instance in references of the works of Lafuente 2008 [127] or Ranzi et al. 2012 [128]. Some published studies based on experimental methods applications were related to hydrogen fuel blends, as those summarized in table 20.

Many of these examples use the hydrogen mole (volume) fractions (already defined in table 1, in chapter 1) as well in the global fuel-air mixture X_{H_2} or in the fuel blend x_{H_2} to characterize the amounts of H_2 addition, $h(vol\%)=100x_{H_2}$ between 0-100%, for equivalence ratio values most of the times falling inside a typical range $\Phi=[0.6, 1.4]$. A few of the consulted studies vary also the oxygen content in the fuel mixtures, as Coppens et al. 2007 [129] and Hermanns et al. 2010 [130].

Table 20Summary of literature references with experimental measurements of laminar burning velocities for **hydrogen blends** in different fuel-air mixtures

Fuel-air mixtures with blends of H ₂ and	Techniques				
	Expanding spherical flame	Counter-flow/stagnation flame	Heat flux/flat flame	Tube burner	Bunsen flame
NG	[6] 2006 Huang et al. [9] 2008 Wang et al. [11-13] 2008,2009 Miao et al. [79] 2011 Tinaut et al.	-	-	-	-
CH₄	[131] 1984 Milton&Keck [132] 1988 Sher&Refael [133] 1989 Refael&Sher [134] 2003 Tanoue et al. [32] 2004 Law&Kwon [53,135,136] 2005,2007,2010 Halter et al. [54] 2006 Ilbas et al. [55] 2007 Mandilas et al. [75,78] 2009 Hu et al. [137] 2009 Tahtouh et al.	[138] 1986 Yu et al. [139] 1991 Liu et al. [140] 2001 Ren et al. [141] 2011 Park et al.	[129,142] 2007 Coppens et al. [143,144,130] 2007,2010 Hermanns et al.	[145] 1959 Scholte &Vaags	-
C ₂ H ₆	[146] 2011 Wu et al.	[147] 2002 Dong et al.	-	-	-
C ₂ H ₄	[32] 2004 Law&Kwon [146] 2011 Wu et al.	-	-	-	-
C ₂ H ₂	[131] 1984 Milton&Keck [146] 2011 Wu et al.	-	-	-	-
C ₃ H ₈	[131] 1984 Milton&Keck [133] 1989 Refael&Sher [32] 2004 Law&Kwon [148,149] 2008 Tang et al.	[138] 1986 Yu et al. [141] 2011 Park et al.	-	-	-
n C ₄ H ₁₀	[150] 2011 Tang et al.	[141] 2011 Park et al.	[151] 1992 Sher&Ozdor	-	-
i C ₆ H ₁₈	[55] 2007 Mandilas et al. [152] 2011 Tahtouh et al.	-	-	-	-
CO	[153] 1994 Mclean et al. [154] 1997 Hassan et al. [155] 2007 Sun et al. [146] 2011 Wu et al.	[156] 1994 Vagelopoulos&Egolfopoulos [157] 2007 Natarajan et al.	-	[158] 1959 Scholte &Vaags	[157] 2007 Natarajan et al. [159] 2009 Dong et al.

In most conventional experimental measurements the initial unburned temperatures were the normal of room ambient about 298-303 K and pressure was typically atmospheric about 0.1 MPa, although several authors deal also with low and elevated pressures, trying to approach to higher cylinder pressures and temperatures that are attained in the combustion chambers for fuel blends with hydrogen combination, as the actual burn rates increase due to hydrogen addition.

The experimental results for hydrocarbon-air mixtures show a weak dependence on hydrogen addition up to percentages about 50% of hydrogen mole fraction and a rapid increase thereafter, mainly beyond values of 80%. As a side remark, it is known that this behavior differs substantially for carbon monoxide (CO), given that the flame speed increases rapidly because the strong catalytic effect on the oxidation of CO with even small amount of hydrogen, Lafuente 2008 [127].

An especial target will be dedicated in this part of the present work to studies that have published laminar burning velocities of fuel-air mixtures of hydrogen enriched natural gas or methane blends. Particularly when H₂ is added to CH₄, according with reviewed experimental studies, an approach to linear increase of the laminar burning velocity occurs with increasing the hydrogen mole fraction in the fuel up to values about $x_{H_2}=0.7$, as was observed by Di-

Sarli&Di-Benedetto 2007 [160]; this enhancement is slight especially at lower equivalence ratios. On the contrary, at high H₂ molar contents $x_{H_2} > 0.85$, the substitution by CH₄ has a strong effect of inhibition on H₂ reactivity. Moreover, when increasing the CH₄ content, a linear decrease takes place that becomes steeper at rich conditions.

The experimental consequences obtained by Sierens&Rosseel 2000 [28] on an ICE with lean blends of NG and hydrogen were consistent with the effects of addition of H₂ and CH₄ on the laminar burning velocity of hybrid mixtures. They showed that there is a very limited improvement in engine efficiency and emissions for hydrogen molar contents in the fuel up to $x_{H_2} = 0.2$. On the other hand, high efficiency and low emissions without abnormal combustion phenomena (knock and backfire events) were found starting from H₂ substitutions by NG of $x_{NG} = 0.2$.

6.2.2. Experimental results of some authors about fuel blends behavior with spherically expanding flames in combustion chambers

In spherical combustion chamber experiments Halter et al. 2005 [53] observed that laminar burning velocity of CH₄-air premixed flames, for a given equivalence ratio, decreased with pressure increase but increased with the percentage of hydrogen addition in the mixture, which results in a reduction of its dependence versus flame stretch and in reduction to the sensitivity to strain rates. The laminar flame thickness, inversely proportional to the laminar burning velocity, decreased with hydrogen addition and with the pressure increase.

Huang et al. 2006 [6] studied the characteristics of laminar flame air mixtures in a constant volume bomb at normal temperature and pressure and their experimental summarized results were as follows, depending of the mixtures equivalence ratio and H₂ addition, showing that the burning velocities increased with the addition of H₂ to NG and that equivalence ratio had greater effect on flame propagation speed of the fuel with low H₂ fraction than that of the fuel with high H₂ fraction.

- For *lean mixture* combustion, flame radius increased with time, but the rate of increase decreased with flame expansion for NG and for mixtures with low H₂ fractions, while a linear correlation exists between flame radius and time at high H₂ fractions. For *rich mixture* combustion, the flame radius showed a slow rate of increase at early stages of flame propagation, and a high rate of increase at late stages of flame propagation for NG and for mixtures with low H₂ fractions, and a linear correlation exists between flame radius and time for mixtures with high H₂ fractions. Combustion at *stoichiometric mixture* demonstrated the linear relationship between flame radius and time for NG-air, H₂-air, and NG-H₂-air flames.
- H₂-air flame gave a very high value of the stretched flame speed compared to those of NG-air flame and NG-H₂-air flames, even at high H₂ fraction. The influence of equivalence ratio on the stretched flame speed was larger than the influence of H₂ addition.
- With the increase of H₂ fractions in mixtures, laminar burning velocities increased exponentially, while the Markstein lengths or associated numbers decreased and flame instability increased. In addition, for a fixed H₂ fraction, the Markstein constants and flame stability increased with the increase of equivalence ratios.

The laminar flame propagation characteristics of premixed NG-H₂-air mixtures in a constant volume combustion bomb were studied by Miao et al. 2008 [11]. Mass burning fluxes and laminar burning velocities were obtained under various H₂ fractions and equivalence ratios, with various initial pressures, while flame stability and their influencing factors (Markstein length, density ratio and flame thickness) were analyzed by the flame images (e.g. [figs. 39 & 40](#)).

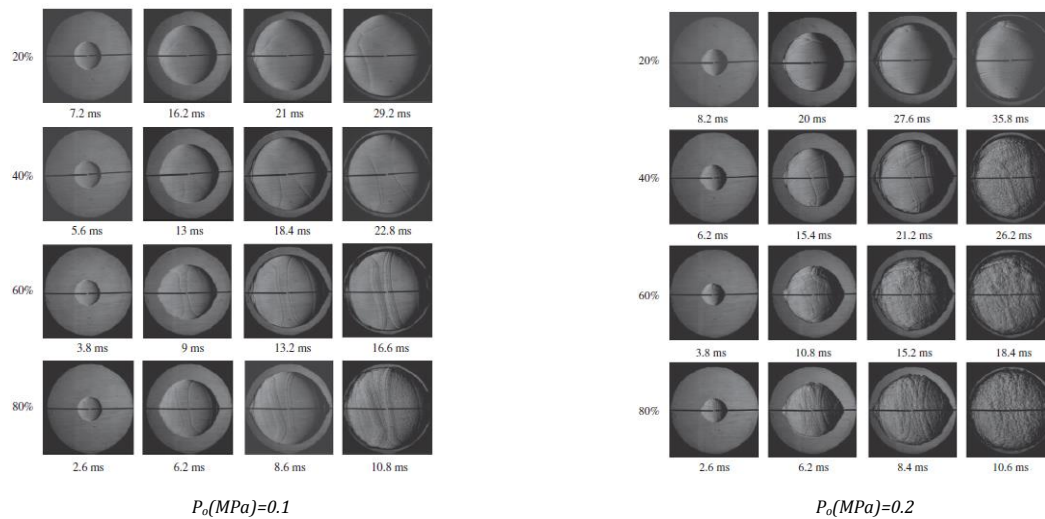


Fig. 39. Spherically expanding flames of hydrogen-methane-air mixtures, recorded by Schlieren cinematography, with H_2 fractions $h(\%) = \{20, 40, 60, 80\}$ for $\Phi = 1$, $T_{u,o}(K) = 300$ and $P_o(MPa) = \{0.1, 0.2\}$ (taken from Miao et al 2008 [11])

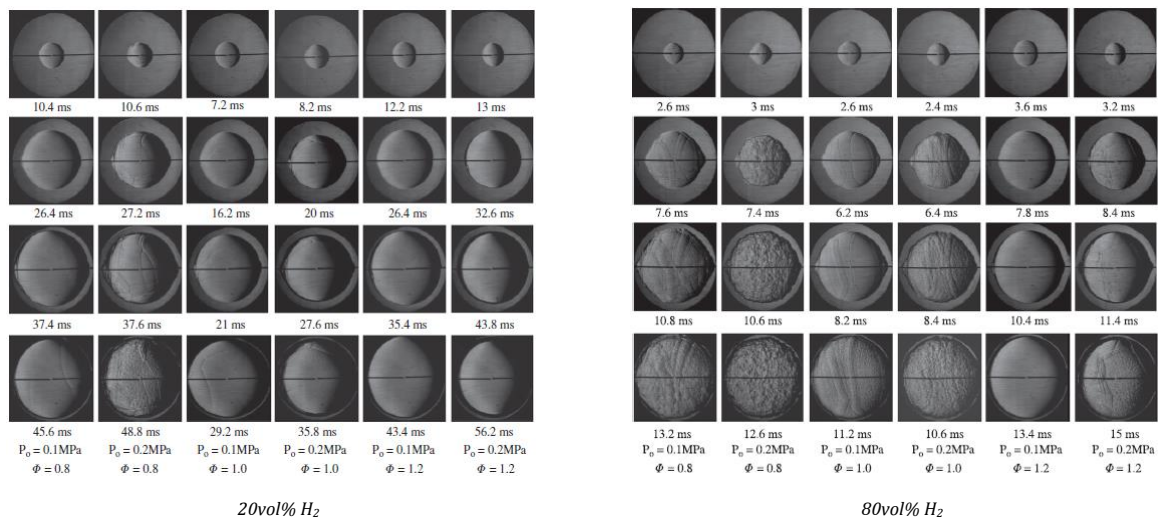


Fig. 40. Spherically expanding flames of hydrogen-methane-air mixtures, recorded by Schlieren cinematography, with H_2 fractions $h(\%) = \{20, 80\}$ for $\Phi = \{0.8, 1, 1.2\}$, $T_{u,o}(K) = 300$ and $P_o(MPa) = \{0.1, 0.2\}$ (taken from Miao et al 2008 [11])

The results showed that H_2 fraction, initial pressure as well as equivalence ratio had combined influence on both un-stretched laminar burning velocity and flame instability, meanwhile flame stability decreased with the increase of initial pressures. These were some main conclusions of these authors:

- Initial pressure, H_2 fraction as well as equivalence ratio exerted a combined influence on un-stretched laminar burning velocity and mass burning flux of these mixtures. Both quickly increased with the increase of H_2 fraction. H_2 addition was especially effective in increasing the burning velocity at rich conditions. At *rich equivalence ratio*, the laminar burning velocity declined with the increase of initial pressure, while at *lean* and *stoichiometric* conditions it tended to increase and then decreased with the increase of initial pressure within the range of the experiments.
- Flame stability decreased with the increase of H_2 fraction and initial pressure. For the case of relatively low H_2 fraction (20%vol) flame stability of relatively lean combustion decreased with

the increase of initial pressure, while for the case of high H₂ fraction (80%vol) flame stability of lean and stoichiometric combustion decreases with the increase of initial pressure. At rich conditions the increase of H₂ fraction exerted less influence on flame stability comparing with that at lean and stoichiometric conditions.

- At large flame radius, flame stability was dominantly influenced by hydrodynamic factors, reflected by both density ratios of unburned gas to burned gas at two sides of flame front and flame thickness. For fixed given equivalence ratio and H₂ fraction, the increase of initial pressure had obvious influence on flame thickness but slight influence on density ratio, that is, flame thickness was more sensitive to the variation of the initial pressure, than to that of the density ratio, and flame thickness decreased with the increase of initial pressure, indicating thereby that flame stability decreased.

The same authors in other experimental work, Miao et al. 2009 [13], studied also the laminar burning velocities of nitrogen diluted H₂-enriched NG in the constant volume bomb at normal, reduced and elevated pressures. Un-stretched flame speeds and burning velocities together with Markstein lengths of stoichiometric mixtures with different H₂ fractions and diluent ratios were obtained under various initial pressures. These were main conclusions:

- The effect of increase in initial pressure on the flame propagation of diluted H₂-enriched NG air mixtures obeyed the same rule of speed and velocity reduction as that of the corresponding non-diluted cases (except when H₂ fractions reach about 80%). Both un-stretched flame speed and un-stretched burning velocity were reduced with the increase of diluent ratio, and increased with the increase of H₂ fraction.

- Within the range of the stoichiometric experiments, the velocity reduction rate due to diluent addition was determined mainly by diluent ratio and H₂ fraction. The effect of initial pressure was considered negligible. The velocity with high H₂ contents was reduced more slowly than that for low H₂ fractions.

- Flame stability decreased with the increase of initial pressure and H₂ fraction, while increased with the diluent gas addition increase. The effect of initial pressure on Markstein length was restrained for the fuel with high H₂ fraction. Under higher initial pressure, Markstein length was less sensitive to the change of diluent ratio than under lower pressure; respectively, Markstein length of a fuel with low H₂ fraction was more sensitive to the change of initial pressure than that of a one with high H₂ fraction.

Analogously, the same authors, Miao et al. 2009 [12] treated the laminar flame propagation characteristics of NG-H₂-air-diluent gas (N₂/CO₂) mixtures, studying in lean, stoichiometric and rich conditions, at various H₂ fractions and diluent ratios, considering the respective effects of N₂ and CO₂ separately. Both un-stretched laminar burning velocities and Markstein lengths were obtained. The results showed that equivalence ratio, H₂ fraction and diluent ratio had combined influence on laminar burning velocity and flame instability. These were main conclusions:

- With same amount of diluent gas, the fuel with higher H₂ fraction had stronger capability to maintain its flame propagation speed than the fuel with lower H₂ fraction; consequently, the former could tolerate higher diluent ratio.

- The un-stretched laminar burning velocity was reduced at a rate that was increased with the increase of the diluent ratio. The reduction effect of diluent ratio on the flame speed was not linear; the quantity of which was determined by not only diluent ratio, but also by H₂ fraction, equivalence ratio and the property of the employed diluent gas. The reduction effect of CO₂ diluent gas was stronger than that of N₂ diluent gas, mainly due to thermal effect because CO₂ has larger specific heat and causes more reduction in temperature.

- The effect of diluent ratio on Markstein length depended on the hydrogen fraction. In the case of the fuel with low H₂ volumetric fraction (20%) flame stability increased with the increase of diluent ratio, while in the case of the fuel with high H₂ volumetric fraction (80%) stability of lean and stoichiometric combustion tended to be slightly decreased with the increase of diluent ratio.

Additionally further study was considered necessary for these authors to be conducted for a better understanding of the effect of diluent gas on the stability of these types of fuel mixtures flames.

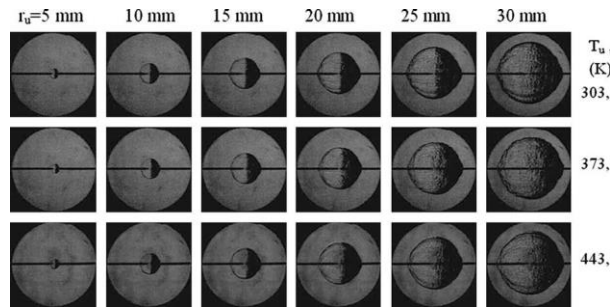


Fig. 41. Spherically expanding flames of hydrogen-methane-air mixtures, recorded by Schlieren cinematography, with H_2 fraction $h(\%)=40$ for $\phi=0.8$, $T_{u,0}(K)=\{303, 373, 443\}$ and $P_0(MPa)=0.5$ (adapted from Hu et al 2009 [76])

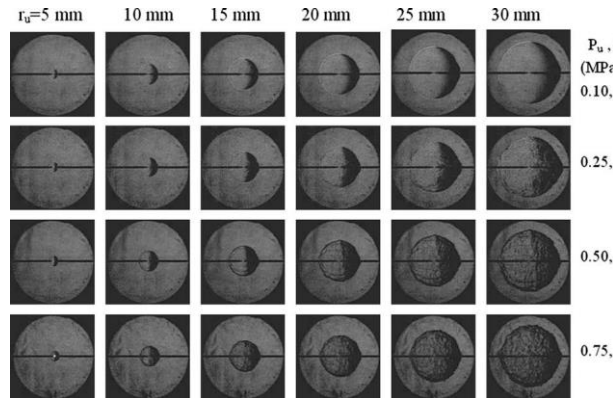


Fig. 42. Spherically expanding flames of hydrogen-methane-air mixtures, recorded by Schlieren cinematography, with H_2 fraction $h(\%)=60$ for $\phi=0.8$, $T_{u,0}(K)=373$ and $P_0(MPa)=\{0.1, 0.25, 0.5, 0.75\}$ (adapted from Hu et al 2009 [76])

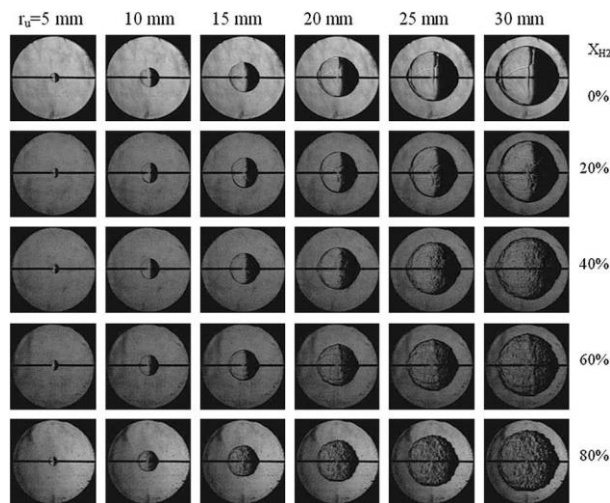


Fig. 43. Spherically expanding flames of hydrogen-methane-air mixtures, recorded by Schlieren cinematography, with H_2 fractions $h(\%)=\{0,20,40,60,80\}$ for $\phi=0.8$, $T_{u,0}(K)=373$ and $P_0(MPa)=0.5$ (adapted from Hu et al 2009 [76])

Hu et al. 2009 [76,78] studied experimentally and experimentally-numerically the lean premixed methane-hydrogen-air flames, their laminar burning velocities and the onset of cellular instabilities. The experimental works using spherically expanding flames (e.g. figs. 41-43) were conducted at different initial temperatures, pressures and hydrogen fractions and their effects were analyzed. Some conclusions were as follows.

- At the regarded lean condition (equivalence ratio of 0.8) significant decrease of critical radius and Markstein length with the increase of hydrogen fraction were presented, indicating the increase in both thermo-diffusive and hydrodynamic instabilities when hydrogen fraction is increased.
- With the increase of initial pressure, advancement of early onset of cellular instability was presented and the critical radius decreased. Markstein lengths decreased with the increase of initial pressure and hydrogen fraction, indicating that the flame instabilities increase with these increases of initial pressure and hydrogen fraction.
- The study showed very slight decrease or no variations in Markstein length at different initial temperatures. The flame instability was insensitive to initial temperature compared to initial pressure.
- The un-stretched flame propagation speeds and the un-stretched laminar burning velocities increased with the increase of initial temperature and hydrogen fraction, and they decreased with the increase of initial pressure.

Other experimental-numerical studies on the laminar premixed methane-hydrogen-air flames in the same constant volume combustion chamber were conducted by Hu et al. 2009 [75] at room temperature and atmospheric pressure. The un-stretched laminar burning velocity and the Markstein length were obtained over a wide range of diverse equivalence ratios and hydrogen fractions, with some additional conclusions.

- The laminar burning velocity increased with the increase of hydrogen fraction and the peak value of the laminar burning velocity shift to the rich mixture side.
- Markstein length showed an increase with the increase of equivalence ratio and the behavior became more remarkable at high equivalence ratio. Markstein lengths of methane-hydrogen-air flames with large hydrogen fraction showed a slow increase with the increase of equivalence ratio as hydrogen-air flames. Inasmuch as Markstein length decreases with the increase of hydrogen fraction, this suggested that the flame front stability enhances with the increase of equivalence ratio but the addition of hydrogen into the methane-air mixtures decreases the flame front stability.

6.3. Theoretical laminar burning velocities from simulation of one-dimensional premixed flames of fuel blends with implemented chemical kinetics schemes

As aforementioned, experimental measurements of the laminar burning velocity have been mostly limited in pressure and temperature and compromised by the effects of flame stretch interaction and instabilities. Computationally, these effects have been avoided in some published works by calculating one-dimensional, planar adiabatic flames using implementations of chemical oxidation mechanisms. The velocity of these flames is the laminar burning velocity by definition. Thus, kinetic models can be used to calculate the laminar burning velocity over a range of engine-like conditions. Laminar burning velocities are fundamentally important in regard to developing and justifying the chemical kinetics mechanisms, as well as in regard to predicting the performance and emissions of combustion systems, Bradley et al. 1998 [119]. Hypothetically, available mathematical expressions of laminar burning velocity, when they were accurately determined, offer the potential for the extraction of kinetic information by comparing the experimentally measured values and numerically simulated calculations. There is an extended agreement that chemical effects dependent on H radicals play a role in both the

promoting effect of hydrogen addition on combustion of hydrocarbons (e.g. methane) and the inhibiting effect, vice versa, of hydrocarbons (e.g. CH₄) on combustion of hydrogen.

Simulations of one dimensional premixed hybrid flames have been performed extensively in the literature and the numerical computations have been carried out with commercial or in-house laminar premixed flame codes in which the detailed kinetic schemes have been implemented. The replacing of overall single-step chemical schemes by the complex chemical reactions have had a huge impact on predictive models, giving better results and demonstrating the general interest of complex chemistry. Some of the codes and mechanisms have been associated to hydrogen hybrid blends applications, as several of those referred in [table 27](#) (chapter 8). Many of these studies were carried out, for instance, with CHEMKIN [\[161-166\]](#) or COSILAB [\[167,168\]](#) codes, and with implementation e.g. of GRI-Mechanism [\[169-171\]](#). Most of these works deal with the simulations of laminar flames on the HC rich side or on the H₂ rich side, but only a few of them identify global behaviors over wide ranges of hydrogen fractions and elevated pressures and temperatures. In particular, not many of the studies deal with the laminar burning velocities at medium hydrogen (molar) contents in the blend, which can be considered interesting in order to clarify how the transition takes place between the other behaviors in both sides.

A benchmark of available kinetic schemes for complex chemistry calculations, to describe premixed combustion of CH₄-H₂ blends, was realized by Bougrine et al. 2011 [\[172\]](#). Several of them were tested against a wide database of laminar flame speed measurements from the literature in order to evaluate and to choose a more relevant mechanism in terms of relevance of the scheme for methane-hydrogen-air-diluents mixture combustion, numerical consistence and robustness of calculations, predicted results accuracy and agreement with experimental data, precision and processing efficiency (directly linked to the number of species and reactions). Their results confirmed, especially regarding flame velocities, a good behavior of GRI-Mech 3.0 of Smith et al. 2011 [\[169,170\]](#) (with 325 elementary chemical reactions with associated rate coefficient expressions and thermochemical parameters for 53 species) compared to measurements of laminar premixed flames at low pressure and temperature, and then this mechanism was considered a reasonable choice to predict laminar flame speeds at high pressure and temperature. The other tested mechanisms were Princeton-Mech of Li et al. 2011 [\[173\]](#) (with 21 species and 93 reactions), USC_II-Mech of Wang et al. 2011 [\[174\]](#) (with 111 species and 784 reactions), and Konnov-Mech 0.5 of Konnov 2011 [\[175\]](#) (with 127 species and 1207 reactions). A database of laminar flame speeds and thicknesses was generated, from priori simulations of one-dimensional premixed flames, using the PREMIX-code/CHEMKIN-II of Kee et al. 1989 [\[162,163\]](#) and considering methane-hydrogen-air-diluents mixtures. The Premix simulation results, using the different chemical schemes, were compared to experimental data collected from an important process of gathering measurements that was carried out. Thus, the good behaviors of the mechanisms were reported for many studies compared to experimental results of laminar premixed flames velocities.

The studies over wide ranges of unburned mixture compositions and thermodynamic conditions, in order to complement experimental measurements as done in the same mentioned work by Bougrine et al. 2011 [\[172\]](#), are not frequent in general in the literature and raise questions around whether the laminar burning velocity may be obtained from the individual constituents, at the same conditions, by varying of the components contents in fuel blends, and about whether there are substantial differences in the calculated trends of this velocity by varying the initial conditions in global ranges and how the tendencies are. The theoretical work of Di-Sarli&Di-Benedetto 2007 [\[160\]](#) was a good sample of a very interesting and important reference, joining objectives and trying to clarify the effects of radicals interactions. They also

looked for the obtaining of correlations for the laminar burning velocity of fuel-blends in air mixtures, in their study considered for different values of equivalence ratio and hydrogen content in the fuel. A code (adopting a hybrid time-integration/Newton-iteration technique to solve the steady-state mass, species and energy conservation equations) was set up to simulate a freely propagating flame (one dimensional, planar, adiabatic, steady, un-stretched laminar flame propagation), derived from the application of PREMIX-module [162]/CHEMKIN-package [165,166] (and implemented detailed reaction scheme of GRI-Mech 3.0 [170,171]) with mixture-averaged formulas for evaluating the transport properties.

6.4. *Mixing-rules calculations to obtain laminar burning velocities of fuel blends*

This section introduces a previous general discussion on the application of mixing rules to the calculation of laminar burning velocities for air mixtures of hydrogen-hydrocarbon combined blends in comparison with its applicability to other types of fuel blends. Chapter 7 will review concrete expressions of some authors, based on some of these types of mixing rules applied to hydrogen-hydrocarbon blends.

The definition and construction of chemical kinetic models for combustion of fuel blends can be very complex, with long calculation times. Other frequent tentative solution is obtaining the laminar burning velocity based on more or less accurate mixing rules, which can determine the laminar burning velocity of the fuel blends based on the corresponding burning velocities of the fuel components without being computationally too demanding. Sufficiently accurate determinations of the laminar burning velocities of the fuel components and the laminar burning velocity of the fuel blends have been requirements practically needed to obtain and compare some mixing rules adequately.

As commented, in the literature there have been published experimental measurements of fuel blends with hydrogen addition, more or less limited in their applicable ranges, and sometimes there have been doubted in the accuracy when measurements on different setups were compared. Actually, not many measurements of fuel blends are available in the published technical articles for wide ranges of conditions, being particularly difficult to be found for engine-like conditions.

On the other hand, functional expressions based on simple mixing rules to predict the laminar burning velocity of (binary, ternary or multicomponent) fuel mixtures can be collated with expressions generated from detailed chemistry and simulations by combustion modeling. Thereby some published works have considered interesting to explore how mixing rules that have been used to estimate those burning velocities, sometimes of practical simplicity, can be consistently compared to the expressions based on the detailed chemical kinetics of the fuel blends.

An overview with considerations of different mixing rules to predict laminar burning velocities was given in the work of Sileghem et al. 2012 [176], more focused on gasoline-alcohol blends as alternative fuels for spark ignition engines but with some interesting considerations in general aspects.

The present work makes a review to compare different laminar burning velocity expressions that have been published about fuel blends of H₂ and other gas fuels, with special attention to NG and particularly to CH₄ as its reference fuel. Among the compared works, those which are based on mixing rules, and were originally tested for fuel blends, were derived either from experimental or modeling data of fuel-air mixtures, giving numerical data for combined mixtures, with their respective implications on the effects of higher temperature and pressure by the performance of the applied mixing rules.

6.4.1. Mixing rules derived from linear and potential rules-like formulas

A pioneering simple empirical mixing rule, giving the maximum burning velocity of a mixture in terms of the maximum burning velocities of the fuel components, was proposed by Payman&Wheeler 1922 [177] based on the weighted average by the concentrations in volume of the components, considering that these formulas do not correspond to conceivable physical systems and that its use has to be restricted to fuels whose burning velocities and flame temperatures do not differ substantially from each other.

Laminar flame speeds of C₁-C₃ hydrocarbons (containing from one to three carbon atoms in its molecule) with hydrogen addition were measured by Yu et al. 1986 [138], Wu et al. 2011 [146], Tang et al. 2011 [150], with the results interpreted on the basis of enhanced kinetic, thermal and transport effects due to the associated increases in the reaction kinetics, adiabatic flame temperature and diffusivity. Burning velocities are mostly governed by the activation energy, the flame temperature and, to a certain extent, the transport properties, with the corresponding kinetic, thermal and transport consequences. Dependent upon the fuel, an enhanced reactivity can be expected, which is the case with hydrogen, Wu et al. 2011 [146]. A lower or higher adiabatic flame temperature, responsible for the thermal effect, can lead to another mixture reactivity, even assuming the same underlying reaction mechanism. Furthermore, dependent upon the diffusivities of the blend components, there can be a modification of the mixture concentration in the flame structure, Tang et al. 2011 [150].

The inherent difficulty in the development of a mixing rule is that various chemical and thermal effects may not be separable for fuel blends because of possible thermo-kinetic couplings. For this reason mixing rules based on the fractions of the fuel components are not expected to be simply linear in the fuel blend composition, Hirasawa et al. 2002 [178], Sileghem et al. 2012 [176], proven by the poor predictions of the mole fraction and mass fraction mixing rules in some cases.

$$u_{L,blend}(\Phi) = \sum_i [z_i \cdot u_{i,i}(\Phi)] \quad i=\{1, N\} \quad (149)$$

$$\text{where } z_i = \{x_i, y_i \text{ or } w_i\} \quad (150)$$

$$\text{with } w_i = [(x_i \cdot ch_i^0) / \sum_j (x_j \cdot ch_j^0)] \quad (151)$$

Here the composition-parameter fraction z_i of the i component can represent either x_i , y_i or w_i : mole (volume) x_i , mass y_i or energy w_i fraction (this latter w_i is based on the combustion heat ch_i^0 of the mixture components).

Hirasawa et al. 2002 [178] developed an empirical mixing rule, dependent upon the mole fraction x_i weighted average of the burning velocities and flame temperatures T_f , based on that the flame temperature has the dominant effect, at atmospheric pressure, on the burning velocity of fuel blends as ethylene/n-butane, ethylene/toluene and n-butane/toluene, where the kinetic coupling hardly affects the burning velocities of the air mixtures of these fuel blends.

$$u_{L,blend} = \Pi_i [u_{i,i}^{\tau_i}] \quad i=\{1, N\} \quad (152)$$

$$\text{where } \tau_i = [(x_i \cdot n_i \cdot T_{f,i}) / (n_{blend} \cdot T_{f,blend})] \quad (153)$$

with n = total number of product moles (including diluents)

Ji et al. 2011 [179] in the same way, also at atmospheric pressure, found that laminar burning velocity of mixtures of n-dodecane/toluene and n-dodecane/methyl-cyclohexane can be predicted using the laminar burning velocities and adiabatic flame temperatures of the components. Kinetic couplings appeared to have a minor effect on flame propagation in those cases.

On the contrary, for the fuel blends of the specific interest of the present work, e.g. hydrogen-methane-air mixtures, the chemical kinetic interactions have the biggest influence, Wu et al. 2011 [146], Tang et al. 2011 [150], Di-Sarli&Di-Benedetto 2007 [160], Bougrine et al. 2011 [172]. Because of its strong reactivity, hydrogen addition enhances flame propagation and extends the flammability limits of the fuel-air mixtures, as described previously.

6.4.2. Mixing rules derived from LeChatelier's rule-like formula

This rule is based on the principle that the equilibrium of a chemical system shifts to counteract an imposed change and a new equilibrium is established when the chemical system at equilibrium experiences the change.

$$[1 / u_{L,blend}(\Phi)] = \sum_i [z_i / u_{L,i}(\Phi)] \quad i=\{1, N\} \quad (154)$$

$$\text{where } z_i = \{x_i, y_i \text{ or } w_i\} \quad (155)$$

$$\text{with } w_i = [(x_i \cdot ch_{i^o}) / \sum_j (x_j \cdot ch_{j^o})] \quad (156)$$

As explained previously, the composition-parameter fraction z_i of the i component can represent either x_i , y_i or w_i : mole (volume) x_i , mass y_i or energy w_i fraction (this latter w_i is based on the combustion heat ch_{i^o} of the mixture components).

According with some published formulations, as Di-Sarli&Di-Benedetto 2007 [160], LeChatelier's rule is simple to apply generating laminar burning velocities expressions for some blends. Because of that, it has been used preferably when the accuracy based in comparison of mixing rules was considered enough.

Sileghem et al. 2012 [176] used LeChatelier's rule (based on the energy fraction w_i) to predict the laminar burning velocity of gasoline-alcohol blends, with this corresponding smallest over-prediction of the laminar burning velocity in comparison with other tested mixing rules. An energy fraction mixing rule, a mixing rule of the type of Hirasawa et al. 2002 [178] and a LeChatelier's rule based on the energy fractions gave the best results in these cases, indicating that the flame temperature is the dominant factor for laminar burning velocity of these types of fuel blends. There were over-predictions, with the shortest one for LeChatelier's rule and the largest one for the energy-fraction mixing rule, with differences considered as very small, and the same trend was seen in both the experimental and modeling data (over-prediction of the laminar burning velocity). Because of the simplicity of LeChatelier's rule, this was considered as preferable by the authors in those cases, pending of other validations. These three mixing rules performed very well for binary, ternary and multicomponent fuels, and particularly for binary blends of fuels even at higher temperature and pressure. LeChatelier's rule based on the energy fraction stood out above the rest for the data used in that study, in both accuracy and simplicity. However, the same authors considered in their work that further validation was needed because of uncertainty limits of both the experimental and modeling results.

In the same previously mentioned study, Sileghem et al. 2012 [176] also commented that these mixing rules do not work precisely for fuel blends when chemical kinetic interactions have the biggest influence, e.g. for hydrogen-methane-air mixtures. Their laminar burning velocities were considered not to be predicted accurately in wide ranges of conditions and composition with the previous mixing rules. This regard was shown, for instance, by a comparison for blends as 70/30% of H₂-CH₄ in a range of equivalence ratio $\Phi=[0.8, 1.2]$ at temperatures of about $T_u(K)=600$ and close to atmospheric pressure $P(MPa)=0.1$ (fig. 44); the observed errors were significant in fact in this appraisal. Chemical kinetic based calculations of this H₂-CH₄ mixture were performed in that study with the GRI-Mech 3.0 mechanism [170].

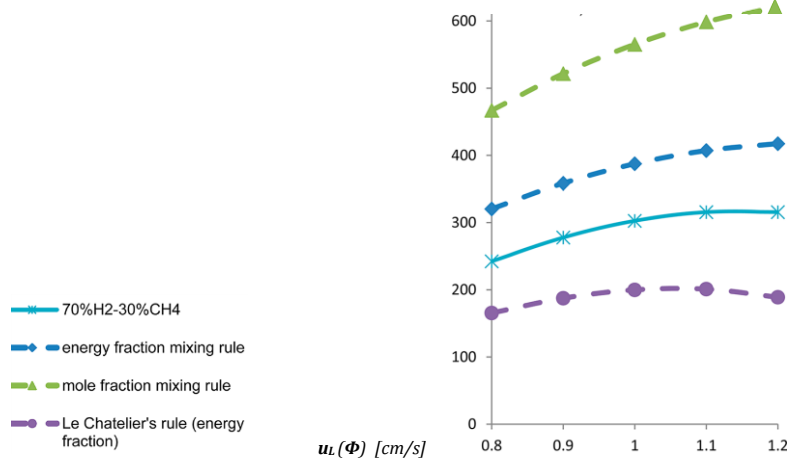


Fig. 44. Laminar burning velocities of a blend of H₂-CH₄ with $x_{H_2}=0.7$; u_{L, H_2-CH_4} (cm/s) versus equivalence ratio $\Phi=[0.8, 1.2]$ for $P(MPa)=0.1$ and $T_u(K)=600$ (taken from Sileghem et al. 2012 [176])

References of chapters six, seven and eight (*after the eighth chapter*)

7. Expressions for laminar burning velocity of hydrogen - natural gas blends

- 7.1. Expressions for laminar burning velocities of hydrogen-hydrocarbon blends escalated linearly with hydrogen content
 - 7.1.1. Specific composition parameters intended for a preferential oxidation of hydrogen in hydrocarbon-based mixtures
 - 7.1.2. Comparison of transport, thermal and kinetic effects of hydrogen addition to hydrocarbon-based mixtures
 - 7.1.3. Adiabatic flame temperature and Zeldovich number for hydrogen addition to methane-based mixtures
- 7.2. Expressions for laminar burning velocities of methane and natural gas fuel-air mixtures escalated exponentially with hydrogen content
 - 7.2.1. Effects of equivalence ratio, temperature and dilution
 - 7.2.2. Concept of dimensionless laminar burning velocity increment
- 7.3. Expressions for laminar burning velocities of hydrogen and methane blends based on linear mixing rules
 - 7.3.1. Non-linear behavior of laminar burning velocities of hydrogen and methane blends
 - 7.3.2. Regimes of laminar burning velocities of hydrogen and methane blends
- 7.4. The role of radicals in the premixed flame reaction zone and interaction on laminar burning velocities
 - 7.4.1. Radicals for combustion of hydrogen-methane fuel-air mixtures
 - 7.4.2. Radicals for combustion of hydrogen-natural gas fuel-air mixtures
- 7.5. Expressions for laminar burning velocities of fuel-air mixtures of hydrogen and methane/natural gas blends based on LeChatelier's rule-like formulas
 - 7.5.1. Applicability of expressions based on LeChatelier's rule in function of equivalence ratio and hydrogen content
 - 7.5.2. Applications of expressions based on LeChatelier's rule at engine-like conditions for spark-ignition engine models

- 7.6. Complex expressions of laminar burning velocity applicable to hydrogen-methane blends at engine-like conditions in complete range of fuel combinations
 - 7.6.1. Effects of equivalence ratio and hydrogen addition
 - 7.6.2. Temperature and pressure effects
 - 7.6.3. Dilution effect of residual gas
 - 7.6.4. Calculation by global correlation compared to simulation based on detailed chemistry

References of chapters six, seven and eight (*after the eighth chapter*)

7. Expressions for laminar burning velocity of hydrogen - natural gas blends

This chapter presents laminar burning velocity expressions derived from several treatments of some authors, at functionally different regimes of hydrogen-hydrocarbon fuel blends, and the corresponding formulations and concepts related with diverse methodologies from room-ambient terms of reference up to engine-like conditions. A summary of the types of these expressions is included in [table 26](#) (at the end of this chapter 7) for fuel blends of H₂ with CH₄ or NG, with their features of applicability depending on composition conditions.

7.1. Expressions for laminar burning velocities of hydrogen-hydrocarbon blends escalated linearly with hydrogen content

First, expressions for augmented laminar burning velocities of hydrocarbon fuel-air mixtures with hydrogen combination are considered almost linearly escalated with virtually defined parameters of hydrogen addition in relatively small proportions.

7.1.1. Specific composition parameters intended for a preferential oxidation of hydrogen in hydrocarbon-based mixtures

Some studies, as Wu et al. 2011 [\[146\]](#) and Tang et al. 2011 [\[150\]](#), following the work of Yu et al. 1986 [\[138\]](#), considered a skewed nature of the hydrogen mole fraction in the fuel blend. They used the initial mole fractions in the global fuel-air mixture of the hydrocarbon fuel and hydrogen addition respectively ([table 1](#), chapter 1).

$$\begin{array}{ll}
 \text{Hydrogen mole fraction in the global fuel-air mixture} & X_{H_2} \equiv X_h \\
 \text{Hydrocarbon mole fraction in the global fuel-air mixture} & X_{HC} = X_f \\
 \text{Fuel blend mole fraction in the global fuel-air mixture} & X_F = X_f + X_h = X_{HC} + X_{H_2} \quad (157)
 \end{array}$$

$$X_f + X_h + X_a = X_F + X_a = 1 \quad (158)$$

On a molar basis, the consumption of hydrogen requires much less oxygen, releases much less heat, and heats up much less of the nitrogen associated with the corresponding amount of oxygen in the air, as compared to a typical hydrocarbon. Thus, the amount of hydrogen addition given as a conventional mole fraction in a fuel blend represents an overestimation of the hydrogen concentration on the flame.

$$\text{Hydrogen molar fraction in the fuel blend} \quad x_{H_2} = (X_{H_2}/X_F) = [X_{H_2}/(X_{H_2} + X_{HC})] \quad (159)$$

$$\text{Hydrocarbon molar fraction in the fuel blend} \quad x_{HC} = (X_{HC}/X_F) = [X_{HC}/(X_{H_2} + X_{HC})] \quad (160)$$

$$x_{HC} + x_{H_2} = 1 \quad (161)$$

For a more balanced quantification of the hydrogen content, Yu et al. 1986 [\[138\]](#) used the symmetrical and adiabatic counter-flow flame to measure the laminar flames speeds of different methane and propane air mixtures, both without and with small amounts of hydrogen addition. Regardless of whether the mixture was lean or rich, they found that the increase of burning

velocity with hydrogen addition can be approximately linearly correlated with the flame speed without hydrogen addition and a single parameter R_h of extent of the hydrogen content, where X_f , X_a and X_h are the initial mole concentrations (fractions) of the C₁-C₃ hydrocarbon fuel, air and hydrogen addition, respectively.

This parameter R_h is the ratio of the amount of hydrogen X_h plus the stoichiometric amount of air $\chi_{stqa,h}$ needed for its total oxidation, to the amount of hydrocarbon X_f plus the remaining available air $\chi_{a,f}$ left for its oxidation.

$$R_h = [(X_h + \chi_{stqa,h}) / (X_f + \chi_{a,f})] \quad (162)$$

$$\text{where } \chi_{a,f} = (X_a - \chi_{stqa,h}) \quad (163)$$

$$\text{and } \chi_{stqa,h} = [X_h / (X_h/X_a)_{stq}] \quad (164)$$

$$\text{with } (X_h/X_a)_{stq} = 0.418 \quad \text{for H}_2 \text{ in air (molar stoichiometric hydrogen-air ratio)}$$

Thus, the numerator of R_h properly accounts for all the gases that participate in the oxidation of hydrogen. Therefore, hydrogen has been considered present only in stoichiometric small quantities (and its combustion requiring e.g. four times less oxygen than methane). It is assumed that there is enough air to facilitate a complete oxidation of hydrogen, while the remaining air is used to oxidize the fuel (e.g. methane); based on this indicator, hydrogen can be considered to be the minor component of the total fuel in the blend.

Although the amount of hydrogen addition is small based on stoichiometry, it is quite significant in terms of the volumetric fraction. So, e.g. for butane, in Tang et al. 2011 [150] the hydrogen addition amount in terms of molar fraction in the fuel blend could be quite substantial, up to $\chi_{H_2}=0.7-0.9$ for a relative amount of hydrogen addition ratio up to $R_h=0.5$, which is the maximum value of this parameter considered in that study.

Other related composition parameter, also defined by Yu et al. 1986 [138], is an effective equivalence ratio Φ_{eF} of the hydrocarbon in the fuel-air mixtures.

$$\Phi_{eF} = [(X_f/\chi_{a,f}) / (X_f/X_a)_{stq}] \quad (165)$$

(where $\chi_{a,f}$ has been previously described when R_h has been defined)

$$\begin{aligned} \text{with } (X_f/X_a)_{stq} = & 0.105 \quad \text{for CH}_4 \text{ in air (molar stoichiometric methane-air ratio)} \\ & 0.070 \quad \text{for C}_2\text{H}_4 \text{ in air (molar stoichiometric ethylene-air ratio)} \\ & 0.418 \quad \text{for C}_3\text{H}_8 \text{ in air (molar stoichiometric propane-air ratio)} \\ & 0.032 \quad \text{for C}_4\text{H}_{10} \text{ in air (molar stoichiometric butane-air ratio)} \\ & 0.420 \quad \text{for CO in air (molar stoichiometric carbon oxide-air ratio)} \end{aligned}$$

It is important to emphasize that these parameters R_h and Φ_{eF} do not represent the actual stoichiometry during the reaction (for example, the hydrocarbon fuel obviously has access to the total amount of air present). It is necessary to insist on that, implicit in the adoption of these parameters, there is the assumption that hydrogen is preferentially oxidized as compared to the hydrocarbon fuel as its consumption is considered stoichiometric and hence complete, leaving the remaining oxygen to react with the HC fuel. While such supposition is reasonable considering the highly reactive and diffusive nature of hydrogen, as compared to the HC fuel, and for relatively small amounts of hydrogen addition, its ultimate justification lies on how well the parameter R_h can provide a more balanced indication of the fact that hydrogen addition is small and hence its effect can be linearly described.

The two concentration parameters, R_h and Φ_{eF} , were intuitively defined to facilitate data reduction and empirical correlation in order to quantify, measure and represent the effects and extent of hydrogen addition. They were also shown and used in several other studies as the developments of Wu et al. 2011 [146] or Tang et al. 2011 [150], whose analysis showed that both Arrhenius (reactivity and temperature) and diffusive contributions to the laminar flame speed are nearly linear functions of the hydrogen addition. These works, for small to moderate amount of hydrogen addition in terms of oxygen consumption, also considered specifically that there should always be enough air to facilitate the complete oxidation of hydrogen.

The laminar flame velocities correlated with R_h and Φ_{eF} are expressed as linear relations in the form defined by Yu et al. 1986 [138] at atmospheric conditions, at pressure $P_o=0.1$ MPa, temperature $T_{u,o}=300$ K.

$$u_{l,o \text{ HC-H}_2}(\Phi_{eF}, R_h; T_{u,o}, P_o) = u_{l,o \text{ HC}}(\Phi_{eF}, R_h=0; T_{u,o}, P_o) + k_h(\Phi_{eF}) \cdot R_h \quad (166)$$

$$\text{where } u_{l,o \text{ HC}}(\Phi_{eF}, R_h=0; T_{u,o}, P_o) = u_{l,o \text{ HC}}(\Phi=\Phi_{eF}; T_{u,o}, P_o) \quad (167)$$

The experimental results by Yu et al. 1986 [138], who estimated $k_h(\Phi_{eF}) \approx 83$ cm/s for methane and propane based mixtures with small variations, for small amounts of hydrogen addition, were numerically reproduced by El-Sherif 2000 [38], who estimated $k_h(\Phi_{eF}) \approx 84$ cm/s for methane-air flames with the following base expression.

$$u_{L,o \text{ CH}_4}(\Phi_{eF}, R_h=0; T_{u,o}, P_o) = u_{L,o \text{ CH}_4}(\Phi=\Phi_{eF}; T_{u,o}, P_o) \quad (168)$$

$$\text{with } u_{L,o \text{ CH}_4}(\Phi=\Phi_{eF}; T_{u,o}, P_o) [\text{cm/s}] = 38 \Phi_{eF}^{-0.35} \text{EXP}[-5.5(\Phi_{eF}-1.1)^2] \quad (169)$$

His assessment of methane burning velocity increment at atmospheric conditions, for $\Phi_{eF}=1$ and $R_h=0.4$, was about twice the corresponding value without hydrogen addition. This was explained as due mainly to the increase of H radical and the consequent enhanced reactivity of chain branching reaction $\text{O}_2+\text{H}\rightarrow\text{O}+\text{HO}$ with a significant role for increasing burning velocity.

For these authors, the hydrogen-augmented flame speeds escalated almost linearly with the defined parameter R_h of hydrogen-addition. Therefore, k_h is a coefficient that represents the sensitivity of the laminar flame velocity to hydrogen addition, with values derived from experimental measurements or by computational simulation calculation. Coefficient k_h actually depends on Φ_{eF} , with minima at about $\Phi_{eF}=1$. The influence of hydrogen addition is stronger for off-stoichiometric conditions, lean burning terms, which in turn implies the minimal influence around stoichiometry, with the weakest dependence on R_h at near stoichiometric conditions.

According to observations of Vagelopoulos et al. 1994 [180], who showed that the laminar flame speed can be overestimated if the distance of the nozzle separation is too short in the experimental counter-flow arrangement, the results of Yu et al. 1986 [138] were probably too high for the laminar burning velocity due to that experiments configuration. This was also considered by Halter et al. 2005 [53] by comparison of their results.

The above linear equations, that are able to take into account the trend of the laminar burning velocity with hydrogen addition on the methane-based fuel, have been considered intrinsically valid only for small hydrogen contents, Di-Sarli&Di-Benedetto 2007 [160], due to the way that the expressions of parameters R_h and Φ_{eF} are defined to account for the composition of the hybrid fuel-air mixtures.

7.1.2. Comparison of transport, thermal and kinetic effects of hydrogen addition to hydrocarbons-based mixtures

Tang et al. 2011 [150] also found, after Sher&Ozdon 1992 [151], that a linear laminar flame speed correlation for n-butane-air mixtures with hydrogen addition again held approximately. With a sensitivity-based analysis, they showed that the kinetic effect was the most prominent for all effective equivalence ratios, followed by the thermal effect that was smaller but still significant, with the transport effect being minimal and substantially smaller. The mixture reactivity is intensified, enhanced through the global activation energy decrease. The temperature is increased, even assuming an underlying reaction mechanism, through the inherently higher adiabatic flame temperature of hydrogen air mixtures as compared to those of the hydrocarbon air mixtures, for the same equivalence ratio. The non-equal diffusion of the mixture concentration in the flame structure is facilitated due to the high mobility of hydrogen gas compared to those of the hydrocarbons and air, through the global Lewis number (respectively very small and large for lean and rich hydrogen air mixtures). All the sensitivity factors at the stoichiometric conditions are one order smaller than those ones at the off-stoichiometric conditions.

$$\text{Laminar burning flux (density-weighted flame speed)} \sim \{Le \text{ EXP}[-E_a/R_o T_{ad}]\}^{(1/2)} \quad (170)$$

In extension, additional computations for other fuels were also performed by Tang et al. 2011 [150], for methane, ethylene and propane air mixtures, and the same extent of linearity was again observed over the same ranges of values for parameters R_h and Φ_{eF} . The behavior of k_h coefficients in terms of the variation with Φ_{eF} was similar for all them, with methane having higher values than butane, propane and ethylene. In fact, the controlling chemistries are quite similar for alkanes, but it is interesting that ethylene had also the same behavior, in spite of being an alkene and its chemistry is distinctively different and its flame speed is much higher. The study assessment was done with a dimensionless coefficient, a normalized sensitivity coefficient K_h , reasoning that methane, having the slowest flame speeds among the considered four hydrocarbons, would be most sensitive to the enhancement of hydrogen addition and therefore had the largest values of $K_h(\Phi_{eF})$. The opposite was held for ethylene, because it had the fastest flame speeds.

$$K_h(\Phi_{eF}) = [k_h(\Phi_{eF}) / u_{L,0}(\Phi_{eF}, R_h=0)] \quad (171)$$

Wu et al. 2011 [146] studied analogously the laminar burning velocities of mixtures of ethane, ethylene, acetylene and carbon monoxide with a small hydrogen addition at atmospheric and elevated pressures. They used expanding spherical flames, with the dual chamber design of Tse et al. 2004 [181], to measure the laminar flames of gas air mixtures with hydrogen addition, by Schlieren images recorded using a high-speed digital camera. Standard air was used as the oxidizer for experimentation at atmospheric pressure. At elevated pressures, oxygen-helium mixtures were used to suppress the onset of cellular instabilities. Effects of hydrogen addition were interpreted through an expression obtained with a one-step overall reaction and constant transport properties, in which the Lewis number Le in combination with the thermal diffusivity D_t , the adiabatic flame temperature T_{ad} and the activation temperature T_a can be considered to represent the diffusion-transport, thermal and kinetic effects. The expression is of this type:

$$\text{Laminar burning velocity} \sim (Le D_t)^{0.5} \text{ EXP}[(1/2)(-T_a/T_{ad})] \quad (172)$$

This equation showed the dominant functional dependence of the laminar burning velocity on the transport and thermo-kinetic parameters and provided a viable expression to guide the interpretation of the flame response to the diffusive and chemical complex processes constituting the flame. The influence of hydrogen addition due to different effects could be evaluated once determined the parameters. Since the kinetic and thermal effects were lumped through the exponential factor, their effects could be treated as a combined Arrhenius effect, and similarly the pre-exponential factor was the representation of the diffusion effect. The evaluation of these governing parameters showed that both the Arrhenius and diffusive contributions to laminar flame velocity were functions of hydrogen addition, which explained the approximate linear identified correlations.

Laminar flame velocities were calculated by Wu et al. 2011 [146] using the CHEMKIN collection codes, PREMIX-module [162] in conjunction with CHEMKIN [163] and TRANSPORT [161] packages. The Transport package [161] was used to evaluate the thermal diffusivity and other transport coefficients that were evaluated at the unburned gas temperature. The effective Lewis numbers for the hybrid mixtures, for $\Phi_{eF} > 1$ and $\Phi_{eF} < 1$ respectively, were given by application of expressions derived from Law et al. 2005 [182] and Bechtold&Matalon 2001 [183] in function of the Lewis numbers of hydrogen, hydrocarbon and oxygen. The solutions were obtained allowing multicomponent formulation of the transport properties and thermal diffusion. The kinetic mechanism employed was the mentioned USC_II-Mech [174] which is a high temperature reaction model consisting of 111 species and 784 reactions, developed for the prediction of H₂/CO/C₁-C₄ hydrocarbon combustion. The adiabatic temperature T_{ad} , and the densities of the unburned ρ_u and burned ρ_b gas mixtures, were evaluated using the STANJAN equilibrium program [184]. The global activation temperature T_a was evaluated following a numerical approach used in Tang et al. 2011 [150] and Jomaas et al. 2007 [185], applied for sufficiently off-stoichiometric mixtures for which the reaction rate is controlled by the deficient reactant, Law 2006 [186], Law&Sung 2000 [187]. Respectively, for the near-stoichiometric mixtures, this temperature T_a was evaluated by interpolation of the results of off-stoichiometric mixtures.

Thus, in a generalization of this kind of treatments, Wu et al. 2011 [146] considered demonstrated experimentally and computationally that the approximately linear correlation between laminar flame speed and H₂ addition, previously observed (by Yu et al. 1986 [138], Sher&Ozdor 1992 [151], Tang et al. 2011 [150]) for hybrid mixtures of methane (C₁), propane (C₃) and n-butane (C₄), could also being largely applied to C₂ fuel hydrocarbons as ethane, ethylene and acetylene at atmospheric pressure, as well as approximately for ethylene and propane at elevated pressures, although relatively limited. Moreover, they considered that, in most cases, H₂ addition enhances burning velocity mainly through the modification of the activation temperature rather than the flame temperature, i.e. the kinetic effect is stronger than the thermal effect. This strong kinetic affects the progress of reactions through pressure variations, which facilitate three-body termination reactions relative to the two-body carrying and branching reactions. Some deviations between measurements and calculations of Wu et al. 2011 [146] suggested to them that a revision of aspects of the mechanism USC_II-Mech [174] was required.

As a side remark comment, on the other hand they observed that the linear correlation did not hold for CO because of the strong kinetic coupling by the catalytic effect of hydrogen, especially for small values of R_h . This effect reduces the activation temperature and increase the Arrhenius factor leading to a highly nonlinear dependence of the laminar flame velocity with hydrogen addition.

7.1.3. Adiabatic flame temperature and Zeldovich number for hydrogen addition to methane-based mixtures

As shown in previous sections, hydrogen addition increases the laminar burning velocity in fuel blends. Some motives may be considered for that increase understanding. One reason is the increase of H radical concentration when hydrogen is added, as it will be seen in section 7.4. Another is the increase of the adiabatic flame temperature T_{ad} as hydrogen is aggregated. Adiabatic flame temperature through Arrhenius kinetics exerts an influence on laminar burning velocity. A clear evidence of such strong dependence was shown e.g. by Hu et al. 2009 [77] for methane-air and hydrogen-air flames. In methane-air mixture, the two factors not only gave the same pattern but they give their peak on the rich side with close equivalence ratios. At the same T_{ad} , laminar burning velocity of fuel-lean mixtures and fuel-rich mixtures almost gave the same value except at high rich conditions. However, in hydrogen-air mixture, this correspondence is offset since T_{ad} has its peak at equivalence ratio $\Phi=1.1$ while the un-stretched laminar burning velocity peaks at $\Phi=1.8$. This sufficiently off-stoichiometric peak at rich side is a consequence of the highly diffusive nature of hydrogen. Specially, since the free-stream Lewis number Le in sufficiently lean and rich hydrogen-air mixtures are about 0.33 and 2.3, respectively, and $u_L \sim Le^{0.5}$, the effect of Le is to reduce un-stretched laminar burning velocity on the fuel-lean side but to increase it on the fuel-rich side, leading to its peak value toward the rich side. The gradient of un-stretched laminar burning velocity on the fuel lean side shows a larger reduction compared with that on the fuel-rich side.

The temperature profiles of the stoichiometric methane-hydrogen-air flames at atmospheric conditions were given by Hu et al. 2009 [77] showing that, at small hydrogen fraction, hydrogen addition had a little influence on the temperature. The equilibrium adiabatic flame temperature increased only 15 K from methane-air flame to methane-hydrogen-air flame with 40% hydrogen fraction but another 120 K increase in temperature was reached when hydrogen fraction was increased from 40% to pure hydrogen-air flame. The plots of un-stretched laminar burning velocity and adiabatic temperature versus hydrogen fraction also showed the same trend.

Asymptotic analyzes of Zeldovich et al. 1985 [188] expressed laminar burning velocity in terms of the square root of Arrhenius expression in adiabatic flame temperature T_{ad} with overall activation energy E_a . Peters&Williams 1987 [189] derived an asymptotic structure of the flame that introduced the inner layer temperature T^0 in fuel consumption. The inner layer temperature represents the crossover temperature between chain-branching reactions and chain-termination reactions, i.e. that characterizes the balance between chain-branching reactions and chain-breaking effect of the fuel consumption and recombination reactions, and was interpreted as the critical temperature "at and above" which chemical reactions take place, Götting et al. 1992 [190]. Within the temperature profile of a premixed flame, it demonstrates a transition position from inert preheat zone to reaction zone, and this is the position where the second derivative vanishes and the gradient gives the maximum value.

The profiles of temperature and its first and second derivatives for stoichiometric methane-hydrogen-air flames were given by Hu et al. 2009 [77] at atmospheric conditions and for different hydrogen fractions showing that T^0 was decreased with the increase of hydrogen fraction and this was consistent with the tendency of overall activation energy E_a . Based on fundamental combustion theory, Warnatz et al. 1998 [191] claimed that the easier occurrence of combustion reaction of H₂-air mixture than that of CH₄-air mixture was due to the lower activation energy of hydrogen compared with that of methane. With the increase of hydrogen fraction, the activation energy E_a of methane-hydrogen mixture was decreased because the critical temperature or the transition temperature T^0 was decreased.

The Zeldovich number Z , already mentioned in section 3.2, is a dimensionless form of overall activation energy. It represents the sensitivity of chemical reactions to the variation of maximum flame temperature, and the inverse of it physically denotes an effective dimensionless width of the reaction zone. This number Z can be calculated (Jomaas et al. 2007 [185], Egolfopoulos&Law 1990 [192], Clavin 1985 [193]) with the values of E_a and T^0 .

$$Z = [(E_a/R) (T_a - T_u) / (T_{ad})^2] \quad (173)$$

Hu et al. 2009 [77] gave the variation of Z against hydrogen fraction for stoichiometric methane-hydrogen-air mixtures at atmospheric conditions. They showed that Z is largely influenced by hydrogen addition. The increase of hydrogen fraction results in decreasing Z because of the decrease of inner flame temperature T^0 . This behavior reflects the controlling influence of the flame temperature, which increases with the increase of hydrogen content. This facilitates the temperature-sensitive two-body branching reactions relative to the temperature-insensitive three-body termination reactions, Jomaas et al. 2007 [185], leading to overall faster reactions and reducing overall activation energy with the increase of hydrogen content.

7.2. Expressions for laminar burning velocities of methane and natural gas fuel-air mixtures escalated exponentially with hydrogen content

The work of Hu et al. 2009 [77] can be regarded as an introductory reference to this section because they proposed, on the basis of the numerical results, the following illustrative correlations for the laminar burning velocities of CH₄ fuel-air mixtures with H₂ blend, for varied discrete values of equivalence ratio $\Phi = \{0.8, 1, 1.2\}$, making difference of linear and exponential behaviors depending on the hydrogen volumetric fraction in its total possible range $x_{H_2} = [0, 1]$, i.e. $h(\text{vol}\%) = 100x_{H_2} = [0, 100]$, at pressure $P_o = 0.1 \text{ MPa}$ and temperature $T_{u,o} = 303 \text{ K}$.

$$u_{l,o \text{ CH}_4\text{-H}_2} (\Phi=0.8, h \leq 40\%; T_{u,o}, P_o) \text{ [cm/s]} = 28.462 + 0.229 h \quad (174)$$

$$u_{l,o \text{ CH}_4\text{-H}_2} (\Phi=1.0, h \leq 40\%; T_{u,o}, P_o) \text{ [cm/s]} = 39.836 + 0.367 h \quad (175)$$

$$u_{l,o \text{ CH}_4\text{-H}_2} (\Phi=1.2, h \leq 40\%; T_{u,o}, P_o) \text{ [cm/s]} = 34.798 + 0.467 h \quad (176)$$

$$u_{l,o \text{ CH}_4\text{-H}_2} (\Phi=0.8, h > 40\%; T_{u,o}, P_o) \text{ [cm/s]} = 37.426 + 0.200 \text{ EXP}[h/15.41042] \quad (177)$$

$$u_{l,o \text{ CH}_4\text{-H}_2} (\Phi=1.0, h > 40\%; T_{u,o}, P_o) \text{ [cm/s]} = 49.842 + 0.812 \text{ EXP}[h/18.28432] \quad (178)$$

$$u_{l,o \text{ CH}_4\text{-H}_2} (\Phi=1.2, h > 40\%; T_{u,o}, P_o) \text{ [cm/s]} = 44.489 + 1.452 \text{ EXP}[h/19.47500] \quad (179)$$

In addition to these expressions proposed by Hu et al. 2009 [77], other expressions that escalate exponentially with the proportion of hydrogen are considered for laminar burning velocities of NG and CH₄ fuel-air mixtures with hydrogen blend, taking into account different effects and conditions.

7.2.1. Effects of equivalence ratio, temperature and dilution

In order to present correlations for CH₄-H₂-air flames over a broad range of hydrogen contents Haniff et al. 1989 [194] presented a burning velocity fourth order polynomial dependent on equivalence ratio and hydrogen content, in a range between $\Phi = [0.85, 1.2]$ and for hydrogen fractions up to $x_{H_2} = 0.372$ at atmospheric conditions.

Coppens et al. 2007 [129,142] and Hermanns et al. 2007,2010 [143,144,130] studied the characteristics of laminar flame air mixtures, by heat flux method at atmospheric pressure, and proposed correlations of the experimental data based on the empirical expression of Gülder 1984 [195] which, in spite of this, did not agree with their more precise measurements of laminar burning velocity of methane-air mixtures. Thus, correlations suitable also for fuel blends, as CH₄-H₂-air, were therefore proposed starting from measurements of laminar burning velocity of these heat flux data, that were comparable with data from Halter et al. 2005 [53] of spherical expanding flames at ambient conditions.

Coppens et al. 2007 [142] presented a relation which took into account the hydrogen content in volumetric percentage $h(\%)=100x_{H_2}$ in the fuel in order to explore and simulate the shift of the maximum burning velocity to higher equivalence ratios, in a range of $\Phi=[0.6, 1.5]$, with increasing hydrogen concentration up to $x_{H_2}=0.35$, at atmospheric condition $P_o=0.1$ MPa and temperature $T_{u,o}=298$ K.

$$u_{l,o \text{ CH}_4\text{-H}_2}(\Phi, h \leq 35\%; T_{u,o}, P_o) \text{ [cm/s]} \\ = (1 + 1.9153 h^{1.533}) 39.0542 \Phi^{-0.4333} \text{ EXP}[-6.0157 (\Phi - 0.0133 h - 1.1)^2] \quad (180)$$

Hermanns et al. 2007 [144] used the same form for a correlation to fit an independent set of experimental data for enriched methane-air burning velocity at standard conditions, in a range of $\Phi=[0.6, 1.5]$ for hydrogen content up to $x_{H_2}=0.4$, with similar but not exactly the same values of the coefficients.

$$u_{l,o \text{ CH}_4\text{-H}_2}(\Phi, h \leq 40\%; T_{u,o}, P_o) \text{ [cm/s]} \\ = (1 + 1.7395 h^{1.3694}) 38.9542 \Phi^{-0.7411} \text{ EXP}[-6.2401 (\Phi - 0.0126 h - 1.106)^2] \quad (181)$$

Later, Hermanns et al. 2010 [130] used another expression of the same form, where the burning velocity at reference conditions is part of a more complex function of a more general burning velocity, for a domain of equivalence ratio $\Phi=[0.7, 1.4]$ and hydrogen content $x_{H_2}=[0, 0.4]$ in hybrid fuel with CH₄, with initial temperatures range $T_u=[298, 418]$. This expressions was applied to different proportions of mixture dilution with nitrogen, varying the relative amount of oxygen in air, in an interval $x_{O_2}=[0.21, 0.16]$, i.e. $x_{N_2}=[0.79, 0.84]$, in addition to the case of normal air with fractions $x_{O_2}=0.21$, $x_{N_2}=0.79$.

$$u_{l \text{ CH}_4\text{-H}_2}(\Phi, h \leq 40\%, x_{O_2}; T_u, P_o) \text{ [cm/s]} \\ = \{1 - (10.7787 - 15.2661 \Phi + 6.9656 \Phi^2) [1 - (x_{O_2}/0.21)]\} \cdot (T_u/T_o)^\alpha \cdot u_{l,o \text{ CH}_4\text{-H}_2}(\Phi, h; T_{u,o}, P_o) \quad (182)$$

$$\text{where } u_{l,o \text{ CH}_4\text{-H}_2}(\Phi, h; T_{u,o}, P_o) \text{ [cm/s]} \\ = (1 + 1.0034 h^{1.358}) 48.8082 \Phi^{-2.187} \text{ EXP}[-6.7619 (\Phi - 0.0002 h - 1.2103)^2] \quad (183)$$

$$\text{and } \alpha(\Phi, h) = 9.1105 - 14.8013 \Phi + 7.2796 \Phi^2 - 0.0028 h \quad (184)$$

This empirical expression was not able to represent the non-linear increase of the burning velocity for hydrogen contents higher than $x_{H_2}=0.4$, as was concluded by the same authors. Moreover, it must not be used for very slow flames having burning velocity below 10 cm/s. The values of the temperature exponent α show a small dependence on the hydrogen content in the fuel. The values of the coefficients for the reference burning velocity varied due to the increasing

amount of them for the more extensive conditions. Nevertheless, these were also limited at atmospheric pressure and thereby without consideration in this formulation of pressure dependence. This correlation has been extended for higher pressures in a more recent work of Bougrine et al. 2011 [172] who have developed a more sophisticated formula that will be explained in section 7.6.

Otherwise, a burning velocity correlation was fitted by Tinaut et al. 2011 [79], also with dependence of the temperature, from constant volume combustion bomb experiments for lean flames of NG-H₂ blends, for fixed equivalence ratio $\Phi=0.8$ and $x_{H_2}=[0, 0.15]$, as small hydrogen contents in hybrid fuel with NG, and with data belonging to an adiabatic curve starting at the ambient conditions of pressure and temperature.

$$u_{q|NG-H_2}(\Phi=0.8, h \leq 15\%; T_u, P_{ad}) \text{ [cm/s]} = (22.7 + 0.2866 h) \cdot (T_u/T_o)^{(1.02 + 0.00293 h)} \quad (185)$$

$$\text{where } P_{ad} = P_o (T_u/T_o)^{[\gamma/(\gamma-1)]} \quad \text{with } \gamma = (c_p/c_v) \quad (186)$$

The temperature exponent of this correlation was linearly dependent, with low increment, on the H₂ percentage $h(\text{vol}\%)=100x_{H_2}$; its range of variation was very small. The pre-potential factor also increased linearly. Thus, the H₂ content increased the burning velocity of NG.

7.2.2. Concept of dimensionless laminar burning velocity increment

Based on experimental data, Huang et al. 2006 [6], fitted a correlation of the un-stretched laminar burning velocity of NG-air mixtures in spherical expanding premixed flames as function of equivalence ratio, in a range $\Phi=[0.6, 1.4]$, for ambient conditions, at a reference initial temperature $T_{u,o}=300 \text{ K}$ and pressure $P_o=0.1 \text{ MPa}$.

$$u_{l,o \text{ NG}}(\Phi, h=0\%; T_{u,o}, P_o) \text{ [cm/s]} = -1.2924 - 96.327 \Phi + 287.6 \Phi^2 - 150.84 \Phi^3 \quad (187)$$

They also fitted another experimental correlation of the un-stretched laminar burning velocity as a function of equivalence ratio for the laminar burning velocity of H₂-air mixtures in spherical expanding premixed flames, in the same ranges and analogous conditions.

$$u_{l,o \text{ H}_2}(\Phi, h=100\%; T_{u,o}, P_o) \text{ [cm/s]} = -267.07 + 835.14 \Phi - 394.46 \Phi^2 + 51.902 \Phi^3 \quad (188)$$

Thus, Huang et al. 2006 [6] studied the laminar flames of air mixtures in a constant volume bomb and proposed an expression showing that the burning velocities increase with the addition of H₂ to NG, according with their experimental results. The provided empirical function, fitted at atmospheric conditions, included the two respective third order polynomial fits (eqs. 187&188) for the pure fuels burning velocities, as parts for pure CH₄-air and pure H₂-air mixtures, respectively, and used the concept of dimensionless increment of laminar burning velocity for NG (CH₄) and H₂ blends, with range $\Delta_{\Delta} u_{L,o \text{ H}_2\text{-NG}}=[0, 1]$. The correlation was an exponential function, which describes the increase in the mixture burning velocity as a function of the hydrogen content in a complete range of application $h(\%)=[0, 100]$.

$$\Delta_{\Delta} u_{L,o \text{ H}_2\text{-NG}}(\Phi, h; T_{u,o}, P_o) = 0.00334 + 0.00737 \text{ EXP}[h/20.38] \quad (189)$$

where

$$\Delta_{\Delta} u_{L,o \text{ H}_2\text{-NG}}(\Phi, h; T_{u,o}, P_o) = [\Delta u_{L,o \text{ H}_2\text{-NG,CH}_4}(\Phi, h; T_{u,o}, P_o) / \Delta u_{L,o \text{ H}_2\text{-CH}_4}(\Phi; T_{u,o}, P_o)] \quad (190)$$

$$\text{with } \Delta u_{L,0 \text{ H}_2\text{-NG_CH}_4}(\Phi, h; T_{u,o}, P_o) = [u_{L,0 \text{ H}_2\text{-NG}}(\Phi, h; T_{u,o}, P_o) - u_{L,0 \text{ CH}_4}(\Phi; T_{u,o}, P_o)] \quad (191)$$

$$\text{and } \Delta u_{L,0 \text{ H}_2\text{_CH}_4}(\Phi; T_{u,o}, P_o) = [u_{L,0 \text{ H}_2}(\Phi; T_{u,o}, P_o) - u_{L,0 \text{ CH}_4}(\Phi; T_{u,o}, P_o)] \quad (192)$$

Fig. 45 illustrates the dimensionless increments of laminar burning velocity increasing exponentially with the increase of H₂ fraction in NG blends with reference to methane. Little variations in the increments were observed among the various equivalence ratios $\Phi=\{0.6, 0.7, 0.8, 0.9, 1, 1.1, 1.2, 1.3, 1.4\}$ for every fixed fraction of H₂, considering as quite small the influence of equivalence ratio on this so-defined dimensionless increment of un-stretched laminar burning velocity for these types of fuel blends in air mixtures.

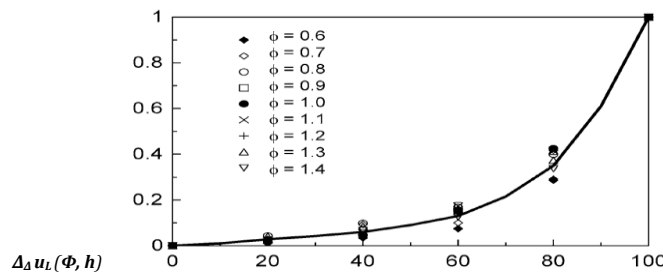


Fig. 45. Dimensionless increment of laminar burning velocity in air mixtures of NG-H₂ fuel blend versus H₂ mole fraction percentage $h(\text{vol}\%)=100x_{\text{H}_2}$; $T_u(K)=300$, $P(\text{MPa})=0.1$ (adapted from Huang et al. 2006 [6] and Ma et al. 2008 [86])

In order to verify the accuracy of the exponential formula, calculated data derived from its application were compared by Ma et al. 2008 [86] with experimental data for equivalence ratios $\Phi=\{0.6, 0.7, 0.8, 0.9, 1, 1.1, 1.2, 1.3, 1.4\}$ and H₂ fractions $x_{\text{H}_2}=\{0.1, 0.2, 0.3, 0.4, 0.5, 0.6, 0.8\}$. The experimental data of laminar burning velocity agreed quite well with the calculated values at low H₂ fractions in an interval $x_{\text{H}_2}=[0, 0.3]$ and for high H₂ contents in a range $x_{\text{H}_2}=[0.6, 1]$. However for medium fractions $x_{\text{H}_2}=(0.3, 0.6)$ the errors were relatively higher (greater than 15%). Thus, Ma et al. 2008 [86] concluded that the accuracy of the exponential formula was high only at low H₂ fractions for $x_{\text{H}_2}=(0, 0.3]$, and especially in the interval where the relative estimated error was lower (less than 8%) for $x_{\text{H}_2}=[0.2, 0.3]$, that is a H₂ fraction range commonly used in hydrogen enriched compressed natural gas (HCNG) engines. This was considered for all values of equivalence ratio but, in spite of that, actually this was specified only valid within a range of $\Phi=[0.6, 1.3]$ because significant errors are incurred for rich mixtures when $\Phi>1.3$. This range has the advantage of being an interval commonly used in HCNG engines, as well.

Although this exponential formula was derived by Huang et al. 2006 [6] from data measured close to atmospheric conditions, Ma et al. 2008 [86] pointed out that it could still be used at more elevated pressure and temperature, because the pressure data predicted with their engine model and using this expression agreed quite well with the experimental data.

$$\begin{aligned} & [u_{L \text{ H}_2\text{-NG or H}_2\text{-CH}_4}(\Phi, h<30\%; T_w, P) - u_{L \text{ CH}_4}(\Phi; T_w, P)] \\ & = [u_{L \text{ H}_2}(\Phi; T_w, P) - u_{L \text{ CH}_4}(\Phi; T_w, P)] \cdot \{0.00334 + 0.00737 \text{ EXP}[h/20.38]\} \end{aligned} \quad (193)$$

Perini et al. 2010 [196] also applied this expression for low values of H₂ content $x_{\text{H}_2}<0.3$, where this is considered of reasonable accuracy, in their combustion model at SIE-like conditions for fuel blends with CH₄.

7.3. Expressions for laminar burning velocities of hydrogen and methane blends based on linear mixing rules

As a simple approach, the expression proposed in the work of Di-Sarli&Di-Benedetto 2007 [160] can be cited. These authors compared their calculated values for H₂-CH₄ air mixtures from the used theoretical one-dimensional premixed flame code with the linear combination, by molar fraction averaging, of the laminar burning velocities of the pure fuel components evaluated at the same equivalence ratio of the hybrid fuel.

$$100 u_{L, H_2-CH_4}(\Phi, h) = [h \cdot u_{L, H_2}(\Phi) + (100-h) \cdot u_{L, CH_4}(\Phi)] \quad (194)$$

The computed values of the mixture laminar burning velocity were always well below those obtained by averaging the respective velocities of the constituent fuel gases in molar proportions. This implies the presence of the strong non-linear effects in chemical kinetics that emphasize the weight of the more slowly reacting methane in the fuel blend combustion.

7.3.1. Non-linear behavior of laminar burning velocities of hydrogen and methane blends

Previous results of El-Sherif 2000 [38] and subsequent results of Hu et al. 2009 [75,77] also showed that, in fact, the values of laminar burning velocities for blends were smaller than those obtained by averaging the laminar burning velocities of the pure fuels according with their molar proportions. El-Sherif found that in lean mixtures the H₂ addition enhanced the CH₄ reactivity slightly, while a strong inhibiting effect of the H₂ substitution by CH₄ was observed at rich conditions. These findings were attributed to changes on both, the H radical concentration and the reactions involving such atoms.

Table 21

Laminar burning velocity trends in different regimes of fuel-air mixtures of H₂-CH₄ blends (adapted from ^aDi-Sarli&Di-Benedetto 2007 [160], ^bHu et al. 2009 [75], ^cHu et al. 2009 [77])

Regime of combustion	H ₂ content	H ₂ mole fraction in the fuel blend x_{H_2}	Laminar burning velocity of the fuel blend $u_{L,F}$
CH ₄ combustion, dominated by CH ₄	Low	^a (0, 0.5) ^b (0, 0.6) ^c (0, 0.4)	Slight linear increase of u_{L,CH_4-H_2} on adding H ₂ in the fuel blend (enhancement especially slight with lean mixtures)
Transition regimes	Medium-high	^a [0.5, 0.9] ^b [0.6, 0.8] ^c [0.4, ~0.8*]	Strongly non-linear (exponential) evolution (complex kinetics behaviors)
H ₂ combustion, restrained by CH ₄	High	^a (0.9, 1) ^b (0.8, 1) ^c (~0.8*, 1)	Sharp linear decrease of u_{L,H_2-CH_4} on adding CH ₄ in the fuel blend (significant decrease stronger at rich conditions)

(* Approximation according to the representations in ^cHu et al. 2009 [77] and related to ^bHu et al. 2009 [75])

7.3.2. Regimes of laminar burning velocities of hydrogen and methane blends

Di-Sarli&Di-Benedetto 2007 [160] identified three regimes in the H₂-CH₄ air mixture flame propagation at atmospheric conditions, at all equivalence ratios (Φ) but depending on the H₂ mole fraction in the fuel blend (x_{H_2}). The two linear trends (of laminar burning velocity with the H₂ molar content in the fuel blend) found in both extreme regimes have been widely recognized in the literature (table 21 and fig. 46). The first $0 < x_{H_2} < 0.5$ and the third $0.9 < x_{H_2} < 1$ regimes are characterized by a linear increase of the laminar burning velocity. These linear evolutions were attributed in the first case to the promoting effect of hydrogen addition in methane and in the

last case to an inhibiting effect due to the addition of methane to hydrogen. In the intermediate regime ($0.5 < x_{H_2} < 0.9$) the evolution is strongly non-linear reflecting complex kinetics behaviors.

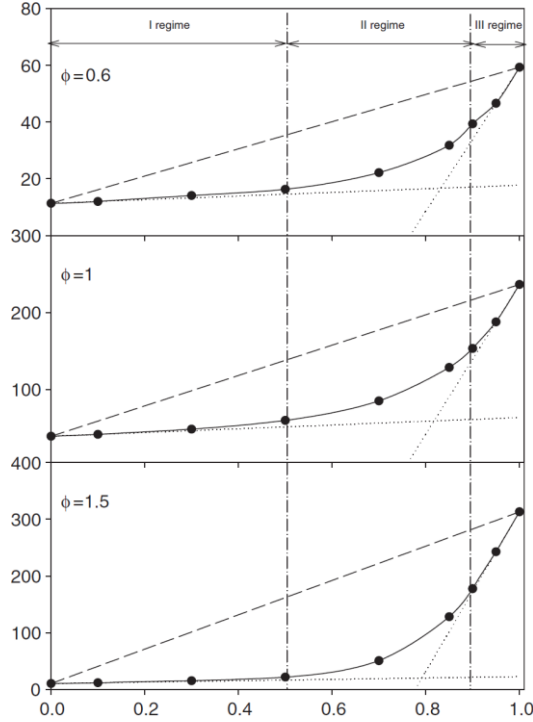


Fig. 46. Laminar burning velocities of fuel blend air mixtures versus the molar hydrogen fraction at atmospheric conditions $u_{L, H_2-CH_4}(\Phi, x_{H_2})$ [cm/s] for $\Phi = \{0.6, 1, 1.5\}$ (taken from Di-Sarli&Di-Benedetto 2007 [160])

Hu et al. 2009 [75] also identified analogous three regimes (table 21) in the H_2 - CH_4 air mixture flame propagation, at room temperature and atmospheric pressure, depending on the H_2 mole fraction in the fuel blend (x_{H_2}). In this study the characterized regimes by the linear increase of the laminar burning velocity are the first in a range $0 < x_{H_2} < 0.6$ and the third in a range $0.8 < x_{H_2} < 1$. In the range of the intermediate regime, $0.6 < x_{H_2} < 0.8$, the evolution is regarded as exponential. In the already referred numerical study by Hu et al. 2009 [77], they distinguished only when hydrogen fractions were respectively less or larger than $x_{H_2} = 0.4$.

Table 22

Relevant reactions involving H atoms for fuel air mixtures of H_2 - CH_4 blends; $T_i = 300$ K, $P = 0.1$ MPa, $\Phi = 1$ (adapted from Bougrine et al. 2011 [172])

H ₂ mole fraction in fuel blend x_{H_2}	Null 0	Medium 0.5	High 0.9	Reaction types
Main elementary reaction steps	H+O ₂ ↔O+OH	H+O ₂ ↔O+OH	H+O ₂ ↔O+OH	Chain branching (r_w) (r_p) (r_a)
	OH+CO↔CO ₂ +H	OH+CO↔CO ₂ +H	OH+CO↔CO ₂ +H	
	HCO+H ₂ O↔H ₂ O+CO+H	HCO+H ₂ O↔H ₂ O+CO+H (OH+H ₂ ↔H ₂ O+H)	(HCO+H ₂ O↔H ₂ O+CO+H) OH+H ₂ ↔H ₂ O+H	
	-	-	H+HO ₂ ↔2 OH	Termination (r_b) (r_c)
	-	-	O+H ₂ ↔OH+H	
	H+CH ₃ +M↔CH ₄ +M	H+CH ₃ +M↔CH ₄ +M	H+CH ₃ +M↔CH ₄ +M	
	H+O ₂ +H ₂ O↔H ₂ O+HO ₂	H+O ₂ +H ₂ O↔H ₂ O+HO ₂	H+O ₂ +H ₂ O↔H ₂ O+HO ₂	
	(H+OH+M↔H ₂ O+M)	(H+OH+M↔H ₂ O+M)	H+OH+M↔H ₂ O+M	
	OH+CH ₄ ↔H ₂ O+CH ₃	-	-	
	-	-	-	

A detailed study of the H₂ addition effect on the combustion was also achieved by Bougrine et al. 2011 [172] to evaluate the main chemical processes (table 22) governing the production of H atoms, as crucial contribution to the laminar flame velocity, and so to understand these three different regimes in the methane-hydrogen flames propagation and to explain the non-linear evolution of the laminar flame velocity.

7.4. The role of radicals in the premixed flame reaction zone and interaction on laminar burning velocities

Hu et al. 2009 [75,77] inferred that the enhancement of chemical reaction with H₂ addition was due to the increase of mole fractions of radicals H, O and OH in the flame as H₂ was added, with an existing strong correlation between burning velocity and maximum H and OH radical concentrations in the reaction zone of premixed flames, as observed by Padley&Sugden 1958 [197] and Butler&Hayhurst 1998 [198]. Moreover, Hu et al. 2009 [75,77] inferred more widely that suppression (or enhancement) of overall chemical reaction with the increase of initial pressure (or respectively temperature and hydrogen fraction) was due to the decrease (or respectively increase) of H, O and OH mole fractions in the flames. High burning velocities corresponded to high radical concentrations in the reaction zone.

Concentrations of some intermediate radicals in methane-hydrogen flames were measured (e.g. by the laser induced fluorescence, Choudhuri&Gollahalli 2000 [199], and the planar laser induced fluorescence spectroscopy, Katoh et al. 2006 [200]) and the studies showed that the concentration of OH increased with the increase of H₂ fraction which is beneficial to improve the burning velocity and reduce emissions, Naha et al. 2005 [201].

7.4.1. Radicals for combustion of hydrogen-methane fuel-air mixtures

From the experimental and numerical studies of methane-hydrogen fuel blends that have been conducted in the literature on laminar burning velocity measurement, intermediate species measurement and chemical kinetics simulation, it is well known that the high burning velocity of H₂-air premixed flames are due to the occurrence of fast exothermic reactions in the low temperature flame regions that require H atoms produced by diffusion from the flame front according to the propagation mechanism of such flames, Kuniishi&Fukutani 1992 [202]. In contrast, CH₄-air premixed flames propagate thanks to the thermal energy transported by conduction from the high to the low temperature regions, hence having much lower flame speeds, Gaydon&Wolfhard 1979 [203].

Bougrine et al. 2011 [172] carried out an abridged sensitivity analysis for laminar burning velocity of stoichiometric methane-hydrogen-air flames, based on normalized sensitivity coefficients (about each reaction rate associated to every considered sensitive reaction step). They compared the mechanisms GRI-Mech 3.0 [170] and Konnov-Mech 0.5 [175] and confirmed that the most sensitive reactions involve H atoms (table 22). Both chemical schemes appeared to show similar behaviors with respect to the addition of H₂ in the fuel blends for stoichiometric and atmospheric operating conditions $T_u(K)=300$, $P(bar)=1$, $\Phi=1$, $x_{H_2}=\{0, 0.5, 0.9\}$. For example, the maximum values of the flame speed sensitivity, with respect to the rate constant of the reaction (r_w) $H+O_2\leftrightarrow O+OH$, were obtained for $x_{H_2}=0.5$ according to both schemes, even though the importance of this reaction seemed to be a bit higher for the GRI-Mech.

Table 23Main elementary reaction steps of fuel air mixtures of **H₂-CH₄** binary blends at atmospheric conditions

H ₂ mole fraction in fuel blend x_{H_2}	H ₂ content	Combustion regime	Stoichiometry Φ	Main elementary reaction steps	Related references
(0, 0.5-0.6)	Low	CH ₄ conversion, dominated by CH ₄ (promotion effect by H ₂ addition)	Independently from stoichiometry	Dominated by step $H+O_2 \leftrightarrow O+OH$, with CH ₄ burning rate high sensitivity (and of general relevance in HC combustions)	[132] 1988 Sher&Refael [133] 1989 Refael&Sher [204] 1999 Warnatz et al. [38] 2000 El Sherif [140] 2001 Ren et al. [205] 2005 Dagaut&Nicolle [206] 2006 Dagaut&Dayma [160] 2007 Di-Sarli&Di-Benedetto [75,78] 2009 Hu et al.
			Lean CH ₄ -air flame $\Phi < 1$ with small H ₂ addition	CH ₄ main consumption via step $OH+CH_4 \leftrightarrow CH_3+H_2O$	[140] 2001 Ren et al. [205] 2005 Dagaut&Nicolle [160] 2007 Di-Sarli&Di-Benedetto [78] 2009 Hu et al.
[0.5-0.6, 0.8-0.9]	Inter-mediate	Transition		(Step $H+O_2 \leftrightarrow O+OH$ with decreased sensitivity factors and comparable or lesser values than those corresponding to other steps)	[160] 2007 Di-Sarli&Di-Benedetto
			Starting from $x_{H_2}=0.7-0.85$ and at all Φ	Non-main role of step $H+O_2 \leftrightarrow O+OH$ in controlling CH ₄ combustion	
(0.8-0.9, 1)	High	H ₂ combustion, restrained by CH ₄ (inhibition effect by CH ₄ addition)		H radicals consumption by steps $H+CH_4 \leftrightarrow CH_3+H_2$ $H+CH_3+(M) \leftrightarrow CH_4+(M)$	[160] 2007 Di-Sarli&Di-Benedetto [75] 2009 Hu et al.
				The bigger sensitivity of CH ₄ conversion at rich conditions and high H ₂ contents to these previous steps (compared to that of stoichiometric and lean flames to steps $H+CH_4 \leftrightarrow CH_3+H_2$ / $OH+CH_4 \leftrightarrow CH_3+H_2O$) enhances the inhibition of the blend combustion by H ₂ substitution with CH ₄ on increasing the equivalence ratio.	
				The lower presence of O ₂ in the rich flames compared to stoichiometric and lean conditions allows the formed CH ₃ radicals accelerating the step $H+CH_3+(M) \leftrightarrow CH_4+(M)$ with respect the oxidation reactions. This determines the more significant decrease of the u_L of rich mixtures.	
			Rich flames $\Phi > 1$	Kinetically dominated by step $H+CH_4 \leftrightarrow CH_3+H_2$ (CH ₃ radicals produced by this step)	
	Stoichiometric flames $\Phi = 1$	Kinetically dominated by step $H+CH_4 \leftrightarrow CH_3+H_2$ (CH ₃ radicals produced by this step and the step $OH+CH_4 \leftrightarrow CH_3+H_2O$)			
	Lean combustion $\Phi < 1$	Kinetically dominated by step $OH+CH_4 \leftrightarrow CH_3+H_2O$ (CH ₃ radicals produced by this step)			

Di-Sarli&Di-Benedetto 2007 [160] performed a wide sensitivity analysis, based on methane mole fraction normalized sensitivity factors, in order to find out the role of radicals interactions in the observed behaviors of combined H₂-CH₄ fuel air-premixed flames. The analysis evaluated the main contributions to kinetic control of elementary reaction steps (tables 23&24.A) affecting the combustion of the blends, at atmospheric conditions $T_u(K)=300$, $P(atm)=1$, for $\Phi=\{0.6, 1, 1.5\}$ and $x_{H_2}=\{0, 0.3, 0.5, 0.7, 0.85, 0.9, 0.95\}$ respectively. Their findings were aimed to the amount of H radicals and their fate through the chain branching and termination reaction steps.

Other sensitivity analysis, also based on methane mole fraction normalized sensitivity factors, in order to deepen in the understanding about the effect of reactions in the system of H₂-CH₄ fuel air-premixed flames, was performed by Hu et al. 2009 [75] evaluating the main contributions to kinetic control of elementary reaction steps (table 24.B) affecting the combustion of the blends, at atmospheric conditions $T_u(K)=303$, $P(MPa)=0.1$, for $\Phi=\{0.8, 1, 1.2\}$ and $x_{H_2}=\{0, 0.1, 0.2, 0.3, 0.4, 0.5, 0.6, 0.7, 0.8, 0.9, 1\}$ respectively. Their findings were aimed to the amounts of H and OH radicals and their share through the chain branching and termination reaction steps. The main consumption reactions of CH₄ in the flame were reaction steps led by H, O and OH to form CH₃. However, the different main elementary reaction steps were not simultaneously involved in the same way at all equivalence ratios, with different kinetic control contributions (table 23).

The predictions in the mentioned numerical study of Hu et al. 2009 [77] showed unstretched laminar burning velocities and peak mole fractions of H+OH radicals for the different hydrogen fractions at three different equivalence ratios $\Phi=\{0.8, 1, 1.2\}$, for $T_{u,o}(K)=303$ and $P_o(MPa)=0.1$. Enhancement of chemical reaction with hydrogen addition resulted from the increase of H, O and OH radical concentrations in the flame as hydrogen was added. Laminar burning velocity was increased with the increase of peak H+OH mole fraction $(x_{[H]}+x_{[OH]})_{max}$ in the reaction zone and strong linear-fit correlations between both were obtained and stated by the following expressions:

$$u_{l,o \text{ CH}_4\text{-H}_2} (\Phi=0.8; x_{[H]}, x_{[OH]}; T_{u,o}, P_o) \text{ [cm/s]} = -16.786 + 5365.323 (x_{[H]} + x_{[OH]})_{max} \quad (195)$$

$$u_{l,o \text{ CH}_4\text{-H}_2} (\Phi=1.0; x_{[H]}, x_{[OH]}; T_{u,o}, P_o) \text{ [cm/s]} = -26.365 + 4821.428 (x_{[H]} + x_{[OH]})_{max} \quad (196)$$

$$u_{l,o \text{ CH}_4\text{-H}_2} (\Phi=1.2; x_{[H]}, x_{[OH]}; T_{u,o}, P_o) \text{ [cm/s]} = -24.373 + 4485.874 (x_{[H]} + x_{[OH]})_{max} \quad (197)$$

The detailed flame structures from predictions were studied by Hu et al. 2009 [77] to gain a better insight on the effect of hydrogen addition on laminar burning velocities. Flame structures of freely propagating methane-air flames with $h(\%)=\{0, 40, 80, 100\}$ of H₂ in the fuel blends for the stoichiometric mixtures with $\Phi=1$ were presented. The final burned gas temperature and the maximum values of H, O, OH radical mole concentration were plotted. Comparison of the temperature distributions showed that the final burnt-gas temperature was increased with the increase of hydrogen fraction. The results showed that for the stoichiometric methane-air flames, the radical OH had the largest maximum concentrations in the flames, with H having a somewhat smaller value in maximum concentration, roughly 10-30% lower than that of OH. Concentrations of O and CH₃ were less than half of OH concentration. However, for the hydrogen-air flames, the largest concentration was that of H radical. The maximum concentrations of H, O and OH in flames were increased with the increase of hydrogen fraction and this fomented the combustion of methane-air flames. The increase in maximum concentration of H and OH would lead to the corresponding increase of the laminar burning velocity of flames, as reported by Kwon&Faeth 2001 [207] about the increase of H peak concentration. For pure hydrogen-air flame and methane-hydrogen-air flame with hydrogen fraction of 80%, the increase of O₂ concentration near the cold boundary of the flame prior to O₂ decreasing approached the reaction zone of the flame. This reflected the dominating effect from the preferential diffusion of fast diffusing reactant H₂ compared to the slow-diffusing reactants CH₄ and O₂, Qiao et al. 2005 [208], resulting in a rapid reduction in H₂ concentration as the mixture approached the active reaction zone.

Table 24Main elementary reaction steps for different mixture conditions of **H₂-CH₄ blends****A.** For atmospheric conditions at temperature $T_u=300$ K and pressure $P=1$ atm (adapted from Di-Sarli&Di-Benedetto 2007 [160])

Mixture conditions	Lean	Stoichiometric	Rich	Reaction types
	$\Phi < 1$ (0.6)	$\Phi = 1$	$\Phi > 1$ (1.5)	
Main elementary reaction steps	H+O ₂ ↔O+OH	H+O ₂ ↔O+OH	H+O ₂ ↔O+OH	Chain branching (r_w)
	OH+CO↔CO ₂ +H	-	-	(r_p)
	OH+CH ₄ ↔H ₂ O+CH ₃	OH+CH ₄ ↔H ₂ O+CH ₃	-	Kinetic control
	-	H+CH ₄ ↔H ₂ +CH ₃	H+CH ₄ ↔H ₂ +CH ₃	"
	[^] H+CH ₃ + <i>(M)</i> ↔CH ₄ + <i>(M)</i>	[^] H+CH ₃ + <i>(M)</i> ↔CH ₄ + <i>(M)</i>	H+CH ₃ + <i>(M)</i> ↔CH ₄ + <i>(M)</i>	Termination (r_b)
	H+O ₂ +H ₂ O↔H ₂ O+HO ₂	-	-	(r_c)

{^} Moderate relevance only for low H₂ contents

B. For conditions at room temperature $T_u=303$ K and atmospheric pressure $P=1$ bar (adapted from Hu et al. 2009 [75])

Mixture conditions	Lean	Stoichiometric	Rich	Reaction types
	$\Phi < 1$ (0.8)	$\Phi = 1$	$\Phi > 1$ (1.2)	
Main elementary reaction steps	H+O ₂ ↔O+OH	H+O ₂ ↔O+OH	H+O ₂ ↔O+OH	Chain branching (r_w)
	OH+CO↔CO ₂ +H	OH+CO↔CO ₂ +H	-	(r_p)
	O+CH ₄ ↔OH+CH ₃	-	-	Kinetic control
	OH+CH ₄ ↔H ₂ O+CH ₃	OH+CH ₄ ↔H ₂ O+CH ₃	-	"
	H+CH ₄ ↔H ₂ +CH ₃	H+CH ₄ ↔H ₂ +CH ₃	H+CH ₄ ↔H ₂ +CH ₃	"
	[^] H+CH ₃ + <i>(M)</i> ↔CH ₄ + <i>(M)</i>	[^] H+CH ₃ + <i>(M)</i> ↔CH ₄ + <i>(M)</i>	H+CH ₃ + <i>(M)</i> ↔CH ₄ + <i>(M)</i>	Termination (r_b)
	H+O ₂ +H ₂ O↔H ₂ O+HO ₂	-	-	(r_c)

{^} Moderate relevance only for low H₂ contents

C. For lean conditions of $\Phi=0.8$ at temperature $T_u=373$ K and pressure $P=5$ bar (adapted from Hu et al. 2009 [78])

Mixture condition	Lean	Reaction types
	$\Phi < 1$ (0.8)	
Main elementary reaction steps	H+O ₂ ↔O+OH	Chain branching (r_w)
	OH+CO↔CO ₂ +H	(r_p)
		Kinetic control
		"
	HO ₂ +CH ₃ ↔OH+CH ₃ O	(r_q)
	OH+CH ₃ ↔H ₂ O+CH ₂ (S)	
	^{^^} HCO+H ₂ O↔H ₂ O+CO+H	
	[^] H+CH ₃ + <i>(M)</i> ↔CH ₄ + <i>(M)</i>	Termination (r_b)
	H+O ₂ +H ₂ O↔H ₂ O+HO ₂	(r_c)
		^{^^} HCO+O ₂ ↔HO ₂ +CO

{^} Moderate relevance only for low H₂ contents, {^^} Very moderate relevance only for low H₂ contents

Another type of sensitivity analysis based on temperature of H₂-CH₄ fuel air-premixed lean flames was performed by Hu et al. 2009 [78] evaluating the main contributions to kinetic control of elementary reaction steps affecting the combustion of the blends at initial conditions $T_u(K)=373$ and $P(MPa)=0.5$, for $\Phi=0.8$ and $x_{H_2}=\{0, 0.2, 0.4, 0.6, 0.8\}$. It was found that the main reactions of hydrocarbon and hydrogen combustion were chain developing or branching and recombination reactions led by H and OH, CO formation reactions in the path of HCO, and CO₂ formation reaction by CO oxidation. The results showed the chain developing and branching reactions that exhibit large positive and negative sensitivities (table 24.C). Laminar burning velocity reflected the competition between the main chain branching reactions and chain recombination reactions. With the increase of initial pressure, the increase rate of recombination reaction is much higher than that of branching reaction, and this induces the reduction of active radicals and reduces the burning velocity. With the increase of initial temperature, the increase rate of branching reaction is larger than that of recombination reaction, and this increases the concentrations of highly reactive radical species and lead to the increase of burning velocity. The chain branching reactions were the temperature-sensitive, two-body reactions, and the recombination reactions were the temperature-insensitive, three-body reactions. The branching reaction and recombination reaction can be enhanced relative to each other by increasing the flame temperature and system pressure, respectively.

The particular flame structures of lean premixed methane-hydrogen-air flame were also calculated in the work of Hu et al. 2009 [78]. They showed the concentration profiles of radical species (H, O and OH) and the maximum values of their mole fractions at different initial conditions $T_u(K)=\{303, 373, 443\}$ and $P(MPa)=\{0.1, 0.25, 0.5, 0.75\}$ for $\Phi=0.8$ and $x_{H_2}=\{0, 0.2, 0.4, 0.6, 0.8\}$. The results showed that in the lean methane-hydrogen-air flame also the radical OH had the largest peak concentrations in the flames, and the concentrations of H and O radicals had roughly 10-30% lower than that of OH in peak concentration. With the increase of initial pressure, the mole fractions of H, O and OH radicals were decreased, while these fractions were increased with the increase of initial temperature. This could be explained as, with the increase of pressure, the chain-recombination-reaction rate would increase more quickly than the chain-branching-reaction rate, and the combined result was the reduction of active radical and the suppression of combustion. Increasing initial temperature would give more increase in the chain-branching-reaction rate than in the chain-recombination-reaction rate, and this produced more radicals that are active and promoted the combustion. They could find that with the increase of hydrogen fraction, the mole fractions of active radicals were also increased. The increase (or decrease) of peak concentration of H and OH would lead a corresponding increase (or decrease) of laminar burning velocity. The results in this study were so consistent with other previous in the literature. They also give the maximum values of H, O and OH radicals at different initial pressures, temperatures and hydrogen fractions. The results showed that the variation trends of maximum mole fractions of H, OH radicals versus initial pressure, temperature and hydrogen fraction were similar to that of laminar burning velocities versus initial pressure, temperature and hydrogen fraction. Thus, they regarded in this study that the analysis of chain mechanism could be validated by this behavior.

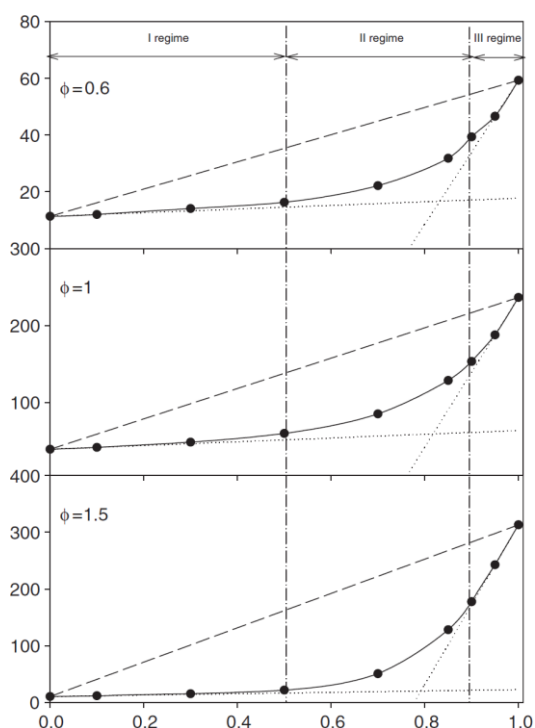


Fig. 46. Laminar burning velocities of fuel blend air mixtures versus the molar hydrogen fraction at atmospheric conditions $u_{L, H_2-CH_4}(\Phi, x_{H_2})$ [cm/s] for $\Phi=\{0.6, 1, 1.5\}$

Fig. 46, from 7.3.2, is repeated here to facilitate a joint comparison (Both figs. 46 & 47 taken from Di-Sarli&Di-Benedetto 2007 [160])

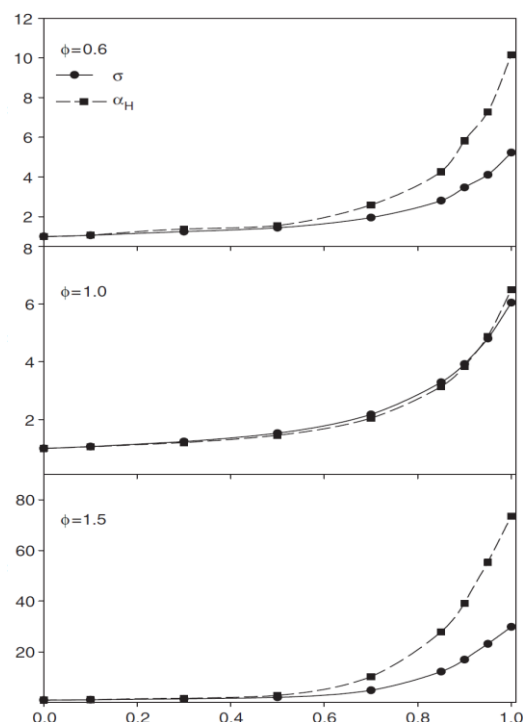


Fig. 47. Normalized burning velocity and radical concentration

Normalized laminar burning velocities of fuel blend $\sigma(\Phi, x_{H_2}) = u_{L, H_2-CH_4}(\Phi, x_{H_2}) / u_{L, CH_4}(\Phi)$
 Normalized maximum H radical (mole fraction) concentration $\alpha_H(\Phi, x_{H_2}) = X_{[H]}^{\max}(H_2-CH_4) / X_{[H]}^{\max}(CH_4)$

Di-Sarli&Di-Benedetto 2007 [160] observed higher differences at rich rather than at lean conditions, considering the laminar burning velocity values of the H₂-CH₄ fuel blend in air mixture normalized (σ) with the corresponding values for pure methane-air flame, in comparison to the normalized maximum concentration (α_H) of H radicals (in mole fractions $X_{[H]max}$) in the reaction zone (eqs. 198&199) as a function of the hydrogen content x_{H_2} (fig. 47) at three values of equivalence ratio Φ .

$$\sigma_{[(H_2-CH_4)/CH_4]}(\Phi, x_{H_2}) = [u_{L, H_2-CH_4}(\Phi, x_{H_2}) / u_{L, CH_4}(\Phi)] \quad (198)$$

$$\alpha_{H, [(H_2-CH_4)/CH_4]} = [X_{[H]max(H_2-CH_4)} / X_{[H]max(CH_4)}] \quad (199)$$

The increase of the laminar burning velocity of hydrogen blends compared to pure methane flames (σ) was obtained by them as equal to that of the H radicals concentration increase (α_H) only at stoichiometric conditions, whatever the H₂ content in the mixture; on the contrary, it was shown to be lower for non-stoichiometric mixtures with hydrogen mole fraction values $x_{H_2} > 0.5$. This was explained by the fact that H radicals (table 24.A) also participate in the termination reactions (r_b) $H+CH_3+(M)\leftrightarrow CH_4+(M)$ and (r_c) $H+O_2+H_2O\leftrightarrow H_2O+HO_2$ that compete (respectively) for H atoms with the chain branching reaction (r_w) $H+O_2\leftrightarrow O+OH$ at lean and rich conditions. Thus, they showed that there is a particularly clear coupling between the burning velocity and the maximum concentration of H atom at stoichiometric conditions, which is a key radical in chain branching reactions.

The work of Di-Sarli&Di-Benedetto 2007 [160] suggested that, with respect to lean and rich flames, at stoichiometric conditions H atoms (table 24.A) are much more prone to consume CH₄ rather than to be involved in the termination reactions r_b and r_c , which decrease the global reactivity; that it is saying the relevant effect of termination reaction r_c on slowing down the methane oxidation for lean hydrogen-natural gas blends, Dagaut&Nicolle 2005 [205].

They also showed that, for the same composition, the H radical concentration is greater in the rich flames than in the lean flames. Then, a larger fraction of H atoms (table 24.A) can be lost by the termination reaction r_b at rich conditions compared to that participating in the termination reaction r_c at lean conditions.

Thus, in qualitative agreement with other literature results as El-Sherif 2000 [38], Di-Sarli&Di-Benedetto 2007 [160] considered that it appears that the addition of H₂ to CH₄ has a weaker promoting effect with lean mixtures, while the inhibiting effect of CH₄ addition on H₂ is stronger at rich conditions, relating these trends to the observed strong dependence on H radicals of the laminar burning velocity of the fuel blend. They could be explained considering that the corresponding variations of the concentration of H radicals are higher on increasing the equivalence ratio, either increasing or decreasing the hydrogen mole fraction in the fuel x_{H_2} starting from a fixed composition.

7.4.2. Radicals for combustion of hydrogen-natural gas fuel-air mixtures

In Bougrine et al. 2011 [172] the effects of fuel de-carbonization by H₂ addition on H radicals production from C₁-C₂ species were investigated using GRI-Mech 3.0 [170] in order to elucidate H₂ addition effects on flame propagation. Previously, several groups, Sabia et al. 2007 [209], De-Ferri eres et al. 2007 [210], working under very different operating conditions (jet stirred reactor versus premixed flame propagation), concluded that H₂ substitution to NG enhances the oxidation pathway (C₁ sequence). However, their results concerning the impact of H₂ on recombination (C₂) pathway could not be directly compared because they were relative to very different fuel compositions, CH₄ in [209] versus CH₄-C₂H₆-C₃H₈ blends in [210].

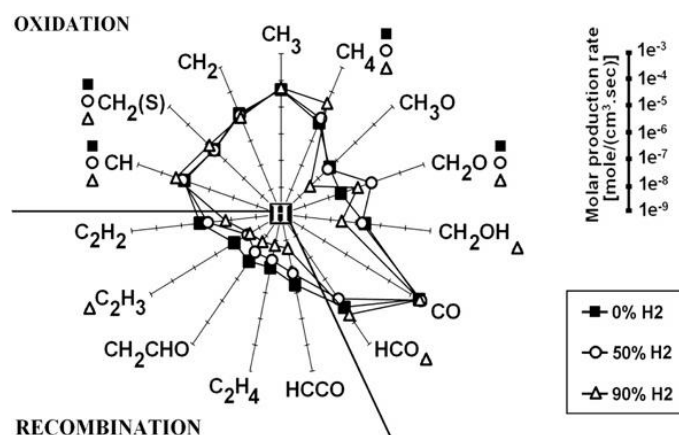


Fig. 48. Main H radical production/consumption rates according to several species at H peak concentration location. Species with symbols are relative to species inhibiting H production at the corresponding $x_{H_2}=\{0, 0.5, 0.9\}$, $\Phi=1$, $P(\text{MPa})=0.1$, $T_u(K)=300$ (taken from Bougrine et al. 2011 [172])

Bougrine et al. 2011 [172] considered the H radicals production or consumption rates from the most significant C_1 - C_2 species, in stoichiometric conditions, at the location of the maximum H concentration (fig. 48). As they noticed, the production or consumption of H radicals is mainly determined by C_1 species, which appear to contribute more and more to H production as x_{H_2} is increased. It is remarkable that H production rate from reactions involving CO is only slightly affected by H_2 addition, whereas some others pathways are strongly affected.

Their work [172] showed in particular the evolution of the molar production and consumption rates of H radicals for the most important C_1 reactions at stoichiometric and atmospheric conditions for the three considered hydrogen amounts $x_{H_2}=\{0, 0.5, 0.9\}$ in the fuel (table 22). Moreover, in order to numerically identify, respectively, the thermal and kinetic effects of H_2 addition, complementary calculations were carried out imposing the temperature profile as well as the inlet mass flow rate corresponding to $x_{H_2}=0.5$ while at the same time keeping the inlet composition of methane at $x_{H_2}=0$. It turned out that the complex evolution of the rate of reaction (r_q) $\text{HCO}+\text{H}_2\text{O}\leftrightarrow\text{H}_2\text{O}+\text{CO}+\text{H}$ could be attributed to a competition between thermal and chemical effects. It appeared that the promoting thermal effect was only partially compensated for by the chemical effect of increasing x_{H_2} from 0 to 0.5. As a result, the overall effect of H_2 addition on HCO profile was promoting, which resulted in an increase of the corresponding rate of reaction. In contrast, the extent of the chemical effect of H_2 addition on CO concentration profile became lower than that of its thermal effect, so that the global effect on CO concentration became reaction inhibiting. However, the rate of reaction (r_p) $\text{OH}+\text{CO}\leftrightarrow\text{CO}_2+\text{H}$ was still enhanced when increasing x_{H_2} from 0 to 0.5 due to the stronger impact of H_2 addition on OH concentration level. Concerning reaction (r_b) $\text{H}+\text{CH}_3(+M)\leftrightarrow\text{CH}_4(+M)$ consuming H radicals, the effect of H_2 addition on CH_3 species concentration appeared of minor importance compared to its leading promoting effect on H radical concentration.

Thus, these analyzes carried out by Bougrine et al. 2011 [172] in stoichiometric conditions and at atmospheric pressure contributed somehow to understand the nonlinear impact of H_2 addition on the laminar flame propagation as x_{H_2} is increased. Anyhow, they considered the nonlinear behavior through the regimes identified by Di-Sarli&Di-Benedetto 2007 [160] in order to develop a complete and sophisticated correlation of laminar burning velocity for methane-hydrogen-air flames, applicable in a large range of compositions and thermodynamic operating conditions, that will be reviewed in section 7.6.

7.5. Expressions for laminar burning velocities of fuel-air mixtures of hydrogen and methane/natural gas blends based on LeChatelier's rule-like formulas

Di-Sarli&Di-Benedetto 2007 [160] tested the feasibility of a LeChatelier's rule-like formula (based on the mole fractions x_i) to predict the laminar burning velocity of hydrogen-methane blends. Comparing the simulation results obtained with the detailed reaction scheme GRI-Mech 3.0 [170] with the values predicted by LeChatelier's rule, the corresponding expression had a good agreement, mainly for lean and stoichiometric conditions, but more significant differences for rich mixtures with high H_2 contents. With this limitation, the proposed formula was successfully applied to mixtures also at higher than atmospheric values, up to $P \leq 10 \text{ atm}$ of initial pressure and $T_u \leq 400 \text{ K}$ of temperature.

$$\begin{aligned}
 & [100 / u_{L,H_2-CH_4}(\Phi \leq 1, h; T_u \leq 400 \text{ K}, P \leq 10 \text{ atm})] \\
 & = [h / u_{L,H_2}(\Phi; T_w, P)] + [(100-h) / u_{L,CH_4}(\Phi; T_w, P)] \quad (200)
 \end{aligned}$$

7.5.1. Applicability of expressions based on LeChatelier's rule in function of equivalence ratio and hydrogen content

Thus, these predictions were considered good at lean and stoichiometric conditions in all regimes, whatever H_2 content, by Di-Sarli&Di-Benedetto 2007 [160]. This was estimated applicable also to rich mixtures in the so-called first regime, and in some extension for H_2 contents up to $h=70\%$, i.e. for $x_{H_2} \leq 0.7$.

$$\begin{aligned}
 & [100 / u_{L,H_2-CH_4}(\Phi, h \leq 70\%; T_u \leq 400 \text{ K}, P \leq 10 \text{ atm})] \\
 & = [h / u_{L,H_2}(\Phi; T_w, P)] + [(100-h) / u_{L,CH_4}(\Phi; T_w, P)] \quad (201)
 \end{aligned}$$

These considerations were given in consistency with the experimental findings of flammability limits for H_2-CH_4 mixtures, in the entire composition range of the hybrid fuel, given at atmospheric pressure by the works of Karim et al. 1985 [211], Wierzba et al. 1986 [212], Wierzba&Ale 2000 [213]. They also compared measured values with calculated simulations according to the LeChatelier's rule.

7.5.2. Applications of expressions based on LeChatelier's rule at engine-like conditions for spark-ignition engine models

Several works in the literature have used LeChatelier's rule-like formulas based on the mole fractions of fuel components, under similar considerations to Di-Sarli&Di-Benedetto 2007 [160], mostly in studies dedicated to simulation with combustion models for SIEs fueled by hydrogen enriched natural gas or methane blends, usually for lean air mixtures, e.g. Ma et al. 2008,2011,2012 [86,89,4] and Perini et al. 2010 [196].

Thus, in order to obtain a correlation of laminar burning velocity valid at intermediate and high hydrogen contents and at different equivalence ratios, Ma et al. 2008 [86] tested for H_2-NG blends the feasibility of a formula analogous to the expression of Di-Sarli&Di-Benedetto 2007 [160] for H_2-CH_4 blends.

$$\begin{aligned}
 & [100 / u_{L, H_2\text{-NG or } H_2\text{-CH}_4}(\Phi \leq 1, h > 30\%; T_w, P)] \\
 & = [h / u_{L, H_2}(\Phi; T_w, P)] + [(100-h) / u_{L, CH_4}(\Phi; T_w, P)]
 \end{aligned} \tag{202}$$

Data calculated by these expressions were compared by Ma et al. 2008 [86] with experimental data for equivalence ratios $\Phi = \{0.6, 0.7, 0.8, 0.9, 1, 1.1, 1.2, 1.3, 1.4\}$ and H_2 fractions $x_{H_2} = \{0.1, 0.2, 0.3, 0.4, 0.5, 0.8\}$. The experimental data of laminar burning velocity under lean and stoichiometric conditions agreed with the calculated values for all fractions of hydrogen content. However, for rich mixtures the differences between the so-calculated and experimental data were significant. These observations were in accordance with conclusions derived from the studies of Di-Sarli&Di-Benedetto 2007 [160] previously reviewed.

Thus, Ma et al. 2008 [86] concluded that the accuracy of the LeChatelier's rule-like formula for medium and high H_2 fractions, $x_{H_2} = [0.4, 0.8]$, was better than for low H_2 fractions. This was considered for all values of equivalence ratio but, in spite of that, actually this mixing rule was specified only valid within a range of $\Phi = [0.6, 1.3]$ because of significant errors are incurred for rich mixtures when $\Phi > 1.3$. As aforementioned, this range has the advantage of being an interval commonly used in HCNG engines.

$$\begin{aligned}
 & [100 / u_{L, H_2\text{-NG or } H_2\text{-CH}_4}(\Phi, 30 < h(\%) \leq 70; T_w, P)] \\
 & = [h / u_{L, H_2}(\Phi; T_w, P)] + [(100-h) / u_{L, CH_4}(\Phi; T_w, P)]
 \end{aligned} \tag{203}$$

Perini et al. 2010 [196] also applied this expression for medium and high values of H_2 content $x_{H_2} > 0.3$, where it is considered of reasonable accuracy, in their combustion model at SIE-like conditions, over a wide range of fuel blends with CH_4 , with the remark of that its reliability at outmost equivalence ratios should be further improved.

Nevertheless, Aliramezani et al. 2013 [24] applied this laminar burning velocity expression to their estimations for low-medium values of H_2 content, in a combustion model of partial stratification charge (PSC) engine, for ultra-lean conditions and H_2 fractions $x_{H_2} = [0, 0.45]$.

7.6. Complex expressions of laminar burning velocity applicable to hydrogen-methane blends at engine-like conditions in complete range of fuel combinations

After the consideration of the linear and LeChatelier's rule-like expressions tested by Di-Sarli&Di-Benedetto 2007 [160] and other authors to predict the laminar burning velocity of H_2 - CH_4 blends, their assessments were that the latter are able to take into account the kinetic interaction between radicals, but when dealing with high H_2 contents ($x_{H_2} > 0.7$) and then higher H radical concentrations, their interaction is considered too strong to be reproduced even by the LeChatelier's rule-like formula, requiring more sophisticated expressions.

Moreover, according with studies in the literature, the simple mixing rules that have estimated only the change of composition are considered not accurate enough to predict the laminar burning velocity of H_2 - CH_4 blends in wide ranges or other conditions. This means that expressions based on mixing rules do not always work as the functions derived from models based on detailed chemical schemes, especially when wide ranges of engine-like conditions have to be taken into account.

An analytical laminar flame burning velocity expression applicable in very wide ranges was developed by Bougrine et al. 2011 [172] using an optimization algorithm. Their phenomenological function was deeply inspired by preceding works and developed from previous simpler correlations of experimental burning velocities for gasoline-ethanol-air-

diluents and methane-hydrogen-air-diluents mixtures. The motivation of that study was to complement experimental measurements, by extracting a wide data base of laminar flame speeds and thicknesses from complex chemistry one-dimensional simulations of premixed laminar flames using the PREMIX code/CHEMKIN package [162,163], in order to extend the domain of validity of experimental correlations to high proportions of H_2 in the fuel, high residual burned gas mass ratios as well as high pressures and temperatures. A wide number of current conditions (fig. 49) were investigated to cover the whole operating range of fuel compositions and thermodynamic parameters of common practical combustion systems in industrial applications such as piston engines, gas turbines, industrial burners, etc. Equivalence ratio Φ was varied from 0.6 to 1.3, hydrogen content in the fuel x_{H_2} from 0 to 1, diluent or residual burned gas mass fraction $f_{res,u(m)}$ from 0 to 30%, temperature of the fresh mixtures T_u from 300 to 950 K and pressure P from 0.1 to 11 MPa.

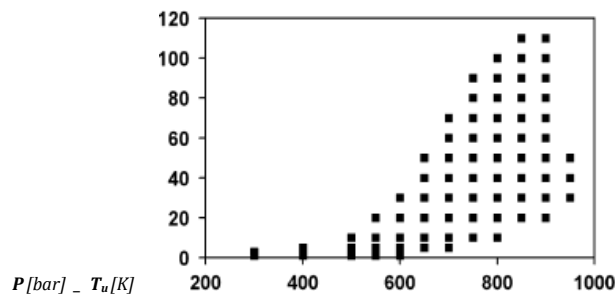


Fig. 49. Map of fresh gases temperature and pressure for one-dimensional premixed simulations (taken from Bougrine et al. 2011 [172])

An assumption in the work of Bougrine et al. 2011 [172] was to approximate diluents as additional nitrogen (N_2). In many combustion systems, such as piston engines or gas turbines, diluents are often composed by products of combustion (CO_2 , H_2O , N_2), as well as residual reactants (fuel, O_2 , N_2) in non-stoichiometric cases. In practice, diluents can be approximated at the first order as nitrogen. This assumption was justified knowing that CO_2 and H_2O have opposite effects on the burning velocity and that N_2 is predominant in mass on CO_2 and H_2O . They compared burning velocities of diluted stoichiometric mixtures when considering residuals as additional N_2 or as additional N_2 , CO_2 and H_2O for several fuel compositions and thermodynamic conditions. In this last case, the residual composition was computed assuming a stoichiometric combustion of the fuel. Except in the case of pure hydrogen, the impact of taking CO_2 and H_2O into account was not significant, which confirmed to these authors the validity of their assumption.

Other assumption treated in depth in [172] was about the molecular diffusivity model. The multicomponent diffusion was not considered, preferring the mixture averaged diffusion model, neglecting then thermo-diffusion (Soret) and mass dispersion (Dufour) effects. They discussed that in spite of that these two effects respectively appear in species and heat flux vectors, and only play a minor role on diffusion mechanisms when the expansion speed of the flame is the first-order, however it should not be neglected in case of the combustion of hydrogen which is highly sensitive to thermo-diffusive instabilities, Gerke et al. 2010 [214]. Nevertheless, the impact of thermal diffusion on hydrogen flame speed was considered mainly clear for rich mixtures, Greenberg 1980 [215]; moreover, they also observed that current thermochemical models cannot reproduce the impact of instabilities on laminar burning velocity like acceleration at high pressure, Gerke et al. 2010 [214]. The impact of using a multicomponent model including Soret-effect was presented for stoichiometric mixtures in atmospheric conditions. For high hydrogen blending rates, accounting for the thermo-diffusive effect had only a slight impact on simulation results, while no significant impact was observed at low hydrogen levels. Thus, it

appeared reasonable to neglect these effects, considering the possible reduction of computational costs. Indeed, the computational cost due to adopting the multicomponent diffusion model in the flame computations could be approximately estimated to be twice or three times the required period to simulate a case without considering these diffusion effects. Moreover, activating the multicomponent diffusion model led to more important number of failed cases when was used that approach, which significantly increased the required global time to treat all the cases.

Experimental and simulated laminar burning velocities for single parameter variations were compared in [172] (e.g. figs. 50-52). Results from simulations were globally in good agreement with many experimental data, showing that the derived dependencies of equivalence ratio Φ , residuals fraction $f_{res,u(m)}$, fresh gases temperature T_u , pressure P and hydrogen content $h=100x_{H_2}$, were satisfactorily captured by the several compared chemical schemes.

However, calculations with GRI-Mech 3.0 [170] scheme seemed slightly overestimate laminar burning velocities. Compared to the other simulations using higher resolution settings, errors remained nevertheless acceptable. It was then noticeable that GRI 3.0 behaved similar to Konnov-Mech 0.5 [175] or USC_II-Mech [174] mechanisms which were build-up with respectively nearly twice as many species and with twice to four times more reactions. On the other hand, the study [172] showed that the Princeton-Mech [173] seemed systematically underestimate laminar burning velocities, pointing out that a minimum level of detail was all the same required to guarantee the computations accuracy. Finally, the GRI 3.0 appeared also more robust than Konnov 0.5; the first showed less than 20% of failed cases against more than 60% for the second. The summarized considerations in [172] confirmed GRI-Mech as a good compromise to predict laminar flame speeds at high pressure and temperature despite a lack of experimental data to validate the scheme over a wider range of P and T_u .

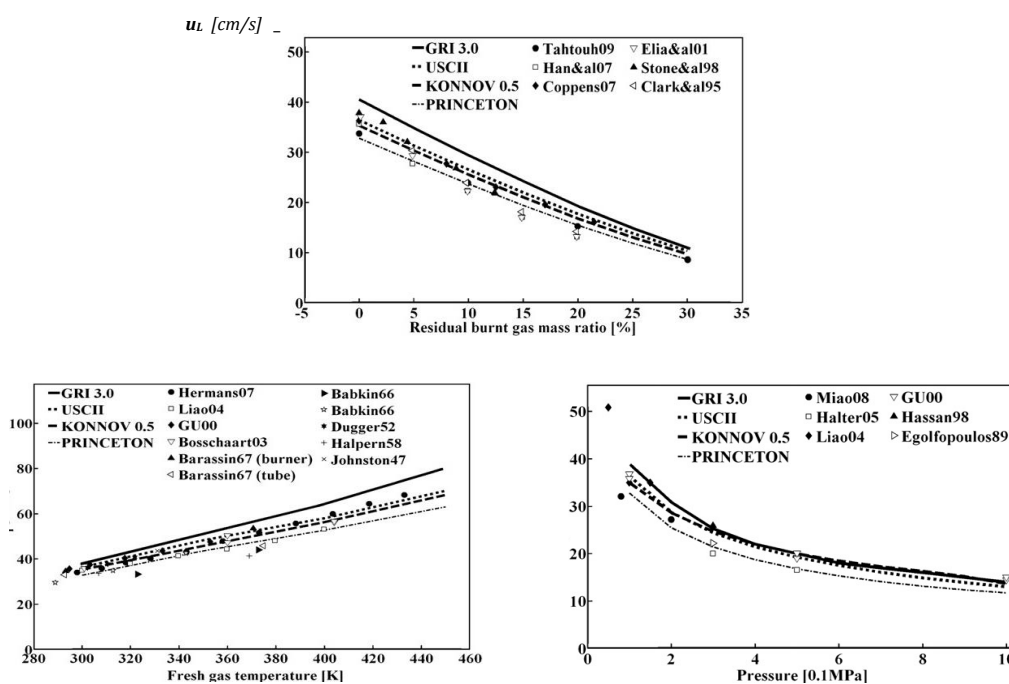


Fig. 50. Comparison of experimental and simulated laminar burning velocities of CH_4 in stoichiometric air mixtures, u_L [cm/s], as respective functions of residuals mass fraction percentage $f_{res,u(m)}$, fresh gas temperature T_u and pressure P , for $T_{u,0}=300$ K, $P_0=0.1$ MPa and $\Phi=1$ (taken from Bougrine et al. 2011 [172])

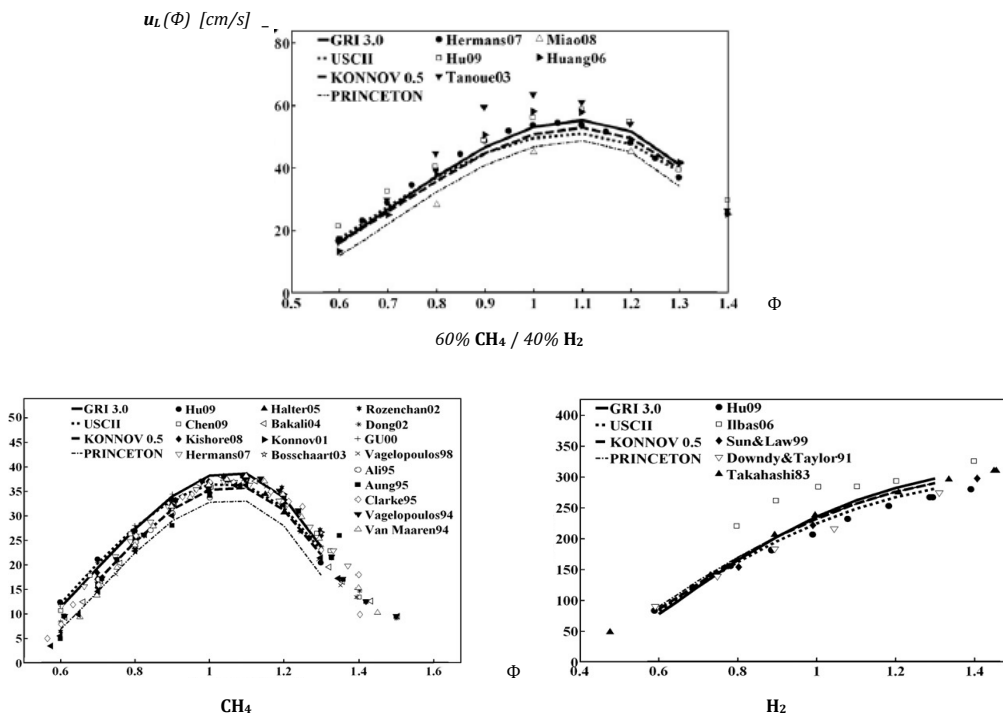


Fig. 51. Comparison of experimental and simulated laminar burning velocities of fuel-air mixtures, u_L [cm/s], as functions of equivalence ratio ϕ , for $T_{u,0}=300$ K and $P_0=0.1$ MPa (taken from Bougrine et al. 2011 [172])

The evolution of the laminar burning velocity with the H_2 proportion in the fuel blend, presented in fig. 52, was explained by Bougrine et al. 2011 [172] as based on the non-linear chemical kinetics processes, according with the three regimes already identified by Di-Sarli&Di-Benedetto 2007 [160] for CH_4 - H_2 flames propagation.

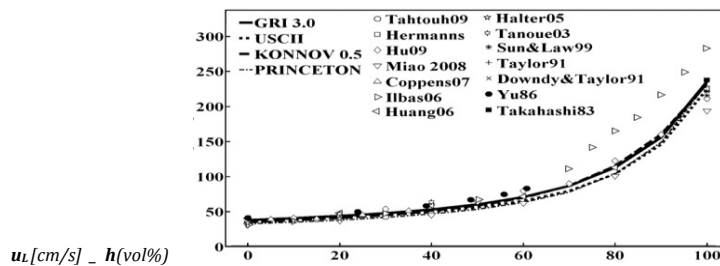


Fig. 52. Comparison of experimental and simulated laminar burning velocities of H_2 - CH_4 blends, u_L [cm/s], as function of volumetric H_2 percentage, for $T_{u,0}=300$ K, $P_0=0.1$ MPa and $\phi=1$ (taken from Bougrine et al. 2011 [172])

The general form of the phenomenological expression for the laminar burning velocity u_L presented by Bougrine et al. 2011 [172] was defined as a global continuous relationship by combination of parametric functions (table 25). These were determined considering the diverse effects of the functional factors and varied conditions, with compilation of the different behaviors that, thus and necessarily, makes complex the correlation. In the following subsections, these effects are reviewed as were considered in the work of these authors for the structuration of their analytical expression.

Table 25Laminar burning velocity analytical expression for **H₂-CH₄ blends** (adapted from Bougrine et al. 2011 [172])

Applicability ranges	P ₀ (bar)	P (bar)	T ₀ (K)	T _u (K)	f _{res,u(m)} (-)	Φ (-)	h=100 x _{H2} (-)%	u _{L,o} (cm/s)	u _L (units)
	1	[1, 110]	300	[300, 950]	[0, 0.3]	[0.6, 1.3]	[0, 100]		
$u_{L,H_2-CH_4}(h, \Phi, f_{res,u(m)}; T_u, P) = (T_u/300)^\alpha \cdot (P/1)^\beta \cdot \zeta(h, \Phi, f_{res,u(m)}; T_u, P) \cdot u_{L,o}$									
					$\alpha_T(T_u; \Phi, h) = [3.2466 - 1.0709(\Phi) + 0.1517(\Phi)^4 - 0.0003201(h) - 1.0359(300/T)^2(\Phi)^2] \cdot \{1 + [0.5(1 + \text{TANH}((h-90)/10))]\} \cdot [-1 + \text{EXP}(-1 + 0.58(T/300)^{0.5})]$				
					$\beta_P(P, T_u; \Phi, h) = [-0.5406 + 0.1347(\Phi) - 0.0125(\Phi)^4 - 0.0005174(h)(\Phi + (1/\Phi))^{0.5} + 0.0002289(T/300)(P/1)(\Phi)^2] \cdot \{1 + [0.5(1 + \text{TANH}((h-90)/10))]\} \cdot [-1 + \text{EXP}(-1.9026 + 0.03556(P/1) - 0.000163(P/1)^2)]$				
					$\Omega_R(h, \Phi; T_u, P) = [4.157 - 1.744(\Phi) + 0.5124(\Phi)^4 - 0.0047(h) - 0.0008694(T/300)(P/1)(\Phi)^2]$				
					$u_{L,o,H_2-CH_4}(\Phi, h) = \{ (1 + 0.00000272 h^{2.897}) 150.817 \Phi^{4.539} \text{EXP}[-2.448(\Phi - 0.0017 h - 0.2248)^2] \} \cdot \{1 + [0.5(1 + \text{TANH}((h-70)/10))]\} \cdot [-1 + 1.4 + 0.000000339(h) - 0.00000117(h)^2 + 0.000000117(h)^3 - 0.0000000375(h)^4 + 0.0000000014(h)^5]$				
					$\zeta(h, \Phi, f_{res,u(m)}; T_u, P) = 1 - \Omega_R f_R(f_{res,u(m)}) = 1 - \Omega_R f_{res,u(m)} [1 - 1.115 f_{res,u(m)} + 1.323 (f_{res,u(m)})^2]$				
					$\cdot \{1 + [0.5(1 + \text{TANH}((h-90)/10))]\} \cdot [-1 + 1.75 - 1.75(\Phi) + 0.625(\Phi)^2 - 0.038(\Phi)^3 + 0.138(\Phi)^4]$				

7.6.1. Effects of equivalence ratio and hydrogen addition

According with [172] the laminar burning velocity $u_{L,o}(\Phi, h)$ of fuel air mixtures of H₂ and CH₄ fuel blends in the reference conditions has not the same response to equivalence ratio variations when varying the fraction of H₂ in the fuel. Indeed, they show that the flame speed promotion is more pronounced to hydrogen addition in rich mixtures than in lean ones. The maximum of the curve is shifted from $\Phi=1.1$ for pure CH₄ to more than 1.4 (between 1.7 and 1.9) for pure H₂.

$$u_{L,o,H_2-CH_4}(\Phi, h) = u_{L,H_2-CH_4}(h, \Phi, f_{res,u(m)}=0; T_{u,o}=300 \text{ K}, P_o=0.1 \text{ MPa}) \quad (204)$$

The expressions of [172] were adapted to hydrogen substitution levels up to $x_{H_2}=1$ (i.e. $h=100\%$) by readjustments of correlation coefficients of Hermanns et al. 2010 [130] (who, as previously Coppens et al. 2007 [142], had improved the Gülder 1984 [195] formulation by adding terms accounting for H₂ addition effect, but only up to $x_{H_2}=0.4$). The optimization was estimated limited by the form of an expression which could hardly reproduce the shift of the optimum equivalence ratio burning velocity notably over $x_{H_2} \approx 0.9$ ($h \approx 90\%$), and a correction term Λ_{U_o} was thereof added to capture the H₂ addition effect over $x_{H_2}=0.7$ ($h=70\%$) by a function $\Psi(h)$ and the equivalence ratio effect over $x_{H_2}=0.9$ ($h=90\%$) by other function $\Theta(\Phi)$, inspired by correlations for hydrogen-air flames of Gerke et al. 2010 [214] and Huang et al. 2006 [6].

$$u_{L,o}(\Phi, h) = \{ (1 + 0.00000272 h^{2.897}) 150.817 \Phi^{4.539} \text{EXP}[-2.448(\Phi - 0.0017 h - 0.2248)^2] \} \cdot \Lambda_{U_o} \quad (205)$$

$$\text{where } \Lambda_{U_o}(\Phi, h) = \{1 + \{0.5 [1 + \text{TANH}((h-70)/10)]\} \cdot [\Psi(h) - 1]\} \cdot \{1 + \{0.5 [1 + \text{TANH}((h-90)/10)]\} \cdot [\Theta(\Phi) - 1]\} \quad (206)$$

$$\text{with } \Psi(h) = 1.4 + 10^{-9} [339(h) - 1170(h)^2 + 117(h)^3 - 3.75(h)^4 + 0.14(h)^5] \quad (207)$$

$$\text{and } \Theta(\Phi) = 1.75 - 1.75(\Phi) + 0.625(\Phi)^2 - 0.038(\Phi)^3 + 0.138(\Phi)^4 \quad (208)$$

The function Λ_{U_0} allowed thus to capture the velocity behavior over $x_{H_2}=0.7$ ($h=70\%$) which corresponds to the two last regimes advocated by Di-Sarli&Di-Benedetto 2007 [160]. The continuity of $u_{L_0}(\Phi, h)$ between the three regimes is ensured by the functions $0.5(1+\text{TANH}((h-70)/10))$ and $0.5(1+\text{TANH}((h-90)/10))$, which also ensure the respective continuities at $x_{H_2}=0.7$ ($h=70\%$) and $x_{H_2}=0.9$ ($h=90\%$), and smooth transitions in between $x_{H_2}=[0.6, 0.8]$ ($h=60-80\%$) or $x_{H_2}=[0.8, 1]$ ($h=80-100\%$) respectively.

7.6.2. Temperature and pressure effects

As commented, the modeling of hydrogen effects was inspired by Gülder 1984 [195] formulations on isooctane-ethanol-air flames, and the expressions of [172] were adapted to H_2 substitution level up to $x_{H_2}=1$ ($h=100\%$) by readjustments of other previous correlations coefficients. Thus, the fresh gas temperature exponent was also adapted from Hermanns et al. 2010 [130], and took into account equivalence ratio and hydrogen addition effects when varying temperature with integration of a term Λ_T for a better fit with simulation results.

$$\alpha_T(T_w; \Phi, h)$$

$$= 10^{-4} [32466 - 10709(\Phi) + 1517(\Phi)^4 - 3.201(h) - 10359(T_o/T)^2(\Phi)^2] \cdot \Lambda_T \quad (209)$$

$$\text{where } \Lambda_T(T_w; h) = 1 + \{0.5 [1 + \text{TANH}((h-90)/10)]\} \cdot \{-1 + \text{EXP}[-1 + 0.58(T/T_o)^{0.5}]\} \quad (210)$$

In spite of that Hermanns et al. 2010 [130] did not consider a pressure effect in laminar burning velocity (that was limited to atmospheric pressure), the expression of [172] for the fresh gas pressure exponent was also determined similarly as function of temperature, equivalence ratio and hydrogen addition effects, with an adjustment term Λ_P .

$$\beta_P(P, T_w; \Phi, h)$$

$$= 10^{-4} [-5406 + 1347(\Phi) - 125(\Phi)^4 - 5.174(h)(\Phi + (1/\Phi))^{0.5} + 2.289(T/T_o)(P/P_o)(\Phi)^2] \cdot \Lambda_P \quad (211)$$

$$\text{where } \Lambda_P(P; h) = 1 + \{0.5 [1 + \text{TANH}((h-90)/10)]\} \cdot \{-1 + \text{EXP}[-1.9026 + 0.03556(P/P_o) - 0.000163(P/P_o)^2]\} \quad (212)$$

The correction function terms Λ_T and Λ_P are thereof added to capture hydrogen addition effects when varying temperature and pressure, respectively, when $x_{H_2}=0.9$ ($h=90\%$).

7.6.3. Dilution effect of residual gas

Concerning the influence of residual burned gases Metghalchi&Keck 1980 [120] noticed a linear decrease of the flame speed when increasing the dilution rate, while Hermanns et al. 2010 [130] recommended to introduce an equivalence ratio dependency.

Miao et al. 2009 [12,13] found that the reduction effect of diluent ratio on flame speed was not linear and determined not only by this, but also by equivalence ratio, hydrogen fraction and the property of diluent gas.

The expression of [172] integrated temperature and pressure terms besides equivalence ratio and hydrogen fraction, leading to a slight improvement of the results. Moreover, they considered that over a residuals fraction of $f_{res,u(m)} \sim 0.35$ the influence of residual burned gases is not linear anymore, and then introduced a polynomial function of the dilution fraction $F_R(f_{res,u(m)})$.

$$\zeta(h, \Phi, f_{res,u(m)}; T_w, P) = [1 - \Omega_R(h, \Phi; T_w, P) \cdot F_R(f_{res,u(m)})] \quad (213)$$

where $\Omega_R(h, \Phi; T_w, P)$

$$= 4.157 - 1.744(\Phi) + 0.5124(\Phi)^4 - 0.0047(h) - 0.0008694(T/T_o)(P/P_o)(\Phi)^2 \quad (214)$$

$$\text{and } F_R(f_{res,u(m)}) = f_{res,u(m)} \cdot [1 - 1.115 f_{res,u(m)} + 1.323(f_{res,u(m)})^2] \quad (215)$$

with $f_{res,u(m)} = [0, 0.3]$

7.6.4. Calculation by global correlation compared to simulation based on detailed chemistry

Bougrine et al. 2011 [172] compared the results of their analytical continuous correlation, over the whole simulated database (62244 operating points), with the corresponding outcomes based on the one dimensional model simulations by PREMIX-code/CHEMKIN package [162,163] with implemented GRI-Mech 3.0 [170]. A very good agreement was observed showing that the influences on the laminar burning velocity u_L of hydrogen content $h(\%)$, equivalence ratio Φ , fresh gas temperature T_w , pressure P and dilution fraction of residual gas $f_{res,u(m)}$ were well reproduced.

$$u_{L, H_2-CH_4}(h, \Phi, f_{res,u(m)}; T_w, P) = (T_w/T_o)^\alpha \cdot (P/P_o)^\beta \cdot [1 - \Omega_R \cdot F_R(f_{res,u(m)})] \cdot u_{L,o}(\Phi, h) \quad (216)$$

Their results exhibited relative errors, on the laminar burning velocity for the whole database, lower than 10% for about 83% of handled points and lower than 5% for about 60% of the points, when the volumetric hydrogen content in the fuel blend is between $0 < x_{H_2} \leq 0.7$. Errors were more important over $x_{H_2} > 0.8$, pointing out the difficulty to well describe the three regimes of the CH_4 - H_2 flame propagation by a single global continuous correlation. These results were satisfactorily regarded by the authors, estimating that the mean error was about 6% globally, and given that the large number of cases treated and the accuracy of chemical mechanisms together with the base experimental inaccuracy, considered by them that could lead to uncertainties of 10% meanwhile.

Table 26Summary of types of expressions of laminar burning velocity for fuel **blends of hydrogen with methane or natural gas**. Features of applicability depending on composition conditions.

Fuel blends	Types of expressions	Applicability observations	Expressions for reference condition	Expressions for wider range of conditions	H ₂ proportion <i>h</i> (vol%)	Equivalence ratio Φ	Dilution <i>f_{res}</i> or EGR	Pressure <i>P</i> (bar)	Temperature <i>T_u</i> (K)	Ref.	Chapter /section
NG or CH ₄ & H ₂	Escalated linearly with hydrogen content.	Intrinsically valid only for relatively small H ₂ contents. Not representative for non-linear behavior at medium-high H ₂ contents.	$u_{l,0 \text{ HC or CH}_4 - \text{H}_2}(\Phi_{ef}, R_h; T_{u,0}, P_0) = u_{l,0 \text{ HC or CH}_4}(\Phi_{ef}; T_{u,0}, P_0) + k_h(\Phi_{ef}) \cdot R_h$	-	Virtually defined parameter <i>R_h</i>	Virtually defined effective parameter Φ_{ef}	-	$P_0 \approx 1$	$T_{u,0} \approx 300$	El-Sherif 2000 [38] Yu et al. 1986 [138] Wu et al. 2011 [146] Tang et al. 2011 [150] Sher&Ozdor 1992 [151] Di-Sarli&Di-Benedetto 2007 [160]	7.1
			$u_{l,0 \text{ NG} - \text{H}_2}(h; T_{u,0}, P_0) = u_{l,0 \text{ NG}}(T_{u,0}, P_0) + ct(\Phi_0) \cdot h$	$u_{l,0 \text{ NG} - \text{H}_2}(h; T_{u,0}, P_{ad}) = (T_u/T_0)^{\alpha(h)}$	$h(\%) \leq 15$	$\Phi_0 = 0.8 < 1$	$P_0 = [3, 5.4]$	$T_{u,0} = [392, 458]$ $T_{u,0} > 500$	Tinaut et al. 2011 [79]	7.2.1	
			$u_{l,0 \text{ CH}_4 - \text{H}_2}(\Phi, h; T_{u,0}, P_0) = u_{l,0 \text{ CH}_4}(\Phi; T_{u,0}, P_0) + k_h(\Phi) \cdot h$	-	$h(\%) < 40$	$\Phi = \{0.8, 1, 1.2\}$	$P_0 \approx 1$	$T_{u,0} \approx 303$	Hu et al. 2009 [77]	7.2	
Escalated linearly with concentration of H and OH radicals.	Based on specific sensitivity analysis in limited ranges of conditions. Higher differences at rich rather than at lean conditions.	$u_{l,0 \text{ CH}_4 - \text{H}_2}(\Phi; X_{[H]}, X_{[OH]}; T_{u,0}, P_0) = ct(\Phi) + ct'(\Phi) [X_{[H]} + X_{[OH]}]_{\max}$	Suppression (or enhancement) of overall chemical reaction with the increase of initial pressure (or respectively temperature and H ₂ fraction) related to the decrease (or respectively increase) of H, O and OH fractions in the flames.	$h(\%) \leq 80$	$\Phi = [0.6, 1.2]$	-	$P_0 \approx 1$ $P < 5$	$T_{u,0} \approx 303$ $T_u < 400$	Hu et al. 2009 [77,78] Di-Sarli&Di-Benedetto 2007 [160]	7.4 7.4.1	
				$h(\%) \leq 35$	$\Phi = [0.6, 1.5]$	-	$P_0 \approx 1$	$T_{u,0} \approx 298$	Coppens et al. 2007 [142]	7.2.1	
Escalated exponentially with hydrogen content.	Not representative for non-exponential behavior at very high H ₂ contents.	$u_{l,0 \text{ CH}_4 - \text{H}_2}(\Phi, h; T_{u,0}, P_0) \sim (\Phi^a, h^b) \cdot \text{EXP}[(\Phi, h)]$	-	$h(\%) \leq 40$	$\Phi = [0.7, 1.4]$	-	$T_{u,0} = [298, 418]$	Hermanns et al. 2007 [144] Hermanns et al. 2010 [130]			
				$u_{l,0 \text{ CH}_4 - \text{H}_2}(\Phi, h; T_{u,0}, P_0) \sim (\Phi^a) \cdot (T_u/T_0)^{\alpha(\Phi, h)}$	-	$h(\%) > 40$	$\Phi = \{0.8, 1, 1.2\}$	$T_{u,0} \approx 303$	Hu et al. 2009 [77]	7.2	
				$u_{l,0 \text{ CH}_4 - \text{H}_2}(\Phi, h; T_{u,0}, P_0) \sim u_{l,0 \text{ CH}_4}(\Phi; T_{u,0}, P_0) + \text{EXP}[(\Phi, h)]$	-	$h(\%) < 40$	$\Phi = [0.6, 1.4]$	$T_{u,0} \approx 300$	Huang et al. 2006 [6]	7.2.2	
				$\Delta_{\Delta} u_{l,0 \text{ NG} - \text{H}_2}(\Phi, h; T_{u,0}, P_0) = ct + \text{EXP}[h]$	$\Delta_{\Delta} u_{l,0 \text{ NG} - \text{H}_2}(\Phi, h; T_u, P) = ct + \text{EXP}[h]$	$h(\%) = [20, 30]$	$\Phi = [0.6, 1.3]$	$P = (5, 70)$	$T_u >$	Ma et al. 2008 [86]	
				-	-	$h(\%) < 30$	$\Phi = [0.6, 1.4]$	$P > 30$	$T_u >$	Perini et al. 2010 [196]	
Linear mixing rules by averaging of constituent fuel gases in their proportions.	Not representative of strong non-linear effects in chemical kinetics, as distinguished in different regimes. Actual values smaller than those obtained by this averaging.	-	-	$100 u_{l, \text{H}_2 - \text{CH}_4}(\Phi, h) = [h \cdot u_{l, \text{H}_2}(\Phi) + (100-h) \cdot u_{l, \text{CH}_4}(\Phi)]$	$h(\%) < 40-60$ $h(\%) > 80-90$	$\Phi = [0.6, 1.5]$ In lean mixtures, the H ₂ addition enhance the CH ₄ reactivity slightly, while a strong inhibiting effect of the H ₂ substitution by CH ₄ is given at rich conditions.	-	$P_0 \approx 1$	$T_{u,0} \approx 300-303$	El-Sherif 2000 [38] Hu et al. 2009 [75,77] Di-Sarli&Di-Benedetto 2007 [160]	7.3 7.3.1 7.3.2

Fuel blends	Types of expressions	Applicability observations	Expressions for reference conditions	Expressions for wider range of conditions	H ₂ proportion <i>h</i> (vol%)	Equivalence ratio Φ	Dilution <i>f_{res}</i> or EGR	Pressure <i>P</i> (bar)	Temperature <i>T_u</i> (K)	Ref.	Chapter /section
NG or CH ₄ & H ₂	Simple mixing rules, mainly based on the composition changes.	No enough accuracy to predict the laminar burning velocity of H ₂ -CH ₄ blends in wide ranges.	Expressions based on mixing rules do not always work as the functions derived from models based on detailed chemical schemes.	Expressions are especially questionable when wide ranges of engine-like conditions have to be taken into account.							7
	Mixing rules by LeChatelier rule-like averaging of constituent fuel gases in their proportions.	Better accuracy for medium-high H ₂ contents than for low proportions. Good agreement, mainly for lean and stoichiometric conditions. More differences for rich mixtures and high %H ₂ . (Significant errors for rich mixtures $\Phi > 1.3$). Less applied for low-medium %H ₂ (e.g. in a PSC engine).	-	$[100 / u_{L,NG \text{ or } CH_4 - H_2}(\Phi, h; T_u, P)] = [h / u_{L,H_2}(\Phi; T_u, P)] + [(100-h) / u_{L,CH_4}(\Phi; T_u, P)]$	<i>h</i> (%)=(0, 100)	$\Phi \leq 1$	-	<i>P</i> ≤ 10 atm	<i>T_u</i> ≤ 400	Di-Sarli&Di-Benedetto 2007 [160]	7.5
					<i>h</i> (%) ≤ 70	$\Phi \leq 1, 1 < \Phi$				Di-Sarli&Di-Benedetto 2007 [160] Karim et al. 1985 [211] Wierzba&Ale 2000 [213]	7.5.1
					<i>h</i> (%) > 30 <i>h</i> (%)=[30, 70]	($\Phi \leq 1$) $\Phi = [0.6, 1.3]$		<i>P</i> ≈ (5, 70)	<i>T_u</i> >	Ma et al. 2008 [86]	7.5.2
					<i>h</i> (%)=[30, 80]	$\Phi = [0.6, 1.4]$		<i>P</i> > 30	<i>T_u</i> >	Perini et al. 2010 [196]	
				<i>h</i> (%)=[0, 45]	$\Phi = [0.75, 1.1]$ $\Phi_{PSC} = [0, 6]$		<i>P</i> >	<i>T_u</i> >	Aliramezani et al. 2013 [24]		
	LeChatelier rule-like expressions.	Ability to take into account the kinetic interaction between radicals.	For high H ₂ contents (<i>x</i> _{H2} > 0.7) and then higher H radical concentrations, their interaction is too strong to be reproduced by LeChatelier's rule.	More sophisticated expressions are required for complete ranges of compositions and thermodynamic conditions, pointing out the difficulty for well describing the three regimes of the CH ₄ -H ₂ flame propagation by a single correlation.							7
	Complex, global and continuous relationships by combination of parametric functions, for application in complete ranges of operative conditions.	Satisfactory results of [172] estimating mean error globally about 6%; meanwhile uncertainties of about 10% due to the large number of cases treated and the no-absolute accuracy of chemical mechanisms together with the base experimental inaccuracy. Relative errors lower than 10% for about 83% of for the whole database, and lower than 5% for about 60% of the handled points, when %H ₂ between <i>h</i> =0-70%, with more error over <i>h</i> >80%.	(Section 7.6.1) $u_{L,0 H_2-CH_4}(\Phi, h; T_{u,0}, P_0)$	(Section 7.6.4) $u_L(\Phi, f_{res,u}; T_u, P) = [T_u/T_0]^{\alpha} \cdot (P/P_0)^{\beta} \cdot \zeta \cdot u_{L,0}$	<i>h</i> (%)=[0, 100]	$\Phi = [0.6, 1.3]$	$f_{res,u(m)} = [0, 30] \%$	<i>P</i> = [1, 110]	<i>T_u</i> = [300, 950]	Bougrine et al. 2011 [172]	7.6
				Relationship to extend the domain of validity of experimental and computational expressions to high proportions of H ₂ in the fuel, high residual burned gas ratios as well as high pressures and temperatures, covering the whole operating range of fuel compositions and thermodynamic parameters of common practical combustion systems (table 25). Expressions for temperature and pressure effects (section 7.6.2) $\alpha_T(T_u; \Phi, h)$ and $\beta_P(P, T_u; \Phi, h)$ and for dilution effect of residual gas (sect. 7.6.3) $\zeta(h, \Phi, f_{res,u(m)}; T_u, P)$.							

References of chapters six, seven and eight (*after the eighth chapter*)

8. Summaries of reviews on other consulted works about combinations of hydrogen - natural gas (*appendix chapter to the fourth part*)

- 8.1. Characteristics and conditions of several works related to combustion of hydrogen combined with methane or natural gas
- 8.2. Conditions related to several works about laminar burning velocity expressions for single methane-air mixtures
- 8.3. Conditions related to several works about laminar burning velocity expressions for single hydrogen-air mixtures

References of chapters six, seven and eight (*fourth part*)

8. Summaries of reviews on other consulted works about combinations of hydrogen - natural gas (appendix chapter to the fourth part)

This chapter 8 summarizes, in tabular and schematic way, other consulted pieces of information of published works that have been considered interesting, in the context of the development of the fourth part of this study, to complement the basis of material reported in chapters 6 and 7.

8.1. Characteristics and conditions of several works related to combustion of hydrogen combined with methane or natural gas

Conditions and some characteristics relative to several works in the literature, related with combustion of hydrogen fuel blends in air mixtures with methane or natural gas and other cases with some other hydrocarbons, are summarized in [table 27](#).

Different kinds of gaseous combinations considered for the fuel blends with hydrogen are included, as well parameters of composition and conditions of pressure and temperature, types of experimental data and simulation results, computational simulations, applications to thermodynamic models and-or calculation codes applied, chemical kinetics mechanisms, laminar burning velocities (theoretical, quasi-laminar or apparent) and other observations.

8.2. Conditions related to several works about laminar burning velocity expressions for single methane-air mixtures

Literature references with expressions for burning velocities of methane-air mixtures and their applicability ranges, for pressures, temperatures, equivalence ratios and residual gas fractions, are summarized in [table 28](#).

8.3. Conditions related to several works about laminar burning velocity expressions for single hydrogen-air mixtures

Literature references with expressions for burning velocities of hydrogen-air mixtures and their applicability ranges, for pressures, temperatures, equivalence ratios and residual gas fractions, are summarized in [table 29](#).

Table 27

Summary of some characteristics relative to several works in the literature related with combustion of **hydrogen fuel blends** in air mixtures **with methane or natural gas** and some cases with other hydrocarbons

Ref.	Gaseous mixtures. Fuel blends of H ₂ with:	Parameters and conditions	Experimental data/ simulation results	Computational simulations, thermodynamic models and-or calculation codes	Chemical kinetics mechanisms	Laminar burning velocities (theoretical, quasi-laminar or apparent)	Observations
Aliramezani et al. 2013 [24]	NG/CH ₄ -air PSC-SIE H ₂ addition	$x_{H_2} = \{0, 0.15, 0.3, 0.45\}$; $x_{CH_4} + x_{H_2} = 1$ $\Phi = \{0.75, 0.8, 0.9, 1, 1.05, 1.1\}$ Engine conditions $\Phi_{PSC} = \{-, 2.38, 3.23, 5.88\}$ (non-PSC, lean PSC, mid PSC, rich PSC)	Simulation results validated with experimental data for NG at lean condition, Reynolds et al. 2005 [216], for wide range of charge stratification.	Thermodynamic-based theoretical 2-Z model including (non-spherical) flame propagation pattern and non-homogeneous charge system	Overall chemical formulas to combustion products (water vapor, hydrogen, methane, oxygen, nitrogen, carbon dioxide and carbon monoxide). Equations of mass balance for oxygen, hydrogen, carbon and nitrogen plus equations provided by equilibrium constants of most probable reactions.	$u_{L,H_2-CH_4}(x_{H_2}, \Phi)$ calculations, for low and medium H ₂ contents, by LeChatelier's rule-like formula, based on Di-Sarli&Di-Benedetto 2007 [160], applying empirical formulas for individual constituents, u_{L,H_2} by Iijima&Takeno 1986 [217] and u_{L,CH_4} by Bougrine et al. 2011 [218]	Approach of partial stratification charge (PSC, relative rich region around the spark plug by micro-direct injection), which improves engine performance by reducing combustion duration, decreasing specific fuel consumption and increasing of IMEP in lean conditions. The increasing of H ₂ content improves the PSC effect of increasing the stability and reliability of ignition and combustion process.
Mariani et al. 2013 [90]	NG-air SIE H ₂ addition	$x_{H_2} = \{0, 0.15, 0.3\}$; $x_{NG} + x_{H_2} = 1$ Engine conditions (different driving cycles) $P_{max} (bar) \leq 40$	Experimental data. Pressure signal measured in the cylinder.	Combustion analysis by processing of the pressure signal	-	-	H ₂ addition resulted in combustion phasing advance, and cyclic variability decreased, particularly at low loads, due to effect of H ₂ on stability. CO ₂ emissions reductions between 3-6% for $h(\%)=15$ and 13-16% for $h(\%)=30$, respectively.
Mariani et al. 2012 [41]		$x_{H_2} = \{0, 0.1, 0.2, 0.3\}$; $x_{H_2} = \{0, 0.3\}$; $x_{NG} + x_{H_2} = 1$ $\Phi = 1$ Engine conditions	Simulations performed at engine-like conditions. <i>MBT</i> ignition timing adopted for all fuels and operating conditions.	Numerical model developed using a 1-D discretization for pipes, and a 0-D model inside cylinders. Combustion analysis by a 2-Z model, Heywood 1988 [99]	Zeldovich mechanism model for nitric oxide formation, Glassman&Yetter 2008 [219]	The models accounts for the effects of H ₂ on laminar flame speed. $u_L(\Phi, f_{res,ui}, T_w, P)$ classical experimental correlation employed in calculations was the given by Heywood 1988 [99]	Consumption performance, engine efficiency and NO _x emissions predictions. Three-way catalyst for efficient exhaust after-treatment. <i>EGR</i> investigated for reducing of NO _x emissions and improving of efficiency.
Morrone& Unich 2009 [66]			<i>MBT</i> spark advance choosing for each fuel.	Combustion model to obtain <i>BMF</i> time evolution	-		Estimation of engine brake efficiency and performance.
Mariani et al. 2008 [65]				Numerical engine model	-		Engine efficiency improving by <i>MBT</i> spark advance, with HCNG blends, more relevant at part loads and for higher H ₂ content.
Sileghem et al. 2012 [176]	CH ₄ -air H ₂ substitution	$x_{H_2} = 0.7$; $x_{CH_4} = 0.3$ $\Phi = \{0.8, 1.2\}$ $T_w(K) = 600$; $P(bar) = 1$	-	Computational 1-D planar adiabatic flame simulation using chemical oxidation mechanism	Implemented detailed reaction scheme GRI-Mech 3.0 [170]	$u_{L,H_2-CH_4}(x_{H_2} = 0.7, \Phi)$ calculations	$u_L(\Phi)$ comparison with some mixing rules calculations based on energy and mole fractions and LeChatelier's rule.

Ma et al. 2012 [4]	NG-air SIE H ₂ addition/ H ₂ substitution	Engine model validation by experimental parameters: $x_{H_2} = \{0, 0.15, 0.3, 0.45, 0.55\}$; $x_{NG} + x_{H_2} = 1$ $\Phi = \{0.67, 0.71, 0.77\}$ Engine conditions $P_i, exp / pred (bar) \approx \{4.8-12.6 / 5.1-12.1\}$ $P_{max, exp} / pred (bar) \approx \{21.2-69.6 / 21.2-68.5\}$	Simulations results compared with experimental (pressure) data from (H)CNG engine performance, in-line six-cylinder, turbocharged intercooled;	Quasi-D combustion model based on fractal geometry implementation	-	$u_{L, HCNG}(x_{H_2}, \Phi)$ calculations by LeChatelier's rule-like formula, based on Di-Sarli & Di-Benedetto 2007 [160], applying empirical formulas for individual constituents, u_{L, H_2} by Göttgens et al. 1992 [190] and u_{L, CH_4} by Müller et al. 1997 [220]	Model simulation predictions of cylinder pressure histories and <i>BMP</i> , compared with experimental results, match quite well except for step of early combustion (over a wide range of loads and engine speeds, and diverse hydrogen blending and fuel to air equivalence ratios).
Ma et al. 2011 [89]		Engine model validation by experimental parameters: $x_{H_2} = \{0, 0.3, 0.55, 1\}$; $x_{NG} + x_{H_2} = 1$ $\Phi = \{0.48, 0.67, 0.71, 0.77\}$ Engine conditions		Improved model about Ma et al. 2008 [86]			
Ma et al. 2008 [86]		Engine model validation by experimental parameters: $x_{H_2} = \{0, 0.1, 0.2, 0.3, 0.4, 0.5\}$; $x_{NG} + x_{H_2} = 1$ $\Phi = \{0.61, 0.62, 0.71, 0.75, 0.77, 0.80, 0.83\}$ Engine conditions $P_i, exp / pred (bar) \approx \{7.2-15.7 / 7.5-15.2\}$ $P_{max, exp} / pred (bar) \approx \{29-60.5 / 28.8-60.1\}$ Experimental comparisons for LeChatelier's rule-like formula: $x_{H_2} = \{0, 0.1, 0.2, 0.3, 0.4, 0.5, 0.8\}$; $x_{NG} + x_{H_2} = 1$ $\Phi = \{0.6, 0.7, 0.8, 0.9, 1, 1.1, 1.2, 1.3, 1.4\}$ $\Phi = [0.6, 1.3]$ Experimental comparisons for exponential formula, Huang et al. 2006 [6]: $x_{H_2} = \{0, 0.1, 0.2, 0.3, 0.4, 0.5, 0.6, 0.8\}$; $x_{NG} + x_{H_2} = 1$ $\Phi = \{0.6, 0.7, 0.8, 0.9, 1, 1.1, 1.2, 1.3, 1.4\}$ $\Phi = [0.6, 1.3]$	Single port injection engine	2-Z quasi-D predictive model to simulate the engine working cycle		$u_{L, HCNG}(x_{H_2}, \Phi)$ calculations by the same LeChatelier's rule-like formula, for medium and high H ₂ contents; and by the exponential formula from Huang et al. 2006 [6], for low H ₂ mole fractions	Simulation and experimental results match quite well except for extremely fuel lean conditions where become severe incomplete combustion problems.
Tinaut et al. 2011 [79]	NG-air SIE H ₂ addition	$x_{H_2} = \{0, 0.03, 0.06, 0.15\}$; $x_{NG} + x_{H_2} = 1$ $\Phi = 0.8$ Engine conditions (different initial T_i, P_i) $T_i(K) = \{392, 458\}$; $P_i(bar) = \{3, 4.6, 5.1, 5.3, 5.4\}$ $T_i(K) > 500$ (for burning velocity correlation)	Combustion chamber, (constant volume bomb) Tinaut et al. 2010 [221], and 4-cylinder engine	Quasi-D predictive model, Horrillo 1998 [222], Tinaut et al. 1999, 2001 [223, 224]	In-house chemical kinetics model (based on Zeldovich extended mechanism)	$u_{fl}(\Phi=0.8, x_{H_2}, T_i)$ T-function in potential form for apparent or quasi-laminar burning velocity	Performance and NO _x & CO exhaust emissions prediction of ICE. Flame speed ratio $FSR = u_{fl} / u_{fl}$
Park et al. 2011 [141]	CH ₄ -air C ₃ H ₈ -air n C ₄ H ₁₀ -air CH ₄ -CO-air C ₃ H ₈ -CO-air n C ₄ H ₁₀ -CO-air	$x_{H_2} = 0.95$; $x_{HC} + x_{H_2} = 1$ $\Phi = \{0.35, 0.65\}$ $T_i(K) = 298$; $P(atm) = 1$ $x_{H_2} = \{0.32, 0.6\}$; $x_{CO} = \{0.58, 0.1\}$; $x_{HC} + x_{H_2} + x_{CO} = 1$ $\Phi = \{0.5, 0.8\}$ $T_i(K) = 298$; $P(atm) = 1$	Twin flame (in opposed jet configuration) with symmetrical planar flames. Variable pressure chamber for propagation and extinction studies.	Numerical simulations by CHEMKIN-PREMIX-TRANSPORT codes [163, 162, 161]	Implemented detailed reaction scheme USC_II-Mech [174]	Experimental and computed laminar flame speeds	Other numerical analysis to investigate at lean operating conditions the performance and emission characteristics of an engine fueled by CH ₄ and CH ₄ -H ₂ blends obtaining an engine efficiency increase of 7% when a 15% H ₂ content was adopted.

Ref.	Gaseous mixtures. Fuel blends of H ₂ with:	Parameters and conditions	Experimental data/ simulation results	Computational simulations, thermo-dynamic models and-or calculation codes	Chemical kinetics mechanisms	Laminar burning velocities (theoretical, quasi-laminar or apparent)	Observations
Bougrine et al. 2011 [172]	CH ₄ -air SIE H ₂ addition/ H ₂ substitution	$x_{H_2} = [0, 1]; x_{CH_4} + x_{H_2} = 1$ $\Phi = [0.6, 1.3]; f_{res,u(m)} = [0, 0.3]$ $T_u(K) = [300, 950]; P(bar) = [1, 110]$	Simulations results compared with a wide data base of experimental measurement from the literature	1-D premixed flames simulation to generate a wide chemical database by PREMIX-code/ CHEMKIN-II [162,163]. Wide range of thermodynamic conditions representative of modern combustion systems	Implemented detailed reaction scheme GRI-Mech 3.0 [170]. Benchmarked with other several kinetic schemes Princeton [173], USC_II [174] and Konnov 0.5 [175].	$u_L(x_{H_2}, \Phi, f_{res,u}; T_w, P)$ continuous and complex expression inspired by other previous works: Gülder 1984 [195], Han et al. 2007 [225], Rahim et al. 2002 [226], Coppens et al. 2007 [142], Hermanns 2007 [144], Hermanns et al. 2010 [130], Huang et al. 2006 [6], Tahtouh et al. 2009 [137], Gerke et al. 2010 [214], Bougrine et al. 2011 [218], & Verhelst et al. 2011 [227]	Phenomenological function extending the ranges of validity domain of the previous works on experimental correlations, to high levels of pressure and temperature, in a generic expression for any fraction of H ₂ content in a fuel blend with CH ₄ , and for high residual burned mass ratios.
Wu et al. 2011 [146]	C ₂ H ₆ -air C ₂ H ₄ -air C ₂ H ₂ -air C ₂ H ₄ -air C ₃ H ₈ -O ₂ -He CO-O ₂ -He	$R_b = [0, 0.5]$ $\Phi_{ef} = \{0.7, 1, 1.6\}$ $T_u(K) = 293 \pm 2; P(atm) = 1$ $R_b = [0, 0.2]$ $\Phi_{ef} = 0.7$ $T_u(K) = 293 \pm 2; P(atm) = 5$ $R_b = [0, 0.4]$ $\Phi_{ef} = 0.6$ $T_u(K) = 293 \pm 2; P(atm) = 20$ $R_b = [0, 0.5]$ $\Phi_{ef} = 1$ $T_u(K) = 293 \pm 2; P(atm) = 20$	Constant pressure dual chamber	CHEMKIN-PREMIX-TRANSPORT codes [163,162,161], STANJAN equilibrium program [184]	Implemented detailed reaction scheme USC_II-Mech [174]	$u_L(R_b, \Phi_{ef})$ linear correlation of burning velocities with small amounts of H ₂ addition	
Tang et al. 2011 [150]	n C ₄ H ₁₀ -air CH ₄ -air C ₂ H ₄ -air C ₃ H ₈ -air	$R_b = [0, 0.5]$ $\Phi_{ef} = [0.6, 1.4]$ $T_u(K) = 298; P(atm) = 1$	Constant pressure dual chamber, Kelley&Law 2009 [228], Tse et al. 2004 [181]. Constant volume cylindrical single chamber, Tang et al. 2008 [149]	1-D freely propagating laminar flame model	Implemented detailed reaction scheme USC_II-Mech [174]	$u_L(R_b, \Phi_{ef})$ linear correlation of burning velocities with small amounts of H ₂ addition	

Perini et al. 2010 [196]	CH ₄ -air SIE H ₂ addition/ H ₂ substitution	$x_{H_2} = \{0, 0.2, 0.4, 1\}$; $x_{H_2} = [0, 1]$; $x_{NG} + x_{H_2} = 1$ $\Phi = \{0.5, 1, 2.3\}$; $\Phi = [0.6, 1.4]$ Engine conditions $T(K) = [1000, 4000]$ $P_{ref}(bar) = 30$	Validation comparing against numerical pressure traces on a standard single-cylinder engine, with references on detailed experimental data from the literature (Bade-Shrestha&Karim 1999,2001 [27,229], Verhelst&Sierens 2007 [230]).	2-Z quasi-D combustion model to simulate engine power cycle (assuming spherical flame and infinitesimal thickness). Fractal geometry based model implemented for turbulence influence on flame evolution. Jointed computations of gaseous mixtures composition and physical mass-averaged thermodynamic properties, by kinetic theory of gases, Verhelst &Sheppard 2009 [231]	Computing for evaluating equilibrium species concentrations of combustion products developed and coupled to the code. Chemical compositions estimated though the application of a chemical equilibrium algorithm with twelve more important species of combustion in air of H ₂ -CH ₄ blends.	$u_{L,H_2-CH_4}(x_{H_2}, \Phi)$ calculations, for medium and high H ₂ contents, by LeChatelier's rule-like formula, based on Di-Sarli&Di-Benedetto 2007 [160], applying empirical formulas for the individual constituents u_{L,H_2} by Verhelst 2005 [232], Verhelst et al. 2005 [125], Gerke 2007 [233] and u_{L,CH_4} by Müller et al. 1997 [220]. $u_{L,H_2-CH_4}(x_{H_2}, \Phi)$ calculations for low H ₂ mole fractions by exponential formula as Ma et al. 2008 [86], Huang et al. 2006 [6]	Model performance and emissions prediction of ICE. Cylinder pressure and NO _x CO pollutant emissions compared with experimental data. Models yield very reasonable trends and accurate predictions, properly capturing the dependence of different hydrogen fraction. Only the NO predictions at very lean mixtures were not satisfactory
Hu et al. 2009 [76]	CH ₄ -air H ₂ addition/ H ₂ substitution	$x_{H_2} = \{0, 0.2, 0.4, 0.6, 0.8\}$; $x_{CH_4} + x_{H_2} = 1$ $\Phi = 0.8$ $T_i(K) = \{303, 373, 443\}$; $P(bar) = \{1, 2.5, 5, 7.5\}$	Cylindrical constant volume combustion chamber	-	-	Experimental un-stretched burning velocities and Markstein constants. Measurements restricted before the occurrence of cellular structure.	Flame stability analysis (Peclet number and influence of hydrodynamic and thermo-diffusive instabilities on transition to cellular flames). Flame photos in a radius range of 5-25 mm to avoid ignition energy and pressure rise effects.
Hu et al. 2009 [78]			Simulations results validated with experimental data at lean condition.	CHEMKIN (with TWOPNT), PREMIX, TRANSPORT codes [163,162,161]	Implemented detailed reaction scheme GRI-Mech 3.0 [170]	Good agreement of computational burning velocities versus the experimental results except at high H ₂ fraction, probably related to the kinetic scheme.	Validation of kinetic mechanism for H ₂ -CH ₄ blends in several conditions (further validations to Ren et al. 2001 [140], Halter et al. 2005 [53], Di-Sarli&Di-Benedetto 2007 [160]).
Hu et al. 2009 [75,77]		$x_{H_2} = \{0, 0.1, 0.2, 0.3, 0.4, 0.5, 0.6, 0.7, 0.8, 0.9, 1\}$; $x_{CH_4} + x_{H_2} = 1$ $\Phi = \{0.4, 0.6, 0.7, 0.8, 0.9, 1, 1.1, 1.2, 1.3, 1.8, 2.2, 3, 4\}$; $\Phi = \{0.8, 1, 1.2\}$ $T_i(K) = 303$; $P(bar) = 1$	Simulations validated with experimental data at stoichiometric and rich conditions and for high H ₂ fractions			$u_L(x_{H_2})$ numerical correlations	
Hu et al. 2009 [14,15]	NG-air SIE H ₂ addition	$x_{H_2} = \{0, 0.1, 0.2, 0.3, 0.4\}$; $x_{NG} + x_{H_2} = 1$ $EGR(\%) = \{0, 5, 10, 15, 20, 30, 35, 40\}$ Engine conditions	Experimental test engine	-	-		Performance and emissions prediction for SIE. EGR investigated for engine efficiency improving and NO _x emissions reducing.

Ref.	Gaseous mixtures. Fuel blends of H ₂ with:	Parameters and conditions	Experimental data/ simulation results	Computational simulations, thermo-dynamic models and-or calculation codes	Chemical kinetics mechanisms	Laminar burning velocities (theoretical, quasi-laminar or apparent)	Observations
Miao et al. 2009 [12]	NG-air H ₂ addition/ H ₂ substitution	$x_{H_2} = \{0.2, 0.8\}$; $x_{N_2} + x_{H_2} = 1$ $\Phi = \{0.8, 1, 1.2\}$; $f_{res,u(v)} = \{0, 0.05, 0.1, 0.15, 0.20, 0.25, 0.3, 0.35, 0.4, 0.45\}$ $T_u(K) = 300$; $P(bar) = 1$	Cylindrical constant volume combustion bomb, based on Law&Kwon 2004 [32]	-	-	Experimental un-stretched burning velocities and Markstein constants.	N ₂ or CO ₂ as diluent gases
Miao et al. 2009 [13]		$x_{H_2} = \{0.2, 0.4, 0.6, 0.8\}$; $x_{N_2} + x_{H_2} = 1$ $\Phi = 1$; $f_{res,u(v)} = \{0, 0.05, 0.1, 0.15, 0.20, 0.25, 0.3\}$ $T_u(K) = 300$; $P(bar) = \{0.8, 1, 1.5, 2\}$				The flame radius was analyzed in a range of 6-25 mm, to avoid the effects of spark and pressure rise	N ₂ as diluent gas
Miao et al. 2008 [11]		$x_{H_2} = \{0, 0.2, 0.4, 0.6, 0.8, 1\}$; $x_{N_2} + x_{H_2} = 1$ $\Phi = \{0.8, 1, 1.2\}$ $T_u(K) = 300$; $P(bar) = \{0.8, 1, 1.5, 2\}$				(based on Bradley et al. 1998 [119], Gu et al. 2000 [234], Lamoureux et al. 2003 [235], Liao et al. 2004 [5])	No diluent gas
Hermanns et al. 2010-2007 [130,144]	CH ₄ -air H ₂ addition	$x_{H_2} = [0, 0.4]$; $x_{CH_4} + x_{H_2} = 1$ $x_{O_2} = [0.16, 0.21]$; $x_{O_2} + x_{N_2} = 1$ $\Phi = [0.6, 1.5]$; $f_{res,u(m)} = [0, 0.25]$ $T_u(K) = [298, 418]$; $P(bar) = 1$ T-dependence determined for $\Phi = \{0.8, 1, 1.2\}$ ($u_L > 5-10$ cm/s, burning velocity constrain as limiting value suitable to predict the flammability limits)	Heat flux method. Data from experiments of Hermanns 2007 [144], Coppens et al. 2007 [129,142] and other experimental data.	-	-	$u_L(\Phi, x_{H_2}; T_u, f_{res,u})$ empirical correlation, extension of Coppens et al. 2007 [142] and based on Metghalchi&Keck 1982 [121] for the temperature dependent part.	Enrichment by H ₂ combined with fuel gas recirculation. Dilution effect weighted with expressions based on Stone et al. 1998 [236], Metghalchi&Keck 1982 [121], Ryan&Lestz [237] 1982. Simulations correlated by the method of least squares (with Matlab [238]), covering the range of experiments, and compared with other experiments and correlations.
Coppens et al. 2007 [129,142]	CH ₄ -air CH ₄ -O ₂ H ₂ addition	$x_{H_2} = [0, 0.35]$; $x_{CH_4} + x_{H_2} = 1$ $x_{O_2} = [0.16, 0.21]$; $x_{O_2} + x_{N_2} = 1$ $\Phi = [0.6, 1.5]$ $T_u(K) = 298$; $P(bar) = 1$				$u_L(\Phi, x_{H_2})$ correlations presented by Coppens et al. 2007 [142] (and by Hermanns 2010,2007 [130,144]) were based on expression proposed by Gilder 1984 [195]	Also considered mixtures of several compositions of CH ₄ -O ₂ with N ₂ dilution.
Di-Sarli&Di-Benedetto 2007 [160]	CH ₄ -air H ₂ addition/ H ₂ substitution	$x_{H_2} = \{0.1, 0.3, 0.5, 0.7, 0.85, 0.9, 0.95\}$; $x_{H_2} = [0, 1]$; $x_{CH_4} + x_{H_2} = 1$ $\Phi = \{0.6, 1, 1.5\}$; $\Phi = [0.6, 3]$ $T_u(K) = \{300, 350, 400\}$; $T_u(K) = [300, 400]$ $P_i(atm) = \{1, 5, 10\}$; $P(atm) = [1, 10]$	Stretch free data for validations based on studies at atmospheric conditions of Halter et al. 2005 [53], Law&Kwon 2004 [32], Yu et al. 1986 [138]	PREMIX module [162], CHEMKIN 4.0.1 package [163,166]	Implemented detailed reaction scheme GRI-Mech 3.0 [170]	$u_L(\Phi, x_{H_2})$ Good agreement of calculated burning velocities with experimental data except at high H ₂ contents, probably related to the kinetic scheme	Validations of kinetic mechanism for H ₂ -CH ₄ blends, in several conditions (further validations to Ren et al. 2001 [140,239])

Mandilas et al. 2007 [55]	CH₄ -air H ₂ addition	$x_{H_2} = 0.3$; $x_{CH_4} + x_{H_2} = 1$ $\Phi = \{0.8, 1, 1.2\}$; $\Phi = \{0.5, 1.4\}$ $T_0(K) = 360$; $P(\text{bar}) = 5$	Expanding spherical flame in a chamber with optical access	-	-	$u_L(\Phi, x_{H_2})$ increment of laminar burning velocity with H ₂ addition mainly for fuel lean and for stoichiometric mixtures. No increase for $\Phi > 1.2$. Earlier onset of instabilities and reduction of Markstein lengths with H ₂ addition.	Flames results more cellular at large radii, with the exception of rich mixtures. Ignition could be performed for $0.6 < \Phi < 1.3$ for pure CH ₄ -air mixtures while were performed with limits extension in $0.1 - 0.5 < \Phi < 1.4$ for CH ₄ -H ₂ -air, for both lean and rich mixtures.
Ilbas et al. 2006 [54]	CH₄ -air H ₂ addition/ H ₂ substitution	$x_{H_2} = \{0, 0.3, 0.7, 1\}$; $x_{H_2} = [0, 1]$; $x_{NG} + x_{H_2} = 1$ $\Phi = \{0.8, 1, 1.1, 1.8, 3.2\}$; $\Phi = \{0.8, 3.2\}$ $T_0(K) = 298$; $P(\text{bar}) = 1$	Expanding spherical flame in a cylindrical explosion bomb with optical access	CHEMKIN [163] code to provide expansion ratios and determine burning velocities from the experimental flame speeds	-	Laminar burning velocity increase and widening of the flammability limits with H ₂ content increasing in the mixture.	Ignition and combustion could not be performed for $\Phi > 1.3$ for pure CH ₄ -air mixtures while were easily performed up to high $\Phi < 3.2$ for CH ₄ -H ₂ -air. H ₂ -CH ₄ blend about 30-70% defined as competitive alternative for flame stability in combustion plants.
Huang et al. 2006 [6]	NG -air H ₂ addition/ H ₂ substitution	$x_{H_2} = \{0, 0.2, 0.4, 0.6, 0.8, 1\}$; $x_{H_2} = [0, 1]$; $x_{NG} + x_{H_2} = 1$ $\Phi = \{0.6, 1, 1.3\}$; $\Phi = \{0.6, 1.4\}$ $T_0(K) = 300$; $P(\text{bar}) = 1$	Constant volume bomb, based on set-up of Law&Kwon 2004 [32]	-	-	$\Delta_s u_L(\Phi, h)$ dimensionless laminar burning velocity increment (in section 7.2.2). Laminar burning velocity exponential increase with H ₂ addition, with increase of instability and decrease of Markstein length. Markstein number and stability increases with Φ increasing for fixed H ₂ fraction.	Combustion characteristics in a DI engine with combustion duration decrease, Huang et al. 2006,2007 [69-72]
Halter et al. 2005 [53,135]	CH₄ -air H ₂ addition	$x_{H_2} = \{0, 0.1, 0.2\}$; $x_{H_2} = [0, 0.2]$; $x_{CH_4} + x_{H_2} = 1$ $\Phi = \{0.8, 1, 1.2\}$; $\Phi = \{0.7, 1.2\}$ $T_0(K) = 298$; $P(\text{bar}) = \{1, 3, 5\}$, $P(\text{bar}) = [1, 5]$	Expanding spherical flame in a combustion chamber with optical access	CHEMKIN-PREMIX codes [163,162]	Implemented detailed reaction scheme GRI-Mech 3.0 [170]	Onset of instabilities at $P(\text{bar}) > 5$ with H ₂ addition. Increase of u_L and reduction of flame dependence on stretch with H ₂ content increase. Burning velocity decreasing with pressure increasing for a given Φ .	Good agreements of calculations and experimental measurements for laminar burning velocities and burned gas Markstein lengths. Transport effects by reduction of Lewis number with H ₂ fraction increase play a role in reducing the flame sensitivity to strain rates.
Law&Kwon 2004 [32]	CH₄ -air C ₂ H ₄ -air C ₃ H ₈ -air H ₂ substitution	$x_{H_2} = \{0.85, 1\}$; $x_{HC} = \{0, 0.5, 0.1, 0.15\}$; $x_{HC} + x_{H_2} = 1$ $\Phi = \{0.6, 1, 1.67\}$ $T_0(K) = 298 \pm 3$; $P(\text{atm}) = 1$	Expanding spherical flame in constant pressure dual chamber, Tse et al. 2004 [181].	CHEMKIN-PREMIX-TRANSPORT codes [163,162,240]	-	The flame radius was analyzed in a range of 5-20 mm, to avoid the effects of spark and wall interference. Small to moderate amount of CH ₄ addition could reduce laminar burning velocities and would suppress the instabilities onset propensity.	Flame temperature decrease remarkably by adding small fraction of HC fuel. Potential of HC addition to suppress explosion hazards.

Ref.	Gaseous mixtures. Fuel blends of H ₂ with:	Parameters and conditions	Experimental data/ simulation results	Computational simulations, thermo-dynamic models and-or calculation codes	Chemical kinetics mechanisms	Laminar burning velocities (theoretical, quasi-laminar or apparent)	Observations
Ren et al. 2001 [140, 239]	CH ₄ -air H ₂ addition	$x_{H_2} = [0, 0.08]$; $x_{CH_4} + x_{H_2} = 1$ $\Phi = \{0.63, 0.68, 0.73\}$; $\Phi = \{0.5, 0.55, 0.6\}$	Experiments on single jet-wall stagnation flow; counter-flow, laser-Doppler velocimetry measurements and chemiluminescence analyzer	Simulations conducted in the opposed-jet, symmetric, twin-flame configuration. CHEMKIN, PREMIX, TRANSPORT codes [163,162,161]	Implemented detailed reaction scheme GRI-Mech 3.0 [170]	With increasing H ₂ content, the laminar flame speed gradually increases.	Validation of kinetic mechanism for H ₂ -CH ₄ blends, in lean conditions, comparing laminar burning velocity computed values with experiments.
Bauer& Forest 2001 [16,29]	CH ₄ -air SIE H ₂ addition/ H ₂ substitution	$x_{H_2} = \{0, 0.2, 0.4, 0.6\}$; $x_{H_2} = [0.1, 0.4]$; $x_{NG} + x_{H_2} = 1$ $\Phi = [0.4, 1.1]$ Engine conditions	Experiments on a single-cylinder research engine	-	-	-	Φ varying from lean values, at low engine loads, to near stoichiometric values, at high loads, in simulations of driving cycles. Reductions in CH ₄ consumption and CO ₂ production, with relatively small change in other pollutant emissions, for H ₂ fuel fractions about 11-35% as optimum considered ranges.
Uykur et al. 2001 [241]	CH ₄ -air H ₂ addition	$x_{H_2} = \{0, 0.1, 0.2\}$; $x_{H_2} = [0.1, 0.2]$; $x_{NG} + x_{H_2} = 1$ $\Phi = \{0.5, 0.6, 0.7, 0.8, 0.9, 1, 1.1, 1.2, 1.3, 1.4, 1.5\}$ $\Phi = [0.5, 1.5]$ $T_i(K) = 298$; $P_i(bar) = 1$	-	Simulation of premixed flame by CHEMKIN III (with TWOPNT), PREMIX codes [242,162]	Implemented detailed reaction scheme GRI-Mech 3.0 [170]	Addition of 10-20% H ₂ in the fuel with small effect in improving flame speed and lean flammability limit properties. Improvements in the flame speeds of CH ₄ -air mixtures by the addition of 10% H ₂ and its associated O ₂ were equivalent to the improvements obtained by the addition of 20% H ₂ only.	The addition of O ₂ and H ₂ in the same ratio as is found in water was shown to be beneficial. The addition of O ₂ substantially increased the NO _x concentrations in near stoichiometric mixtures, but no increase in NO _x was predicted for lean mixtures. CO emissions were reduced when H ₂ displaced C-containing fuels.
El-Sherif 2000 [38]	CH ₄ -air H ₂ addition CO addition	$R_{O_2} = [0, 0.4]$ $\Phi_{eff} = [0.6, 1.2]$ $T_i(K) = 300$; $P(atm) = 1$ $R_{CO} = [0, 0.4]$ $\Phi_{eff} = [0.62, 1.2]$ $T_i(K) = 300$; $P(atm) = 1$	Experimental data from the symmetrical adiabatic counter-flow arrangement of the study by Yu et al. 1986 [138] in the literature Experimental data from the counter-flow twin flame and laser-Doppler velocimetry by Vagelopoulos& Egolfopoulos 1994 [156] in the literature	In-house 1-D laminar flame model with incorporated representation of transport fluxes	Chemical kinetics mechanism (59 reactions among 25 chemical species, involving CH ₄ -H ₂ -CO-NO _x chemistry)	$u_L(\Phi_{eff}, R_{O_2})$ linear correlation of burning velocities with addition of H ₂ in small amounts $u_L(\Phi_{eff}, R_{CO})$ linear correlation of burning velocities with addition of CO in small amounts	Validation experimental data El-Sherif 1998 [45] and other checking mechanisms as GRI-Mech 2.11 [170], Leeds (Pilling et al.) [243], etc. $k_i(\Phi_{eff}) = 84$ cm/s $k_{CO}(\Phi_{eff}) = 40$ cm/s

Hoekstra et al. 1996 [56]	NG-air	$x_{H_2} = \{0, 0.11, 0.2, 0.28, 0.36\}$; $x_{H_2} = [0.28, 0.36]$; $x_{NG} + x_{H_2} = 1$	Experimental test engine V8	-	-	-	Extremely low levels of NO _x were possible with acceptably moderate increases in un-burned HC using 28% and 36% H ₂ supplementation. Significant reduction for 30% H ₂ and engine running near the lean limit.
	SIE	$\Phi = \{0.625, 0.67, 0.75, 0.833, 0.87, 0.91, 0.95, 1, 1.1, 1.25\}$					
	H ₂ addition	Engine conditions					
Yu et al. 1986 [138]	CH ₄ -air	$x_{H_2} = [0, 0.7]$; $R_b = [0, 0.5]$ $\Phi_{ef} = [0.51, 1.37]$	Experimental data from the symmetrical adiabatic counter-flow twin-flame	-	-	$u_l(\Phi_{ef}, R_b)$ linear correlation of burning velocities with stoichiometric addition of H ₂ in small amounts. Flame speeds extrapolated to zero stretch rate.	Stretch free results covering the range $x_{H_2} = (0.2, 0.7)$ $k_b(\Phi_{ef}) = 83 \text{ cm/s}$
	H ₂ addition	$T_i(K) = 300$; $P(atm) = 1$					
	C ₃ H ₈ -air	$R_b = [0, 0.25]$ extended to 1 for the leanest case $\Phi_{ef} = 0.5$; $\Phi_{ef} = [0.5, 1.5]$					
	H ₂ addition	$T_i(K) = 300$; $P(atm) = 1$					

Table 28
Summary of literature references with expressions for burning velocities of **methane-air mixtures**. Applicability ranges

Ref./ year	Authors	P bar	T _u K	P _o bar	T _o K	Φ (-)	f _{res,u} (-)	
[218] 2011	Bougrine, Richard, Veynante	[0, 110]	[0, 950]	1	300	[0.6, 1.3]	[0, 0.25]	(f _{u,m})
[127] 2008	Lafuente	[1, 6] [5, 35]	[330, 480] [500, 680]	1 5	300 500	[0.7, 1.2] [0.8, 1.05]	0	-
[225] 2007	Han, Checkel, Fleck, Nowicki	[1, 5.1]	[298, 473]	1.01325	298	1	0	-
[244] 2006	Tinaut, Melgar, Giménez, Díez	[8, 45]	[600, 1300]	1	298	[0.8, 1.2]	0	-
[245] 2006	Rahim, Elia, Ulinski, Metghalchi	[1, 40.5]	[298, 650]	1.01325	298	[0.8, 1.2]	0	-
[6] 2006	Huang, Zhang, Zeng, Liu, Wang, Jiang	1	300	(1)	(300)	[0.6, 1.4]	0	-
[5] 2004	Liao, Jiang, Cheng	[0.5, 1.5]	[300, 400]	1	300	[0.6, 1.4] [0.7, 1.2]	0 [0, 0.3]	- (f _{u,v})
[195] 2004	Gülder	1.01325	298	(1.01325)	(298)	[0.8, 1.3]	0	-
[246] 2003	Dahoe, De-Goey	[1, 8.7] [0.4, 5.1] [0.3, 30.4]	[298.15, 800] [298, 700] [291, 500]	1 1.01325 1.01325	(298.15) 298 291	[0.67, 1.36] [0.8, 1.5] [0.8, 1.3]	0	-
[234] 2000	Gu, Haq, Lawes, Wooley	[1, 10]	[300, 400]	1	298	{0.8, 1, 1.2}	0	-
[236] 1998	Stone, Clarke, Bethwick	[0.5, 10.4]	[295, 454]	1	298	[0.6, 1.4]	[0, 0.6]	(f _{u,m})
[220] 1997	Müller, Bolling, Peters	[1, 40]	[298, 800]	(1)	(298)	[0.6, 1]	0	-
[190] 1992	Göttgens, Mauss, Peters	[1, 40]	[298, 800]	(1)	(298)	[0.4, 1]	0	-
[217] 1986	Iijima, Takeno	[0.5, 30.4]	[291, 500]	1.01325	291	[0.8, 1.3]	0	-
[247] 1981	Sharma, Agrawal, Gupta	[1, 8.1]	[300, 600]	(1.01325)	300	[0.8, 1.2]	0	-
[248] 1980	Rallis, Garforth	[1, 4.1]	[300, 430]	(1.01325)	(298)	1	0	-
[249] 1978	Tsatsaronis	[0.1, 10.1] 1.01325	298 [300, 430]	(1.01325)	(298)	1	0	-
[250] 1972	Andrews, Bradley	[5.1, 101.3] 1.01325 1.01325	298 [100, 600] [300, 1000]	(1.01325)	(298)	1	0	-
[251] 1967	Barassin, Lisbet, Combourieu, Laffitte	1.01325	[293, 532]	(1.01325)	(293)	1	0	-
[252] 1966	Babkin, Kozachenko	[1, 23.3] [23.3, 70.9]	[323, 473]	(1.01325)	100	1	0	-
[253] 1961	Agnew, Graiff	[0.5, 20.3]	298	(1.01325)	(298)	1	0	-
[254] 1952	Dugger	1.01325	[141, 615]	(1.01325)	(298)	1	0	-
[255] 1951	Smith, Agnew	[0.1, 20.3]	298	(1.01325)	(298)	1	0	-

Table 29
Summary of literature references with expressions for burning velocities of **hydrogen-air mixtures**. Applicability ranges

Ref./ year	Variables & units <i>Authors</i>	P	T _u	P _o	T _o	Φ	f _{res,u}	
		bar	K	bar	K	(-)	(-)	
[131] 1984	Milton, Keck	[0.5, 7.1]	[298, 550]	1.01325	298	1	0	-
[127] 2008	Lafuente	[1, 7]	[330, 500]	1	300	1	0	-
[217] 1986	Iijima, Takeno	[0.5, 25.3]	[291, 500]	1.01325	291	[0.5, 4]	0	-
[190] 1992	Göttgens, Mauss, Peters	[1, 40]	[298, 500]	(1)	(298)	[0.4, 1]	0	-
[256] [232] 2003-05	Verhelst, Sierens (Yetter <i>et al.</i> / O'Conaire <i>et al.</i>)	[1, 16]	[300, 800]	1	300	[0.33, 1]	[0, 0.3]	(f _{u,v})
[257] 2008	D'Errico, Onorati, Ellgas	[1, <60] (16)	[500, 900]	(1)	(300)	[0.36, 1]	[0, 0.5]	(f _{u,m})
[125] [232] [230] 2005-07	Verhelst; Wooley, Lawes, Sierens	[1, 10]	[300, 430]	5	365	[0.3, 1]	[0, 0.3]	(f _{u,v})
[258] 2008	Knop, Benkenida, Jay, Colin	[1, 10]	[300, <1000]	1.01325	298	[0.25, <5]	[0, 0.3]	(f _{u,v})
[259] * 2007	Bradley, Lawes, Liu, Verhelst, Wooley (O'Conaire <i>et al.</i> / Konnov)	{1, 5, 10}	{300, 365}	(1)	{300, 365}	[0.3, 1]	0	-
[126] 2009	Hu, Huang, He, Miao	[1, 80]	[303, 950]	1	303	1	-	-
[214] 2010	Gerke, Steurs, Rebecchi, Boulouchos (O'Conaire <i>et al.</i>)	[<10, >45] [>1, 80]	[<350, >700] [>300, <900]	20 20	600 500	[<0.36, >2.5] [0.4, 3.75]	[0, 0.3] [0, 0.3]	(f _{u,m}) (f _{u,m})
[227] 2011	Verhelst, T'Joel, Vancoillie, Demuynck (Konnov)	[5, 45]	[500, 900]	1	300	[0.33, 5]	[0, 0.5]	(f _{u,v})
[172] 2011	Bougrine, Richard, Nicolle, Veynante	[1, 110]	[300, 950]	1	300	[0.6, 1.3]	[0, 0.3]	(f _{u,m})

(*) Without an analytical correlation

References of chapters six, seven and eight (*fourth part*)

- [1] **Cho HM, He BQ.** Spark ignition natural gas engines – a review. *Energy Conversion and Management* 2007;48(2):608-18.
- [2] **Naber JD, Siebers DL, Di-Julio SS, Westbrook CK.** Effects of natural gas composition on ignition delay under diesel conditions. *Combustion and Flame* 1994;99:192-200.
- [3] **Jessen PF, Melvin A.** Combustion fundamentals relevant to the burning of natural gas. *Progress in Energy and Combustion Science* 1977;4(2):239-55.
- [4] **Ma F, Li S, Zhao J, Qi Z, Deng J, Naeve N, He Y, Zhao S.** A fractal-based quasi-dimensional combustion model for SI engines fueled by hydrogen compressed natural gas. *International Journal of Hydrogen Energy* 2012;37:9892-901.
- [5] **Liao SY, Jiang DM, Cheng Q.** Determination of laminar burning velocities for natural gas. *Fuel* 2004;83(9):1247-50.
- [6] **Huang Z, Zhang Y, Zeng K, Liu B, Wang Q, Jiang D.** Measurements of laminar burning velocities for natural gas-hydrogen-air mixtures. *Combustion and Flame* 2006;146:302-11.
- [7] **Huang B, Hu E, Huang Z, Zeng J, Liu B, Jiang D.** Cycle-by-cycle variations in a spark ignition engine fueled with natural gas-hydrogen blends combined with EGR. *International Journal of Hydrogen Energy* 2009;34:8405-14.
- [8] **Wang J, Huang Z, Fang Y, Liu B, Zeng K, Miao H, Jiang D.** Combustion behaviors of a direct-injection engine operating on various fractions of natural gas-hydrogen blends. *International Journal of Hydrogen Energy* 2007;32(15):3555-64.
- [9] **Wang J, Huang Z, Miao H, Wang X, Jiang D.** Characteristics of direct injection combustion fueled by natural gas-hydrogen mixtures using a constant volume vessel. *International Journal of Hydrogen Energy* 2008;33:1947-56.
- [10] **Wang J, Chen H, Liu B, Huang Z.** Study of cycle-by-cycle variations of a spark ignition engine fueled with natural gas-hydrogen blends. *International Journal of Hydrogen Energy* 2008;33(18):4876-83.
- [11] **Miao H, Jiao Q, Huang Z, Jiang D.** Effect of initial pressure on laminar combustion characteristics of hydrogen enriched natural gas. *International Journal of Hydrogen Energy* 2008;33:3876-85.
- [12] **Miao H, Jiao Q, Huang Z, Jiang D.** Measurement of laminar burning velocities and Markstein lengths of diluted hydrogen-enriched natural gas. *International Journal of Hydrogen Energy* 2009;34:507-18.
- [13] **Miao H, Ji M, Jiao Q, Huang Q, Huang Z.** Laminar burning velocity and Markstein length of nitrogen diluted natural gas/hydrogen/air mixtures at normal, reduced and elevated pressures. *International Journal of Hydrogen Energy* 2009;34:3145-55.
- [14] **Hu E, Huang Z, Liu B, Zheng J, Gu X, Huang B.** Experimental investigation on performance and emissions of a spark-ignition engine fueled with natural gas-hydrogen blends combined with EGR. *International Journal of Hydrogen Energy* 2009;34(1):528-39.
- [15] **Hu E, Huang Z, Liu B, Zheng J, Gu X.** Experimental study on combustion characteristics of a spark-ignition engine fueled with natural gas-hydrogen blends combining with EGR. *International Journal of Hydrogen Energy* 2009;34(2):1035-44.
- [16] **Bauer CG, Forest TW.** Effect of hydrogen addition on the performance of methane-fueled vehicles. Part I: effect on S.I. engine performance. *International Journal of Hydrogen Energy* 2001;26:55-70.
- [17] **Karim GA.** Hydrogen as a spark ignition engine fuel. *International Journal of Hydrogen Energy* 2003;28:569-77.
- [18] **Verhelst S, Wallner T.** Hydrogen-fueled internal combustion engines. *Progress in Energy and Combustion Science* 2009;35:490-527.
- [19] **Gorensek MB, Forsberg CW.** Relative economic incentives for hydrogen from nuclear, renewable, and fossil energy sources. *International Journal of Hydrogen Energy* 2009;34:4237-42.
- [20] **Das LM, Gulati R, Gupta PK.** A comparative evaluation of the performance characteristics of a spark ignition engine using hydrogen and compressed natural gas as alternative fuels. *International Journal of Hydrogen Energy* 2000;25:783-93.
- [21] **Verhelst S, Sierens R.** Hydrogen engine specific properties. *International Journal of Hydrogen Energy* 2001;26:987-90.

- [22] **Heffel JW.** NO_x emission reduction in a hydrogen fueled internal combustion engine at 3000 rpm using exhaust gas recirculation. *International Journal of Hydrogen Energy* 2003;28:1285-92.
- [23] **Mohammadi A, Shioji M, Nakai Y, Ishikura W, Tabo E.** Performance and combustion characteristics of a direct injection SI hydrogen engine. *International Journal of Hydrogen Energy* 2007;32:296-304.
- [24] **Aliramezani M, Chitsaz I, Mozafari AA.** Thermodynamic modeling of partially stratified charge engine characteristics for hydrogen-methane blends at ultra-lean conditions. *International Journal of Hydrogen Energy* 2013;38:10640-47.
- [25] **Schefer RW, Wicksall DM, Agrawal AK.** Combustion of hydrogen enriched methane in a lean premixed swirl-stabilized burner. *Proceedings of the 29th international symposium on combustion* 2002;843-51.
- [26] **Bell SR, Gupta M.** Extension of the lean operating limit for natural gas fueling of a spark ignited engine using hydrogen blending. *Combustion Science and Technology* 1997;123:23-48.
- [27] **Bade-Shrestha SO, Karim GA.** Hydrogen as an additive to methane for spark ignition engine applications. *International Journal of Hydrogen Energy* 1999;24:577-86.
- [28] **Sierens R, Rosseel E.** Variable composition hydrogen/natural gas mixtures for increased engine efficiency and decreased emissions. *Journal of Engineering for Gas Turbines and Power* 2000;122:135-40.
- [29] **Bauer CG, Forest TW.** Effect of hydrogen addition on the performance of methane-fueled vehicles. Part II: driving cycle simulations. *International Journal of Hydrogen Energy* 2001;26:71-90.
- [30] **Verhelst S, Sierens R.** Aspects concerning the optimization of a hydrogen fueled engine. *International Journal of Hydrogen Energy* 2001;26:981-5.
- [31] **Goltsov VA, Veziroglu TN, Goltsova LF.** Hydrogen civilization of the future – a new conception of the IAHE. *International Journal of Hydrogen Energy* 2006;31:153-9.
- [32] **Law CK, Kwon OC.** Effects of hydrocarbon substitution on atmospheric hydrogen-air flame propagation. *International Journal of Hydrogen Energy* 2004;29(8):867-79.
- [33] **Gruber F, Herdin G, Klausner J, Robitschko R.** Use of hydrogen and hydrogen mixtures in a gas engine. *Proceedings of the 1st international symposium on hydrogen internal combustion engines, Graz, Austria* 2006;34-48.
- [34] **Wallner T, Lohse-Busch H, Ng H, Peters RW.** Results of research engine and vehicle drive cycle testing during blended hydrogen-methane operation. *Proceedings of National Hydrogen Association Annual Conference, San Antonio, Texas, 2007.*
- [35] **Wallner T, Ng H, Peters RW.** The effects of blending hydrogen with methane on engine operation, efficiency and emissions. *SAE Paper 2007-01-0474, 2007.*
- [36] **Eichlseder H, Wallner T, Freymann R, Ringler J,** The potential of hydrogen internal combustion engines in a future mobility scenario. *SAE Paper 2003-01-2267, 2003.*
- [37] **Karim GA, Wierzba I, Al-Alousi Y.** Methane-hydrogen mixtures as fuels. *International Journal of Hydrogen Energy* 1996;21(7):625-31.
- [38] **El-Sherif SA.** Control of emissions by gaseous additives in methane-air and carbon monoxide-air flames. *Fuel* 2000;79:567-75.
- [39] **Ortenzi F, Chiesa M, Scarcelli R, Pede G.** Experimental tests of blends of hydrogen and natural gas in light-duty vehicles. *International Journal of Hydrogen Energy* 2008;33:3225-9.
- [40] **Larsen JF, Wallace JS.** Comparison of emissions and efficiency of a turbocharged lean-burn natural gas and hythane-fueled engine. *Journal of Engineering for Gas Turbines and Power* 1997;119(1):218-26.
- [41] **Mariani A, Morrone B, Unich A.** Numerical evaluation of internal combustion spark ignition engines performance fueled with hydrogen-natural gas blends. *International Journal of Hydrogen Energy* 2012;37:2644-54.
- [42] **Klell M, Eichlseder H, Sartory M.** Mixtures of hydrogen and methane in the internal combustion engine – synergies, potential and regulations. *International Journal of Hydrogen Energy* 2012;37:11531-40.
- [43] **Ristovski ZD, Morawska L, Hitchins J, Thomas S, Greenaway C, Gilbert D.** Particle emissions from compressed natural gas engines. *Journal of Aerosol Science* 2000;31:403-13.
- [44] **Prati MV, Mariani A, Torbati R, Unich A, Costagliola MA, Morrone B.** Emissions and combustion behavior of a bi-fuel gasoline and natural gas spark ignition engine. *SAE International Journal Fuels Lubricants* 2011;4:328-38.

- [45] **El-Sherif SA.** Effects of natural gas composition on the nitrogen oxide, flame structure and burning velocity under laminar premixed flame conditions. *Fuel* 1998;77:1539-47.
- [46] **Mello P, Pelliza G, Cataluna R, Da-Silva R.** Evaluation of the maximum horsepower of vehicles converted for use with natural gas fuel. *Fuel* 2006;85:2180-6.
- [47] **Huang Z, Shiga S, Ueda T, Jingu N, Nakamura H, Ishima T, Obokata T, Tsue M, Kono M.** A basic behavior of CNG DI combustion in a spark ignited rapid compression machine. *JSME International Journal, Series B, Fluids and Thermal Engineering* 2002;45(4):891-900.
- [48] **Ben L, Dacros NR, Truquet R, Charnay G.** Influence of air/fuel ratio on cyclic variation and exhaust emission in natural gas SI engine, SAE Paper 992901; 1999.
- [49] **Rousseau S, Lemoult B, Tazerout M.** Combustion characteristics of natural gas in a lean burn spark-ignition engine. *Proceedings of the Institution of Mechanical Engineers, Part D, Journal of Automobile Engineering* 1999;213(D5):481-9.
- [50] **Das A, Watson HC.** Development of a natural gas spark ignition engine for optimum performance. *Proceedings of the Institution of Mechanical Engineers, Part D, Journal of Automobile Engineering* 1997;211:361-78.
- [51] **Blarigan PV, Keller JO.** A hydrogen-fueled internal combustion engine designed for single speed power operation. *International Journal of Hydrogen Energy* 2002;23(7):603-9.
- [52] **Akansu SO, Dulger A, Kahraman N.** Internal combustion engines fueled by natural gas-hydrogen mixtures. *International Journal of Hydrogen Energy* 2004;29(14):1527-39.
- [53] **Halter F, Chauveau C, Djebaili-Chaumeix N, Gökalp I.** Characterization of the effects of pressure and hydrogen concentration on laminar burning velocities of methane-hydrogen-air mixtures. *Proceedings of the Combustion Institute* 2005;30:201-8.
- [54] **Ilbas M, Crayford AP, Yilmaz I, Bowen PJ, Syred N.** Laminar-burning velocities of hydrogen-air and hydrogen-methane-air mixtures: an experimental study. *International Journal of Hydrogen Energy* 2006;31:1768-79.
- [55] **Mandilas C, Ormsby MP, Sheppard CGW, Woolley R.** Effects of hydrogen addition on laminar and turbulent premixed methane and iso-octane/air flames. *Proceedings of the Combustion Institute* 2007;31:1443-50.
- [56] **Hoekstra RL, Blarigan PV, Mulligan N.** NO_x emissions and efficiency of hydrogen, natural gas, and hydrogen/natural gas blended fuels. SAE Paper 961103; 1996.
- [57] **Rakopoulos CD, Kyritsis DC.** Hydrogen enrichment effects on the second law analysis of natural and landfill gas combustion in engine cylinders. *International Journal of Hydrogen Energy* 2006;31:1384-93.
- [58] **Schefer RW.** Hydrogen enrichment for improved lean flame stability. *International Journal of Hydrogen Energy* 2003;28:1131-41.
- [59] **Choudhuri AR, Gollahalli SR.** Stability of hydrogen-hydrocarbon blended fuel flames. *AIAA Journal of Propulsion and Power* 2003;19(2):220-5.
- [60] **Hawkes ER, Chen JH.** Direct numerical simulation of hydrogen-enriched lean premixed methane-air flames. *Combustion and Flame* 2004;138:242-58.
- [61] **Sankaran R, Im HG.** Effect of hydrogen addition on the flammability limit of stretched methane-air premixed flames. *Combustion Science and Technology* 2006;178:1585-611.
- [62] **Munshi S.** Medium-heavy duty hydrogen enriched natural gas spark ignition IC engine operation. *Proceedings of the 1st international symposium on hydrogen internal combustion engines, Graz, Austria* 2006;71-82.
- [63] **Nagalingam B, Duebel F, Schmillen K.** Performance study using natural gas, hydrogen supplemented natural gas and hydrogen in AVL research engine. *International Journal of Hydrogen Energy* 1983;8(9):715-20.
- [64] **Hoekstra RL, Collier K, Mulligan N, Chew L.** Experimental study of a clean burning vehicle fuel. *International Journal of Hydrogen Energy* 1995;20:737-45.
- [65] **Mariani A, Morrone B, Unich A.** Numerical modeling of internal combustion engines fueled by hydrogen-natural gas blends. *ASME international mechanical engineering congress exposition; 2008.*
- [66] **Morrone B, Unich A.** Numerical investigation on the effects of natural gas and hydrogen blends on engine combustion. *International Journal of Hydrogen Energy* 2009;34:4626-34.
- [67] **Sita-Rama-Raju AV, Ramesh A, Nagalingam B.** Effect of hydrogen induction on the performance of a natural-gas fueled lean-burn SI engine. *Journal of the Energy Institute* 2000;73(496):143-8.

- [68] **Wong YK, Karim GA.** An analytical examination of the effects of hydrogen addition on cyclic variations in homogeneously charged compression-ignition engines. *International Journal of Hydrogen Energy* 2000;25(12):1217-24.
- [69] **Huang Z, Liu B, Zeng K, Huang Y, Jiang D, Wang X, et al.** Experimental study on engine performance and emissions for an engine fueled with natural gas-hydrogen mixtures. *Energy & Fuels* 2006;20(5):2131-6.
- [70] **Huang Z, Wang J, Liu B, Zeng K, Yu K, Jiang D.** Combustion characteristics of a direct-injection engine fueled with natural gas-hydrogen mixtures. *Energy & Fuels* 2006;20(2):540-6.
- [71] **Huang Z, Wang J, Liu B, Zeng K, Yu K, Jiang D.** Combustion characteristics of a direct-injection engine fueled with natural gas-hydrogen blends under various injection timings. *Energy & Fuels* 2006;20(4):1498-504.
- [72] **Huang Z, Wang J, Liu B, Zeng K, Yu K, Jiang D.** Combustion characteristics of a direct-injection engine fueled with natural gas-hydrogen blends under different ignition timings. *Fuel* 2007;86:381-7.
- [73] **Bysveen M.** Engine characteristics of emissions and performance using mixtures of natural gas and hydrogen. *International Journal of Hydrogen Energy* 2007;32(4):482-9.
- [74] **Liu B, Huang Z, Zeng K, Chen H, Wang X, Miao H, et al.** Experimental study on emissions of a spark-ignition engine fueled with natural gas-hydrogen blends. *Energy & Fuels* 2008;22(1):273-7.
- [75] **Hu E, Huang Z, He J, Jin C, Zheng J.** Experimental and numerical study on laminar burning characteristics of premixed methane-hydrogen-air flames. *International Journal of Hydrogen Energy* 2009;34(11):4876-88.
- [76] **Hu E, Huang Z, He J, Zheng J, Miao H.** Measurements on laminar burning velocities and onset of cellular instabilities of methane-hydrogen-air flames at elevated pressure and temperatures. *International Journal of Hydrogen Energy* 2009;34:5574-84.
- [77] **Hu E, Huang Z, Zheng J, Li Q, He J.** Numerical study on laminar burning velocity and NO formation of premixed methane-hydrogen-air flames. *International Journal of Hydrogen Energy* 2009;34:6545-57.
- [78] **Hu E, Huang Z, He J, Miao H.** Experimental and numerical study on lean premixed methane-hydrogen-air flames at elevated pressure and temperatures. *International Journal of Hydrogen Energy* 2009;34:6951-60.
- [79] **Tinaut FV, Melgar A, Giménez B, Reyes M.** Prediction of performance and emissions of an engine fueled with natural gas/hydrogen blends. *International Journal of Hydrogen Energy* 2011;36:947-56.
- [80] **Wang J, Huang Z, Zheng J, Miao H.** Effect of partially premixed and hydrogen addition on natural gas direct injection lean combustion. *International Journal of Hydrogen Energy* 2009;34:9239-47.
- [81] **Wang X, Zhang H, Yao B, Lei Y, Sun X, Wang D, Ge Y.** Experimental study on factors affecting lean combustion limit of SI engine fueled with compressed natural gas and hydrogen blends. *Energy* 2012;38:58-65.
- [82] **Ma F, Wang Y, Liu HQ, Li Y, Wang JJ, Zhao S.** Experimental study on thermal efficiency and emission characteristics of a lean burn hydrogen enriched natural gas engine. *International Journal of Hydrogen Energy* 2007;32(18):5067-75.
- [83] **Ma F, Liu H, Wang Y, Li Y, Wang JJ, Zhao S.** Combustion and emission characteristics of a port-injection HCNG engine under various ignition timings. *International Journal of Hydrogen Energy* 2008; 33(2):816-22.
- [84] **Ma F, Wang Y, Liu H, Li Y, Wang J, Ding S.** Effects of hydrogen addition on cycle-by-cycle variations in a lean burn natural gas spark-ignition engine. *International Journal of Hydrogen Energy* 2008;33(2):823-31.
- [85] **Ma F, Wang Y.** Study on the extension of lean operation limit through hydrogen enrichment in a natural gas spark ignition engine. *International Journal of Hydrogen Energy* 2008;33(4):1416-24.
- [86] **Ma F, Wang Y, Wang M, Liu H, Wang J, Ding S, et al.** Development and validation of a quasi-dimensional combustion model for SI engines fueled by HCNG with variable hydrogen fractions. *International Journal of Hydrogen Energy* 2008;33:4863-75.
- [87] **Ma F, Liu H, Wang Y, Wang J, Ding S, Zhao S.** A quasi-dimensional combustion model for SI engine fueled by hydrogen enriched compressed natural gas. *SAE Paper* 2008-01-1633, 2008.

- [88] **Ma F, Wang M.** Performance and emission characteristics of a turbocharged spark-ignition hydrogen-enriched compressed natural gas engine under wide open throttle operating conditions. *International Journal of Hydrogen Energy* 2010;35:12502-9.
- [89] **Ma F, Deng J, Qi Z, Li S, Cheng R, Yang H, Zhao S.** Study on the calibration coefficients of a quasi-dimensional model for HCNG engine. *International Journal of Hydrogen Energy* 2011;33:9278-85.
- [90] **Mariani A, Prati MV, Unich A, Morrone B.** Combustion analysis of a spark ignition i.c. engine fueled alternatively with natural gas and hydrogen-natural gas blends. *International Journal of Hydrogen Energy* 2013;38:1616-23.
- [91] **Phillips JN, Roby RJ.** Hydrogen-enriched natural gas offers economic NO_x reduction alternative. *Power Engineering (Barrington, Illinois)* 2000;104(5):3.
- [92] **Raman V, Hansel J, Fulton J, Lynch F, Bruderly D.** Hythane – An ultraclean transportation fuel. *Proceedings of 10th World Hydrogen Conference, Cocoa Beach, Florida, USA, 1994.*
- [93] **Genovese A, Contrisciani N, Ortenzi F, Cazzola V.** On road experimental tests of hydrogen-natural gas blends on transit buses. *International Journal of Hydrogen Energy* 2011;36:1775-83.
- [94] **Allenby S, Chang WC, Megaritis A, Wyszynski ML.** Hydrogen enrichment: a way to maintain combustion stability in a natural gas fueled engine with exhaust gas recirculation, the potential of fuel reforming. *Proceedings of the Institution of Mechanical Engineers, Part D: Journal of Automobile Engineering* 2001;215(3):405–18.
- [95] **Dimopoulos P, Bach C, Soltic P, Boulouchos K.** Hydrogen-natural gas blends fuelling passenger car engines: combustion, emissions and well-to-wheels assessment. *International Journal of Hydrogen Energy* 2008;33(23):7224-36.
- [96] **Dimopoulos P, Rechsteiner C, Soltic P, Laemmle C, Boulouchos K.** Increase of passenger car engine efficiency with low engine-out emissions using hydrogen–natural gas mixtures: a thermodynamic analysis. *International Journal of Hydrogen Energy* 2007;32(14):3073-83.
- [97] **Ivanic Z, Ayala F, Goldwit J, Heywood JB.** Effects of hydrogen enhancement on efficiency and NO_x emissions of lean and EGR-diluted mixtures in a SI engine. *SAE paper 2005-01-0253, 2005.*
- [98] **Blarigan PV, Keller JO.** A hydrogen-fueled internal combustion engine designed for single speed-power operation. *Journal of Engineering for Gas Turbines and Power* 2003;125(3):783–90.
- [99] **Heywood JB.** *Internal combustion engine fundamentals.* McGraw-Hill, New-York; 1988.
- [100] **Sen AK, Longwic R, Litak G, Górski K.** Analysis of cycle-to-cycle pressure oscillations in a diesel engine. *Mechanical Systems and Signal Processing* 2008;22(2):362-73.
- [101] **Galloni E.** Analyses about parameters that affect cyclic variation in a spark ignition engine. *Applied Thermal Engineering Journal* 2009;29(5-6):1131-7.
- [102] **Tinaut FV, Giménez B, Horrillo A, Cabaco G.** Use of multi-zone combustion models to analyze and predict the effect of cyclic variations on SI engines. *SAE Paper 2000-1-0961, 2000.*
- [103] **Litak G, Kaminski T, Czarnigowski J, Zukowski D, Wendeker M.** Cycle-to-cycle oscillations of heat release in a spark ignition engine. *Meccanica* 2007;42:423-33.
- [104] **Litak G, Kaminski T, Rusinek R, Czarnigowski J, Wendeker M.** Patterns in the combustion process in a spark ignition engine. *Chaos, Solitons & Fractals* 2008;35(3):578-85.
- [105] **Litak G, Kaminski T, Czarnigowski J, Sen A, Wendeker M.** Combustion process in a spark ignition engine: analysis of cyclic peak pressure and peak pressure angle oscillations. *Meccanica* 2009;44:1-11.
- [106] **Selim MY.** Effect of engine parameters and gaseous fuel type on the cyclic variability of dual fuel engines. *Fuel* 2005;84(7-8):961-71.
- [107] **Hill PG.** Cyclic variations and turbulence structure in spark ignition engines. *Combust Flame* 1988;72(1):73-89.
- [108] **Hill PG, Kapil A.** The relationship between cyclic variations in spark-ignition engines and the small structure of turbulence. *Combust Flame* 1989;78(2):237-47.
- [109] **Sen AK, Zheng J, Huang Z.** Dynamics of cycle-to-cycle variations in a natural gas direct-injection spark-ignition engine. *Applied Energy* 2011;88(7):2324-34.
- [110] **Ebrahimi R, Desmet B.** An experimental investigation on engine speed and cyclic dispersion in an HCCI engine. *Fuel* 2010;89(8):2149-56.
- [111] **Sen A, Litak G, Edwards K, Finney C, Daw C, Wagner R.** Characteristics of cyclic heat release variability in the transition from spark ignition to HCCI in a gasoline engine. *Applied Energy* 2011;88(5):1649-55.

- [112] **Vermorel O, Richard S, Colin O, Angelberger C, Benkenida A, Veynante S.** Towards the understanding of cyclic variability in a spark ignited engine using multi-cycle LES. *Combustion and Flame* 2009;156(8):1525-41.
- [113] **Curto-Risso P, Medina A, Hernández AC, Guzmán-Vargas L, Angulo-Brown F.** On cycle-to-cycle heat release variations in a simulated spark ignition heat engine. *Applied Energy* 2011;88(5):1557-67.
- [114] **Turns SR.** An introduction to combustion. McGraw-Hill, New-York, 2000.
- [115] **Tinaut FV, Reyes M, Giménez B, Pérez A.** Characterization of combustion process and cycle-to-cycle variations in a spark ignition engine fueled with natural gas/hydrogen mixtures. Scientific conference on Combustion and related fields -SPEIC14- Towards Sustainable Combustion, Lisboa. Nov 19-21, 2014.
- [116] **Wang J, Huang Z, Miao H, Wang X, Jiang D.** Study of cyclic variations of direct-injection combustion fueled with natural gas-hydrogen blends using a constant volume vessel. *International Journal of Hydrogen Energy* 2008;33:7580-91.
- [117] **Reyes M, Melgar A, Pérez A, Giménez B.** Study of the cycle-to-cycle variations of an internal combustion engine fueled with natural gas-hydrogen blends from the diagnosis of combustion pressure. *International Journal of Hydrogen Energy* 2013;38:15477-87.
- [118] **Bilgin A.** Geometric features of the flame propagation process for an SI engine having dual ignition system. *International Journal of Energy Research* 2002;26(11):987-1000.
- [119] **Bradley D, Hicks RA, Lawes M, Sheppard CGW, Woolley R.** The measurement of laminar burning velocities and Markstein numbers, for iso-octane/air and iso-octane/n-heptane/air mixtures, at elevated temperatures and pressures, in an explosion bomb. *Combustion and Flame* 1998;115(1-2):126-44.
- [120] **Metghalchi M, Keck JC.** Laminar burning velocity of propane-air mixtures at high temperature and pressure. *Combustion and Flame* 1980;38:143-54.
- [121] **Metghalchi M, Keck JC.** Burning velocities of mixtures of air with methanol, isooctane, and indolene at high pressure and temperature. *Combustion and Flame* 1982;48:191-210.
- [122] **Bradley D, Gaskell PH, Gu XJ.** Burning velocities, Markstein lengths, and flame quenching for spherical methane-air flames: a computational study. *Combustion and Flame* 1996;104(1-2):176-98.
- [123] **Sun CJ, Sung CJ, He L, Law CK.** Dynamics of weakly stretched flames quantitative description and extraction of global flame parameters. *Combustion and Flame* 1999;118:108-28.
- [124] **Reyes M.** Characterization of the combustion and auto-ignition processes of liquid fuels in homogeneous mixtures for using in internal combustion engines running in HCCI mode (Spanish). PhD thesis 2008, University of Valladolid (Spain).
- [125] **Verhelst S, Woolley R, Lawes M, Sierens R.** Laminar and unstable burning velocities and Markstein lengths of hydrogen-air mixtures at engine-like conditions. *Proceedings of the Combustion Institute* 2005;30:209-16.
- [126] **Hu EJ, Huang ZH, He JJ, Miao HY.** Experimental and numerical study on laminar burning velocities and flame instabilities of hydrogen-air mixtures at elevated pressures and temperatures. *International Journal of Hydrogen Energy* 2009;34:8741-55.
- [127] **Lafuente A.** Methodology for the laminar burning velocity diagnosis in mixtures of fuels from the instantaneous pressure in a constant volume combustion bomb (Spanish). PhD thesis 2008, University of Valladolid (Spain).
- [128] **Ranzi E, Frassoldati A, Grana R, Cuoci A, Faravelli T, Kelley AP, Law CK.** Hierarchical and comparative kinetic modeling of laminar flame speeds of hydrocarbon and oxygenated fuels. *Progress in Energy and Combustion Science* 2012;38(4):468-501.
- [129] **Coppens FHV, de Ruyck J, Konnov AA.** The effects of composition on burning velocity and nitric oxide formation in laminar premixed flames of $\text{CH}_4+\text{H}_2+\text{O}_2+\text{N}_2$. *Combustion and Flame* 2007;149(4):409-17.
- [130] **Hermanns RTE, Konnov AA, Bastiaans RJM, De-Goey LPH, Lucka K, Köhne H.** Effects of temperature and composition on the laminar burning velocity of $\text{CH}_4+\text{H}_2+\text{O}_2+\text{N}_2$ flames. *Fuel* 2010;89:114-21.
- [131] **Milton BE, Keck JC.** Laminar burning velocities in stoichiometric hydrogen and hydrogen-hydrocarbon gas mixtures. *Combustion and Flame* 1984;58:13-22.

- [132] **Sher E, Refael S.** A simplified reaction scheme for the combustion of hydrogen enriched methane-air flame. *Combustion Science and Technology* 1988;59:371-89.
- [133] **Refael S, Sher E.** Reaction kinetics of hydrogen-enriched methane-air and propane-air flames. *Combustion and Flame* 1989;78:326-38.
- [134] **Tanoue K, Goto S, Shimada F, Hamatake T.** Effects of hydrogen addition on stretched premixed laminar methane flames. 1st Report, effects on laminar burning velocity. *Transactions of JSME* 2003;69:162-8.
- [135] **Halter F, Chauveau C, Gokalp I.** Characterization of the effects of hydrogen addition in premixed methane-air flames. *Journal of Hydrogen Energy* 2007;32:2585-92.
- [136] **Halter F, Tahtouh T, Mounaim-Rousselle C.** Nonlinear effects of stretch on the flame front propagation. *Combustion and Flame* 2010;157:1825-32.
- [137] **Tahtouh T, Halter F, Samson E, Mounaim-Rousselle C.** Effects of hydrogen addition and nitrogen dilution on the laminar flame characteristics of premixed methane-air flames. *International Journal of Hydrogen Energy* 2009;34:8329-38.
- [138] **Yu G, Law CK, Wu CK.** Laminar flame speeds of hydrocarbon-air mixtures with hydrogen addition. *Combustion and Flame* 1986;63:339-47.
- [139] **Liu Y, Lenze B, Leuckel W.** Investigation on the laminar and turbulent burning velocities of premixed lean and rich flames of methane-hydrogen-air mixtures. *Progress in Astronautics and Aeronautics* 1991;131:259-74.
- [140] **Ren JY, Qin W, Egolfopoulos FN, Tsotsis TT.** Strain-rate effects on hydrogen-enhanced lean premixed combustion. *Combustion and Flame* 2001;124:717-20.
- [141] **Park O, Veloo PS, Liu N, Egolfopoulos FN.** Combustion characteristics of alternative gaseous fuels. *Proceedings of the Combustion Institute* 2011;33:887-94.
- [142] **Coppens FHV, de Ruyck J, Konnov AA.** Effects of hydrogen enrichment on adiabatic burning velocity and NO formation in methane-air flames. *Thermal and Fluid Science* 2007;31(5):437-44.
- [143] **Hermanns RTE, Konnov AA, Bastiaans RJM, De-Goey LPH.** Laminar burning velocities of diluted hydrogen-oxygen-nitrogen mixtures. *Energy Fuels* 2007;21(4):1977-81.
- [144] **Hermanns RTE.** Laminar burning velocities of methane-hydrogen-air mixtures. PhD thesis 2007. Eindhoven University, Universal Press, Veenendaal, Netherlands.
- [145] **Scholte TG, Vaags PB.** Burning velocities of mixtures of hydrogen, carbon monoxide and methane with air. *Combustion and Flame* 1959;3:511-24.
- [146] **Wu FJ, Kelley AP, Tang CL, Zhu DL, Law CK.** Measurements and correlation of laminar flame speeds of CO and C₂-hydrocarbons with hydrogen addition at atmospheric and elevated pressures. *International Journal of Hydrogen Energy* 2011;36:13171-80.
- [147] **Dong Y, Vagelopoulos CM, Spedding GR, Egolfopoulos FN.** Measurement of laminar flame speeds through digital particle image velocimetry: mixtures of methane and ethane with hydrogen, oxygen, nitrogen, and helium. *Proceedings of the Combustion Institute*; 2002:1419-26.
- [148] **Tang C, Huang Z, Jin C, He J, Wang J, Wang X, et al.** Laminar burning velocities and combustion characteristics of propane-hydrogen-air premixed flames. *International Journal of Hydrogen Energy* 2008;33:4906-14.
- [149] **Tang C, He J, Huang Z, Jin C, Wang J, Wang X, et al.** Measurements of laminar burning velocities and Markstein lengths of propane-hydrogen-air mixtures at elevated pressures and temperatures. *International Journal of Hydrogen Energy* 2008;33:7274-85.
- [150] **Tang C, Huang Z, Law CK.** Determination, correlation, and mechanistic interpretation of effects of hydrogen addition on laminar flame speeds of hydrocarbon-air mixtures. *Proceedings of the Combustion Institute* 2011;33:921-8.
- [151] **Sher E, Ozdor N.** Laminar burning velocities of n-butane-air mixtures enriched with hydrogen. *Combustion and Flame* 1992;89:214-20.
- [152] **Tahtouh T, Halter F, Mounaim-Rousselle C.** Laminar premixed flame characteristics of hydrogen blended isooctane-air-nitrogen mixtures. *International Journal of Hydrogen Energy* 2011;36:985-91.
- [153] **McLean IC, Smith DB, Taylor SC.** The use of carbon monoxide-hydrogen burning velocities to examine the rate of the CO+OH reaction. *Proceedings of the 25th international symposium on combustion* 1994;749-57.
- [154] **Hassan MI, Aung KT, Faeth GM.** Properties of laminar premixed CO-H₂-air flames at various pressures. *Journal of Propulsion and Power* 1997;13(2):239-45.

- [155] Sun H, Yang SI, Jomaas G, Law CK. High-pressure laminar flame speeds and kinetic modeling of carbon monoxide – hydrogen combustion. *Proceedings of the Combustion Institute* 2007;31:439-46.
- [156] Vagelopoulos CM, Egolfopoulos FN. Laminar flame speeds and extinction strain rates of mixtures of carbon monoxide with hydrogen, methane and air. *Proceedings of the 25th international symposium on combustion* 1994;1317-23.
- [157] Natarajan J, Lieuwen T, Seitzman J. Laminar flame speeds of H₂-CO mixtures: effect of CO₂ dilution, preheat temperature, and pressure. *Combustion and Flame* 2007;151:104-19.
- [158] Scholte TG, Vaags PB. The influence of small quantities of hydrogen and hydrogen compounds on the burning velocity of carbon monoxide-air flames. *Combustion and Flame* 1959;3:503-10.
- [159] Dong C, Zhou Q, Zhao Q, Zhang Y, Xu T, Hui S. Experimental study on the laminar flame speed of hydrogen-carbon monoxide-air mixtures. *Fuel* 2009;88:1858-63.
- [160] Di-Sarli V, Di-Benedetto A. Laminar burning velocity of hydrogen-methane-air premixed flames. *International Journal of Hydrogen Energy* 2007;32:637-46.
- [161] Kee RJ, Rupley FM, Miller JA. **TRANSPORT (CHEMKIN Collection part)**: A Fortran computer code package for the evaluation of gas-phase viscosities, conductivities and diffusion coefficients. Sandia National Laboratories, Albuquerque, New Mexico, 1983; Report SAND 83-8209.
- [162] Kee RJ, Grcar JF, Smooke MD, Miller JA. **PREMIX (CHEMKIN Collection part)**: A Fortran program for modeling steady laminar one-dimensional premixed flames. Sandia National Laboratories, Albuquerque, New Mexico, 1985; Report SAND 85-8240.
- [163] Kee RJ, Rupley FM, Miller JA. **CHEMKIN_II (CHEMKIN Collection part)**: A Fortran chemical kinetics package for the analysis of gas-phase chemical kinetics. Sandia National Laboratories, Albuquerque, New Mexico, 1989; Report SAND 89-8009.
- [164] Kee RJ, Rupley FM, Miller JA, Coltrin ME, Grcar JF, Meeks E, Moffat HK, Lutz AE, Dixon-Lewis G, Smooke MD, Warnatz J, Evans GH, Larson RS, Mitchell RE, Petzold LR, Reynolds WC, Caracotsios M, Stewart WE, Glarborg P, Wang C, Adigun O. A software package for the analysis of gas-phase chemical kinetics and plasma kinetics. CHEMKIN program & subroutine library. CHEMKIN Collection part, Release 3.6, Reaction Design, Inc. San Diego, California, 2000.
- [165] Kee RJ, Rupley FM, Miller JA, Coltrin ME, Grcar JF, Meeks E, Moffat HK, Lutz AE, Dixon-Lewis G, Smooke MD, Warnatz J, Evans GH, Larson RS, Mitchell RE, Petzold LR, Reynolds WC, Caracotsios M, Stewart WE, Glarborg P, Wang C, Adigun O, Houf WG, Chou CP, Miller SF, Ho P, Young DJ. CHEMKIN Software, Release 4.0, Reaction Design, Inc. San Diego, California, 2004.
- [166] CHEMKIN (4.0.1). Theory manual [chapter 12]; 2004.
- [167] Rogg B. **COSILAB, RUN-1DL**: Cambridge universal laminar flame code. Cambridge University, Department of Engineering Report 1991; CUED/A-THERMO/TR39.
- [168] Rogg B. **COSILAB, RUN-1DL**: The Cambridge universal laminar flamelet computer code. Reduced kinetic mechanisms for applications in combustion systems, Appendix C. Springer-Verlag, Berlin-Heidelberg-NewYork, 1993.
- [169] Smith GP, Golden DM, Frenklach M, Moriarty NW, Eiteneer B, Goldenberg M, Bowman CT, Hanson RK, Song S, Gardiner WCjr, Lissianski VV, Qin Z. **GRI-Mech**: An optimized detailed chemical reaction mechanism for methane combustion, 1995; Report GRI-95/0058.
- [170] **GRI-Mech**. http://www.me.berkeley.edu/gri_mech/releases.html/, 2011.
- [171] Frenklach M, Bowman T, Smith G, Gardiner B. The “**GRI-Mech_3.0**” chemical kinetic mechanism, 1999.
- [172] Bougrine S, Richard S, Nicolle A, Veynante D. Numerical study of laminar flame properties of diluted methane-hydrogen-air flames at high pressure and temperature using detailed chemistry. *International Journal of Hydrogen Energy* 2011;36:12035-47.
- [173] Li J, Zhao Z, Kazakov A, Dryer FL. **Princeton-Mech**. <http://www.princeton.edu/wcombust/database/files/other/>, 2011.
- [174] Wang H, You X, Joshi AV, Davis SG, Laskin A, Egolfopoulos FN, et al. **USC_II-Mech**. High-temperature combustion reaction model of H₂/CO/C₁-C₄ compounds. http://ignis.usc.edu/USC_Mech-II.htm/, 2011.
- [175] Konnov AA. **Konnov-Mech_5.0**. <http://homepages.vub.ac.be/~akonnov/>, 2011.
- [176] Sileghem L, Vancoillie J, Demuyneck J, Galle J, Verhelst S. Alternative fuels for spark-ignition engines: Mixing rules for the laminar burning velocity of gasoline-alcohol blends. *Energy Fuels* 2012;26:4721-7.

- [177] **Payman W, Wheeler RV.** The combustion of complex gaseous mixtures. *Fuel* 1922;1:185.
- [178] **Hirasawa T, Sung CJ, Joshi A, Yang Z, Wang H, Law CK.** Determination of laminar flame speeds using digital particle image velocimetry: Binary fuel blends of ethylene, n-butane, and toluene. *Proceedings of the Combustion Institute* 2002;29:1427-34.
- [179] **Ji C, Egolfopoulos FN.** Flame propagation of mixtures of air with binary liquid fuel mixtures. *Proceedings of the Combustion Institute* 2011;33(1):955-61.
- [180] **Vagelopoulos CM, Egolfopoulos FN, Law CK.** Further considerations on the determination of laminar flame speeds with the counter-flow twin-flame technique. *Proceedings of the Combustion Institute* 1994;25:1341-7.
- [181] **Tse SD, Zhu D, Law CK.** Optically accessible high-pressure combustion apparatus. *Review of Scientific Instruments* 2004;75(1):233-9.
- [182] **Law CK, Jomaas G, Bechtold JK.** Cellular instabilities of expanding hydrogen-propane spherical flames at elevated pressures: theory and experiment. *Proceedings of the Combustion Institute* 2005;30(1):159-67.
- [183] **Bechtold JK, Matalon M.** The dependence of the Markstein Length on stoichiometry. *Combustion and Flame* 2001;127:1906-13.
- [184] **Lutz AE, Rupley FM, Kee RJ, Reynolds WC.** EQUIL: a program (CHEMKIN implementation of STANJAN) for computing chemical equilibria. Sandia National Laboratories Report, 1998.
- [185] **Jomaas G, Law CK, Bechtold JK.** On transition to cellularity in expanding spherical flames. *Journal of Fluid Mechanics* 2007;583:1-26.
- [186] **Law CK.** *Combustion physics.* Cambridge University Press, 2006.
- [187] **Law CK, Sung CJ.** Structure, aerodynamics and geometry of premixed flamelets. *Progress in Energy and Combustion Science* 2000;26(4-6):459-505.
- [188] **Zeldovich YB, Barenblatt GI, Librovich VB, Makhviladze GM.** *The mathematical theory of combustion and explosions.* Plenum Press, New-York, 1985.
- [189] **Peters N, Williams FA.** The asymptotic structure of stoichiometric methane-air flames. *Combustion and Flame* 1987;68(2):185-207.
- [190] **Göttgens J, Mauss F, Peters N.** Analytic approximations of burning velocities and flame thicknesses of lean hydrogen, methane, ethylene, ethane, acetylene and propane flames. *Proceedings of the Combustion Institute* 1992;24:129-35.
- [191] **Warnatz J, Maas U, Dibble RW.** *Combustion: physical and chemical fundamentals, modeling and simulation, experiments, pollutant formation.* Springer-Verlag, Berlin-Heidelberg-NewYork, 1998.
- [192] **Egolfopoulos FN, Law CK.** Chain mechanisms in the overall reaction orders in laminar flame propagation. *Combustion and Flame* 1990;80(1):7-16.
- [193] **Clavin P.** Dynamic behavior of premixed flame fronts in laminar and turbulent flows. *Progress in Energy and Combustion Science* 1985;11(1):1-59.
- [194] **Haniff MS, Melvin A, Smith DB, Williams A.** The burning velocities of methane and SNG mixtures with air. *Journal of Institute of Energy* 1989;62:229-36.
- [195] **Gülnder L.** Effect of initial mixture temperature on flame speed of methane-air, propane-air and ethylene-air mixtures. SAE 841000, 1984.
- [196] **Perini F, Paltrinieri F, Mattarelli E.** A quasi-dimensional combustion model for performance and emissions of SI engines running on hydrogen-methane blends. *International Journal of Hydrogen Energy* 2010;35:4687-701.
- [197] **Padley PJ, Sugden TM.** Chemiluminescence and radical re-combination in hydrogen flames. *Proceedings of the Combustion Institute* 1958;7(1):235-42.
- [198] **Butler CJ, Hayhurst AN.** Measurements of the concentrations of free hydrogen atoms in flames from observations of ions: correlation of burning velocities with concentrations of free hydrogen atoms. *Combustion and Flame* 1998;115(1-2):241-52.
- [199] **Choudhuri AR, Gollahalli SR.** Laser induced fluorescence measurements of radical concentrations in hydrogen-hydrocarbon hybrid gas fuel flames. *International Journal of Hydrogen Energy* 2000;25(11):1119-27.
- [200] **Katoh A, Oyama H, Kitagawa K, Gupta AK.** Visualization of OH radical distribution in a methane-hydrogen mixture flame by isotope shift-planar laser induced fluorescence spectroscopy. *Combustion Science and Technology* 2006;178(12):2061-74.
- [201] **Naha S, Briones AM, Aggarwal SK.** Effect of fuel blends on pollutant emissions in flames. *Combustion Science and Technology* 2005;177(1):183-220.

- [202] **Kunioshi N, Fukutani S.** Fuel mixing effects on propagation of premixed flames, II. Hydrogen+methane flames. *Bulletin of the Chemical Society of Japan* 1992;65:2573-7.
- [203] **Gaydon AG, Wolfhard HG.** *Flames*. Chapman&Hall, London, 1979.
- [204] **Warnatz J, Maas U, Dibble RW.** *Combustion*. Springer-Verlag, Berlin-Heidelberg-NewYork, 1999.
- [205] **Dagaut P, Nicolle A.** Experimental and detailed kinetic modeling study of hydrogen-enriched natural gas blend oxidation over extended temperature and equivalence ratio ranges. *Proceedings of the Combustion Institute* 2005;30(2):2631-8.
- [206] **Dagaut P, Dayma G.** Hydrogen-enriched natural gas blend oxidation under high-pressure conditions: experimental and detailed chemical kinetic modeling. *International Journal of Hydrogen Energy* 2006;31(4):505-15.
- [207] **Kwon OC, Faeth GM.** Flame-stretch interactions of premixed hydrogen-fueled flames: measurements and predictions. *Combustion and Flame* 2001;124:590-610.
- [208] **Qiao L, Kim CH, Faeth GM.** Suppression effects of diluents on laminar premixed hydrogen-oxygen-nitrogen flames. *Combustion and Flame* 2005;143(1-2):79-96.
- [209] **Sabia P, De-Joannon M, Romano E, Cavaliere A.** Hydrogen enriched methane mild combustion in a well stirred reactor. *Proceedings of the European Combustion Meeting ECM* 2007.
- [210] **De-Ferrières S, El-Bakali A, Lefort B, Montero M, Pauwels JF.** Investigation of laminar low pressure stoichiometric $\text{CH}_4\text{-C}_2\text{H}_6\text{-C}_3\text{H}_8\text{-O}_2\text{-N}_2$ and $\text{CH}_4\text{-C}_2\text{H}_6\text{-C}_3\text{H}_8\text{-H}_2\text{-O}_2\text{-N}_2$ flames. *Proceedings of the European Combustion Meeting ECM* 2007.
- [211] **Karim GA, Wierzba I, Boon S.** Some considerations of the lean flammability limits of mixtures involving hydrogen. *International Journal of Hydrogen Energy* 1985;10:117-23.
- [212] **Wierzba I, Karim GA, Cheng H.** The rich flammability limits of fuel mixtures containing hydrogen. *American Institute of Chemical Engineers Symposium Series* 1986;82:104-10.
- [213] **Wierzba I, Ale BB.** Rich flammability limits of fuel mixtures involving hydrogen at elevated temperatures. *International Journal of Hydrogen Energy* 2000;25:75-80.
- [214] **Gerke U, Steurs K, Rebecchi P, Boulouchos K.** Derivation of burning velocities of premixed hydrogen-air flames at engine-relevant conditions using a single-cylinder compression machine with optical access. *International Journal of Hydrogen Energy* 2010;35:2566-77.
- [215] **Greenberg JB.** On the prediction of thermal diffusion effects in laminar one-dimensional flames. *Combustion Science and Technology* 1980;24:83-8.
- [216] **Reynolds CCO, Evans RL, Andreassi L, Cordiner S, Mulone V.** The effect of varying the injected charge stoichiometry in a partially stratified charge natural gas engine. *SAE Paper* 2005-01-0247, 2005.
- [217] **Iijima T, Takeno T.** Effects of temperature and pressure on burning velocity. *Combustion and Flame* 1986;65:35-43.
- [218] **Bougrine S, Richard S, Veynante D.** On the combination of complex chemistry with a 0-D coherent flame model to account for the fuel properties in spark ignition engines simulations: Application to methane-air-diluents mixtures. *Proceedings of the Combustion Institute* 2011;33:3123-30.
- [219] **Glassman I, Yetter RA.** *Combustion*. Academic Press Elsevier. New York, 2008.
- [220] **Müller UC, Bollig M, Peters N.** Approximations for burning velocities and Markstein numbers for lean hydrocarbon and methanol flames. *Combustion and Flame* 1997;108:349-56.
- [221] **Tinaut FV, Melgar A, Giménez B, Reyes M.** Characterization of the combustion of biomass producer gas in a constant volume combustion bomb. *Fuel* 2010;89:724-31.
- [222] **Horrillo A.** Utilization of multi-zone models for the prediction of the pollutant emissions in the exhaust process in spark ignition engines (Spanish). PhD thesis 1998, University of Valladolid (Spain).
- [223] **Tinaut FV, Melgar A, Horrillo AJ.** Utilization of a quasi-dimensional model for predicting pollutant emissions in SI engines. *SAE Paper* 1999-01-0223, 1999.
- [224] **Tinaut FV, Melgar A, Giménez B, Horrillo AJ.** Comparison of the performance of spark-ignition engines fed with producer gas and other conventional fuels by the utilization of a predictive multi-zone model. *Venezuela, V-Congreso Iberoamericano de Ingeniería Mecánica*; 2001.
- [225] **Han P, Checkel MD, Fleck BA, Nowicki NL.** Burning velocity of methane-diluent mixture with reformer gas addition. *Fuel* 2007;86(4):585-96.
- [226] **Rahim F, Elia M, Ulinski M, Metghalchi M.** Burning velocity measurements of methane-oxygen-argon mixtures and an application to extend methane-air burning velocity measurements. *International Journal of Engine Research* 2002;3(2):81-92.

- [227] **Verhelst S, T'Joel C, Vancoillie J, Demuyneck J.** A correlation for the laminar burning velocity for use in hydrogen spark-ignition engine simulation. *International Journal of Hydrogen Energy* 2011;36:957-74.
- [228] **Kelley AP, Law CK.** Nonlinear effects in the extraction of laminar flame speeds from expanding spherical flames. *Combustion and Flame* 2009;156(9):1844-51.
- [229] **Bade-Shrestha SO, Karim GA.** Predicting the effects of the presence of diluents with methane on spark ignition engine performance. *Applied Thermal Engineering* 2001;21:331-42.
- [230] **Verhelst S, Sierens R.** A quasi-dimensional model for the power cycle of a hydrogen fueled ICE. *International Journal of Hydrogen Energy* 2007;32:3545-54.
- [231] **Verhelst S, Sheppard CGW.** Multi-zone thermodynamic modeling of spark-ignition engine combustion – An overview. *Energy Conversion and Management* 2009;50:1326-35.
- [232] **Verhelst S.** A study of the combustion in hydrogen fueled internal combustion engines. PhD thesis 2005, Ghent University, Belgium.
- [233] **Gerke U.** Numerical analysis of mixture formation and combustion in a hydrogen direct-injection internal combustion engine. PhD thesis 2007, Swiss Federal Institute of Technology, Zurich, Switzerland.
- [234] **Gu XJ, Haq MZ, Lawes M, Woolley R.** Laminar burning velocity and Markstein lengths of methane-air mixtures. *Combustion and Flame* 2000;121(1-2):41-58.
- [235] **Lamoureux N, Djebäyli-Chaumeix N, Paillard CE.** Laminar flame velocity determination for H₂-air-He-CO₂ mixtures using the spherical bomb method. *Experimental Thermal and Fluid Science* 2003;27(4):385-93.
- [236] **Stone R, Clarke A, Beckwith P.** Correlations for the laminar burning velocity of methane-diluent-air mixtures obtained in free fall experiments. *Combustion and Flame* 1998;114:546–55.
- [237] **Ryan TW, Lestz SS.** The laminar burning velocity of iso-octane, n-heptane, methanol, methane, and propane at elevated temperature and pressures in the presence of a diluent. SAE 800103./ SAE Transactions, Detroit, Michigan, 1980;Vol.89.
- [238] **Matlab.** The language of technical computing, <http://www.mathworks.com/>; 2011.
- [239] **Ren JY, Qin W, Egolfopoulos FN, Mak H, Tsotsis TT.** Methane reforming and its potential effect on the efficiency and pollutant emissions of lean methane-air combustion. *Chemical Engineering Science* 2001;56:1541-9.
- [240] **Kee RJ, Dixon-Lewis G, Warnatz J, Coltrin ME, Miller JA.** **TRANSPORT (CHEMKIN Collection part):** A Fortran computer code package for the evaluation of gas-phase, multicomponent transport properties. Sandia National Laboratories, Albuquerque, New Mexico, 1986; Report SAND 86-8246.
- [241] **Uykur C, Henshaw PF; Ting DSK, Barron RM.** Effects of addition of electrolysis products on methane-air premixed laminar combustion. *International Journal of Hydrogen Energy* 2001;26:265-73.
- [242] **Kee RJ, Rupley FM, Meeks E, Miller JA.** **CHEMKIN_III:** A Fortran chemical kinetics package for the analysis of gas-phase chemical and plasma kinetics. Sandia National Laboratories, 1996; Report SAND 96-8216.
- [243] **Pilling MJ, Turanyi T, Hughes KJ.** The Leeds methane oxidation mechanism, [www:http://chem.leeds.ac.uk/Combustion/](http://chem.leeds.ac.uk/Combustion/). Html, 1996.
- [244] **Tinaut FV, Melgar A, Horrillo AJ, Díez A.** Method for predicting the performance of an internal combustion engine fueled by producer gas and other low heating value gases. *Fuel Processing Technology* 2006;87:135-42.
- [245] **Rahim F.** Determination of burning speed for methane-oxidizer-diluent mixtures. PhD thesis 2002, Northeastern University, Boston, Massachusetts.
- [246] **Dahoe AE, De-Goey LPH.** On the determination of the laminar burning velocity from closed vessel gas explosions. *Journal of Loss Prevention in the Process Industries* 2003;16:457-78.
- [247] **Sharma SP, Agrawal DD, Gupta CP.** The pressure and temperature dependence of burning velocity in a spherical combustion bomb. *Proceedings of the 18th international symposium on combustion*, The Combustion Institute 1981.
- [248] **Rallis CJ, Garforth AM.** The determination of laminar burning velocity. *Progress in Energy and Combustion Science* 1980;6:303-29.
- [249] **Tsatsaronis, G.** Prediction of propagating laminar flames in methane, oxygen, nitrogen mixtures. *Combustion and Flame* 1978;33:217-39.

- [250] **Andrews** GE, **Bradley** D. The burning velocity of methane-air mixture. *Combustion and Flame* 1972;19:275-88.
- [251] **Barassin** A, **Lisbet** R, **Combourieu** J, **Laffitte** P. Etude de l'influence de la temperature initiale sur la vitesse normale de deflagration de melanges methane-air en fonction de la concentration. *Bulletin de la Societe Chimique de France* 1967; 104(7):2521-6.
- [252] **Babkin** VS, **Kozachenko** LS. Study of normal burning velocity in methane-air mixtures at high pressures. *Fizika Goreniya i Vzryva* 1966;3(2):77-86. (English translation: *Combustion, Explosion and Shock Waves* 1966;2:46-52).
- [253] **Agnew** JT, **Graiff** LB. The pressure dependence of laminar burning velocity by the spherical bomb method. *Combustion and Flame* 1961;5:209-19.
- [254] **Dugger** GL. Effect of initial mixture temperature on flame speed of methane-air, propane-air and ethylene-air mixtures. NACA report of investigations 1061, Lewis Flight Propulsion Laboratory, Cleveland, Ohio, 1952.
- [255] **Smith** D, **Agnew** JT. The effect of pressure on the laminar burning velocity of methane-oxygen-nitrogen mixtures. *Proceedings of the 6th international symposium on combustion*, The Combustion Institute 1951;83-88.
- [256] **Verhelst** S, **Sierens** R. A laminar burning velocity correlation for hydrogen-air mixtures valid at spark-ignition engine conditions. ASME Spring Engine Technology Conference paper ICES2003-555, Salzburg, Austria, 2003.
- [257] **D'Errico** G, **Onorati** A, **Ellgas** S. 1D-thermo-fluid dynamic modeling of an SI single-cylinder H₂ engine with cryogenic port injection. *International Journal of Hydrogen Energy* 2008;33:5829-41.
- [258] **Knop** V, **Benkenida** A, **Jay** S, **Colin** O. Modeling of combustion and nitrogen oxide formation in hydrogen-fueled internal combustion engines within a 3D-CFD code. *International Journal of Hydrogen Energy* 2008;33:5083-97.
- [259] **Bradley** D, **Lawes** M, **Liu** K, **Verhelst** S, **Woolley** R. Laminar burning velocities of lean hydrogen-air mixtures at pressures up to 1 Mpa. *Combustion and Flame* 2007;149(1-2):162-72.

9. Conclusions

- 9.1. General aspects of laminar burning velocity of fuel blends of hydrogen in relation to methods of obtaining
- 9.2. Characteristics of specific expressions of laminar burning velocity for hydrogen-air mixtures
- 9.3. Trends of laminar burning velocity of hydrogen-methane blends for the regimes related to hydrogen contents
- 9.4. Characteristics of diverse expressions of laminar burning velocity for fuel blends of hydrogen and natural gas
 - 9.4.1. Simple expressions for laminar burning velocity of fuel blends of hydrogen and natural gas
 - 9.4.2. Global expressions for laminar burning velocity of fuel blends of hydrogen and natural gas in complete ranges of conditions for fuel composition and thermodynamic variables
- 9.5. Proposals for future developments

References of chapter nine (*fifth part*)

9. Conclusions

In this final chapter of conclusions derived from the various parts of this work, we focus mostly on two perspectives: on one hand, on considerations of issues related to different methods of deduction of expressions of laminar burning velocities for hydrogen and mixtures with methane or natural gas and, on the other hand, on considerations of different types of expressions and specific expressions applicable to various contents of hydrogen in mixtures, from only hydrogen up to methane, covering each possible combination.

9.1. *General aspects of laminar burning velocity of fuel blends of hydrogen in relation to methods of obtaining*

A research target is obtaining values of the laminar burning velocity of hydrogen mixtures, at elevated pressures and temperatures, such as occurring in ICE, and to account for the effect of residual gases derived of exhaust gas recirculation. The definition and validation of laminar burning velocity of fuel-air mixtures is not easy when trying to find accurate experimental data from blends of gaseous fuels combined with hydrogen as one of the constituents, being also insufficiently comprehensive and representative in general. An important reason for this is that generating enough experimental data is difficult, especially for engine-like conditions, mainly trying to cover the many possibilities of composition for mixtures of several components in the fuel blends, with hydrogen and hydrocarbons as methane or natural gas at varied and elevated pressures and temperatures.

The experimental values of the burning velocity depend significantly on the apparatus and **measurement techniques**. The burning velocities obtained by optical techniques (flame speed in unburned zone) depend on the specific methodologies and are different from those obtained by pressure registering (burned mass fractions) combined with thermodynamic models. Measurements based on flame images are sensitive to the means by which the flame front is recorded and to the location within the flame of the recorded property (refractive index gradients, species concentrations, etc.). The results are influenced by image resolution, methods of flame edge detection and calculation procedures. On the other hand, measurements based on pressure registers are sensitive to the accuracy of transducers and recorders, particularly at the early stages of the flame growth. In addition, when burning velocities have to be obtained from pressure by means of thermodynamic models, additional hypotheses and computation procedures must be considered, thus introducing new sources of error.

Moreover, in any experimental device, especially for hydrogen combustion, the effects of **stretch, instabilities and cellularity** are present. The experimental measurements are affected by accelerating effects of flame stretch and thermo-diffusive and hydrodynamic instabilities, which obviously are not covered by purely kinetic schemes. The stretch effect on burning velocities should be quantified, at least, to attain stretch-free laminar burning velocities properly defined. The effects of stretch rate are more significant at low pressure and temperature than at engine-like conditions, where Markstein numbers (the Markstein length over the flame thickness) are lower and neglecting stretch effects may be considered not too important in practice. On the other hand, laminar flames are more prone to instability and cellularity at engine-like conditions, with flame surface increasing and burning velocity enhancing. Thus, the presence of flame stretch in most experimental set-ups and the unstable nature of high-pressure flames make experimental determination very difficult.

Experimental measurements of burning velocities at elevated pressures and mainly for lean to stoichiometric fuel to air equivalence ratios have only been possible in the published experiences by making semi-theoretical considerations for the arising **hydrodynamic and thermo-diffusive instabilities**. The starting point for such correction for instabilities has to be the accurate measurement of the critical radius at which the flame speed increases up due to flame instabilities. This has enabled to find the critical values of Peclet number (the flame radius over the flame thickness), together with inner and outer cut-off wavelengths of instability. Measurements of flame speed within the stretched stable regime of flame propagation, between the end of spark ignition and the onset of unstable propagation, have enabled strain rate Markstein numbers to be found.

All these measurements require, for instance, very high frame speed cinematography. Nevertheless, as the pressure increases, the enhancement of flame speed due to instabilities occurs earlier in the flame propagation process, making the accurate consideration for the instabilities more important. With increasing pressure, the time interval for stable flame propagation is reduced, between the end of spark and the development of cellularity, making the accurate estimation of Markstein number nearly impossible. As the interval becomes even shorter, the measurement of laminar burning velocity becomes unreliable, throwing into question the interest of this parameter for high pressure and unstable flames, as suggested by some authors. As stable laminar flames will not exist at engine conditions, it can be argued that the laminar burning velocity, i.e. the “pure or ideal” burning velocity u_l of stable planar flames, loses their validity as input for combustion models. Consequently, the data at engine conditions that can be found in the specific literature are either “**apparent**” laminar burning velocities (i.e. not “stable and stretch-free”) or are associated with uncertainties.

Thus, technical limits of measurements at **high pressures and temperatures**, as well as hydrodynamic and thermo-diffusive instabilities appearing in such conditions, prevent the acquisition of reliable results in terms of burning velocities, restraining the domain of validity of hypothetical laminar flame speed empirical correlations to few bars and hundreds of Kelvin. These limits are even more important when the reactivity of the considered fuel or fuel blend is high. The **highly explosive nature** of pure hydrogen makes measurements even more complicated.

In this context, data for purely laminar burning velocities at engine conditions are relevant, to be able to assess the effect of instabilities, or to provide an unambiguous reference for measured or modeled turbulent burning velocities. However, **theoretical treatments** are usually required because of the important **experimental limitations** (due to instabilities and stretch interactions, cellularity phenomena, etc.) depending on fuels properties, mixtures composition ranges and thermodynamic conditions. As mentioned, approaches have been shown in literature that use **stability theory** to compute burning velocities for stable flames, from measured data of unstable flame propagation and, on the other hand, inversely relevant unstable burning velocities have been computed from stable data. Such data have been generated by using **chemical kinetic calculations**, but they have also required the computation of Markstein lengths, although the validity of the used reaction schemes is difficult to assess, because of the lack of experimental data to validate the schemes.

Development of internal combustion engines is frequently based on a link between **experimental testing and numerical simulation**. Multidimensional and one-dimensional thermo-fluid dynamic models are commonly used to design optimizations through prediction of flows. Some numerical simulation works use specialized codes and packages. With these ones, freely propagating adiabatic, premixed, un-stretched planar flames have been simulated in some important studies. Thus, in order to complement experimental measurements, the developments in technical works of the literature have frequently led to using **models of theoretical one-**

dimensional premixed flames and schemes of detailed chemistry. The measured values of burning velocity in general are comparatively higher than the predicted by chemical kinetic models in the literature but, inside the error margins, they are considered with analogous trends at high pressures. The drawback for many types of fuel blends is that the definition of chemical kinetic models is usually complex, with long calculation times, and few models exist for these cases. Thereby studies over complete or wide ranges of unburned mixture compositions and thermodynamic conditions are not found in publications very often.

Other options in the literature are developed by obtaining the **laminar burning velocity of blends** from corresponding **laminar burning velocities of the individual constituents**, at the same conditions, by varying their contents in the blends composition and by modifying the initial conditions in some limited ranges. Their viability and accuracy can be checked by comparison of results, but not many accurate reference data are available for fuel blends in wide ranges of conditions, and also are particularly scarce at engine-like conditions.

On the other hand, expressions based e.g. on weighted averages of concentrations of hydrogen-hydrocarbon components would have to be restricted to fuels in blends with burning velocities and flame temperatures that should not differ substantially from each other, which is not the general case. Furthermore, modifications of the mixtures concentration in the flame structures can happen depending upon the diffusivities of the blend components and their differences. Moreover, the chemical kinetic interactions have a big influence with strong reactivity of hydrogen, which enhances flames propagations.

From all these previous considerations, this Thesis reports an overview of **expressions of laminar burning velocities of hydrogen-air mixtures**, obtained from authors who have used complementary chemical kinetic calculations, using reaction schemes that were validated, at least partially, against burning velocity measurements at increased temperature and pressure. These expressions have been processed analytically, for a wide range of conditions representative of engine-premixed combustion, and compared with some expressions from older works, purely experimental or defined in conditions that are more limited. The attention given to the analytical formulations of the fitted expressions arises from the fact that analytical expressions are more easily implemented in codes, and conveniently allow comparisons with existing and future expressions of laminar burning velocity for hydrogen-air mixtures and other mixtures in air of blends of hydrogen and other gases.

Purely experimentally based expressions published in literature are shown less suitable than the derived in conjunction with detailed kinetics results, because of the mentioned associated uncertainties to hydrogen-air flames. In spite of that, kinetic schemes cannot be estimated as absolutely accurate input data to predict actual burning speeds, since their behavior often differs from experiments (for example, they predict a pure decrease of the laminar flame speed with increasing pressure whatever the fuel-air equivalence ratio). In summary, the **expressions obtained from some numerical works**, based on partial validations by experimental data or engine codes, in conjunction with kinetic models, are considered more suitable to be used.

As complementary information, in addition to other references given along this Thesis, essential recommendations for the development of **accurate kinetic models** are given e.g. by Egolfopoulos et al. 2014 [1] in order to increase data fidelity and reduce **experimental uncertainties due to non-quantified physical effects, inherent instrument limitations, data processing and data interpretation.**

Finally, also as complements to other references already reported, some remarks that can be very helpful on other development applications, are offered by Sánchez&Williams 2014 [2] (Sánchez et al. 1997 [3]) from viewpoints of safety and energy production, including problems

and prospects for hydrogen usage. An example of the work of these mentioned authors is a comprehensive review of the more recent advances in understanding of flammability characteristics of hydrogen, with an updated exposition of the elementary schemes of hydrogen oxidation, chemical kinetic results and evaluated selections of reaction-rate parameters. Some of the hydrogen mechanisms that are reviewed have been quite recently released or complemented, e.g. those of Konnov 2004,2008 [4,5], Hong et al. 2010-2103 [6-10], Burke et al. 2012,2013 [11-12], Keromnes et al. 2013 [13], etc. The mechanism of Burke et al. was primarily made for high-pressure combustion. The model of Keromnes et al. was validated against the high-pressure burning velocity data of Burke et al. 2009 [14] and Tse et al. 2000 [15], and was used later to support measurements at elevated temperatures by Krejci et al. 2013 [16].

9.2. Characteristics of specific expressions of laminar burning velocity for hydrogen-air mixtures

As mentioned, a first goal of this work is to identify published expressions of hydrogen-air laminar burning velocity, relevant for their possible uses in new developments about fuel-air mixtures of hydrogen as pure fuel or as a component in fuel blends (e.g. with methane or natural gas) regarding the origins of their methodological definitions and the ranges and influence of each input parameter (fuel air equivalence ratio Φ , fresh gas temperature T_u , pressure P , and residual gas fraction $f_{res,u}$).

This Thesis reviews expressions of laminar burning velocity, derived from experimental and numerical studies on hydrogen-air flames that had been published. Special attention is given to expressions valid for pressures and temperatures in the so-called **engine-like conditions** (up to about 5 MPa and 900 K), in order to allow computation of hydrogen combustion in engines as well as to increase the understanding of hydrogen-air mixtures combustion at those conditions. Velocity expressions of these kinds are conceptually described in chapters 3 and 4 and more particularly in chapter 5 (tables 10-16). The reviewed expressions are based on diverse data, used for the correlation of laminar burning velocities determined by different origin methods. Some of them are based on an experimental methodology while others are based on reaction mechanisms of several origins. In order to provide a better understanding of the involved methods, the basic concepts of laminar combustion have been reviewed, including aspects such as instabilities and stretch effects. An additional overview on the calculated **experimental and numerical data** of the published laminar burning velocities of hydrogen-air mixtures has been done, and a homogenization and standardization of notations and nomenclature has been included in chapter 3 and section 5.2 in order to facilitate understanding the actual meaning and comparing the expressions.

Twelve analytical expressions have been chosen, as the most interesting published in the bibliography, among the works of many authors. These analytical expressions are fully detailed in section 5.3, with their corresponding ranges of applicability in section 5.4. These twelve selected expressions (functions of pressure, temperature, fuel to air equivalence ratio and residual gas fraction) have been numerically processed and graphically represented, with a wide set of results in operating conditions that have been estimated significant according with all the previous considerations.

According to considerations in section 5 and the predicted results for the conditions of this work, the expressions that are considered **more appropriate** for all ranges are the proposed by Gerke et al. 2010 [17(III.2)] and the proposed by Verhelst et al. 2011 [18(III.3)]. Additionally, the expression proposed by Bougrine et al. 2011 [19(III.12)] has a very wide range of validity and is directly applicable to the combustion in-air of hydrogen-methane blends.

The expression based on chemical kinetic calculations from O'Conaire et al. [20(III.139)] given by Gerke et al. 2010 [17(III.2)] predicts the burning velocity well in its ranges of pressure (1-80 bar) and temperature (300-900 K), with trends of values that are coherent with those predicted by the expression of Verhelst et al. 2011 [18(III.3)] in its respective ranges of pressure (5-45 bar) and temperature (500-900 K). The latter expression is based on Konnov's mechanisms [4(III.47),5(III.125)], which are favorably reputed for higher pressures, while O'Conaire et al. mechanisms [20(III.139)] are considered adequate at more moderated pressures.

Both expressions [17(III.2)] and [18(III.3)] are applicable in wide ranges of spark ignition engine conditions, include the dependence on equivalence ratios and residuals dilution fractions, and provide similar values in the somehow narrower ranges of temperature and pressure of [III.3]. Their results are also close for elevated values of temperature and pressure and even for moderate lean equivalence ratios and significant rates of residual gases.

The expression of Göttgens et al. 1992 [21(III.9)] could be a supplementary option for the intervals of low pressure, lower than engine-like conditions, and temperature less than 500 K, but it is limited for lean to stoichiometric equivalence ratios and does not include the residual gas fraction.

In cases of utilization of the expression of Gerke et al. 2010 [17(III.2)], the more elaborated form of the *residuals function factor* proposed by Verhelst et al. 2011 [18(III.3)] could be applied as an alternative (instead of the suggested in [17(III.2)] previously, adapted from other work of Verhelst et al. 2005,2007 [22,23(III.7,14)]), although this recommendation has not been checked in the present review. Furthermore, in accordance with this and as a tentative conclusion, it can be said that, since the influence of residual gases on combustion velocity is incorporated in the expression of Verhelst et al. 2011 [18(III.3)] in the form of a separate correction term, then this term could easily be introduced in other velocity expressions.

The application of the expression due to Bougrine et al. 2011 [19(III.12)] may be very practical when required for computations of burning velocity in *very wide ranges* reaching very elevated pressures and temperatures. Its applicability range is more extended than the ones allowed by other expressions, and starts even from atmospheric conditions or low pressures, where its velocity results are better in agreement with the trends of other authors' results than the values given e.g. by the expression of Gerke et al. 2010 [17(III.2)]. The burning velocity expression due to Bougrine et al. 2011 [19(III.12)], as an optimized combination of other expressions, including the expressions of Gerke et al. 2010 [17(III.2)] and Verhelst et al. 2011 [18(III.3)], allows with a single generic expression a wide extension of the validity ranges, reaching up to high levels of pressure $P(\text{bar})=[1, 110]$ and temperature $T(\text{K})=[300, 950]$, for any fraction of hydrogen content from 100 to 0% in fuel blends with methane (Bougrine et al. 2011 [24(III.142)]). The expression [19(III.12)] is interesting also for its equivalence ratio range $\Phi=[0.6, 1.3]$, that covers well out of stoichiometric conditions, although it does not extend up to very rich mixtures. The expression is suitable in order to be applied in the context of air mixtures with natural gas and hydrogen blends, as concluded in section 9.4.2.

In summary, the expressions provided by Gerke et al. 2010 [17(III.2)], Verhelst et al. 2011 [18(III.3)], and Bougrine et al. 2011 [19(III.12)], offer *consistent and useful results* for calculating laminar burning velocity of hydrogen-air mixtures, with an additional advantage of the ultimate expression of being valid for calculating laminar burning velocities of mixtures of hydrogen-methane-air, also with consistent and very useful results for sufficiently complete ranges, even at engine-like conditions, and with acceptable accuracy if compared to other formulations based on simple or complex mixing rules, that perhaps in origin are easier to apply but restricted to more partial ranges of variables, as explained in section 9.4.

9.3. Trends of laminar burning velocity of hydrogen-methane blends for the regimes related to hydrogen contents

Three different modes of behavior have been identified in the literature for the velocity of propagation of flames with H₂-CH₄-air mixtures, at room temperatures and atmospheric pressure, for all values of equivalence ratio but depending on the **hydrogen mole fraction** in the fuel blend.

Two **linear** trends of laminar burning velocity with the hydrogen volumetric contents in the fuel blend are widely recognized, corresponding to two types of proportions of hydrogen in methane:

- a first regime, for low and medium contents of hydrogen, of about $x_{H_2}=[0; 0.4-0.6]$;
- a second regime, for very high or predominant contents, of about $x_{H_2}=(0.8-0.9; 1]$.

Both regimes are characterized by linear evolutions of the laminar burning velocity although with different slopes.

However, in a central part of values of hydrogen-methane proportion, the laminar burning velocity evolution is otherwise strongly nonlinear, assimilated as **quasi-exponential**, reflecting complex kinetics behaviors,

- and a third regime, for medium and high contents of hydrogen, of about $x_{H_2}=(0.5; 0.9)$.

The mentioned two linear regimes of laminar burning velocity for the hydrogen-methane blends have been respectively attributed, in a case, to the **enhancing effect of hydrogen addition** in methane and, in the other case, to an **inhibiting effect of the addition of methane** to hydrogen. Thus, the regime of combustion dominated by methane is characterized by a slight linear increase when adding hydrogen in the blend. Moreover, the regime of hydrogen combustion inhibited by methane, known sometimes as dominated by hydrogen, is characterized by a sharp linear decrease when adding methane.

The increase of laminar burning velocity by hydrogen addition is widely justified by the increase of reactive radicals and the rise of adiabatic flame temperature. Hydrogen addition enhances slightly the methane reactivity in lean mixtures, while the inhibiting effect of methane addition to hydrogen is much stronger for rich conditions.

9.4. Characteristics of diverse expressions of laminar burning velocity for fuel blends of hydrogen and natural gas

A summary of types of these expressions is included in [table 26](#) (at the end of chapter 7) for fuel blends of hydrogen with methane or natural gas, with their features of applicability depending on composition conditions.

Here are some particular conclusions that are summarized for diverse types of simple expressions, i.e. linear, exponential and LeChatelier's rule-like formulas. Afterwards other conclusions are also given for expressions that are more complex.

9.4.1. Simple expressions for laminar burning velocity of fuel blends of hydrogen and natural gas

Different linear, exponential and LeChatelier's rule-like formulas have been respectively proposed by many authors to predict the laminar burning velocity of H₂-CH₄ or H₂-NG blends. According with the literature, simplified formulations and **simple mixing rules** based on the change in composition are considered not accurate enough to predict the laminar burning

velocity of fuel blends in wide ranges. Therefore, simple expressions can be used only in specific ranges when applied.

General simple rules have been questioned in part because of the applicability in limited ranges of compositions and thermodynamic conditions. The functional relationships based on simple rules do not work as well as the formulas derived from models based on detailed chemical schemes, especially when wide ranges of engine-like conditions have to be taken into account.

Some developments, such as based on the **rule of LeChatelier**, can be extrapolated for use at high pressures and temperatures, including for engine conditions. Applications that are made for calculations of laminar burning velocities of blends of fuels, e.g. hydrogen and methane or natural gas, may offer different accuracies. They can be more or less acceptable, according to whether linking of results of the individual expressions of laminar burning velocity (corresponding to each one of the integrated fuels through the considered average rule) is more or less appropriate. The accuracy of such formulas for fuel blends, so resulting from combining of the characteristic expressions of the components of the fuel blend, also depends on the setting of the combination of respective accuracies of the original expressions with respect to their own applicability intervals. These ranges should be large enough, to facilitate a reasonable use in common of combining expressions, and should be taken in their matching portion, for coupling the use with a medium stringency, analytically at least. In any case, this type of methodology, just by itself, does not include the effects of interactions of the combined fuels in the mixture; therefore, its accuracy is relatively conditioned by this fact.

- **Linear expressions of laminar burning velocities for hydrogen-hydrocarbon blends**

The intense non-linear effects of chemical kinetics make difficult to obtain accurately simple linear expressions, since reaction kinetics of methane is much slower than that of hydrogen in the fuel blend combustion. This explains big differences between the values of laminar burning velocities computed by other methods and those obtained by linear averaging of the velocities of the constituent fuel gases in molar proportions.

The linear expressions of laminar flame velocity based on some virtually defined parameters have been considered intrinsically valid only for low hydrogen contents. These parameters are such as an effective equivalence ratio (Φ_{eF}) associated to a ratio R_h (of the amount of hydrogen plus the stoichiometric amount of air needed for its total oxidation, to the amount of hydrocarbon plus the remaining available air left for its oxidation). These formulations are related to some specific coefficients of sensitivity to hydrogen content (which e.g. can take into account the trend of the laminar burning velocity with hydrogen addition on the methane-based fuel). Their limited validity for low hydrogen proportion is due to the inherent performance of the expressions of these parameters, adopted in that form to define effective virtual compositions of the hybrid-fuel mixtures with air. With these limitations and some deviations between experimental measurements and numerical calculations, these approximate linear correlations, between laminar flame speeds and hydrogen addition, have been respectively applied in the literature for combined mixtures of methane (C_1), ethane, ethylene and acetylene (C_2), propane (C_3) and n-butane (C_4), at atmospheric pressure. In addition, this type of correlations has also been considered, although less accurate, for ethylene and propane at relatively limited elevated pressures.

- **Exponential expressions of laminar burning velocities for hydrogen-natural gas blends**

Some formulas, based on experimental data, consider dimensionless increments of the laminar burning velocities of methane or natural gas when hydrogen is added. Their trends are

markedly exponential with the increase of the hydrogen fraction. This agrees quite well with calculated values at low hydrogen fractions, for intervals of molar content in the fuel blend of about $x_{H_2}=[0; 0.3-0.4]$, and for high proportions, in ranges about $x_{H_2}=(0.6-0.7; 1]$. However, the errors are relatively higher for intermediate fractions of about $x_{H_2}=(0.3; 0.7)$.

These exponential expressions have usually been obtained from data measured close to atmospheric conditions, but they have also been used at more elevated pressures and temperatures, because experimental results of pressure agree quite well with engine models predictions for low values of hydrogen content, $x_{H_2}<0.3$, where this kind of expression is considered of reasonable accuracy, in combustion at SIE-like conditions for fuel blends with methane. Thus, the accuracy of these expressions is considered to be high only for low hydrogen fractions, in usual ranges of equivalence ratio about $\Phi=[0.6, 1.3]$, and sometimes with a lower error particularly in narrow intervals, e.g. about $x_{H_2}=[0.2, 0.3]$, included in ranges of hydrogen contents commonly used in natural gas engines.

- ***Average expressions based on LeChatelier's rule applied to laminar burning velocities for hydrogen-natural gas blends***

LeChatelier's rule-like formulas, based on mole fractions of the fuel components to predict the laminar burning velocity of hydrogen and methane or natural gas blends, have been tried by some authors, showing the feasibility of this type of expressions to obtain correlations of laminar burning velocities. In the literature, the formulas based on LeChatelier's rule assumptions have been preferably used when the accuracy based in composition of mixing rules has been considered enough but, even in this case, it is considered that accurate results cannot be predicted over complete ranges of conditions.

Their results can be valid at different equivalence ratios and hydrogen contents, particularly for intermediate and high hydrogen fractions, with better accuracies for values $x_{H_2}>0.3-0.4$. The corresponding expressions by LeChatelier's rule application have been considered good at lean and stoichiometric conditions in all regimes, with good agreement between the predicted values with either experimental data or simulation results obtained through detailed reaction schemes. However, there are more significant differences for rich mixtures with high hydrogen contents; when predictions are made for rich mixtures, they are considered applicable only for limited ranges of hydrogen fraction, in some extensions up to $x_{H_2}\leq 0.7$ at most. Thus, formulas of this kind are successfully applied on wide ranges of fuel blends of hydrogen with methane, even at higher than atmospheric conditions, and are considered of reasonable accuracy when used with combustion models at SIE-like conditions, for equivalence ratio ranges of about $\Phi=[0.6, 1.3]$, with limitations about their reliability for other different equivalence ratios.

9.4.2. Global expressions for laminar burning velocity of fuel blends of hydrogen and natural gas in complete ranges of conditions for fuel composition and thermodynamic variables

Thus, according with literature assessments, some expressions as the based on the LeChatelier's rule provide suitable predictions, in better accordance with the reactions kinetic behavior than other types of expressions. However, when dealing with hydrogen contents greater than $x_{H_2}>0.7$, and thereby with associated higher H radical concentrations, their interaction is too strong to be reproduced by simple expressions, even by the LeChatelier's rule, requiring more sophisticated expressions.

Not many studies have been able to extend the options covering all the different regimes simultaneously. Some of them have done so through expressions that are more complex and, in some cases, are valid for wider and more complete ranges. However, arranging simple

combination rules for the laminar burning velocity of fuel blends in air mixtures, with constituents as diverse as H_2 and CH_4 (or NG), has not been given as an easy task in the literature, because the individual components are not only chemically dissimilar but also have different transport properties. Another difficulty to present accurate correlations for these mixtures arises due to the different stoichiometry requirements of the fuel components. Formulas for the prediction of burning velocities become necessarily complex, mostly when broad ranges are required as for engine-like conditions. Relationships could be simplified when only relatively small amounts of hydrogen are present in the fuel blends.

Some detailed studies from the literature, carried out more frequently starting at stoichiometric and atmospheric conditions, report evaluations of main chemical processes governing the production of hydrogen radicals, as key contributor to the laminar flame velocity. Few of them jointly consider the three regimes of the methane-hydrogen blends. The complete analyzes, when available, contribute to quantify the non-linear impact on the expanding laminar flame. They also help to understand the evolutions of the laminar burning velocity due to the hydrogen content effect on the fuel blends. The general studies are interesting for common systems of combustion in industrial applications, because of the scarcity of global expressions of laminar flame velocity fully applicable in wide operating ranges of fuels composition and thermodynamic variables, which is due to the large number of sets of current conditions that have to be investigated.

When the different behaviors through the three regimes are simultaneously taken into account, then this leads to the development of complex expressions of laminar burning velocity for methane-hydrogen-air flames. Such is the case of the phenomenological formula, widely described in section 7.6 and partially used in chapter 5, with a general form that has been defined by Bougrine et al. by combination of parametric functions. These were determined considering the diverse effects of the functional factors and varied conditions, with compilation of the different behaviors contrasted by one-dimensional simulations of premixed laminar flames and through complex chemistry, ensuring the respective continuities at $x_{H_2}=0.7$ and $x_{H_2}=0.9$ and also smooth transitions in $x_{H_2}=[0.6, 0.8]$ and $x_{H_2}=[0.8, 1]$ respectively. This relationship is applicable even in large ranges of compositions and thermodynamic operating conditions, such as the characteristics of SIE or gas turbines, and extends the domain of validity of experimental correlations to high proportions of hydrogen in the fuel, high ratios of residual burned gas as well as high pressures and temperatures. Thus, this expression can be very useful, specially to be used on its application for new developments of this kind, and as an input data in combustion models, for other types of studies.

9.5. Proposals for future developments

Some future developments that can be proposed are studies for obtaining the combustion behavior of diverse fuel mixtures containing hydrogen, extended to considering other variables, e.g. ignition delay times.

On the other hand, additionally to all expressions of laminar burning velocity that have been analyzed in this Thesis for mixtures of gaseous fuels (single hydrogen and blends of hydrogen and natural gas/methane), other expressions can also be developed on the basis of the use of mixing rules (as functions of fractions of volume, mass or energy, with formulas of direct or indirect averaging). These expressions could then be used for applications of a wide variety of mixtures of the mentioned fuels and for other fuels.

In another context, reviewing and applying more recent methodologies in the literature can be useful to obtain specific experimental laminar burning velocities from spherically expanding flames, as done for instance by Jayachandran et al. 2014,2015 [25,26] (e.g. for ethylene and n-heptane). This can allow comparing updated discussions with the considerations used as example in section 3 (as illustration of some conventional developments), since recent studies involve additional insights about the limitations of experimental determinations of burning velocity, e.g. using spherically expanding flames.

Moreover, new in-depth developments of kinetic models, with more accurate values of the rate constants, and validations of the rates of elementary chemical reactions at elevated pressure and temperature, with the concentrations of species and their gradients, are also challenging for combustion chemistry research in laminar flames. In addition, fully detailed descriptions of molecular transport phenomena and chemical kinetics are interesting for flame modeling, as well as new possible advances in experiments of laminar flame with implications for the combustion chemistry of hydrogen and many varied blends with other fuels. Relative studies about the effects of initial and boundary conditions on flames structure at high pressures and temperatures, with particular analysis of physical parameters, are also of interest.

References of chapter nine (*fifth part*)

- [1] **Egolfopoulos FN, Hansen N, Ju Y, Kohse-Höinghaus K, Law CK, Qi F.** Advances and challenges in laminar flame experiments and implications for combustion chemistry. *Progress in Energy and Combustion Science* 2014;43:36-67.
- [2] **Sánchez AL, Williams FA.** Recent advances in understanding of flammability characteristics of hydrogen. *Progress in Energy and Combustion Science* 2014;41:1-55.
- [3] **Sánchez AL, Liñán A, Williams FA.** A generalized Burke-Schumann formulation for hydrogen-oxygen diffusion flames maintaining partial equilibrium of the shuffle reactions. *Combustion Science and Technology* 1997;123:317-45.
- [4] **Konnov AA.** Refinement of the kinetic mechanism of hydrogen combustion. *Journal of Advances in Chemical Physics* 2004;23:5-18.
[III.47]
- [5] **Konnov AA.** Remaining uncertainties in the kinetic mechanism of hydrogen combustion. *Combustion and Flame* 2008;152:507-28.
[III.125]
- [6] **Hong Z, Davidson DF, Hanson RK.** An improved H₂/O₂ mechanism based on recent shock tube-laser absorption measurements. *Combustion and Flame* 2011;158:633-44.
- [7] **Hong Z, Davidson DF, Barbour EA, Hanson RK.** A new shock tube study of the H+O₂→OH+O reaction rate using tunable diode laser absorption of H₂O near 2.5 μm. *Proceedings of the Combustion Institute* 2011;33:309-16.
- [8] **Hong Z, Lam KY, Sur R, Wang S, Davidson DF, Hanson RK.** On the rate constants of OH+HO₂→H₂O+O₂: a comprehensive study of H₂O₂ thermal decomposition using multi-species laser absorption. *Proceedings of the Combustion Institute* 2013;34:565-71.
- [9] **Hong Z, Cook RD, Davidson DF, Hanson RK.** A shock tube study of the OH+H₂O₂→H₂O+HO₂ and H₂O₂+M→2OH+M using laser absorption of H₂O and OH. *Journal of Physical Chemistry* 2010;114:5718-27.
- [10] **Hong Z, Vasu SS, Davidson DF, Hanson RK.** Experimental study of the rate of OH+HO₂→H₂O+O₂ at high temperatures using the reverse reaction. *Journal of Physical Chemistry* 2010;114:5520-5.
- [11] **Burke MP, Chaos M, Ju Y, Dryer FL, Klippenstein SJ.** Comprehensive H₂/O₂ kinetic model for high-pressure combustion. *International Journal of Chemical Kinetics* 2012;44:444-74.
- [12] **Burke MP, Klippenstein SJ, Harding LB.** A quantitative explanation for the apparent anomalous temperature dependence of OH+HO₂→H₂O+O₂ through multi-scale modeling. *Proceedings of the Combustion Institute* 2013;34:547-55.
- [13] **Kéromnès A, Metcalfe WK, Heufer KA, Donohoe N, Das AK, Sung CJ, et al.** An experimental and detailed chemical kinetic modeling study of hydrogen and syngas mixture oxidation at elevated pressures. *Combustion and Flame* 2013;160:995-1011.
- [14] **Burke MP, Chen Z, Ju Y, Dryer FL.** Effect of cylindrical confinement on the determination of laminar flame speeds using outwardly propagating flames. *Combustion and Flame* 2009;156:771-9.
- [15] **Tse SD, Zhu DL, Law CK.** Morphology and burning rates of expanding spherical flames in H₂-O₂-inert mixtures up to 60 atmospheres. *Proceedings of the Combustion Institute* 2000;28:1793-800.
[III.96]
- [16] **Krejci MC, Mathieu O, Vissotski AJ, Ravi S, Sikes TG, Petersen EL, et al.** Laminar flame speed and ignition delay time data for the kinetic modeling of hydrogen and syngas fuel blends. *Journal Engineering Gas Turbines Power* 2013;135:021503.
- [17] **Gerke U, Steurs K, Rebecchi P, Boulouchos K.** Derivation of burning velocities of premixed hydrogen-air flames at engine-relevant conditions using a single-cylinder compression machine with optical access. *International Journal of Hydrogen Energy* 2010;35:2566-77.
[III.2];[IV.214]
- [18] **Verhelst S, T'Joel C, Vancoillie J, Demuyneck J.** A correlation for the laminar burning velocity for use in hydrogen spark-ignition engine simulation. *International Journal of Hydrogen Energy* 2011;36:957-74.
[III.3];[IV.227]

- [19] **Bougrine S, Richard S, Nicolle A, Veynante D.** Numerical study of laminar flame properties of diluted methane-hydrogen-air flames at high pressure and temperature using detailed chemistry. *International Journal of Hydrogen Energy* 2011;36:12035-47.
[III.12];[IV.172]
- [20] **O'Conaire M, Curran HJ, Simmie JM, Pitz WJ, Westbrook CK.** A comprehensive modeling study of hydrogen oxidation. *International Journal of Chemical Kinetics* 2004;36(11):603-22.
[III.139]
- [21] **Göttgens J, Mauss F, Peters N.** Analytic approximations of burning velocities and flame thicknesses of lean hydrogen, methane, ethylene, ethane, acetylene and propane flames. *Proceedings of the Combustion Institute* 1992;24:129-35.
[III.9];[IV.190]
- [22] **Verhelst S, Woolley R, Lawes M, Sierens R.** Laminar and unstable burning velocities and Markstein lengths of hydrogen-air mixtures at engine-like conditions. *Proceedings of the Combustion Institute* 2005;30:209-16.
[III.7];[IV.125]
- [23] **Verhelst S, Sierens R.** A quasi-dimensional model for the power cycle of a hydrogen fueled ICE. *International Journal of Hydrogen Energy* 2007;32:3545-54.
[III.14];[IV.230]
- [24] **Bougrine S, Richard S, Veynante D.** On the combination of complex chemistry with a 0-D coherent flame model to account for the fuel properties in spark ignition engines simulations: Application to methane-air-diluents mixtures. *Proceedings of the Combustion Institute* 2011;33:3123-30.
[III.142];[IV.218]
- [25] **Jayachandran J, Zhao R, Egolfopoulos FN.** Determination of laminar flame speeds using stagnation and spherically expanding flames: Molecular transport and radiation effects. *Combustion and Flame* 2014;161:2305-2316.
- [26] **Jayachandran J, Lefebvre A, Zhao R, Halter F, Varea E, Renou B, Egolfopoulos FN.** A study of propagation of spherically expanding and counter-flow laminar flames using direct measurements and numerical simulations. *Proceedings of the Combustion Institute* 2015;35:695-702.

Lists of figures and tables

Summaries of all figures and tables (*in their sequential orders, respectively*)

Figures

- Fig. 1. Ideal laminar burning velocity u_l
- Fig. 2. Laminar burning velocity u_{ne} based on flame mass flux \dot{m}_e of unburned reactants entrainment
- Fig. 3. Laminar burning velocity u_{nr} based on flame mass flux \dot{m}_r of burned reacted products
- Fig. 4. Flame speed s_n and gas expansion velocity v_g
- Fig. 5. Sketch of a section of an ideal laminar flame front
- Fig. 6. Sketch of a section of a laminar flame front
- Fig. 7. Radially unstable flame front sketch
- Fig. 8. Transversely unstable flame front sketch
- Fig. 9. Radially and transversely unstable flame front sketch
- Fig. 10. Unsteady flame front sketch
- Fig. 11. Wrinkled flame front sketch
- Fig. 12. Cellular flame front sketch
- Fig. 13. Scheme of hydrodynamic instability growth mechanism (adapted from Law&Sung 2000 [III.54])
- Fig. 14. Schematics of diffusion of heat and mass in thermo-diffusive instability
- Fig. 15. Comparative schemes of thermal and mass diffusion-lengths
- Fig. 16. Instabilities correction
- Fig. 17. Stretch correction
- Fig. 18. Sketch of a theoretical laminar flame front with an infinite radius
- Fig. 19. Flame instabilities
- Fig. 20. Flame wrinkling and cracking
- Fig. 21. Flame cellularity
- Fig. 22. Localized turbulization of the flame
- Fig. 23. Limiting wavenumbers in peninsula of instability (adapted from Al-Shahrany et al. 2005 [III.68])
- Fig. 24. Spherically expanding flames of hydrogen and propane air mixtures recorded by Schlieren cinematography (taken from Matalon 2007 [III.99] and Law 2006 [III.57])
- Fig. 25. Propagation of hydrogen flames recorded by Schlieren cinematography (adapted from Verhelst 2005 [III.13])
- Fig. 26. Propagation of hydrogen flame recorded by OH-chemiluminescence (taken from Gerke et al. 2010 [III.2])
- Fig. 27. Hydrogen-air mixture laminar burning velocity $u(P)$ and $u(T_w)$ graphs for $\Phi=0.5$ & $EGR=0$
- Fig. 28. Hydrogen-air mixture laminar burning velocity $u(P)$ and $u(T_w)$ graphs for $\Phi=0.9$ & $EGR=0$
- Fig. 29. Hydrogen-air mixture laminar burning velocity $u(P)$ and $u(T_w)$ graphs for $\Phi=1$ & $EGR=0$
- Fig. 30. Hydrogen-air mixture laminar burning velocity $u(P)$ and $u(T_w)$ graphs for $\Phi=1.3$ & $EGR=0$
- Fig. 31. Hydrogen-air mixture laminar burning velocity $u(P)$ and $u(T_w)$ graphs for $\Phi=1.75$ & $EGR=0$
- Fig. 32. Hydrogen-air mixture laminar burning velocity $u(P)$ and $u(T_w)$ graphs for $\Phi=2$ & $EGR=0$
- Fig. 33. Hydrogen-air mixture laminar burning velocity $u(P)$ and $u(T_w)$ graphs for $\Phi=3.3$ & $EGR=0$
- Fig. 34. Hydrogen-air mixture laminar burning velocity $u(P)$ and $u(T_w)$ graphs for $\Phi=1$ & $EGR=0.15$
- Fig. 35. Hydrogen-air mixture laminar burning velocity $u(P)$ and $u(T_w)$ graphs for $\Phi=1$ & $EGR=0.30$
- Fig. 36. Hydrogen-air mixture laminar burning velocity $u(P)$ and $u(T_w)$ graphs for $\Phi=1$ & $EGR=0.40$

- Fig. 37. Hydrogen-air mixture laminar burning velocity $u(T)$ and $u(P)$ graphs for $\Phi=1$ & $EGR=0$ and adiabatically related P - T values ($\gamma=1.4$).
- Fig. 38. Hydrogen-air mixture laminar burning velocity $u(\Phi)$ and $u(EGR)$ graphs for $T_u=\{300, 500\}$ K & $P=\{1, 6, 10\}$ bar
- Fig. 39. Spherically expanding flames of hydrogen-methane-air mixtures, recorded by Schlieren cinematography, with H_2 fractions $h(\%)=\{20, 40, 60, 80\}$ for $\Phi=1$, $T_{u,o}(K)=300$ and $P_o(MPa)=\{0.1, 0.2\}$ (taken from Miao et al 2008 [IV.11])
- Fig. 40. Spherically expanding flames of hydrogen-methane-air mixtures, recorded by Schlieren cinematography, with H_2 fractions $h(\%)=\{20, 80\}$ for $\Phi=\{0.8, 1, 1.2\}$, $T_{u,o}(K)=300$ and $P_o(MPa)=\{0.1, 0.2\}$ (taken from Miao et al 2008 [IV.11])
- Fig. 41. Spherically expanding flames of hydrogen-methane-air mixtures, recorded by Schlieren cinematography, with H_2 fraction $h(\%)=40$ for $\Phi=0.8$, $T_{u,o}(K)=\{303, 373, 443\}$ and $P_o(MPa)=0.5$ (adapted from Hu et al 2009 [IV.76])
- Fig. 42. Spherically expanding flames of hydrogen-methane-air mixtures, recorded by Schlieren cinematography, with H_2 fraction $h(\%)=60$ for $\Phi=0.8$, $T_{u,o}(K)=373$ and $P_o(MPa)=\{0.1, 0.25, 0.5, 0.75\}$ (adapted from Hu et al 2009 [IV.76])
- Fig. 43. Spherically expanding flames of hydrogen-methane-air mixtures, recorded by Schlieren cinematography, with H_2 fractions $h(\%)=\{0, 20, 40, 60, 80\}$ for $\Phi=0.8$, $T_{u,o}(K)=373$ and $P_o(MPa)=0.5$ (adapted from Hu et al 2009 [IV.76])
- Fig. 44. Laminar burning velocities of a blend of H_2 - CH_4 with $x_{H_2}=0.7$; u_{L, H_2-CH_4} (cm/s) versus equivalence ratio $\Phi=\{0.8, 1.2\}$ for $P(MPa)=0.1$ and $T_u(K)=600$ (taken from Sileghem et al. 2012 [IV.176])
- Fig. 45. Dimensionless increment of laminar burning velocity in air mixtures of NG- H_2 fuel blend versus H_2 mole fraction percentage $h(vol\%)=100x_{H_2}$; $T_u(K)=300$, $P(MPa)=0.1$ (adapted from Huang et al. 2006 [IV.6] and Ma et al. 2008 [IV.86])
- Fig. 46. Laminar burning velocities of fuel blend air mixtures versus the molar hydrogen fraction at atmospheric conditions $u_{L, H_2-CH_4}(\Phi, x_{H_2})$ [cm/s] for $\Phi=\{0.6, 1, 1.5\}$ (taken from Di-Sarli&Di-Benedetto 2007 [IV.160])
- Fig. 47. Normalized burning velocity and radical concentration: Normalized laminar burning velocities of fuel blend $\sigma(\Phi, x_{H_2})=u_{L, H_2-CH_4}(\Phi, x_{H_2})/u_{L, CH_4}(\Phi)$. Normalized maximum H radical (mole fraction) concentration $\alpha_H(\Phi, x_{H_2})=x_{[H]max(H_2-CH_4)}/x_{[H]max(CH_4)}$ (taken from Di-Sarli&Di-Benedetto 2007 [IV.160])
- Fig. 48. Main H radical production or consumption rates according to several species at H peak concentration location. Species with symbols are relative to species inhibiting H production at the corresponding H_2 rate for $T_u(K)=300$, $P(MPa)=0.1$, $\Phi=1$, $x_{H_2}=\{0, 0.5, 0.9\}$ (taken from Bougrine et al. 2011 [IV.172])
- Fig. 49. Map of fresh gases temperature and pressure for one-dimensional premixed simulations (taken from Bougrine et al. 2011 [IV.172])
- Fig. 50. Comparison of experimental and simulated laminar burning velocities of CH_4 in stoichiometric air mixtures, u_L [cm/s], as respective functions of residuals mass fraction percentage $f_{res,u(m)}$, fresh gas temperature T_u and pressure P , for $T_{u,o}=300$ K, $P_o=0.1$ MPa and $\Phi=1$ (taken from Bougrine et al. 2011 [IV.172])
- Fig. 51. Comparison of experimental and simulated laminar burning velocities of fuel air-mixtures, u_L [cm/s], as functions of equivalence ratio Φ , for $T_{u,o}=300$ K and $P_o=0.1$ MPa (taken from Bougrine et al. 2011 [IV.172])
- Fig. 52. Comparison of experimental and simulated laminar burning velocities of H_2 - CH_4 blends, u_L [cm/s], as function of volumetric H_2 percentage, for $T_{u,o}=300$ K, $P_o=0.1$ MPa and $\Phi=1$ (taken from Bougrine et al. 2011 [IV.172])

Tables

Table 1.	Composition terms for air mixtures of hydrogen and fuel blends.
Table 2.	Natural gas compositions.
A.	Approximate ranges of hydrocarbon (HC) components in composition of different NG types from diverse origins (adapted from Naber et al. 1994 [II.2]).
B.	Approximate ranges of composition of other minor components in different NG types from diverse sources (adapted from Jessen&Melvin 1977 [II.3]).
C.	Usual NG composition (adapt. from Huang et al. 2006,2009 [II.6,7], Wang et al. 2007,2008 [II.8-10], Miao et al. 2008,2009 [II.11-13], Hu et al. 2009 [II.14,15]).
D.	Particular NG sample type composition (measurements from chromatographic analysis in a continuous supply line in Valladolid; April 2011).
Table 3	Hydrogen properties compared to other gases: properties of hydrogen, methane and iso-octane as pure fuels and in fuel-air mixtures (adapted from Bauer&Forest 2001 [II.16], Karim 2003 [II.17], Wang et al. 2008 [II.9], Huang et al. 2009 [II.7], Hu et al. 2009 [II.14,15], Verhelst&Wallner 2009 [II.18]).
Table 4	Simple schemes of combustion for hydrogen-air mixtures. Burned gas compositions as a function of fuel to air equivalence ratio Φ with product moles evaluation for each mole of fuel.
Table 5.	Summary of some effects of fuel composition parameters on the combustion performance and emissions in spark ignition engines for premixed blends of natural gas and hydrogen.
Table 6.	Compared diffusivities of hydrogen, methane and propane in fuel-air mixtures (adapted from Law&Sung 2000 [III.54]).
Table 7.	Flame conditions regarding to instabilities phenomena (some combinations of cases).
Table 8.	Flame trends with stretch interactions (some combinations of cases).
Table 9.	Flame front speed corrections of instabilities and stretch effects.
Table 10.	Summary of particular characteristics of the methodologies used in the definition and some applications of reviewed expressions of laminar burning velocity for hydrogen-air mixtures.
Table 11.	Nomenclature relations and notations of the reviewed expressions of laminar burning velocity for hydrogen-air mixtures. Parametric and functional dependences (based on their respective data origins, derived from conceptually varied methodological sources).
Table 12.	Summary of complex unified notations of table 11, for the reviewed expressions of laminar burning velocity with their functional dependences.
Table 13.	Dependences of exponents and coefficients appearing in the reviewed expressions of laminar burning velocity.
Table 14.	Dependences of factors and functions in the reviewed expressions of laminar burning velocity.
Table 15.	Expressions of laminar burning velocity for hydrogen-air mixtures (applicability ranges in table 16).
Table 16.	Applicability ranges of the reviewed expressions of laminar burning velocity for hydrogen-air mixtures (analytical expressions in table 15).
Table 17.	Summary of conditions considered in this study for the comparison of expressions of laminar burning velocity.
Table 18.	Summary of charts indicating the functional dependences represented for the reviewed expressions of laminar burning velocity.
Table 19.	Values of temperature T and pressure P related by an adiabatic compression ($\gamma=c_p/c_v=1.4$) for the expressions of laminar burning velocity in charts of fig. 37 (A,A';B,B').
Table 20.	Summary of literature references with experimental measurements of laminar burning velocities for hydrogen blends in different fuel-air mixtures.

- Table 21.** Laminar burning velocity trends in different regimes of fuel-air mixtures of H₂-CH₄ blends (adapted from Di-Sarli&Di-Benedetto 2007 [IV.160], Hu et al. 2009 [IV.75], Hu et al. 2009 [IV.77]).
- Table 22.** Relevant reactions involving H atoms for fuel-air mixtures of H₂-CH₄ blends; $T_u=300\text{ K}$, $P=0.1\text{ MPa}$, $\Phi=1$ (adapted from Bougrine et al. 2011 [IV.172]).
- Table 23.** Main elementary reaction steps of fuel-air mixtures of H₂-CH₄ binary blends at atmospheric conditions.
- Table 24.** Main elementary reaction steps for different mixture conditions of H₂-CH₄ blends.
- A.** For atmospheric conditions at temperature $T_u=300\text{ K}$ and pressure $P=1\text{ atm}$ (adapted from Di-Sarli&Di-Benedetto 2007 [IV.160]).
 - B.** For conditions at room temperature $T_u=303\text{ K}$ and atmospheric pressure $P=1\text{ bar}$ (adapted from Hu et al. 2009 [IV.75]).
 - C.** For lean conditions of $\Phi=0.8$ at increased temperature $T_u=373\text{ K}$ and pressure $P=5\text{ bar}$ (adapted from Hu et al. 2009 [IV.78]).
- Table 25.** Laminar burning velocity analytical expression for H₂-CH₄ blends (adapted from Bougrine et al. 2011 [IV.172]).
- Table 26.** Summary of types of expressions of laminar burning velocity for fuel blends of hydrogen with methane or natural gas. Features of applicability depending on composition conditions.
- Table 27.** Summary of some characteristics relative to several works in the literature related with combustion of hydrogen fuel blends in air mixtures with methane or natural gas and some cases with other hydrocarbons.
- Table 28.** Summary of literature references with expressions for burning velocities of methane-air mixtures. Applicability ranges.
- Table 29.** Summary of literature references with expressions for burning velocities of hydrogen-air mixtures. Applicability ranges.

Bibliography

General summary of all parts references (*in alphabetical order*)

A

- [1] **Addabbo R, Bechtold JK, Matalon M.** Wrinkling of spherically expanding flames. Proceedings of the Combustion Institute 2002; 29(2):1527-35.
[III.104]
- [2] **Agnew JT, Graiff LB.** The pressure dependence of laminar burning velocity by the spherical bomb method. Combustion and Flame 1961;5:209-19.
[IV.253]
- [3] **Akansu SO, Dulger A, Kahraman N.** Internal combustion engines fueled by natural gas-hydrogen mixtures. International Journal of Hydrogen Energy 2004;29(14):1527-39.
[II,IV.52]
- [4] **Aldredge RC, Zuo B.** Flame acceleration associated with the Darrieus-Landau instability. Combustion and Flame 2001;127:2091-101.
[III.91]
- [5] **Aliramezani M, Chitsaz I, Mozafari AA.** Thermodynamic modeling of partially stratified charge engine characteristics for hydrogen-methane blends at ultra-lean conditions. International Journal of Hydrogen Energy 2013;38:10640-47.
[II,IV.24]
- [6] **Allenby S, Chang WC, Megaritis A, Wyszynski ML.** Hydrogen enrichment: a way to maintain combustion stability in a natural gas fueled engine with exhaust gas recirculation, the potential of fuel reforming. Proceedings of the Institution of Mechanical Engineers, Part D: Journal of Automobile Engineering 2001;215(3):405-18.
[II,IV.94]
- [7] **Al-Shahrany AS, Bradley D, Lawes M, Liu K, Woolley R.** Darrieus-Landau and thermo-acoustic instabilities in closed vessel explosions. Combustion Science and Technology 2006;178:1771-802.
[III.69]
- [8] **Al-Shahrany AS, Bradley D, Lawes M, Woolley R.** Measurement of unstable burning velocities of Isooctane-air mixtures at high pressure and the derivation of laminar burning velocities. Proceedings of the Combustion Institute 2005;30:225-32.
[III.68]
- [9] **Andrews GE, Bradley D.** Determination of burning velocities: A critical review. Combustion and Flame 1972;18(1):133-53.
[III.105]
- [10] **Andrews GE, Bradley D.** The burning velocity of methane-air mixture. Combustion and Flame 1972;19:275-88.
[IV.250]
- [11] **Aung KT, Hassan MI, Faeth GM.** Effects of pressure and nitrogen dilution on flame stretch interactions of laminar premixed H₂-O₂-N₂ flames. Combustion and Flame 1998;112:1-15.
[III.79]
- [12] **Aung KT, Hassan MI, Faeth GM.** Flame stretch interactions of laminar premixed hydrogen-air flames at normal temperature and pressure. Combustion and Flame 1997;109(1-2):1-24.
[III.114]
- [13] **Aung KT, Hassan MI, Kwon S, Tseng LK, Kwon OC, Faeth GM.** Flame/stretch interaction in laminar and turbulent premixed flames. Combustion Science and Technology 2002;174:61-99.
[III.64]

B

- [14] **Babkin VS, Kozachenko LS.** Study of normal burning velocity in methane-air mixtures at high pressures. Fizika Goreniya i Vzryva 1966;3(2):77-86. (English translation: Combustion, Explosion and Shock Waves 1966;2:46-52).
[IV.252]
- [15] **Bade-Shrestha SO, Karim GA.** Hydrogen as an additive to methane for spark ignition engine applications. International Journal of Hydrogen Energy 1999;24:577-86.
[II,IV.27]

- [16] **Bade-Shrestha SO, Karim GA.** Predicting the effects of the presence of diluents with methane on spark ignition engine performance. *Applied Thermal Engineering* 2001;21:331-42.
[IV.229]
- [17] **Barassin A, Lisbet R, Combourieu J, Laffitte P.** Etude de l'influence de la temperature initiale sur la vitesse normale de deflagration de melanges methane-air en fonction de la concentration. *Bulletin de la Societe Chimique de France* 1967; 104(7):2521-6.
[IV.251]
- [18] **Bauer CG, Forest TW.** Effect of hydrogen addition on the performance of methane-fueled vehicles. Part I: effect on S.I. engine performance. *International Journal of Hydrogen Energy* 2001;26:55-70.
[II,IV.16];[III.16]
- [19] **Bauer CG, Forest TW.** Effect of hydrogen addition on the performance of methane-fueled vehicles. Part II: driving cycle simulations. *International Journal of Hydrogen Energy* 2001;26:71-90.
[II,IV.29]
- [20] **Bechtold JK, Matalon M.** Hydrodynamic and diffusion effects on the stability of spherically expanding flames. *Combustion and Flame* 1987;67(1):77-90.
[III.49]
- [21] **Bechtold JK, Matalon M.** The dependence of the Markstein Length on stoichiometry. *Combustion and Flame* 2001;127:1906-13.
[III.75];[IV.183]
- [22] **Bell SR, Gupta M.** Extension of the lean operating limit for natural gas fueling of a spark ignited engine using hydrogen blending. *Combustion Science and Technology* 1997;123:23-48.
[II,IV.26]
- [23] **Ben L, Dacros NR, Truquet R, Charnay G.** Influence of air/fuel ratio on cyclic variation and exhaust emission in natural gas SI engine, SAE Paper 992901; 1999.
[II,IV.48]
- [24] **Bilgin A.** Geometric features of the flame propagation process for an SI engine having dual ignition system. *International Journal of Energy Research* 2002;26(11):987-1000.
[IV.118]
- [25] **Blarigan PV, Keller JO.** A hydrogen-fueled internal combustion engine designed for single speed power operation. *International Journal of Hydrogen Energy* 2002;23(7):603-9.
[II,IV.51]
- [26] **Blarigan PV, Keller JO.** A hydrogen-fueled internal combustion engine designed for single speed-power operation. *Journal of Engineering for Gas Turbines and Power* 2003;125(3):783-90.
[II,IV.98]
- [27] **Blint RJ.** The relationship of the laminar flame width to flame speed. *Combustion Science and Technology* 1986;49:79-92.
[III.83]
- [28] **Bougrine S, Richard S, Nicolle A, Veynante D.** Numerical study of laminar flame properties of diluted methane-hydrogen-air flames at high pressure and temperature using detailed chemistry. *International Journal of Hydrogen Energy* 2011;36:12035-47.
[III.12];[IV.172];[V.19]
- [29] **Bougrine S, Richard S, Veynante D.** On the combination of complex chemistry with a 0-D coherent flame model to account for the fuel properties in spark ignition engines simulations: Application to methane-air-diluents mixtures. *Proceedings of the Combustion Institute* 2011;33:3123-30.
[III.142];[IV.218];[V.24]
- [30] **Bradley D, Cresswell TM, Puttock JS.** Flame acceleration due to flame-induced instabilities in large-scale explosions. *Combustion and Flame* 2001;124:551-9.
[III.92]
- [31] **Bradley D, Gaskell PH, Gu XJ, Sedaghat A.** Flame instabilities in large scale atmospheric gaseous explosions. 4th International Seminar on Fire and Explosion Hazards, Londonderry, Northern Ireland, 2003.
[III.78]
- [32] **Bradley D, Gaskell PH, Gu XJ.** Burning velocities, Markstein lengths, and flame quenching for spherical methane-air flames: a computational study. *Combustion and Flame* 1996;104(1-2):176-98.

- [III.25];[IV.122]
- [33] **Bradley D, Harper CM.** The development of instabilities in laminar explosion flames. *Combustion and Flame* 1994;99(3-4):562-72.
[III.98]
- [34] **Bradley D, Hicks RA, Lawes M, Sheppard CGW, Woolley R.** The measurement of laminar burning velocities and Markstein numbers, for iso-octane/air and iso-octane/n-heptane/air mixtures, at elevated temperatures and pressures, in an explosion bomb. *Combustion and Flame* 1998;115(1-2):126-44.
[III.26];[IV.119]
- [35] **Bradley D, Lawes M, Liu K, Verhelst S, Woolley R.** Laminar burning velocities of lean hydrogen-air mixtures at pressures up to 1 MPa. *Combustion and Flame* 2007;149(1-2):162-72.
[III.45];[IV.259]
- [36] **Bradley D, Sheppard CGW, Wooley R, Greenhalgh DA, Lockett RD.** The development and structure of flame instabilities and cellularity, at low Markstein numbers in explosions. *Combustion and Flame* 2000;122:195-209.
[III.77]
- [37] **Bradley D.** How fast can we burn? *Proceedings of the Combustion Institute* 1992;24:247-62.
[III.106]
- [38] **Bradley D.** Instabilities and flame speeds in large-scale premixed gaseous explosions. *Philosophical Transactions of the Royal Society of London* 1999;357:3567-81.
[III.100]
- [39] **Brewster S, Bleachmore C.** Dilution strategies for load and NO_x management in a hydrogen fueled direct injection engine. SAE 2007-01-4097, 2007.
[III.198]
- [40] **Burke MP, Chaos M, Ju Y, Dryer FL, Klippenstein SJ.** Comprehensive H₂/O₂ kinetic model for high-pressure combustion. *International Journal of Chemical Kinetics* 2012;44:444-74.
[V.11]
- [41] **Burke MP, Chen Z, Ju Y, Dryer FL.** Effect of cylindrical confinement on the determination of laminar flame speeds using outwardly propagating flames. *Combustion and Flame* 2009;156:771-9.
[V.14]
- [42] **Burke MP, Klippenstein SJ, Harding LB.** A quantitative explanation for the apparent anomalous temperature dependence of OH+HO₂→H₂O+O₂ through multi-scale modeling. *Proceedings of the Combustion Institute* 2013;34:547-55.
[V.12]
- [43] **Burks TL, Oran ES.** A computational study of the chemical kinetics of hydrogen combustion. NRL Memorandum Report 1981;NRL-44-0572-0-1.
[III.171]
- [44] **Butler CJ, Hayhurst AN.** Measurements of the concentrations of free hydrogen atoms in flames from observations of ions: correlation of burning velocities with concentrations of free hydrogen atoms. *Combustion and Flame* 1998;115(1-2):241-52.
[IV.198]
- [45] **Bychkov VV, Liberman MA.** Dynamics and stability of premixed flames. *Physics Reports* 2000;325:115-237.
[III.53]
- [46] **Bysveen M.** Engine characteristics of emissions and performance using mixtures of natural gas and hydrogen. *International Journal of Hydrogen Energy* 2007;32(4):482-9.
[II,IV.73]

C

- [47] **CHEMKIN (4.0.1).** Theory manual [chapter 12]; 2004.
[IV.166]
- [48] **Chen Z, Burke MP, Ju Y.** Effects of Lewis number and ignition energy on the determination of laminar flame speed using propagating spherical flames. *Proceedings of the Combustion Institute* 2009;32(1):1253-60.

- [III.121]
- [49] **Cho** HM, **He** BQ. Spark ignition natural gas engines - a review. *Energy Conversion and Management* 2007;48(2):608-18.
[II,IV.1]
- [50] **Choudhuri** AR, **Gollahalli** SR. Laser induced fluorescence measurements of radical concentrations in hydrogen-hydrocarbon hybrid gas fuel flames. *International Journal of Hydrogen Energy* 2000;25(11):1119-27.
[IV.199]
- [51] **Choudhuri** AR, **Gollahalli** SR. Stability of hydrogen-hydrocarbon blended fuel flames. *AIAA Journal of Propulsion and Power* 2003;19(2):220-5.
[II,IV.59]
- [52] **Chung**, SH, **Chung** DH, **Fu** C, **Cho** P. Proceedings of seminar on combustion phenomena in IC engines. Korean Society of Mechanical Engineers, Seoul, 1995;29.
[III.81]
- [53] **Clavin** P. Dynamic behavior of premixed flame fronts in laminar and turbulent flows. *Progress in Energy and Combustion Science* 1985;11(1):1-59.
[III.42];[IV.193]
- [54] **Colin** O, **Benkenida** A, **Angelberger** C. ECFM_3D modeling of mixing, ignition and combustion phenomena in highly stratified gasoline engines. *Oil Gas Science Technology* 2003;58:47-62.
[III.156]
- [55] **Combustion Technology** group, Technical University of Eindhoven. <http://www.Combustion.tue.nl>.
[III.185]
- [56] **Coppens** FHV, de **Ruyck** J, **Konnov** AA. Effects of hydrogen enrichment on adiabatic burning velocity and NO formation in methane-air flames. *Thermal and Fluid Science* 2007;31(5):437-44.
[III.190];[IV.142]
- [57] **Coppens** FHV, de **Ruyck** J, **Konnov** AA. The effects of composition on burning velocity and nitric oxide formation in laminar premixed flames of $\text{CH}_4+\text{H}_2+\text{O}_2+\text{N}_2$. *Combustion and Flame* 2007;149(4):409-17.
[IV.129]
- [58] **Cuenot** B, **Egolfopoulos** FN, **Poinsot** T. Direct numerical simulation of stagnation-flow premixed flames transition from planar to Bunsen flames and the direct measurement of laminar flame speeds. 2nd Joint Meeting of the Combustion Institute US Sections, 2000;134.
[III.23]
- [59] **Curtis** AR, **Sweetenham** WP. FACSIMILE release H user's manual. AERE report R11771, 1987. <http://www.esm-software.com>.
[III.147]
- [60] **Curto-Risso** P, **Medina** A, **Hernández** AC, **Guzmán-Vargas** L, **Angulo-Brown** F. On cycle-to-cycle heat release variations in a simulated spark ignition heat engine. *Applied Energy* 2011;88(5):1557-67.
[II,IV.113]

D

- [61] **D'Errico** G, **Ferrari** G, **Onorati** A, **Cerri** T. Modeling the pollutant emissions from a S.I. engine. SAE 2002-01-0006, 2002.
[III.182]
- [62] **D'Errico** G, **Lucchini** T. A combustion model with reduced kinetic schemes for S.I. engines fueled with compressed natural gas. SAE 2005-01-1123, 2005.
[III.183]
- [63] **D'Errico** G, **Onorati** A, **Ellgas** S, **Obieglo** A. Thermo-fluid dynamic simulation of a SI single-cylinder H_2 engine and comparison with experimental data. ASME Engine Technology Conference, Aachen, Germany. ICES2006-1311, 2006.
[III.184]

- [64] **D'Errico G, Onorati A, Ellgas S.** 1D-thermo-fluid dynamic modeling of an SI single-cylinder H₂ engine with cryogenic port injection. *International Journal of Hydrogen Energy* 2008;33:5829-41. [\[III.11\]](#); [\[IV.257\]](#)
- [65] **Dagaut P, Dayma G.** Hydrogen-enriched natural gas blend oxidation under high-pressure conditions: experimental and detailed chemical kinetic modeling. *International Journal of Hydrogen Energy* 2006;31(4):505-15. [\[IV.206\]](#)
- [66] **Dagaut P, Nicolle A.** Experimental and detailed kinetic modeling study of hydrogen-enriched natural gas blend oxidation over extended temperature and equivalence ratio ranges. *Proceedings of the Combustion Institute* 2005;30(2):2631-8. [\[IV.205\]](#)
- [67] **Dahoe AE, De-Goey LPH.** On the determination of the laminar burning velocity from closed vessel gas explosions. *Journal of Loss Prevention in the Process Industries* 2003;16:457-78. [\[III.31\]](#); [\[IV.246\]](#)
- [68] **Dahoe AE.** Laminar burning velocities of hydrogen-air mixtures from closed vessel gas explosions. *Journal of Loss Prevention in the Process Industries* 2005;18:152-66. [\[III.32\]](#)
- [69] **Das A, Watson HC.** Development of a natural gas spark ignition engine for optimum performance. *Proceedings of the Institution of Mechanical Engineers, Part D, Journal of Automobile Engineering* 1997;211:361-78. [\[II,IV.50\]](#)
- [70] **Das LM, Gulati R, Gupta PK.** A comparative evaluation of the performance characteristics of a spark ignition engine using hydrogen and compressed natural gas as alternative fuels. *International Journal of Hydrogen Energy* 2000;25:783-93. [\[II,IV.20\]](#)
- [71] **Davis SG, Joshi AV, Wang H, Egolfopoulos F.** An optimized kinetic model of H₂-CO combustion. *Proceedings of the Combustion Institute* 2005;30:1283-92. [\[III.46\]](#)
- [72] **De-Ferrières S, El-Bakali A, Lefort B, Montero M, Pauwels JF.** Investigation of laminar low pressure stoichiometric CH₄-C₂H₆-C₃H₈-O₂-N₂ and CH₄-C₂H₆-C₃H₈-H₂-O₂-N₂ flames. *Proceedings of the European Combustion Meeting ECM* 2007. [\[IV.210\]](#)
- [73] **De-Goey LPH, Thije-Boonkkamp JHM.** A flamelet description of premixed laminar flames and the relation with flame stretch. *Combustion and Flame* 1999;119:253-71. [\[III.66\]](#)
- [74] **Desantes JM, Molina S.** Introduction to combustion. In: Payri F, Desantes JM, editors. *Reciprocating internal combustion engines* (Spanish). Valencia Polytechnic University publication, Reverté publisher 2011 (2nd imprint 2012);chapt.13. [\[III.36\]](#)
- [75] **Dimopoulos P, Bach C, Soltic P, Boulouchos K.** Hydrogen-natural gas blends fuelling passenger car engines: combustion, emissions and well-to-wheels assessment. *International Journal of Hydrogen Energy* 2008;33(23):7224-36. [\[II,IV.95\]](#)
- [76] **Dimopoulos P, Rechsteiner C, Soltic P, Laemmle C, Boulouchos K.** Increase of passenger car engine efficiency with low engine-out emissions using hydrogen-natural gas mixtures: a thermodynamic analysis. *International Journal of Hydrogen Energy* 2007;32(14):3073-83. [\[II,IV.96\]](#)
- [77] **Di-Sarli V, Di-Benedetto A.** Laminar burning velocity of hydrogen-methane-air premixed flames. *International Journal of Hydrogen Energy* 2007;32:637-46. [\[IV.160\]](#)
- [78] **Dixon-Lewis G, Williams A.** Some observations on the structure of a slow-burning flame supported by the reaction between hydrogen and oxygen at atmospheric pressure. *Proceedings of the Combustion Institute* 1963;9:576-84. [\[III.166\]](#)
- [79] **Dixon-Lewis G.** Chemical mechanism and properties of freely propagating hydrogen oxygen supported flames. *Archivum Combustionis* 1984;4:279-96.

- [III.167]
- [80] **Dong C, Zhou Q, Zhao Q, Zhang Y, Xu T, Hui S.** Experimental study on the laminar flame speed of hydrogen-carbon monoxide-air mixtures. *Fuel* 2009;88:1858-63.
[IV.159]
- [81] **Dong Y, Vagelopoulos CM, Spedding GR, Egolfopoulos FN.** Measurement of laminar flame speeds through digital particle image velocimetry: mixtures of methane and ethane with hydrogen, oxygen, nitrogen, and helium. *Proceedings of the Combustion Institute*; 2002:1419-26.
[IV.147]
- [82] **Dowdy DD, Smith D, Taylor SC, Williams A.** The use of expanding spherical flames to determine burning velocities and stretch effects in hydrogen air mixtures. *Proceedings of the Combustion Institute* 1990;23:325-32.
[III.112]
- [83] **Driscoll JF.** Turbulent premixed combustion: flamelet structure and its effect on turbulent burning velocities. *Progress in Energy and Combustion Science* 2008;34:91-134.
[III.101]
- [84] **Dugger GL.** Effect of initial mixture temperature on flame speed of methane-air, propane-air and ethylene-air mixtures. NACA report of investigations 1061, Lewis Flight Propulsion Laboratory, Cleveland, Ohio, 1952.
[IV.254]

E

- [85] **Ebrahimi R, Desmet B.** An experimental investigation on engine speed and cyclic dispersion in an HCCI engine. *Fuel* 2010;89(8):2149-56.
[II,IV.110]
- [86] **Egolfopoulos FN, Hansen N, Ju Y, Kohse-Höinghaus K, Law CK, Qi F.** Advances and challenges in laminar flame experiments and implications for combustion chemistry. *Progress in Energy and Combustion Science* 2014;43:36-67.
[V.1]
- [87] **Egolfopoulos FN, Law CK.** An experimental and computational study of the burning rates of ultra-lean to moderately-rich H₂-O₂-N₂ laminar flames with pressure variations. *Proceedings of the Combustion Institute* 1991;23(1):333-40.
[III.113]
- [88] **Egolfopoulos FN, Law CK.** Chain mechanisms in the overall reaction orders in laminar flame propagation. *Combustion and Flame* 1990;80(1):7-16.
[III.38];[IV.192]
- [89] **Eichseder H, Wallner T, Freymann R, Ringler J,** The potential of hydrogen internal combustion engines in a future mobility scenario. SAE Paper 2003-01-2267, 2003.
[II,IV.36]
- [90] **El-Sherif SA.** Control of emissions by gaseous additives in methane-air and carbon monoxide-air flames. *Fuel* 2000;79:567-75.
[II,IV.38]
- [91] **El-Sherif SA.** Effects of natural gas composition on the nitrogen oxide, flame structure and burning velocity under laminar premixed flame conditions. *Fuel* 1998;77:1539-47.
[II,IV.45]
- [92] **Ern A, Giovangigli V, Eglib,** A general purpose Fortran library for multicomponent transport property evaluation, CERMICS Internal Report 96-51, 1996. Ecole Nationale des Ponts et Chaussées, Marne, France. <http://www.blanche.Polytechnique.fr/www.eglib>.
[III.186]

F

- [93] **FIRE** version 8.2 manual, 2003. AVL List GmbH. <http://www.avl.com>.
[III.153]

- [94] **FLUENT** (Ansys) flow modeling simulation software. Inc. Modeling premixed combustion. User's manual 2003. <http://www.fluent.com>.
[III.154]
- [95] **Frassoldati A, Faravelli T, Ranzi E. Dsmoke**: A wide range modeling study of NO_x formation and nitrogen chemistry in hydrogen combustion. *International Journal of Hydrogen Energy* 2006;31:2310-28.
[III.172]
- [96] **Frenklach M, Bowman T, Smith G, Gardiner B. GRI-Mech** version 3.0, 1999.
[III.144]
- [97] **Frenklach M, Bowman T, Smith G, Gardiner B.** The "GRI-Mech_3.0" chemical kinetic mechanism, 1999.
[IV.171]
- [98] **Frenklach M, Wang H, Rabinowitz MJ.** Optimization and analysis of large chemical kinetic mechanisms using the solution mapping method-combustion of methane. *Progress in Energy Combustion Science*, 1992;18:47-73.
[III.159]

G

- [99] **Galloni E.** Analyses about parameters that affect cyclic variation in a spark ignition engine. *Applied Thermal Engineering Journal* 2009;29(5-6):1131-7.
[II,IV.101]
- [100] **Gaydon AG, Wolfhard HG.** *Flames*. Chapman&Hall, London, 1979.
[IV.203]
- [101] **Genovese A, Contrisciani N, Ortenzi F, Cazzola V.** On road experimental tests of hydrogen-natural gas blends on transit buses. *International Journal of Hydrogen Energy* 2011;36:1775-83.
[II,IV.93]
- [102] **Gerke U, Boulouchos K, Wimmer A.** Numerical analysis of the mixture formation and combustion process in a direct injected hydrogen internal combustion engine. *Proceedings 1st international symposium on hydrogen internal combustion engines*. Graz, Austria, 2006;94-106.
[III.176]
- [103] **Gerke U, Steurs K, Rebecchi P, Boulouchos K.** Derivation of burning velocities of premixed hydrogen-air flames at engine-relevant conditions using a single-cylinder compression machine with optical access. *International Journal of Hydrogen Energy* 2010;35:2566-77.
[III.2];[IV.214];[V.17]
- [104] **Gerke U.** Numerical analysis of mixture formation and combustion in a hydrogen direct-injection internal combustion engine. PhD thesis 2007, Swiss Federal Institute of Technology, Zurich, Switzerland.
[III.122];[IV.233]
- [105] **Gillespie L, Lawes M, Sheppard CGW, Woolley R.** Aspects of laminar and turbulent burning velocity relevant to SI engines. SAE 2000-01-0192, 2000./ *SAE Transactions* 109 (section 3) 2001:13-33. In: Oppenheim AK, Stodolsky F, editors. *Advances in combustion*. Society of Automotive Engineers, SAE SP-1492, 2000;1-22.
[III.22]
- [106] **Glassman I, Yetter RA.** *Combustion*. Academic Press Elsevier. New York, 2008.
[IV.219]
- [107] **Glassman I.** *Combustion*. Academic Press Inc. Orlando, Florida, 1997.
[III.34]
- [108] **Goltsov VA, Veziroglu TN, Goltsova LF.** Hydrogen civilization of the future – a new conception of the IAHE. *International Journal of Hydrogen Energy* 2006;31:153-9.
[II,IV.31]
- [109] **Gorensek MB, Forsberg CW.** Relative economic incentives for hydrogen from nuclear, renewable, and fossil energy sources. *International Journal of Hydrogen Energy* 2009;34:4237-42.
[II,IV.19]

- [110] **Göttgens J, Mauss F, Peters N.** Analytic approximations of burning velocities and flame thicknesses of lean hydrogen, methane, ethylene, ethane, acetylene and propane flames. Proceedings of the Combustion Institute 1992;24:129-35.
[III.9];[IV.190];[V.21]
- [111] **Greenberg JB.** On the prediction of thermal diffusion effects in laminar one-dimensional flames. Combustion Science and Technology 1980;24:83-8.
[IV.215]
- [112] **GRI-Mech.** http://www.me.berkeley.edu/gri_mech/releases.html/, 2011.
[IV.170]
- [113] **Groff EG.** The cellular nature of confined spherical propane-air flames. Combustion and Flame 1982;48:51-62.
[III.89]
- [114] **Gruber F, Herdin G, Klausner J, Robitschko R.** Use of hydrogen and hydrogen mixtures in a gas engine. Proceedings of the 1st international symposium on hydrogen internal combustion engines, Graz, Austria 2006;34-48.
[II,IV.33]
- [115] **Gu XJ, Haq MZ, Lawes M, Woolley R.** Laminar burning velocity and Markstein lengths of methane-air mixtures. Combustion and Flame 2000;121(1-2):41-58.
[III.55];[IV.234]
- [116] **Gülder L.** Effect of initial mixture temperature on flame speed of methane-air, propane-air and ethylene-air mixtures. SAE 841000, 1984.
[III.188];[IV.195]

H

- [117] **Halter F, Chauveau C, Djebaili-Chaumeix N, Gökalp I.** Characterization of the effects of pressure and hydrogen concentration on laminar burning velocities of methane-hydrogen-air mixtures. Proceedings of the Combustion Institute 2005;30:201-8.
[II,IV.53]
- [118] **Halter F, Chauveau C, Gokalp I.** Characterization of the effects of hydrogen addition in premixed methane-air flames. Journal of Hydrogen Energy 2007;32:2585-92.
[IV.135]
- [119] **Halter F, Tahtouh T, Mounaim-Rousselle C.** Nonlinear effects of stretch on the flame front propagation. Combustion and Flame 2010;157:1825-32.
[IV.136]
- [120] **Han P, Checkel MD, Fleck BA, Nowicki NL.** Burning velocity of methane-diluent mixture with reformer gas addition. Fuel 2007;86(4):585-96.
[III.189];[IV.225]
- [121] **Haniff MS, Melvin A, Smith DB, Williams A.** The burning velocities of methane and SNG mixtures with air. Journal of Institute of Energy 1989;62:229-36.
[IV.194]
- [122] **Hassan MI, Aung KT, Faeth GM.** Properties of laminar premixed CO-H₂-air flames at various pressures. Journal of Propulsion and Power 1997;13(2):239-45.
[IV.154]
- [123] **Hawkes ER, Chen JH.** Direct numerical simulation of hydrogen-enriched lean premixed methane-air flames. Combustion and Flame 2004;138:242-58.
[II,IV.60]
- [124] **Heffel JW.** NO_x emission reduction in a hydrogen fueled internal combustion engine at 3000 rpm using exhaust gas recirculation. International Journal of Hydrogen Energy 2003;28:1285-92.
[II,IV.22]
- [125] **Hermanns RTE, Konnov AA, Bastiaans RJM, De-Goey LPH, Lucka K, Köhne H.** Effects of temperature and composition on the laminar burning velocity of CH₄+H₂+O₂+N₂ flames. Fuel 2010;89:114-21.
[III.192];[IV.130]

- [126] **Hermanns RTE, Konnov AA, Bastiaans RJM, De-Goey LPH.** Laminar burning velocities of diluted hydrogen-oxygen-nitrogen mixtures. *Energy Fuels* 2007;21(4):1977-81.
[III.119];[IV.143]
- [127] **Hermanns RTE.** Laminar burning velocities of methane-hydrogen-air mixtures. PhD thesis 2007. Eindhoven University, Universal Press, Veenendaal, Netherlands.
[III.191],[IV.144]
- [128] **Hertzberg M.** Selective diffusional demixing: occurrence and size of cellular flames. *Progress in Energy Combustion Science* 1989;15:203-39.
[III.61]
- [129] **Heywood JB.** Internal combustion engine fundamentals. McGraw-Hill, New-York; 1988.
[III.33];[II,IV.99]
- [130] **Hilbert R, Tap F, El-Rabii H, Thévenin D.** Impact of detailed chemistry and transport models on turbulent combustion simulations. *Progress in Energy and Combustion Science* 2004;30:61-117.
[III.157]
- [131] **Hill PG, Kapil A.** The relationship between cyclic variations in spark-ignition engines and the small structure of turbulence. *Combust Flame* 1989;78(2):237-47.
[II,IV.108]
- [132] **Hill PG.** Cyclic variations and turbulence structure in spark ignition engines. *Combust Flame* 1988;72(1):73-89.
[II,IV.107]
- [133] **Hirasawa T, Sung CJ, Joshi A, Yang Z, Wang H, Law CK.** Determination of laminar flame speeds using digital particle image velocimetry: Binary fuel blends of ethylene, n-butane, and toluene. *Proceedings of the Combustion Institute* 2002;29:1427-34.
[IV.178]
- [134] **Hoekstra RL, Blarigan PV, Mulligan N.** NO_x emissions and efficiency of hydrogen, natural gas, and hydrogen/natural gas blended fuels. SAE Paper 961103; 1996.
[II,IV.56]
- [135] **Hoekstra RL, Collier K, Mulligan N, Chew L.** Experimental study of a clean burning vehicle fuel. *International Journal of Hydrogen Energy* 1995;20:737-45.
[II,IV.64]
- [136] **Hong Z, Cook RD, Davidson DF, Hanson RK.** A shock tube study of the $\text{OH}+\text{H}_2\text{O}_2\rightarrow\text{H}_2\text{O}+\text{HO}_2$ and $\text{H}_2\text{O}_2+\text{M}\rightarrow 2\text{OH}+\text{M}$ using laser absorption of H₂O and OH. *Journal of Physical Chemistry* 2010;114:5718-27.
[V.9]
- [137] **Hong Z, Davidson DF, Barbour EA, Hanson RK.** A new shock tube study of the $\text{H}+\text{O}_2\rightarrow\text{OH}+\text{O}$ reaction rate using tunable diode laser absorption of H₂O near 2.5 μm. *Proceedings of the Combustion Institute* 2011;33:309-16.
[V.7]
- [138] **Hong Z, Davidson DF, Hanson RK.** An improved H₂/O₂ mechanism based on recent shock tube-laser absorption measurements. *Combustion and Flame* 2011;158:633-44.
[V.6]
- [139] **Hong Z, Lam KY, Sur R, Wang S, Davidson DF, Hanson RK.** On the rate constants of $\text{OH}+\text{HO}_2\rightarrow\text{H}_2\text{O}+\text{O}_2$: a comprehensive study of H₂O₂ thermal decomposition using multi-species laser absorption. *Proceedings of the Combustion Institute* 2013;34:565-71.
[V.8]
- [140] **Hong Z, Vasu SS, Davidson DF, Hanson RK.** Experimental study of the rate of $\text{OH}+\text{HO}_2\rightarrow\text{H}_2\text{O}+\text{O}_2$ at high temperatures using the reverse reaction. *Journal of Physical Chemistry* 2010;114:5520-5.
[V.10]
- [141] **Horrillo A.** Utilization of multi-zone models for the prediction of the pollutant emissions in the exhaust process in spark ignition engines (Spanish). PhD thesis 1998, University of Valladolid (Spain).
[III.21];[IV.222]
- [142] **Hu E, Huang Z, He J, Jin C, Zheng J.** Experimental and numerical study on laminar burning characteristics of premixed methane-hydrogen-air flames. *International Journal of Hydrogen Energy* 2009;34(11):4876-88.

- [143] [\[II,IV.75\]](#)
Hu E, Huang Z, He J, Miao H. Experimental and numerical study on lean premixed methane-hydrogen-air flames at elevated pressure and temperatures. *International Journal of Hydrogen Energy* 2009;34:6951-60.
[\[II,IV.78\]](#)
- [144] **Hu E, Huang Z, He J, Zheng J, Miao H.** Measurements on laminar burning velocities and onset of cellular instabilities of methane-hydrogen-air flames at elevated pressure and temperatures. *International Journal of Hydrogen Energy* 2009;34:5574-84.
[\[II,IV.76\]](#)
- [145] **Hu E, Huang Z, Liu B, Zheng J, Gu X, Huang B.** Experimental investigation on performance and emissions of a spark-ignition engine fueled with natural gas-hydrogen blends combined with EGR. *International Journal of Hydrogen Energy* 2009;34(1):528-39.
[\[II,IV.14\]](#)
- [146] **Hu E, Huang Z, Liu B, Zheng J, Gu X.** Experimental study on combustion characteristics of a spark-ignition engine fueled with natural gas-hydrogen blends combining with EGR. *International Journal of Hydrogen Energy* 2009;34(2):1035-44.
[\[II,IV.15\]](#)
- [147] **Hu E, Huang Z, Zheng J, Li Q, He J.** Numerical study on laminar burning velocity and NO formation of premixed methane-hydrogen-air flames. *International Journal of Hydrogen Energy* 2009;34:6545-57.
[\[II,IV.77\]](#)
- [148] **Hu E, Huang ZH, He JJ, Jin C, Zheng JJ.** Experimental and numerical study on laminar burning characteristics of premixed methane-hydrogen-air flames. *International Journal of Hydrogen Energy* 2009;34(11):4876-88.
[\[III.18\]](#)
- [149] **Hu E, Huang ZH, He JJ, Miao HY.** Experimental and numerical study on laminar burning velocities and flame instabilities of hydrogen-air mixtures at elevated pressures and temperatures. *International Journal of Hydrogen Energy* 2009;34:8741-55.
[\[III.1\];\[IV.126\]](#)
- [150] **Huang B, Hu E, Huang Z, Zeng J, Liu B, Jiang D.** Cycle-by-cycle variations in a spark ignition engine fueled with natural gas-hydrogen blends combined with EGR. *International Journal of Hydrogen Energy* 2009;34:8405-14.
[\[II,IV.7\]](#)
- [151] **Huang J, Bushe WK.** Experimental and kinetic study of autoignition in methane-ethane and methane-propane-air mixtures under engine-relevant conditions. *Combustion and Flame* 2006;144:74-88.
[\[III.141\]](#)
- [152] **Huang Z, Liu B, Zeng K, Huang Y, Jiang D, Wang X, et al.** Experimental study on engine performance and emissions for an engine fueled with natural gas-hydrogen mixtures. *Energy & Fuels* 2006;20(5):2131-6.
[\[II,IV.69\]](#)
- [153] **Huang Z, Shiga S, Ueda T, Jingu N, Nakamura H, Ishima T, Obokata T, Tsue M, Kono M.** A basic behavior of CNG DI combustion in a spark ignited rapid compression machine. *JSME International Journal, Series B, Fluids and Thermal Engineering* 2002;45(4):891-900.
[\[II,IV.47\]](#)
- [154] **Huang Z, Wang J, Liu B, Zeng K, Yu K, Jiang D.** Combustion characteristics of a direct-injection engine fueled with natural gas-hydrogen mixtures. *Energy & Fuels* 2006;20(2):540-6.
[\[II,IV.70\]](#)
- [155] **Huang Z, Wang J, Liu B, Zeng K, Yu K, Jiang D.** Combustion characteristics of a direct-injection engine fueled with natural gas-hydrogen blends under various injection timings. *Energy & Fuels* 2006;20(4):1498-504.
[\[II,IV.71\]](#)
- [156] **Huang Z, Wang J, Liu B, Zeng K, Yu K, Jiang D.** Combustion characteristics of a direct-injection engine fueled with natural gas-hydrogen blends under different ignition timings. *Fuel* 2007;86:381-7.
[\[II,IV.72\]](#)

- [157] **Huang Z, Zhang Y, Zeng K, Liu B, Wang Q, Jiang D.** Measurements of laminar burning velocities for natural gas-hydrogen-air mixtures. *Combustion and Flame* 2006;146:302-11.
[III.193];[II,IV.6]
- [158] **Hughes KJ, Turanyi T, Clague AR, Pilling MJ.** Development and testing of a comprehensive chemical mechanism for the oxidation of methane. *International Journal of Chemical Kinetics* 2001;33(9):513-38.
[III.164]

I

- [159] **Iijima T, Takeno T.** Effects of temperature and pressure on burning velocity. *Combustion and Flame* 1986;65:35-43.
[III.4];[IV.217]
- [160] **Ilbas M, Crayford AP, Yilmaz I, Bowen PJ, Syred N.** Laminar-burning velocities of hydrogen-air and hydrogen-methane-air mixtures: an experimental study. *International Journal of Hydrogen Energy* 2006;31:1768-79.
[II,IV.54]
- [161] **Ivanic Z, Ayala F, Goldwit J, Heywood JB.** Effects of hydrogen enhancement on efficiency and NO_x emissions of lean and EGR-diluted mixtures in a SI engine. SAE paper 2005-01-0253, 2005.
[II,IV.97]

J

- [162] **Jayachandran J, Lefebvre A, Zhao R, Halter F, Varea E, Renou B, Egolfopoulos FN.** A study of propagation of spherically expanding and counter-flow laminar flames using direct measurements and numerical simulations. *Proceedings of the Combustion Institute* 2015;35:695-702.
[IV.26]
- [163] **Jayachandran J, Zhao R, Egolfopoulos FN.** Determination of laminar flame speeds using stagnation and spherically expanding flames: Molecular transport and radiation effects. *Combustion and Flame* 2014;161:2305-2316.
[V.25]
- [164] **Jamel MAM.** PhD thesis 1984, University of Leeds.
[III.82]
- [165] **Jessen PF, Melvin A.** Combustion fundamentals relevant to the burning of natural gas. *Progress in Energy and Combustion Science* 1977;4(2):239-55.
[II,IV.3]
- [166] **Ji C, Egolfopoulos FN.** Flame propagation of mixtures of air with binary liquid fuel mixtures. *Proceedings of the Combustion Institute* 2011;33(1):955-61.
[IV.179]
- [167] **Jomaas G, Law CK, Bechtold JK.** On transition to cellularity in expanding spherical flames. *Journal of Fluid Mechanics* 2007;583:1-26.
[IV.185]
- [168] **Joulin G, Mitani T.** Linear stability analysis of two-reactant flames. *Combustion and Flame* 1981;40:235-46.
[III.60]

K

- [169] **Kadowaki S, Hasegawa T.** Numerical simulation of dynamics of premixed flames, flame instability and vortex-flame interaction. *Progress in Energy and Combustion Science* 2005;31:193-241.
[III.95]
- [170] **Kadowaki S, Suzukia H, Kobayashi H.** The unstable behavior of cellular premixed flames induced by intrinsic instability. *Proceedings of the Combustion Institute* 2005;30:169-76.
[III.93]

- [171] **Kadowaki S.** Body-force effect on the cell formation of premixed flames. *Combustion and Flame* 2001;124:409-21.
[III.94]
- [172] **Karim GA, Wierzba I, Al-Alousi Y.** Methane-hydrogen mixtures as fuels. *International Journal of Hydrogen Energy* 1996;21(7):625-31.
[II,IV.37]
- [173] **Karim GA, Wierzba I, Boon S.** Some considerations of the lean flammability limits of mixtures involving hydrogen. *International Journal of Hydrogen Energy* 1985;10:117-23.
[IV.211]
- [174] **Karim GA.** Hydrogen as a spark ignition engine fuel. *International Journal of Hydrogen Energy* 2003;28:569-77.
[II,IV.17]
- [175] **Katoh A, Oyama H, Kitagawa K, Gupta AK.** Visualization of OH radical distribution in a methane-hydrogen mixture flame by isotope shift-planar laser induced fluorescence spectroscopy. *Combustion Science and Technology* 2006;178(12):2061-74.
[IV.200]
- [176] **Kee RJ, Dixon-Lewis G, Warnatz J, Coltrin ME, Miller JA.** TRANSPORT (CHEMKIN Collection part): A Fortran computer code package for the evaluation of gas-phase, multicomponent transport properties. Sandia National Laboratories, Albuquerque, New Mexico, 1986; Report SAND 86-8246.
[IV.240]
- [177] **Kee RJ, Grcar JF, Smooke MD, Miller JA.** PREMIX (CHEMKIN Collection part): A Fortran program for modeling steady laminar one-dimensional premixed flames. Sandia National Laboratories, Albuquerque, New Mexico, 1985; Report SAND 85-8240.
[III.129];[IV.162]
- [178] **Kee RJ, Miller JA, Evans G, Dixon-Lewis G.** A computational model of the structure and extinction of strained opposed flow, premixed methane air flame. *Proceedings of the Combustion Institute* 1988;22:1479-94.
[III.130]
- [179] **Kee RJ, Rupley FM, Meeks E, Miller JA.** CHEMKIN_III: A Fortran chemical kinetics package for the analysis of gas-phase chemical and plasma kinetics. Sandia National Laboratories, 1996; Report SAND 96-8216.
[IV.242]
- [180] **Kee RJ, Rupley FM, Miller JA, Coltrin ME, Grcar JF, Meeks E, Moffat HK, Lutz AE, Dixon-Lewis G, Smooke MD, Warnatz J, Evans GH, Larson RS, Mitchell RE, Petzold LR, Reynolds WC, Caracotsios M, Stewart WE, Glarborg P, Wang C, Adigun O.** A software package for the analysis of gas-phase chemical kinetics and plasma kinetics. CHEMKIN program & subroutine library. CHEMKIN Collection part, Release 3.6, Reaction Design, Inc. San Diego, California, 2000.
[III.132];[IV.164]
- [181] **Kee RJ, Rupley FM, Miller JA, Coltrin ME, Grcar JF, Meeks E, Moffat HK, Lutz AE, Dixon-Lewis G, Smooke MD, Warnatz J, Evans GH, Larson RS, Mitchell RE, Petzold LR, Reynolds WC, Caracotsios M, Stewart WE, Glarborg P, Wang C, Adigun O, Houf WG, Chou CP, Miller SF, Ho P, Young DJ.** CHEMKIN Software, Release 4.0, Reaction Design, Inc. San Diego, California, 2004.
[III.133];[IV.165]
- [182] **Kee RJ, Rupley FM, Miller JA.** CHEMKIN_II (CHEMKIN Collection part): A Fortran chemical kinetics package for the analysis of gas-phase chemical kinetics. Sandia National Laboratories, Albuquerque, New Mexico, 1989; Report SAND 89-8009.
[III.131];[IV.163]
- [183] **Kee RJ, Rupley FM, Miller JA.** TRANSPORT (CHEMKIN Collection part): A Fortran computer code package for the evaluation of gas-phase viscosities, conductivities and diffusion coefficients. Sandia National Laboratories, Albuquerque, New Mexico, 1983; Report SAND 83-8209.
[IV.161]
- [184] **Kelley AP, Law CK.** Nonlinear effects in the extraction of laminar flame speeds from expanding spherical flames. *Combustion and Flame* 2009;156(9):1844-51.
[IV.228]

- [185] **Kéromnès A, Metcalfe WK, Heufer KA, Donohoe N, Das AK, Sung CJ**, et al. An experimental and detailed chemical kinetic modeling study of hydrogen and syngas mixture oxidation at elevated pressures. *Combustion and Flame* 2013;160:995-1011.
[V.13]
- [186] **Kim TJ, Yetter RA, Dryer FL**. New results on moist CO oxidation: high pressure, high temperature experiments and comprehensive kinetic modeling. *Proceedings of the Combustion Institute* 1994;25:759-66.
[III.71]
- [187] **Klell M, Eichseder H, Sartory M**. Mixtures of hydrogen and methane in the internal combustion engine - synergies, potential and regulations. *International Journal of Hydrogen Energy* 2012;37:11531-40.
[II,IV.42]
- [188] **Knop V, Benkenida A, Jay S, Colin O**. Modeling of combustion and nitrogen oxide formation in hydrogen-fueled internal combustion engines within a 3D-CFD code. *International Journal of Hydrogen Energy* 2008;33:5083-97.
[III.6];[IV.258]
- [189] **Kobayashi H, Kawazoe H**. Flame instability effects on the smallest wrinkling scale and burning velocity of high pressure turbulent premixed flames. *Proceedings of the Combustion Institute* 2000;28:375-82.
[III.80]
- [190] **Konnov AA, Dyakov IV**. Measurement of propagation speeds in adiabatic cellular premixed flames of CH₄-O₂-CO₂. *Experimental Thermal and Fluid Science* 2005;29:901-7.
[III.90]
- [191] **Konnov AA**. Development and validation of a detailed reaction mechanism for the combustion modeling. *Eurasian Chemico-Technological Journal*, 2000;2:257-64. <http://homepages.vub.ac.be/~akonnov/>.
[III.163]
- [192] **Konnov AA. Konnov-Mech_5.0**. <http://homepages.vub.ac.be/~akonnov/>, 2011.
[III.196];[IV.175]
- [193] **Konnov AA**. Refinement of the kinetic mechanism of hydrogen combustion. *Journal of Advances in Chemical Physics* 2004;23:5-18.
[III.47];[V.4]
- [194] **Konnov AA**. Remaining uncertainties in the kinetic mechanism of hydrogen combustion. *Combustion and Flame* 2008;152:507-28.
[III.125];[V.5]
- [195] **Koroll GW, Kumar RK, Bowles EM**. Burning velocities of hydrogen-air mixtures. *Combustion and Flame* 1993;94:330-40.
[III.111]
- [196] **Krejci MC, Mathieu O, Vissotski AJ, Ravi S, Sikes TG, Petersen EL**, et al. Laminar flame speed and ignition delay time data for the kinetic modeling of hydrogen and syngas fuel blends. *Journal Engineering Gas Turbines Power* 2013;135:021503.
[V.16]
- [197] **Kull HJ**. Theory of the Rayleigh-Taylor instability. *Physics Reports (Review Section of Physics Letters)* 1991;206(5):197-325.
[III.51]
- [198] **Kunioshi N, Fukutani S**. Fuel mixing effects on propagation of premixed flames, II. Hydrogen+methane flames. *Bulletin of the Chemical Society of Japan* 1992;65:2573-7.
[IV.202]
- [199] **Kuo KK**. Principles of combustion. Wiley&Sons Inc. New York, 1986.
[III.35]
- [200] **Kwon OC, Faeth GM**. Flame-stretch interactions of premixed hydrogen-fueled flames: measurements and predictions. *Combustion and Flame* 2001;124:590-610.
[III.97];[IV.207]
- [201] **Kwon OC, Rozenchan G, Law CK**. Cellular instabilities and self-acceleration of outwardly propagating spherical flames. *Proceedings of the Combustion Institute* 2002;29(2):1775-83.

[III.58]

- [202] **Kwon S, Tseng LK, Faeth GM.** Laminar burning velocities and transition to unstable flames in H₂-O₂-N₂ and C₃H₈-O₂-N₂ mixtures. *Combustion and Flame* 1992;90:230-46.

[III.62]

L

- [203] **Lafuente A.** Methodology for the laminar burning velocity diagnosis in mixtures of fuels from the instantaneous pressure in a constant volume combustion bomb (Spanish). PhD thesis 2008, University of Valladolid (Spain).

[III.8];[IV.127]

- [204] **Lamoureux N, Djebāyli-Chaumeix N, Paillard CE.** Laminar flame velocity determination for H₂-air-He-CO₂ mixtures using the spherical bomb method. *Experimental Thermal and Fluid Science* 2003;27(4):385-93.

[III.117];[IV.235]

- [205] **Larsen JF, Wallace JS.** Comparison of emissions and efficiency of a turbocharged lean-burn natural gas and hythane-fueled engine. *Journal of Engineering for Gas Turbines and Power* 1997;119(1):218-26.

[II,IV.40]

- [206] **Law CK, Jomaas G, Bechtold JK.** Cellular instabilities of expanding hydrogen-propane spherical flames at elevated pressures: theory and experiment. *Proceedings of the Combustion Institute* 2005;30(1):159-67.

[III.84];[IV.182]

- [207] **Law CK, Kwon OC.** Effects of hydrocarbon substitution on atmospheric hydrogen-air flame propagation. *International Journal of Hydrogen Energy* 2004;29(8):867-79.

[III.56];[II,IV.32]

- [208] **Law CK, Sung CJ.** Structure, aerodynamics and geometry of premixed flamelets. *Progress in Energy and Combustion Science* 2000;26(4-6):459-505.

[III.54];[IV.187]

- [209] **Law CK.** *Combustion physics.* Cambridge University Press, 2006.

[IV.186]

- [210] **Law CK.** Dynamics of stretched flames. *Proceedings of the Combustion Institute* 1988;22:1381-402.

[III.50]

- [211] **Law CK.** Propagation, structure, and limit phenomena of laminar flames at elevated pressures. *Combustion Science and Technology* 2006;178:335-60.

[III.57]

- [212] **Lawrence Livermore National Laboratory, Chemistry and Materials Science Web site:** <http://www.cms.llnl.gov/>.

[III.165]

- [213] **Li J, Zhao Z, Kazakov A, Dryer FL. Princeton-Mech.** <http://www.princeton.edu/wcombust/database/files/other/>, 2011.

[III.197];[IV.173]

- [214] **Liao SY, Jiang DM, Cheng Q.** Determination of laminar burning velocities for natural gas. *Fuel* 2004;83(9):1247-50.

[II,IV.5]

- [215] **Lipatnikov AN, Chomiak J.** Molecular transport effects on turbulent flame propagation and structure. *Progress in Energy and Combustion Science* 2005;31:1-73.

[III.102]

- [216] **Lipatnikov AN, Chomiak J.** Turbulent flame speed and thickness: phenomenology, evaluation, and application in multi-dimensional simulations. *Progress in Energy and Combustion Science* 2002;28:1-74.

[III.103]

- [217] **Litak G, Kaminski T, Czarnigowski J, Sen A, Wendeker M.** Combustion process in a spark ignition engine: analysis of cyclic peak pressure and peak pressure angle oscillations. *Meccanica* 2009;44:1-11.

- [II,IV.105]
- [218] **Litak G, Kaminski T, Czarnigowski J, Zukowski D, Wendeker M.** Cycle-to-cycle oscillations of heat release in a spark ignition engine. *Meccanica* 2007;42:423-33.
[II,IV.103]
- [219] **Litak G, Kaminski T, Rusinek R, Czarnigowski J, Wendeker M.** Patterns in the combustion process in a spark ignition engine. *Chaos, Solitons & Fractals* 2008;35(3):578-85.
[II,IV.104]
- [220] **Liu B, Huang Z, Zeng K, Chen H, Wang X, Miao H, et al.** Experimental study on emissions of a spark-ignition engine fueled with natural gas-hydrogen blends. *Energy & Fuels* 2008;22(1):273-7.
[II,IV.74]
- [221] **Liu DDS, MacFarlane R.** Laminar burning velocities of hydrogen-air and hydrogen-air-steam flames. *Combustion and Flame* 1983;49:59-71.
[III.110]
- [222] **Liu Y, Lenze B, Leuckel W.** Investigation on the laminar and turbulent burning velocities of premixed lean and rich flames of methane-hydrogen-air mixtures. *Progress in Astronautics and Aeronautics* 1991;131:259-74.
[IV.139]
- [223] **Lutz AE, Rupley FM, Kee RJ, Reynolds WC.** EQUIL: a program (CHEMKIN implementation of STANJAN) for computing chemical equilibria. Sandia National Laboratories Report, 1998.
[IV.184]

M

- [224] **Ma F, Deng J, Qi Z, Li S, Cheng R, Yang H, Zhao S.** Study on the calibration coefficients of a quasi-dimensional model for HCNG engine. *International Journal of Hydrogen Energy* 2011;33:9278-85.
[II,IV.89]
- [225] **Ma F, Li S, Zhao J, Qi Z, Deng J, Naeve N, He Y, Zhao S.** A fractal-based quasi-dimensional combustion model for SI engines fueled by hydrogen compressed natural gas. *International Journal of Hydrogen Energy* 2012;37:9892-901.
[II,IV.4]
- [226] **Ma F, Liu H, Wang Y, Li Y, Wang JJ, Zhao S.** Combustion and emission characteristics of a port-injection HCNG engine under various ignition timings. *International Journal of Hydrogen Energy* 2008; 33(2):816-22.
[II,IV.83]
- [227] **Ma F, Liu H, Wang Y, Wang J, Ding S, Zhao S.** A quasi-dimensional combustion model for SI engine fueled by hydrogen enriched compressed natural gas. SAE Paper 2008-01-1633, 2008.
[II,IV.87]
- [228] **Ma F, Wang M.** Performance and emission characteristics of a turbocharged spark-ignition hydrogen-enriched compressed natural gas engine under wide open throttle operating conditions. *International Journal of Hydrogen Energy* 2010;35:12502-9.
[II,IV.88]
- [229] **Ma F, Wang Y, Liu H, Li Y, Wang J, Ding S.** Effects of hydrogen addition on cycle-by-cycle variations in a lean burn natural gas spark-ignition engine. *International Journal of Hydrogen Energy* 2008;33(2):823-31.
[II,IV.84]
- [230] **Ma F, Wang Y, Liu HQ, Li Y, Wang JJ, Zhao S.** Experimental study on thermal efficiency and emission characteristics of a lean burn hydrogen enriched natural gas engine. *International Journal of Hydrogen Energy* 2007;32(18):5067-75.
[II,IV.82]
- [231] **Ma F, Wang Y, Wang M, Liu H, Wang J, Ding S, et al.** Development and validation of a quasi-dimensional combustion model for SI engines fueled by HCNG with variable hydrogen fractions. *International Journal of Hydrogen Energy* 2008;33:4863-75.
[II,IV.86]
- [232] **Ma F, Wang Y.** Study on the extension of lean operation limit through hydrogen enrichment in a natural gas spark ignition engine. *International Journal of Hydrogen Energy* 2008;33(4):1416-24.

- [II,IV.85]
- [233] **Maas U, Warnatz J.** Ignition processes in hydrogen-oxygen mixtures. *Combustion and Flame* 1988;74:53-69.
[III.169]
- [234] **Mandilas C, Ormsby MP, Sheppard CGW, Woolley R.** Effects of hydrogen addition on laminar and turbulent premixed methane and iso-octane/air flames. *Proceedings of the Combustion Institute* 2007;31:1443-50.
[II,IV.55]
- [235] **Manton J, Von-Elbe G, Lewis B.** Burning-velocity measurements in a spherical vessel with central ignition. *Proceedings of the Combustion Institute* 1953;4:358-63.
[III.86]
- [236] **Manton J, Von-Elbe G, Lewis B.** Non-isotropic propagation of combustion waves in explosive gas mixtures and the development of cellular flames. *Journal of Chemical Physics* 1952;20(1):153-7.
[III.48]
- [237] **Mariani A, Morrone B, Unich A.** Numerical evaluation of internal combustion spark ignition engines performance fueled with hydrogen-natural gas blends. *International Journal of Hydrogen Energy* 2012;37:2644-54.
[II,IV.41]
- [238] **Mariani A, Morrone B, Unich A.** Numerical modeling of internal combustion engines fueled by hydrogen-natural gas blends. ASME international mechanical engineering congress exposition; 2008.
[II,IV.65]
- [239] **Mariani A, Prati MV, Unich A, Morrone B.** Combustion analysis of a spark ignition i.c. engine fueled alternatively with natural gas and hydrogen-natural gas blends. *International Journal of Hydrogen Energy* 2013;38:1616-23.
[II,IV.90]
- [240] **Marinov NM, Curran H.J, Pitz WJ, Westbrook CK.** Chemical kinetic modeling of hydrogen under conditions found in internal combustion engines. *Energy and Fuels* 1998;12:78-82.
[III.135]
- [241] **Marinov NM, Westbrook CK, Pitz WJ.** Detailed and global kinetics model for hydrogen. *Transport phenomena in combustion*, Taylor&Francis, Washington, Columbia, 1996;Vol.1.
[III.134]
- [242] **Markstein GH.** Cell structure of propane flames burning in tubes. *Journal of Chemical Physics* 1949;17(4):428-9.
[III.85]
- [243] **Matalon M.** Intrinsic flame instabilities in premixed and nonpremixed combustion. *Annual Review of Fluid Mechanics* 2007;39:163-91.
[III.99]
- [244] **Matlab.** The language of technical computing, <http://www.mathworks.com/>; 2011.
[III.187];[IV.238]
- [245] **Mclean IC, Smith DB, Taylor SC.** The use of carbon monoxide-hydrogen burning velocities to examine the rate of the CO+OH reaction. *Proceedings of the 25th international symposium on combustion* 1994;749-57.
[IV.153]
- [246] **Mello P, Pelliza G, Cataluna R, Da-Silva R.** Evaluation of the maximum horsepower of vehicles converted for use with natural gas fuel. *Fuel* 2006;85:2180-6.
[II,IV.46]
- [247] **Messner D, Wimmer A, Gerke U, Gerbig F.** Application and validation of the 3D CFD method for a hydrogen fueled IC engine with internal mixture formation. SAE 2006-01-0448, 2006.
[III.175]
- [248] **Metghalchi M, Keck JC.** Burning velocities of mixtures of air with methanol, isooctane, and indolene at high pressure and temperature. *Combustion and Flame* 1982;48:191-210.
[III.28];[IV.121]
- [249] **Metghalchi M, Keck JC.** Laminar burning velocity of propane-air mixtures at high temperature and pressure. *Combustion and Flame* 1980;38:143-54.

- [III.27];[IV.120]
- [250] **Miao H, Ji M, Jiao Q, Huang Q, Huang Z.** Laminar burning velocity and Markstein length of nitrogen diluted natural gas/hydrogen/air mixtures at normal, reduced and elevated pressures. *International Journal of Hydrogen Energy* 2009;34:3145-55.
[II,IV.13];[III.74]
- [251] **Miao H, Jiao Q, Huang Z, Jiang D.** Effect of initial pressure on laminar combustion characteristics of hydrogen enriched natural gas. *International Journal of Hydrogen Energy* 2008;33:3876-85.
[II,IV.11];[III.72]
- [252] **Miao H, Jiao Q, Huang Z, Jiang D.** Measurement of laminar burning velocities and Markstein lengths of diluted hydrogen-enriched natural gas. *International Journal of Hydrogen Energy* 2009;34:507-18.
[II,IV.12];[III.73]
- [253] **Miller JA, Bowman CT.** Mechanism and modeling of nitrogen chemistry in combustion. *Progress in Energy and Combustion Science* 1989;15:287-8.
[III.160]
- [254] **Miller JA, Mitchell RE, Smooke MD, Kee RJ.** Towards a comprehensive chemical kinetic mechanism for the oxidation of acetylene. *Proceedings of the Combustion Institute* 1982;19:181-96.
[III.161]
- [255] **Milton BE, Keck JC.** Laminar burning velocities in stoichiometric hydrogen and hydrogen-hydrocarbon gas mixtures. *Combustion and Flame* 1984;58:13-22.
[III.5];[IV.131]
- [256] **Mohammadi A, Shioji M, Nakai Y, Ishikura W, Tabo E.** Performance and combustion characteristics of a direct injection SI hydrogen engine. *International Journal of Hydrogen Energy* 2007;32:296-304.
[II,IV.23]
- [257] **Morrone B, Unich A.** Numerical investigation on the effects of natural gas and hydrogen blends on engine combustion. *International Journal of Hydrogen Energy* 2009;34:4626-34.
[II,IV.66]
- [258] **Mosbacher D, Wehrmeyer J, Pitz R, Sung CJ, Byrd J.** Experimental and numerical investigation of premixed cylindrical flames. *American Institute of Aeronautics and Astronautics, AIAA2002-0481*, 2002.
[III.136]
- [259] **Müller UC, Bollig M, Peters N.** Approximations for burning velocities and Markstein numbers for lean hydrocarbon and methanol flames. *Combustion and Flame* 1997;108:349-56.
[IV.220]
- [260] **Munshi S.** Medium-heavy duty hydrogen enriched natural gas spark ignition IC engine operation. *Proceedings of the 1st international symposium on hydrogen internal combustion engines, Graz, Austria* 2006;71-82.
[II,IV.62]

N

- [261] **Naber JD, Siebers DL, Di-Julio SS, Westbrook CK.** Effects of natural gas composition on ignition delay under diesel conditions. *Combustion and Flame* 1994;99:192-200.
[II,IV.2]
- [262] **Nagalingam B, Duebel F, Schmillen K.** Performance study using natural gas, hydrogen supplemented natural gas and hydrogen in AVL research engine. *International Journal of Hydrogen Energy* 1983;8(9):715-20.
[II,IV.63]
- [263] **Naha S, Briones AM, Aggarwal SK.** Effect of fuel blends on pollutant emissions in flames. *Combustion Science and Technology* 2005;177(1):183-220.
[IV.201]
- [264] **Natarajan J, Lieuwen T, Seitzman J.** Laminar flame speeds of H₂-CO mixtures: effect of CO₂ dilution, preheat temperature, and pressure. *Combustion and Flame* 2007;151:104-19.
[IV.157]

O

- [265] **O'Conaire M, Curran HJ, Simmie JM, Pitz WJ, Westbrook CK.** A comprehensive modeling study of hydrogen oxidation. *International Journal of Chemical Kinetics* 2004;36(11):603-22.
[III.139];[V.20]
- [266] **Ortenzi F, Chiesa M, Scarcelli R, Pede G.** Experimental tests of blends of hydrogen and natural gas in light-duty vehicles. *International Journal of Hydrogen Energy* 2008;33:3225-9.
[II,IV.39]

P

- [267] **Padley PJ, Sugden TM.** Chemiluminescence and radical re-combination in hydrogen flames. *Proceedings of the Combustion Institute* 1958;7(1):235-42.
[IV.197]
- [268] **Palm-Leis A, Strehlow RA.** On the propagation of turbulent flames. *Combustion and Flame* 1969;13:111-29.
[III.88]
- [269] **Pareja J, Burbano HJ, Ogami Y.** Measurements of the laminar burning velocity of hydrogen-air premixed flames. *International Journal of Hydrogen Energy* 2010;35:1812-8.
[III.120]
- [270] **Park O, Veloo PS, Liu N, Egolfopoulos FN.** Combustion characteristics of alternative gaseous fuels. *Proceedings of the Combustion Institute* 2011;33:887-94.
[IV.141]
- [271] **Parlange JY.** Influence of preferential diffusion on the stability of a laminar flame. *Journal of Chemical Physics* 1968;48(4):1843-9.
[III.87]
- [272] **Payman W, Wheeler RV.** The combustion of complex gaseous mixtures. *Fuel* 1922;1:185.
[IV.177]
- [273] **Perini F, Paltrinieri F, Mattarelli E.** A quasi-dimensional combustion model for performance and emissions of SI engines running on hydrogen-methane blends. *International Journal of Hydrogen Energy* 2010;35:4687-701.
[III.17];[IV.196]
- [274] **Peters N, Rogg B,** editors. *Reduced kinetic mechanisms for applications in combustion systems.* Springer-Verlag, Berlin Heidelberg New York; 1992.
[III.180]
- [275] **Peters N, Williams FA.** The asymptotic structure of stoichiometric methane-air flames. *Combustion and Flame* 1987;68(2):185-207.
[III.44];[IV.189]
- [276] **Phillips JN, Roby RJ.** Hydrogen-enriched natural gas offers economic NO_x reduction alternative. *Power Engineering (Barrington, Illinois)* 2000;104(5):3.
[II,IV.91]
- [277] **Pilling MJ, Turanyi T, Hughes KJ.** The Leeds methane oxidation mechanism, [www:http://chem.leeds.ac.uk/Combustion/](http://chem.leeds.ac.uk/Combustion/).html, 1996.
[IV.243]
- [278] **Pitsch H, Bollig M.** **FLAMEMASTER:** A computer code for homogeneous and one-dimensional laminar flame calculation. Institut für Technische Mechanik, 1994. RWTHAachen. <http://www.Lavision.de>.
[III.146]
- [279] **Prati MV, Mariani A, Torbati R, Unich A, Costagliola MA, Morrone B.** Emissions and combustion behavior of a bi-fuel gasoline and natural gas spark ignition engine. *SAE International Journal Fuels Lubricants* 2011;4:328-38.
[II,IV.44]

Q

- [280] **Qiao L, Kim CH, Faeth GM.** Suppression effects of diluents on laminar premixed hydrogen-oxygen-nitrogen flames. *Combustion and Flame* 2005;143(1-2):79-96.
[III.118],[IV.208]
- [281] **Qin X, Kobayashi H, Niioka T.** Laminar burning velocity of hydrogen-air premixed flames at elevated pressure. *Experimental Thermal and Fluid Science* 2000;21:58-63.
[III.181]

R

- [282] **Rahim F, Elia M, Ulinski M, Metghalchi M.** Burning velocity measurements of methane-oxygen-argon mixtures and an application to extend methane-air burning velocity measurements. *International Journal of Engine Research* 2002;3(2):81-92.
[III.137]
- [283] **Rahim F, Elia M, Ulinski M, Metghalchi M.** Burning velocity measurements of methane-oxygen-argon mixtures and an application to extend methane-air burning velocity measurements. *International Journal of Engine Research* 2002;3(2):81-92.
[IV.226]
- [284] **Rahim F.** Determination of burning speed for methane-oxidizer-diluent mixtures. PhD thesis 2002, Northeastern University, Boston, Massachusetts.
[III.30],[IV.245]
- [285] **Rakopoulos CD, Kyritsis DC.** Hydrogen enrichment effects on the second law analysis of natural and landfill gas combustion in engine cylinders. *International Journal of Hydrogen Energy* 2006;31:1384-93.
[II,IV.57]
- [286] **Rallis CJ, Garforth AM, Steinz JA.** Laminar burning velocity of acetylene-air mixtures by the constant volume method. *Combustion and Flame* 1965;9:345-56.
[III.24]
- [287] **Rallis CJ, Garforth AM.** The determination of laminar burning velocity. *Progress in Energy and Combustion Science* 1980;6:303-29.
[IV.248]
- [288] **Raman V, Hansel J, Fulton J, Lynch F, Bruderly D.** Hythane - An ultraclean transportation fuel. Proceedings of 10th World Hydrogen Conference, Cocoa Beach, Florida, USA, 1994.
[II,IV.92]
- [289] **Ranzi E, Frassoldati A, Grana R, Cuoci A, Faravelli T, Kelley AP, Law CK.** Hierarchical and comparative kinetic modeling of laminar flame speeds of hydrocarbon and oxygenated fuels. *Progress in Energy and Combustion Science* 2012;38(4):468-501.
[IV.128]
- [290] **Rao S, Rutland CJ.** A flamelet time scale model for non-premixed combustion including unsteady effects. *Combustion and Flame* 2003;133:189-91.
[III.151]
- [291] **Refael S, Sher E.** Reaction kinetics of hydrogen-enriched methane-air and propane-air flames. *Combustion and Flame* 1989;78:326-38.
[IV.133]
- [292] **Ren JY, Qin W, Egolfopoulos FN, Mak H, Tsotsis TT.** Methane reforming and its potential effect on the efficiency and pollutant emissions of lean methane-air combustion. *Chemical Engineering Science* 2001;56:1541-9.
[IV.239]
- [293] **Ren JY, Qin W, Egolfopoulos FN, Tsotsis TT.** Strain-rate effects on hydrogen-enhanced lean premixed combustion. *Combustion and Flame* 2001;124:717-20.
[IV.140]
- [294] **Reyes M, Melgar A, Pérez A, Giménez B.** Study of the cycle-to-cycle variations of an internal combustion engine fueled with natural gas-hydrogen blends from the diagnosis of combustion pressure. *International Journal of Hydrogen Energy* 2013;38:15477-87.

- [II,IV.117]
- [295] **Reyes M.** Characterization of the combustion and auto-ignition processes of liquid fuels in homogeneous mixtures for using in internal combustion engines running in HCCI mode (Spanish). PhD thesis 2008, University of Valladolid (Spain).
[IV.124]
- [296] **Reynolds CCO, Evans RL, Andreassi L, Cordiner S, Mulone V.** The effect of varying the injected charge stoichiometry in a partially stratified charge natural gas engine. SAE Paper 2005-01-0247, 2005.
[IV.216]
- [297] **Ristovski ZD, Morawska L, Hitchins J, Thomas S, Greenaway C, Gilbert D.** Particle emissions from compressed natural gas engines. Journal of Aerosol Science 2000;31:403-13.
[II,IV.43]
- [298] **Rogg B. COSILAB, RUN-1DL:** Cambridge universal laminar flame code. Cambridge University, Department of Engineering Report 1991; CUED/A-THERMO/TR39.
[III.143];[IV.167]
- [299] **Rogg B. COSILAB, RUN-1DL:** The Cambridge universal laminar flamelet computer code. Reduced kinetic mechanisms for applications in combustion systems, Appendix C. Springer-Verlag, Berlin-Heidelberg-NewYork, 1993.
[III.148];[IV.168]
- [300] **Ronney PD.** A perspective on the microgravity role in combustion research. Combustion and Flame 1999;116:317-8.
[III.52]
- [301] **Rousseau S, Lemoult B, Tazerout M.** Combustion characteristics of natural gas in a lean burn spark-ignition engine. Proceedings of the Institution of Mechanical Engineers, Part D, Journal of Automobile Engineering 1999;213(D5):481-9.
[II,IV.49]
- [302] **Rozenchan G, Zhu DL, Law CK, Tse SD.** Outward propagation, burning velocities, and chemical effects of methane flames up to 60 atm. Proceedings of the Combustion Institute 2002;29:1461-69.
[III.138]
- [303] **Ryan TW, Lestz SS.** The laminar burning velocity of iso-octane, n-heptane, methanol, methane, and propane at elevated temperature and pressures in the presence of a diluent. SAE 800103./ SAE Transactions, Detroit, Michigan, 1980;Vol.89.
[III.29],[IV.237]

S

- [304] **Sabia P, De-Joannon M, Romano E, Cavaliere A.** Hydrogen enriched methane mild combustion in a well stirred reactor. Proceedings of the European Combustion Meeting ECM 2007.
[IV.209]
- [305] **Safari H, Jazayeri S, Ebrahimi R.** Potentials of NO_x emission reduction methods in SI hydrogen engines: simulation study. International Journal of Hydrogen Energy 2009;34:1015-25.
[III.173]
- [306] **Sánchez AL, Lépinette A, Bollig M, Liñán A, Lázaro B.** The reduced kinetic description of lean premixed combustion. Combustion and Flame 2000;123:436-64.
[III.150]
- [307] **Sánchez AL, Liñán A, Williams FA.** A generalized Burke-Schumann formulation for hydrogen-oxygen diffusion flames maintaining partial equilibrium of the shuffle reactions. Combustion Science and Technology 1997;123:317-45.
[V.3]
- [308] **Sánchez AL, Williams FA.** Recent advances in understanding of flammability characteristics of hydrogen. Progress in Energy and Combustion Science 2014;41:1-55.
[V.2]
- [309] **Sankaran R, Im HG.** Effect of hydrogen addition on the flammability limit of stretched methane-air premixed flames. Combustion Science and Technology 2006;178:1585-611.
[II,IV.61]

- [310] **Saxena P, Williams FA.** Testing a small detailed Chemical-kinetic mechanism for the combustion of hydrogen and carbon monoxide. *Combustion and Flame* 2006;145:316-23.
[\[III.126\]](#)
- [311] **Schefer RW, Wicksall DM, Agrawal AK.** Combustion of hydrogen enriched methane in a lean premixed swirl-stabilized burner. *Proceedings of the 29th international symposium on combustion* 2002;843-51.
[\[II,IV.25\]](#)
- [312] **Schefer RW.** Hydrogen enrichment for improved lean flame stability. *International Journal of Hydrogen Energy* 2003;28:1131-41.
[\[II,IV.58\]](#)
- [313] **Scholte TG, Vaags PB.** Burning velocities of mixtures of hydrogen, carbon monoxide and methane with air. *Combustion and Flame* 1959;3:511-24.
[\[IV.145\]](#)
- [314] **Scholte TG, Vaags PB.** The influence of small quantities of hydrogen and hydrogen compounds on the burning velocity of carbon monoxide-air flames. *Combustion and Flame* 1959;3:503-10.
[\[IV.158\]](#)
- [315] **Selim MY.** Effect of engine parameters and gaseous fuel type on the cyclic variability of dual fuel engines. *Fuel* 2005;84(7-8):961-71.
[\[II,IV.106\]](#)
- [316] **Sen A, Litak G, Edwards K, Finney C, Daw C, Wagner R.** Characteristics of cyclic heat release variability in the transition from spark ignition to HCCI in a gasoline engine. *Applied Energy* 2011;88(5):1649-55.
[\[II,IV.111\]](#)
- [317] **Sen AK, Longwic R, Litak G, Górski K.** Analysis of cycle-to-cycle pressure oscillations in a diesel engine. *Mechanical Systems and Signal Processing* 2008;22(2):362-73.
[\[II,IV.100\]](#)
- [318] **Sen AK, Zheng J, Huang Z.** Dynamics of cycle-to-cycle variations in a natural gas direct-injection spark-ignition engine. *Applied Energy* 2011;88(7):2324-34.
[\[II,IV.109\]](#)
- [319] **Seshadri KA, Williams FA.** *Turbulent reacting flows.* Academic Press, London; 1994.
[\[III.43\]](#)
- [320] **Sharma SP, Agrawal DD, Gupta CP.** The pressure and temperature dependence of burning velocity in a spherical combustion bomb. *Proceedings of the 18th international symposium on combustion,* The Combustion Institute 1981.
[\[IV.247\]](#)
- [321] **Sher E, Ozdor N.** Laminar burning velocities of n-butane-air mixtures enriched with hydrogen. *Combustion and Flame* 1992;89:214-20.
[\[IV.151\]](#)
- [322] **Sher E, Refael S.** A simplified reaction scheme for the combustion of hydrogen enriched methane-air flame. *Combustion Science and Technology* 1988;59:371-89.
[\[IV.132\]](#)
- [323] **Sierens R, Rosseel E.** Variable composition hydrogen/natural gas mixtures for increased engine efficiency and decreased emissions. *Journal of Engineering for Gas Turbines and Power* 2000;122:135-40.
[\[II,IV.28\]](#)
- [324] **Sileghem L, Vancoillie J, Demuyneck J, Galle J, Verhelst S.** Alternative fuels for spark-ignition engines: Mixing rules for the laminar burning velocity of gasoline-alcohol blends. *Energy Fuels* 2012;26:4721-7.
[\[IV.176\]](#)
- [325] **Simmie JM.** Detailed chemical kinetic models for the combustion of hydrocarbon fuels. *Progress in Energy and Combustion Science* 2003;29:599-634.
[\[III.158\]](#)
- [326] **Sita-Rama-Raju AV, Ramesh A, Nagalingam B.** Effect of hydrogen induction on the performance of a natural-gas fueled lean-burn SI engine. *Journal of the Energy Institute* 2000;73(496):143-8.
[\[II,IV.67\]](#)

- [327] **Smallbone AJ, Tsuneyoshi K, Kitagawa T.** Turbulent and stable-unstable laminar burning velocity measurements from outwardly propagating spherical hydrogen-air flames at elevated pressures. *Journal of Thermal Science and Technology* 2006;1:31-41.
[III.109]
- [328] **Smith D, Agnew JT.** The effect of pressure on the laminar burning velocity of methane-oxygen-nitrogen mixtures. *Proceedings of the 6th international symposium on combustion, The Combustion Institute* 1951;83-88.
[IV.255]
- [329] **Smith GP, Golden DM, Frenklach M, Moriarty NW, Eiteneer B, Goldenberg M, et al. GRI-Mech.** http://www.me.berkeley.edu/gri_mech/releases.html/, 2011.
[III.145]
- [330] **Smith GP, Golden DM, Frenklach M, Moriarty NW, Eiteneer B, Goldenberg M, Bowman CT, Hanson RK, Song S, Gardiner WCjr, Lissianski VV, Qin Z. GRI-Mech:** An optimized detailed chemical reaction mechanism for methane combustion. Report GRI-95/0058, 1995.
[IV.169]
- [331] **Somers LMT. CHEM1D** The simulation of flat flames with detailed and reduced chemical models. PhD thesis 1994. Eindhoven Technical University, Netherlands. TU/e. <http://yp.wtb.tue.nl/showabstract.php/1684>.
[III.149]
- [332] **STAR-CD** version 3.15 PROSTAR. CD-adapco Group. <http://www.cd-adapco.com>.
[III.155]
- [333] **Stone R, Clarke A, Beckwith P.** Correlations for the laminar burning velocity of methane-diluent-air mixtures obtained in free fall experiments. *Combustion and Flame* 1998;114:546-55.
[IV.236]
- [334] **Strehlow RA, Savage LD.** The concept of flame stretch. *Combustion and Flame* 1978;31:209-11.
[III.65]
- [335] **Ströhle J, Myhrvold T.** An evaluation of detailed reaction mechanisms for hydrogen combustion under gas turbine conditions. *International Journal of Hydrogen Energy* 2007;32:125-35.
[III.128]
- [336] **Sun CJ, Law CK.** On the nonlinear response of stretched premixed flames. *Combustion and Flame* 2000;121:236-48.
[III.70]
- [337] **Sun CJ, Sung CJ, He L, Law CK.** Dynamics of weakly stretched flames quantitative description and extraction of global flame parameters. *Combustion and Flame* 1999;118:108-28.
[III.59];[IV.123]
- [338] **Sun H, Yang SI, Jomaas G, Law CK.** High-pressure laminar flame speeds and kinetic modeling of carbon monoxide - hydrogen combustion. *Proceedings of the Combustion Institute* 2007;31:439-46.
[IV.155]

T

- [339] **Tahtouh T, Halter F, Mounaïm-Rousselle C.** Laminar premixed flame characteristics of hydrogen blended isooctane-air-nitrogen mixtures. *International Journal of Hydrogen Energy* 2011;36:985-91.
[IV.152]
- [340] **Tahtouh T, Halter F, Samson E, Mounaïm-Rousselle C.** Effects of hydrogen addition and nitrogen dilution on the laminar flame characteristics of premixed methane-air flames. *International Journal of Hydrogen Energy* 2009;34:8329-38.
[III.194];[IV.137]
- [341] **Takeno T, Iijima T.** First specialist meeting of the combustion Institute, French section 1981;55.
[III.179]
- [342] **Tang C, He J, Huang Z, Jin C, Wang J, Wang X, et al.** Measurements of laminar burning velocities and Markstein lengths of propane-hydrogen-air mixtures at elevated pressures and temperatures. *International Journal of Hydrogen Energy* 2008;33:7274-85.

- [IV.149]
- [343] **Tang C, Huang Z, Jin C, He J, Wang J, Wang X**, et al. Laminar burning velocities and combustion characteristics of propane-hydrogen-air premixed flames. *International Journal of Hydrogen Energy* 2008;33:4906-14.
[IV.148]
- [344] **Tang C, Huang Z, Law CK**. Determination, correlation, and mechanistic interpretation of effects of hydrogen addition on laminar flame speeds of hydrocarbon-air mixtures. *Proceedings of the Combustion Institute* 2011;33:921-8.
[IV.150]
- [345] **Tanoue K, Goto S, Shimada F, Hamatake T**. Effects of hydrogen addition on stretched premixed laminar methane flames. 1st Report, effects on laminar burning velocity. *Transactions of JSME* 2003;69:162-8.
[IV.134]
- [346] **Taylor SC**. Burning velocity and the influence of flame stretch. PhD thesis 1991, University of Leeds, United Kingdom.
[III.115]
- [347] **Tien JH, Matalon M**. On the burning velocity of stretched flames. *Combustion and Flame* 1991;84:238-48.
[III.76]
- [348] **Tinaut FV, Giménez B, Horrillo A, Cabaco G**. Use of multi-zone combustion models to analyze and predict the effect of cyclic variations on SI engines. SAE Paper 2000-1-0961, 2000.
[II,IV.102]
- [349] **Tinaut FV, Giménez B, Iglesias D, Lawes M**. Experimental determination of the burning velocity of mixtures of n-heptane and toluene in engine-like conditions. *Flow, Turbulence and Combustion* 2012;89(2):183-213.
[III.123]
- [350] **Tinaut FV, López JJ**. Combustion in spark ignition engines. In: Payri F, Desantes JM, editors. *Reciprocating internal combustion engines (Spanish)*. Valencia Polytechnic University publication, Reverté publisher 2011 (2nd imprint 2012); chapt.18.
[III.19]
- [351] **Tinaut FV, Melgar A, Giménez B, Horrillo AJ**. Comparison of the performance of spark-ignition engines fed with producer gas and other conventional fuels by the utilization of a predictive multi-zone model. *Venezuela, V-Congreso Iberoamericano de Ingeniería Mecánica*; 2001.
[IV.224]
- [352] **Tinaut FV, Melgar A, Giménez B, Reyes M**. Characterization of the combustion of biomass producer gas in a constant volume combustion bomb. *Fuel* 2010;89:724-31.
[IV.221]
- [353] **Tinaut FV, Melgar A, Giménez B, Reyes M**. Prediction of performance and emissions of an engine fueled with natural gas/hydrogen blends. *International Journal of Hydrogen Energy* 2011;36:947-56.
[II,IV.79]
- [354] **Tinaut FV, Melgar A, Horrillo AJ, Díez A**. Method for predicting the performance of an internal combustion engine fueled by producer gas and other low heating value gases. *Fuel Processing Technology* 2006;87:135-42.
[IV.244]
- [355] **Tinaut FV, Melgar A, Horrillo AJ**. Utilization of a quasi-dimensional model for predicting pollutant emissions in SI engines. SAE Paper 1999-01-0223, 1999.
[IV.223]
- [356] **Tinaut FV, Reyes M, Giménez B, Pérez A**. Characterization of combustion process and cycle-to-cycle variations in a spark ignition engine fueled with natural gas/hydrogen mixtures. *Scientific conference on Combustion and related fields -SPEIC14- Towards Sustainable Combustion*, Lisboa. Nov, 2014.
[II,IV.115]
- [357] **Tsatsaronis, G**. Prediction of propagating laminar flames in methane, oxygen, nitrogen mixtures. *Combustion and Flame* 1978;33:217-39.
[IV.249]

- [358] **Tse SD, Zhu D, Law CK.** Optically accessible high-pressure combustion apparatus. Review of Scientific Instruments 2004;75(1):233-9.
[IV.181]
- [359] **Tse SD, Zhu DL, Law CK.** Morphology and burning rates of expanding spherical flames in H₂-O₂-inert mixtures up to 60 atmospheres. Proceedings of the Combustion Institute 2000;28:1793-800.
[III.96];[V.15]
- [360] **Tseng LK, Ismail MA, Faeth GM.** Laminar burning velocities and Markstein numbers of hydrocarbon-air flames. Combustion and Flame 1993;95:410-26.
[III.63]
- [361] **Turns SR.** An introduction to combustion. McGraw-Hill, New-York, 2000.
[II,IV.114];[III.37]

U

- [362] **Uykur C, Henshaw PF; Ting DSK, Barron RM.** Effects of addition of electrolysis products on methane-air premixed laminar combustion. International Journal of Hydrogen Energy 2001;26:265-73.
[IV.241]

V

- [363] **Vagelopoulos CM, Egolfopoulos FN, Law CK.** Further considerations on the determination of laminar flame speeds with the counter-flow twin-flame technique. Proceedings of the Combustion Institute 1994;25:1341-7.
[III.107]
- [364] **Vagelopoulos CM, Egolfopoulos FN, Law CK.** Further considerations on the determination of laminar flame speeds with the counter-flow twin-flame technique. Proceedings of the Combustion Institute 1994;25:1341-7.
[IV.180]
- [365] **Vagelopoulos CM, Egolfopoulos FN.** Direct experimental determination of laminar flame speeds. Proceedings of the Combustion Institute 1998;27(1):513-9.
[III.108]
- [366] **Vagelopoulos CM, Egolfopoulos FN.** Laminar flame speeds and extinction strain rates of mixtures of carbon monoxide with hydrogen, methane and air. Proceedings of the 25th international symposium on combustion 1994;1317-23.
[IV.156]
- [367] **Verhelst S, Sheppard CGW.** Multi-zone thermodynamic modeling of spark-ignition engine combustion - An overview. Energy Conversion and Management 2009;50:1326-35.
[III.20];[IV.231]
- [368] **Verhelst S, Sierens R.** A laminar burning velocity correlation for hydrogen-air mixtures valid at spark-ignition engine conditions. ASME Spring Engine Technology Conference paper ICES2003-555, Salzburg, Austria, 2003.
[III.10];[IV.256]
- [369] **Verhelst S, Sierens R.** A quasi-dimensional model for the power cycle of a hydrogen fueled ICE. International Journal of Hydrogen Energy 2007;32:3545-54.
[III.14];[IV.230];[V.23]
- [370] **Verhelst S, Sierens R.** Aspects concerning the optimization of a hydrogen fueled engine. International Journal of Hydrogen Energy 2001;26:981-5.
[II,IV.30]
- [371] **Verhelst S, Sierens R.** Hydrogen engine specific properties. International Journal of Hydrogen Energy 2001;26:987-90.
[II,IV.21]
- [372] **Verhelst S, T'Joel C, Vancoillie J, Demuyneck J.** A correlation for the laminar burning velocity for use in hydrogen spark-ignition engine simulation. International Journal of Hydrogen Energy 2011;36:957-74.

- [III.3];[IV.227];[V.18]
- [373] **Verhelst S, Wallner T.** Hydrogen-fueled internal combustion engines. *Progress in Energy and Combustion Science* 2009;35:490-527.
[II,IV.18];[III.15]
- [374] **Verhelst S, Woolley R, Lawes M, Sierens R.** Laminar and unstable burning velocities and Markstein lengths of hydrogen-air mixtures at engine-like conditions. *Proceedings of the Combustion Institute* 2005;30:209-16.
[III.7];[IV.125];[V.22]
- [375] **Verhelst S.** A study of the combustion in hydrogen fueled internal combustion engines. PhD thesis 2005, Ghent University, Belgium.
[III.13];[IV.232]
- [376] **Vermorel O, Richard S, Colin O, Angelberger C, Benkenida A, Veynante S.** Towards the understanding of cyclic variability in a spark ignited engine using multi-cycle LES. *Combustion and Flame* 2009;156(8):1525-41.
[II,IV.112]

W

- [377] **Wallner T, Lohse-Busch H, Ng H, Peters RW.** Results of research engine and vehicle drive cycle testing during blended hydrogen-methane operation. *Proceedings of National Hydrogen Association Annual Conference, San Antonio, Texas, 2007.*
[II,IV.34]
- [378] **Wallner T, Ng H, Peters RW.** The effects of blending hydrogen with methane on engine operation, efficiency and emissions. *SAE Paper 2007-01-0474, 2007.*
[II,IV.35]
- [379] **Wang H, You X, Joshi AV, Davis SG, Laskin A, Egolfopoulos FN, et al. USC_II-Mech.** High-temperature combustion reaction model of H₂/CO/C₁-C₄ compounds. http://ignis.usc.edu/USC_Mech-II.htm/, 2011.
[III.195];[IV.174]
- [380] **Wang J, Chen H, Liu B, Huang Z.** Study of cycle-by-cycle variations of a spark ignition engine fueled with natural gas-hydrogen blends. *International Journal of Hydrogen Energy* 2008;33(18):4876-83.
[II,IV.10]
- [381] **Wang J, Huang Z, Fang Y, Liu B, Zeng K, Miao H, Jiang D.** Combustion behaviors of a direct-injection engine operating on various fractions of natural gas-hydrogen blends. *International Journal of Hydrogen Energy* 2007;32(15):3555-64.
[II,IV.8]
- [382] **Wang J, Huang Z, Miao H, Wang X, Jiang D.** Characteristics of direct injection combustion fueled by natural gas-hydrogen mixtures using a constant volume vessel. *International Journal of Hydrogen Energy* 2008;33:1947-56.
[II,IV.9]
- [383] **Wang J, Huang Z, Miao H, Wang X, Jiang D.** Study of cyclic variations of direct-injection combustion fueled with natural gas-hydrogen blends using a constant volume vessel. *International Journal of Hydrogen Energy* 2008;33:7580-91.
[II,IV.116]
- [384] **Wang J, Huang Z, Zheng J, Miao H.** Effect of partially premixed and hydrogen addition on natural gas direct injection lean combustion. *International Journal of Hydrogen Energy* 2009;34:9239-47.
[II,IV.80]
- [385] **Wang X, Zhang H, Yao B, Lei Y, Sun X, Wang D, Ge Y.** Experimental study on factors affecting lean combustion limit of SI engine fueled with compressed natural gas and hydrogen blends. *Energy* 2012;38:58-65.
[II,IV.81]
- [386] **Warnatz J, Maas U, Dibble RW.** *Combustion.* Springer-Verlag, Berlin-Heidelberg-NewYork, 1999.
[IV.204]
- [387] **Warnatz J, Maas U, Dibble RW.** *Combustion: physical and chemical fundamentals, modeling and simulation, experiments, pollutant formation.* Springer-Verlag, Berlin-Heidelberg-NewYork, 1998.

- [IV.191]
- [388] **Warnatz J, Maas U.** Technische Verbrennung: Grundlagen, Modellbildung, Schadstoffentstehung. Springer-Verlag, Berlin Heidelberg New York, 1993;101-4.
[III.162]
- [389] **Warnatz J.** Concentration, pressure and temperature dependence of the flame velocity in hydrogen-oxygen-nitrogen mixtures. Combustion Science and Technology 1981;26:203-13.
[III.168]
- [390] **Wierzba I, Ale BB.** Rich flammability limits of fuel mixtures involving hydrogen at elevated temperatures. International Journal of Hydrogen Energy 2000;25:75-80.
[IV.213]
- [391] **Wierzba I, Karim GA, Cheng H.** The rich flammability limits of fuel mixtures containing hydrogen. American Institute of Chemical Engineers Symposium Series 1986;82:104-10.
[IV.212]
- [392] **Williams FA, Grcar JF.** A hypothetical burning-velocity formula for very lean hydrogen-air flames. Proceedings of the Combustion Institute 2009;32:1351-7.
[III.124]
- [393] **Williams FA.** Combustion theory. Addison-Wesley, Reading, Massachusetts, 1985.
[III.41]
- [394] **Williams FA.** Detailed and reduced chemistry for hydrogen autoignition. Journal of Loss Prevention in the Process Industries 2008;21:131-5.
[III.127]
- [395] **Williams FA.** Progress in knowledge of flamelet structure and extinction. Progress in Energy and Combustion Science 2000;26:657-82.
[III.67]
- [396] **Wimmer A, Wallner T, Ringler J, Gerbig F.** Hydrogen-direct injection, a highly promising combustion concept. SAE 2005-01-0108; 2005.
[III.174]
- [397] **Wong YK, Karim GA.** An analytical examination of the effects of hydrogen addition on cyclic variations in homogeneously charged compression-ignition engines. International Journal of Hydrogen Energy 2000;25(12):1217-24.
[II,IV.68]
- [398] **Wu CK, Law CK.** On the determination of laminar flame speeds from stretched flames. Proceedings of the Combustion Institute 1984;20:1941-9.
[III.116]
- [399] **Wu FJ, Kelley AP, Tang CL, Zhu DL, Law CK.** Measurements and correlation of laminar flame speeds of CO and C₂-hydrocarbons with hydrogen addition at atmospheric and elevated pressures. International Journal of Hydrogen Energy 2011;36:13171-80.
[IV.146]
- [400] **Wu MS, Liu JB, Ronney PD.** Numerical simulation of diluent effects on flame balls. Proceedings of the Combustion Institute 1998;27:2543-50.
[III.152]

X

[...] (No references with initial letter -X-)

Y

- [401] **Yetter RA, Dryer FL, Rabitz H.** A comprehensive reaction mechanism for carbon monoxide/hydrogen/oxygen kinetics. Combustion Science and Technology 1993,1991;79:97-128.
[III.170]
- [402] **Yu G, Law CK, Wu CK.** Laminar flame speeds of hydrocarbon-air mixtures with hydrogen addition. Combustion and Flame 1986;63:339-47.
[IV.138]

Z

- [403] **Zeldovich YB, Barenblatt GI, Librovich VB, Makhviladze GM.** The mathematical theory of combustion and explosions. Plenum Press, New-York, 1985.
[\[III.40\]](#); [\[IV.188\]](#)
- [404] **Zeldovich YB, Sadovnikov PYA, Frank-Kamenetskii DA.** Oxidation of nitrogen in combustion, translated by Shelef M. Moscow Academy of Science, 1947.
[\[III.178\]](#)
- [405] **Zeldovich YB.** Structure and stability of steady laminar flames at moderately large Reynolds numbers. *Combustion and Flame* 1981;40:225-34.
[\[III.39\]](#)
- [406] **Zhao Z, Li J, Kazakov A, Dryer FL, Zeppieri SP, Dryer FL.** Burning velocities and a high-temperature skeletal kinetic model for n-decane. *Combustion Science and Technology* 2005;177:89-106.
[\[III.140\]](#)
- [407] **Zimont V, Lipatnikov A.** A numerical model of premixed turbulent combustion of gases. *Chemical Physics Report* 1995;14: 993-1025.
[\[III.177\]](#)

Nomenclature

Glossary of abbreviations, acronyms, symbols and others (*in alphabetical orders*)

Abbreviations

BMF	burned mass fraction
CFD	computational fluid dynamics
CI/CIE	compression-ignition/ engine
CNG	compressed natural gas
CoV	coefficient of variation
$C_xH_yO_z$	generic fuel
D	dimensional
DI	direct injection
EGR	exhaust gas recirculation
FC	fuel cell
FSR	flame speed ratio
HC	hydrocarbon
HC/THC	hydrocarbon fuel or hydrocarbon emissions/ total unburned hydrocarbons
HCCI/	homogeneous charge compression-ignition/
HCCIE	engine
HCNG	hydrogen enriched compressed natural gas
H_2 ICE/SIE	hydrogen-fueled ICE/SIE
IC/ICE	internal combustion/ engine
IMEP	indicated mean effective pressure
MAXP	maximum pressure
MFBR	mass fraction burning rate
NG	natural gas
PSC	partial stratification charge/ engine
SI/SIE	spark-ignition/ spark ignited engine
Z	zone

Symbols

A	area, section
c	specific heat capacity
ct	constant
d	fractal dimension
D	diffusivity
E	activation energy
f, F	fuel; fuel blend
f, F	factor; function
F	function $F(T_w, P, 1/\Phi, f_{res})$
f, g	fractions
F_R	function $F_R(f_{res,u(m)})$
$f_r, f_{res}, f_{res,u}$	residual gas content
$f_{res,u(m)}, f_{u,m}$	residual gas fraction on mass basis
$f_{res,u(v)}, f_{u,v}$	residual gas fraction on volume basis
\hat{h}	hydrogen content
h	hydrogen volumetric fraction (%) in fuel
k	rate coefficient
k_h	coefficient of sensitivity to hydrogen addition of the laminar flame velocity
K_h	dimensionless-normalized coefficient of sensitivity to hydrogen addition of the laminar flame velocity
M	third body in chemical reaction; molecular weight
m	mass

n	moles number; normal unit vector
n	reaction order; wavenumber
P	gas pressure
r	flame radius
R	universal gas constant
R_h	hydrogen composition parameter
S_n	flame speed affected by stretch and instabilities
S	instability-free flame speed, corrected for instabilities but not stretch-free
S_s	moderate-instability flame speed, stretch-free by correction
S_s	stretch-free and instability-free flame speed (by both corrections)
t	time
T	gas temperature
u	burning velocity
u_l	laminar burning velocity free of effects of stretch and instabilities or theoretically one-dimensional
u_L	laminar burning velocity (one-dimensional flame) computed by kinetics or theoretical quasi laminar obtained from chemical kinetics calculations and numerical extension of some experimental data
u_{ne}	normal burning velocity of entrainment (of unburned reactants), affected by stretch and instabilities (image record)
u_{nr}	normal burning velocity of reaction (to burned products), affected by stretch and instabilities (pressure record)
u_s	moderate-instability laminar burning velocity, stretch-free by correction
U_s	stretch-free and instability-free laminar burning velocity (by both corrections)
v	velocity
vol	volumetric
Vol	volume
x	volumetric (molar) fraction in a fuel blend
X	volumetric (molar) fraction in a fuel-air mixture
y	mass fraction in a fuel blend
Y	mass fraction in a fuel-air mixture

Greek and other symbols

α	temperature exponent
α_H	normalized maximum concentration (mole fraction) of H radicals
α_T	function $\alpha_T(T_u; \Phi, h)$
β	pressure exponent
β_P	function $\beta_P(P, T_u; \Phi, h)$
γ	ratio of specific heat capacities c_p/c_v
Γ	function $\Gamma(f_{res,u(m)})$
Γ_w	normalized unstable wavelength scale
δ	flame thickness
Δ	increment
Δ_Δ	dimensionless-increment
ϵ	stoichiometric coefficient
ζ	function $\zeta(\Phi, f_{res}; T_u, P)$ or $\zeta(h, \Phi, f_{res,u}; T_u, P)$
η	function
Θ	function $\Theta(\Phi)$
κ	flame stretch rate, stretch factor
λ	air to fuel equivalence ratio
λ_{tc}	thermal conductivity
λ_w	unstable wavelength scale

Λ_P	function $\Lambda_P(P; h)$
Λ_T	function $\Lambda_T(T_w; h)$
Λ_{U_0}	function $\Lambda_{U_0}(\Phi, h)$
ν	kinematic viscosity
Π	multiplication
ρ	gas density
ρ_a	air density
ρ_b	burned gas density
ρ_u	unburned gas density
ζ	function $\zeta(T_w, P; \Phi)$
σ	expansion (density) ratio ρ_u/ρ_b
σ	normalized laminar burning velocity of fuel blend
Σ	summation
Φ	fuel to air equivalence ratio
Φ_{eF}	effective parameter of fuel-air equivalence ratio
$\chi_{a,f}$	assumption of remaining available air left for hydrocarbon oxidation in combustion of a hydrocarbon-hydrogen blend $(X_a - \chi_{stqa,h})$
$\chi_{stqa,h}$	assumption of stoichiometric amount of air needed for hydrogen total oxidation in combustion of a hydrocarbon-hydrogen blend $[X_h / (X_h/X_a)_{stq}]$
ψ	function
Ψ	function $\Psi(h)$
ω	reaction rate
Ω_R	function $\Omega_R(T_w, P, \Phi, h)$

Subscripts & superscripts

a	air; activation
ad	adiabatic
b	subscript of global Markstein length-number
bv	burning velocity
c	potentially affected by cellularity
cr, cl, ct	critical, critical cellular, critical turbulent
d, dil	dilution, diluent
def, lim	limiting or deficient reactant
e	entrainment (consumption)
exc	excess reactant
f	fuel; flame
g	gas (expansion)
h	hydrogen
hd	hydrodynamic
i, j	species
imep	indicated mean effective pressure
l	laminar (ideal flame; free of stretch and instability)
L	laminar (theoretical; one-dimensional flame computed by kinetics)
m	mass
max	maximum
maxp	maximum pressure
n	normal
o	reference condition
0	inner layer conditions
p	at constant pressure
qL	theoretical quasi laminar obtained from chemical kinetics calculations
qN	quasi laminar or apparent obtained from experimental data

r	reacted (burned products)
r, θ , ϑ	spherical coordinates
s	extrapolated to zero stretch rate
se,ce; sr,cr	subscripts of Markstein lengths and numbers (associated respectively to u_{ne} and u_{nr})
se,sr; ce,cr	subscripts associated to strain rate effect or curvature effect, respectively
st, stq	stoichiometric
stqa	stoichiometric amount of air
t	thermal; turbulent
td; md	thermo-diffusive; mass-diffusive
u; b	unburned; burned
v	at constant volume
vol, v	volumetric
w,y,z	mathematical exponents of parameters

Other notations

Ka	Karlovitz number
l	Markstein lengths (for moderate instability)
L	Markstein lengths (in absence of instability)
Le	Lewis number
Ma	Markstein number
Pe	Peclet number
Re	Reynolds number
Pr	Prandtl number
Z, Ze	Zeldovich numbers

